frontiers | Research Topics

Adaptation of halophilic/halotolerant microorganisms and their applications

Edited by
Furkan Orhan, Rosa María Martínez-Espinosa, Sudhir K. Upadhyay and Sumit Kumar

Published in
Frontiers in Microbiology

ISSN 1664-8714
ISBN 978-2-8325-3422-9
DOI 10.3389/978-2-8325-3422-9

About Frontiers

Frontiers is more than just an open access publisher of scholarly articles: it is a pioneering approach to the world of academia, radically improving the way scholarly research is managed. The grand vision of Frontiers is a world where all people have an equal opportunity to seek, share and generate knowledge. Frontiers provides immediate and permanent online open access to all its publications, but this alone is not enough to realize our grand goals.

Frontiers journal series

The Frontiers journal series is a multi-tier and interdisciplinary set of open-access, online journals, promising a paradigm shift from the current review, selection and dissemination processes in academic publishing. All Frontiers journals are driven by researchers for researchers; therefore, they constitute a service to the scholarly community. At the same time, the *Frontiers journal series* operates on a revolutionary invention, the tiered publishing system, initially addressing specific communities of scholars, and gradually climbing up to broader public understanding, thus serving the interests of the lay society, too.

Dedication to quality

Each Frontiers article is a landmark of the highest quality, thanks to genuinely collaborative interactions between authors and review editors, who include some of the world's best academicians. Research must be certified by peers before entering a stream of knowledge that may eventually reach the public - and shape society; therefore, Frontiers only applies the most rigorous and unbiased reviews. Frontiers revolutionizes research publishing by freely delivering the most outstanding research, evaluated with no bias from both the academic and social point of view. By applying the most advanced information technologies, Frontiers is catapulting scholarly publishing into a new generation.

What are Frontiers Research Topics?

Frontiers Research Topics are very popular trademarks of the *Frontiers journals series*: they are collections of at least ten articles, all centered on a particular subject. With their unique mix of varied contributions from Original Research to Review Articles, Frontiers Research Topics unify the most influential researchers, the latest key findings and historical advances in a hot research area.

Find out more on how to host your own Frontiers Research Topic or contribute to one as an author by contacting the Frontiers editorial office: frontiersin.org/about/contact

Adaptation of halophilic/halotolerant microorganisms and their applications

Topic editors

Furkan Orhan — Ağrı İbrahim Çeçen University, Türkiye
Rosa María Martínez-Espinosa — University of Alicante, Spain
Sudhir K. Upadhyay — Veer Bahadur Singh Purvanchal University, India
Sumit Kumar — Amity University, India

Citation

Orhan, F., Martínez-Espinosa, R. M., Upadhyay, S. K., Kumar, S., eds. (2023). *Adaptation of halophilic/halotolerant microorganisms and their applications*. Lausanne: Frontiers Media SA. doi: 10.3389/978-2-8325-3422-9

Table of contents

frontiers | Frontiers in Microbiology

TYPE Editorial
PUBLISHED 22 August 2023
DOI 10.3389/fmicb.2023.1252921

OPEN ACCESS

EDITED AND REVIEWED BY
Andreas Teske,
University of North Carolina at Chapel Hill, United States

*CORRESPONDENCE
Furkan Orhan
furkan_orhan@hotmail.com

RECEIVED 04 July 2023
ACCEPTED 11 August 2023
PUBLISHED 22 August 2023

CITATION
Martínez-Espinosa RM, Kumar S, Upadhyay SK and Orhan F (2023) Editorial: Adaptation of halophilic/halotolerant microorganisms and their applications. *Front. Microbiol.* 14:1252921. doi: 10.3389/fmicb.2023.1252921

Editorial: Adaptation of halophilic/halotolerant microorganisms and their applications

Rosa María Martínez-Espinosa[1,2], Sumit Kumar[3], Sudhir K. Upadhyay[4] and Furkan Orhan[5]*

[1]Department of Biochemistry, Molecular Biology, Edaphology, and Agricultural Chemistry, Faculty of Sciences, University of Alicante, Alicante, Spain, [2]Applied Biochemistry Research Group, Multidisciplinary Institute for Environmental Studies "Ramón Margalef" University of Alicante, Alicante, Spain, [3]Amity Institute of Biotechnology, Amity University, Noida, Uttar Pradesh, India, [4]Department of Environmental Science, Veer Bahadur Singh Purvanchal University, Jaunpur, Uttar Pradesh, India, [5]Faculty of Arts and Science, Department of Molecular Biology and Genetics, Ağrı Ibrahim Çeçen University, Ağrı, Türkiye

KEYWORDS

halophilic, enzyme, compatible solutes, bioactive compounds, PGP

Editorial on the Research Topic
Adaptation of halophilic/halotolerant microorganisms and their applications

In hypersaline soils and waters, microorganisms surviving in these ecosystems must deal with excess salt in addition to any other factors limiting survival. Halophilic and halotolerant microorganisms use a variety of strategies to maintain osmotic equilibrium across their cell membranes and prevent the loss of cytoplasmic water. Among these strategies, modifications at molecular levels affecting proteins and RNA/DNA, salt-in adaptation, compatible solute adaptation, and salt-stable cell surface and membranes are included.

Due to their physiological adaptations, halophilic/halotolerant microorganisms have great potential for diverse applications. The Research Topic "*Adaptation of halophilic/halotolerant microorganisms and their applications*" includes review and original research articles on the uses of halotolerant and halophilic microorganisms in a variety of fields, including agriculture, medicine, pharmaceuticals, industry, food, and waste treatments such as the degradation of hydrocarbons, and saline wastewater treatment.

Halotolerant and halophilic microorganisms have developed versatile molecular mechanisms for coping with saline stress, and many of these molecular adaptations have potential applications in biotechnology. Within this context, Zhou et al. have explored the mechanisms of halotolerance in six type strains of *Pontixanthobacter* and *Allopontixanthobacter* by comparative genome analysis. Genes directly connected to halotolerance include those involved in osmolytes synthesis, membrane permeability control, ions transport, intracellular signaling, polysaccharide biosynthesis, and SOS response. Similar gene content has been described previously in other bacteria, thus reinforcing the idea that these are the main mechanisms explaining halotolerance. The authors are linking genome-wide co-occurrence, genetic diversity, and physiological characteristics of these bacteria.

Metagenomics as a culture-independent tool has also been employed to harness the biotechnological potential of halophiles. On similar lines, Jeilu et al. identified novel carbohydrate-degrading enzymes using functional metagenomic analysis in samples from Ethiopian Soda Lakes. A total of 378 genes mostly belonging to multiple Glycoside Hydrolases (GH) were identified. Most GH genes were of bacterial origin, predominantly of the *Halomonas* genus. Biochemical analysis of amylase, cellulase, and pectinase revealed them to be polyextremophilic with activity at high temperatures, pH, and salt concentrations. Such properties are relevant for enzymatic applications, particularly in lignocellulosic biorefinery.

To explore polysaccharide-hydrolyzing genomic potential of cultured haloarchaea, Elcheninov et al. reported a comparative genomic analysis of 155 haloarchaeal bacterial strains including seven different genera as *Natronolimnobius*, *Halococcoides*, *Halosimplex*, *Natronobiforma*, *Halomicrobium* and *Natrarchaeobius*. The authors observed an overpresentation of cellulase genes (GH9, GH12, and GH5) in the cellulotrophic haloarchaea genomes compared to cellulotrophic archaea on a per-genome basis. The research findings also indicated variations in CAZymes profiles among the groups (neutrophilic and alkaliphilic haloarchaea), relating to genome size, the number of genes involved in import mechanisms, and central metabolism of sugars.

The study by Tu et al. used cultivation and high-throughput sequencing techniques to investigate the microbial community of Dingyuan Salt Mine, and to study the effects of long-term brine storage on the microbial community. The dominant bacterial species in fresh brine were *Cyanobium* PCC-6307 spp., *Aeromonas* spp. and *Pseudomonas* spp., whereas the dominant archaea were *Natronomonas* spp., *Halapricum* spp., and *Halomicrobium* spp. After 3-year storage, the microbial community shifted toward *Salinibacter* spp. and *Alcanivorax* spp. as dominant bacterial species and *Natronomonas* spp. and *Halorientalis* spp. as archaeal species. Long-term storage of brine resulted in increased biomass but species diversity declined. This study also led to the isolation of 12 possible new species belonging to 3 genera of halophilic archaea.

Halophiles have also been a great repository for valuable bioactive compounds of pharmaceutical importance. In this context, Karthik et al. investigated the potential of mangrove microbe *Glutamicibacter mysorens* for antimicrobial and anticancer properties, and demonstrated anticancer activity of intracellular metabolites on prostate cancer cells. Low molecular weight compounds Kinetin-9- ribose and Embinin were identified by Liquid Chromatography–Mass Spectrometry (LC–MS) study. Thus, *G. mysorens* is a promising source for low molecular weight bioactive molecules with therapeutic potential.

The review of Moopantakath et al. demonstrated the ecology and diversity of haloarchaeal microorganisms, their strategies in coping with stress, haloarchaea biotechnological significance (anticancer compounds, antimicrobial compounds, antioxidant compounds), hydrolytic enzymes, biodegradable and biocompatible polymers, and synthesis and application of bioactive nanoparticles from haloarchaeal microorganisms.

Haloarchaea are a promising group of microorganisms for biotechnological applications, showing metabolic capabilities of interest for industrial processes within the circular economy, for example the biodegradation and use of the two dominant biomass polysaccharides on the planet, cellulose and chitin. Related to polysaccharide biodegradation, Sorokin et al. conducted a selective enrichment on a wide polysaccharide spectrum aiming at the isolation of novel metabolic and taxonomic groups of haloarchaea from hypersaline lakes. By using an array of commercially available homo- and heteropolysaccharides to enrich hydrolytic haloarchaea, the authors isolated a range of halo- and natronoarchaea, including previously described taxa and several new genus-level lineages. This study demonstrates previously unrecognized microbial potential for utilization of a broad range of natural polysaccharides in hypersaline habitats.

One is the major compatible solutes produced by halophiles is ectoine. Using the ectoine-excreting strain *Halomonas elongata* KB2.13, Hobmeier et al. demonstrated two methods of ectoine production, based on Oxaloacetate-enhanced precursor and on over-expression of transporter [transporter for ectoine accumulation (Tea ABC)]. Both techniques have the potential to significantly increase ectoine production and excretion. This increase was initially attributed to the absence of phosphoenolpyruvate carboxykinase, which converts the oxaloacetate (OAA) into Phospoenolpyruvate (PEP), thus removing feedback inhibition and allowing the unconverted OAA to enter the TCA cycle for ectoine production. The excretion rate of ectoine was significantly enhanced three-fold when both TeaBC subunits, a transporter responsible for ectoine uptake, were overexpressed in the absence of the substrate-binding protein TeaA. The main subunit TeaC showed an extracellular ectoine concentration per dry weight that was roughly five times higher than TeaBC shortly after its expression was induced. Since both approaches are complementary, they are promising solutions for metabolic engineering challenges.

In deep shale reservoirs, salinity and hydraulic retention time (HRT) have an impact on *Halanaerobium* cell membrane structure, which in turn affects microbial development and physiology and causes biogeochemical responses. The variations in the membrane fatty acid chemistry of *H. congolense* WG10 caused by salt and HRT have been addressed by Ugwuodo et al.. Notably, *H. congolense* WG10 increases the amount of polyunsaturated fatty acids in its membrane under suboptimal salt concentrations, which appears to increase its fluidity and thickness. Mean chain length and double bond index are used as proxies for the fluidity and thickness of the membrane, respectively. Thus, natural and human-made variables may alter the chemistry of membrane fatty acids in persistent microbial taxa that are important to maintain physical and biogeochemical equilibrium of fractured shale, with implications for human health.

The review article of Ramasamy and Mahawar offers novel perspectives on the role of halotolerant (HT) bacteria linked to crop plants in boosting their resistance to salinity stress. The paper also identifies several issues with halotolerant plant growth promoting Rhizobacteria (HT-PGPR)'s application in the agricultural sector and suggests scientific ways to solve them to advance sustainable agriculture in the future.

Based on research conducted by John et al. the inoculation of *Vigna mungo* L., a legume, with halotolerant plant growth promoting rhizobacteria (HT-PGPR) isolated from *Sesuvium portulacastrum*, led to increased shoot length and vigor index, indicating a potential enhancement in salt tolerance for the plant. Moreover, the salt tolerant bacterial inoculation led to enhancements in grain yield, shoot length, chlorophyll content, and photosynthetic rate, while also reducing the enzymatic activity of catalase and superoxide dismutase, suggesting improved stress tolerance. The research findings also suggest that HT-PGPRs can be a cost-effective and ecologically sustainable approach to enhance crop productivity in high saline conditions. The use of such rhizobacteria holds significant promise for sustainable agricultural practices in salt-affected regions.

In conclusion, most saline ecosystems of our planet are still unexplored for both basic and applied sciences studies. The study of the microbiome of these environments by culture-dependent and -independent techniques will reveal a great deal of microbial diversity. Furthermore, these halophilic microbes can be a biotechnologically useful source of robust enzymes and of pharmaceutical molecules with potential for industry, agriculture, and environmental bioremediation. Research carried out on halophiles to date has established that halophiles can serve as an important tool for biological interventions.

Author contributions

All authors listed have made a substantial, direct, and intellectual contribution to the work and approved it for publication.

Conflict of interest

The authors declare that the research was conducted in the absence of any commercial or financial relationships that could be construed as a potential conflict of interest.

Publisher's note

All claims expressed in this article are solely those of the authors and do not necessarily represent those of their affiliated organizations, or those of the publisher, the editors and the reviewers. Any product that may be evaluated in this article, or claim that may be made by its manufacturer, is not guaranteed or endorsed by the publisher.

frontiers | Frontiers in Microbiology

TYPE Original Research
PUBLISHED 25 August 2022
DOI 10.3389/fmicb.2022.968983

OPEN ACCESS

EDITED BY
Sudhir K. Upadhyay,
Veer Bahadur Singh Purvanchal University, India

REVIEWED BY
Devendra Jain,
Maharana Pratap University of Agriculture & Technology, India
Antonio Ventosa,
Sevilla University, Spain

*CORRESPONDENCE
Alberto Marin-Sanguino
alberto.marin@udl.cat

SPECIALTY SECTION
This article was submitted to Extreme Microbiology, a section of the journal Frontiers in Microbiology

RECEIVED 14 July 2022
ACCEPTED 29 July 2022
PUBLISHED 25 August 2022

CITATION
Hobmeier K, Oppermann M, Stasinski N, Kremling A, Pflüger-Grau K, Kunte HJ and Marin-Sanguino A (2022) Metabolic engineering of *Halomonas elongata*: Ectoine secretion is increased by demand and supply driven approaches.
Front. Microbiol. 13:968983.
doi: 10.3389/fmicb.2022.968983

Metabolic engineering of *Halomonas elongata*: Ectoine secretion is increased by demand and supply driven approaches

Karina Hobmeier[1], Martin Oppermann[1], Natalie Stasinski[1], Andreas Kremling[1], Katharina Pflüger-Grau[1], Hans Jörg Kunte[2] and Alberto Marin-Sanguino[1,3]*

[1]Professorship for Systems Biotechnology, Technical University of Munich, Garching, Germany, [2]Division Biodeterioration and Reference Organisms, Bundesanstalt für Materialforschung und-prüfung (BAM), Berlin, Germany, [3]Departament de Ciències Mèdiques Bàsiques, Universitat de Lleida, Lleida, Spain

The application of naturally-derived biomolecules in everyday products, replacing conventional synthetic manufacturing, is an ever-increasing market. An example of this is the compatible solute ectoine, which is contained in a plethora of treatment formulations for medicinal products and cosmetics. As of today, ectoine is produced in a scale of tons each year by the natural producer *Halomonas elongata*. In this work, we explore two complementary approaches to obtain genetically improved producer strains for ectoine production. We explore the effect of increased precursor supply (oxaloacetate) on ectoine production, as well as an implementation of increased ectoine demand through the overexpression of a transporter. Both approaches were implemented on an already genetically modified ectoine-excreting strain *H. elongata* KB2.13 (Δ*teaABC* Δ*doeA*) and both led to new strains with higher ectoine excretion. The supply driven approach led to a 45% increase in ectoine titers in two different strains. This increase was attributed to the removal of phosphoenolpyruvate carboxykinase (PEPCK), which allowed the conversion of 17.9% of the glucose substrate to ectoine. For the demand driven approach, we investigated the potential of the TeaBC transmembrane proteins from the ectoine-specific Tripartite ATP-Independent Periplasmic (TRAP) transporter as export channels to improve ectoine excretion. In the absence of the substrate-binding protein TeaA, an overexpression of both subunits TeaBC facilitated a three-fold increased excretion rate of ectoine. Individually, the large subunit TeaC showed an approximately five times higher extracellular ectoine concentration per dry weight compared to TeaBC shortly after its expression was induced. However, the detrimental effect on growth and ectoine titer at the end of the process hints toward a negative impact of TeaC overexpression on membrane integrity and possibly leads to cell lysis. By using either strategy, the ectoine synthesis and excretion in *H. elongata* could be boosted drastically. The inherent complementary nature of these approaches point at a coordinated implementation of both as a promising strategy

for future projects in Metabolic Engineering. Moreover, a wide variation of intracelllular ectoine levels was observed between the strains, which points at a major disruption of mechanisms responsible for ectoine regulation in strain KB2.13.

KEYWORDS

biochemistry, biotechnology, ectoine, *Halomonas elongata*, halophiles, metabolic engineering, microbiology

1. Introduction

The osmoadaptation strategy used by many bacteria and methanogenic archaea is the intracellular accumulation of osmolytes to balance the turgor pressure experienced in saline environments (Galinski, 1995). These osmoprotective organic compounds are called "compatible solutes" due to their compatibility with cell metabolism even at high concentrations (Brown, 1976). One of the most widespread compatible solutes is the aspartate-derivative ectoine (1,4,5,6,tetra-2-methyl-4-pyrimidonecarboxylic acid) (Galinski et al., 1985). Ectoine is biotechnologically relevant as protectant and stabilizer of proteins and other biomolecules against a wide range of adverse environmental factors like salinity but also heat, desiccation, freezing, thawing, and ionizing radiation. In addition to its function as a bioprotector, ectoine and its derivative hydroxyectoine have been proposed as potential drugs for diseases, such as Alzheimer's and rhinoconjunctivitis (Kanapathipillai et al., 2005; Salapatek et al., 2011; Bilstein et al., 2021). Moreover, its stabilizing effect was also observed on whole cells against stresses like radiation or cytotoxins (Lippert and Galinski, 1992; Kempf and Bremer, 1998; Pastor et al., 2010; Schröter et al., 2017). For these reasons, around 15,000 tons of ectoine are produced every year, and its price is close to 1,000 USD/Kg (Liu et al., 2021). The moderate halophilic gammaproteobacterium *Halomonas elongata* DSM 2581 (Vreeland et al., 1980) is able to grow at elevated salt concentrations due to the *de novo* synthesis of ectoine as its main compatible solute. A variety of strains of *H. elongata* are used as cell factories to produce ectoine for pharmaceutical and cosmetical use (Lentzen and Schwarz, 2006; Kunte et al., 2014) and a variety of other products (Ye and Chen, 2021). Additionally, there is an active interest in finding or creating other bacteria able to produce ectoine (Gießelmann et al., 2019; Wang et al., 2021).

Bioprocesses must often compete with chemical synthesis based on cheap petrochemicals, this creates a constant pressure to keep optimizing the overall process and streamlining metabolism to maximize the achievable product yield. Manipulating metabolic fluxes is not trivial due to the abundant and often unknown mechanisms by which the cell regulates them to meet its needs. The complexity of metabolic regulation and the need to address it at a systems level was recognized long time ago (Savageau, 1971, 1976) and confirmed by the failure of early attempts to increase metabolic fluxes by directly overexpressing a few key enzymes (Ruijter et al., 1997). Even nowadays, regulatory feedback loops are common obstacles metabolic engineering has to deal with Yu et al. (2021). Early concepts dealing with metabolism as a system based on supply and demand blocks (Hofmeyr and Cornish-Bowden, 2000) highlighted the need to look beyond the pathways, into the global economy of the cell. In the case of ectoine, its intracellular concentration is tightly controlled to balance the external salt concentration (Dötsch et al., 2008; Czech et al., 2018). Since artificial increases in metabolic fluxes producing ectoine are very likely to be countered by feedback mechanisms, rational manipulation of the fluxes is a challenging but feasible approach to improve ectoine production (Ma et al., 2020). Unlike the well studied end-product inhibition pattern commonly found in amino acid synthesis (Savageau, 1975; Alves and Savageau, 2000), whatever mechanism the cell uses for ectoine homeostasis needs to ensure ectoine concentration to be adjustable across a broad range to enable adaptation to different salinities and other environmental conditions. Although the detailed mechanisms controlling ectoine synthesis have not been completely elucidated, it is known that *H. elongata* prioritizes the uptake of compatible solutes from the medium over *de novo* ectoine synthesis and it has been proposed that the export of ectoine to the periplasmic space and subsequent re-uptake into the cytoplasm may be part of the regulatory loop (Grammann et al., 2002; Kunte, 2006). The existence of this traffic of ectoine between compartments and its nature as an aspartate derivative places ectoine synthesis within a tightly regulated metabolic environment.

Since the whole aspartate family of amino acids has oxaloacetate as a precursor, the *de novo* synthesis of ectoine elevates the demand for it and withdraws carbon from the TCA cycle. The anaplerotic node that is responsible for the replenishment of TCA cycle intermediates gains a special position in the *H. elongata* central metabolism when grown on glycolytic carbon sources. The anaplerotic role is shared between the phosphoenolpyruvate carboxylase (Ppc) and the reversible

membrane-associated Na^+-pump oxaloacetate decarboxylase (Oad). Ppc is thermodynamically more favorable, but Oad is directly coupled to the sodium driving force, ensuring a sufficient increase in anaplerotic flux for ectoine synthesis depending on the sodium gradient with this alternative pathway (Hobmeier et al., 2020). The remaining enzymes involved in this part of the metabolic network, to which we will refer from now on as the PEP-PYR-OAA node, are the PEP carboxykinase (PckA) and the malic enzymes (MaeA and MaeB). PckA catalyzes the irreversible decarboxylation of oxaloacetate to phosphoenol-pyruvate, consuming ATP in the process (Sauer and Eikmanns, 2005). The PckA-mediated reaction is really only necessary when the cell grows on gluconeogenetic carbon sources, but it has been shown to be active in other bacteria during glycolytic growth as well (Chao and Liao, 1994; Yang et al., 2003). The futile cycle created by the simultaneous activity of Ppc and PckA is a sink for ATP and prevents accumulation of oxaloacetate, making PckA a promising target for flux optimization. The malic enzymes are normally also gluconeogenetic enzymes converting malate to pyruvate (Sauer and Eikmanns, 2005). In *H. elongata*, there are two isoenzymes present, namely *maeA* (HELO_3817), which corresponds to *sfcA* in *E. coli*, and *maeB* (HELO_3763). They have different cofactor specificities with *maeA* being linked to NAD and *maeB* to NADP. For both isoenzymes an oxaloacetate-decarboxylating activity is described as possible in the literature, meaning not only malate but also oxaloacetate can be used as a substrate (Sauer and Eikmanns, 2005). This again constitutes a competing pathway for ectoine synthesis. However, enzyme assays only showed *in vitro* activity for the NADP-dependent isoenzyme MaeB.

Besides accumulating in the cytoplasm and being diluted by growth, ectoine has other possible metabolic fates. Ectoine can be used as a carbon source by *H. elongata* through an independent degradation pathway (Schwibbert et al., 2011), or it can also be exported to the periplasm through a not yet identified transporter (Vandrich et al., 2020) and then taken up through the ectoine-specific TRAP transporter encoded in the *teaABC* operon. The discovery of this cycle was possible through the modified *"leaky mutant"* strain KB2.13 (*H. elongata* DSM 2581, Δ*teaABC* Δ*doeA*) which, true to its name, leaks ectoine into its surroundings (Kunte et al., 2002; Kunte, 2006) due to the deletion of the *teaABC* operon (Grammann et al., 2002; Kunte et al., 2014). The additional deletion of the ectoine hydrolase gene *doeA* abolishes ectoine degradation and prevents this strain from consuming ectoine (Schwibbert et al., 2011). It is noteworthy that the leaky phenotype can already be observed after solely removing the periplasmic substrate-binding protein (SBP), TeaA, but leaving the small and large transmembrane subunits (TeaB and TeaC) intact. Since the TRAP is a secondary transporter and it is not driven by ATP hydrolysis, but a by an ion gradient (Kunte et al., 2002), both transmembrane proteins could potentially facilitate the bidirectional transport of ectoine in the absence of the SBP TeaA.

The aim of this work was to explore the potential for increased ectoine production in the industrial producer strain *H. elongata*. To achieve this goal, we used two complementary strategies that aim at a rational manipulation of the relevant fluxes: increasing the supply of precursors and boosting the demand for the end-product.

2. Materials and methods

2.1. *H. elongata* strains and growth experiments

The *H. elongata* strains used in this work are derived from the modified strain *H. elongata* KB2.13 (Δ*teaABC* Δ*doeA*; Kunte et al., 2002; Kunte, 2006), and are listed in Table 1. Further modifications were introduced using homologous recombination as detailed below. All *H. elongata* strains were routinely grown at 30°C and under shaking at 220 r.p.m. in liquid media LB (Miller) enriched with 1 M NaCl or MM63 minimal medium [KH_2PO_4 100 mM, $(NH_4)_2SO_4$ 15 mM, KOH 75 mM, NaCl variable (from 0.17 to 2 M depending on the experiment), carbon source (glucose or acetate depending on the experiment) 27.75 mM, $MgSO_4 \cdot 7\ H_2O$ 1 mM, $FeSO_4 \cdot 7\ H_2O$ 0.004 mM] (Larsen et al., 1987). In general, three biological replicates were always used in each growth experiment for each strain and condition except for the ectoine secretion experiments with TeaBC, TeaB, and TeaC. Here, six replicates were used in the pre-culture steps in order to induce the heterologous gene expression in three while leaving three others uninduced as references.

In the first step of the growth experiments, for each biological replicate a single colony was taken from a solid agar plate and grown in 3 mL liquid LB medium enriched with 1 M NaCl. Subsequently, an aliquot of this overnight culture was taken to inoculate 3 mL MM63 minimal medium with 1 M NaCl and either glucose or acetate as carbon source in a 1:100 ratio. This culture was then again used to inoculate a subsequent MM63 culture with an adjusted inoculum volume to achieve an OD_{600} of 0.01 in the new culture. This third pre-culture differs slightly from experiment to experiment since it is used to adjust the cultures to the respective main culture medium. In case of the microtiter plate screenings, four 3 mL MM63 minimal medium cultures with each containing a different NaCl concentration (0.17, 0.5, 1, and 2 M) and the carbon source used in the previous step were inoculated. For all shake flask experiments with the general MM63 minimal medium (not SO_4-limited medium) the same medium as in the previous pre-culture step (1 M NaCl) was used. for the ectoine excretion experiment with SO_4-limited medium, a SO_4-limited MM63 minimal medium with 1 M NaCl and glucose was used to

TABLE 1 Summary of all modified strains characterized in this work based on the parental strain KB2.13 (*H. elongata* DSM 2581, Δ*teaABC* Δ*doeA*). Most experiments presented in this work were performed with the in frame null mutations, only the screening in microtitter plate was done with the marker replacement strains for convenience. No phenotypic differences were observed between the marker replacement strains and their corresponding in-frame full deletion strains.

Strain	Genotype *H. elongata* KB2.13	Type of modification	Phenotype compared to KB2.13
KH1.1	Δ*pckA*	In-frame null mutation	Reduced growth rate on glucose, no differences growing on acetate, increased ectoine excretion (compared to KB2.13)
KH1.2	Δ*pckA*::Sm^R	Marker replacement of PckA	Resistant against streptomycin, reduced growth rate on glucose especially at low salinities but shorter lag phase than KH1.1, no differences growing on acetate
KH2.1	Δ*pckA*Δ*maeB*	In-frame null mutation	Reduced growth rate on glucose especially at low salinities, no differences growing on acetate, same ectoine synthesis as KH1.1
KH2.2	Δ*pckA* Δ*maeB*::Sm^R	Marker replacement of *maeB*	Resistant against streptomycin, reduced growth rate on glucose especially at low salinities, no differences growing on acetate
KH3.1	Δ*pckA*Δ*ppc*	In-frame null mutation	Reduced growth rate on glucose especially at low salinities, no differences growing on acetate, higher ectoine excretion than KB2.13

inoculate another 3 mL pre-culture step in MM63 SO_4-limited minimal medium with glucose, until the final inoculation of the main culture. During the transfers, the cultures were kept in exponential growth at all times and the final transfer to the main culture was performed with an adjusted inoculation volume reaching an initial OD_{600} of 0.01 in the main culture medium.

The screening experiments were carried out in sterile 96-well plates (Greiner, Germany) with a filling volume of 0.2 mL per well and the four NaCl concentrations (0.17, 0.5, 1, and 2 M) already used in the pre-culture for each replicate. As a blank as well as sterile control, wells with the sterile medium were measured in parallel. The measurements were performed in an automated microplate reader (Tecan, Austria) at 30°C, which was set to shake briefly and measure the OD_{600} in regular intervals every 10 min. The OD_{600} evolution was followed for a time frame of ∼16–24 h until the stationary phase was reached.

Shake flask experiments were routinely performed in 500 mL flasks with 10% working volume incubated in a rotary shaker. The OD_{600} was followed using a spectrometer (Eppendorf, Germany). Ectoine samples were either taken in the late exponential phase as external concentration in relation to the biomass (g/gDW) or after complete consumption of the carbon source as titer (g/L). In the ectoine secretion experiments specifically, after inoculation the cultures were grown to an OD_{600} of 0.1 as an adaptation phase, which lasted ∼7 h. After reaching OD_{600} 0.01 half of the cultures were induced with 0.1 mM 3-methylbenzoic acid (3-MB) diluted in ethanol (EtOH). The same volume of EtOH solvent, which was used for induction, was added to the remaining uninduced references without 3-MB. During the overexpression of TeaBC, 1 mL samples for ectoine detection were taken at three time points in the late exponential phase. In the experiment overexpressing TeaB and TeaC individually, the ectoine was measured at one time point in the late exponential phase as well as the titers.

2.2. Genome modification using homologous recombination

The genome modifications, marker replacement with a Sm^R cassette (*aadA*) from pSEVA434 (Silva-Rocha et al., 2013) and in-frame null mutations, were performed using homologous recombination (Martínez-García and de Lorenzo, 2011). The method established for *Pseudomonas putida* was adapted as detailed in Hobmeier et al. (2020). First an integration vector (Supplementary Table 1) specific for the modification and targeted gene was constructed *via* Gibson Assembly using the oligonucleotides specified in Supplementary Table 1. For the deletion of *ppc*, the previously constructed plasmid pSEVA_Δppc described in Hobmeier et al. (2020) was used. After generating the integration vector, it was transferred into the *H. elongata* respective strain by triparental mating. After successful integration of the vector into the genome a second conjugal transfer of the expression plasmid pSW-2 for the homing endonuclease I-SceI was carried out. Subsequently, the recombination event was triggered by induction of I-SceI expression, which causes double-strand breaks in the genome at the specific recognition sites introduced together with the integration plasmid. The mutant strains were selected based on the desired phenotype and the correct genotype was verified using polymerase chain reaction (PCR) and

sequencing (Eurofins Genomics, Germany). All used enzymes were purchased from New England Biolabs (USA).

2.3. Construction of the expression vectors for TeaBC, TeaB, and TeaC

The expression vectors were constructed *via* Gibson Assembly using the oligonucleotides specified in Supplementary Table 1. The oligonucleotides were designed to regenerate the restriction sites used to linearize the plasmid pSEVA438 (Silva-Rocha et al., 2013) which was used as backbone. pSEVA438 already harbors the inducible XylS/Pm promoter with an empty multiple cloning site. The plasmid was linearized using the restriction sites *SacI* and *HindIII* for the expression plasmids pSEVA438-*teaBC* and pSEVA438-*teaC*. For pSEVA438-*teaB* the combination *SacI* and *PstI* was used. The inserts were generated by PCR amplification using the protocol specified by the manufacturer. Using the oligonucleotides, the synthetic ribosomal binding site (5' aggaggcttcat 3') was inserted for each construct to facilitate translation. The Gibson Assembly reaction was carried out as specified in the manufacturer's protocol and transformed into TSS-competent *E. coli* DH5α λ*pir* cells (Chung et al., 1989) described in detail by Hobmeier et al. (2020). The correct genotypes were verified using PCR and sequencing (Eurofins Genomics, Germany). All applied enzymes were purchased from New England Biolabs (USA).

2.4. Transcriptomic analysis

The collection of RNA for transcriptomic analysis was part of the experiment described in Hobmeier et al. (2022). In this work, we add the data for strain KH1.1, which has not been published before. The parental strain KB2.13 (*H. elongata* DSM 2581 Δ*teaABC* Δ*doeA*) and derivative KH1.1 (*H. elongata* KB2.13 Δ*pckA*) were grown in 50 mL scale as described earlier in MM63 minimal medium with 1 M NaCl and glucose. After reaching an OD_{600} of ∼0.5, well within the exponential growth phase, samples were taken and treated with RNAprotect reagent (Qiagen, Germany). Subsequently, the RNA was isolated using the Macherey-Nagel NucleoSpin RNA kit (Macherey-Nagel, Germany) and sent to GATC Biotech company (Germany). They generated a strand-specific cDNA library and performed the RNA-sequencing at the company facilities using the Illumina NovaSeq 6000 S4 XP. The obtained FASTQ files were comprised of paired-end reads with lengths of 150 bp. The data was further processed as described in Hobmeier et al. (2022). The resulting transcript per million (TPM) were then analyzed regarding differential expression of genes based on a log2-fold change (log2-FC) of |1.5| between strains using Python scripts. For clustering, Principal Component Analysis (PCA) was applied to the set of TPM counts for all conditions: wild type *H. elongata* DSM 2581 (Wt) on glucose and acetate, KB2.13 strain on glucose and KH1.1 on glucose (three replicates each). In order to cluster genes by their response to different conditions and not by their overall level of expression, the first principal component was not used to compute distances in the clustering process.

2.5. Ectoine detection via RP-HPLC

The quantification of extracellular ectoine was performed using reverse-phase (RP) high performance liquid chromatography (HPLC) analysis, which has been described in detail in Hobmeier et al. (2020). However, since the secreted ectoine in the medium was measured no extraction was needed. After sampling, the biomass was separated by centrifugation for 5 min at 15,000 × g and 25°C and the supernatant was carefully transferred into a new tube. The supernatant was then diluted 1:10 with the mobile phase (acetonitrile/phosphate) and analyzed using a reverse phase column (Nucleodur 100 5 NH2 RP CC 125/4, Macherey-Nagel). With a UV-detector the absorption of ectoine at a wavelength of 210 nm was recorded. Ectoine samples were taken either in the late exponential phase or after the end of the batch process. Samples taken during the growth phase were normed using the biomass at the time of sampling (gram per gram dry weight, g/gDW) by applying the previously determined OD_{600} to ash free dry weight correlation published by Hobmeier et al. (2020). Because the measured OD_{600} values after reaching the stationary phase are not reliable the amount of produced ectoine at the end of the process was determined as the final ectoine titer (g/L).

3. Results

3.1. Growth and salt tolerance of modified strains

We screened various *H. elongata* knockout mutants with modifications in the PEP-PYR-OAA node in comparison to KB2.13, from which they are derived. In detail, these strains are KH1.2 with a marker replacement in phosphoenolpyruvate carboxykinase (Δ*pckA*::Sm^R), KH2.2 with a null mutation in *pckA* and a marker replacement in NADP-dependent malic enzyme (Δ*pckA*Δ*maeB*::Sm^R), and finally KH3.1 with null mutations in phosphoenolpyruvate carboxykinase and phosphoenolpyruvate carboxylase (Δ*pckA*Δ*ppc*). The impact on physiology and ectoine synthesis due to these modifications are explored in the following. The determined growth rates are shown in Figure 1. The reference strain (KB2.13) is illustrated in gray. The knockout mutants KH1.2, KH2.2, and KH3.1 are depicted in orange, green, and blue, respectively.

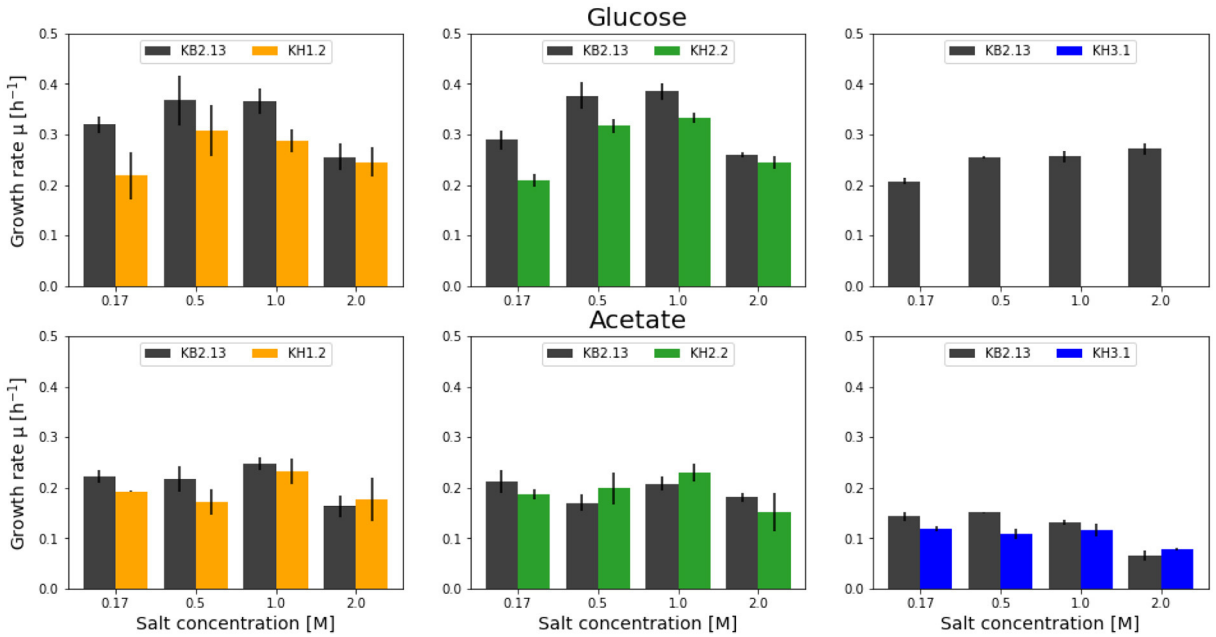

FIGURE 1
Overview of the growth rates achieved by the modified strains KH1.2 (KB2.13, Δ*pckA*::Sm^R) (orange), KH2.2 (KB2.13, Δ*pckA* Δ*maeB*::Sm^R) (green), and KH3.1 (KB2.13, Δ*pckA*Δ*ppc*) (blue) in microtiter plate screenings growing on glucose (top) and acetate (bottom). For each screening the parental strain, KB2.13 (*Halomonas elongata* DSM 2581, Δ*teaABC* Δ*doeA*) (gray) is grown in parallel as reference. The deleted genes *pckA*, *ppc* and *maeB* encode phosphoenolpyruvate carboxykinase, phosphoenolpyruvate carboxylase, and the NADP-dependent malic enzyme, respectively.

3.1.1. KH1.2—Phosphoenolpyruvate carboxykinase deletion strain

In the literature, the PckA-mediated reaction is generally designated as a gluconeogenetic reaction. But the disruption in *H. elongata* KB2.13 had an impact on its growth behavior specifically with glucose as substrate. Across a range of salt concentrations, spanning from low salinity at 0.17 M NaCl, the plateau of salt optimum from ~0.5 to 1 M NaCl, and up to high salinity at 2 M NaCl, the KH1.2 strain grew significantly slower than the parental strain KB2.13 in all salt concentrations except high salt (2 M NaCl). In contrast, with the gluconeogenetic substrate acetate a significant reduction in growth rate was only observed at low salt (0.17 M NaCl).

3.1.2. KH2.2—Phosphoenolpyruvate carboxykinase and NADP-dependent malic enzyme deletion strain

The main role of the NADP-dependent malic enzyme MaeB lies in the production of NADPH during growth on acetate (Wang et al., 2011). The growth rates of the double knockout strain KH2.2 was very similar to KB2.13. Growing on acetate no significant differences were found. The biggest impact of the *maeB* deletion occurred with glucose as carbon substrate. Only at low salinity (0.17 M NaCl) a reduced growth rate was observed.

3.1.3. KH3.1—Phosphoenolpyruvate carboxykinase and phosphoenolpyruvate carboxylase deletion strain

Phosphoenolpyruvate carboxylase is one of the two enzymes carrying the anaplerotic flux in *H. elongata*. In KH3.1, both carboxylating and decarboxylating reactions between phosphoenolpyruvate and oxaloacetate are abolished. Therefore, glycolytic fluxes necessarily have to pass through the ATP-forming pyruvate kinase to pyruvate before anaplerosis is possible. For this strain, no growth with glucose could be determined up until 18 h after inoculation. However, in the previous pre-culture steps using the same growth medium growth on glucose was observed. It has already been shown in Hobmeier et al. (2020) that the removal of phosphoenolpyruvate carboxylase leads to a rather unstable phenotype with an increased lag phase and high variability in growth rates. KH3.1 was often unable to grow on glucose in microtiter plate. However, it grew well with acetate as carbon source, albeit with a reduced growth rate at lower salt concentrations of 0.17 and 0.5 M NaCl.

3.1.4. Growth and ectoine homeostasis in batch cultures

The growth of the deletion mutants on glycolytic substrate was further verified in shake flask experiments at the salt optimum 1 M NaCl. The growth rates for the deletion strains KH1.1 and KH2.1 (in-frame null mutations) in relation to the parental strain KB2.13 was determined in four distinct batch experiments. KB2.13 grew significantly faster with an average growth rate of 0.467 ± 0.044 h^{-1}. KH1.1 and KH2.1 both showed the same average growth rate of 0.345 ± 0.051 and 0.348 ± 0.057 h^{-1}, respectively. Therefore, the reduced growth can be attributed directly to the loss of phosphoenolpyruvate carboxykinase. Also, for this mutant a longer lag phase was observed. Even though the additional deletion of *maeB* does not affect the growth rate, there is a noticeable impact on the lag phase. The prolonged lag phase observed for KH1.1 is shortened in KH2.1 and it can commence growth faster after inoculation.

The additional deletion of phosphoenolpyruvate carboxylase in strain KH3.1, was introduced to shed light on the phenotype of KH1.1 growing with glucose as carbon substrate. The growth deficit observed for KH3.1 with glucose was shown to be an artifact associated to cultivation on microtiter plate. However, compared to KB2.13 and KH1.1 the growth rate was found to be considerably reduced at only 0.238 ± 0.010 h^{-1} on glucose. Strain KH1.1 grew at a growth rate of 0.303 ± 0.036 h^{-1}, and the fastest growth rate was as always observed for KB2.13 at 0.450 ± 0.004 h^{-1}. The diminished growth rate after deletion of Ppc is not surprising since it is thought to carry a major portion of the anaplerotic flux during glycolytic growth even though the alternative Oad can take over a portion of the flux at the applied salt concentration 1 M NaCl (Hobmeier et al., 2020). In the late exponential phase, an intracellular ectoine content of 0.018 ± 0.002 g/gDW was determined for KB2.13 and a much higher content of 0.080 ± 0.016 g/gDW for KH1.1. The deletion of *ppc* led to a decrease in ectoine content to 0.051 ± 0.009 g/gDW. However, this is still a 2.8-fold increase compared to KB2.13. These important variations in ectoine concentration point toward a major disruption of the regulatory mechanisms that normally keep ectoine homeostasis. Growth on the gluconeogenetic substrate acetate was not expected to be affected by Ppc and indeed, all strains exhibited very similar growth rates on acetate, with growth rates of 0.237 ± 0.003, 0.227 ± 0.004, and 0.222 ± 0.004 h^{-1} for KB2.13, KH1.1, and KH3.1. This was also reflected in the intracellular ectoine content with 0.019 ± 0.002, 0.023 ± 0.001, and, again, 0.023 ± 0.001 g/gDW, respectively.

3.2. Ectoine excretion in KH1.1 (Δ*pckA*) and KH2.1 (Δ*pckA*Δ*maeB*)

Ectoine analytics in shake flask experiments is challenging due to the low biomass achieved in such cultures, which leads to ectoine accumulation being at the lower end of the HPLC detection limit during the exponential growth phase. Since the genetic background of all the strains discussed in this work includes an impaired ectoine catabolic pathway (Δ*doeA*), it was possible to compare cultures grown into the stagnation phase. The titers after the end of the process are the maximal final concentrations achievable from the applied substrate. To further increase ectoine yields, an experiment in a SO_4-limited medium was carried out. Based on a standard biomass formula of $CH_{1.6}O_{0.37}N_{0.26}S_{0.006}$ (Battley, 1991) the amount of sulfate in the medium was adjusted to limit the maximum biomass to an OD_{600} of 2. As can be seen in Figures 2, 3, the growth of KB2.13, KH1.1, and KH2.1 compared to each other coincided with the pattern observed in the regular minimal medium with KB2.13 growing significantly faster at 0.512 ± 0.035 h^{-1} and both

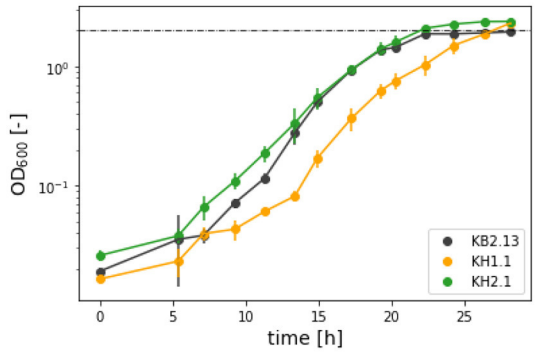

FIGURE 2
OD_{600} evolution in half-logarithmic depiction for the ectoine synthesis experiment in SO_4-limited medium with the strains KB2.13 (*Halomonas elongata* DSM 2581, Δ*teaABC* Δ*doeA*) (gray), KH1.1 (KB2.13, Δ*pckA*) (orange), and KH2.1 (KB2.13, Δ*pckA* Δ*maeB*) (green).

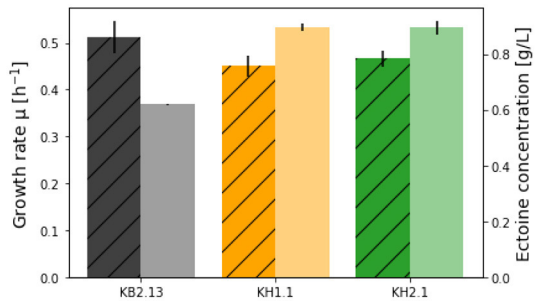

FIGURE 3
Growth rates (striped bars) and ectoine titers (no pattern) achieved in the SO_4-limited medium with the strains KB2.13 (*Halomonas elongata* DSM 2581, Δ*teaABC* Δ*doeA*) (gray), KH1.1 (KB2.13, Δ*pckA*) (orange), and KH2.1 (KB2.13, Δ*pckA* Δ*maeB*) (green).

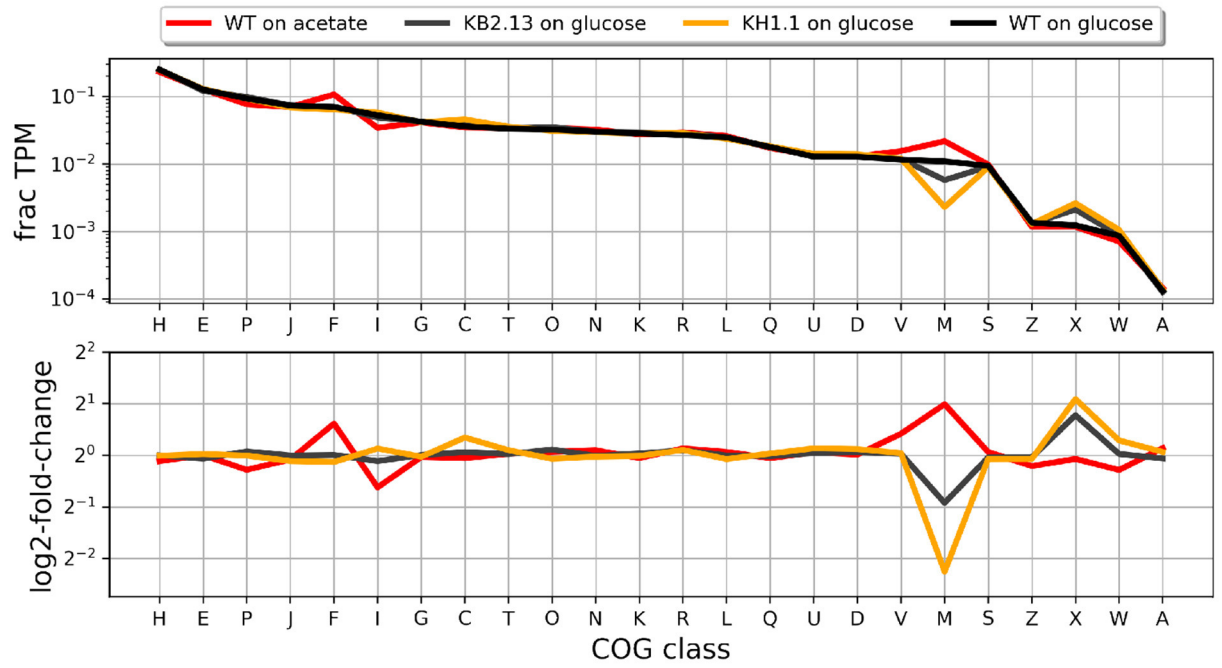

FIGURE 4
Fraction of the transcriptome occupied by each COG class in each experiment (upper panel) and log2-fold-change for each case with respect to the wild type *Halomonas elongata* DSM 2581 growing on glucose. The strains are KB2.13 (*Halomonas elongata* DSM 2581, Δ*teaABC* Δ*doeA*) (gray) and KH1.1 (KB2.13, Δ*pckA*) (orange).

modified strains at similar growth rates of $0.450 \pm 0.024\ h^{-1}$ for KH1.1 and $0.466 \pm 0.017\ h^{-1}$ for KH2.1. As mentioned before, the deletion of *maeB* in KH2.1 leads to a reduced lag phase, which is apparent in the growth curves depicted in Figure 3. Another interesting finding here is that the evolution of OD_{600} for KB2.13 stops precisely at the theoretically determined limit of OD_{600} 2, but the modified strains eventually exceeded the OD_{600} limit (Figure 2). This hints toward possible changes in the biomass composition. A tendency of the modified strains to accumulate PHB would be consistent with these results as well as previous observations of *H. elongata*'s behavior under stress (Hobmeier et al., 2022). The available data on the transcriptome of KH1.1 do not provide enough evidence to confirm this since the upregulation of *phbC* in this strain amounts to a log2-fold-change of 1.3, which is close but still below the chosen threshold of 1.5 for differential expression.

After 48 h the final ectoine titers in the medium were measured for all strains. With 5 g/L glucose KB2.13 produced 0.619 ± 0.002 g/L. The modified strains reached considerably higher titers of 0.895 ± 0.012 g/L for KH1.1 and 0.894 ± 0.025 g/L for KH2.1. This equates to a 45 % increase in ectoine titer. The improvement is clearly caused by the disruption of the PckA futile cycle and the additional removal of NADP-ME has no impact on ectoine synthesis.

3.3. RNA-Seq analysis of modified strain KH1.1

During the RNA-Seq experiments described by Hobmeier et al. (2022), RNA was also collected from KH1.1. Figure 4 shows the distribution of COG classes in the transcriptome of this strain in relation to those of the previous publication. The profiles suggest that the changes in transcription levels grouped by COG class that appear in KB2.13 become more prominent after the additional deletion of *pckA* in strain KH1.1.

In general, the transcription profile of KH1.1 changes more with respect to the parental strain (KB2.13) than that strain did with respect to the wild type. Genes showing a log2-fold-change larger than 1.5 between strains, were clustered by their pattern of transcription as described in materials and methods (see Supplementary material for details). The two larger clusters were formed by genes involved in chemotaxis (33 genes) and flagellar motility (17 genes).

All these genes have been previously found to be already close or beyond the threshold of down-regulation in KB2.13 and also severely down-regulated by cells growing on low-salinity. The down-regulation of these genes in KH1.1 with respect to its parental strain KB2.13 is even more prominent. The next few clusters in size include a large number of uncharacterized or poorly annotated genes. For instance, the third largest cluster

includes 17 genes which are poorly characterized except, for two genes involved in the degradation of ectoine: *doeB* and *doeC*. These genes are clearly down-regulated in KB2.13 (in which *doeA* is deleted) but seem unaffected by the deletion of *pckA* in the KH1.1 strain. The down-regulation in KB2.13 is most likely a direct consequence of the *doeA* deletion. The next cluster with 14 genes includes *teaD* (Schweikhard et al., 2010) which shows increased transcription in the KB2.13 strain and a series of genes that are up-regulated exclusively in KH1.1. The up-regulation of *teaD* can also be attributed to the introduced modifications in KB2.13. Due to the deletion of *teaABC* the adjacent open reading frame *teaD* directly underlies the *tea* operon promoters resulting in an artificial overexpression. The remaining genes only affected in KH1.1 include *acnA*, which encodes for the TCA cycle enzyme aconitase, the chaperone (*clpB*), the cold-shock protein (*cspA4*), and a APC family transporter (HELO_1536). Smaller clusters normally involve well annotated genes. Cluster 13 is formed by consecutive genes *putP* and *putA* involved in proline metabolism, as well as HELO_1459 coding for an OmpW family protein and HELO_2165A coding for a UspA domain protein. These genes are up-regulated in KH1.1 and also show a similar behavior in the wild type growing on acetate or in low salinity. Cluster 14 contains only two consecutive genes HELO_4326 and HELO_4327 coding for a tryptophan synthase and they are down-regulated both in strain KH1.1 and again in the wild type growing on acetate or in low salinity. A similar behavior is exhibited by the two genes in cluster 12: NAD-dependent acetaldehyde dehydrogenase HELO_2817 (*acoD*) and alcohol dehydrogenase HELO_2818 (*adh2*) except these two genes are up-regulated at low salinity. The genes for the multidrug efflux pump AcrAB (HELO_3739 and HELO_3738) is up-regulated exclusively in KH1.1. This transporter facilitates the energy-dependent vertical transport of diverse compounds from the cytoplasm directly into the extracellular space (Du et al., 2014).

3.4. Ectoine excretion *via* transmembrane proteins TeaB and/or TeaC

As a way to avoid potential feedback inhibition by ectoine on its own synthesis, we explored ways to enhance ectoine removal from the cytoplasm. This action on demand was implemented independently from the supply oriented method shown above, but both approaches are clearly complementary. The mechanisms that secretes ectoine to the periplasm has not yet been fully characterized. It has been established that 20% of this flux is carried by the mechanosensitive channels, but the remaining 80% goes through an as yet unidentified transporter (Vandrich et al., 2020). Therefore, the removal of ectoine was implemented using the channel building proteins of the ectoine specific TRAP transporter: TeaB and TeaC. Since this channel is a symporter of ectoine with sodium, ectoine export through this method involves overcoming the sodium gradient and adding a sodium export flux. The single knockout of the periplasmic substrate binding protein (SBP) TeaA already results in the same leaky phenotype as the complete removal of the *tea* operon (HELO_4274-6). Without the specific SBP the re-uptake of ectoine is disrupted and accumulates in the periplasm over time, leading to a constant loss of ectoine into the extracellular space.

We tested the induced overexpression of both membrane proteins in strain KB2.13, in which the *tea* operon is deleted and, thus, TeaA is not present. Three different plasmids based on the pSEVA architecture were assembled with *teaBC*, *teaB*, or *teaC* under the inducible XylS/Pm promoter. To rule out any impact of the inducer or solvent, their impact was also examined in KB2.13 but no significant differences in ectoine secretion between untreated cultures, cultures treated with only solvent (EtOH), and cultures treated with the inducer (0.1 mM 3-methyl-benzoic acid in EtOH) could be detected (see Supplementary material).

First, the effect of the complete transmembrane complex TeaBC was investigated. After inoculation, initially the cultures were left uninduced for a period of ∼7 h in order for the cultures to adapt. Up to an OD_{600} of 0.1 all KB2.13 (pSEVA438-*teaBC*) replicates grew with the same growth rate of 0.468 ± 0.010 h^{-1}. After induction of half of the cultures with 0.01 mM inducer at OD_{600} 0.01 this exponential growth continued for 3 h until the late exponential phase was reached after ∼10 h. From then on, the uninduced cultures showed a growth rate of 0.299 ± 0.011 h^{-1} and the induced cultures a slightly slower (16.7%) growth rate of 0.249 ± 0.006 h^{-1}. Regarding the ectoine concentration in the medium, the induced *teaBC* expressing cultures (green) during the late exponential phase accumulated ectoine at an increased rate of 0.078 g/L extracellular ectoine per g/L dry weight, in contrast to the uninduced cultures (black) with a rate of only 0.027 g/L (Figure 5A). This translates into an almost 3-fold increase of ectoine secretion caused by the TeaBC channels.

Cultures of KB2.13 harboring either the pSEVA438-*teaB* or pSEVA438-*teaC* expression plasmid were grown in parallel. After an initial growth period of ∼7 h for adaptation after inoculation, half of the cultures for each expression plasmid were induced (0.01 mM 3-MB in EtOH) upon reaching an OD_{600} of 0.1. Up to this point, the growth rates of all cultures regardless of the plasmid were the same with an average of 0.545 ± 0.040 h^{-1}. Again, the exponential growth continued at the same growth rate for about 3 h. After 10 h upon reaching the late exponential growth phase, the growth rates decreased with uninduced cultures harboring pSEVA438-*teaB* having a growth rate at 0.380 ± 0.013 h^{-1} and the uninduced cultures harboring pSEVA438-*teaC* having a growth rate at 0.381 ± 0.013 h^{-1}. Even though the strains have different expression plasmids, the uninduced growth rates were essentially the same. This suggests a very tight control of heterologous expression using the XylS/Pm promoter system in *H. elongata* with a low basal expression similar to *P. putida*, from which this expression

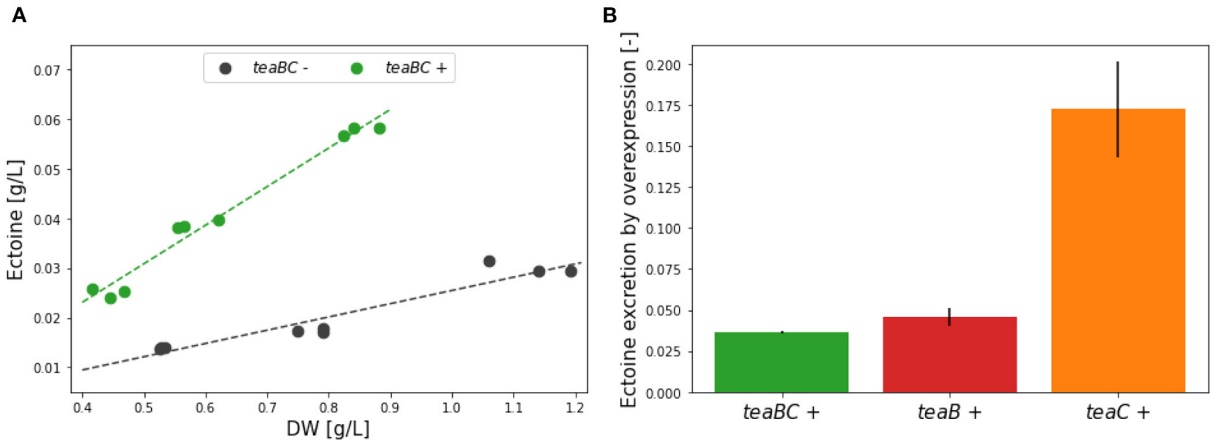

FIGURE 5
(A) Ectoine accumulation rates for the overexpression of *teaBC* (green, induced) and the uninduced control (gray) in the late exponential phase. The rates were calculated for three biological replicates at three time points. **(B)** Comparison of the accumulated ectoine in the medium in the late exponential phase after 13 h of process time for the overexpression of the genes encoding the transmembrane proteins: *teaBC* (green), *teaB* (red), and *teaC* (orange). All genes were introduced using pSEVA438 plasmids under the inducible XylS/Pm promoter (see text for details).

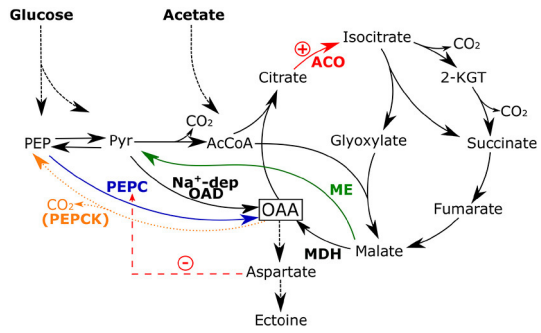

FIGURE 6
Fluxes around the PEP-PYR-OAA node in KH1.1 caused by the deletion of PEPCK (orange, dashed line). An increase in aspartate could lead to the inhibition of PEPC. RNA-Seq revealed the upregulation of ACO in this mutant, which could be linked to an increased flux through the glyoxylate shunt. The flux toward the TCA cycle might hinder ME activity due to mass action. Thus, MAL could be increasingly channeled toward oxaloacetate *via* MDH.

system originates (Kessler et al., 1994; Gawin et al., 2017). Surprisingly, the cultures expressing *teaB* also grew at a similar, only slightly reduced rate ($0.328 \pm 0.021\ h^{-1}$) compared to the uninduced cultures. In contrast, the expression of *teaC* caused a drastic drop to about half of the growth rate ($0.189 \pm 0.047\ h^{-1}$). The synthesis of TeaC seems to impose a much higher burden on the cell compared to the small subunit TeaB. The concentration of secreted ectoine per dry weight into the medium after 13 h was compared for the *teaB*, *teaC*, and *teaBC* expression from both batch experiments. Therefore, the ectoine concentration was normed using the uninduced references. As shown in Figure 5B, TeaC facilitates almost 4–5 times the amount that is secreted with either TeaB or TeaBC. But it is not entirely clear how the overexpression of *teaC* impacts cell viability as the growth rate is extremely reduced to about 50%. Additionally, the measured ectoine titers for TeaB and TeaC after 30 h show no significant difference. The final ectoine titer achieved for TeaB was 0.259 ± 0.022 g/L and for TeaC 0.278 ± 0.03 g/L. For the uninduced references lower titers of 0.163 ± 0.003 g/L (TeaB) and 0.163 ± 0.005 g/L (TeaC) were determined. It is possible that the expression of TeaC leads to a loss of membrane integrity. Cell lysis upon induction could explain the strong increase of extracellular ectoine after 13 h. However, as *teaC*-overexpressing cells produce less cell mass due to lysis, *teaB*-overexpressing cells catch up until no differences are found in ectoine titers after 30 h.

4. Conclusions

This work has shown two different approaches to increase the synthesis and excretion of ectoine in *H. elongata*. These two strategies clearly complement each other, but were implemented separately to assess their viability. Both approaches have clearly shown to be able to increase the flux toward ectoine and to be promising steps toward strain improvement. Moreover, the phenotypes of the strains created provide further insight on the regulation of intracellular ectoine levels and salt adaptation in *H. elongata*. All the strains were created from a parental strain (KB2.13) that leaks ectoine as a result of a deletion of the TRAP transporter TeaABC.

The first strategy was to increase the supply of oxaloacetate as a central precursor for ectoine synthesis. This was implemented by disrupting the PEP-PYR-OAD node (see Figure 6) that connects glycolysis and the TCA cycle, which

has been described as a major switching point for the flux distribution within carbon metabolism (Sauer and Eikmanns, 2005). *H. elongata* utilizes various reactions to adequately split the available carbon flux between feeding the catabolic section of the TCA cycle and the anaplerotic reactions that replenish the carbon skeletons lost to anabolic processes. The deletion of the gene for PEPCK, *pckA*, resulted in a strain (KH1.1) that not only secretes ectoine at a higher rate, but also accumulates it in a higher concentration in the cytoplasm. The subsequent deletion of NADP-dependent ME (MaeB) in KH1.1 resulted in a new strain (KH2.1) which grew at similar rates on glucose and acetate as its parental strain, but had considerably shorter lag phases. Moreover, strain KH3.1 (lacking PckA and Ppc) also had intracellular ectoine concentrations different from the previously mentioned KH1.1 and the parental KB2.13. The fact that intracellular ectoine levels, normally strictly controlled, are significantly different between these strains indicates that the mechanisms controlling ectoine levels in the wild type are no longer functional in all the strains discussed above, probably including the original KB2.13. This has important implications since it simplifies further improvement on ectoine production and supports the hypothesis that the circulation of ectoine between cytoplasm and periplasm fulfils a regulatory function. If PHB accumulation is confirmed in the two strains, a further improvement could be easily obtained from disrupting the PHB synthesis pathway.

The second strategy, increasing ectoine export, also proved able to increase the flux through the pathway and therefore enhance production. This strategy was implemented through overexpression of the TeaBC channel. It is noteworthy that, even though this implementation is not optimal due to the potential coupling between ectoine export and sodium extrusion, it still resulted in a clear improvement of ectoine secretion. This promises high rewards for further work on engineering a more efficient transporter.

Data availability statement

The RNAseq data generated in this study has been uploaded to SRA and can be accessed under the accession number PRJNA803715.

Author contributions

AM-S, AK, and HK obtained the funding. HK, KH, and AM-S conceptualized the research. AM-S, KP-G, and KH supervised the work. KH, MO, and NS carried out the experiments. KH and AM-S analyzed the data. KH wrote the first draft of the manuscript. AM-S and HK participated in the elaboration of subsequent versions. All authors read and approved the final version of the manuscript.

Funding

This work has been funded by the German Federal Ministry of Education and Research (BMBF) through project HOBBIT (031B03).

Conflict of interest

Authors KH, KP-G, AK, and AM-S are the authors of European patent application EP3833753 (A1)—2021-06-16. An improved method to produce chemical compounds derived from oxaloacetate by microorganisms.

The remaining authors declare that the research was conducted in the absence of any commercial or financial relationships that could be construed as a potential conflict of interest.

Publisher's note

Supplementary material

The Supplementary Material for this article can be found online at: https://www.frontiersin.org/articles/10.3389/fmicb.2022.968983/full#supplementary-material

SUPPLEMENTARY TABLE 1
Summary of all used oligonucleotides in this work.

SUPPLEMENTARY TABLE 2
TPM data in pseudocounts [$\log_2(n+1)$] as averages of three biological replicates.

SUPPLEMENTARY TABLE 3
DESeq results comparing KB2.13 vs Wild type *Halomonas elongata*.

SUPPLEMENTARY TABLE 4
DESeq results comparing KH1.1 vs KB2.13.

SUPPLEMENTARY TABLE 5
Clusters.

References

Alves, R. and Savageau, M. A. (2000). Effect of overall feedback inhibition in unbranched biosynthetic pathways. *Biophys. J.* 79, 2290–2304. doi: 10.1016/S0006-3495(00)76475-7

Battley, E. H. (1991). Calculation of the heat of growth of *Escherichia coli* K-12 on succinic acid. *Biotechnol. Bioeng.* 37, 334–343. doi: 10.1002/bit.260370407

Bilstein, A., Heinrich, A., Rybachuk, A., and Mösges, R. (2021). Ectoine in the treatment of irritations and inflammations of the eye surface. *BioMed Res. Int.* 2021:8885032. doi: 10.1155/2021/8885032

Brown, A. D. (1976). Microbial water stress. *Bacteriol. Rev.* 40, 803–846. doi: 10.1128/br.40.4.803-846.1976

Chao, Y. P. and Liao, J. C. (1994). Metabolic responses to substrate futile cycling in *Escherichia coli*. *J. Biol. Chem.* 269, 5122–5126. doi: 10.1016/S0021-9258(17)37663-9

Chung, C. T., Niemela, S. L., and Miller, R. H. (1989). One-step preparation of competent *Escherichia coli*: transformation and storage of bacterial cells in the same solution. *Proc. Natl. Acad. Sci. U.S.A.* 86, 2172–2175. doi: 10.1073/pnas.86.7.2172

Czech, L., Hermann, L., Stöveken, N., Richter, A. A., Höppner, A., Smits, S. H., et al. (2018). Role of the extremolytes ectoine and hydroxyectoine as stress protectants and nutrients: genetics, phylogenomics, biochemistry, and structural analysis. *Genes* 9:177. doi: 10.3390/genes9040177

Dötsch, A., Severin, J., Alt, W., Galinski, E. A., and Kreft, J.-U. (2008). A mathematical model for growth and osmoregulation in halophilic bacteria. *Microbiology* 154(Pt 10), 2956–2969. doi: 10.1099/mic.0.2007/012237-0

Du, D., Wang, Z., James, N. R., Voss, J. E., Klimont, E., Ohene-Agyei, T., et al. (2014). Structure of the AcrAB-TolC multidrug efflux pump. *Nature* 509, 512–515. doi: 10.1038/nature13205

Galinski, E. A., Pfeiffer, H. P., and Trüper, H. G. (1985). 1,4,5,6-tetrahydro-2-methyl-4-pyrimidinecarboxylic acid. A novel cyclic amino acid from halophilic phototrophic bacteria of the genus *Ectothiorhodospira*. *Eur. J. Biochem.* 149, 135–139. doi: 10.1111/j.1432-1033.1985.tb08903.x

Galinski, E. A. (1995). "Osmoadaptation in bacteria," in *Advances in Microbial Physiology, Vol. 37 of Advances in Microbial Physiology* (Cambridge, MA: Academic Press, Elsevier), 273–328. doi: 10.1016/S0065-2911(08)60148-4

Gawin, A., Valla, S., and Brautaset, T. (2017). The XylS/Pm regulator/promoter system and its use in fundamental studies of bacterial gene expression, recombinant protein production and metabolic engineering. *Microb. Biotechnol.* 10, 702–718. doi: 10.1111/1751-7915.12701

Gießelmann, G., Dietrich, D., Jungmann, L., Kohlstedt, M., Jeon, E. J., Yim, S. S., et al. (2019). Metabolic engineering of *Corynebacterium glutamicum* for high-level ectoine production: design, combinatorial assembly, and implementation of a transcriptionally balanced heterologous ectoine pathway. *Biotechnol. J.* 14:1800417. doi: 10.1002/biot.201800417

Grammann, K., Volke, A., and Kunte, H. J. (2002). New type of osmoregulated solute transporter identified in halophilic members of the bacteria domain: TRAP transporter TeaABC mediates uptake of ectoine and hydroxyectoine in *Halomonas elongate* DSM 2581T. *J. Bacteriol.* 184, 3078–3085. doi: 10.1128/JB.184.11.3078-3085.2002

Hobmeier, K., Cantone, M., Nguyen, Q. A., Pflüger-Grau, K., Kremling, A., Kunte, H.-J., et al. (2022). Adaptation to varying salinity in *Halomonas elongate*: much more than ectoine accumulation. *Front. Microbiol.* 13:846677. doi: 10.3389/fmicb.2022.846677

Hobmeier, K., Goëss, M. C., Sehr, C., Schwaminger, S., Berensmeier, S., Kremling, A., et al. (2020). Anaplerotic pathways in *Halomonas elongate*: the role of the sodium gradient. *Front. Microbiol.* 11:561800. doi: 10.3389/fmicb.2020.561800

Hofmeyr, J.-H. S., and Cornish-Bowden, A. (2000). Regulating the cellular economy of supply and demand. *FEBS Lett.* 476, 47–51. doi: 10.1016/S0014-5793(00)01668-9

Kanapathipillai, M., Lentzen, G., Sierks, M., and Park, C. B. (2005). Ectoine and hydroxyectoine inhibit aggregation and neurotoxicity of Alzheimer?s β-amyloid. *FEBS Lett.* 579, 4775–4780. doi: 10.1016/j.febslet.2005.07.057

Kempf, B., and Bremer, E. (1998). Uptake and synthesis of compatible solutes as microbial stress responses to high-osmolality environments. *Arch. Microbiol.* 170, 319–330. doi: 10.1007/s002030050649

Kessler, B., Timmis, K. N., and de Lorenzo, V. (1994). The organization of the Pm promoter of the TOL plasmid reflects the structure of its cognate activator protein XylS. *Mol. Gen. Genet.* 244, 596–605. doi: 10.1007/BF00282749

Kunte, H. J. (2006). Osmoregulation in bacteria: compatible solute accumulation and osmosensing. *Environ. Chem.* 3:94. doi: 10.1071/EN06016

Kunte, H. J., Trüper, H. G., and Stan-Lotter, H. (2002). "Halophilic microorganisms," in *Astrobiology* (Berlin: Springer), 185–200. doi: 10.1007/978-3-642-59381-9_13

Kunte, H. J., Lentzen, G., and Galinski, E. (2014). Industrial production of the cell protectant ectoine: protection mechanisms, processes, and products. *Curr. Biotechnol.* 3, 10–25. doi: 10.2174/2211550111302660037

Larsen, P. I., Sydnes, L. K., Landfald, B., and Ström, A. R. (1987). Osmoregulation in *Escherichia coli* by accumulation of organic osmolytes: betaines, glutamic acid, and trehalose. *Arch. Microbiol.* 147, 1–7. doi: 10.1007/BF00492896

Lentzen, G., and Schwarz, T. (2006). Extremolytes: natural compounds from extremophiles for versatile applications. *Appl. Microbiol. Biotechnol.* 72, 623–634. doi: 10.1007/s00253-006-0553-9

Lippert, K., and Galinski, E. (1992). Enzyme stabilization be ectoine-type compatible solutes: protection against heating, freezing and drying. *Appl. Microbiol. Biotechnol.* 37, 61–65. doi: 10.1007/BF00174204

Liu, M., Liu, H., Shi, M., Jiang, M., Li, L., and Zheng, Y. (2021). Microbial production of ectoine and hydroxyectoine as high-value chemicals. *Microb. Cell Fact.* 20, 1–11. doi: 10.1186/s12934-021-01567-6

Ma, H., Zhao, Y., Huang, W., Zhang, L., Wu, F., Ye, J., et al. (2020). Rational flux-tuning of halomonas bluephagenesis for co-production of bioplastic phb and ectoine. *Nat. Commun.* 11, 1–12. doi: 10.1038/s41467-020-17223-3

Martínez-García, E., and de Lorenzo, V. (2011). Engineering multiple genomic deletions in Gram-negative bacteria: analysis of the multi-resistant antibiotic profile of *Pseudomonas putida* KT2440. *Environ. Microbial.* 13, 2702–2716. doi: 10.1111/j.1462-2920.2011.02538.x

Pastor, J. M., Salvador, M., Argando na, M., Bernal, V., Reina-Bueno, M., Csonka, L. N., et al. (2010). Ectoines in cell stress protection: uses and biotechnological production. *Biotechnol. Adv.* 28, 782–801. doi: 10.1016/j.biotechadv.2010.06.005

Ruijter, G., Panneman, H., and Visser, J. (1997). Overexpression of phosphofructokinase and pyruvate kinase in citric acid-producing *Aspergillus niger*. *Biochim. Biophys. Acta* 1334, 317–326. doi: 10.1016/S0304-4165(96)00110-9

Salapatek, A., Bates, M., Bilstein, A., and Patel, D. (2011). Ectoin®, a novel, non-drug, extremophile-based device, relieves allergic rhinoconjunctivitis symptoms in patients in an environmental exposure chamber model. *J. Allergy Clin. Immunol.* 127:AB202. doi: 10.1016/j.jaci.2010.12.803

Sauer, U., and Eikmanns, B. J. (2005). The pep-pyruvate-oxaloacetate node as the switch point for carbon flux distribution in bacteria. *FEMS Microbiol. Rev.* 29, 765–794. doi: 10.1016/j.femsre.2004.11.002

Savageau, M. A. (1971). Concepts relating the behavior of biochemical systems to their underlying molecular properties. *Arch. Biochem. Biophys.* 145, 612–621. doi: 10.1016/S0003-9861(71)80021-8

Savageau, M. A. (1975). Optimal design of feedback control by inhibition. *J. Mol. Evol.* 5, 199–222. doi: 10.1007/BF01741242

Savageau, M. A. (1976). *Biochemical Systems Analysis: A Study of Function and Design in Molecular Biology*. Reading, MA: Addison-Wesley.

Schröter, M.-A., Meyer, S., Hahn, M. B., Solomun, T., Sturm, H., and Kunte, H.-J. (2017). Ectoine protects DNA from damage by ionizing radiation. *Sci. Rep.* 7, 1–7. doi: 10.1038/s41598-017-15512-4

Schweikhard, E. S., Kuhlmann, S. I., Kunte, H.-J., Grammann, K., and Ziegler, C. M. (2010). Structure and function of the universal stress protein TeaD and its role in regulating the ectoine transporter TeaABC of *Halomonas elongate* DSM 2581T. *Biochemistry* 49, 2194–2204. doi: 10.1021/bi9017522

Schwibbert, K., Marin-Sanguino, A., Bagyan, I., Heidrich, G., Lentzen, G., Seitz, H., et al. (2011). A blueprint of ectoine metabolism from the genome of the industrial producer *Halomonas elongate* DSM 2581T. *Environ. Microbiol.* 13, 1973–1994. doi: 10.1111/j.1462-2920.2010.02336.x

Silva-Rocha, R., Martínez-García, E., Calles, B., Chavarría, M., Arce-Rodríguez, A., de Las Heras, A., et al. (2013). The standard European vector architecture (SEVA): a coherent platform for the analysis and deployment of complex prokaryotic phenotypes. *Nucl.Acids Res.* 41, D666?-D675. doi: 10.1093/nar/gks1119

Vandrich, J., Pfeiffer, F., Alfaro-Espinoza, G., and Kunte, H. J. (2020). Contribution of mechanosensitive channels to osmoadaptation and ectoine excretion in *Halomonas elongate*. *Extremophiles* 24, 421–432. doi: 10.1007/s00792-020-01168-y

Vreeland, R. H., Lichtfield, C. D., Martin, E. L., and Elliot, E. (1980). *Halomonas elongata*, a new genus and species of extremely salt-tolerant bacteria. *Int. J. Syst. Bacteriol*. 30, 485–495. doi: 10.1099/00207713-30-2-485

Wang, B., Wang, P., Zheng, E., Chen, X., Zhao, H., Song, P., et al. (2011). Biochemical properties and physiological roles of nadp-dependent malic enzyme in *Escherichia coli*. *J. Microbiol*. 49, 797–802. doi: 10.1007/s12275-011-0487-5

Wang, D., Chen, J., Wang, Y., Du, G., and Kang, Z. (2021). Engineering *Escherichia coli* for high-yield production of ectoine. *Green Chem. Eng*. doi: 10.1016/j.gce.2021.09.002

Yang, C., Hua, Q., Baba, T., Mori, H., and Shimizu, K. (2003). Analysis of *Escherichia coli* anaplerotic metabolism and its regulation mechanisms from the metabolic responses to altered dilution rates and phosphoenolpyruvate carboxykinase knockout. *Biotechnol. Bioeng*. 84, 129–144. doi: 10.1002/bit.10692

Ye, J.-W., and Chen, G.-Q. (2021). *Halomonas* as a chassis. *Essays Biochem*. 65, 393–403. doi: 10.1042/EBC20200159

Yu, S., Zheng, B., Chen, Z., and Huo, Y.-X. (2021). Metabolic engineering of *Corynebacterium glutamicum* for producing branched chain amino acids. *Microb. Cell Fact*. 20, 1–14. doi: 10.1186/s12934-021-01721-0

frontiers | Frontiers in Microbiology

TYPE Original Research
PUBLISHED 02 September 2022
DOI 10.3389/fmicb.2022.975271

OPEN ACCESS

EDITED BY
Sumit Kumar,
Indian Institute of Technology Delhi, India

REVIEWED BY
Ram Karan,
King Abdullah University of Science and Technology, Saudi Arabia
Noha M. Mesbah,
Suez Canal University, Egypt

*CORRESPONDENCE
Jing Han
hanjing@im.ac.cn
Shaoxing Chen
chensx@ahnu.edu.cn

SPECIALTY SECTION
This article was submitted to Extreme Microbiology, a section of the journal Frontiers in Microbiology

RECEIVED 22 June 2022
ACCEPTED 05 August 2022
PUBLISHED 02 September 2022

CITATION
Tu D, Ke J, Luo Y, Hong T, Sun S, Han J and Chen S (2022) Microbial community structure and shift pattern of industry brine after a long-term static storage in closed tank. *Front. Microbiol.* 13:975271. doi: 10.3389/fmicb.2022.975271

Microbial community structure and shift pattern of industry brine after a long-term static storage in closed tank

Demei Tu[1], Juntao Ke[1], Yuqing Luo[1], Tao Hong[1], Siqi Sun[2], Jing Han[3]* and Shaoxing Chen[1,3]*

[1]College of Life Sciences, Anhui Normal University, Wuhu, China, [2]Anhui Jiaotianxiang Biological Technology Co., Ltd., Xuancheng, China, [3]State Key Laboratory of Microbial Resources, Institute of Microbiology, Chinese Academy of Sciences, Beijing, China

Brine from Dingyuan Salt Mine (Anhui, China), an athalassohaline hypersaline environment formed in the early tertiary Oligocene, is used to produce table salt for hundreds of millions of people. However, halophiles preserved in this niche during deposition are still unknown. Here, we employed cultivation and high-throughput sequencing strategies to uncover the microbial community and its shift after a long-term storage in the brine collected from Dingyuan Salt Mine. High-throughput sequencing showed (1) in the fresh brine (2021), *Cyanobium_stocktickerPCC-6307* spp. (8.46%), *Aeromonas* spp. (6.91%) and *Pseudomonas* spp. (4.71%) are the dominant species in bacteria while *Natronomonas* spp. (18.89%), *Halapricum* spp. (13.73%), and *Halomicrobium* spp. (12.35%) in archaea; (2) after a 3-year-storage, *Salinibacter* spp. (30.01%) and *Alcanivorax* spp. (14.96%) surpassed *Cyanobium_stocktickerPCC-6307* spp. (8.46%) becoming the dominant species in bacteria; *Natronomonas* spp. are still the dominant species, while *Halorientalis* spp. (14.80%) outnumbered *Halapricum* spp. becoming the dominant species in archaea; (3) *Alcanivorax* spp. and *Halorientalis* spp. two hydrocarbons degrading microorganisms were enriched in the brine containing hydrocarbons. Cultivation using hypersaline nutrient medium (20% NaCl) combined with high-throughput 16S rRNA gene sequencing showed that (1) the biomass significantly increased while the species diversity sharply declined after a 3-year-storage; (2) *Halorubrum* spp. scarcely detected from the environment total stocktickerDNA were flourishing after cultivation using AS-168 or NOM medium; (3) twelve possible new species were revealed based on almost full-length 16S rRNA gene sequence similarity search. This study generally uncovered the microbial community and the dominant halophiles in this inland athalassohaline salt mine, and provided a new insight on the shift pattern of dominant halophiles during a long-term storage, which illustrated the shaping of microorganisms in the unique environment, and the adaptation of microbe to the specific environment.

KEYWORDS

salt mine, hypersaline environment, halophiles, haloarchaea, microbial community, archaea

Introduction

Hypersaline ecosystems are widespread across the globe, including a wide variety of habitats such as hypersaline lakes, solar salterns, soils, and ancient salt deposits (Oren, 2011). In addition to high salt concentrations, high pH, and low oxygen concentrations are also characteristics of these extreme environments (Naghoni et al., 2017). Although the conditions are harsh, and even high salinity is fatal to most organisms, a large number of halophilic archaea, halophilic and salt-tolerant bacteria still exist in these environments (Oren, 2002; Fendrihan et al., 2006; Naghoni et al., 2017), which play a vital role in global biogeochemical cycles (Mani et al., 2012).

In recent years, the diversity of microorganisms in various hypersaline environments has been studied, but these studies have mainly focused on saline lakes, solar salterns, saline soils (Ben Abdallah et al., 2018; Gomez-Villegas et al., 2018; Bachran et al., 2019; Couto-Rodríguez and Montalvo-Rodríguez, 2019; Nan et al., 2020; Sáenz de Miera et al., 2021). It is worth noting that salt mine, a unique habitat formed tens of millions of years ago, is also an important representative of the hypersaline environment (Chen et al., 2019). For instance, brine from Dingyuan Salt Mine (Dongxing Town, Dingyuan County, Anhui Province, China), an athalassohaline hypersaline environment, is used to produce table salt for hundreds of millions of people. However, current analysis of microbial communities in this kind of environment is limited. Actually, salt mines are rich in microbial resources. For example, the study of halophilic microorganisms in salt mines can not only reveal the evolution and adaptation mechanism of life in extreme environments, but also shows importance in the breeding, development and utilization of microorganisms (Chen et al., 2019).

At present, high-throughput sequencing technology has been applied to investigate microbial communities in different hypersaline environments (Genderjahn et al., 2018; Perez-Fernandez et al., 2019; Zhu et al., 2020). Compared to traditional methods, it has emerged as a reliable tool for investigating differences in microbial community species diversity and structure in any given habitat (Boutaiba et al., 2011), because the culture-independent method of amplicon sequencing appears to be more efficient than the traditional culture-dependent methods (Gibtan et al., 2017). However, culture-dependent method is still a necessary means to acquire valuable microbial strains with potential for new applications and to understand their ecophysiological and environmental functions (Vandamme et al., 1996; Sfanos et al., 2005). For example, the use of traditional culture techniques and the development of new media are encouraged to find novel pure isolates with desired physiological and metabolic characteristics (Rohban et al., 2009).

Therefore, in this study, high-throughput sequencing, clone library and traditional culture-dependent approaches were combined to analyze the microbial diversity of brine (long-term indoor sealed static storage and freshly collected brines) from Dingyuan Salt Mine in Anhui Province (China). The microbial community composition and diversity in this environment were explored using culture-independent and culture-dependent methods, and different results for characterizing microbial communities were compared. In addition, microbial interactions and keystone taxa in complex environments were identified and inferred using co-occurrence network analysis method. The results of this study expand our knowledge on microbial ecology in hypersaline environments.

Materials and methods

Sampling site description and sample collection

Brine samples were collected from Dingyuan Salt Mine located in Dongxing town, Dingyuan county, Anhui Province, China (117.4956E, 32.5066N) (**Supplementary Figures 1a,b**). Geographic location of the sampling site was generated with ArcGIS 10.2 software[1]. This sampling site is an athalassohaline hypersaline environment derived from a long-term evaporation and sedimentation of inland saline streams and lakes (Chen et al., 2019). Two brine samples, C4 and C5, were collected in August 2018, and the other three samples, C1, C2, and C3, were collected in July 2021. All these five samples were collected from the same site as shown in **Supplementary Figures 1a,b** and **Figure 1A**. And these brine samples were held using sterile plastic containers (10 L), and were brought back to the laboratory within a few hours. In particular, the two samples (C4 and C5) were stored in sealed plastic tanks for approximately 3 years in our laboratory without any manual intervention at perennial room temperature (20–25°C). And one-fifth of the volume of air existed in the upper layer of the tanks.

Physicochemical properties determination

The pH of these brine samples value was measured by a Delta 320 pH meter (Mettler-Toledo, Zurich, Switzerland). Additionally, chemical composition of them was performed by a commercial analytical laboratory based on standardized methods (Beijing Zhongkebaice Technology Service Co., Ltd., Beijing, China). Nitrate ion (NO_3^-) concentration was measured by ion-chromatography on an ICS-1500 (Dionex, Sunnyvale, CA, United States). The content of metallic elements such as magnesium (Mg), iron (Fe), and potassium

1 https://desktop.arcgis.com/en/

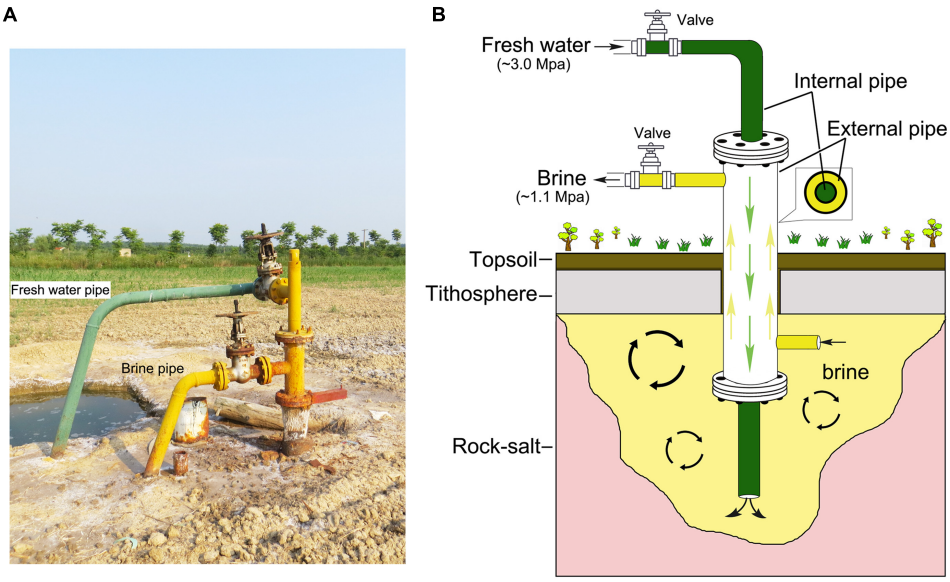

FIGURE 1
Landscape of the sampling site and brine production mode. **(A)** The surrounding landscape of the sampling site. The fresh water (green pipe) with high pressure was pumped into the underground salt mine and the industry brine (yellow pipe) with relative low pressure flowed out. **(B)** The working principle of rock salt mining is fresh water-in (green, ~3.0 Mpa) and brine-out (yellow, ~1.1 Mpa). Green arrows indicate the direction of fresh water in the internal pipe, and the yellow arrows indicate the direction of industry brine in the external pipe.

(K) were determined by inductively coupled plasma atomic emission spectrometry (ICP-AES) using an OPTIMA 5300 DV spectrometer (Perkin Elmer, Norwalk, CT, United States).

Cultivation, isolation, and identification of halophilic microorganisms

The brine samples were cultured in two different hypersaline media AS-168 and NOM (pH = 7.5) (Han et al., 2007; Cui et al., 2012). Besides, solid media were made by adding 15.0 g agar powder to each liter of liquid medium prior to autoclaving. Then, 200 μL of above brine samples were pipetted and spread onto AS-168 and NOM agar plates (three plates for each sample). Finally, all plates sealed with parafilm were put into a ziplock bag to keep moisture during a long-term cultivation. After 3–4 weeks cultivation at 37°C, numerous halophilic or salt tolerant microorganisms were obtained.

Colonies, developed from the above operation with different color, transparency and size, were sorted out. After successive streaking, pure cultures were subjected to identification. Polymerase chain reaction (PCR) amplification of the 16S rRNA gene was performed using universal primers F8/R1462 (**Supplementary Table 1**; Lizama et al., 2001) and 27F/1492R (**Supplementary Table 1**; Lane, 1991) for archaea and bacterial respectively.

The PCR products were sequenced using the corresponding PCR primers (Sangon Biotech, Shanghai, China) after agarose gel electrophoresis. The assembled almost full-length 16S rRNA gene sequences (>1,300 nt) were used as queries to match the public database using Basic Local Alignment Search Tool (BLAST)[2]. To determine the taxonomic position of these strains, 97% of 16S rRNA gene sequence similarity was taken as species boundary.

Total DNA extraction, 16S rRNA gene amplification, and high-throughput DNA sequencing

To analyze the microbial community of culture-dependent approach, colonies grown on AS-168 and NOM agar plates were collected by washing with 20% (w/v) sterilized NaCl solution. With this approach, cells of C1, C2, and C3 washed from AS-168 plates were blended into a tube as one sample (C1-3-AS168). Samples C4-5-AS168 and C4-5-NOM were obtained by the same method. Total DNA of these three samples was extracted using TIANamp Bacteria DNA Kit in accordance with the instruction (TIANGEN, Beijing, China).

To explore the microbial community of culture-independent approach, several related environmental samples such as brines, fresh water used to produce brine, ddH_2O used to dissolve DNA, and routine lab air containing microorganisms were involved in the process of total environmental DNA

2 https://blast.ncbi.nlm.nih.gov/Blast.cgi

extraction. Each sample (1 L) was filtered through a 0.22 μm membrane filter (as for lab air sample, an equal filtrating time with ddH_2O was used). Then, the filter membrane of each sample was cut into small pieces, from which the total environmental DNA was extracted using the DNeasy PowerSoil Pro Kit (QIAGEN, Dusseldorf, Germany) according to the manufacturer's instructions. Although long-term storage enables the formation of endospore in bacteria, the DNA extraction kit used in this study was also able to isolate total DNA *via* bead-beating from bacterial endospores (Redweik et al., 2020). Thus, differences in microbial diversity in different brine samples can be well characterized. Subsequently, all the harvested DNA samples were detected using 1% agarose gel electrophoresis, and the purity and concentration were determined by a NanoDrop-2000 (Thermo Fisher Scientific, Waltham, MA, United States).

The V3-V4 regions of bacterial and archaeal 16S rRNA genes from samples C1∼C5 were amplified using primer pairs 338F/806R (468 nt) for Bacteria, and Arch349F/Arch806R (457 nt) for Archaea, respectively (**Supplementary Table 1**; Derakhshani et al., 2016). Then, the 16S rRNA gene amplicons were subjected to high-throughput DNA sequencing on the Illumina Novaseq 6000 platform in Biomarker Biotech Co., Ltd. (Beijing, China).

Clone library construction

In order to reveal the alteration of haloarchaeal community after a 3-year indoor storage in the brine sample in species level, the primer pair F8/R1462 (**Supplementary Table 1**; Lizama et al., 2001) was used to amplify the nearly full length of haloarchaeal 16S rRNA gene. C1-3 was made by blending the total DNA of C1, C2 and C3 in identical volume; and the C4-5 was generated in the similar way. One microliter of C1-3 or C4-5 was used as template in PCR amplification. The 16S rRNA gene was purified using MonPur^{TM} Gel & PCR Purification Kit (Monad, Shanghai, China) after DNA electrophoresis. The purified DNA fragments were inserted into pMD18T vector (TaKaRa, Tokyo, Japan) for DNA sequencing. Then, the nearly full-length 16S rRNA gene sequences were used to determine the taxonomic status *via* sequence similarity search against public database using BLAST as well.

Data analysis

For the purpose of obtaining clean reads, Trimmomatic (version 0.33) (Bolger et al., 2014) software was used to filter the raw reads, and Cutadapt (version 1.9.1) (Martin, 2011) software was used to identify and remove primer sequences. Next, clean reads from each sample were spliced and filtered by using Usearch (version 10) (Edgar, 2010) software. Finally, effective reads for further analysis were obtained by removing the chimeras with software UCHIME (version 4.2) (Edgar et al., 2011). Operational taxonomic units (OTUs) were obtained by clustering effective reads at a similarity threshold of 97% (Stackebrandt and Goebel, 1994). Using SILVA as the reference database, the Naive Bayesina classifier was used to indicate the OTU's taxonomic status (Quast et al., 2012). According to the OTU information, QIIME software was used to generate species abundance tables at different taxonomic levels (Caporaso et al., 2010). The R language tool was used to draw the community structure figures of the samples at each taxonomic level (R Core Team, 2013). The alpha diversity indexes of the samples were evaluated by using the QIIME2 software (Hall and Beiko, 2018) and the rarefaction curve were generated with the R language tool (R Core Team, 2013). One-way analysis of variance was performed using SPSS 23.0 (Kirkpatrick, 2015) for counting DNA concentration and Shannon index of different samples, and *post-hoc* Scheffe test was used for pairwise comparisons. The level of significance was set at 0.05. Independent samples *t*-test was performed using SPSS 23.0 (Kirkpatrick, 2015) for the inorganic ion concentrations of samples C1-3 and C4-5, the level of significance was set at 0.05. The results obtained by clone library and culture-dependent methods were counted, and the bioinformatics analysis images were drawn using the Origin software (Edwards, 2002). According to the abundance and changes of each species in each sample, Spearman's rank correlation analysis was performed (Corder and Foreman, 2014). Then, the data with significant and robust correlations ($\rho > 0.7$ and $P < 0.05$) were screened, and the correlation network diagram was drawn based on Python.

Results

Physicochemical characteristics of brine samples

Brine samples were collected from Dingyuan Salt Mine located in Dongxing Town, Dingyuan County, Anhui Province, China (**Supplementary Figures 1a,b**). The physicochemical properties of these brine samples are shown in **Table 1**. The pH

TABLE 1 Physicochemical properties of brines.

Item	C1[a]	C2[a]	C3[a]	C4[b]	C5[b]
Mg (mg/L)	7.452	7.610	7.011	7.112	7.031
K (mg/L)	213.5	221.2	211.9	210.8	215.4
Fe (mg/L)	0.222	0.267	0.151	0.236	0.214
NO_3^- (mg/L)	9.790	9.716	8.201	9.625	8.096
pH	8.09	8.11	7.99	8.19	8.17

[a]Brine collected in July, 2021.
[b]Brine collected in August, 2018.

of brine samples varies from 7.99 to 8.19, indicating that these brine samples are slightly alkaline. The concentration of nitrate ion in these five brine samples ranges from 8.1 to 9.8 mg/L. In addition, the concentrations of magnesium, potassium, and iron in samples C1-3 and C4-5 were not significantly different ($p < 0.05$).

Total environmental DNA extracted from different brine samples

Total environmental DNA extracted from different brine samples is shown in **Supplementary Table 2** and **Figure 2A**. The results revealed that the environmental DNA extracted from the samples collected in 2018 (C4-5) was 2–3 times higher than that from samples collected in 2021 (C1-3), which indicates that the biomass accumulated greatly after 3 years of indoor static and closed storage. The DNAs in the ddH_2O used in environmental DNA extraction and room air samples were much lower than those in the brine samples in order of magnitudes. The DNA concentrations in the different samples (**Figure 2A**) were significantly different, demonstrating that there was a significant difference in DNA concentrations between the samples C4-5 and samples C1-3. Similarly, DNA concentrations in samples (C1-5) were all significantly different from sample freshwater (FW) which was pumped in to dissolve solid salt mine to produce brine. It was worth noting that the DNA concentration of the sample FW was much higher than that of the brine samples (C1-5). Additionally, the PCR amplification experiments indicated that no haloarchaeal DNA was detected or the amount of haloarchaeal DNA was below the limit of PCR detection in the samples ddH_2O, room air and FW (**Figure 2B**), illustrating a low experimental contamination.

Species diversity indices

High-throughput sequencing was performed on brine samples (C1-5), fresh water (FW), and samples collected after the halophiles in brine were cultured in medium (Cx-168 and Cx-NOM). Sequences obtained from the quality filtering were

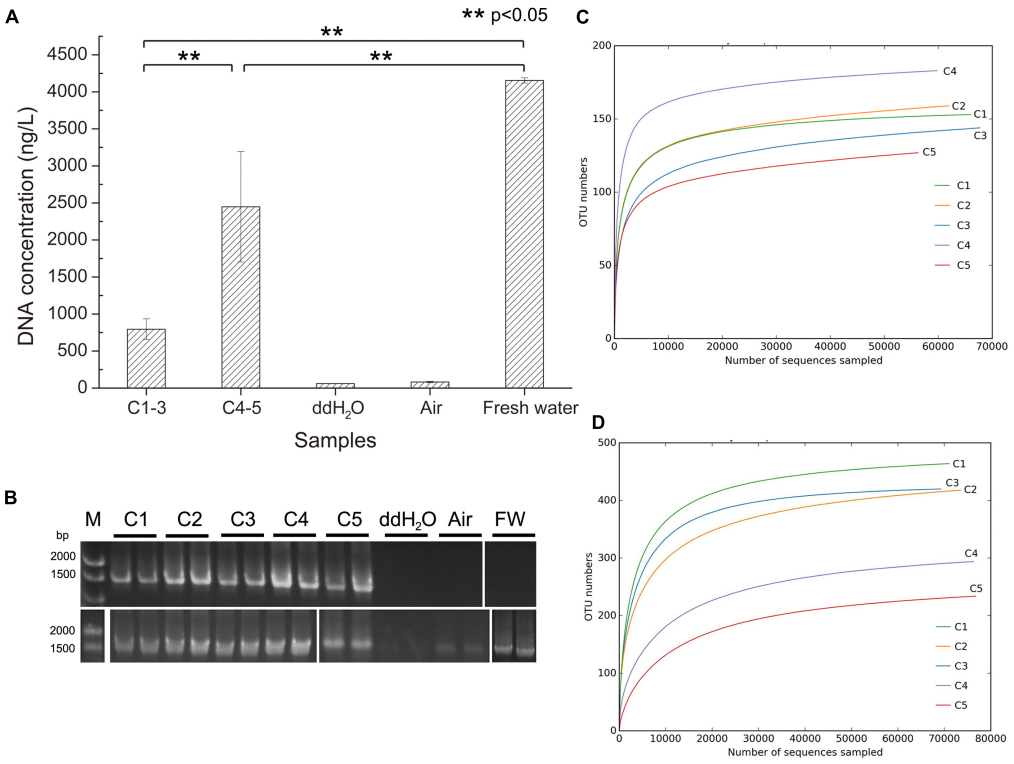

FIGURE 2
Total environmental DNA extraction and 16S RNA amplicon sequencing rarefaction curves. **(A)** The total DNA was extracted from 1 L of the corresponding samples except from the air in the lab with suction filtration approach. C1-3, three brine samples (C1, C2, and C3) collected in July 2021; C4-5, two brine samples (C4 and C5) collected in August 2018; ddH_2O, distilled water; Air, time duration of lab air suction filtration was the same as ddH_2O; Fresh water, the natural water source used to dissolve salt mines for brine production. $^{**}p < 0.05$, significant difference. **(B)** These extracted environmental DNA was used as PCR template for amplifying haloarchaeal (upper row) and bacterial (bottom row) 16S rRNA gene using F8/R1462 and 27F/1492R, respectively. FW, fresh water; DNA ladder was shown on the left. **(C)** Rarefaction curve of archaeal 16S RNA amplicon sequencing. **(D)** Rarefaction curve of bacterial 16S RNA amplicon sequencing. OTU, operational taxonomic unit.

trimmed, after which the high-quality ones were obtained for further analysis. In the culture-independent approach, 398,634 and 399,340 high-quality reads were obtained with archaeal and bacterial 16S rRNA gene primer sets, respectively. For samples collected from culture-dependent of brine, 366,127 high-quality reads were obtained with archaeal 16S rRNA gene primer set. Interestingly, the number of OTUs of archaea in samples C1-3 and C4-5 was not significantly different, but the number of OTUs of bacteria in samples C1-3, C4-5 and FW was significantly different ($p < 0.05$) (**Supplementary Figure 2**). OTUs were grouped at the 97% similarity cut off, and diversity indices and richness estimates were calculated for each sample (**Supplementary Table 3**).

The coverage values of all samples exceeded 0.99 (**Supplementary Table 3**), indicating that the sequencing results can adequately reflect the diversity and structure of microbial community. Similarly, the rarefaction curves for all samples including freshwater samples (FW) were approaching saturation as the sequencing deepens, suggesting sequencing depth was adequate (**Figures 2C,D** and **Supplementary Figures 3a,b**). The Chao1, ACE, Simpson and Shannon indices for bacterial communities in samples C1-3 were higher than those in samples C4-5, especially the Shannon index was significantly different ($p < 0.05$) (**Supplementary Table 3** and **Figure 3A**). However, C4 exhibited higher Chao1, ACE and Shannon indices compared to other brine samples when using archaeal primers.

For culture-dependent approach (Cx-168 and Cx-NOM), there was no significant difference in the species diversity ($p < 0.05$) (**Supplementary Table 3** and **Figure 3B**). Interestingly, the bacterial diversity of samples C1-3 was higher than that of Archaea, while it was opposite in samples C4-5.

Microbial community structure revealed by culture-independent approach

Community structure of bacteria and archaea at the phylum, family, and genus level

According to the classification based on the 16S rRNA gene sequence similarity (V3 + V4), a total of 28 bacterial phyla, 218 bacterial families and 345 bacterial genera were identified. The top 10 bacterial classes in different brine samples are vividly exhibited in **Figures 4A–C**. As shown in **Figure 4A**, the bacterial community in C1-3 was dominated by phyla Proteobacteria (53.61%), Bacteroidetes (20.85%) and Cyanobacteria (12.04%), followed by Firmicutes (5.90%) and Actinobacteria (2.21%). Coincidentally, the dominant phyla in C4-5 were also Proteobacteria and Bacteroidetes, accounting for 32.22% and 51.99%, respectively. On the other hand, the dominant phyla in freshwater samples (FW) were also Proteobacteria (42.99%), Actinobacteria (27.88%) and Bacteroidetes (12.41%) (**Supplementary Figure 4**). It's obvious that although samples C1-3, C4-5 and FW shared the similar dominant phyla, the proportion of them was quite different. For instance, the proportions of phyla Proteobacteria, Cyanobacteria, Firmicutes and Actinobacteria in C4-5 were lower than in C1-3, indicating that their abundance decreased during a long-term indoor

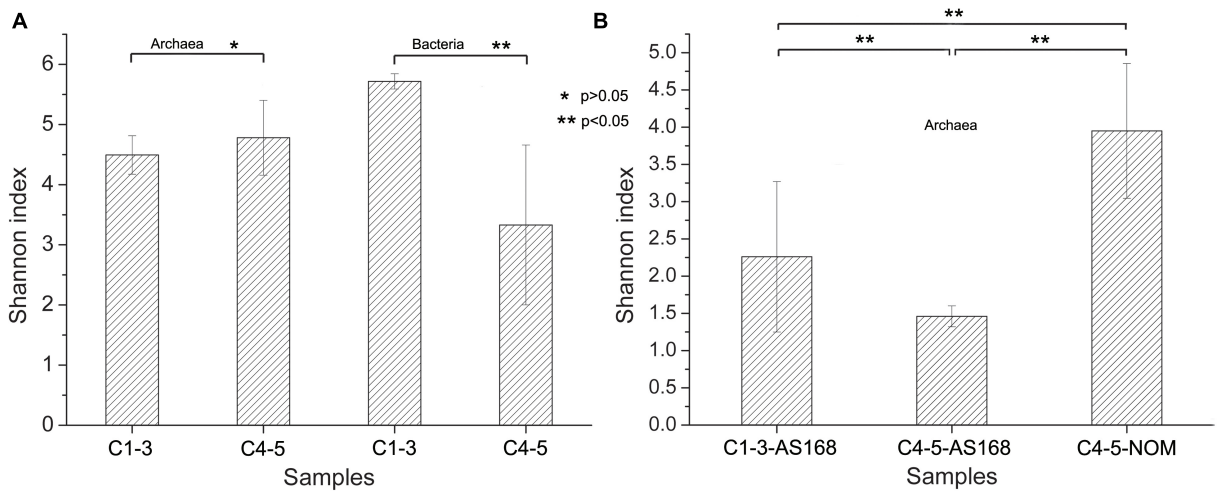

FIGURE 3
Species diversity of different brine samples revealed by Shannon index. The species diversity was shown using 16S rRNA-based high-throughput sequencing technology under culture-independent **(A)** and culture-dependent approaches **(B)**. *$p > 0.05$, **$p < 0.05$. Archaea, archaeal 16S rRNA gene primers were used; Bacteria, bacterial 16S rRNA gene primers were used; AS-168 medium, colonies grown on the AS-168 medium were collected for the archaeal 16S rRNA-based high-throughput sequencing; NOM medium, colonies grown on the NOM medium were collected for the archaeal 16S rRNA-based high-throughput sequencing; C1-3, three samples collected in July 2021; C4-5, two samples collected in August 2018.

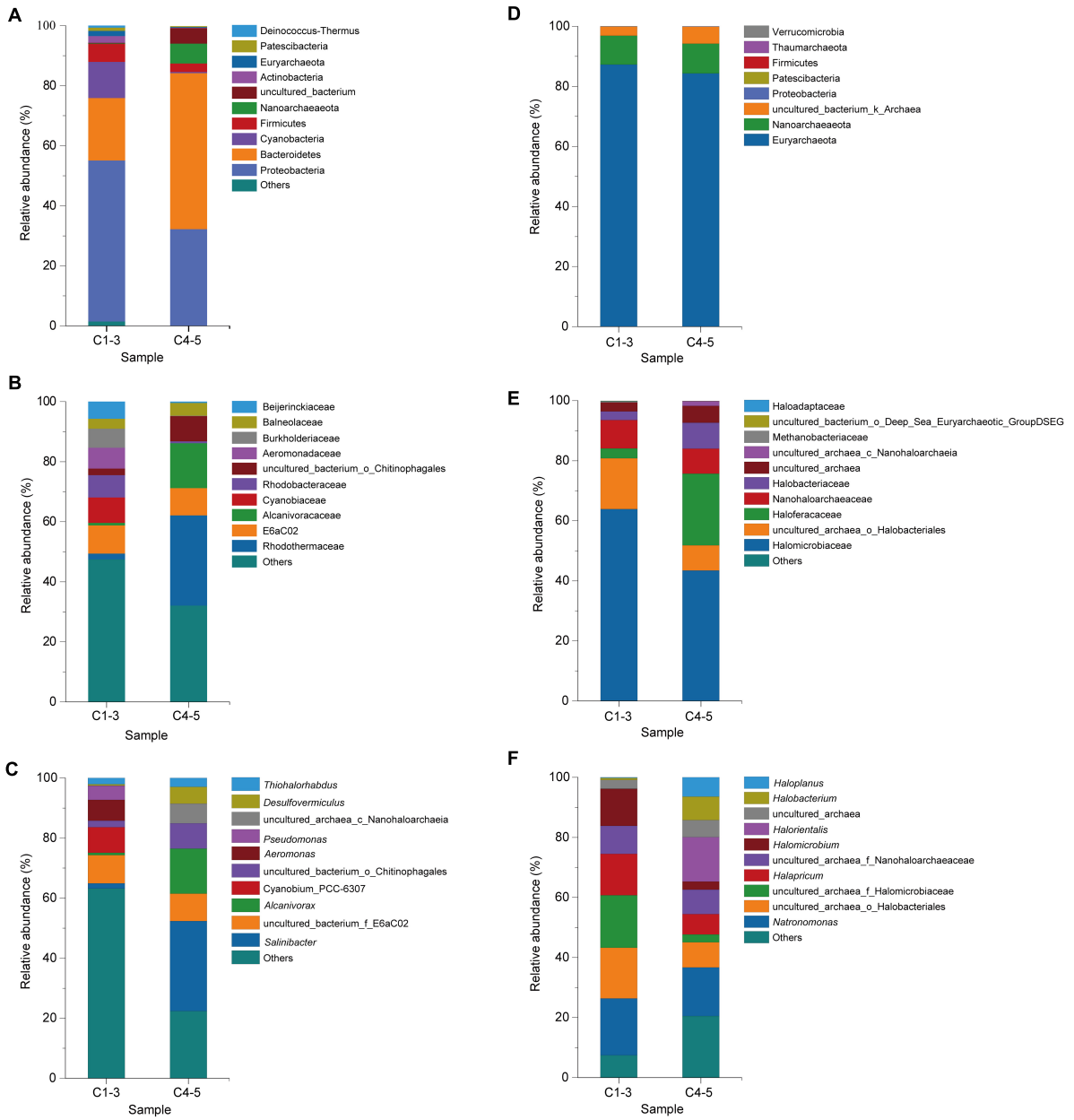

FIGURE 4
Microbial community of brine samples revealed by 16S rRNA gene sequencing under culture-independent strategy. The community composition of bacteria in brine samples was shown at the phylum **(A)**, family **(B)**, and genus **(C)** levels; while composition of archaea in the brine samples was also shown at the phylum **(D)**, family **(E)**, and genus **(F)** levels; C1-3, three brine samples collected in July 2021; C4-5, two brine samples collected in August 2018.

static and closed storage. Conversely, the proportion of Bacteroidetes in C4-5 community increased significantly. At the family level, families *E6aC02*, *Cyanobiaceae*, *Rhodobacteraceae*, *Aeromonadaceae*, and *Burkholderiaceae* were the top five dominant taxa in C1-3, but only constituted 38.56% of the total taxa. However, *Rhodothermaceae* (30.01%) was dominant in C4-5 at the family level, followed by families *Alcanivoracaceae* (14.96%) and *E6aC02* (9.10%). Detailed analysis of the bacterial community composition at the genus level revealed that some genera were dominant in C1-3 with a higher proportion, while presenting a much lower proportion in C4-5 or even below detection limit. For example, genera *Cyanobium_PCC-6307* (8.46%), *Aeromonas* (6.91%), and *Pseudomonas* (4.71%) were the dominant genera in C1-3, but almost undetectable in C4-5. Genus *Salinibacter* (30.01%) was the most common in C4-5, followed by genus *Alcanivorax* (14.96%). Apparently,

during a long-term indoor storage, genera *Salinibacter*, *Alcanivorax* and *Desulfovermiculus* were flourishing, while genera *Cyanobium_PCC-6307*, *Aeromonas* and *Pseudomonas* were experiencing a recession or even extinction.

Archaeal taxa at the phylum level and family level are shown in **Figures 4D,E**, respectively. The representative archaeal phyla in C1-3 and C4-5 were Euryarchaeota and Nanoarchaeaeota, accounting for 96.90% and 94.24% of the total OTUs, respectively. At the family level, *Halomicrobiaceae* (63.81%) and *Nanohaloarchaeaceae* (9.45%) were the top dominant families in C1-3. The most abundant family in C4-5 was *Halomicrobiaceae* (43.43%), followed by the family *Nanohaloarchaeaceae* (23.89%). Furthermore, it showed that families *Haloferacaceae* and *Halobacteriaceae* were more abundant in C4-5 than C1-3, while families *Halomicrobiaceae* and *Nanohaloarchaeaceae* were the opposite. To better explain the structure of the archaeal community in different brines, the relative abundance and classification of OTUs were analyzed at the genus level (**Figure 4F**). Genera *Natronomonas* (18.89%), *Halapricum* (13.73%) and *Halomicrobium* (12.35%) were the dominant genera in C1-3. In C4-5, the top dominant taxa were genera *Natronomonas* (16.18%), *Halorientalis* (14.80%), *Halobacterium* (7.82%), *Haloplanus* (6.46%) and *Halomicrobium* (2.67%). It was found that the abundance of genera *Halapricum* and *Halomicrobium* decreased sharply after a long-term indoor storage, while genera *Halorientalis*, *Halobacterium*, and *Haloplanus* became dominant.

Community composition of haloarchaea at the genus level revealed by limited clone sequencing

The limited clone library strategy sequenced 185 clones selected randomly from samples C1, C2, C3, C4, and C5. These 185 sequenced 16S rRNA gene sequences belonged to 25 genera (**Figure 5**). Among them, genera *Halorientalis* (29.83%), *Salinirussus* (16.66%), *Natronomonas* (14.16%) and *Halomicrobium* (9.24%) were the dominant groups with a relative higher proportion in C1-3. In C4-5, genus *Halovenus* (28.75%) accounted for the highest proportion, followed by genera *Halorientalis* (21.79%), *Natronomonas* (21.07%), and *Haloplanus* (8.39%). Intriguingly, genus *Halomicrobium* accounting for 9.24% in C1-3 was not detected in C4-5. However, genus *Haloplanus* accounting for 8.39% in C4-5 was not detected in C1-3. Thus, the patterns of change for genera *Halomicrobium* and *Haloplanus* were the opposite.

Sequence similarity search of these cloned 16S rRNA gene sequences against public database using Basic Local Alignment Search Tool (BLAST; see text footnote 2) revealed that the majority of these cloned sequences showed a relatively lower sequence identity (<95%). It supposed that there were a large number of potential new species or genera in hypersaline environments. Meanwhile, these results also indicated that high through-put sequencing and cloning library were both culture-independent methods showing a significant difference in revealing microbial community structure.

Microbial community structure uncovered by culture-dependent methods

Halophilic microbes in different brine samples were cultivated by using AS-168 and NOM media, respectively. On AS-168 agar plates, it was evident that the number and species of halophilic microorganisms from C4-5 exceeded those from C1-3 (**Figure 6A**). The chocolate-colored with white surrounding colonies cultivated from C1-3 belonged to the genus *Salicola*, which were completely absent in C4-5 on AS-168 agar plates.

To gain more information, colonies grown on AS-168 and NOM agar plates were washed with 20% (w/v) sterilized NaCl solution and then collected for high-throughput sequencing using archaeal 16S rRNA gene primers. The top 10 archaeal genera detected in different medium are shown in **Figure 6B**. Genera *Halorubrum* (47.23%), *Natronomonas* (24.78%) and *Halopenitus* (10.73%) were the dominant Haloarchaea in C1-3-AS168. Similarly, genus *Halorubrum* (88.69%) was also determined to be the most dominant group in C4-5-AS168, followed by genera *Halobellus* (4.56%) and *Halopenitus* (4.25%). Although genus *Halorubrum* showed the highest richness in both C1-3-AS168 and C4-5-AS168, the proportion varied from different sample sets. Genera *Natronomonas* (24.37%), *Halorubrum* (17.91%) and *Haloarcula* (12.81%) were the dominant genera in C4-5-NOM. Among them, *Natronomonas* and *Haloarcula* were more abundant in C4-5-NOM than C4-5-AS168, indicating that NOM medium was more suitable for their growth. Compared to NOM medium, AS-168 was a eutrophic environment. It reflected that as a typical chemoheterotrophic halophilic archaeon, *Halorubrum* spp. may prefer a eutrophic environment. Generally, oligotrophic environments were more suitable for the isolation of more different halophilic archaea (**Figure 6B**).

Through cultivation and a series of streaking, 62 halophilic microorganisms including 12 possible new species (sequence identity < 97.5%, see "Data availability statement") were isolated from different brine samples by using AS-168 and NOM media. Next, they were classified into 10 genera such as *Halorubrum*, *Halorientalis*, *Natronomonas*, and *Halovibrio* based on the 16S rRNA gene sequence similarity search (**Figure 6C**).

Microbial co-occurrence network analyses

The bacterial genera and archaea genera with a relative abundance more than 0.1% were selected as study objects, and the potential interactions of these taxa were analyzed.

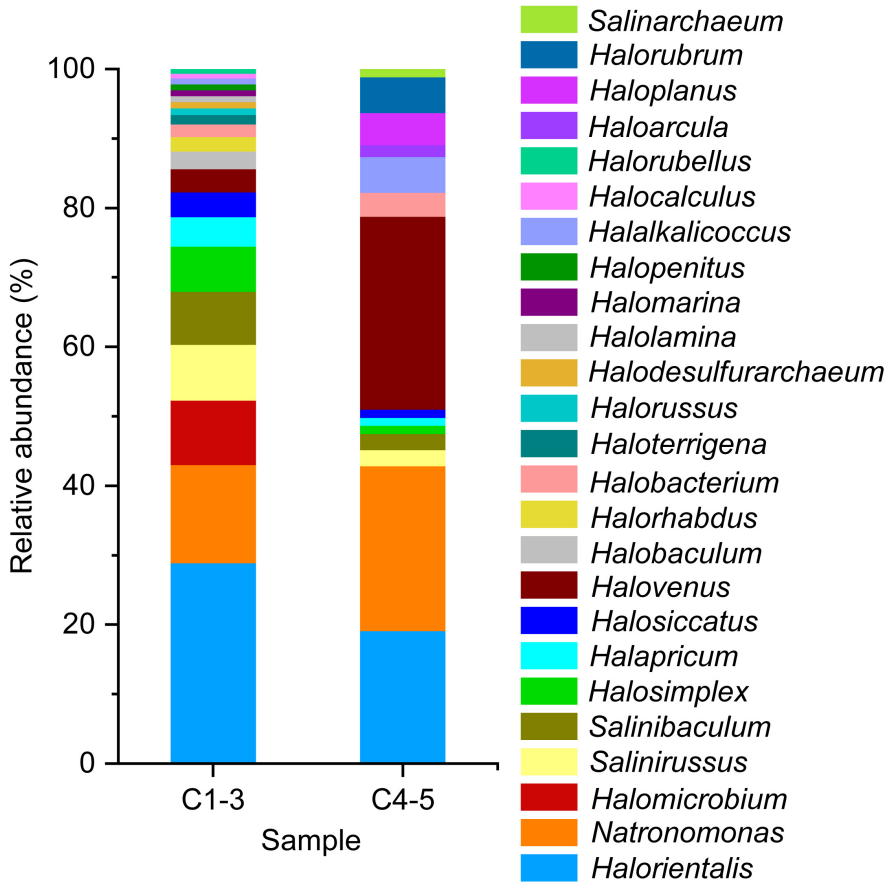

FIGURE 5
Haloarchaeal composition in brine samples revealed by clone library at the genus level under culture-independent approach. Almost complete length of the 16S rRNA gene was obtained by using F8 and R1462 primer pair. C1-3, three brine samples collected in July 2021; C4-5, two brine samples collected in August 2018.

Co-occurrence network taxa were highly significant network hubs ($\rho > 0.7$, $p < 0.05$; **Figures 7A,B**). The bacterial network consisted of 52 nodes and 100 edges, and the average degree and the clustering coefficient were 3.85 and 1.29, respectively. In the bacterial network, most of the correlations were positive (positive correlation ratio: 91%, **Figure 7A**). The nodes in the bacterial network were divided into 10 bacterial phyla. Among them, Proteobacteria accounted for 53.85% of all nodes, showing a strong intra-phylum correlation. However, members of Actinobacteria and Bacteroidetes showed more positive correlations with other bacterial genera, especially with Proteobacteria. The top nine keystone genera with the highest number of connections in the bacterial network were *Ralstonia*, *Rhodobaculum*, *uncultured_bacterium_f_Rhodobacteraceae*, *Salinarimonas*, *Paracoccus*, *Cyanobacterium_PCC-10605*, *uncultured_bacterium_f_Balneolaceae*, *Algoriphagus*, and *Cyanobium_PCC-6307*.

The archaeal network was composed of 26 nodes and 100 edges, and the average degree and clustering coefficient were 7.69 and 0.61, respectively (**Figure 7B**). Among the only three Archaeal phyla, the Euryarchaeota was the most dominant, accounting for 80.76% of all nodes. The next was Nanoarchaeaeota (15.38%), which had the highest number of associations with Euryarchaeota. The top five genera with the most connections in the archaeal network were *Haloplanus*, *uncultured_bacterium_f_Halofracaceae*, *Halobacterium*, *Halapricum*, and *Halorientalis*.

Discussion

The Dingyuan Salt Mine in Anhui Province, located in central China, is endowed with the characteristics of continental basin deposits, whose salt-bearing layer was formed in the Early Tertiary Oligocene and is dominated by river-lake facies deposition (**Supplementary Figures 1a,b**; Chen et al., 2019). At present, water dissolution (fresh water-in and brine-out) is the main method for salt mining (**Figures 1A,B**). In detail, the mining process involves injecting fresh water (solvent) into the deposit to dissolve salt minerals *in situ* into a flowing solution

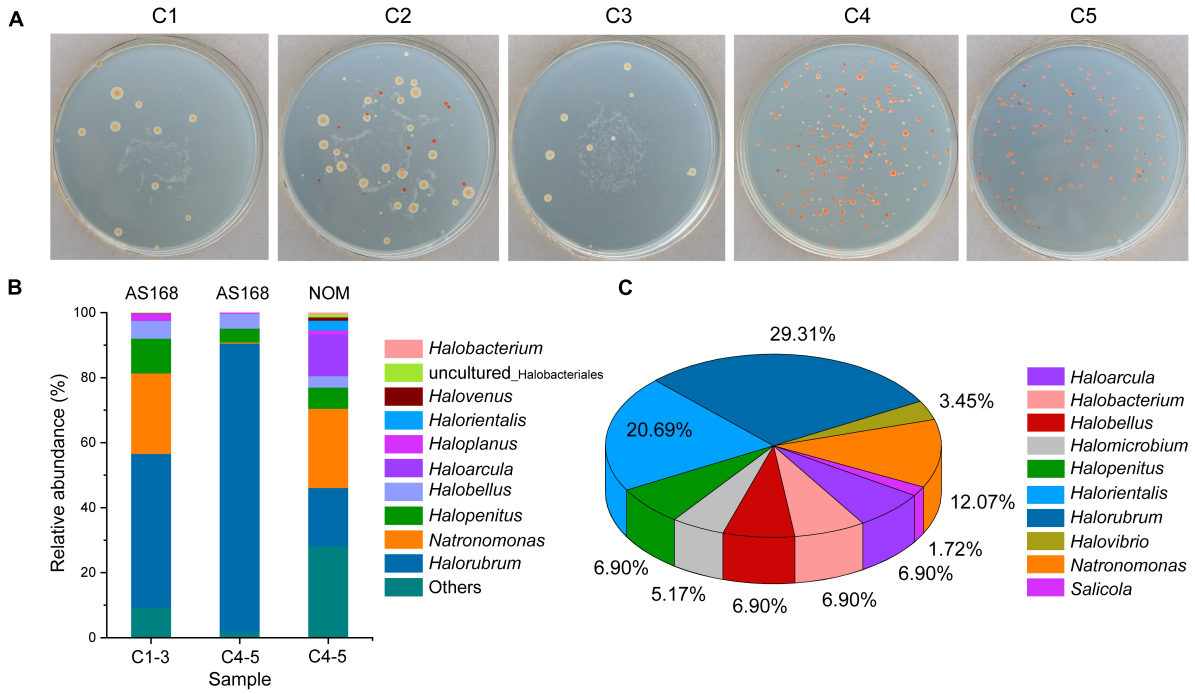

FIGURE 6
Halophilic archaea and halotolerant bacteria isolated from brine samples. Cultivation of halophilic microbes from brine samples using the AS-168 agar plates **(A)**. Cultures grown on the AS-168 and NOM agar plates were collected by washing with 20% (w/v) sterilized NaCl solution for archaeal 16S rRNA gene (V3 + V4) high-throughput sequencing **(B)**. Microbial composition of randomly isolated strains identified by sequencing the almost complete 16S rRNA gene combined with sequence similarity search **(C)**. C1-3, three brine samples including C1, C2, and C3 collected in July 2021; C4-5, two brine samples including C4 and C5 collected in August 2018.

(brine), and then the brine coming out (Wang, 1999). In this study, the composition of microbial communities in brines after long-term indoor static and closed storage (C4-5) and in freshly collected brines (C1-3) was preliminarily compared by a combination of culture-independent and culture-dependent methods. Environmental conditions such as high salinity, hypoxia, and slightly alkaline pH are driving factors shaping microbial community structure and forming corresponding adaptability after long-term indoor sealed storage in this study.

It is widely acknowledged that salinity is an important factor affecting the richness and diversity of bacteria and archaea (Kalwasinska et al., 2017; Banda et al., 2021). The DNA concentration of freshwater samples (FW) used to dissolve the rock salt buried underground in this study is significantly higher than that of brine samples (C1-5) ($p < 0.05$; **Supplementary Table 2** and **Figure 2A**), illustrating that microorganisms in freshwater declined steeply or even disappeared after entering a hypersaline environment. Besides, it also means that environmental filtering prevents the efficient colonization and persistence of non-tolerant species in hypersaline environments (Triado-Margarit et al., 2019). It is worth noting that the bacterial diversity of samples C1-3 is higher than that of archaea, which is in the opposite manner for samples C4-5 (**Supplementary Table 3** and **Figure 3A**). And the diversity of bacterial community in samples C1-3 is significantly higher than that in samples C4-5 ($p < 0.05$; **Supplementary Table 3** and **Figure 3A**). It is worth noting that some of the error bars in **Figures 2A**, **3A,B** vary greatly, which may be caused by the small sample size. However, the tendency reflected by the differences between these samples (C1-3 and C4-5) are still obvious and persuasive. The result showed that the diversity of bacterial communities in the brine samples decreased significantly after long-term indoor sealed storage. At the phylum level, long-term indoor sealed storage profoundly altered bacterial community structure, i.e., the relative abundance of some bacterial communities varied much more than archaeal communities (**Figures 4A,D**). At the same time, studies have shown that archaea can withstand environmental stress better than bacteria, and obtain a stable community structure within a certain time-frame (de León-Lorenzana et al., 2017; Mani et al., 2020). Therefore, we believe that archaea in brine samples are more adaptive than bacteria in the hypersaline environment under a long-term indoor sealed storage condition.

In this paper, bacterial and archaeal communities in different brine samples were analyzed by Illumina high-throughput sequencing technology. Overall, the bacterial communities in the brine samples are mainly composed

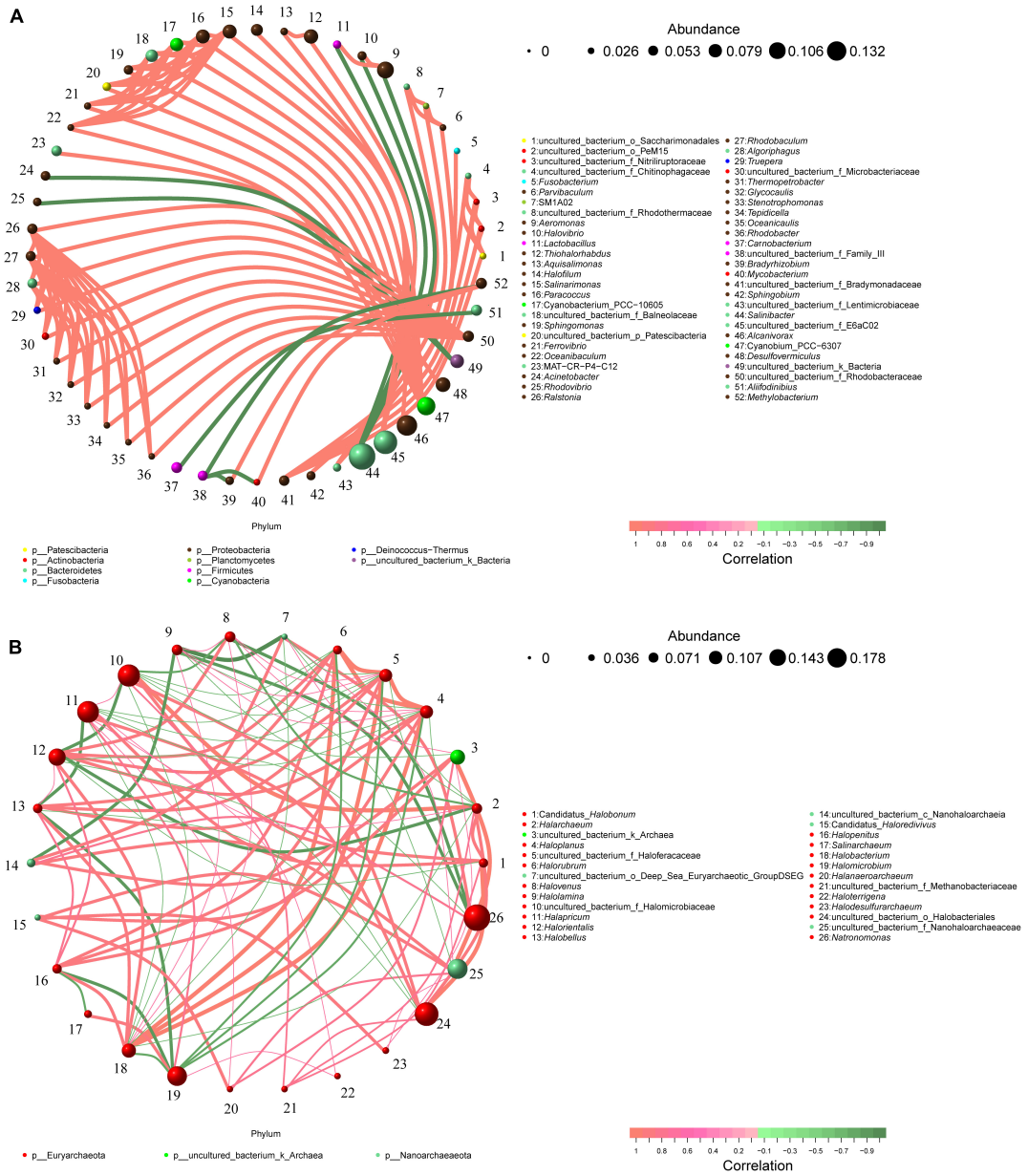

FIGURE 7
Co-occurrence networks of microbial communities in different brine samples based on correlation analysis. The nodes in network are colored by phylum. Co-occurrence networks of bacterial communities **(A)** and archaea communities **(B)**; The connections indicate strong spearman's ($\rho > 0.7$) and significant ($p < 0.05$) correlations. The size of each node is proportional to the relative abundance of specific genus.

of Proteobacteria and Bacteroidetes (**Figure 4A**), which is consistent with other researches (Boujelben et al., 2012; Kalwasinska et al., 2018; Mazière et al., 2021). In fact, Proteobacteria and Bacteroidetes are also the dominant phyla in other saline waters (Boujelben et al., 2012; Kalwasinska et al., 2018; Cardoso et al., 2019), playing an important role in carbon and nitrogen cycling (Bernhard et al., 2012; Wong et al., 2015). The result also shows that these brine samples have the characteristics of dominant bacterial taxa commonly found in other hypersaline environments.

Further analysis reveals that although samples C1-3 and C4-5 shared the same dominant bacterial phyla, their relative abundances are quite different (**Figure 4A**). As it shows in the result that the abundance of Proteobacteria may decrease greatly after long-term indoor sealed storage, whereas the abundance of Bacteroidetes is the opposite. Similarly, genera *Salinibacter* and *Alcanivorax* are dominant in C4-5, but less abundant

in C1-3 (**Figure 4C**). *Cyanobium_PCC-6307*, *Aeromonas* and *Pseudomonas* are the dominant genera in C1-3, but are barely detectable in C4-5 (**Figure 4C**). Among them, genus *Salinibacter* is an extreme halophilic genus with archaeal properties in Bacteroidetes, also an important part of bacterial communities in various high-salt environments (Bachran et al., 2019; Perez-Fernandez et al., 2019; Cycil et al., 2020). *Salinibacter* spp. generally, requires light-driven pumps for growth and maintenance of ion gradients across the cell membrane (Doğan and Kocabaş, 2021). The low levels of genus *Salinibacter* in C1-3 may be attributed to relatively lower levels of solar radiation and lower temperatures (Kalwasinska et al., 2018). Meanwhile, the enrichment of genus *Salinibacter* is also one of the reasons for the largest proportion of Bacteroidetes in C4-5.

Compared with bacterial taxa, fewer Archaeal phyla can be found in these samples, with most of the sequences belonging to Euryarchaeota, followed by Nanoarchaeaeota (**Figure 4D**). And the relative abundance difference of the dominant phyla in samples C1-3 and C4-5 is small (**Figure 4D**). However, the opposite is true at the genus level. The relative abundance of genera *Halapricum* and *Halomicrobium* in samples C1-3 is much higher than those in samples C4-5, while the relative abundance of genera *Halorientalis*, *Halobacterium* and *Haloplanus* in samples C4-5 is much higher than those in samples C1-3 (**Figure 4F**). Interestingly, genus *Natronomonas* dominates in all samples (**Figure 4F**). As observed elsewhere, genus *Natronomonas* is one of the most successful ecological taxa able to survive in hypersaline environments (Chen et al., 2020; Banda et al., 2021; Satari et al., 2021; Zhu et al., 2021).

It should not be ignored that species in genera *Alcanivorax* and *Halorientalis* were blooming in hypersaline environment in long-term indoor storage, becoming the dominant genera (**Figures 4C,F**). Genus *Alcanivorax* is a ubiquitous marine hydrocarbonoclastic genus, which dominates in many oil-contaminated environments (Scoma and Boon, 2016). Known for its preference for metabolizing hydrocarbons and crude oil derivatives (Zadjelovic et al., 2020). And the members of genus *Halorientalis* were also reported to be capable of degrading hydrocarbons (Khalid et al., 2021). It is worth noting that the formation process of rock salt and petroleum is always closely related. Petroleum consisting of hydrocarbons with different carbon chain length is covered by a thick stratum of salt. Hydrocarbons with a relatively low density can leak into the upper salt stratum through cracks created by geological movements (Sonnenfeld and Perthuisot, 1984). Additionally, previous studies have shown that the Hefei Basin (Anhui province, China), where the Dingyuan Salt Mine is located, exhibits ideal geological conditions for petroleum formation (Jia et al., 2001; Dai et al., 2011). The brine sample smelled of petrol. Therefore, the brine samples are likely to contain petroleum and hydrocarbons, and such favorable environmental conditions may lead to the enrichment of genera *Alcanivorax* and *Halorientalis*. Hydrocarbons degrading microorganisms were enriched in the presence of favorable substrates during a relative long period of storage.

Clone library technology has been widely used to study microbial communities in different habitats (Jones et al., 2009; Xiao et al., 2013; Wang et al., 2018; Chen et al., 2020), which is also applied in this study. It can be found that the dominant genus with the highest proportion in C1-3 is genus *Halorientalis*, while in C4-5 it is genus *Halovenus* (**Figure 5**), which is inconsistent with the high-throughput sequencing results. Previous studies have also shown that the diversity of microbial communities can fluctuate severely along with the size of the clone library (Li et al., 2017). Therefore, it is normal to get different results between the two methods.

With the development of molecular methods, culture-independent methods are considered more effective than culture-dependent methods (Dakal and Arora, 2012), because the latter can only detect 1–5% of all microorganisms in the sample (Ma et al., 2015). Nevertheless, the methods of culture-dependent are still an indispensable technique to acquire microbial species with tremendous application potential and to understand their ecophysiological and environmental functions (Vandamme et al., 1996; Sfanos et al., 2005). In this study, genera *Halorubrum*, *Halobellus*, and *Halopenitus* are the dominant taxa in C4-5-AS168, but genera *Natronomonas*, *Halorubrum*, and *Haloarcula* have a higher proportion in C4-5-NOM (**Figure 6B**). Among them, the relative abundance of genus *Halorubrum* in C4-5-AS168 is nearly five times that in C4-5-NOM, indicating that the eutrophic environment of AS-168 may make it more competitive.

Furthermore, a large proportion of microbial species are uncultured, which tends to make some opportunistic species predominant in isolates. Therefore, culture-dependent approaches introduce numerous biases, and generally do not select the most abundant taxa in the environment. Rather, they select the microorganisms that grow best under the culture conditions used. The results often differ from the actual distribution of microbial taxa in the environment (Henriet et al., 2014; Naghoni et al., 2017). In this study, a total of 62 halophilic microorganisms including 12 possible new species (sequence identity $< 97.5\%$) isolated from the two media belong to 10 genera (**Figure 6C**). Notably, their sequence similarity search based on 16S rRNA gene sequences all show relatively higher sequence identity ($>95\%$). However, most of the 16S rRNA gene sequences obtained by clone library approach exhibit a lower sequence identity ($<95\%$). The unpredictable alteration of template may happen in different cycles during the PCR amplification in clone library construction, which tends to form a larger number of chimeras. Therefore, clone library approach based on PCR amplification of total environmental DNA may severely overestimate the species diversity (Stevens et al., 2013).

Co-occurrence networks can reveal interactions between different taxa in microbial communities, which can be competitive or cooperative (Faust and Raes, 2012;

He et al., 2019). In this study, the positive correlation among bacterial networks is 91% (**Figure 7A**), while that among archaeal networks is only 64% (**Figure 7B**). This suggests that bacterial communities in brine samples are more likely than archaeal communities to survive in harsh environments through synergies. In addition, genera *Ralstonia*, *Rhodobaculum*, *uncultured_bacterium_f_Rhodobacteraceae*, *Salinarimonas*, *Paracoccus*, *Cyanobacterium_PCC-10605*, *uncultured_bacterium_f_Balneolaceae*, *Algoriphagus* and *Cyanobium_PCC-6307* are found to be highly associated taxa in the bacterial network. Similarly, genera *Haloplanus*, *uncultured_bacterium_f_Halofracaceae*, *Halobacterium*, *Halapricum* and *Halorientalis* are more connected in the archaeal network. These microbial taxa are considered as keystone taxa due to their highly connected nodes (Hu et al., 2018; Guo et al., 2019). Compared with other taxa in the network, these taxa may play a vital part in maintaining the stability of ecological network structure and function (Faust and Raes, 2012; Shi et al., 2019).

Interestingly, the average relative abundances of keystone taxa (except genus *Cyanobium_PCC-6307*) in the bacterial network were fairly low (0.81%∼2.51%). The results indicated the significance of low-abundance genera in bacterial communities. Although the abundance of such genera may not be high, more attention should be paid to them being the key nodes in bacterial communities (Guo et al., 2019). However, the average relative abundances of keystone genera (except *uncultured_bacterium_f_Halofracaceae*) in archaeal network ranged from 2.71% to 10.95%. The result of archaea is different from Bacteria in network. The dominant archaea are also key nodes in archaeal network. These differences may be attributed to the different adaptation mechanisms of bacteria and archaea, which are beneficial to their survival and development of their respective taxa. On the other hand, members of the genera *Salinarimonas* and *Paracoccus* were previously isolated in oil-contaminated environments, indicating their role in hydrocarbon bioremediation (Zhang et al., 2020; Procópio, 2021). And bacteria belonging to *Algoriphagus* were also confirmed as an oil-degrading bacterium (Wang et al., 2014). Meanwhile, members of the genera *Halobacterium* and *Halorientalis* were reported to be capable of degrading hydrocarbons (Kumar et al., 2020). Therefore, these keystone taxa may play important roles in ecological processes, especially in the remediation of oil-polluted hypersaline environments.

Conclusion

In this work, the microorganisms in the brine of salt mine were studied in details for the first time by combining culture-independent and culture-dependent methods. Our conclusions are:

(1) After long-term indoor airtight storage, the species diversity of bacterial communities in brine samples decreased significantly ($p < 0.05$), while that of archaeal communities did not change significantly. The composition of the dominant bacterial and archaeal phyla in different samples was similar, but their relative abundances of dominant phyla are significantly different. Among them, halotolerant genera *Salinibacter* and *Natronomonas* were the predominant inhabitants in brine samples, suggesting that they play a crucial role in this environment.

(2) A total number of 62 halophilic microorganisms including 12 possible new species (sequence identity < 97.5%) belong to 10 genera were isolated from brine of inland salt mine through culture-dependent method before these inhibiting species went extinct with salt mining. Extremophiles from hypersaline environment are of great significance in special biotechnological applications, and in understanding their ecophysiological and environmental functions.

(3) Network analysis showed that the bacteria in brine samples were more likely than the archaea to survive in harsh environments through synergies. Keystone taxa with highly connected nodes (such as genera *Ralstonia*, *Rhodobaculum*, *Haloplanus*, etc.) play an important role in maintaining the stability of ecological network structure and function.

(4) The brine samples are likely to contain petroleum and hydrocarbons, and such favorable environmental conditions led to the enrichment of specific genera *Alcanivorax* and *Halorientalis*, which are capable of degrading hydrocarbons. In addition, the genera *Salinarimonas*, *Paracoccus*, *Algoriphagus* and *Halobacterium* in keystone taxa also have this ability. The interesting phenomenon reflects that these taxa may have significant contributions in the bioremediation of oil-contaminated hypersaline environments.

Overall, the results of this study will expand the understanding of microbial diversity in extreme environments. On the other hand, it is conducive to explore the functional roles or environmental niches inhabited by various microorganisms in extreme environments.

Data availability statement

The datasets presented in this study can be found in online repositories. The names of the repository/repositories and accession number(s) can be found below (check **Supplementary Table 4** for details): NCBI -

(1) PRJNA787045 (https://submit.ncbi.nlm.nih.gov/subs/sra/SUB10779502/overview);

(2) PRJNA791781 (https://submit.ncbi.nlm.nih.gov/subs/sra/SUB10837144/overview);

(3) PRJNA787012 (https://submit.ncbi.nlm.nih.gov/subs/sra/SUB10721350/overview);

(4) PRJNA787052 (https://submit.ncbi.nlm.nih.gov/subs/sra/SUB10779714/overview);

(5) OM184316-OM184500 (https://submit.ncbi.nlm.nih.gov/subs/genbank/SUB10907784/overview);

(6) OL979230-OL979291 (Possible new species: OL979250, OL979251, OL979252, OL979254, OL979260, OL979266, OL979267, OL979268, OL979269, OL979280, OL979282, and OL979283) (https://submit.ncbi.nlm.nih.gov/subs/genbank/SUB10837125/overview).

Author contributions

SC and JH: conceptualization and funding acquisition. SC, SS, DT, JK, YL, and TH: data curation. SC, SS, and DT: investigation. SC and DT: methodology. SC, DT, and JK: writing – original draft. SC, JH, DT, and JK: writing – review and editing. All authors have read and agreed to the published version of the manuscript.

Funding

This work was supported by grants from the Anhui Provincial Key Laboratory of the Conservation and Exploitation of Biological Resources (swzy202011 to SC), the Excellent Young Talents Fund Project for Universities in Anhui Province (gxyqZD2017011 to SC), the Natural Science Foundation of Anhui Province (2208085MC39 to SC), the Opening Project of the State Key Laboratory of Microbial Resources (SKLMR-20220702 to SC), and the National Natural Science Foundation of China (Grant Numbers 31970031 and 91751201 to JH).

Acknowledgments

The authors gratefully acknowledge Feng Li from Dingyuan Salt Mine for assisting in brine sampling and Tao Pan from Anhui Normal University for analyzing part of the data.

Conflict of interest

SS was employed by Anhui Jiaotianxiang Biological Technology Co., Ltd.

The remaining authors declare that the research was conducted in the absence of any commercial or financial relationships that could be construed as a potential conflict of interest.

Publisher's note

Supplementary material

The Supplementary Material for this article can be found online at: https://www.frontiersin.org/articles/10.3389/fmicb.2022.975271/full#supplementary-material

References

Bachran, M., Kluge, S., Lopez-Fernandez, M., and Cherkouk, A. (2019). Microbial diversity in an arid, naturally saline environment. *Microb. Ecol.* 78, 494–505. doi: 10.1007/s00248-018-1301-2

Banda, J. F., Zhang, Q., Ma, L., Pei, L., Du, Z., Hao, C., et al. (2021). Both pH and salinity shape the microbial communities of the lakes in Badain Jaran Desert, NW China. *Sci. Total Environ.* 791:148108. doi: 10.1016/j.scitotenv.2021.148108

Ben Abdallah, M., Karray, F., Kallel, N., Armougom, F., Mhiri, N., Quéméneur, M., et al. (2018). Abundance and diversity of prokaryotes in ephemeral hypersaline lake Chott El Jerid using Illumina Miseq sequencing, DGGE and qPCR assays. *Extremophiles* 22, 811–823. doi: 10.1007/s00792-018-1040-9

Bernhard, A. E., Marshall, D., and Yiannos, L. (2012). Increased variability of microbial communities in restored salt marshes nearly 30 years after tidal flow restoration. *Estuaries Coasts* 35, 1049–1059.

Bolger, A. M., Lohse, M., and Usadel, B. (2014). Trimmomatic: A flexible trimmer for Illumina sequence data. *Bioinformatics* 30, 2114–2120.

Boujelben, I., Gomariz, M., Martínez-García, M., Santos, F., Peña, A., López, C., et al. (2012). Spatial and seasonal prokaryotic community dynamics in ponds of increasing salinity of Sfax solar saltern in Tunisia. *Antonie Van Leeuwenhoek* 101, 845–857. doi: 10.1007/s10482-012-9701-7

Boutaiba, S., Hacene, H., Bidle, K. A., and Maupin-Furlow, J. A. (2011). Microbial diversity of the hypersaline sidi ameur and himalatt salt lakes of the algerian sahara. *J. Arid Environ.* 75, 909–916. doi: 10.1016/j.jaridenv.2011.04.010

Caporaso, J. G., Kuczynski, J., Stombaugh, J., Bittinger, K., Bushman, F. D., Costello, E. K., et al. (2010). QIIME allows analysis of high-throughput community sequencing data. *Nat. Methods* 7, 335–336.

Cardoso, D. C., Cretoiu, M. S., Stal, L. J., and Bolhuis, H. (2019). Seasonal development of a coastal microbial mat. *Sci. Rep.* 9, 1–14.

Chen, L., Li, F., Sun, S., Xu, Y., and Chen, S. (2019). Species-diversity of culturable halophilic microorganisms isolated from Dingyuan salt mine, Anhui. *Microbiol. China* 46:12.

Chen, S., Xu, Y., and Helfant, L. (2020). Geographical isolation, buried depth, and physicochemical traits drive the variation of species diversity and prokaryotic community in three typical hypersaline environments. *Microorganisms* 8, 2–14. doi: 10.3390/microorganisms8010120

Corder, G. W., and Foreman, D. I. (2014). *Nonparametric Statistics: A Step-By-Step Approach*. Hoboken, NJ: John Wiley & Sons.

Couto-Rodríguez, R. L., and Montalvo-Rodríguez, R. (2019). Temporal analysis of the microbial community from the crystallizer ponds in Cabo Rojo, Puerto Rico, using metagenomics. *Genes* 10:422. doi: 10.3390/genes10060422

Cui, H. L., Mou, Y. Z., Yang, X., Zhou, Y. G., Liu, H. C., and Zhou, P. J. (2012). Halorubellus salinus gen. nov., sp. nov. and Halorubellus litoreus sp. nov., novel halophilic archaea isolated from a marine solar saltern. *Syst. Appl. Microbiol.* 35, 30–34. doi: 10.1016/j.syapm.2011.08.001

Cycil, L. M., DasSarma, S., Pecher, W., McDonald, R., AbdulSalam, M., and Hasan, F. (2020). Metagenomic insights into the diversity of halophilic microorganisms indigenous to the karak salt mine, Pakistan. *Front. Microbiol.* 11:1567. doi: 10.3389/fmicb.2020.01567

Dai, Y., Hu, W., Tang, J., Peng, G., and Yan, F. (2011). Tectonic evolution, differential deformation and gas exploration prospect of Hefei basin. *Geol. China* 38, 1584–1592.

Dakal, T. C., and Arora, P. K. (2012). Evaluation of potential of molecular and physical techniques in studying biodeterioration. *Rev. Environ. Sci. Biotechnol.* 11, 1–34.

de León-Lorenzana, A. S., Delgado-Balbuena, L., Domínguez-Mendoza, C., Navarro-Noya, Y. E., Luna-Guido, M., and Dendooven, L. (2017). Reducing salinity by flooding an extremely alkaline and saline soil changes the bacterial community but its effect on the archaeal community is limited. *Front. Microbiol.* 8:466. doi: 10.3389/fmicb.2017.00466

Derakhshani, H., Tun, H. M., and Khafipour, E. (2016). An extended single-index multiplexed 16S rRNA sequencing for microbial community analysis on MiSeq illumina platforms. *J. Basic Microbiol.* 56, 321–326. doi: 10.1002/jobm.201500420

Doğan, S. Ş, and Kocabaş, A. (2021). Metagenomic assessment of prokaryotic diversity within hypersaline Tuz Lake, Turkey. *Microbiology* 90, 647–655.

Edgar, R. C. (2010). Search and clustering orders of magnitude faster than BLAST. *Bioinformatics* 26, 2460–2461.

Edgar, R. C., Haas, B. J., Clemente, J. C., Quince, C., and Knight, R. (2011). UCHIME improves sensitivity and speed of chimera detection. *Bioinformatics* 27, 2194–2200. doi: 10.1093/bioinformatics/btr381

Edwards, P. M. (2002). Origin 7.0: Scientific graphing and data analysis software. *J. Chem. Inf. Comput. Sci.* 42, 1270–1271.

Faust, K., and Raes, J. (2012). Microbial interactions: From networks to models. *Nat. Rev. Microbiol.* 10, 538–550.

Fendrihan, S., Legat, A., Pfaffenhuemer, M., Gruber, C., Weidler, G., Gerbl, F., et al. (2006). Extremely halophilic archaea and the issue of long-term microbial survival. *Rev. Environ. Sci. Biotechnol.* 5, 203–218. doi: 10.1007/s11157-006-0007-y

Genderjahn, S., Alawi, M., Mangelsdorf, K., Horn, F., and Wagner, D. (2018). Desiccation- and saline-tolerant bacteria and archaea in kalahari pan sediments. *Front. Microbiol.* 9:2082. doi: 10.3389/fmicb.2018.02082

Gibtan, A., Park, K., Woo, M., Shin, J. K., Lee, D. W., Sohn, J. H., et al. (2017). Diversity of extremely halophilic archaeal and bacterial communities from commercial salts. *Front. Microbiol.* 8:799. doi: 10.3389/fmicb.2017.00799

Gomez-Villegas, P., Vigara, J., and Leon, R. (2018). Characterization of the microbial population inhabiting a solar saltern pond of the odiel marshlands (SW Spain). *Mar. Drugs* 16:332. doi: 10.3390/md16090332

Guo, X. P., Yang, Y., Niu, Z. S., Lu, D. P., Zhu, C. H., Feng, J. N., et al. (2019). Characteristics of microbial community indicate anthropogenic impact on the sediments along the Yangtze Estuary and its coastal area, China. *Sci. Total Environ.* 648, 306–314. doi: 10.1016/j.scitotenv.2018.08.162

Hall, M., and Beiko, R. G. (2018). "16S rRNA gene analysis with QIIME2," in *Microbiome Analysis*, eds R. Beiko, W. Hsiao, and J. Parkinson (Berlin: Springer), 113–129.

Han, J., Lu, Q., Zhou, L., Zhou, J., and Xiang, H. (2007). Molecular characterization of the phaEC Hm genes, required for biosynthesis of poly (3-hydroxybutyrate) in the extremely halophilic archaeon Haloarcula marismortui. *Appl. Environ. Microbiol.* 73, 6058–6065. doi: 10.1128/AEM.00953-07

He, H., Fu, L., Liu, Q., Fu, L., Bi, N., Yang, Z., et al. (2019). Community structure, abundance and potential functions of bacteria and archaea in the sansha yongle blue hole, xisha, south china sea. *Front. Microbiol.* 10:2404. doi: 10.3389/fmicb.2019.02404

Henriet, O., Fourmentin, J., Delince, B., and Mahillon, J. (2014). Exploring the diversity of extremely halophilic archaea in food-grade salts. *Int. J. Food Microbiol.* 191, 36–44. doi: 10.1016/j.ijfoodmicro.2014.08.019

Hu, Y., Bai, C., Cai, J., Dai, J., Shao, K., Tang, X., et al. (2018). Co-occurrence network reveals the higher fragmentation of the bacterial community in Kaidu River than its tributaries in Northwestern China. *Microbes Environ.* 33, 127–134. doi: 10.1264/jsme2.ME17170

Jia, H., Liu, G., Zhang, Y., and Zhang, R. (2001). The formation mechanism of the Hefei basin and its oil and gas exploration prospect. *Geol. Anhui* 11, 9–18.

Jones, R. T., Robeson, M. S., Lauber, C. L., Hamady, M., Knight, R., and Fierer, N. (2009). A comprehensive survey of soil acidobacterial diversity using pyrosequencing and clone library analyses. *ISME J.* 3, 442–453. doi: 10.1038/ismej.2008.127

Kalwasinska, A., Deja-Sikora, E., Burkowska-But, A., Szabo, A., Felfoldi, T., Kosobucki, P., et al. (2018). Changes in bacterial and archaeal communities during the concentration of brine at the graduation towers in Ciechocinek spa (Poland). *Extremophiles* 22, 233–246. doi: 10.1007/s00792-017-0992-5

Kalwasinska, A., Felfoldi, T., Szabo, A., Deja-Sikora, E., Kosobucki, P., and Walczak, M. (2017). Microbial communities associated with the anthropogenic, highly alkaline environment of a saline soda lime, Poland. *Antonie Van Leeuwenhoek* 110, 945–962. doi: 10.1007/s10482-017-0866-y

Khalid, F. E., Lim, Z. S., Sabri, S., Gomez-Fuentes, C., Zulkharnain, A., and Ahmad, S. A. (2021). Bioremediation of diesel contaminated marine water by bacteria: A review and bibliometric analysis. *J. Mar. Sci. Eng.* 9:155.

Kirkpatrick, L. A. (2015). *A Simple Guide to IBM SPSS Statistics-Version 23.0*. Boston, MA: Cengage Learning.

Kumar, S., Zhou, J., Li, M., Xiang, H., and Zhao, D. (2020). Insights into the metabolism pathway and functional genes of long-chain aliphatic alkane degradation in haloarchaea. *Extremophiles* 24, 475–483. doi: 10.1007/s00792-020-01167-z

Lane, D. (1991). "16S/23S rRNA sequencing," in *Nucleic Acid Techniques In Bacterial Systematics*, eds E. Stackebrandt and M. Goodfellow (New York, N: John Wiley and Sons), 115–175.

Li, Q., Zhang, B., Wang, L., and Ge, Q. (2017). Distribution and diversity of bacteria and fungi colonizing ancient Buddhist statues analyzed by high-throughput sequencing. *Int. Biodeterior. Biodegrad.* 117, 245–254. doi: 10.1371/journal.pone.0163287

Lizama, C., Monteoliva-Sánchez, M., Prado, B., Ramos-Cormenzana, A., Weckesser, J., and Campos, V. (2001). Taxonomic study of extreme halophilic archaea isolated from the "Salar de Atacama", Chile. *Syst. Appl. Microbiol.* 24, 464–474. doi: 10.1078/0723-2020-00053

Ma, Y., Zhang, H., Du, Y., Tian, T., Xiang, T., Liu, X., et al. (2015). The community distribution of bacteria and fungi on ancient wall paintings of the Mogao Grottoes. *Sci. Rep.* 5, 1–9. doi: 10.1038/srep07752

Mani, K., Salgaonkar, B. B., Das, D., and Bragança, J. M. (2012). Community solar salt production in Goa, India. *Aquat. Biosyst.* 8, 1–8.

Mani, K., Taib, N., Hugoni, M., Bronner, G., Bragança, J. M., and Debroas, D. (2020). Transient dynamics of archaea and bacteria in sediments and brine across a salinity gradient in a solar saltern of Goa, India. *Front. Microbiol.* 11:1891. doi: 10.3389/fmicb.2020.01891

Martin, M. (2011). Cutadapt removes adapter sequences from high-throughput sequencing reads. *EMBnet J.* 17, 10–12. doi: 10.1089/cmb.2017.0096

Mazière, C., Agogué, H., Cravo-Laureau, C., Cagnon, C., Lanneluc, I., Sablé, S., et al. (2021). New insights in bacterial and eukaryotic diversity of microbial mats inhabiting exploited and abandoned salterns at the Ré Island (France). *Microbiol. Res.* 252:126854. doi: 10.1016/j.micres.2021.126854

Naghoni, A., Emtiazi, G., Amoozegar, M. A., Cretoiu, M. S., Stal, L. J., Etemadifar, Z., et al. (2017). Microbial diversity in the hypersaline Lake Meyghan, Iran. *Sci. Rep.* 7:11522. doi: 10.1038/s41598-017-11585-3

Nan, L., Guo, Q., and Cao, S. (2020). Archaeal community diversity in different types of saline-alkali soil in arid regions of Northwest China. *J. Biosci. Bioeng.* 130, 382–389. doi: 10.1016/j.jbiosc.2020.06.001

Oren, A. (2002). Diversity of halophilic microorganisms: Environments, phylogeny, physiology, and applications. *J. Ind. Microbiol. Biotechnol.* 28, 56–63. doi: 10.1038/sj/jim/7000176

Oren, A. (2011). Thermodynamic limits to microbial life at high salt concentrations. *Environ. Microbiol.* 13, 1908–1923.

Perez-Fernandez, C. A., Iriarte, M., Rivera-Perez, J., Tremblay, R. L., and Toranzos, G. A. (2019). Microbiota dispersion in the Uyuni salt flat (Bolivia) as determined by community structure analyses. *Int. Microbiol.* 22, 325–336. doi: 10.1007/s10123-018-00052-2

Procópio, L. (2021). The oil spill and the use of chemical surfactant reduce microbial corrosion on API 5L steel buried in saline soil. *Environ. Sci. Pollut. Res.* 28, 26975–26989. doi: 10.1007/s11356-021-12544-2

Quast, C., Pruesse, E., Yilmaz, P., Gerken, J., Schweer, T., Yarza, P., et al. (2012). The SILVA ribosomal RNA gene database project: Improved data processing and web-based tools. *Nucleic Acids Res.* 41, D590–D596. doi: 10.1093/nar/gks1219

R Core Team (2013). *R: A Language And Environment For Statistical Computing*. Vienna: R Foundation for Statistical Computing.

Redweik, G. A., Kogut, M. H., Arsenault, R. J., and Mellata, M. (2020). Oral treatment with ileal spores triggers immunometabolic shifts in chicken gut. *Front. Vet. Sci.* 7:629. doi: 10.3389/fvets.2020.00629

Rohban, R., Amoozegar, M. A., and Ventosa, A. (2009). Screening and isolation of halophilic bacteria producing extracellular hydrolyses from Howz Soltan Lake, Iran. *J. Ind. Microbiol. Biotechnol.* 36, 333–340. doi: 10.1007/s10295-008-0500-0

Sáenz de Miera, L. E., Gutiérrez-González, J. J., Arroyo, P., Falagán, J., and Ansola, G. (2021). Prokaryotic community diversity in the sediments of saline lagoons and its resistance to seasonal disturbances by water level cycles. *J. Soils Sediments* 21, 3169–3184.

Satari, L., Guillen, A., Latorre-Perez, A., and Porcar, M. (2021). Beyond Archaea: The Table Salt Bacteriome. *Front. Microbiol.* 12:714110. doi: 10.3389/fmicb.2021.714110

Scoma, A., and Boon, N. (2016). Osmotic stress confers enhanced cell integrity to hydrostatic pressure but impairs growth in Alcanivorax borkumensis SK2. *Front. Microbiol.* 7:729. doi: 10.3389/fmicb.2016.00729

Sfanos, K., Harmody, D., Dang, P., Ledger, A., Pomponi, S., McCarthy, P., et al. (2005). A molecular systematic survey of cultured microbial associates of deep-water marine invertebrates. *Syst. Appl. Microbiol.* 28, 242–264. doi: 10.1016/j.syapm.2004.12.002

Shi, Y., Fan, K., Li, Y., Yang, T., He, J. S., and Chu, H. (2019). Archaea enhance the robustness of microbial co-occurrence networks in Tibetan Plateau soils. *Soil Sci. Soc. Am. J.* 83, 1093–1099.

Sonnenfeld, P., and Perthuisot, J.-P. (1984). *Brines And Evaporites*. Hoboken, NJ: Wiley.

Stackebrandt, E., and Goebel, B. M. (1994). Taxonomic note: A place for DNA-DNA reassociation and 16S rRNA sequence analysis in the present species definition in bacteriology. *Int. J. Syst. Bacteriol.* 44, 846–849.

Stevens, J. L., Jackson, R. L., and Olson, J. B. (2013). Slowing PCR ramp speed reduces chimera formation from environmental samples. *J. Microbiol. Methods* 93, 203–205. doi: 10.1016/j.mimet.2013.03.013

Triado-Margarit, X., Capitan, J. A., Menendez-Serra, M., Ortiz-Alvarez, R., Ontiveros, V. J., Casamayor, E. O., et al. (2019). A Randomized Trait Community Clustering approach to unveil consistent environmental thresholds in community assembly. *ISME J.* 13, 2681–2689. doi: 10.1038/s41396-019-0454-4

Vandamme, P., Pot, B., Gillis, M., De Vos, P., Kersters, K., and Swings, J. (1996). Polyphasic taxonomy, a consensus approach to bacterial systematics. *Microbiol. Rev.* 60, 407–438.

Wang, H., Gilbert, J. A., Zhu, Y., and Yang, X. (2018). Salinity is a key factor driving the nitrogen cycling in the mangrove sediment. *Sci. Total Environ.* 631-632, 1342–1349.

Wang, Q. (1999). Development of water-soluble-mining technology in China's salt industry. *China-Min. Mag.* 5, 36–41.

Wang, W., Zhong, R., Shan, D., and Shao, Z. (2014). Indigenous oil-degrading bacteria in crude oil-contaminated seawater of the Yellow sea, China. *Appl. Microbiol. Biotechnol.* 98, 7253–7269. doi: 10.1007/s00253-014-5817-1

Wong, H. L., Smith, D. L., Visscher, P. T., and Burns, B. P. (2015). Niche differentiation of bacterial communities at a millimeter scale in Shark Bay microbial mats. *Sci. Rep.* 5, 1–17. doi: 10.1038/srep15607

Xiao, W., Wang, Z. G., Wang, Y. X., Schneegurt, M. A., Li, Z. Y., Lai, Y. H., et al. (2013). Comparative molecular analysis of the prokaryotic diversity of two salt mine soils in southwest China. *J. Basic Microbiol.* 53, 942–952. doi: 10.1002/jobm.201200200

Zadjelovic, V., Chhun, A., Quareshy, M., Silvano, E., Hernandez-Fernaud, J. R., Aguilo-Ferretjans, M. M., et al. (2020). Beyond oil degradation: Enzymatic potential of Alcanivorax to degrade natural and synthetic polyesters. *Environ. Microbiol.* 22, 1356–1369. doi: 10.1111/1462-2920.14947

Zhang, Y. X., Li, X., Li, F. L., Ma, S. C., Zheng, G. D., Chen, W. F., et al. (2020). Paracoccus alkanivorans sp. nov., isolated from a deep well with oil reservoir water. *Int. J. Syst. Evol. Microbiol.* 70, 2312–2317. doi: 10.1099/ijsem.0.004036

Zhu, D., Han, R., Long, Q., Gao, X., Xing, J., Shen, G., et al. (2020). An evaluation of the core bacterial communities associated with hypersaline environments in the Qaidam Basin, China. *Arch. Microbiol.* 202, 2093–2103. doi: 10.1007/s00203-020-01927-7

Zhu, D., Shen, G., Wang, Z., Han, R., Long, Q., Gao, X., et al. (2021). Distinctive distributions of halophilic Archaea across hypersaline environments within the Qaidam Basin of China. *Arch. Microbiol.* 203, 2029–2042. doi: 10.1007/s00203-020-02181-7

frontiers | Frontiers in Microbiology

TYPE Original Research
PUBLISHED 10 November 2022
DOI 10.3389/fmicb.2022.1023575

OPEN ACCESS

EDITED BY
Sudhir K. Upadhyay,
Veer Bahadur Singh Purvanchal University, India

REVIEWED BY
Jamie Hinks,
Nanyang Technological University, Singapore
Ali Asger Bhojiya,
U.S. Ostwal Science, Arts & Commerce College, India

*CORRESPONDENCE
Paula J. Mouser
paula.Mouser@unh.edu

SPECIALTY SECTION
This article was submitted to Extreme Microbiology, a section of the journal Frontiers in Microbiology

RECEIVED 19 August 2022
ACCEPTED 17 October 2022
PUBLISHED 10 November 2022

CITATION
Ugwuodo CJ, Colosimo F, Adhikari J, Shen Y, Badireddy AR and Mouser PJ (2022) Salinity and hydraulic retention time induce membrane phospholipid acyl chain remodeling in *Halanaerobium congolense* WG10 and mixed cultures from hydraulically fractured shale wells. *Front. Microbiol.* 13:1023575. doi: 10.3389/fmicb.2022.1023575

Salinity and hydraulic retention time induce membrane phospholipid acyl chain remodeling in *Halanaerobium congolense* WG10 and mixed cultures from hydraulically fractured shale wells

Chika Jude Ugwuodo[1,2], Fabrizio Colosimo[3], Jishnu Adhikari[4], Yuxiang Shen[5], Appala Raju Badireddy[5] and Paula J. Mouser[2]*

[1]Natural Resources and Earth Systems Science, University of New Hampshire, Durham, NH, United States, [2]Department of Civil and Environmental Engineering, University of New Hampshire, Durham, NH, United States, [3]New England Biolabs, Ipswich, MA, United States, [4]Sanborn, Head and Associates, Inc., Concord, NH, United States, [5]Department of Civil and Environmental Engineering, University of Vermont, Burlington, VT, United States

Bacteria remodel their plasma membrane lipidome to maintain key biophysical attributes in response to ecological disturbances. For *Halanaerobium* and other anaerobic halotolerant taxa that persist in hydraulically fractured deep subsurface shale reservoirs, salinity, and hydraulic retention time (HRT) are important perturbants of cell membrane structure, yet their effects remain poorly understood. Membrane-linked activities underlie *in situ* microbial growth kinetics and physiologies which drive biogeochemical reactions in engineered subsurface systems. Hence, we used gas chromatography–mass spectrometry (GC–MS) to investigate the effects of salinity and HRT on the phospholipid fatty acid composition of *H. congolense* WG10 and mixed enrichment cultures from hydraulically fractured shale wells. We also coupled acyl chain remodeling to membrane mechanics by measuring bilayer elasticity using atomic force microscopy (AFM). For these experiments, cultures were grown in a chemostat vessel operated in continuous flow mode under strict anoxia and constant stirring. Our findings show that salinity and HRT induce significant changes in membrane fatty acid chemistry of *H. congolense* WG10 in distinct and complementary ways. Notably, under nonoptimal salt concentrations (7% and 20% NaCl), *H. congolense* WG10 elevates the portion of polyunsaturated fatty acids (PUFAs) in its membrane, and this results in an apparent increase in fluidity (homeoviscous adaptation principle) and thickness. Double bond index (DBI) and mean chain length (MCL) were used as proxies for membrane fluidity and thickness, respectively. These results provide new insight into our understanding of how environmental and engineered factors might disrupt the physical and biogeochemical equilibria of fractured shale by inducing physiologically relevant changes in the membrane fatty acid chemistry of persistent microbial taxa.

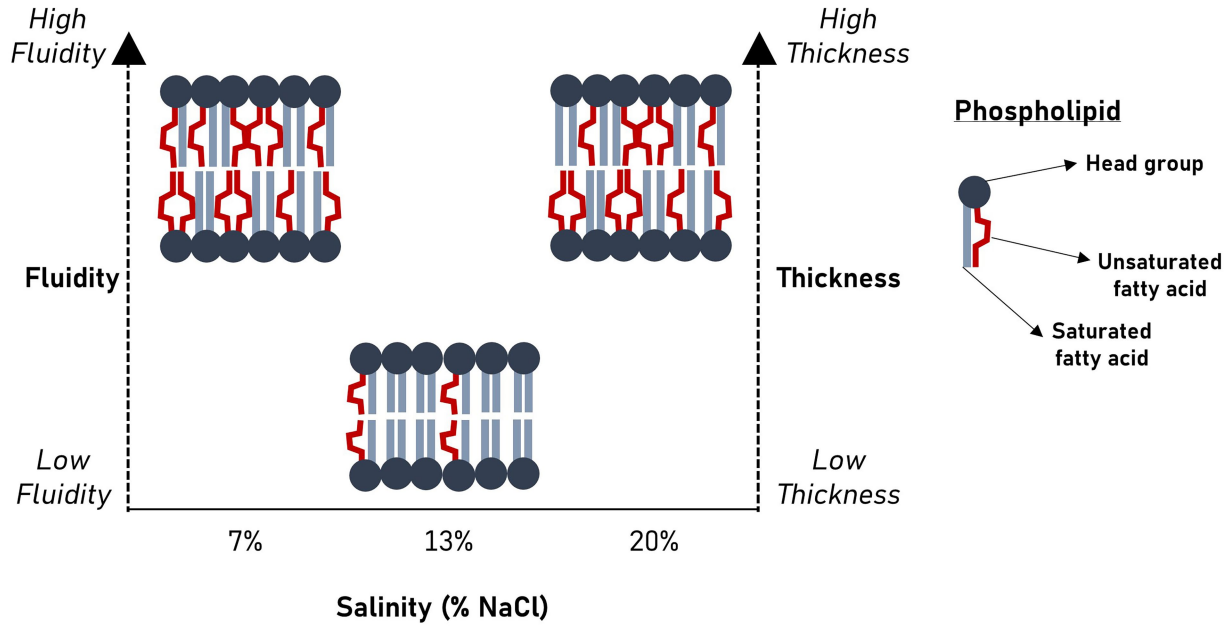

GRAPHICAL ABSTRACT
Salinity significantly alters membrane bilayer fluidity and thickness in *Halanaerobium congolense* WG10.

KEYWORDS

membrane adaptation, *Halanaerobium*, fractured shale, lipids, salinity, hydraulic retention time, fatty acid methyl ester

Introduction

Deep subsurface shale is increasingly being engineered in the United States (US EIA, 2020) and globally using horizontal drilling and hydraulic fracturing, to meet rising demands for energy. Shale reservoirs accounted for 79% of total dry natural gas production in the US in 2020 and are projected to continue to supply most of the dry natural gas through 2050 (US EIA, 2021). During hydraulic fracturing, a water-based "fracking" fluid is injected downhole to extend fracture networks on low-permeability subterranean formations (Stemple et al., 2021). Communities of microbes are introduced into engineered shale with prefracturing fluid, drilling mud, and impoundment water (Gaspar et al., 2014) where they colonize the reservoir (Cluff et al., 2014; Daly et al., 2016). Over time, they become major drivers of subsurface biogeochemistry, with negative consequences for efficient energy recovery and ecosystem health, including biofouling (Booker et al., 2017) and pore clogging (Jones et al., 2021). Fractured shale is a hostile and highly dynamic environment, characterized by a myriad of stressors including brine-level salinities. In addition, well flow rates vary, due to natural deterioration as well as seasonal controls. These unstable environmental and engineered conditions perturb the microbiome, necessitating adaptive changes including adjustments in plasma membrane features. Microbial activities in subsurface energy systems hamper natural gas production, which is a cleaner alternative to other fossil fuels such as coal (Hayhoe et al., 2002; Jaramillo et al., 2007; Burney, 2020). Therefore, to meet the United Nation's Sustainable Development Goal 7 – affordable and clean energy (Racioppi et al., 2020) – it is imperative to advance our understanding of how persistent taxa in underground hydrocarbon systems respond to ecosystem changes.

Hydraulic fracturing fluids have relatively low salt concentrations, typically <5,000 ppm total dissolved solids (Zeng et al., 2020). However, the salinity of flowback and produced water, which is co-collected with natural gas, ranges from 40,000 to 70,000 mg/L (Zolfaghari et al., 2016), and could be much higher depending on the geochemistry of the formation (Stewart et al., 2015). The high salinity of produced water derives from several geo-physicochemical mechanisms including mixing of fracturing fluids with formation brine (Rowan et al., 2015), and dissolution of salts and minerals on fractured surfaces (Ghanbari et al., 2013; Ghanbari and Dehghanpour, 2015). Members of halotolerant and thermotolerant bacterial and archaeal taxa including *Halanaerobium*, *Marinobacter*, *Methanohalophilus*,

Methanolobus, *Halomonadaceae* and *Halobacteroidaceae*, adapt to these subsurface conditions and dominate the fractured shale ecosystem (Daly et al., 2016). The genus *Halanaerobium* has been identified and recovered from several geographically and geologically distinct subsurface hydrocarbon reservoirs (Jones et al., 2021), indicating it is an important representative taxon in these systems for understanding microbial growth kinetics, roles in subsurface biogeochemistries and responses to physicochemical fluctuations.

Salinity is a topic of global interest (Upadhyay and Chauhan, 2022), transcending engineered subsurface hydrocarbon systems. Notably, salinity affects the productivity of agricultural soils (Singh et al., 2022), thus, threatens food security, which is a critical United Nation's Sustainable Development Goal (Upadhyay and Chauhan, 2022). Natural causes of soil salinization include mineral weathering, dissolution of fossil salts, rain deposition, and upwards migration of saline groundwater by capillary action (Das et al., 2020). Moreover, anthropogenic management practices especially irrigation, represent a significant source of inorganic salts to soils (Yu et al., 2021). Salinity levels beyond their tolerance thresholds challenge the viability and physiologies of plants and microorganisms, which dominate the biota of the soil matrix. Several studies have linked high salinity to reduced microbial diversity in forest, desert and agro-based systems (Rath et al., 2019; Zhang et al., 2019; Yu et al., 2021). In addition, the availability of micronutrients such as iron (Fe) to plants is impeded by high salt levels (Abbas et al., 2015; Singh et al., 2022). Therefore, salt tolerance is a highly desirable trait in microorganisms and plants in the face of increasing salinization and aridification of global soils. Halotolerant and halophilic species are able to sustain microbial functions and help plants acquire micronutrients whose availabilities are limited in salinity degraded soils (Abbas et al., 2015; Singh et al., 2022; Upadhyay et al., 2022).

The microbial plasma membrane protects the cell from external stressors and mediates critical physiologies, including transport, metabolism, signaling, aggregation and cell-surface interactions (Hurdle et al., 2011). In most microbes, it makes up the cell envelope alongside a peptidoglycan-based cell wall and in a few taxa, other structural layers such as the capsule. In Gram negative bacteria, a second membrane, regarded as the outer membrane (OM) which is rich in lipopolysaccharides, lies outside the thin sheet of peptidoglycan. Most archaea have a single membrane and are covered by a paracrystalline protein layer (Konings et al., 2002; Albers and Meyer, 2011). The plasma membrane is composed of lipids, proteins, and occasionally sugars. A unit membrane is basically a fluid matrix of lipids to which proteins are either attached loosely or enmeshed – the so called "fluid mosaic model" proposed by Singer and Nicolson (1972). The main constituents of the bacterial membrane lipidome are glycerophospholipids which comprise a hydrophilic polar head group covalently linked to hydrophobic fatty acid tails. Phospholipid fatty acids (PLFAs) differ in chain length, saturation, structural configuration, and functional groups. Membrane functions are associated with the activities of peripheral and integral proteins, which in turn depend on biophysical properties such as phase behavior, bilayer symmetry, viscosity, curvature, thickness and elasticity (Chwastek et al., 2020). To a large extent, these properties are collectively dictated by the bilayer lipidome (Klose et al., 2013).

Microorganisms remodel their membrane lipidome to maintain key biophysical properties (Klose et al., 2013; Levental et al., 2017; Chwastek et al., 2020) in response to external stressors. This involves reconfiguration and reorganization of head groups and/or hydrophobic tails. Both fluidity and phase behavior, are important for biological membrane function (Winnikoff et al., 2021). Fluidity affects permeability (Lande et al., 1995) and plays an important role in cellular respiration (Budin et al., 2018), while phase controls lipid raft (floating microdomain) formation (Simons and Vaz, 2004), as well as membrane fusion and budding (Siegel and Epand, 1997). Homeoviscous adaptation, the biochemical mechanism to maintain cell membrane viscosity, mainly depends on the nature of phospholipid fatty acids (Winnikoff et al., 2021). Induced changes in membrane fatty acid composition are common in microorganisms (Fan and Evans, 2015; Chwastek et al., 2020; Winnikoff et al., 2021), including subsurface-dwelling bacteria (Grossi et al., 2010; Fichtel et al., 2015; Roumagnac et al., 2020).

The membrane lipids of moderately and extremely halophilic bacteria are acutely sensitive to salinity (Kates, 1986). However, the effects of salt stress on biological membranes have not been studied as extensively as the effects of temperature and pressure. In halophilic phototrophic bacteria including *Ectothiorhodospira* sp., *Chromatium purpuratum*, *Rhodobacter adriaticus* and *Rhodopseudomonas marina*, salt-induced trends in membrane fatty acid composition were dependent on the optimum growth salinity (Imhoff and Thiemann, 1991). Suboptimal salt concentrations led to acyl chain shortening and increase in unsaturation (Imhoff and Thiemann, 1991). In other halotolerant bacteria, *Vibrio* sp. (Hanna et al., 1984) and *Planococcus* sp. (Miller and Leschine, 2005), proportions of branched chain fatty acids (BCFAs) and cyclic fatty acids increased with salt concentration. These adaptive strategies fluidize the membrane and depress its gel point (Kates, 1986; Winnikoff et al., 2021).

In addition to changes in salinity as the shale well develops, the flow rate of natural gas and produced water is subject to considerable temporal fluctuations. Naturally, constant production leads to an exponential decline in natural gas recovery. In addition, well flow rates are intentionally adjusted according to energy demands from consumers (Sherven et al., 2013). For instance, due to lower demands during warmer months, production of natural gas and co-eluting fluids are typically reduced by "turning back" the well. There is a relationship between well flow rate and fluid residence time in hydraulically fractured shale reservoirs, termed hydraulic retention time (HRT): HRT is increased by lower flows and vice versa. Fluid residence time, in the context of fractured subsurface systems and continuous culture reactors, can affect

microbial specific growth rate (Rodrigues et al., 2012) and biomass yields. However, the effects of HRT on biological membranes, especially in high salinity environments, remain largely unexplored.

For *Halanaerobium* and other persistent microbial taxa of fractured shale, salinity, and hydraulic retention time (HRT) are important perturbants of cell membrane structure. Hence, we investigated the effects of salinity and HRT on membrane fatty acid composition and elasticity of *Halanaerobium congolense* WG10 and mixed enrichment cultures from hydraulically fractured wells in West Virginia, United States. This study provides new insight into our growing understanding of how environmental and engineered factors might disrupt the physical and biogeochemical equilibria of fractured shale by inducing physiologically relevant changes in the membrane fatty acid chemistry of persistent microbial taxa.

Materials and methods

Growth experiments

Cultures of *Halanaerobium congolense* WG10 (NCBI Assembly accession number: GCA_900102605.1), previously isolated from a Utica-Point Pleasant natural gas well (Booker et al., 2017), were grown in triplicate using chemostat bioreactors (Sartorius Biostat® Q-plus, Germany) at 40°C under three salinities (7%, 13%, and 20%) and three hydraulic retention times (HRTs; 19.2, 24, and 48 h). Produced fluid samples were obtained from the gas-water separator of hydraulically fractured natural gas wells in the Appalachian Basin (Marcellus Shale Energy and Environmental Laboratory – MSEEL, Morgantown, WV). The fluids were filtered on site using 0.45 μm PES filters (EMD Millipore, Burlington, MA, United States) and stored in 1 L sterile amber glass containers. Samples were preserved at 4°C until analysis. Produced fluid enrichment (mixed) cultures were cultivated in triplicate at 40°C under two HRTs (24 h and 48 h). For both culture types: eight (8) days after steady state was attained, cells were pelleted *via* centrifugation at 4,000*g* for 30 min; excess supernatant was removed before storage at −80°C. Tubes containing frozen cells were recovered and left to thaw at room temperature in a laminar flow hood. Then the culture pellets were aseptically transferred to a 15 ml muffled glass tube.

Lipid extraction and fatty acid methylation

Samples were sequentially extracted ultrasonically according to a modified Bligh and Dyer procedure (Bligh and Dyer, 1959) using three solvent mixtures – dichloromethane (DCM): methanol (MeOH): phosphate buffer, 1:2:0.8 (v/v/v); DCM: MeOH: trichloroacetic acid (TCAA) buffer, 1:2:0.8 (v/v/v); and DCM: MeOH, 5:1 (v/v; Cequier-Sánchez et al., 2008). Phosphate buffer (0.05 M) was prepared by adding 4.35 g of dibasic potassium phosphate (K_2HPO_4) with 500 ml of HPLC-grade water and neutralizing to pH 7.4 with 1 N hydrochloric acid. Trichloroacetic acid buffer (0.05 M) was prepared by adding 0.8169 g of TCAA with 100 ml of HPLC-grade water and neutralized with 10 N sodium hydroxide (NaOH) solution to pH of 2.0. Both buffers were washed with DCM (5% of buffer volume) by shaking the mixture vigorously and storing for 5-h at room temperature to allow for complete phase separation.

Exactly 4 ml of DCM: MeOH: phosphate buffer was added to the 15 ml tubes containing culture pellets. To this mixture, 50 μl of 50 pmol per μl of internal standard 1,2-dinonadecanoyl-*sn*-glycero-3-phosphocholine (Avanti Polar Lipids) was added. The tube was shaken, vortexed for 15 s and sonicated in an ultrasonicator bath for 10 min. It was centrifuged for 10 min at 3000 rpm and the supernatant was transferred into a muffled 250 ml glass separatory funnel. This procedure was repeated once with DCM: MeOH: phosphate buffer, and the resulting supernatant was added to the same collecting funnel. The samples were then extracted twice each with DCM: MeOH: TCAA buffer and DCM: MeOH, following the same protocol. The separatory funnel containing the mixture of supernatants was shaken vigorously for 15 s and let to rest overnight to split phase. The organic phase was collected into another muffled separatory funnel, and the aqueous phase was re-extracted with DCM. The pool of organic phases was washed with HPLC-grade water and evaporated to near dryness with a high-purity nitrogen blowdown evaporator at 37°C. The resulting total lipid extract (TLE) was reconstituted with 1 ml of hexane and stored at −20°C until further use.

Total lipid extracts were sequentially fractionated on an activated silicic acid column into fractions of different polarities using hexane, chloroform, acetone, and methanol. The methanol fraction containing phospholipids was evaporated to dryness using a N_2 gas blowdown evaporator, then resuspended with 500 μl of methanol and 1 ml of methanolic potassium hydroxide. The mixture was vortexed for 30 s and incubated at 60°C for 30 min. After cooling, 2 ml of hexane was added prior to neutralization with 200 μl of 1 N acetic acid. Then, 2 ml of Milli-Q® nanopure distilled water was added to break phase. The samples were vortexed for 30 s and centrifuged for 5 min at 2,000 rpm to separate the phases. The upper (organic) phase was transferred to a muffled volatile organic carbon (VOC) vial and the lower phase was re-extracted with 2 ml of hexane. The solution containing fatty acid methyl ester (FAME) extracts was evaporated to dryness using a N_2 gas blowdown evaporator and redissolved in 300 μl of hexane. The hexane containing FAMEs was transferred to a GC vial and preserved at −20°C until analysis.

GC–MS analysis, lipid identification, and quantification

Aliquots (1 μl) of hexane containing FAMEs were analyzed using a Thermo Scientific Trace 1300 gas chromatograph (GC) coupled to a Thermo Scientific ISQ 7000 single quadrupole

mass spectrometer (MS). The chromatograph was equipped with a cyanopropylphenyl-based phase column (TRACE™ TR-FAME 30 m, 0.25 mm I.D. × 0.25 μm film thickness), specifically designed for the separation of FAMEs. The GC was programmed to run at 60°C for 2 min, then the temperature was increased at a rate of 10°C per min to 150°C; this was followed by a second ramp to 312°C, at 3°C per min. The final operating temperatures of the injector and detector were 230°C and 300°C, respectively.

FAMEs were identified and quantified using the following external standards (Matreya LLC, State College, Pennsylvania, United States): Bacterial Acid Methyl Ester CP Mixture (BacFAME [1114]), Polyunsaturated FAME Mixture 2 (PUFA-2 [1081]) and Polyunsaturated FAME Mixture 3 (PUFA-3 [1177]). These standards contained FAMEs ranging from 11 to 22 carbons in length and had representative saturates, monounsaturates and polyunsaturates. Identities of FAMEs were initially checked against the NIST17 mass spectral library and confirmed using matching external standards. To quantify FAMEs, each peak was integrated, and its area was compared to the external standard. For FAMEs without matching external standards, the response factor (RF) from the most structurally related FAME standard was used for quantitation (Lewe et al., 2021).

Calculation of double bond index and mean acyl chain length

Double bond index (DBI) reflects the degree of membrane phospholipid unsaturation and was calculated using the formula (Vornanen et al., 1999):

$$\frac{\sum(\text{number of double bonds in fatty acid})\times(\text{abundance (mol\%)})}{\sum\text{abundance (mol\%) of all fatty acids in the culture sample}}$$

Mean chain length (MCL) was calculated as (Vornanen et al., 1999):

$$\frac{\sum(\text{hydrocarbon chain length of fatty acid})\times(\text{abundance (mol\%)})}{\sum\text{abundance (mol\%) of all fatty acids in the culture sample}}$$

Atomic force microscopy

To determine membrane elasticity, cultures of *H. congolense* WG10 were fixed onto 0.2 μm polycarbonate membranes (Sterlitech, Kent, WA) by vacuum filtration at 40 psi. Force measurements were performed with MFP-3D-BIOTM Atomic Force Microscope in contact or tapping mode, with polystyrene particle (25 μm) probes with a spring constant of 165.00 pN/nm (Novascan, Boone, IA). A scan rate of 0.15 Hz and a force distance of 1.00 μm were applied. Force map was set at a scan size of 40.00 μm, a scan time of 3.705 min, over a region of four points by four points. Measurements were performed in triplicates, and the pixels related to bacteria were selected empirically based on the range of the elasticity.

Statistical analyses

Peak intensities were converted to molar concentrations using standard calibration curves, then normalized to percent abundance, sample-wise. All statistical analyses and graphing were done in the R environment version 4.1.2. Normality in data distribution was evaluated using Shapiro–Wilk test. To statistically compare two treatment groups, a two-tailed unpaired Student's *t*-test was performed. One-way analysis of variance (ANOVA) was applied to comparisons of multiple groups using a Tukey's honest significance test (HSD) post-hoc analysis. Variations were considered statistically significant at $p \leq 0.05$.

Results

Composition of fatty acid methyl esters

We determined relative molar abundances of individual fatty acid methyl esters (FAMEs) that underpin the structural effects of salinity and HRT on the membranes of these dominant shale taxa. Figure 1 shows that in pure cultures of *H. congolense* WG10 cultivated at 40°C under three salinities (7%, 13%, and 20%) and HRTs (19.2, 24, and 48 h), a total of 39 FAMEs were detected. Meanwhile, only 26 FAMEs were found in the produced fluid mixed culture samples enriched at the same temperature (40°C) under similar HRT gradients (24 and 48 h; Supplementary Table).

Among the 39 fatty acids found in *H. congolense* WG10 across treatment conditions, C14:0 had the highest overall mean abundance (~30%). Of the five fatty acid classes identified, saturated fatty acid (SFA) was the most abundant (~51%), followed by polyunsaturated fatty acid (PUFA; ~26%). For the mixed cultures, C13:0 had the highest overall mean abundance (~28%), and similar to *H. congolense* WG10, SFA was the dominant PLFA class (~68%).

Only nine (9) out of the 39 fatty acids in *H. congolense* WG10 varied significantly with salinity at constant temperature (40°C) and HRT (24 h). Their trends are shown in Figure 2. Among these, three monounsaturated FAMEs [C14:1ω5 ($p = 0.018$), C15:1ω5c ($p = 0.025$) and C16:1ω9c ($p = 0.023$)] significantly increased with salinity (Figures 2A–C). Two others, C17:0 ($p = 0.011$) and C20:4ω6 ($p = 0.047$), significantly progressively decreased as salinity increased (Figures 2D,H). The rest of the fatty acids that varied (C18:0, C18:1ω7c, C18:2ω4 and C22:4ω6c) showed a non-linear pattern of change with salinity – an increase in abundance with increase in salinity from 7% to 13% NaCl, followed by a decline as salinity

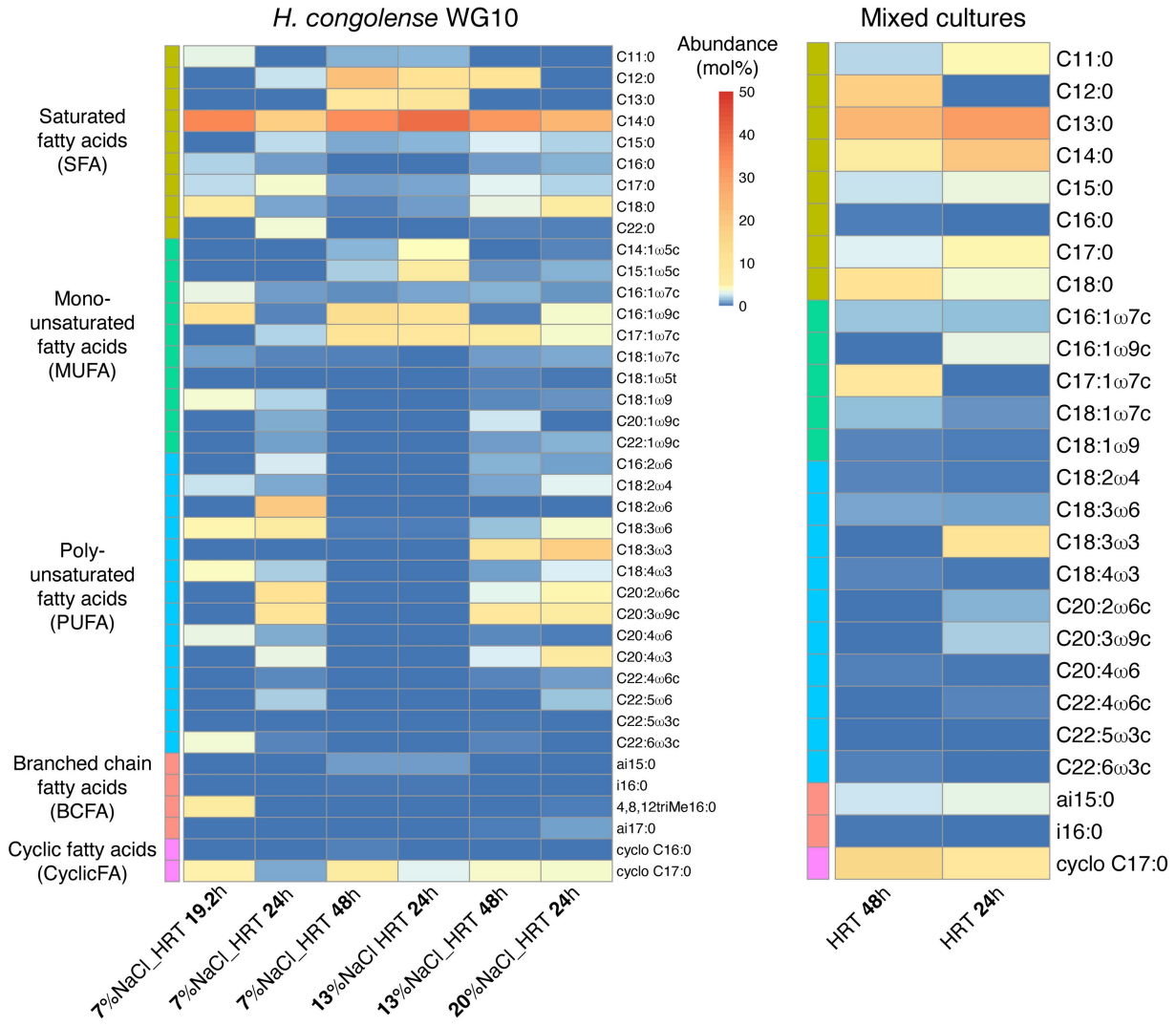

FIGURE 1
Heatmap distribution of individual phospholipid fatty acids in *Halanaerobium congolense* WG10 and fluid enrichment (mixed) cultures grown at 40°C under different salinities and HRTs. Fatty acids are sorted by class, then chain length and number of double bonds.

was further increased to 20% (Figures 2E–G,I). These results imply that unsaturated species are the centerpiece of salinity-induced adjustments to membrane fatty acid chemistry in *H. congolense* WG10. They also indicate complex metabolic exchanges among fatty acids, such as the probable oxidation and desaturation of C17:0 fatty acid to form shorter-chained monounsaturated moieties under increasing salinities.

None of the 39 fatty acids in *H. congolense* WG10 varied significantly with HRT at constant temperature (40°C) and salinity (13% NaCl). Moreover, only one fatty acid, C17:0, showed a significant variation with HRT in *H. congolense* WG10 grown at 40°C and 7% salinity (data not shown). None of the 26 fatty acids found in the mixed cultures varied significantly with HRT (data not shown). This suggests that HRT, which controls cellular growth rate and extent of exposure to toxic metabolic by-products in the reactor, co-ordinately rather than discretely modulates or very minimally influences the plasma membrane fatty acid composition of shale taxa.

Membrane unsaturation and thickness are increased in *Halanaerobium congolense* WG10 under nonoptimal salinities, but are variably affected by HRT

Figure 3 shows the effects of salinity and HRT on the mean chain length (MCL) and double bond index (DBI) of membrane phospholipids in *H. congolense* WG10. Both parameters varied significantly with salinity at constant growth temperature (40°C) and HRT (24 h; Figure 3A). As salinity increased from 7% to 13% NaCl, there was a significant decrease in both mean chain length

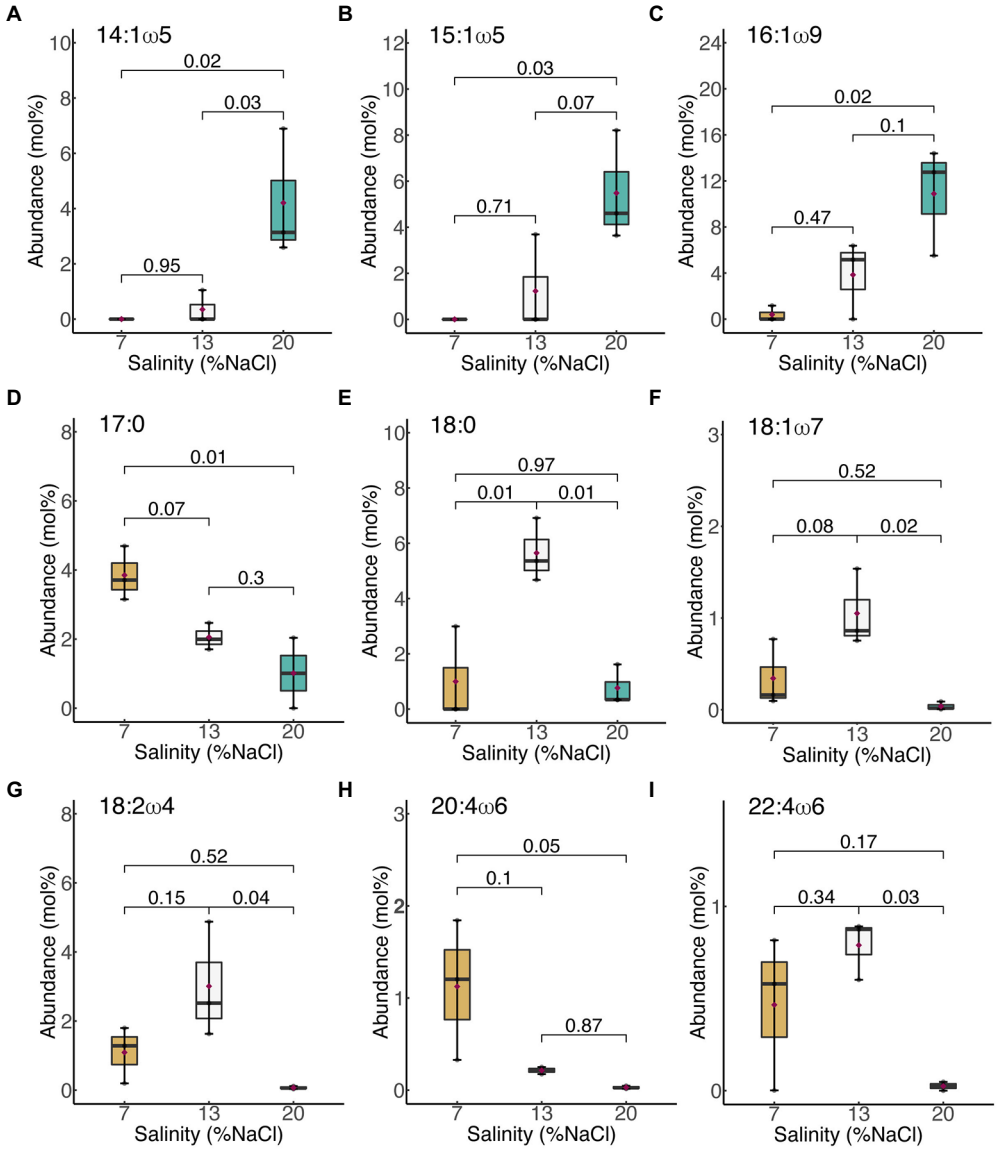

FIGURE 2
Membrane-derived fatty acids that significantly varied with salinity in *H. congolense* WG10. **(A)** 14:1ω5; **(B)** 15:1ω5c; **(C)** 16:1ω9c; **(D)** 17:0; **(E)** 18:0; **(F)** 18:1ω7c; **(G)** 18:2ω4; **(H)** 20:4ω6; **(I)** 22:4ω6c. Fatty acids are arranged by chain length then by number of double bonds. *p*-Values are obtained from one-way ANOVA of independent groups. Variation is considered significant at $\alpha \leq 0.05$.

($p = 0.0003$) and DBI ($p = 0.009$). However, a further increase in salt concentration from 13% to 20% produced the opposite effect, where both mean chain length and DBI increased. There was no significant difference in chain length or DBI between the two nonoptimal salinity conditions (7% and 20%). *Halanaerobium congolense* WG10 also adjusted the mean chain length and DBI of its membrane phospholipids in response to HRT at constant temperature (40°C) and salinity (7% or 13%). At 7%, MCL and DBI significantly decreased with HRT (Figure 3B), while at 13% salinity, *H. congolense* WG10 significantly increased the MCL and DBI of its membrane as HRT increased (Figure 3C). There was no significant variation in either MCL or DBI with HRT (24 versus 48 h) in the mixed cultures (Supplementary Figure S1).

SFAs and MUFAs in the plasma membrane of *Halanaerobium congolense* WG10 are exchanged for PUFAs under nonoptimal salinities

We examined the effects of salinity and HRT on the relative molar abundances of each of five major fatty acid classes: saturated, monounsaturated, polyunsaturated, branched chain and cyclic. As shown in Figure 4, a significant increase in the membrane saturated fatty acid (SFA; $p = 0.03$) content of *H. congolense* WG10 was observed when salinity was increased from 7% to 13% NaCl. This was accompanied by a more significant decline ($p = 0.006$) in the polyunsaturated fatty acid (PUFA)

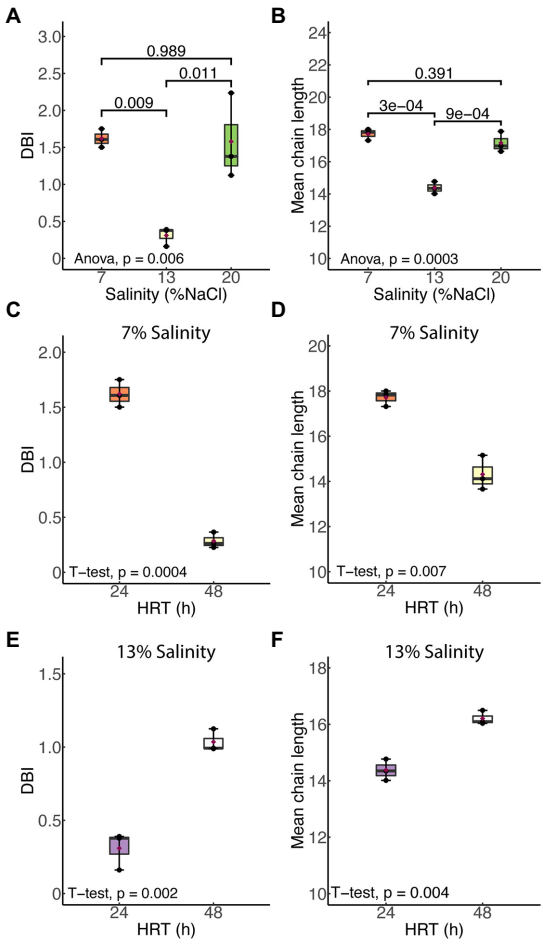

FIGURE 3
Mean chain length (MCL) and double bond index (DBI) of membrane phospholipids in *H. congolense* WG10 responded distinctly to salinity **(A,B)** and hydraulic retention time (HRT). The effect of HRT was evaluated at two discrete salinities – 7% **(C,D)** and 13% **(E,F)**. *p*-Values are obtained from one-way ANOVA of multiple independent groups or Student's *t*-test of two independent groups. Variation is considered statistically significant at $\alpha \leq 0.05$.

fraction. With a further increase in salinity from 13% to 20%, SFA significantly dropped ($p = 0.046$) while PUFA increased ($p = 0.017$). The membrane monounsaturated fatty acid (MUFA) composition of *H. congolense* WG10 varied similarly as the SFA fraction, except that its decline as salinity increased from 13% to 20% was not statistically significant. There was no significant variation in all three PLFA classes between 7% and 20% salinities. Changes in the molar abundances of branched chain fatty acids (BCFAs) and cyclic fatty acids, with salinity, were not statistically significant.

Membrane SFA and MUFA compositions of *H. congolense* WG10 grown at constant temperature (40°C) and salinity (7%), increased significantly as HRT was increased from 24 to 48 h. This was accompanied by a significant decline ($p = 0.016$) in the PUFA content (Figure 5A). Relative molar abundances of both BCFA and cyclic FA did not significantly vary with HRT (data not shown). In contrast, when grown at the same temperature and 13% NaCl, none of the membrane fatty acid classes in *H. congolense* WG10 varied significantly with HRT, except for PUFA whose abundance significantly increased as HRT was increased from 24 to 48 h (Figure 5B). For the mixed cultures, HRT did not produce significant variations in the molar abundances of any of the fatty acid classes (Supplementary Figure S2).

Membrane elasticity in *Halanaerobium congolense* WG10 does not significantly vary with salinity and HRT

To couple changes in fatty acid composition to a physiologically-relevant aspect of membrane mechanics, we measured the bilayer elasticity of *H. congolense* WG10 grown at 40°C under varying salnities (7%, 13%, and 20% NaCl) and hydraulic retention times (19.2, 24, and 48 h), using atomic force microscopy (data not shown). ANOVA revealed that neither salinity nor HRT induced significant changes in membrane elasticity. However, mean Young's Modulus (a measure of stiffness) at 13% salinity was considerably lower than at 7% and 20%, a similar pattern of variation with membrane polyunsaturated fatty acid composition, suggesting that PUFA modulates membrane elasitcity in *H. congolense* WG10.

Discussion

Salinity and hydraulic retention time influence membrane fatty acid chemistry in *Halanaerobium congolense* WG10

Our findings show that *Halanaerobium congolense* WG10 remodels its membrane fatty acid composition in response to variations in salinity and hydraulic retention time (HRT). To curtail the confounding effect of changes in the microbial lipidome due to growth phase progression (Berezhnoy et al., 2022) rather than induced by bioreactor growth conditions, we used a chemostat system for culture cultivation and harvested cells after they had attained steady state at which point, the specific growth rate is constant and equal to the dilution rate. Being a continuous culture system, cultures were sustained in a prolonged exponential growth phase until harvested at steady state. In general, salinity had a more pronounced and consistent impact than HRT. We used mean chain length (MCL) and double bond index (DBI; Figure 3) as proxies to quantify the effects of both perturbants on critical aspects of cell membrane structure and properties, in lieu of biophysical experimentation. DBI is a measure of degree of unsaturation and by implication bilayer viscosity/fluidity (Berezhnoy et al., 2022). Chain length, on the other hand, estimates membrane thickness. Fluidity and thickness affect the biological functions of the membrane. Salinity and HRT induced significant changes in membrane fatty acid composition of

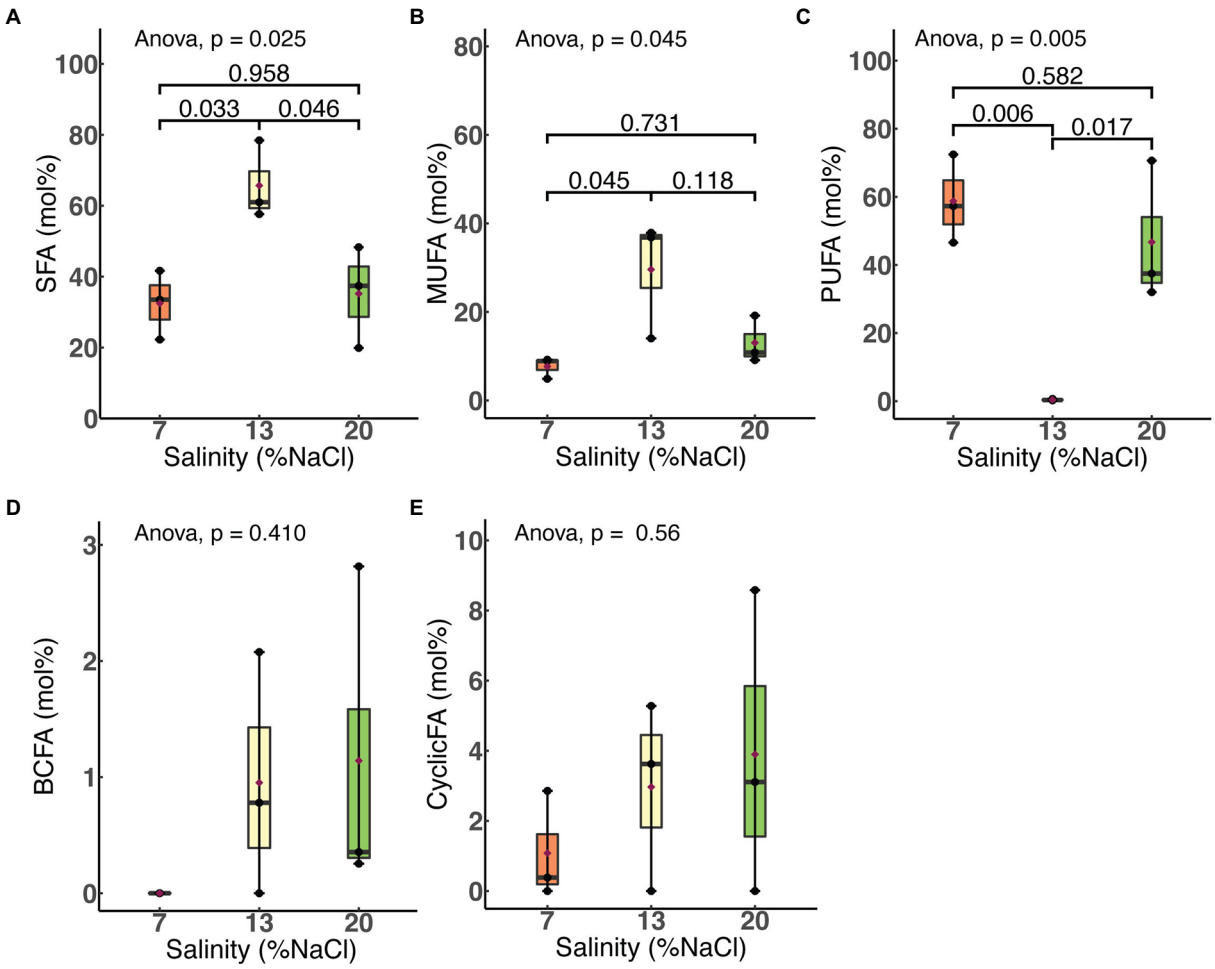

FIGURE 4
Variations in molar abundances of membrane phospholipid fatty acid classes in *H. congolense* WG10 with salinity at constant temperature (40°C) and HRT (24h). *p*-Values are obtained from one-way ANOVA of independent groups. Variation is considered significant at $\alpha \leq 0.05$. SFA, Saturated fatty acid; MUFA, Monounsaturated fatty acid; PUFA, Polyunsaturated fatty acid; BCFA, Branched chain fatty acid; CyclicFA, Cyclic fatty acid.

H. congolense WG10 which reflected on mean chain length and DBI. Accordingly, the membrane appeared to be thicker and more fluid under low (7% NaCl) and high salt stresses (20% NaCl), compared to optimal salinity (13% NaCl). Also, at optimal salinity, membrane thickness and fluidity increased with HRT. The specific growth rate of cultures in a chemostat is lower at higher HRT. Therefore, our fluidity trend observation contrasts in principle with the findings of a prior study which reported that saturated fatty acid (SFA)/double bond equivalent (DBE) ratio increased as the growth rates of two *E. coli* strains plateaued into the stationary phase (Berezhnoy et al., 2022). This indicates that, in the current study, because growth rate variations were domiciled within the prolonged log phase, membrane lipidome changes is due to other growth-related metabolic distresses rather than stationarity. Taken together, our findings imply that a thicker and fluidized membrane is essential to effective adaptation of *H. congolense* WG10 to osmotic and metabolic stresses. In contrast, membrane fatty acid composition of the mixed cultures of persistent shale taxa was not significantly altered by HRT (Supplementary Figures). It is rational to think that in general, shale microbial communities are better able to resist the impacts of ecological disturbances (external stressors) than isolated species, hence the minimal adaptive changes in membrane chemistry.

Thirty-nine (39) phospholipid fatty acids were found at variable abundances in *H. congolense* WG10 grown at 40°C under different salinities (7%, 13%, and 20%) and hydraulic retention times (19.2, 24, and 48 h; Figure 1). These fatty acids belong to five classes – saturated fatty acid (SFA), monounsaturated fatty acid (MUFA), polyunsaturated fatty acid (PUFA), branched chain fatty acid (BCFA) and cyclic fatty acid (CFA). The relatively low amounts of BCFAs and CFAs could be due to the maintenance of cultures in a prolonged exponential growth phase in the chemostats. Cyclopropanation has been reported to increase with growth progression in *E. coli* such that the lipidome is dominated by lipids with CFA chains during the late stationary phase (Berezhnoy et al., 2022). Only 26 of these 39 fatty

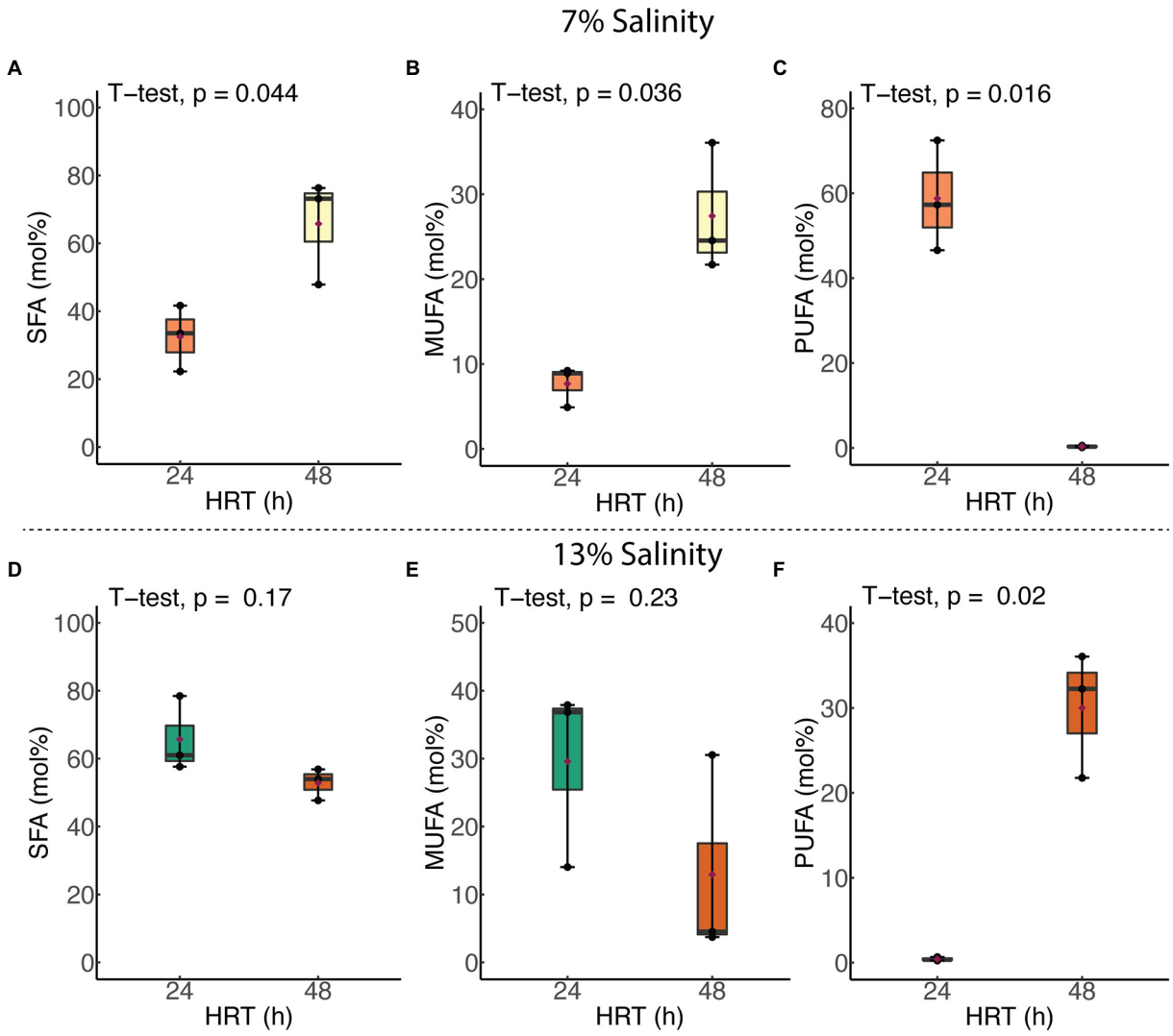

FIGURE 5
Variations in abundances of membrane PLFA classes in *H. congolense* WG10 with hydraulic retention time at constant temperature (40°C), evaluated at two different salinities – 7% **(A–C)** and 13% **(D–F)**. *p*-Values are obtained from student's *t*-test of independent groups. Variation is considered significant at $\alpha \leq 0.05$. SFA, Saturated fatty acid; MUFA, Monounsaturated fatty acid; PUFA, Polyunsaturated fatty acid.

acids were found in the mixed culture samples grown at 40°C under varying HRTs (24 and 48 h; Figure 1). We believe that the fatty acid compositional trends observed in these shale taxa are mainly driven by lipid metabolism as opposed to "diet." Metabolic pathways for fatty acid biosynthesis and post-synthetic modifications exist in bacteria and begin with the conversion of acetyl-CoA to malonyl-CoA (Cronan and Thomas, 2009). After malonyl-CoA condenses with an acyl carrier protein (ACP), the central pathway devolves into several branches that lead to the synthesis of major fatty acids. Fatty acid metabolism in all organisms is globally regulated at various genetic and metabolic levels (Fujita et al., 2007). Faced with changing subsurface conditions, *H. congolense* WG10 and other persistent shale taxa potentially deploy these regulatory mechanisms to modulate fatty acid composition, to maintain functionally-relevant biophysical properties of the plasma membrane.

Membrane polyunsaturated fatty acid (PUFA) composition did not correlate with salinity in *H. congolense* WG10 grown at 40°C and 24 h HRT. Bilayer PUFA abundance during growth at 13% NaCl was significantly lower than at 7% and 20% (Figure 4). Considering that 13% is the optimal growth salinity, this trend indicates that *H. congolense* WG10 adapts to low (7%) and high (20%) salt stress by increasing its membrane PUFA composition. Similarly, a halotolerant bacterium, *Rhodococcus erythropolis*, had significantly higher amounts of membrane derived PUFAs when grown under low (1%) and high (7.5%) osmotic stress, compared to growth at optimal salinity (2.5%; de Carvalho et al., 2014). The observation that none of the individual PUFAs which varied significantly with salinity in *H. congolense* WG10 (C18:2ω4, C20:4ω6, and C22:4ω6c) followed this trend (Figure 2) suggests that they

might be functionally interchangeable and regulated as a group rather than as discrete entities (Winnikoff et al., 2021).

Previously thought incapable (Okuyama et al., 2007), bacteria (especially halophiles and psychrophiles) are now well known to incorporate polyunsaturated fatty acids (PUFAs) into their membrane lipidome (Russel and Nichols, 1999; Nichols and McMeekin, 2002; Jadhav et al., 2010; de Carvalho et al., 2014; Moi et al., 2018). Accordingly, we found 14 PUFAs in *H. congolense* WG10 and 10 in the mixed cultures. Their chain lengths ranged from 18 to 22 and number of double bonds varied from 2 to 6. We believe functional metabolic pathways for *de novo* synthesis of PUFAs exist in these persistent shale taxa. Generally, there are two pathways for PUFA synthesis in bacteria – aerobic and anaerobic. The aerobic mechanism begins with a saturated fatty acid and involves repeating steps of desaturation and elongation (Zhu et al., 2006). On the other hand, the anaerobic pathway involves the actions of polyketide synthase (PKS)-related enzymes, also called PUFA synthases (Zhang et al., 2021). A combination of genetic and biochemical approaches is required to confirm the existence and operation of one or both pathways in *H. congolense* WG10. Meanwhile, an NCBI nucleotide search confirmed the presence of a regulator of polyketide synthase expression gene (GenBank: PUU90574.1) in a metagenome-assembled genome (MAG) belonging to *Halanaerobium* sp. isolated from a hydraulically fractured shale well, suggesting this pathway may exist in this genus.

Shale microbes may also possibly acquire exogenous polyunsaturated fatty acids (PUFAs) from their surroundings. This scavenging behavior is not unthinkable among microbes and have been reported in several bacterial species including halotolerant *Vibrio* (Smith et al., 2021), as well as *Pseudomonas*, *Acinetobacter*, *Escherichia and Klebsiella* (Eder et al., 2017; Moravec et al., 2017; Baker et al., 2018; Hobby et al., 2019; Herndon et al., 2020; Zang et al., 2021). In this hypothetical scenario, exogenous PUFAs would likely come from the oil and gas reservoirs. Organisms of the candidate phyla radiation (CPR) and DPANN radiation residing within the deep continental subsurface have been suggested to scavenge, use and modify molecular lipids from external sources (Probst et al., 2020).

The effects of HRT (24 and 48 h) on membrane PUFA composition of *H. congolense* WG10 is discriminated by salinity (Figure 5). When growing at 7% NaCl, total PUFA abundance declines significantly with HRT whereas at 13%, it increases with HRT. Hydraulic retention time (HRT) – the inverse of dilution rate – is a critical microbial growth parameter in continuous culture systems. At abnormally high HRT (in this case 48 h), the dilution rate likely falls below the bacterium's maximum specific growth rate, upsetting the exponential phase dynamics. Despite being a self-adjusting system, with longer medium residence time in the chemostat, there is substrate depletion and possibly accumulation of toxic metabolic by-products (Foustoukos and Pérez-Rodríguez, 2015). These conditions exert physiological stress on *H. congolense* WG10, prompting membrane acyl chain remodeling to achieve desired biophysical attributes of the bilayer. This translates to increasing membrane PUFA composition when growing at optimal salinity (13% NaCl), but the opposite when subjected to hypoosmotic stress (7% NaCl; Figure 5). We are not exactly sure why this discrepancy exists.

Like PUFA, membrane saturated fatty acid (SFA) and monounsaturated fatty acid (MUFA) compositions of *H. congolense* WG10 did not correlate with salinity at constant temperature (40°C) and HRT (24 h). However, unlike PUFA, molar abundances of SFA and MUFA at 13% NaCl were significantly higher than at 7% and 20% (Figure 4). This inverse relationship between PUFA and SFA/MUFA implies that when confronting low (7%) or high (20%) salt stress, *H. congolense* WG10 exchanges significant amounts of SFAs and MUFAs in its membrane lipidome with PUFAs. This exact same response was reported in the halotolerant bacteria, *Rhodococcus erythropolis* (de Carvalho et al., 2014). Similarly, in *H. congolense* WG10 growing at optimal salinity (13%), membrane PUFA composition was significantly increased under high HRT, even though concomitant reductions in the abundances of SFAs and MUFAs were not statistically significant (Figure 5B).

It is our hypothesis that, just like other bacteria (de Carvalho et al., 2014), *H. congolense* WG10 constitutively expresses desaturases and elongases, which are quickly activated when needed to convert saturated and monounsaturated fatty acids to polyunsaturated fatty acids. We believe that stearoyl-CoA desaturase plays a key role in membrane PUFA biosynthesis in *H. congolense* WG10 growing under salt-stressed conditions, based on the observation that out of the 7 SFAs and MUFAs that varied significantly with salinity (Figure 2), only C18 fatty acids – C18:0 and C18:1ω7c – were downregulated at 7% and 20% salinity compared to 13%. (Figure 2). Stearoyl-CoA desaturase introduces double bonds into C18 fatty acyl chains. Many marine bacteria express elongases and desaturases, including the soluble stearoyl-CoA desaturase and membrane-bound acyl-CoA desaturases (Moi et al., 2018; Berezhnoy et al., 2022).

Rationalizing membrane acyl chain remodeling in *Halanaerobium congolense* WG10

Now, we turn to common hypotheses of membrane lipidome remodeling to attempt a rationalization of the responses of *H. congolense* WG10 to changes in salinity and hydraulic retention time (HRT). Both factors are relevant for hydraulic fracturing of deep subsurface shale and appeared to exert selective forces on membrane fatty acid composition of *H. congolense* WG10. First, our findings seem to align with the homeoviscous principle, which argues that membrane lipidome remodeling is driven by the need to maintain fluidity within a narrow range (Sinensky, 1974; Ernst et al., 2016). We quantitatively estimated degree of unsaturation as double bond index (DBI). Higher DBI connotes higher unsaturation and by implication lower viscosity/higher fluidity (Berezhnoy et al., 2022). Due to kinks in their hydrocarbon chains caused by the presence of double bonds, unsaturated fatty acids pack at relatively low densities, hence, promote membrane transition to the disordered liquid-crystalline phase. As shown in Figure 3, *H. congolense* WG10 adapted

to low and high salt stress by further desaturating its membrane lipidome thereby increasing the fluidity of the bilayer matrix. This was also the response when the cells were challenged by an abnormally high hydraulic retention time (HRT) when growing at optimal temperature and salinity (Figure 3B). Fluidity determines ease of lateral diffusion of macromolecules in the bilayer matrix (Ballweg et al., 2020), and hence affects the spatial orientation, folding and functions of membrane proteins. Perhaps, *H. congolense* WG10 increases bilayer fluidity to spatially reorient thus functionalize or inhibit a cohort of membrane proteins such as sensors, kinases, channels, and transporters. Moreover, under high salinity stress, an increase in membrane fluidity might be necessary to counteract the gelation effect of monovalent cations (Russell, 1989; Seddon, 1990; Imhoff and Thiemann, 1991). However, the homeoviscous principle does not explain why *H. congolense* WG10 opted to increase membrane fluidity with polyunsaturated fatty acids (PUFAs) and not monounsaturated fatty acids. In fact, monounsaturation is sufficient for a bacterium to achieve its desired level of bilayer fluidity as introducing more than one double bond into a membrane fatty acid moiety exerts no additive effect on liquid-crystalline to gel transition (Russel and Nichols, 1999).

This gap in logic can be filled by the second hypothesis of membrane lipidome remodeling – the homeophasic principle. This principle holds that lipidome readjustment is geared toward controlling phase behavior (Linden et al., 1973). Membrane lipids can self-assemble into other supramolecular structures besides the bilayer, including micelles, cubic and hexagonal phases (Ernst et al., 2016). Predominance of non-bilayer phases negatively affects the biophysical properties and functions of the membrane (Russel and Nichols, 1999). While monounsaturated phospholipids favor the formation of non-bilayer phases, PUFAs allow just enough molecular motion to provide fluidity while preventing deleterious transition to inverted phases (Russel and Nichols, 1999). Therefore, it is apparent that *H. congolense* WG10 achieves sufficient fluidity while maintaining its bilayer structure under stress by increasing membrane PUFA composition.

Beyond regulating fluidity and phase behavior, PUFAs are known to alter other mechanical and biophysical properties of the membrane, including elasticity, thickness and curvature (Bruno et al., 2007). Membrane elasticity of *H. congolense* WG10, which we experimentally measured using atomic force microscopy (AFM), did not significantly vary with either HRT or salinity. On the other hand, we used mean phospholipid chain length as a quantitative estimate of bilayer thickness and found it to be significantly variant and positively correlated with membrane PUFA composition across gradients of salinity and hydraulic retention time (Figures 3–5). Hydrophobic thickness of bilayer membranes affects bending rigidity (Bermúdez et al., 2004), permeability (Discher et al., 1999) and elasticity (Bermudez et al., 2002). These properties, in turn, modulate the configuration and functions of membrane proteins including transporters and channels (Bruno et al., 2007). Hence, through several possible mechanistic and chemical processes, polyunsaturated fatty acids stabilize the bilayer membrane of *H. congolense* WG10 and endow it with biophysical attributes needed for adaptation to salinity-and HRT-induced perturbations. Differential gene expression analysis, proteomics and/or lipidomics investigations would shed more light on these underlying mechanisms.

Conclusion

For *H. congolense* WG10 which persists in hydraulically fractured shale wells, salinity and hydraulic retention time (HRT) significantly influence membrane fatty acid composition and mechanics, and therefore, alter bilayer biophysics. Under non-optimal salinities, *H. congolense* WG10 increases the fluidity and thickness of the plasma membrane by elevating its PUFA composition. On the other hand, the effects of HRT on membrane fatty acid chemistry in *H. congolense* is less pronounced and discriminated by salinity level. The functions of the membrane, which include transport, metabolism, respiration, and cell-surface interactions, rely on the maintenance of optimal biophysical states. This study has demonstrated, under a simulated laboratory setting, how salinity and well flow rates affect the plasma membrane fatty acid chemistry of persistent shale taxa. This fundamental mechanistic insight will underlie efforts toward advancing our understanding of how environmental and engineered factors influence the physical and biogeochemical equilibria of subsurface hydrocarbon systems by inducing physiologically relevant changes in membrane features of resident taxa.

Data availability statement

The original contributions presented in the study are included in the article/Supplementary material, further inquiries can be directed to the corresponding author.

Author contributions

PM conceived and designed the study. JA, FC, and CU conducted the laboratory experiments. CU and FC processed the raw MS data. AB and YS conducted the AFM studies and processed the data. CU performed the statistical analyses and wrote the first draft of the manuscript. CU and PM developed the manuscript figures. All authors revised, read, and approved the submitted version of the manuscript.

Funding

This work was funded by the U.S. Department of Energy, Office of Science, Office of Biological and Environmental Research (BER), and the Established Program to Stimulate Competitive Research (EPSCoR) (award number DESC0019444).

Acknowledgments

We are grateful to Jenna Luek for providing very helpful comments on data analysis and interpretation of results.

Conflict of interest

FC is currently employed by New England Biolabs, Ipswich, MA, United States. JA is employed by Sanborn, Head and Associates Inc., Concord, NH, United States.

The remaining authors declare that the research was conducted in the absence of any commercial or financial relationships that could be construed as a potential conflict of interest.

Publisher's note

All claims expressed in this article are solely those of the authors and do not necessarily represent those of their affiliated organizations, or those of the publisher, the editors and the reviewers. Any product that may be evaluated in this article, or claim that may be made by its manufacturer, is not guaranteed or endorsed by the publisher.

Supplementary material

The Supplementary material for this article can be found online at: https://www.frontiersin.org/articles/10.3389/fmicb.2022.1023575/full#supplementary-material

References

Abbas, G., Saqib, M., Akhtar, J., and Haq, M. A. (2015). Interactive effects of salinity and iron deficiency on different rice genotypes. *J. Plant Nutr. Soil Sci.* 178, 306–311. doi: 10.1002/jpln.201400358

Albers, S.-V., and Meyer, B. H. (2011). The archaeal cell envelope. *Nat. Rev. Microbiol.* 9, 414–426. doi: 10.1038/nrmicro2576

Baker, L. Y., Hobby, C. R., Siv, A. W., Bible, W. C., Glennon, M. S., Anderson, D. M., et al. (2018). Pseudomonas aeruginosa responds to exogenous polyunsaturated fatty acids (PUFAs) by modifying phospholipid composition, membrane permeability, and phenotypes associated with virulence. *BMC Microbiol.* 18:117. doi: 10.1186/s12866-018-1259-8

Ballweg, S., Sezgin, E., Doktorova, M., Covino, R., Reinhard, J., Wunnicke, D., et al. (2020). Regulation of lipid saturation without sensing membrane fluidity. *Nat. Commun.* 11:756. doi: 10.1038/s41467-020-14528-1

Berezhnoy, N. V., Cazenave-Gassiot, A., Gao, L., Foo, J. C., Ji, S., Regina, V. R., et al. (2022). Transient complexity of *E. coli* Lipidome is explained by fatty acyl synthesis and Cyclopropanation. *Meta* 12:784. doi: 10.3390/metabo12090784

Bermudez, H., Brannan, A. K., Hammer, D. A., Bates, F. S., and Discher, D. E. (2002). Molecular weight dependence of polymersome membrane structure, elasticity, and stability. *Macromolecules* 35, 8203–8208. doi: 10.1021/ma020669l

Bermúdez, H., Hammer, D. A., and Discher, D. E. (2004). Effect of bilayer thickness on membrane bending rigidity. *Langmuir* 20, 540–543. doi: 10.1021/la035497f

Bligh, E. G., and Dyer, W. J. (1959). A rapid method of total lipid extraction and purification. *Can. J. Biochem. Physiol.* 37, 911–917. doi: 10.1139/o59-099

Booker, A. E., Borton, M. A., Daly, R. A., Welch, S. A., Nicora, C. D., Hoyt, D. W., et al. (2017). Sulfide generation by dominant *Halanaerobium* microorganisms in hydraulically fractured shales. *mSphere* 2, e00257–e00217. doi: 10.1128/mSphereDirect.00257-17

Bruno, M. J., Koeppe, R. E., and Andersen, O. S. (2007). Docosahexaenoic acid alters bilayer elastic properties. *Proc. Natl. Acad. Sci. U. S. A.* 104, 9638–9643. doi: 10.1073/pnas.0701015104

Budin, I., de Rond, T., Chen, Y., Chan, L. J. G., Petzold, C. J., and Keasling, J. D. (2018). Viscous control of cellular respiration by membrane lipid composition. *Science* 362, 1186–1189. doi: 10.1126/science.aat7925

Burney, J. A. (2020). The downstream air pollution impacts of the transition from coal to natural gas in the United States. *Nat. Sustain.* 3, 152–160. doi: 10.1038/s41893-019-0453-5

Cequier-Sánchez, E., Rodríguez, C., Ravelo, A. G., and Zárate, R. (2008). Dichloromethane as a solvent for lipid extraction and assessment of lipid classes and fatty acids from samples of different natures. *J. Agric. Food Chem.* 56, 4297–4303. doi: 10.1021/jf073471e

Chwastek, G., Surma, M. A., Rizk, S., Grosser, D., Lavrynenko, O., Rucińska, M., et al. (2020). Principles of membrane adaptation revealed through environmentally induced bacterial Lipidome remodeling. *Cell Rep.* 32:108165. doi: 10.1016/j.celrep.2020.108165

Cluff, M. A., Hartsock, A., MacRae, J. D., Carter, K., and Mouser, P. J. (2014). Temporal changes in microbial ecology and geochemistry in produced water from hydraulically fractured Marcellus shale gas wells. *Environ. Sci. Technol.* 48, 6508–6517. doi: 10.1021/es501173p

Cronan, J. E., and Thomas, J. (2009). Bacterial fatty acid synthesis and its relationships with polyketide synthetic pathways. *Methods Enzymol.* 459, 395–433. doi: 10.1016/S0076-6879(09)04617-5

Daly, R. A., Borton, M. A., Wilkins, M. J., Hoyt, D. W., Kountz, D. J., Wolfe, R. A., et al. (2016). Microbial metabolisms in a 2.5-km-deep ecosystem created by hydraulic fracturing in shales. *Nat. Microbiol.* 1, 1–9. doi: 10.1038/nmicrobiol.2016.146

Das, R. S., Rahman, M., Sufian, N. P., Rahman, S. M. A., and Siddique, M. A. M. (2020). Assessment of soil salinity in the accreted and non-accreted land and its implication on the agricultural aspects of the Noakhali coastal region. *Bangladesh. Heliyon.* 6:e04926. doi: 10.1016/j.heliyon.2020.e04926

de Carvalho, C. C. C. R., Marques, M. P. C., Hachicho, N., and Heipieper, H. J. (2014). Rapid adaptation of Rhodococcus erythropolis cells to salt stress by synthesizing polyunsaturated fatty acids. *Appl. Microbiol. Biotechnol.* 98, 5599–5606. doi: 10.1007/s00253-014-5549-2

Discher, B. M., Won, Y. Y., Ege, D. S., Lee, J. C., Bates, F. S., Discher, D. E., et al. (1999). Polymersomes: tough vesicles made from diblock copolymers. *Science* 284, 1143–1146. doi: 10.1126/science.284.5417.1143

Eder, A. E., Munir, S. A., Hobby, C. R., Anderson, D. M., Herndon, J. L., Siv, A. W., et al. (2017). Exogenous polyunsaturated fatty acids (PUFAs) alter phospholipid composition, membrane permeability, biofilm formation and motility in *Acinetobacter baumannii*. *Microbiology* 163, 1626–1636. doi: 10.1099/mic.0.000556

Ernst, R., Ejsing, C. S., and Antonny, B. (2016). Homeoviscous adaptation and the regulation of membrane lipids. *J. Mol. Biol.* 428, 4776–4791. doi: 10.1016/j.jmb.2016.08.013

Fan, W., and Evans, R. M. (2015). Turning up the heat on membrane fluidity. *Cells* 161, 962–963. doi: 10.1016/j.cell.2015.04.046

Fichtel, K., Logemann, J., Fichtel, J., Rullkötter, J., Cypionka, H., and Engelen, B. (2015). Temperature and pressure adaptation of a sulfate reducer from the deep subsurface. *Front. Microbiol.* 6:1078. doi: 10.3389/fmicb.2015.01078

Foustoukos, D. I., and Pérez-Rodríguez, I. (2015). A continuous culture system for assessing microbial activities in the Piezosphere. *Appl. Environ. Microbiol.* 81, 6850–6856. doi: 10.1128/AEM.01215-15

Fujita, Y., Matsuoka, H., and Hirooka, K. (2007). Regulation of fatty acid metabolism in bacteria. *Mol. Microbiol.* 66, 829–839. doi: 10.1111/j.1365-2958.2007.05947.x

Gaspar, J., Mathieu, J., Yang, Y., Tomson, R., Leyris, J. D., Gregory, K. B., et al. (2014). Microbial dynamics and control in shale gas production. *Environ. Sci. Technol. Lett.* 1, 465–473. doi: 10.1021/ez5003242

Ghanbari, E., Abbasi, M. A., Dehghanpour, H., and Bearinger, D. (2013). "Flowback volumetric and chemical analysis for evaluating load recovery and its impact on early-time production." *SPE Unconventional Resources Conference Canada, Calgary, Alberta, Canada, November 2013.*

Ghanbari, E., and Dehghanpour, H. (2015). Impact of rock fabric on water imbibition and salt diffusion in gas shales. *Int. J. Coal Geol.* 138, 55–67. doi: 10.1016/j.coal.2014.11.003

Grossi, V., Yakimov, M. M., Al Ali, B., Tapilatu, Y., Cuny, P., Goutx, M., et al. (2010). Hydrostatic pressure affects membrane and storage lipid compositions of the piezotolerant hydrocarbon-degrading Marinobacter hydrocarbonoclasticus strain #5. *Environ. Microbiol.* 12, 2020–2033. doi: 10.1111/j.1462-2920.2010.02213.x

Hanna, K., Bengis-Garber, C., Kushner, D. J., Kogut, M., and Kates, M. (1984). The effect of salt concentration on the phospholipid and fatty acid composition of the moderate halophile vibrio costicola. *Can. J. Microbiol.* 30, 669–675. doi: 10.1139/m84-100

Hayhoe, K., Kheshgi, H. S., Jain, A. K., and Wuebbles, D. J. (2002). Substitution of natural gas for Coal: climatic effects of utility sector emissions. *Clim. Chang.* 54, 107–139. doi: 10.1023/A:1015737505552

Herndon, J. L., Peters, R. E., Hofer, R. N., Simmons, T. B., Symes, S. J., and Giles, D. K. (2020). Exogenous polyunsaturated fatty acids (PUFAs) promote changes in growth, phospholipid composition, membrane permeability and virulence phenotypes in *Escherichia coli*. *BMC Microbiol.* 20:305. doi: 10.1186/s12866-020-01988-0

Hobby, C. R., Herndon, J. L., Morrow, C. A., Peters, R. E., Symes, S. J. K., and Giles, D. K. (2019). Exogenous fatty acids alter phospholipid composition, membrane permeability, capacity for biofilm formation, and antimicrobial peptide susceptibility in *Klebsiella pneumoniae*. *MicrobiologyOpen* 8:e00635. doi: 10.1002/mbo3.635

Hurdle, J. G., O'Neill, A. J., Chopra, I., and Lee, R. E. (2011). Targeting bacterial membrane function: an underexploited mechanism for treating persistent infections. *Nat. Rev. Microbiol.* 9, 62–75. doi: 10.1038/nrmicro2474

Imhoff, J. F., and Thiemann, B. (1991). Influence of salt concentration and temperature on the fatty acid compositions of Ectothiorhodospira and other halophilic phototrophic purple bacteria. *Arch. Microbiol.* 156, 370–375. doi: 10.1007/BF00248713

Jadhav, V. V., Jamle, M. M., Pawar, P. D., Devare, M. N., and Bhadekar, R. K. (2010). Fatty acid profiles of PUFA producing Antarctic bacteria: correlation with RAPD analysis. *Ann. Microbiol.* 60, 693–699. doi: 10.1007/s13213-010-0114-4

Jaramillo, P., Griffin, W. M., and Matthews, H. S. (2007). Comparative life-cycle air emissions of coal, domestic natural gas, LNG, and SNG for electricity generation. *Environ. Sci. Technol.* 41, 6290–6296. doi: 10.1021/es063031o

Jones, A. A., Pilloni, G., Claypool, J. T., Paiva, A. R., and Summers, Z. M. (2021). Evidence of sporulation capability of the ubiquitous oil reservoir microbe *Halanaerobium congolense*. *Geomicrobiol J.* 38, 283–293. doi: 10.1080/01490451.2020.1842944

Kates, M. (1986). Influence of salt concentration on membrane lipids of halophilic bacteria. *FEMS Microbiol. Rev.* 39, 95–101. doi: 10.1111/j.1574-6968.1986.tb01848.x

Klose, C., Surma, M. A., and Simons, K. (2013). Organellar lipidomics--background and perspectives. *Curr. Opin. Cell Biol.* 25, 406–413. doi: 10.1016/j.ceb.2013.03.005

Konings, W. N., Albers, S.-V., Koning, S., and Driessen, A. J. M. (2002). The cell membrane plays a crucial role in survival of bacteria and archaea in extreme environments. *Antonie Van Leeuwenhoek* 81, 61–72. doi: 10.1023/A:1020573408652

Lande, M. B., Donovan, J. M., and Zeidel, M. L. (1995). The relationship between membrane fluidity and permeabilities to water, solutes, ammonia, and protons. *J. Gen. Physiol.* 106, 67–84. doi: 10.1085/jgp.106.1.67

Levental, K. R., Surma, M. A., Skinkle, A. D., Lorent, J. H., Zhou, Y., Klose, C., et al. (2017). ω-3 polyunsaturated fatty acids direct differentiation of the membrane phenotype in mesenchymal stem cells to potentiate osteogenesis. *Sci. Adv.* 3:eaao1193. doi: 10.1126/sciadv.aao1193

Lewe, N., Hermans, S., Lear, G., Kelly, L. T., Thomson-Laing, G., Weisbrod, B., et al. (2021). Phospholipid fatty acid (PLFA) analysis as a tool to estimate absolute abundances from compositional 16S rRNA bacterial metabarcoding data. *J. Microbiol. Methods* 188:106271. doi: 10.1016/j.mimet.2021.106271

Linden, C. D., Wright, K. L., McConnell, H. M., and Fox, C. F. (1973). Lateral phase separations in membrane lipids and the mechanism of sugar transport in Escherichia coli. *Proc. Natl. Acad. Sci. U. S. A.* 70, 2271–2275. doi: 10.1073/pnas.70.8.2271

Miller, K., and Leschine, S. (2005). A halotolerantPlanococcus from Antarctic Dry Valley soil. *Curr. Microbiol.* 11, 205–209. doi: 10.1007/BF01567161

Moi, I. M., Leow, A. T. C., Ali, M. S. M., Rahman, R. N. Z. R. A., Salleh, A. B., and Sabri, S. (2018). Polyunsaturated fatty acids in marine bacteria and strategies to enhance their production. *Appl. Microbiol. Biotechnol.* 102, 5811–5826. doi: 10.1007/s00253-018-9063-9

Moravec, A. R., Siv, A. W., Hobby, C. R., Lindsay, E. N., Norbash, L. V., Shults, D. J., et al. (2017). Exogenous polyunsaturated fatty acids impact membrane remodeling and affect virulence phenotypes among pathogenic vibrio species. *Appl. Environ. Microbiol.* 83, e01415–e01417. doi: 10.1128/AEM.01415-17

Nichols, D. S., and McMeekin, T. A. (2002). Biomarker techniques to screen for bacteria that produce polyunsaturated fatty acids. *J. Microbiol. Methods* 48, 161–170. doi: 10.1016/S0167-7012(01)00320-7

Okuyama, H., Orikasa, Y., Nishida, T., Watanabe, K., and Morita, N. (2007). Bacterial genes responsible for the biosynthesis of Eicosapentaenoic and docosahexaenoic acids and their heterologous expression. *Appl. Environ. Microbiol.* 73, 665–670. doi: 10.1128/AEM.02270-06

Probst, A. J., Elling, F. J., Castelle, C. J., Zhu, Q., Elvert, M., Birarda, G., et al. (2020). Lipid analysis of CO2-rich subsurface aquifers suggests an autotrophy-based deep biosphere with lysolipids enriched in CPR bacteria. *ISME J.* 14, 1547–1560. doi: 10.1038/s41396-020-0624-4

Racioppi, F., Martuzzi, M., Matić, S., Braubach, M., Morris, G., Krzyżanowski, M., et al. (2020). Reaching the sustainable development goals through healthy environments: are we on track? *Eur. J. Pub. Health* 30, i14–i18. doi: 10.1093/eurpub/ckaa028

Rath, K. M., Fierer, N., Murphy, D. V., and Rousk, J. (2019). Linking bacterial community composition to soil salinity along environmental gradients. *ISME J.* 13, 836–846. doi: 10.1038/s41396-018-0313-8

Rodrigues, M. E., Costa, A. R., Henriques, M., Azeredo, J., and Oliveira, R. (2012). Wave characterization for mammalian cell culture: residence time distribution. *New Biotechnol.* 29, 402–408. doi: 10.1016/j.nbt.2011.10.006

Roumagnac, M., Pradel, N., Bartoli, M., Garel, M., Jones, A. A., Armougom, F., et al. (2020). Responses to the hydrostatic pressure of surface and subsurface strains of Pseudothermotoga elfii revealing the Piezophilic nature of the strain originating from an oil-producing well. *Front. Microbiol.* 11:588771. doi: 10.3389/fmicb.2020.588771

Rowan, E. L., Engle, M. A., Kraemer, T. F., Schroeder, K. T., Hammack, R. W., and Doughten, M. W. (2015). Geochemical and isotopic evolution of water produced from middle Devonian Marcellus shale gas wells, Appalachian basin, Pennsylvania. *AAPG Bull.* 99, 181–206. doi: 10.1306/07071413146

Russel, N. J., and Nichols, D. S. (1999). Polyunsaturated fatty acids in marine bacteria – a dogma rewritten. *Microbiology* 145, 767–779. doi: 10.1099/13500872-145-4-767

Russell, N. J. (1989). Adaptive modifications in membranes of halotolerant and halophilic microorganisms. *J. Bioenerg. Biomembr.* 21, 93–113. doi: 10.1007/BF00762214

Seddon, J. M. (1990). Structure of the inverted hexagonal (HII) phase, and non-lamellar phase transitions of lipids. *Biochim. Biophys. Acta* 1031, 1–69. doi: 10.1016/0304-4157(90)90002-t

Sherven, B., Mudry, D., and Majek, A. (2013). Automation maximizes performance for shale wells. *Oil Gas J.* 111, 1–4.

Siegel, D. P., and Epand, R. M. (1997). The mechanism of lamellar-to-inverted hexagonal phase transitions in phosphatidylethanolamine: implications for membrane fusion mechanisms. *Biophys. J.* 73, 3089–3111. doi: 10.1016/S0006-3495(97)78336-X

Simons, K., and Vaz, W. L. C. (2004). Model systems, lipid rafts, and cell membranes. *Annu. Rev. Biophys. Biomol. Struct.* 33, 269–295. doi: 10.1146/annurev.biophys.32.110601.141803

Sinensky, M. (1974). Homeoviscous adaptation–a homeostatic process that regulates the viscosity of membrane lipids in Escherichia coli. *Proc. Natl. Acad. Sci. U. S. A.* 71, 522–525. doi: 10.1073/pnas.71.2.522

Singer, S. J., and Nicolson, G. L. (1972). The fluid mosaic model of the structure of cell membranes. *Science* 175, 720–731. doi: 10.1126/science.175.4023.720

Singh, P., Chauhan, P. K., Upadhyay, S. K., Singh, R. K., Dwivedi, P., Wang, J., et al. (2022). Mechanistic insights and potential use of Siderophores producing microbes in rhizosphere for mitigation of stress in plants grown in degraded land. *Front. Microbiol.* 13:898979. doi: 10.3389/fmicb.2022.898979

Smith, D. S., Houck, C., Lee, A., Simmons, T. B., Chester, O. N., Esdaile, A., et al. (2021). Polyunsaturated fatty acids cause physiological and behavioral changes in vibrio alginolyticus and Vibrio fischeri. *MicrobiologyOpen* 10:e1237. doi: 10.1002/mbo3.1237

Stemple, B., Tinker, K., Sarkar, P., Miller, J., Gulliver, D., and Bibby, K. (2021). Biogeochemistry of the Antrim shale natural gas reservoir. *ACS Earth Space Chem.* 5, 1752–1761. doi: 10.1021/acsearthspacechem.1c00087

Stewart, B. W., Chapman, E. C., Capo, R. C., Johnson, J. D., Graney, J. R., Kirby, C. S., et al. (2015). Origin of brines, salts and carbonate from shales of the Marcellus formation: evidence from geochemical and Sr isotope study of sequentially extracted fluids. *Appl. Geochem.* 60, 78–88. doi: 10.1016/j.apgeochem.2015.01.004

Upadhyay, S. K., and Chauhan, P. K. (2022). Optimization of eco-friendly amendments as sustainable asset for salt-tolerant plant growth-promoting bacteria mediated maize (Zea Mays L.) plant growth, Na uptake reduction and saline soil restoration. *Environ. Res.* 211:113081. doi: 10.1016/j.envres.2022.113081

Upadhyay, S. K., Srivastava, A. K., Rajput, V. D., Chauhan, P. K., Bhojiya, A. A., Jain, D., et al. (2022). Root exudates: mechanistic insight of plant growth promoting Rhizobacteria for sustainable crop production. *Front. Microbiol.* 13:916488. doi: 10.3389/fmicb.2022.916488

US EIA (2020). US oil and gas Wells by production rate – U.S. Energy Information Administration (EIA). Available at: https://www.eia.gov/petroleum/wells/index.php (Accessed October 14, 2021).

US EIA (2021). Annual Energy Outlook 2021. Available at: https://www.eia.gov/outlooks/aeo/ (Accessed December 24, 2021).

Vornanen, M., Tiitu, V., Käkelä, R., and Aho, E. (1999). Effects of thermal acclimation on the relaxation system of crucian carp white myotomal muscle. *J. Exp. Zool.* 284, 241–251. doi: 10.1002/(SICI)1097-010X(19990801)284:3<241::AID-JEZ1>3.0.CO;2-G

Winnikoff, J. R., Haddock, S. H. D., and Budin, I. (2021). Depth-and temperature-specific fatty acid adaptations in ctenophores from extreme habitats. *J. Exp. Biol.* 224:jeb242800. doi: 10.1242/jeb.242800

Yu, X., Jin, Z., and Wang, H. (2021). Effect of saline water for drip irrigation on microbial diversity and on fertility of Aeolian Sandy soils. *Diversity* 13:379. doi: 10.3390/d13080379

Zang, M., MacDermott-Opeskin, H., Adams, F. G., Naidu, V., Waters, J. K., Carey, A. B., et al. (2021). The membrane composition defines the spatial organization and function of a major *Acinetobacter baumannii* drug efflux system. *MBio* 12, e01070–e01021. doi: 10.1128/mBio.01070-21

Zeng, L., Reid, N., Lu, Y., Hossain, M. M., Saeedi, A., and Xie, Q. (2020). Effect of the fluid–shale interaction on salinity: implications for high-salinity Flowback water during hydraulic fracturing in shales. *Energy Fuel* 34, 3031–3040. doi: 10.1021/acs.energyfuels.9b04311

Zhang, K., Shi, Y., Cui, X., Yue, P., Li, K., Liu, X., et al. (2019). Salinity is a key determinant for soil microbial communities in a desert ecosystem. *mSystems* 4, e00225–e00218. doi: 10.1128/mSystems.00225-18

Zhang, M., Zhang, H., Li, Q., Gao, Y., Guo, L., He, L., et al. (2021). Structural insights into the *trans-acting* Enoyl reductase in the biosynthesis of long-chain polyunsaturated fatty acids in *Shewanella piezotolerans*. *J. Agric. Food Chem.* 69, 2316–2324. doi: 10.1021/acs.jafc.0c07386

Zhu, K., Choi, K.-H., Schweizer, H. P., Rock, C. O., and Zhang, Y.-M. (2006). Two aerobic pathways for the formation of unsaturated fatty acids in Pseudomonas aeruginosa. *Mol. Microbiol.* 60, 260–273. doi: 10.1111/j.1365-2958.2006.05088.x

Zolfaghari, A., Dehghanpour, H., Noel, M., and Bearinger, D. (2016). Laboratory and field analysis of flowback water from gas shales. *J. Unconv. Oil Gas Resour.* 14, 113–127. doi: 10.1016/j.juogr.2016.03.004

frontiers | Frontiers in Microbiology

TYPE Original Research
PUBLISHED 23 November 2022
DOI 10.3389/fmicb.2022.1059347

OPEN ACCESS

EDITED BY
Rosa María Martínez-Espinosa,
University of Alicante, Spain

REVIEWED BY
Vikram Hiren Raval,
Gujarat University, India
Heng-Lin Cui,
Jiangsu University, China

*CORRESPONDENCE
Dimitry Y. Sorokin
soroc@inmi.ru;
d.sorokin@tudelft.nl

SPECIALTY SECTION
This article was submitted to Extreme Microbiology, a section of the journal Frontiers in Microbiology

RECEIVED 01 October 2022
ACCEPTED 07 November 2022
PUBLISHED 23 November 2022

CITATION
Sorokin DY, Elcheninov AG, Khijniak TV, Kolganova TV and Kublanov IV (2022) Selective enrichment on a wide polysaccharide spectrum allowed isolation of novel metabolic and taxonomic groups of haloarchaea from hypersaline lakes.
Front. Microbiol. 13:1059347.
doi: 10.3389/fmicb.2022.1059347

Selective enrichment on a wide polysaccharide spectrum allowed isolation of novel metabolic and taxonomic groups of haloarchaea from hypersaline lakes

Dimitry Y. Sorokin[1,2]*, Alexander G. Elcheninov[1], Tatiana V. Khijniak[1], Tatiana V. Kolganova[3] and Ilya V. Kublanov[1,4]

[1]Winogradsky Institute of Microbiology, Federal Research Centre of Biotechnology, Russian Academy of Sciences, Moscow, Russia, [2]Department of Biotechnology, Delft University of Technology, Delft, Netherlands, [3]Institute of Bioengineering, Federal Research Centre of Biotechnology, Russian Academy of Sciences, Moscow, Russia, [4]Faculty of Biology, Lomonosov Moscow State University, Moscow, Russia

Extremely halophilic archaea (haloarchaea) of the class *Halobacteria* is a dominant group of aerobic heterotrophic prokaryotic communities in salt-saturated habitats, such as salt lakes and solar salterns. Most of the pure cultures of haloarchaea were enriched, isolated, and cultivated on rich soluble substrates such as amino acids, peptides or simple sugars. So far, the evidences on the capability of haloarchaea to use different polysaccharides as growth substrates remained scarce. However, it is becoming increasingly obvious that these archaea can also actively participate in mineralization of complex biopolymers, in particular cellulose and chitin–two dominant biomass polysaccharides on the planet. Here we used an array of commercially available homo- and heteropolysaccharides to enrich hydrolytic haloarchaea from hypersaline salt lakes with neutral pH and from alkaline soda lakes. This resulted in isolation of a range of halo- and natrono-archaea, respectively, belonging to already described taxa as well as several new genus-level lineages. In some cases, the isolates enriched with different polysaccharides happened to be closely related, thus representing generalistic ecotype, while the others were narrow specialists. In general, soda lakes yielded a broader range of polysaccharide-utilizing specialists in comparison to neutral salt lakes. The results demonstrated a significant diversity of halo(natrono)archaea with a previously unrecognized potential for utilization of a broad range of natural polysaccharides in hypersaline habitats.

KEYWORDS

halo(natrono)archaea, hypersaline lakes, soda lakes, polysaccharides, hydrolytic

Introduction

Hypersaline lakes and solar salterns at its final evaporation stage represent unique salt-saturated habitats dominated by extremely halophilic microbial communities among which the extremely halophilic archaea of the class *Halobacteria* is the particularly successful group (Cui and Dyall-Smith, 2021). These archaea (at least those known in culture) are mostly aerobic organoheterotrophs, utilizing simple soluble organic compounds, such as amino acids and sugars (Andrei et al., 2012; Oren, 2013, 2015; Grant and Jones, 2016). Haloarchaea typically have very high cell density that gives the characteristic reddish color to hypersaline brines in intracontinental athalassic lakes and thalassic endeavaporite pools of the marine solar salt concentrators. Only handful of cultivated haloarchaeal species can grow with polymeric substances, such as starch, proteins or olive oil (Bhatnagar et al., 2005; Enache and Kamekura, 2010; Moshfegh et al., 2013; Selim et al., 2014; Amoozegar et al., 2017). Recently, this spectrum has been expanded by recalcitrant insoluble polysaccharides, such as cellulose and chitin as well as some other partially soluble polysaccharides, such as galactomannan and xylan. Utilization of native insoluble forms of cellulose has recently been shown for the neutrophilic genera *Halococcoides*, *Halomicrobium*, and *Halosimplex* (Sorokin et al., 2015, 2019a, 2020a) and for two genera of natronoarchaea from soda lakes–*Natronolimnobius* and *Natronobiforma* (Sorokin et al., 2015, 2018, 2019b). The ability to use chitin as the growth substrate has been proven for the neutrophilic genera *Halomicrobium* and *Salinarchaeum* and for the natronoarchael genus *Natrarchaeobius* (Sorokin et al., 2015, 2019c, 2020b; Minegishi et al., 2017). Finally, growth with locust bean galacto-beta-1,4-mannan was shown for the neutrophilic genera *Natronoarchaeum* and *Haloarcula* (Shimane et al., 2010; Enomoto et al., 2020).

The potential of haloarchaea to utilize various recalcitrant polysaccharides produced mostly by plants and algae is of significant interest both for fundamental understanding of their functional importance for the organic matter mineralization in hypersaline environments and also by regarding them as a source of extremely halo(alkali)stable extracellular hydrolases which have important application potential in production of biofuel from lignocellulosic wastes because this process often starts with a decrystallization pretreatment step, performed either with alkali or ionic liquids (Kaar and Holtzapple, 2000; Zavrel et al., 2010; Begemann et al., 2011).

In this work, the search for polysaccharide-utilizing haloarchaea was extended beyond the most abundant cellulose and chitin. For this, a range of commercially available polysaccharides of plant and microbial origin was used for selective enrichment and further isolation in pure cultures of halo(natrono)archaea able to utilize these polymers as growth substrate. The *de novo* sequenced genomes of these strains allowed to establish their phylogenies as well as to detect the genes, encoding enzymes responsible for their polysacharidolytic capacities. The results demonstrated significant diversity of polysaccharide-specialized haloarchaea belonging to already described genera and species (mostly for salt lakes) and several new genera (mostly among natronoarchaea), all of which have enzymatic repertoire sufficient for decomposition of the respective polysaccharides.

Experimental procedures

Samples

Sediment (top 3 cm) and brine samples were obtained from five hypersaline chloride-sulfate lakes with neutral pH in Kulunda Steppe (Altai, Russia) and from hypersaline alkaline (soda) lakes in Kulunda Steppe (three lakes), northeastern Mongolia (two lakes) and North America (California, two lakes) (Sorokin et al., 2015). Two "master mixes," one for each type of lakes, were created by mixing equal parts of sediments and brines from each lake and used at 5% (v/v) for primary enrichments.

Enrichment and growth conditions

The neutrophilic haloarchaea originated from salt lakes were enriched, purified and further cultivated in a neutral base medium 1 with the following composition (g l^{-1}): 230 NaCl, 5 KCl, 0.2 NH_4Cl, 2.5 K_2HPO_4, pH 6.8. After sterilization, the base was supplemented with vitamin and trace metal mix (Pfennig and Lippert, 1966) (1 ml l^{-1} each) and 2 mM $MgSO_4$. For the soda lake enrichments and further cultivation of alkaliphilic natronoarchaea, a sodium carbonate/bicarbonate-based medium 2 containing 4 M total Na^+ [(g l^{-1}): 190 Na_2CO_3, 30 $NaHCO_3$, 16 NaCl, 5 KCl and 1 K_2HPO_4, final pH 10 after sterilization] was supplemented with the same additions as for the medium 1, except that the amount of Mg was two times lower and that 4 mM NH_4Cl was added after sterilization. This alkaline medium was mixed 1:3 with the neutral medium 1, resulting in the final pH of 9.6.

Polysaccharides (Sigma-Aldrich and Megazyme; **Supplementary Table 1**) were either added from suspensions in sterile distilled water (when heat sterilization was not possible) or from 5% heat-sterilized (110°C for 20 min) stocks to a final concentration of 0.5 g l^{-1}. At the stage of initial enrichments and further 1:100 transfers, a mixture of streptomycin and kanamycin (final concentration 100 mg l^{-1}) was added to suppress bacterial development. Cultivation was performed in 30 ml bottles sealed with gray-rubber septa (to prevent evaporation) containing 10 ml medium at 35°C on a rotary shaker at 150 rpm. Solid media were prepared by 3:2 (v:v)

mixing of the fully prepared liquid media with 4% washed agar at 50°C. Solid NaCl was added to the portions of liquid media before heating to bring the salinity back to 4 M of total Na^+ after agar addition. For isolation of pure cultures, the initial positive enrichments were passed 2 times into new media containing target polysaccharides at 1:100 dilution to obtain sediment-free cultures, followed with dilution to extinction series and finally plating the maximal positive dilutions onto solid media with the same composition. The dominant colony types or those showed visible signs of polymer degradation (where possible) were picked up with sterile Pasteur capillary with pooled tips under control of binocular and placed into liquid media. Only those cultures which showed vigorous growth in liquid media were further purified by repeating the colony formation procedure. The purity of isolates were confirmed by microscopy, 16S-rRNA gene sequencing (Sanger and amplicon profiling) and in several cases by full genome sequencing.

Polysaccharide utilization activity

The main indication of polysaccharide utilization was consistent microbial growth in liquid culture whereby the polysaccharide in question served as the sole carbon and energy source. In addition, whenever it was possible, the hydrolytic activities of spot-colonies were also visualized on agar plates, either by formation of clearance zones (amorphous cellulose, beta-mannan) or reagent-developed hydrolysis zone: Lugol solution for starch, pullulan and pectin and Congo Red/1 M NaCl for xylan, xyloglucan, arabonoxylan, and glucomannan.

Genomic sequencing and phylogenetic analysis

Genomic DNA isolation, DNA library preparation, sequencing as well as genome assembly were performed as described earlier (Sorokin et al., 2022a).

Phylogenomic analysis based on the "ar122" set of conserved single copy archaeal proteins (Rinke et al., 2021) was performed as follows: the protein sequences were identified and aligned in *in silico* proteomes of the type species of all genera within *Halobacteria* class (non-type species were taken for *Halalkalicoccus* and *Natronoarchaeum* genera because the genomes of the type species were not available) using the GTDB-tk v.1.7.0 with reference data v.202 (Chaumeil et al., 2019). The maximum likelihood tree was inferred using the RAxML v.8.2.12 (Stamatakis, 2014) with the PROTGAMMAILG model of amino acid substitution; support values were calculated from the 1000 rapid bootstrap replications. The phylogenetic tree was polished using iTOL v.6.5.8 (Letunic and Bork, 2019).

Genome analysis

The genomes were annotated with NCBI Prokaryotic Genome Annotation Pipeline (Tatusova et al., 2016). Carbohydrate-active enzymes (CAZymes) including glycosidases, polysaccharide lyases, carbohydrate esterases, glycosyl transferases, and carbohydrate oxidases genes were predicted using dbCAN2 script v2.0.11 (Zhang et al., 2018) with HMMER v3.3 (Mistry et al., 2013) with default thresholds. The most probable activities of identified CAZymes (excluding glycosyl transferases, for which the manual verification of the predictions was not performed) were predicted using BLAST search against Swiss-Prot database (Boutet et al., 2016).

Genbank accession numbers

The 16S rRNA gene sequences generated in this study were deposited in the GenBank under accession numbers ON787970-ON788000. The whole genome sequence are available in GenBank under the following accession numbers: JAOPJY000000000, JAOPJZ000000000, JAOPKA000000000, JAOPKB000000000, JAOPKC000000000, JAOPKD000000000, and JAOPKE000000000.

Results

Polysaccharide-utilizing haloarchaea from hypersaline lakes with neutral pH

Positive enrichment cultures from salt lakes were obtained with 13 out of 18 polysaccharide compounds tested. The fastest development (maximal growth yield was achieved after 1 week) was observed with starch-like compounds (amylopectin, pullulan, and glycogen), while the slowest (up to a month)–with insoluble beta-linked polysaccharides (beta-mannan and curdlan). Other positive cultures showed growth in between 2 and 3 weeks. All positive primary enrichments were transferred into a sediment-free stage after 2–3 consecutive 1:100 (v:v) transfers on the same synthetic medium and acquired pink coloration with a domination of polymorphic flat cells characteristic of haloarchaea accompanied by visible degradation of substrates in case of insoluble polysaccharides. Further dilutions to extinction were performed without antibiotics and were generally positive up to 10^{-8}–10^{-9}. Final purification was achieved by isolation of individual colonies on solid media. Pure cultures of polysacharidolytic haloarchaea were obtained from those colony morphotype(s) (not always dominant ones) which consistently grew back in liquid medium with the target polysaccharide used in the enrichment. The list of isolates is given in **Table 1**.

All isolates selected on alpha-bonded polysaccharides belonged to the well-characterized genera of haloarchaea, for some of which utilization of starch is known. However, to our knowledge, the capacity to utilize arabinan and arabinoxylan has never been shown/tested for any cultivated species of haloarchaea. This is also true for *Halorhabdus tiamateia*, a broadly-specialized polysaccharidolytic haloarchaeon, according to our current results (**Table 1**) and previous studies (Wainø and Ingvorsen, 2003; Werner et al., 2014). However, its ability to grow on levan (beta-fructan) was not known before. Isolates belonging to the genus *Natronoarchaeum* were second after *Halorhabdus* by the number of isolated strains and were selected with four polysaccharides, including pullulan, beta-galactan, galactomannan, and curdlan. While utilization of galactomannan has already been reported for *N. mannanilyticum* (Shimane et al., 2010), growth with beta-1,4-galactan and beta-1,3-glucans, such as curdlan, have never been observed in any pure cultures of haloarchaea. Same is true for other two beta-1,4-bonded polysaccharides, including xyloglucan and beta-mannan. Looking from the taxonomical perspective, only two insoluble polysaccharides, mannan (consisted of beta-1,4-linked mannose) and curdlan (consisted of beta-1,3-linked glucose) (**Table 1**) resulted in selection of new genus-level isolates from the neutral salt lakes.

The cross-specificity for various polysaccharides supporting growth of the neutrophilic haloarchaea selected with a single polymer is shown in **Figure 1**. All five species enriched on alpha-glucans utilized soluble starch and five out of the six alpha-glucan specialists also grew with arabinoxylan which has alpha-bonded arabinose residues in the side chains. In

TABLE 1 Polysaccharide-utilizing neutrophilic haloarchaea enriched and isolated from hypersaline salt lakes with neutral pH.

Polysaccharide	Isolates	Identification by 16S rRNA gene sequence		Spectrum of utilized polysaccharides	
		Closest cultured relative	% identity	Stable growth in liquid culture	Colony activity (zone of hydrolysis, mm/2–3 weeks)
Alpha-glucans					
Amylopectin	HArc-St	*Natrinema salaciae*	99	Amp/Sst/Glc/Arx	nd/41/nd
Pullulan	HArc-pul1	*Haloferax alexandrinus*	100	Pul/Sst/Arx	30/20/nd
	HArc-pul2	*Natronoarchaeum rubrum*	99	Pul/Sst/Arx/Gtm/Glt/Crd	45/50/nd
Glycogen	HArc-glc1	*Halorubrum alkalophilum*	99	Glc/Sst	nd/22
	HArc-glc2	*"Halobacterium hubeiense"*	99	Glc/Sst/Arx	nd/15
Arabinan	HArc-arb1-5	*"Halobacterium hubeiense"*	99	Arb/Arx/Xyl	nd/40/20
Dextran	No isolates; not utilized by any isolates				
Beta-fructans					
Levan	HArc-lev	*Halorhabdus tiamatea*	99	Lev/Sst/Arx/Pul/Xyl	nd/23
Inulin	No isolates; not utilized by any isolates				
Beta-bonded polysaccharides					
Pectic galactan	HArc-glct1	*Natronoarchaeum rubrum*	99	Glt/Pul/Sst/Arx/Pul/Xyl	20/30/10/20/20/30
Beta-mannan	**HArc-m1***	*Halovarius/Haloterrigena*	**94–95**	Man/Gcm/Arx/Xyl/Xgl/Ac	20/20/30/30/nd/32/15
Glucomannan	HArc-gm1/3/4	*Halorhabdus tiamatea*	99	Pul/Sst/Arx/Xyl	30/40/30/30
	HArc-gm2	*Halomicrobium zhouii*	99	Gcm/Man/Arx/Xyl/Ac/Lam/Bgl	20/8/40/30/7/nd/nd
Galactomannan	HArc-glctm2	*Haloarcula hispanica*	97.3	Gtm/Glt/Pul/Sst	nd/nd/18/12
	HArc-glctm4	*Natronoarchaeum rubrum*	99		
Xylan	HArc-x1/2	*Halorubrum tebenquichense*	100	Xyl/Arx	30/22
Xyloglucan	HArc-xlg1	*Halorhabdus tiamatea*	99.8	Xgl/Arx/Xyl	nd/25/10
Arabinoxylan	HArc-ax1/3	*Halorhabdus tiamatea*	99.7	Pul/Sst/Arx/Xyl	27/34/25/32
Curdlan	HArc-curdl1	*Haloferax sulfurifontis*	97.6	Crd/Pch/Lam/Pul(w)	nd
	HArc-curdl4	*Natronoarchaeum rubrum*	99	Crd/Pch/Lam/Pul(w)	nd/nd/nd/16
	HArc-curdl5-1	*Halapricum salinarum*	**95**	Crd/Pch/Lam/Sst(w)/Inl/Glc	nd
Arabinogalactan	No isolates; not utilized by any isolates				
Alginate					
Pectin					

Polysaccharides: Sst, soluble starch; Glc, glycogen; Pul, pullulan; Lev, levan; Inl, inulin; Amp, amylopectin; Arb, arabinan; Arx, arabinoxylan; Gcm, glucomannan; Gtm, galactomannan; Glt, galactan; Xyl, xylan; Xlg, xyloglucan; Ac, amorphous cellulose; Lam, laminarin; Crd, curdlan; Pch, pachyman; Blg, Barley glucan; nd, test is not possible; potential new genera are in bold. *This isolate was similar to AArc-m2/3/4 isolated on mannan from soda lakes (see **Table 2**).

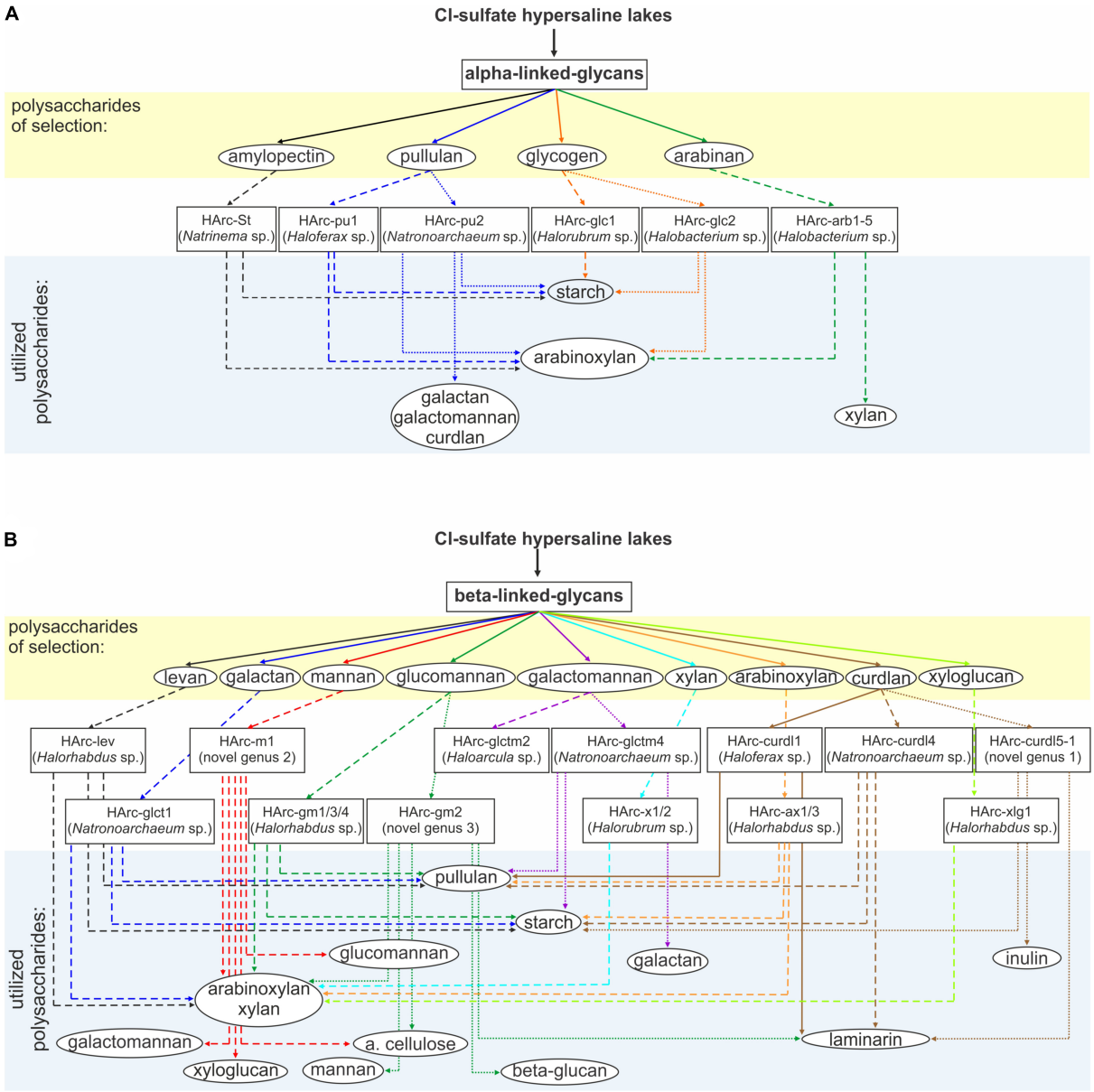

FIGURE 1
Schematic representation of selective enrichments of haloarchaea from hypersaline salt lakes on **(A)** alpha-bonded and **(B)** beta-bonded polysaccharides. Assignment to the novel genus was based on protein sequence-based phylogenomic analysis and 16S rRNA gene sequence identity values.

turn, a single case of cross-specificity was also observed in *Halobacterium* strains which were selected with both glycogen (HArc-glc2) and arabinan (HArc-arb1-5) (Figure 1A).

Among the haloarchaeal strains selected with various beta-bonded polysaccharides the most common cross-substrates were xylan and arabinoxylan, while alpha-glucans (starch and pullulan) were only utilized by a few beta-glucan specialists (Figure 1B). Two out of the three isolates enriched with either mannan (HArc-m1) or glucomannan (HArc-gm2) were able to grow with amorphous cellulose indicating related selectivity of these beta-1,4 backbone polysaccharides. The *Halomicrobium* strain HArc-gm2 selected with glucomannan was identical in its 16S rRNA gene sequence to *Halomicrobium* sp. HArcel3–the cellulose-enriched haloarchaeon most closely related to *H. zhouii* (Sorokin et al., 2015). We tested the type strain *H. zhouii* JCM 17095 and it appeared to be able to grow with amorphous cellulose as well.

Strain HArc-m1 was identical (according to the 16S rRNA gene sequence analysis) to several natronoarchaeal isolates enriched from soda lakes with beta-1,4 mannan

backbone polysaccharides (see below) confirming a link between the cellulose and the beta-mannan selectivity. This pattern has already been observed in cellulotrophic *Natronobiforma cellulositropha* which was enriched on cellulose but can also grow with beta-mannan (Sorokin et al., 2018). Furthermore, HArc-m1 is the only strain enriched from the neutral salt lakes being closely related to isolates from soda lakes representing quite a rare example in our long-term work with hypersaline lakes. It is also worth to notice that, in this particular case, the substrate selectivity (mannan) overruled the dominant selective factor – the nature of sodium salt (chloride vs. carbonate) and, therefore, the considerable difference in the pH-osmotic pressure combination. Growth experiments confirmed that strain HArc-m1 can indeed grow both at neutral pH and up to pH 9.5, thus being a facultative alkaliphile.

Polysaccharide-utilizing natronoarchaea from hypersaline soda lakes

Positive stable enrichment cultures from soda lakes were obtained with 14 out of 16 polysaccharides tested (pullulan and arabinogalactan were not tested). Similar for salt lakes, alginate and pectin enrichments were negative. Another similarity was the fastest growth (1 week) of the starch-like alpha-glucans (amylopectin and glycogen) and the slowest growth (up to a month) of the insoluble beta-linked-glycans (beta-mannan and curdlan) and α-1,6-glucan dextran (which was negative in case of salt lake samples) utilizing enrichment cultures. However, in contrast to salt lakes further dilution to extinction from the soda lake enrichments had still to be done in the presence of antibiotics since in their absence the cultures were rapidly overrun by bacteria. It was even necessary to add antibiotics to the solid media at the final stage of pure culture isolation. The contaminating bacteria mostly belonged to the genus *Halomonas* which were unable to grow on the target polysaccharide but most probably scavenged the hydrolysis products. The *Halomonas* colonies were easily distinguished from the pink-orange colonies of natronoarchaea which helped to purify the latter, although, in most cases only 1-2 types of such colonies grew back in the liquid medium with the target polysaccharide. The list of isolated polysaccharide-utilizing natronoarchaea is given in **Table 2**.

Four different alpha-bonded glucans and fructans resulted in selection of seven isolates, of which, all except two belonged to know genera. Two isolates enriched and isolated either on amylopectin or inulin were identical in their 16S rRNA gene sequences and represented a novel genus and species *Natronocalculus amylovorans* (Sorokin et al., 2022a). The other three amylopectin-utilizing isolates were closely related to each other and to a facultively anaerobic sulfur-respiring amylolytic *Natranaeroarchaeum sulfidigenes* (Sorokin et al., 2022b). Together with the isolate AArc-lev selected with beta-fructan–levan (**Table 2**) those four strains have recently been described as a new species *Natranaeroarchaeum aerophilus* (Sorokin et al., 2022b). So, there seems to be a connection in starch-like alpha-glucans and beta-fructans selectivity among natronoarchaea.

Interestingly, although glycogen is structurally similar to amylopectin (both are branched alpha-glucans), the two glycogen-selected natronoarchaeal isolates from the genera *Natronococcus* and *Natronorubrum* were not related to above-mentioned new taxa. But all four were able to grow with soluble starch and pullulan, similar to the members of the genus *Natronococcus* which are well-known for their ability to utilize starch and to produce alkalistable amylases (Kobayashi et al., 1992; Kanal et al., 1995).

To our knowledge, dextrans have never been shown or even suspected to support growth of any known *Halobacteria* species, while it was mentioned among positive substrates in anaerobic hyperthermophilic archaea *Desulfurcococcus fermentas* (Perevalova et al., 2005), *D. kamchatkensis* (Kublanov et al., 2009), *Thermoccoccus sibiricus* (Mardanov et al., 2009), and *Thermococcus* sp. strain 2319 × 1 (Gavrilov et al., 2016). While starch-like polysaccharides can have side branches with alpha-bonded glucose other than α-1,4, none but dextrans have the α-1,6 backbone, which probably makes them difficult substrates for hydrolytic archaea. From two forms of the cyanobacterial dextran tested in this work (19.5 and 200 kDa), only the low molecular weight variety resulted in a positive enrichment and isolation of a single natronoarchaeal strain AArc-dxtr1 representing a distant novel species in the genus *Saliphagus* (**Table 2**).

Finally, an alpha-1,5-arabinan enrichment from soda lakes yielded a stable binary culture impossible to separate by serial dilutions. Plating showed two distinctive types of colonies: a dominant type with small red colonies and less abundant larger and nearly colorless colonies. Both grew back in liquid pure cultures with arabinan. Interestingly, the arabinan utilization in the liquid culture inoculated with the colorless colonies resulted in a formation of soluble yellow-brownish product, while the red colonies culture supernatant remained colorless. The isolate AArc-arb3/5 with colorless colonies was identified as a novel *Natrialba* species (with the highest 16S rRNA sequence identity of 97% to "*N. wudunaoensis*"), while the second isolate AArc-arb1/2/6 with red colonies was closely related to the known species *Natronolimnobius baerhuensis*.

The natronoarchaea selected from soda lakes on various beta-bonded polysaccharides can be divided into two major groups: preferably xylanolytic and cellulo-/mannanolytic (**Table 2**). The xylanolytics selected on either xylan, arabinoxylan and galactan belonged to the known genus *Natronolimnobius*. Xyloglucan, galactomannan, and mannan

10.3389/fmicb.2022.1059347

TABLE 2 Polysaccharide-utilizing natronoarchaea enriched and isolated from hypersaline soda lakes.

Polysaccharide	Isolates	Identification by 16S rRNA gene sequence		Spectrum of utilized polysaccharides	
		Closest cultured relative	% identity	Stable growth in liquid culture	Colony activity (zone of hydrolysis, mm/2–3 weeks)
Alpha-glucans					
Amylopectin	AArc-St1-1	*"Natranaeroarchaeum*	99.4	Amp/Sst/Pul/Cdx/Lev	nd/35/23/nd/nd
	AArc-St1-2	*sulfidigenes"*	98.5	Amp/Sst/Pul/Cdx/Inl	nd/19/15/nd/nd
	AArc-St1-3	*"Natronocalculus*	99.1		
	AArc-St2	*amylolyticus"*	**100**		
Pullulan	Was not tested since AArc-St isolates were able to utilize pullulan				
Glycogen	AArc-glc1/2/4	*Natronococcus amylolyticus*	99	Glc/Sst/Arx/Xyl/Gcm	nd/23/25/15/20
	AArc-glc3	*Natronorubrum tibetense*	100	Glc/Sst	nd/25
Dextran	**AArc-dxtr1**	*Saliphagus infecundisoli*	96.8	Dxt/Arx/Sst(w)/Inl/Gcm(w)	nd/30/12/nd/8
Arabinan	AArc-arb1/2/6	*Natronolimnobius baerhuensis*	99	Arb/Arx/Arg/Xyl/Gcm(w)	nd/30/nd/9/11/5
	AArc-arb3/5	*Natrialba magadii*	96.4	Arb/Arx/Xyl	nd/15/25
Beta-fructans					
Levan	AArc-lev1	= AArc-St1-1	99	Lev/Sst	nd/20
Inulin	AArc-in1	= AArc-dxtr1	99.8	Inl/Sst/Dxt (weak)	nd/20/nd
	AArc-in2	=AArc-St2		Inl/Sst//Pul	nd/15/20
Beta-bonded polysaccharides					
Pectic galactan	AArc-glct1	*Natronolimnobius baerhuensis*	100	Glt/Arx/Xyl/Gcm/Arg	Nd/30/25/10/nd
Beta-mannan	AArc-m1	*Natronococcus amylolyticus*	99	Man/Arx/Xgl/Gcm	18/20/20/25
	AArc-m2/3/4*	*Halovarius/Haloterrigena*	**94–95**	Man/Gcm/Arx/Xyl/Xgl/Ac	20/20/30/30/20/20
	AArc-m6	*Natronobiforma cellulositropha*	100	Man/Arx/Xyl/Gcm/Ac	12/12/10/12/32
Glucomannan	**AArc-gm3/4/5-2**	**=AArc-m2/3/4**	100	Gcm/Man/Arx/Xyl/Cel	15/10/22/18/22
	AArc-gm6	*Natronobiforma cellulositropha*	100		
Galactomannan	**AArc-glctm3/4/8**	*Natronococcus amylolyticum*	99	Gtm/Gcm/Sst/Inl	nd/18/20/nd
	AArc-glctm5	**=AArc-m2/3/4**	**100**		
Xyloglucan	**AArc-xg1-1**	**=AArc-m2/3/4**	**100**	Xgl/Xyl/Arx/Ac/Man	15/7/22/12/8
Xylan arabinoxylan	AArc-x1/2/3/4	*Natronolimnobius baerhuensis*	99	Xyl/Arx/Ac/Sst	35/18/12/18
	AArc-ax1/2/3		99	Arx/Xyl/Arg	30/20/nd
Curdlan	**AArc-curdl1**	*Halostagnicola alkaliphila*	**95**	Crd/Pch/Lam/Gtm/Sst	nd/nd/nd/nd/15
Arabinogalactan	Was not tested since several other AArc isolates were able to utilize it				
Alginate	No isolates; not utilized by any isolates				
Pectin	There was some growth in primary enrichment but it was not reproduced further in sediment-free transfers				

See Table 1. w, weak growth; *This isolate was similar to HArc-m1 isolated on mannan from salt lakes (see Table 1). Bold values indicate potentially new genera.

enrichments were all dominated by a novel genus-level lineage to which a facultatively alkaliphilic strain HArc-m1 (see above; Table 2) also belonged. Furthermore, a less abundant component in the galactomannan enrichment was identified as a member of the genus *Natronococcus*. A dominant organism in a glucomannan enrichment was identical to the cellulose/mannan-specialized *Natronobiforma cellulositropha* (Sorokin et al., 2018). This is similar to the selectivity of glucomannan in salt lakes resulted in isolation of a cellulolytic haloarchaeon HArc-gm2 closely related to cellulotrophic *Halomicrobium* HArcel3 dominating in cellulose enrichments from hypersaline lakes (Sorokin et al., 2015).

Curdlan, a beta-1,3-glucan homopolysacharide, selected a single natronoarchael strain representing a new genus lineage of the polysaccharide-utilizing archaea. The enrichment culture was very slow in development resulting in degradation of antibiotics and massive development of bacteria belonging to *Halomonas*. Several repeated attempts with sequential addition of antibiotics resulted in the sufficient enrichment of the archaeal component appropriate for further purification on a solid medium. Despite its general chemical similarity to cellulose, curdlan molecules have a different physical structure (helical in contrast to flat ribbon cellulose fibrils) (Deslandes et al., 1980). Altogether, its structural characteristics, both primary and secondary, as well as low occurrence in nature makes it highly selective substrate in comparison with the more common beta-1,4 glucans. We did not manage to find any published data on curdlan utilization in haloarchaea. On the other hand, two out of ten CAZymes families (GH81 and GH16) including members with the endo-β-1,3-glucanase activities (EC 3.2.1.39) have archaeal representatives. While archaeal representatives of the GH81 family are known exclusively by the presence of the respective genes in their genomes, a single archaeal GH16 glycosidase from *Pyrococcus furiosus* (Gueguen et al., 1997) was characterized as a laminarinase able to hydrolyze laminarin, lichenan, and barley β-glucan. However, no information of its capability to hydrolyze curdlan was provided. It should be noted that the halo- and natronoarchaea enriched and isolated on curdlan in the course of this work were capable to grow on laminarin, a soluble beta-1,3/1,6 glucan.

The growth cross-specificity for various polysaccharides among the natronoarchaeal isolates is shown in **Figure 2**. From the strains isolated on alpha-bonded polysaccharides, the amylolytics were most restricted in their polymer-utilizing profiles with only beta-fructans as the alternative substrates. The only exception was *Natronococcus* AArc-glc1/2/4, isolated on glycogen and able to grow with a few beta-1,4 bonded polysaccharides. On the other hand, strains selected with other alpha-bonded polysaccharides, such as dextran and arabinan, were all able to utilize xylan and arabinoxylan and one of them also grew with arabinogalactan (**Figure 2A**).

Among the strains selected with beta-bonded polysaccharides, the most narrowly specialized was strain AArc-curdl1 isolated on curdlan: it only grew with two other polysaccharides with the beta-1,3-backbone (pachyman and laminarin) and on starch (**Figure 2B**). In contrast, the natronoarchaea enriched with various beta-1,4-bonded polysaccharides had a broader substrate range with xylan and arabonoxylan being the most common cross-substrates among them. Similar to the salt lake isolates, the soda lake strains selected with beta-1,4 mannan and glucomannan were also capable of growth on native celluloses. On the other hand, in contrast to salt lakes, the same taxa were also selected on galactomannan. This difference is significant, taking into account importance of cellulose for natural habitats but the reason for this is not clear yet.

Phylogenomic and functional genomic analysis

Genomes of seven stains were *de novo* sequenced and assembled. Quality check of the assemblies revealed high completeness (99–100%) and low contamination (0-1.87%) levels what makes them suitable for both phylogenomic and functional analyses (**Supplementary Table 2**). Genome sizes varied from 2.81 to 5.59 Mbp while the G + C contents for different genomes were 59.2–66%.

Phylogenomic analysis showed that the novel polysaccharidolytic strains are uniformly dispersed within the *Halobacteria* tree (**Figure 3**). Strain AArc-St1-1 belonged to the genus *Natranaeroarchaeum* and is recently described as a new species *N. aerophilus* (Sorokin et al., 2022b), while strain AArc-St2 is described as a novel genus and species *Natronocalculus amylovorans* (Sorokin et al., 2022a). Strain HArc-gm2 was most closely related to the members of the genus *Halosiccatus*. The neutrophilic curdlan-utilizing haloarchaea strains HArc-curdl5-1 and HArc-curdl7 are most closely related to the genus *Halapricum*. The nearest relatives of AArc-dxtr1 are among the *Halostagnicola* species, while AArc-xg1-1, AArc-m2/3/4 and AArc-cudrl1 are related to the cellulolytic *Natronobiforma*. Establishing the exact taxonomic rank (novel species or genus) of these novel haloa(natrono)archaea will need a more in-depth phenotypic and chemotaxonomical characterization.

Polysaccharide-utilizing haloarchaea must have a set of carbohydrate active enzymes (CAZymes), as a prerequisite for successful decomposition of insoluble and soluble poly- and oligosaccharides. Indeed, the sequenced genomes encoded all types of the CAZymes: glycosidases (GH), polysaccharide lyases (PL), glycosyl transferases (GT), carbohydrate esterases (CE), carbohydrate oxidases (AA) as well as carbohydrate-binding modules (CBM). The detailed analysis was focused on GHs and PLs (**Figure 4**; **Supplementary Table 3**) due to their major role in polysaccharide depolymerization.

Closely related neutrophilic strains HArc-curld5-1 and HArc-curdl7 enriched on curdlan had identical CAZyme repertoires. Their capability to degrade curdlan as well as pachyman and laminarin is due to the action of endo-beta-1,3(4)-glucanase (GH81), beta-1,3-glucan phosphorylase (GH161) and beta-glucosidase (GH3). Both strains also grew on starch by means of fourteen alpha-amylases (GH13), three oligo-1,6-glucosidases (GH13), two glucoamylases (GH15), and a 4-alphaglucanotransferase encoded in their genomes. The genome of alkaliphilic strain AArc-curld1 also isolated on curdlan had a smaller set of genes for respective enzymes yet it included an essential endo-beta-1,3(4)-glucanase (GH81)

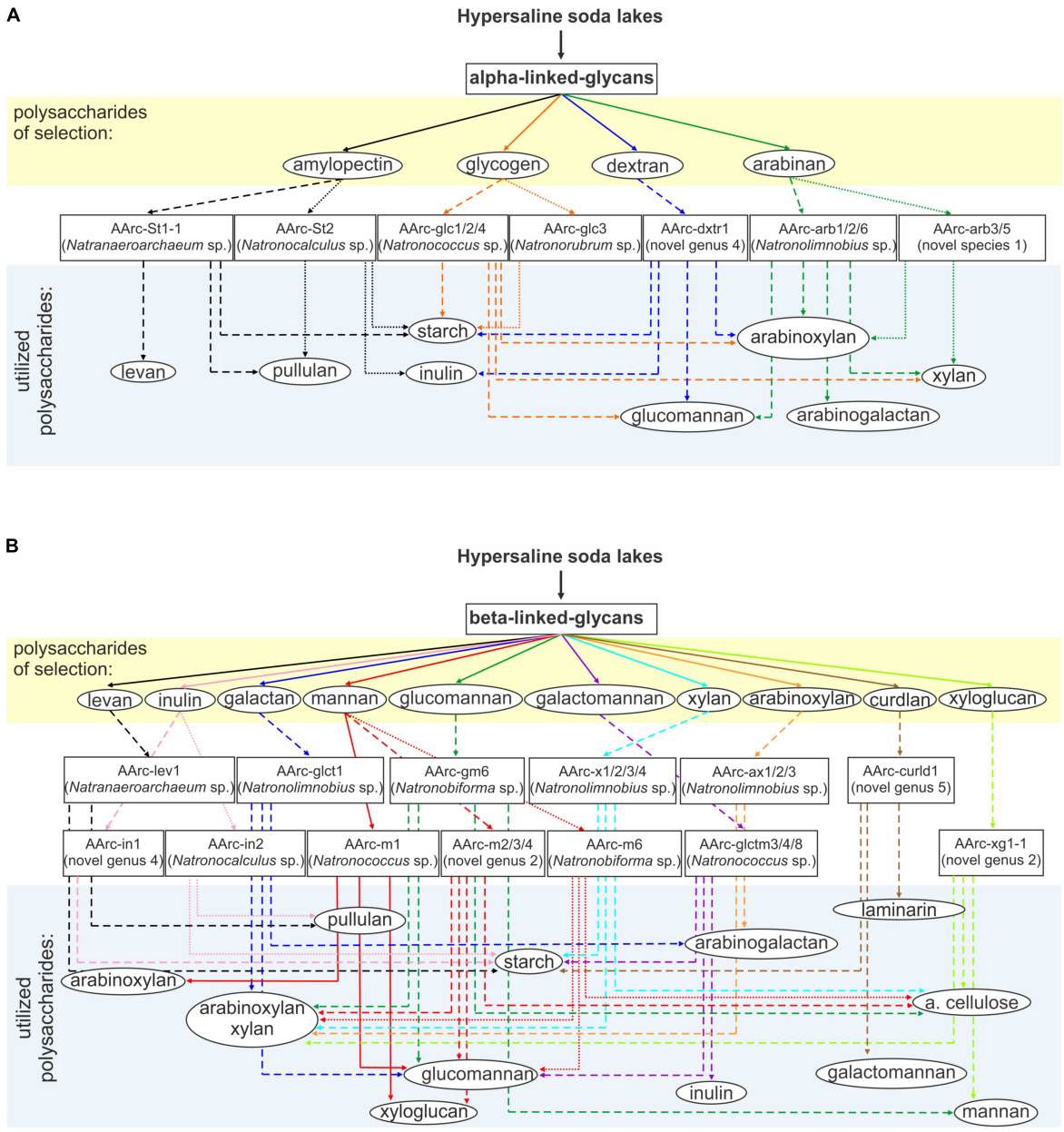

FIGURE 2
Schematic representation of selective enrichments of natronoarchaea from hypersaline soda lakes on **(A)** alpha-bonded and **(B)** beta-bonded polysaccharides. Assignment to the novel genus was based on protein sequence-based phylogenomic analysis and 16S rRNA gene sequence identity values (for strain AArc-arb3/5 only 16S rRNA gene sequence identity values were used).

and a beta-glucosidase (GH3). A neopullulanase (GH13), three alpha-amylases (GH13), a 4-alphaglucanotransferase (GH77), and two glucoamylases (GH15) apparently allowed the strain to utilize soluble starch.

The neutrophilic strain HArcl-gm2 isolated on glucomannan has a machinery for its decomposition including endo-beta-1,4-mannosidase (GH5), several endoglucanases (four from the GH5 and one from the GH9 families), two beta-mannosidases (GH2) and a beta-glucosidase (GH3). The strain also can utilize laminarin and beta-glucan due to the presence of the endo-beta-1,3(4)-glucanase (GH81); xylan and arabinoxylan by means of endoxylanases (seven enzymes from GH10 and three from GH11), beta-xylosidases (GH3), and arabinosidases (GH43 and GH51) responsible for hydrolysis of side chains of arabinoxylan.

Comparative genomic analysis of closely related natronarchaeal strains AArc-xg1-1 (isolated on xyloglucan) and AArc-m2/3/4 (isolated on beta-1,4-mannan) showed

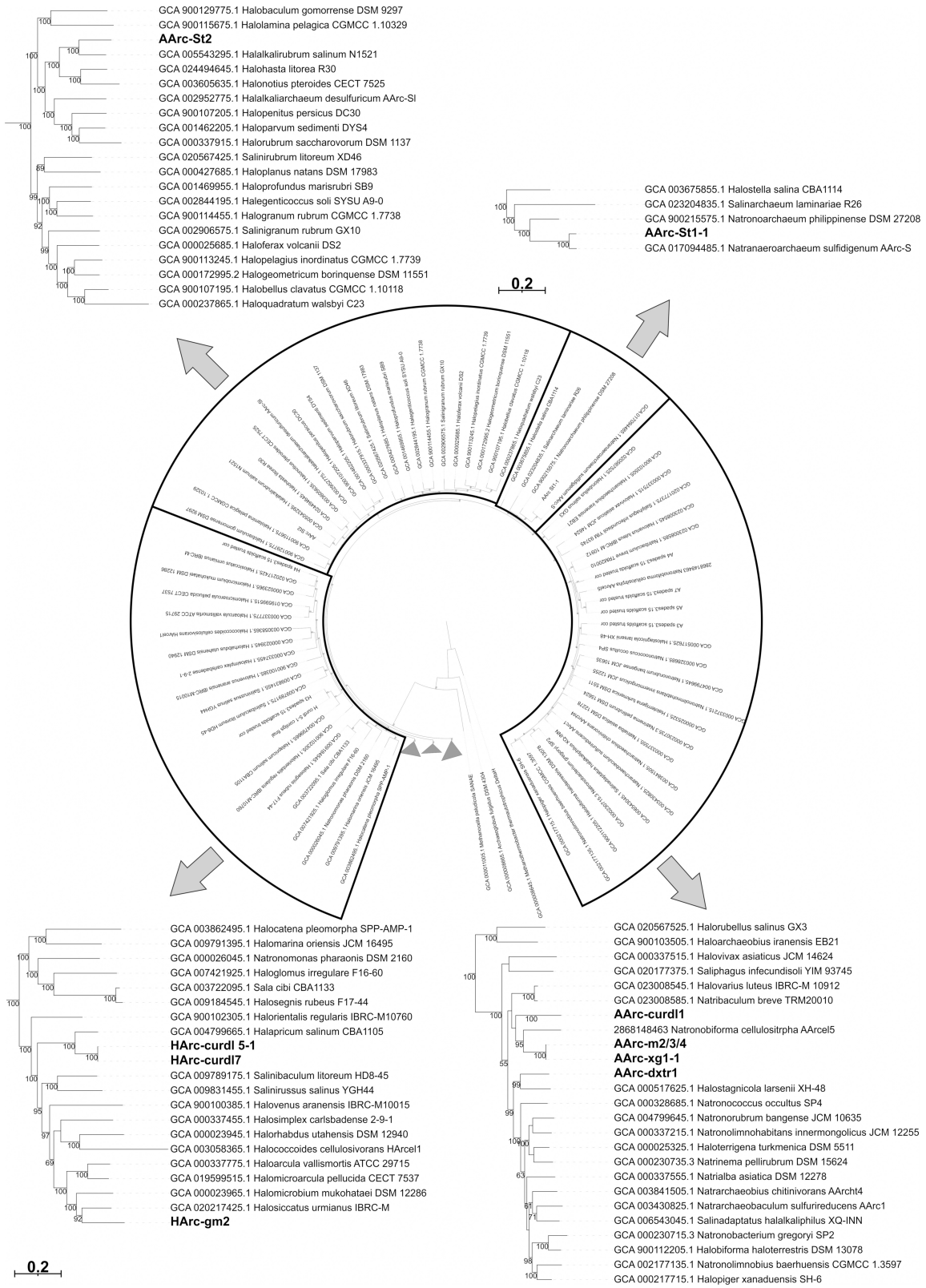

FIGURE 3
Maximum likelihood phylogenomic tree showing position of polysaccharide-utilizing halo(natrono)archaea enriched from hypersaline lakes within the class *Halobacteria*. Sequences of 122 conserved archaeal proteins were used to infer the tree.

10.3389/fmicb.2022.1059347

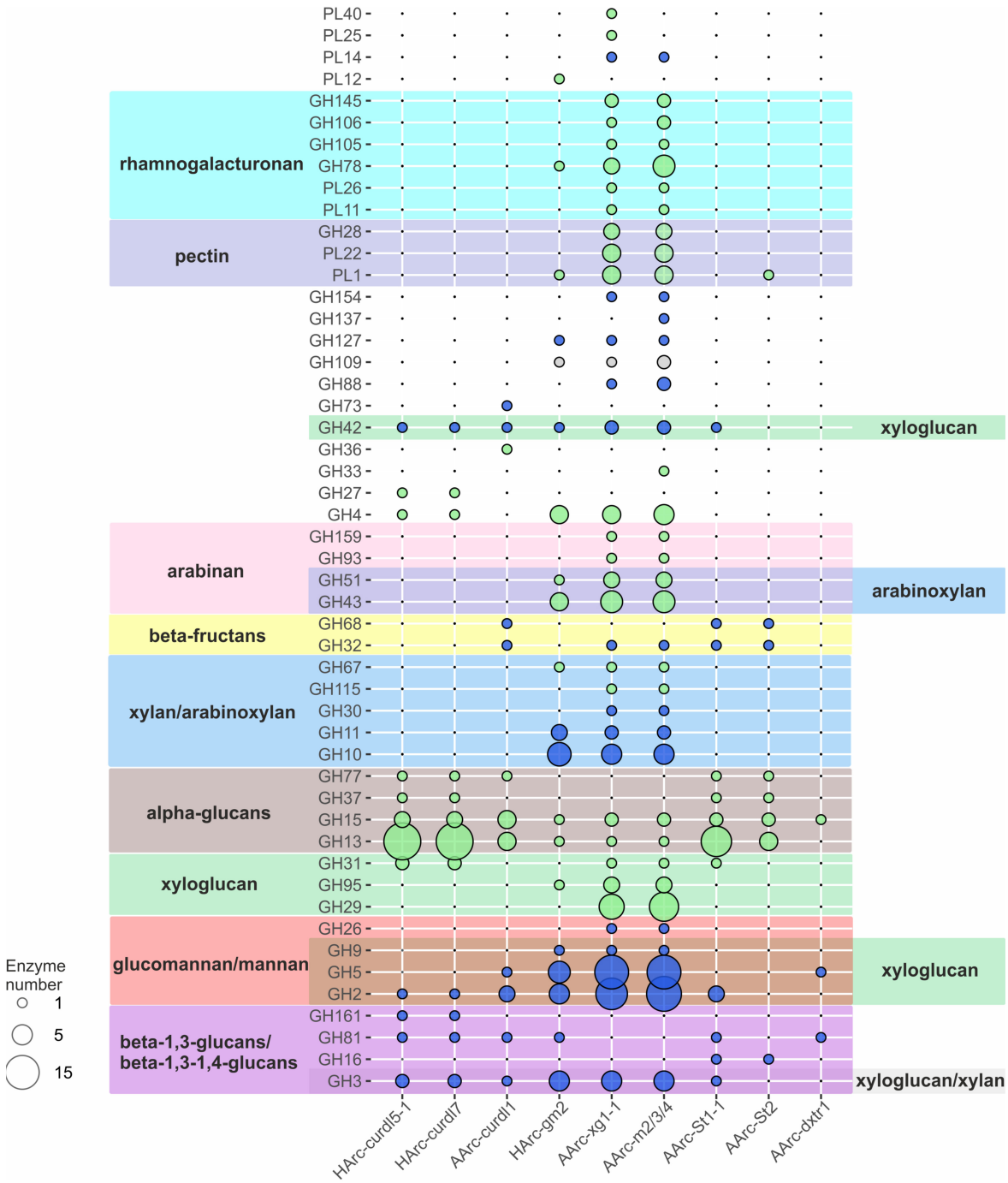

FIGURE 4
Sets of GH and PL genes found in the genomes of novel polysaccharidolytic haloarchaea. Size of bubbles indicate number of enzymes; the color of bubbles indicate the prevailing type of glycosidic bonds hydrolyzed by the enzymes (alpha-bonds—green, beta-bonds—blue, both—gray). Color of background indicates these CAZymes families contains the characterized enzyme(s) capable of depolymerization of respective polysaccharides. No color means the activities, characteristic to these families are not directly linked to the substrates used in this work.

a nearly identical and the largest CAZyme sets among the studied haloarchaea. In particular, the genes encoding several endo-beta-1,4-mannosidases (five enzymes from GH5 family and one from GH26), two beta-mannosidases (GH2), endoglucanases (10 proteins from GH5 and one enzyme from GH9), three beta-glucosidases (GH3 family), endo-beta-1,4-xylanases (5 enzymes from GH10 and two enzymes from GH11), beta-xylosidase (GH3) were found. Moreover, the

genes of enzymes known to degrade galacturonate-containing polymers (polygalacturonate, pectin, rhamnogalacturonan) were also detected: three polygalacturonases (GH28), putative pectate lyases (four proteins from PL1 family and four from PL22), two rhamnogalacturonan lyases (PL11, PL26) as well as arabinan-hydrolyzing enzymes (six proteins from GH43, three GH51 enzymes and one enzyme from GH93). However, none of these isolates grew with either pectins, polygalacturonate, rhamnogalacturonan, or arabinan. This example clearly demonstrates that functional conclusions based solely on the genomic evidence should be considered only as preliminary.

The genome of the natronarchaeal amylolytic strain AArc-St1-1 (*Natranaeroarcheum aerophilus*, Sorokin et al., 2022a) contains a large number of genes coding for alpha-bond degrading glycosidases, including ten alpha-amylases (GH13 family), two oligo-1,6-glucosidases (GH13), 4-alpha-glucanotransferase (GH77), glucoamylase (GH15), and trehalase (GH37). Finally, two beta-fructosidases (GH32 and GH68) were also found, apparently allowing the strain to grow on levan. Also, two beta-1,3(4)-glucanases (GH16, GH81), beta-glucosidase/beta-xylosidase (GH3), beta-mannosidase (GH2), alpha-xylosidase (GH31), and several beta-galactosidases (GH2 and GH42 families) genes were present. Another amylolytic strain AArc-St2 (*Natronocalculus amylovorans*) possessed similar CAZymes set (alpha-glucan-specific enzymes from GH13, GH15 and GH77 families as well beta-fructosidases) but the number of alpha-amylases and oligo-1,6-glucosidases was significantly lower (Sorokin et al., 2020a). Despite the presence of genes for putative GH16 beta-glucanase and PL1 pectate lyase, no growth was observed on their specific substrates including beta-glucan, lichenan, curdlan, pachyman, or pectin.

Only three GH genes and no PL genes were found in the genome of dextran-utilizing natronoarchaeon AArc-dxtr1: trehalase (GH15), endoglucanase (GH5), and beta-1,3(4)-glucanase (GH81). The typical dextran-degrading enzymes from GH13, GH49, GH66, or GH70 families a were not encoded and it might be only speculated that dextran is hydrolyzed as a result of side activity of a GH15 enzyme since this family is known to contain glucodextranases (Mizuno et al., 2004). An endoglucanase and a beta-1,3(4)-glucanase could be responsible for hydrolysis of glucomannan and arabinoxylan which this organism can also utilize.

Altogether, the repertoire of CAZymes within the *in silico* proteomes of the nine polysacharidolytic halo/natronoarchaea analyzed in this work (summarized on **Figure 4**) was mostly consistent with their polysaccharide untilization spectrum. In total, the number of CAZyme genes found in the studied HArcel/AArcel strains greatly varied from 30 (strain AArc-St2) to 160 (strain AArc-m2/3/4). Closely related strains isolated with the same (HArc-curld5-1 and HArc-curdl7) or different (AArc-xg1-1 and AArc-m2/3/4) substrates may have identical or similar CAZymes gene sets indicating that a selection substrate will not necessarily lead to isolation of a distinctive phylogenetic lineage. At the same time, despite that the phylogenetically distant strains enriched and isolated with the same polysaccharide have different CAZymes sets, they all had similar patterns of particular CAZymes responsible for the hydrolysis of selective substrate. Surprisingly, the genomes of several isolates including AArc-xg1-1, AArc-m2/3/4, AArc-St2, and HArc-gm2 also contained polysaccharide lyases genes which are nearly unknown within the Archaeal kingdom. However, the growth experiments revealed that none of those strains can grow on alginate, pectin, polygalacturonate or rhamnogalacturonan indicating that these enzymes might have an unknown activity in halophilic archaea. This is also substantiated by the fact that all our attempts to enrich pectin- or alginate-utilizing haloarchaea failed so far. Among the possible reasons might be that these uronic acids-based polysaccharides are hardly present in hypersaline habitats or that hypersalinity changes the chemical properties and enzyme accessibility of the polymers. On the other hand, the high diversity of hydrolytic haloarchaea with the potential to utilize various polysacchirides with different types of glycosidic bonds indicate that such substrates might be available in hypersaline habitats. One of the most probable source of these polymers are external terrestrial plants growing in the area surrounding hypersaline lakes.

Conclusion

The obtained results allow to significantly extend the knowledge on polysaccharide-utilizing capabilities of haloarchaea and archaea in general. Selective enrichment approach leaded to recover the so called "best-fit" organisms specialized on a narrow-specialized conversion of a particular substrate. In case of polysaccharides, however, most of the haloarchaeal isolates enriched with a certain substrate were still able to utilize several other polymers. It was also found that polymers with the alpha-1,4 or beta-1,4 linkage backbones more often resulted in positive enrichments than with other types of linkage, such as the alpha-1,6- or beta-1,3 bonding. Finally, no haloarchaea, growing on uronic acid-based polysaccharides (pectin and alginate), commonly utilized by bacteria, were isolated.

In the course of this work, the first haloarchaea able to grow on such recalcitrant polysaccharides as dextran, curdlan, xyloglucan, and beta-mannan were isolated. The enlarged variety of polysaccharidolytic halo(natrono)archaea recovered from hypersaline lakes with novel substrate utilization specificities is offering a good opportunity for further studies of their extremely halo(alkali)stable hydrolases, both in fundamental enzymology research and prospective application.

Data availability statement

The datasets presented in this study can be found in online repositories. The names of the repository/repositories and accession number(s) can be found in the article/ **Supplementary material**.

Author contributions

DS and TVKh were responsible for microbiology work. AE and IK analyzed the genomes and run phylogenetic analysis. TVKo was responsible for 16S rRNA gene sequencing and identification of the isolates. DS, AE, and IK wrote the manuscript. All authors contributed to the article and approved the submitted version.

Funding

This work was supported by the Russian Science Foundation (grant 20-14-00250) and by the Russian Ministry of Science and Higher Education (field and primary enrichment work).

Conflict of interest

The authors declare that the research was conducted in the absence of any commercial or financial relationships that could be construed as a potential conflict of interest.

Publisher's note

All claims expressed in this article are solely those of the authors and do not necessarily represent those of their affiliated organizations, or those of the publisher, the editors and the reviewers. Any product that may be evaluated in this article, or claim that may be made by its manufacturer, is not guaranteed or endorsed by the publisher.

Supplementary material

The Supplementary Material for this article can be found online at: https://www.frontiersin.org/articles/10.3389/fmicb.2022.1059347/full#supplementary-material

References

Amoozegar, M. A., Siroosi, M., Atashgahi, S., Smidt, H., and Ventosa, A. (2017). Systematics of haloarchaea and biotechnological potential of their hydrolytic enzymes. *Microbiology* 163, 623–645. doi: 10.1099/mic.0.000463

Andrei, A. Ş, Banciu, H. L., and Oren, A. (2012). Living with salt: Metabolic and phylogenetic diversity of archaea inhabiting saline ecosystems. *FEMS Microbiol. Lett.* 330, 1–9. doi: 10.1111/j.1574-6968.2012.02526.x

Begemann, M. B., Mormile, M. R., Paul, V. G., and Vidt, D. J. (2011). "Potential enhancement of biofuel production through enzymatic biomass degradation activity and biodiesel production by halophilic microorganisms," in *Halophiles and hypersaline environments: Current research and future trends*, eds A. Ventosa, A. Oren, and Y. Ma (Heidelberg: Springer), 341–357.

Bhatnagar, T., Boutaiba, S., Hacene, H., Cayol, J.-L., Fardeau, M.-L., Ollivier, B., et al. (2005). Lipolytic activity from halobacteria: Screening and hydrolase production. *FEMS Microbiol. Lett.* 248, 133–140.

Boutet, E., Lieberherr, D., Tognolli, M., Schneider, M., Bansal, P., Bridge, A. J., et al. (2016). UniProtKB/Swiss-Prot, the manually annotated section of the uniprot knowledgebase: How to use the entry view. *Methods Mol. Biol.* 1374, 23–54. doi: 10.1007/978-1-4939-3167-5_2

Chaumeil, P.-A., Mussig, A. J., Hugenholtz, P., and Parks, D. H. (2019). GTDB-Tk: A toolkit to classify genomes with the genome taxonomy database. *Bioinformatics* 36, 1925–1927. doi: 10.1093/bioinformatics/btz848

Cui, H. L., and Dyall-Smith, M. L. (2021). Cultivation of halophilic archaea (class *Halobacteria*) from thalassohaline and athalassohaline environments. *Mar. Life Sci. Technol.* 3, 243–251.

Deslandes, Y., Marchessault, R. H., and Sarko, A. (1980). Triple-helical structure of (1/3)-b-D-glucan. *Macromolecules* 13, 1466–1471.

Enache, M., and Kamekura, M. (2010). Hydrolytic enzymes of halophilic microorganisms and their economic values. *Rom. J. Biochem.* 47, 47–59. doi: 10.1002/bit.27639

Enomoto, S., Shimane, Y., Ihara, K., Kamekura, M., Itoh, T., Ohkuma, M., et al. (2020). *Haloarcula mannanilytica* sp. nov., a galactomannan-degrading haloarchaeon isolated from commercial salt. *Int. J. Syst. Evol. Microbiol.* 70, 6331–6337. doi: 10.1099/ijsem.0.004535

Gavrilov, S. N., Stracke, C., Jensen, K., Menzel, P., Kallnik, V., Slesarev, A., et al. (2016). Isolation and characterization of the first xylanolytic hyperthermophilic euryarchaeon *Thermococcus* sp. Strain 2319x1 and its unusual multidomain glycosidase. *Front. Microbiol.* 7:552. doi: 10.3389/fmicb.2016.00552

Grant, W. D., and Jones, B. E. (2016). "Bacteria, *Archaea and viruses of soda lakes*," in *Soda Lakes of East Africa*, ed. M. Schagerl (Berlin: Springer International Publishing), 97–147.

Gueguen, Y., Voorhorst, W. G. B., van der Oost, J., and de Vos, W. M. (1997). Molecular and biochemical characterization of an endo-β-1,3-glucanase of the hyperthermophilic archaeon *Pyrococcus furiosus*. *J. Biol. Chem.* 272, 31258–31264.

Kaar, W. E., and Holtzapple, M. T. (2000). Using lime pretreatment to facilitate the enzymic hydrolysis of corn stover. *Biomass Bioenergy* 18, 189–199.

Kanal, H., Kobayashi, T., Aono, R., and Kudo, T. (1995). *Natronococcus amylolyticus* sp. nov., a haloalkaliphilic archaeon. *Int. J. Syst. Bacteriol.* 45, 762–766. doi: 10.1099/00207713-45-4-762

Kobayashi, T., Kanai, H., Hayashi, T., Akiba, T., Akaboshi, R., and Horikoshi, K. (1992). Haloalkaliphilic maltotriose-forming α-amylase from the archaebacterium *Natronococcus* sp. strain Ah-36. *J. Bacteriol.* 174, 3439–3444. doi: 10.1128/jb.174.11.3439-3444.1992

Kublanov, I. V., Bidjieva, S. K. H., Mardanov, A. V., and Bonch-Osmolovskaya, E. A. (2009). *Desulfurococcus kamchatkensis* sp. nov., a novel hyperthermophilic protein-degrading archaeon isolated from a Kamchatka hot spring. *Int. J. Syst. Evol. Microbiol.* 59, 1743–1747.

Letunic, I., and Bork, P. (2019). Interactive tree of life (iTOL) v4: Recent updates and new developments. *Nucleic Acids Res.* 47:W256–W259. doi: 10.1093/nar/gkz239

Mardanov, A. V., Ravin, N. V., Svetlitchnyi, V. A., Beletsky, A. V., Miroshnichenko, M. L., Bonch-Osmolovskaya, E. A., et al. (2009). Metabolic versatility and indigenous origin of the archaeon *Thermococcus sibiricus*, isolated

from a Siberian oil reservoir, as revealed by genome analysis. *Appl. Environ. Microbiol.* 75, 4580–4588. doi: 10.1128/AEM.00718-09

Minegishi, H., Enomoto, S., Echigo, A., Shimane, Y., Kondo, Y., Inoma, A., et al. (2017). *Salinarchaeum chitinilyticum* sp. nov., a chitin-degrading haloarchaeon isolated from commercial salt. *Int. J. Syst. Evol. Microbiol.* 67, 2274–2278. doi: 10.1099/ijsem.0.001941

Mistry, J., Finn, R. D., Eddy, S. R., Bateman, A., and Punta, M. (2013). Challenges in homology search: HMMER3 and convergent evolution of coiled-coil regions. *Nucleic Acids Res.* 41:e121. doi: 10.1093/nar/gkt263

Mizuno, M., Tonozuka, T., Suzuki, S., Uotsu-Tomita, R., Kamitori, S., Nishikawa, A., et al. (2004). Structural insights into substrate specificity and function of glucodextranase. *J. Biol. Chem.* 279, 10575–10583. doi: 10.1074/jbc.M310771200

Moshfegh, M., Shahverdi, A. R., Zarrini, G., and Faramarzi, M. A. (2013). Biochemical characterization of an extracellular polyextremophilic α-amylase from the halophilic archaeon *Halorubrum xinjiangense*. *Extremophiles* 17, 677–687. doi: 10.1007/s00792-013-0551-7

Oren, A. (2013). "Life at high salt concentrations," in *The Prokaryotes: Prokaryotic Communities and Ecophysiology*, eds E. Rosenberg, E. F. DeLong, S. Lory, E. Stackebrandt, and F. Thompson (Berlin: Springer Berlin Heidelberg), 421–440.

Oren, A. (2015). Halophilic microbial communities and their environments. *Curr. Opin. Biotechnol.* 33, 119–124.

Perevalova, A. A., Svetlichny, V. A., Kublanov, I. V., Chernyh, N. A., Kostrikina, N. A., Tourova, T. P., et al. (2005). *Desulfurococcus fermentans* sp. nov., a novel hyperthermophilic archaeon from a Kamchatka hot spring, and emended description of the genus *Desulfurococcus*. *Int. J. Syst. Evol. Microbiol.* 55, 995–999. doi: 10.1099/ijs.0.63378-0

Pfennig, N., and Lippert, K. D. (1966). Über das vitamin B_{12}-bedürfnis phototropher schwefelbakterien. *Arch. Microbiol.* 55, 245–256.

Rinke, C., Chuvochina, M., Mussig, A. J., Chaumeil, P.-A., Davín, A. A., Waite, D. W., et al. (2021). A standardized archaeal taxonomy for the genome taxonomy database. *Nat. Microbiol.* 6, 946–959. doi: 10.1038/s41564-021-00918-8

Selim, S., Hagagy, N., Aziz, M. A., El-Meleigy, E.-S., and Pessione, E. (2014). Thermostable alkaline halophilic-protease production by *Natronolimnobius* innermongolicus WN18. *Nat. Prod. Res.* 28, 1476–1479.

Shimane, Y., Hatada, Y., Minegishi, H., Mizuki, T., and Echigo, A. (2010). *Natronoarchaeum mannanilyticum* gen. nov., sp. nov., an aerobic, extremely halophilic archaeon isolated from commercial salt. *Int. J. Syst. Evol. Microbiol.* 60, 2529–2534. doi: 10.1099/ijs.0.016600-0

Sorokin, D. Y., Elcheninov, A. G., Khizhniak, T. V., Koenen, M., Bale, N. J., Damsté, J. S. S., et al. (2022a). *Natronocalculus amylovorans* gen. nov., sp. nov., and *Natranaeroarchaeum aerophilus* sp. nov., dominant culturable amylolytic natronoarchaea from hypersaline soda lakes in southwestern Siberia. *Syst. Appl. Microbiol.* 45:126336. doi: 10.1016/j.syapm.2022.126336

Sorokin, D. Y., Yakimov, M. M., Messina, E., Merkel, A. Y., Koenen, M., Bale, N. J., et al. (2022b). *Natranaeroarchaeum sulfidigenes* gen. nov., sp. nov., carbohydrate-utilizing sulfur-respiring *Haloarchaeon* from Hypersaline lakes, a member of a new family *Natronoarchaeaceae* fam. nov. in the order *Halobacteriales*. *Syst. Appl. Microbiol.* 45:126356. doi: 10.1016/j.syapm.2022.126356

Sorokin, D. Y., Khijniak, T. V., Kostrikina, N. A., Elcheninov, A. G., Toshchakov, S. V., Bale, N. J., et al. (2018). *Natronobiforma cellulositropha* gen. nov., sp. nov., a novel haloalkaliphilic member of the family *Natrialbaceae* (class *Halobacteria*) from hypersaline alkaline lakes. *Syst. Appl. Microbiol.* 41, 355–362. doi: 10.1016/j.syapm.2018.04.002

Sorokin, D. Y., Khijniak, T. V., Kostrikina, N. A., Elcheninov, A. G., Toshchakov, S. V., Bale, N. J., et al. (2019a). *Halococcoides cellulosivorans* gen. nov., sp. nov., an extremely halophilic cellulose-utilizing haloarchaeon from Hypersaline lakes. *Int. J. Syst. Evol. Microbiol.* 69, 1327–1335. doi: 10.1099/ijsem.0.003312

Sorokin, D. Y., Kublanov, I. V., Elcheninov, A. G., and Oren, A. (2019b). *Natronobiforma. In: Bergey's Manual of Systematics of Archaea and Bacteria*. Hoboken: John Wiley & Sons, Inc, doi: 10.1002/9781118960608.gbm01838

Sorokin, D. Y., Elcheninov, A. G., Toshchakov, S. V., Bale, N. J., Sinninghe Damsté, J. S., Khijniak, T. V., et al. (2019c). *Natrarchaeobius chitinivorans* gen. nov., sp. nov., and *Natrarchaeobius halalkaliphilus* sp. nov., alkaliphilic, chitin-utilizing haloarchaea from hypersaline alkaline lakes. *Syst. Appl. Microbiol.* 42, 309–318. doi: 10.1016/j.syapm.2019.01.001

Sorokin, D. Y., Merkel, A. Y., Kublanov, I. V., and Oren, A. (2020a). *Halococcoides. In: Bergey's Manual of Systematics of Archaea and Bacteria*. Hoboken: John Wiley & Sons, Inc, doi: 10.1002/9781118960608.gbm01944

Sorokin, D. Y., Merkel, A. Y., Kublanov, I. V., and Oren, A. (2020b). *Natrarchaeobius. In: Bergey's Manual of Systematics of Archaea and Bacteria*. Hoboken: John Wiley & Sons, Inc, doi: 10.1002/9781118960608.gbm01945

Sorokin, D. Y., Toshchakov, S. V., Kolganova, T. V., and Kublanov, I. V. (2015). Halo(natrono)archaea isolated from hypersaline lakes utilize cellulose and chitin as growth substrates. *Front. Microbiol.* 6:942. doi: 10.3389/fmicb.2015.00942

Stamatakis, A. (2014). RAxML version 8: A tool for phylogenetic analysis and post-analysis of large phylogenies. *Bioinformatics* 30, 1312–1313. doi: 10.1093/bioinformatics/btu033

Tatusova, T., DiCuccio, M., Badretdin, A., Chetvernin, V., Nawrocki, E. P., Zaslavsky, L., et al. (2016). NCBI prokaryotic genome annotation pipeline. *Nucleic Acids Res.* 44, 6614–6624. doi: 10.1093/nar/gkw569

Wainø, M., and Ingvorsen, K. (2003). Production of β-xylanase and β-xylosidase by the extremely halophilic archaeon *Halorhabdus utahensis*. *Extremophiles* 7, 87–93.

Werner, J., Ferrer, M., Michel, G., Mann, A. J., Huang, S., and Juarez, S. (2014). *Halorhabdus tiamatea*: Proteogenomics and glycosidase activity measurements identify the first cultivated euryarchaeon from a deep-sea anoxic brine lake as potential polysaccharide degrader. *Environ. Microbiol.* 16, 2525–2537. doi: 10.1111/1462-2920.12393

Zavrel, M., Bross, D., Funke, M., Büchs, J., and Spiess, A. C. (2010). High-throughput screening for ionic liquids dissolving (ligno-)cellulose. *Bioresour. Technol.* 100, 2580–2587.

Zhang, H., Yohe, T., Huang, L., Entwistle, S., Wu, P., Yang, Z., et al. (2018). dbCAN2: A meta server for automated carbohydrate-active enzyme annotation. *Nucleic Acids Res.* 46:W95–W101. doi: 10.1093/nar/gky418

frontiers | Frontiers in Microbiology

TYPE Original Research
PUBLISHED 07 December 2022
DOI 10.3389/fmicb.2022.1059061

OPEN ACCESS

EDITED BY
Sumit Kumar,
Amity University,
India

REVIEWED BY
Vikram Hiren Raval,
University School of Sciences, Gujarat University, India
Digvijay Verma,
Babasaheb Bhimrao Ambedkar University, India

*CORRESPONDENCE
Oliyad Jeilu
Oliyad.jeilu.oumer@slu.se

SPECIALTY SECTION
This article was submitted to Extreme Microbiology, a section of the journal Frontiers in Microbiology

RECEIVED 30 September 2022
ACCEPTED 11 November 2022
PUBLISHED 07 December 2022

CITATION
Jeilu O, Simachew A, Alexandersson E, Johansson E and Gessesse A (2022) Discovery of novel carbohydrate degrading enzymes from soda lakes through functional metagenomics. *Front. Microbiol.* 13:1059061. doi: 10.3389/fmicb.2022.1059061

Discovery of novel carbohydrate degrading enzymes from soda lakes through functional metagenomics

Oliyad Jeilu[1,2]*, Addis Simachew[1], Erik Alexandersson[3], Eva Johansson[2] and Amare Gessesse[1,4]

[1]Institute of Biotechnology, Addis Ababa University, Addis Ababa, Ethiopia, [2]Department of Plant Breeding, Swedish University of Agricultural Sciences, Lomma, Sweden, [3]Department of Plant Protection Biology, Swedish University of Agricultural Sciences, Lomma, Sweden, [4]Department of Biological Sciences and Biotechnology, Botswana International University of Science and Technology, Palapye, Botswana

Extremophiles provide a one-of-a-kind source of enzymes with properties that allow them to endure the rigorous industrial conversion of lignocellulose biomass into fermentable sugars. However, the fact that most of these organisms fail to grow under typical culture conditions limits the accessibility to these enzymes. In this study, we employed a functional metagenomics approach to identify carbohydrate-degrading enzymes from Ethiopian soda lakes, which are extreme environments harboring a high microbial diversity. Out of 21,000 clones screened for the five carbohydrate hydrolyzing enzymes, 408 clones were found positive. Cellulase and amylase, gave high hit ratio of 1:75 and 1:280, respectively. A total of 378 genes involved in the degradation of complex carbohydrates were identified by combining high-throughput sequencing of 22 selected clones and bioinformatics analysis using a customized workflow. Around 41% of the annotated genes belonged to the Glycoside Hydrolases (GH). Multiple GHs were identified, indicating the potential to discover novel CAZymes useful for the enzymatic degradation of lignocellulose biomass from the Ethiopian soda Lakes. More than 73% of the annotated GH genes were linked to bacterial origins, with *Halomonas* as the most likely source. Biochemical characterization of the three enzymes from the selected clones (amylase, cellulase, and pectinase) showed that they are active in elevated temperatures, high pH, and high salt concentrations. These properties strongly indicate that the evaluated enzymes have the potential to be used for applications in various industrial processes, particularly in biorefinery for lignocellulose biomass conversion.

KEYWORDS

extremophiles, glycoside hydrolases, lignocellulose biomass, halophiles, soda lakes, CAZymes, functional metagenomics

Introduction

The most abundant bioresource on Earth, lignocellulosic biomass, has an annual global yield of up to 1.3 billion tons (Baruah et al., 2018; Zoghlami and Paës, 2019). Lignocellulosic biomass is mainly composed of polysaccharides (cellulose and hemicelluloses) and lignin (an aromatic polymer). Hydrolysis of the polysaccharide component of lignocellulosic biomass releases fermentable sugars (Anwar et al., 2014), which can produce renewable energy and chemicals (Abdel-Hamid et al., 2013). Such production can reduce dependence on fossil fuels, decrease greenhouse gas emissions, and mitigate climate change (Kabeyi and Olanrewaju, 2022).

Hydrolysis of lignocellulosic biomass can be done through acid or enzymatic hydrolysis. The acid hydrolysis effectively breaks down the polysaccharides into their monomeric sugars. However, it leads to the generation of inhibitors in subsequent fermentation (Oriez et al., 2019) and contributes to environmental pollution (Jönsson and Martín, 2016). Therefore, enzymatic hydrolysis, often carried out under relatively mild reaction conditions, offers an eco-friendly and efficient method for the hydrolysis of lignocellulosic biomass (Ellilä et al., 2019). In practice, the complete breakdown of lignocellulosic polysaccharides to their monomeric components requires the synergistic action of multiple enzymes, known as Carbohydrate-Active enZymes (CAZymes) (Bredon et al., 2018; Liew et al., 2022).

Industrial processes for lignocellulosic biomass degradation has to operate at high temperatures to increase substrate accessibility. In addition, alkali pretreatment is used to enhance the internal surface area of hemicelluloses while removing acetyl groups and uronic acids (Baruah et al., 2018; Lu et al., 2021; Sun et al., 2021; Verma, 2021). Therefore, enzymes that have activity and stability in an alkaline pH range and/or at high temperatures have a potential for hydrolysis of lignocellulosic biomass (Ariaeenejad et al., 2020; Mamo, 2020). However, most known cellulases and hemicellulases are obtained from mesophilic organisms and have their optimum activity and stability around ambient temperature and in a neutral pH range (Collins et al., 2005; Ben Hmad and Gargouri, 2017). To date, relatively few alkaline active and thermostable cellulases and hemicellulases have been reported (Shuddhodana et al., 2018; Verma, 2021). Furthermore, a significant hurdle to the large-scale conversion of lignocellulose to biofuels is the scarcity of low-cost enzymes capable of effectively depolymerizing biomass (Kern et al., 2013). Thus, there is a high need to search for novel enzymes not only to enhance bioconversion but also to in order to make the process more environmentally friendly and cost-effective (Fongaro et al., 2020; Verma and Satyanarayana, 2020; Verma, 2021). One of the best strategies to obtain such enzymes is to search for lignocellulose polysaccharide degrading enzymes from extreme environments such as soda lakes (Berini et al., 2017a; Cabrera and Blamey, 2018).

Soda lakes are unique poly-extreme environments, mainly characterized by high alkalinity and salinity (Schagerl, 2016) and harbor unique and diverse microbial communities (Lanzén et al., 2013; Sorokin et al., 2015; Grant and Jones, 2016). These microbial communities from soda lakes provide a one-of-a-kind source of enzymes (Antony et al., 2013) with properties that allow them to endure the rigorous industrial conversion of lignocellulose biomass into fermentable sugars. Cellulases, hemicellulases, and other carbohydrate polymer degrading enzymes produced by microorganisms from these habitats are expected to be active and stable under extreme conditions prevalent in the soda lakes.

Although most of the known industrial enzymes are obtained from microorganisms through pure culture isolation and screening (Martin and Vandenbol, 2016), recent estimates show that more than 99% of microorganisms in the environment are uncultivable through conventional microbiological methods (Berini et al., 2017a). Thus, in recent years the advent of metagenomics has provided a powerful tool to access the genetic and metabolic diversity of microorganisms in any environment, bypassing the limitations of the current culture-dependent approaches (Berini et al., 2017a; Ngara and Zhang, 2018; Pabbathi et al., 2021). Functional metagenomics is a method that clones the environmental DNA into a suitable vector to create a library and which is then transformed into a host, such as *E. coli*. This library is then screened for various enzymatic activities (Simon and Daniel, 2011; Coughlan et al., 2015; Lam et al., 2015; Sysoev et al., 2021). Through functional metagenomics, novel biocatalysts, including lipases (Privé et al., 2015), cellulases (Voget et al., 2006), amylases (Vester et al., 2015), and chitinases (Berini et al., 2017b) have been discovered.

Whereas CAZymes from ruminants (Wang et al., 2013, 2019; Shen et al., 2020), lignocellulosic biomass wastes (Montella et al., 2017), and soil (López-Mondéjar et al., 2020), have already been thoroughly explored, investigations of CAZymes produced by microbial communities of soda lakes remain scarce. Thus, the main objective of this study was to search for CAZymes from the Ethiopian Rift Valley soda lakes using functional metagenomics.

Materials and methods

Sampling site and sample collection

Water and sediment samples were collected from three soda lakes in the East African Rift Valley: Lakes Abijata (7°37′0″N, 38°36′0″E), Chitu (7°24′14″N, 38°25′15″E), and Shala (7°25′29″N, 38°36′57″E), using sterile Niskin bottles (Ocean Scientific International Ltd., Hampshire, United Kingdom) and polyethylene bags, respectively. The water samples were filtered within 24 h of sample collection, using a polycarbonate filter membrane (0.22 μm pore size, 47 mm diameter; GE, IL, United States) to harvest the biomass for metagenomic DNA extraction.

Isolation of high molecular weight DNA

Metagenomic DNA was extracted from water and sediment samples according to Øvreås et al. (2003) and Verma and Satyanarayana (2011), respectively, with some modifications

described below. Briefly, about 250 µl solution of 1 mg/ml Lysozyme and 0.5 mg/ml RNase (Thermo Scientific, Massachusetts, United States) was added to the microbial biomass on the polycarbonate filter membrane and incubated for 15 min at 37°C. The filter was then treated with 10 µl of 1 mg/ml Proteinase K (Thermo Scientific, Massachusetts, United States) and incubated for 15 min at 37°C. Afterwards, 250 µl of pre-heated 10% sodium dodecyl sulfate (SDS; *w*/*v*) was added and incubated for 15 min at 55°C. About 80 µl of 5 M NaCl and 100 µl of 1% cetyltrimethylammonium bromide (CTAB; *w*/*v*) were added and incubated for 10 min at 65°C; followed by the addition of 750 µl chloroform/isoamyl alcohol (24:1). The mixture was centrifuged at 12,000 × *g* for 15 min, and then a 0.6 volume of isopropanol was added to precipitate the aqueous layer. Finally, the mixture was centrifuged at 12000 *g* for 15 min, and the pellet was washed with 70% (*v*/*v*) ethanol, dried at room temperature, and dissolved in 10 mM TE buffer (pH 8.0). To extract DNA from sediment samples, about 10 g of sediment was suspended in 13.5 ml of extraction buffer (1%CTAB, *w*/*v*), 100 mM Tris (pH 8.0), 100 mM NaH_2PO_4 (pH 8.00), 100 mM EDTA, 1.5 M NaCl). Then, 50 µl of 10 mg/ml proteinase K (Thermo Scientific, Massachusetts, United States) was added, and the mixture was incubated at 37°C for 30 min. After that, 1.5 ml of 20% SDS was added and incubated for 2 h at 65°C. The samples were centrifuged at 4,000 × *g* for 20 min at room temperature to separate the sediment remnants from the cell lysates. The cell lysates were mixed with an equal proportion of phenol, chloroform, and isoamyl alcohol (25:24:1) and were centrifuged at 16,000 × *g* for 5 min. Then, the DNA in the aqueous layer was precipitated by adding 0.6 volumes of isopropanol and recovered by centrifuging at 16,000 × *g* for 10 min. Finally, the pellet was washed with 70% (*v*/*v*) ethanol, dried by air, and dissolved in 10 mM TE buffer (pH 8.0). The quantification and quality control of extracted DNA were performed using a Nanodrop (Thermo Scientific, Massachusetts, United States) and gel electrophoresis with 0.8% agarose gel (Thermo Scientific, Massachusetts, United States).

Construction of the metagenomic library

The metagenomic libraries were constructed by the CopyControl™ Fosmid Library Production Kit (Epicentre, Madison, United States) according to the manufacturer's protocol. Briefly, the high molecular weight metagenomic DNA was sheared to the appropriate size by passing it through a 200-µl small-bore pipette tip a few times and then end-repaired using the CopyControl blunt-end repair kit (Epicentre, Madison, United States). The end-repaired DNA was loaded onto a 1% low-melting-point agarose gel for 16–20 h at 35 voltage in 1× TAE buffer. The DNA fragments that were run parallel to the 40 kb Fosmid control DNA were excised from the gel without UV light. The DNA from the excised gel was recovered using the GELase protocol (Epicentre, Madison, United States), followed by a conventional phenol:chloroform:isoamyl alcohol (24:24:1) extraction to remove the enzymes, and the DNA was precipitated using isopropanol. The resultant DNA pellet was resuspended in 10 mM TE (pH 8.0), and the yield and size of the DNA were validated by running an aliquot down the gel. The end-repaired DNA was ligated to the CopyControl pCC1FOS (Epicentre, Madison, United States) vector at a 10:1 vector-to-insert DNA ratio. The ligated DNA was then packaged into the MaxPlax lambda phage heads (Epicentre, Madison, United States). The lambda phage packaged DNA was then infected into *E. coli* cells (EPI100-T1R Plating Strain, Epicentre, Madison, United States), mixed 2–3 times by inverting the tubes and incubated for 30 min at room temperature. The infected cells were then plated on prewarmed Luria-Bertani (LB) agar plates (supplemented with 12.5 µg/ml Chloramphenicol) and incubated at 37°C for 16–20 h. After the quality control, single colonies were manually transferred to individual wells on a 384-well microtiter plate (Thermofisher, Madison, United States) with 60 µl LB medium supplemented with 12.5 µg/ml chloramphenicol and 20% glycerol. The library was duplicated from each master plate and kept at −80°C for further screening.

Functional screening of specific genes in the fosmid library

The library was replicated to LB agar plates supplemented with soluble starch (1%; Sigma-Aldrich, Missouri, United States), carboxyl methylcellulose (1%; CMC, Sigma-Aldrich, Missouri, United States), pectin (1%; Sigma-Aldrich, Missouri, United States), and xylan (1%; Sigma-Aldrich, Missouri, United States), to detect amylase, cellulase, pectinase, and xylanase activities, respectively. Whereas to detect β-glucosidase activity, LB agar plates were supplemented with esculin hydrate (0.1%; Sigma-Aldrich, Missouri, United States) and ferric ammonium citrate (0.25%; Sigma-Aldrich, Missouri, United States). In addition, LB agar plates were supplemented with chloramphenicol (12.5 µg/ml) and Autoinduction solution (0.2%; Epicentre, Madison, United States). Then, the plates were incubated at 37°C for 2–7 days. For the identification of cellulase and xylanase-positive clones, the method proposed by Teather and Wood (1982) was used, where the colonies were washed off the agar plates with ddH_2O to permit a homogeneous penetration of the staining dye into the medium. Thereafter, the agar plates were stained with 0.2% Congo red solution for 30 min. After the solution was poured off, the agar plates were de-stained up to 3 times for 30 min with 1 M NaCl. Positive clones were detected by forming a yellow halo against a red background. The β-glucosidase activity was detected according to Eberhart et al. (1964) method, where clones exhibiting a black halo around their colonies were selected as positive for β-glucosidase activities. Amylase activity was detected by staining the plates with KI/I_2 solution. A colorless halo surrounded positive colonies on a dark purple background (Sharma et al., 2010).

Fosmid DNA extraction and sequencing

A total of 22 fosmid clones with positive enzyme activities were selected, cultured and induced to a high copy number using the 500×Copy Control Fosmid Autoinduction Solution (Epicentre, Madison, United States) at 37°C overnight (16–20 h) with 12.5 μg/ml chloramphenicol and vigorous shaking (225–250 rpm). Fosmid DNA was extracted using a GenElute Plasmid Miniprep Kit (Sigma-Aldrich, Missouri, United States) according to the manufacturer's protocol. The quality of extracted DNA was checked using a Nanodrop and sent to BGI Genomics for whole-genome sequencing. The *E. coli* whole genome resequencing was performed using the paired-end 150 bp method using the DNBSEQ™ platform.

Bioinformatics analysis

De-novo assembly

An in-house workflow was developed to analyze the whole genome sequences of the fosmids.[1] Briefly, whole genome sequencing (WGS) raw reads Quality Check (QC) was performed with the FastQC tool (Andrews, 2010), and multiple samples were processed with MultiQC (Ewels et al., 2016). All reads from independent 22 fosmid clones were mapped to the *E. coli* reference genome (EPI100-T1R Plating Strain, Epicenter Biotechnologies) using Bowtie2 (Langmead and Salzberg, 2013) and reads were sorted with SAMtools (Danecek et al., 2021). Reads that did not map to the *E. coli* genome were further used for de-novo assembly with SPAdes v3.15.3 and metaplasmidspades (Bankevich et al., 2012). Further, the CopyControl pCC1FOS (Epicenter Biotechnologies) vector backbone sequences were removed from the assembled contigs. NCBI-Blast-v2.9.0+ and Bedtools-v2.27.1 were used for processing assemblies.

Gene prediction, taxonomy, and functional annotation

Functional annotation of the assembled fosmid contigs were performed using RASTtk (Brettin et al., 2015) webserver, and cross-validation of predicted coding DNA sequence (CDS) using TransDecoder-v5.5.0.[2] Then, carbohydrate-active enzymes (Cantarel et al., 2009) annotation was conducted using hmmscan (Version 3.3 b2) against CAZy database (version 2021). Kraken2 (version 2.0.8) (Wood et al., 2019) was applied for taxonomic sequence classification using the Minikraken2_v1_8GB database. Finally, KronaTools v2.7.1 (Ondov et al., 2011) was used to visualize taxonomies.

Preparation of cell culture for enzymatic assay

Among the enzymes screened, amylase, cellulase, and pectinase were selected based on their potential application in complex carbohydrate degradation and their enzymatic activity studied. These positive clones were preliminarily assessed based on their clearing zone diameter, and the top four clones in each enzyme were chosen for further characterization. Positive clones (pectinase, cellulase, and amylase) were inoculated in LB media (50 ml) containing chloramphenicol (12.5 μg/ml) and Autoinduction solution (0.2%), supplemented with 1% of their respective substrates (Pectin/carboxyl methylcellulose/soluble starch). Then, the inoculated media were incubated at 37°C, 200 rpm for 3–5 days, and after incubation, centrifuged at 5,000 × *g* and 4°C for 30 min. The supernatant (crude cell-free extract) was used as a crude enzyme cti fraction for further analysis.

Enzyme assays

Enzyme activity was measured following the dinitrosalicylic acid (DNS) method (Miller, 1959). The standard assay mixture contains 100 μl of the enzyme or crude cell-free extract and 250 μl of the substrate (1% in a final volume of 0.5 ml), and 150 μl McIlvaine buffer. Carboxymethyl cellulose (CMC), pectin, and soluble starch were used as substrates for cellulase, pectinase, and amylase, respectively. The mixture was incubated at 37°C for 15 min, then 750 μl DNS reagent was added, and the samples were boiled at 100°C for 15 min. After cooling down on the ice, the samples were centrifuged at 16,000 × *g* for 2 min to precipitate falling proteins. The samples were transferred to cuvettes, and absorbance was measured at 540 nm (Thermo Scientific). The pH range of the enzyme was determined by measuring standard assay activity between pH 7.0 and 10.5 using 50 mM of appropriate buffers. The temperature range of the enzyme activity was determined by assaying at temperatures between 30 and 75°C. The effect of salt on enzyme activities was investigated by incorporating 0-3M of NaCl into the reaction mixture.

Results

Construction and functional screening of metagenomic libraries

Metagenomic libraries with more than 21,000 clones were generated from three Ethiopian soda lakes (Table 1). At the time of sampling, the salinity of the lakes ranged from 3% (Lake Shala) to 15% (Lake Abijata) and pH from 9.3 (Lake Shala) to 10.0 (Lake Chitu). The number of clones picked from each sample site ranges from 1,440 (Lake Abijata) to 10,368 (Lake Shala; Table 1).

Among all the clones screened (>21,000) for the five hydrolytic enzymes, a total of 408 clones were positive for at least one of the hydrolytic enzymes tested (Figure 1). A relatively high number of clones (281 clones, 1.33% hit ratio) were positive for cellulase, followed by amylase (75 clones, 0.36% hit ratio),

1 https://github.com/gvarmaslu/WGS-fosmid-project
2 http://transdecoder.github.io

10.3389/fmicb.2022.1059061

β-glucosidase (20 clones, 0.1% hit ratio), pectinase (15 clones, 0.07% hit ratio) and 12 positives for xylanase (12 clones, 0.06% hit ratio; Table 2).

Analysis of fosmid insert sequences and detection of carbohydrate-active enzymes

A total of 22 clones that were positive for the enzymes mentioned above were selected and subjected to sequencing. After bioinformatics sequence analysis and assembly, the insert sizes were between 30,230 and 44,461 base pairs. Each library contained clones with average size inserts of approximately 35 kb, yielding approximately 0.74 GB of the total cloned genomic DNA per library. A total of 1,233 open reading frames (ORFs) were predicted from the fosmid clones (Table 3). Then, the carbohydrate-active enzyme (CAZy) database was used to annotate the predicted ORFs, resulting in 378 encoding genes with potential functions predicted (Supplementary Table 1). All the detected genes coding for CAZymes were further assigned to six functional classes: 10 Auxiliary Activities (AAs), 61 Carbohydrate-Binding Modules (CBMs), 24 Carbohydrate Esterases (CEs), 156 Glycoside Hydrolases (GHs), 118 Glycosyl transferases (GTs), and 9 Polysaccharide Lysases (PLs; Table 3).

TABLE 1 Physical parameters of the studied soda lakes of Ethiopia with the number of metagenomics libraries constructed.

Sample site	pH	Salinity (%)	Number of clones
Abijata	9.5	15	1,440
Chitu	10	6	9,216
Shala	9.3	3	10,368
	Total		21,024

Glycoside hydrolase enzymes

GHs were the most abundant class, representing 40% of the identified carbohydrate-degrading enzymes (Table 4; Supplementary Table 1). These GHs were categorized into 38 GH families. The most abundant GH families were GH2, GH3, GH5, GH12, GH13, and GH28. About 10% of the GH families belonged to the GH3 family, which encodes β-glucosidase (EC 3.2.1.21), and N-acetyl-β-D-glucosaminidases (EC 3.2.1.30). The GH5 family representing Cellulase (EC 3.2.1.4) were the second most abundant GH family, representing 8% of the total families. About 5% of the GH families were found to belong to the GH28, a family

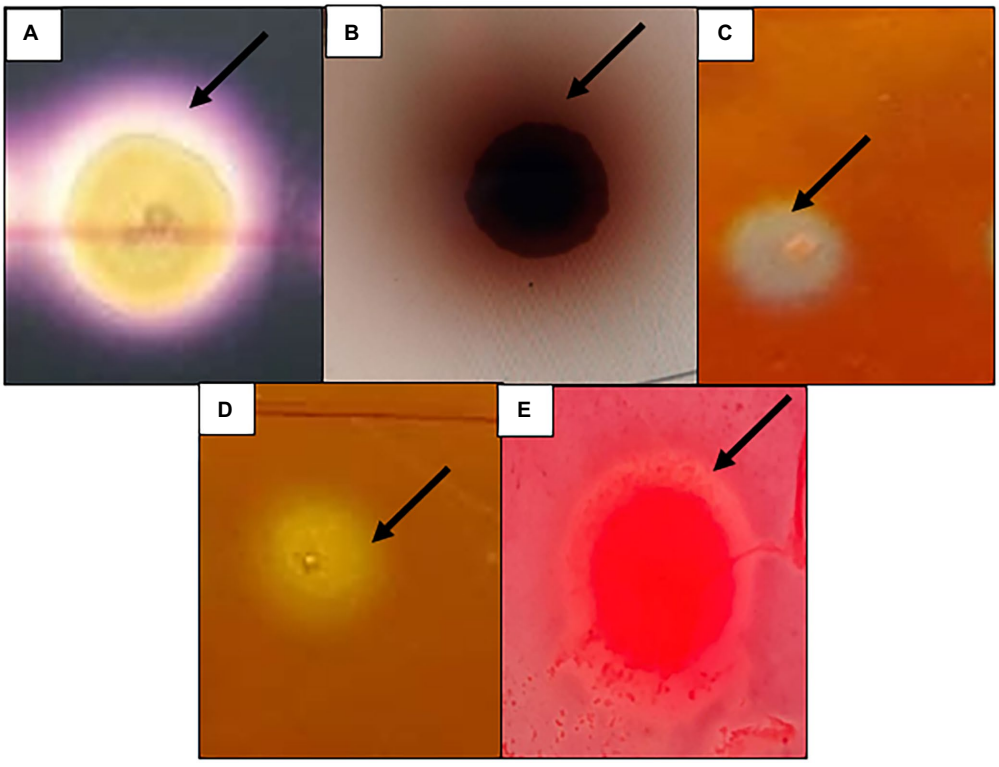

FIGURE 1
Functional screening of the metagenomics library constructed from Ethiopian soda lakes showing positive for **(A)** Amylase, **(B)** β-glucosidase, **(C)** Cellulase, **(D)** Pectinase, **(E)** Xylanase.

10.3389/fmicb.2022.1059061

that contains pectinase polygalacturonase enzymes. Starch degrading enzymes such as alpha-amylases (GH13) were also abundant (4%; Figure 2).

Tracking the microbial sources of the annotated GH genes

The microbial source of the annotated GH genes were predicted, and more than 73% of the genes aligned to bacterial sources. However, there were no organism hits for about 27% of the annotated GH genes. Most of the bacterial genes at the class level belonged to the *Gammaproteobacterial* and at the genera level to *Halomonas* (Supplementary Figure 1).

TABLE 2 Hit ratios of the screened hydrolytic enzymes.

Enzyme	Hit ratio
Amylase	1:280
B-glucosidase	1:1051
Cellulase	1: 75
Pectinase	1:1402
Xylanase	1: 1752

Expression and characterization of selected enzymes

Cellulase

Further studies on the effect of pH, temperature, and salt concentration on the cellulase activities of the selected clones (F8, F9, F17, and F22) showed that the clone F8 had its optimum cellulase activity at pH 9.5, whereas clones F17 and F9 showed the optimum activity at pH 8.5 (Figure 3A). All clones showed their optimum cellulase activity at 37°C (Figure 3B). The optimum cellulase activities for all clones were at 0M NaCl, while the clone F17 maintained 75% of the cellulase activity up to 3 M salt concentration (Figure 3C).

Amylase

Studies on the effect of pH, temperature and salinity on the amylase activity of four screened fosmid clones (F13, F15, F17, and F22) showed that all four clones, except for F22, had the maximum amylase activity at pH 8.5 (Figure 4A), and that the clones F17, F13, and F15 showed the optimum amylase activity at 55, 50, and 45°C, respectively (Figure 4B). Furthermore, these amylase-positive clones showed increasing relative amylase activity with increased salinity (Figure 4C).

TABLE 3 The DNA Insert size of each fosmid in base pairs, the number of ORFs, and detected CAZyme classes.

Fosmid clones	Contig size (bp)	GC (%)	ORFs	AAs	CBMs	CEs	GHs	GTs	PL	Total CAZYmes
F1	39,939	59.81	77	0	0	5	5	0	0	10
F2	33,919	44.52	34	0	0	0	10	17	0	28
F3	30,230	53.28	34	0	1	0	0	0	0	1
F4	43,585	63.87	75	0	1	1	2	5	0	9
F6	31,316	52.00	36	2	15	4	27	11	1	60
F8	36,493	47.93	39	0	3	1	11	9	1	25
F9	36,313	57.36	67	1	2	1	7	4	2	17
F10	44,461	64.38	79	0	1	1	5	2	0	10
F11	31,461	64.19	72	0	0	0	1	0	0	1
F13	37,445	65.37	83	0	2	1	6	4	0	13
F14	36,784	60.12	68	0	1	2	5	6	0	14
F15	42,189	65.68	87	1	2	0	4	6	3	16
F16	33,691	49.63	39	0	1	1	4	1	0	7
F17	35,026	58.60	58	0	5	2	7	4	0	18
F18	35,903	56.98	68	0	3	0	8	4	1	16
F19	35,357	51.12	44	0	0	1	9	7	0	17
F20	31,419	65.25	72	0	3	0	3	7	0	13
F21	33,565	49.65	39	0	1	1	4	7	0	13
F22	35,225	52.03	40	1	3	4	14	6	0	28
F23	36,297	47.81	28	1	15	1	18	6	1	42
F24	38,076	53.27	40	0	0	0	3	9	0	16
F25	30,893	52.05	54	0	0	1	2	2	0	5
Total			1,233	10	61	27	156	117	9	378

ORFs, open reading frames; AAs, auxiliary activities; CBMs, carbohydrate-binding modules; CEs, carbohydrate esterases; GHs, glycoside hydrolases; GTs, Glycosyl transferases; PLs, polysaccharide lyases

TABLE 4 Carbohydrate degrading enzymes detected in the fosmid clones (the complete list in Supplementary Table).

GH family	Fosmid	Hit accession	Identity (%)	Predicted enzyme
GH3	F17	ATH78710.1	96.8	β-glucosidase
GH103	F24	AVI63997.1	86.4	Peptidoglycan lytic
	F11	AXY42412.1	85.5	transglycosylase
GH13	F15	AHO18837.1	69.0	α-amylase
GH73	F19	AZU02762.1	51.9	Lysozyme
GH47	F13	CBX90714.1	47.8	α-mannosidase
GH2	F15	ACR62057.1	47.5	β-galactosidase
GH3	F9	SQK97389.1	46.3	β-glucosidase
GH13	F13	QTJ41571.1	46.0	α-amylase
GH78	4F4	ACT97502.1	43.0	α-L-rhamnosidase
GH43	F14	BBI53471.1	42.0	β-xylosidase
GH3	F22	SQK97389.1	40.7	β-glucosidase
	F6	SQK97389.1	40.5	
GH5	F8	QXC62151.1	40.4	Cellulase
GH38	F1	QJS43890.1	40.1	α-mannosidase
GH140	F22	QJW98933.1	39.6	β-1,2-apiosidase
	F6			
GH53	F22	QKX57828.1	39.5	Endo-β-1,4-
GH53	F6			galactanase
GH55	F25	ATI54262.1	39.4	Exo-β-1,3-glucanase
GH5	F25	QXC62151.1	39.4	Cellulase
GH103	F20	BCX45957.1	38.1	Peptidoglycan lytic
				transglycosylase
GH92	F17	AGB27560.1	38.1	α-1,2-mannosidase
GH51	F17	QKX56076.1	37.9	Endoglucanase
GH5	F10	QXC62151.1	37.6	Cellulase
GH51	F19	QKX56076.1	37.4	Endoglucanase
GH55	F14	AOW25396.1	36.7	Exo-β-1,3-glucanase
GH5	F23	QXC62151.1	36.0	Cellulase
GH99	F13	CAZ29389.1	36.0	α-1,2-mannosidase
GH3	F10	SQK97389.1	35.8	β-glucosidase
GH37	F19	AWO98658.1	35.4	α-trehalase
GH5	F9	QXC62151.1	35.4	Cellulase
GH23	F9	APT58734.1	35.4	Lysozyme
GH51	F8	QKX56076.1	35.0	Endoglucanase

EC, Enzyme commission number.

Pectinase

Studies on the pectinase activity of four fosmid clones (F2, F6, F18, and F23) showed that the clones F18 and F23 had their optimum pectinase activity at pH 9.5 (Figure 5A) and that all four clones had optimum pectinase activity at 65°C (Figure 5B). When different salt concentrations were added, clone F18 showed enhanced pectinase activity, while others retained more than 75% of the pectinase activity up to 3M salt concentrations (Figure 5C).

Discussion

Despite the potential of soda lakes as sources of unique extremozymes, only a few enzymes have so far been identified from these ecosystems. Previously, carbohydrate-degrading enzymes, i.e., xylanase (Gessesse and Mamo, 1998), amylases (Martins et al., 2001), and cellulase (Minig et al., 2009), have been discovered from Ethiopian soda lakes. However, these studies have been based on conventional culture-dependent approaches, in which most microorganisms are unable to grow, thereby limiting the identification of novel enzymes (Culligan et al., 2014). In this study of the Ethiopian soda lakes, we used a functional metagenomics approach to discover carbohydrate-degrading enzymes (CAZymes) to circumvent this limitation.

The DNA extracted from the Ethiopian soda lakes was used to construct metagenomic libraries, which generated clones that produced carbohydrate-degrading enzymes. The hit ratios obtained for the hydrolytic enzymes, especially cellulase and amylase, were high (1:75 and 1:280, respectively) compared to many previous reports in other environments (Ferrer et al., 2012; Nguyen et al., 2012; Liu et al., 2015; Wang et al., 2015; Maruthamuthu et al., 2016). The functional screening approach has previously been reported to be superior in finding genes producing functional products, which increases the potential to uncover entirely new classes of enzymes that lack homologies to previously identified sequences (Culligan et al., 2014; Berini et al., 2017a). The high hit ratios of this study might largely be attributed to the source of the metagenome, i.e., the abundance and diversity of microorganisms producing the different carbohydrate-degrading enzymes in the Ethiopian soda lakes. The Ethiopian soda lakes are characterized by high primary production due to the presence of a dense population of haloalkaliphilic cyanobacteria (Wood et al., 1984; Grant and Sorokin, 2011), which in turn support a diverse group of heterotrophic prokaryotes (Lanzén et al., 2013; Grant and Jones, 2016). Since some of the heterotrophic microorganisms are involved in nutrient recycling released by dead cells, many of them are expected to produce different hydrolytic enzymes, including those involved in the hydrolysis of complex carbohydrates, such as cellulose, hemicellulose, pectin and starch (Jones and Grant, 1999; Sorokin and Kuenen, 2005; Sorokin et al., 2014). The presence of a diverse group of heterotrophs producing the above enzymes might, in turn, lead to an observed high hit ratio.

The complete breakdown of lignocellulosic polymers requires the synergistic action of multiple CAZymes (Bredon et al., 2018; Liew et al., 2022), i.e., mainly consisting of the Glycoside Hydrolases (GHs) families such as cellulase, xylanase, hemicellulase, and pectinase (Rastogi and Shrivastava, 2020; Shrivastava, 2020). About 41% of the CAZymes database annotated genes obtained from the Ethiopian soda lakes have been shown to belong to GHs. GHs are the best-described families of carbohydrate-degrading enzymes due to their high prevalence and broad distribution across genomes (Berlemont and Martiny, 2015; Stewart et al., 2018; Wang et al., 2019). Microorganisms in soda lakes degrade complex polysaccharides, releasing short metabolizable oligosaccharides into the lake environment. Detecting multiple GH enzymes, including GH5, GH3, GH13, GH43, and GH28, indicates the relevance of these enzymes to the ecosystems of the soda lakes and their carbon cycle. The short

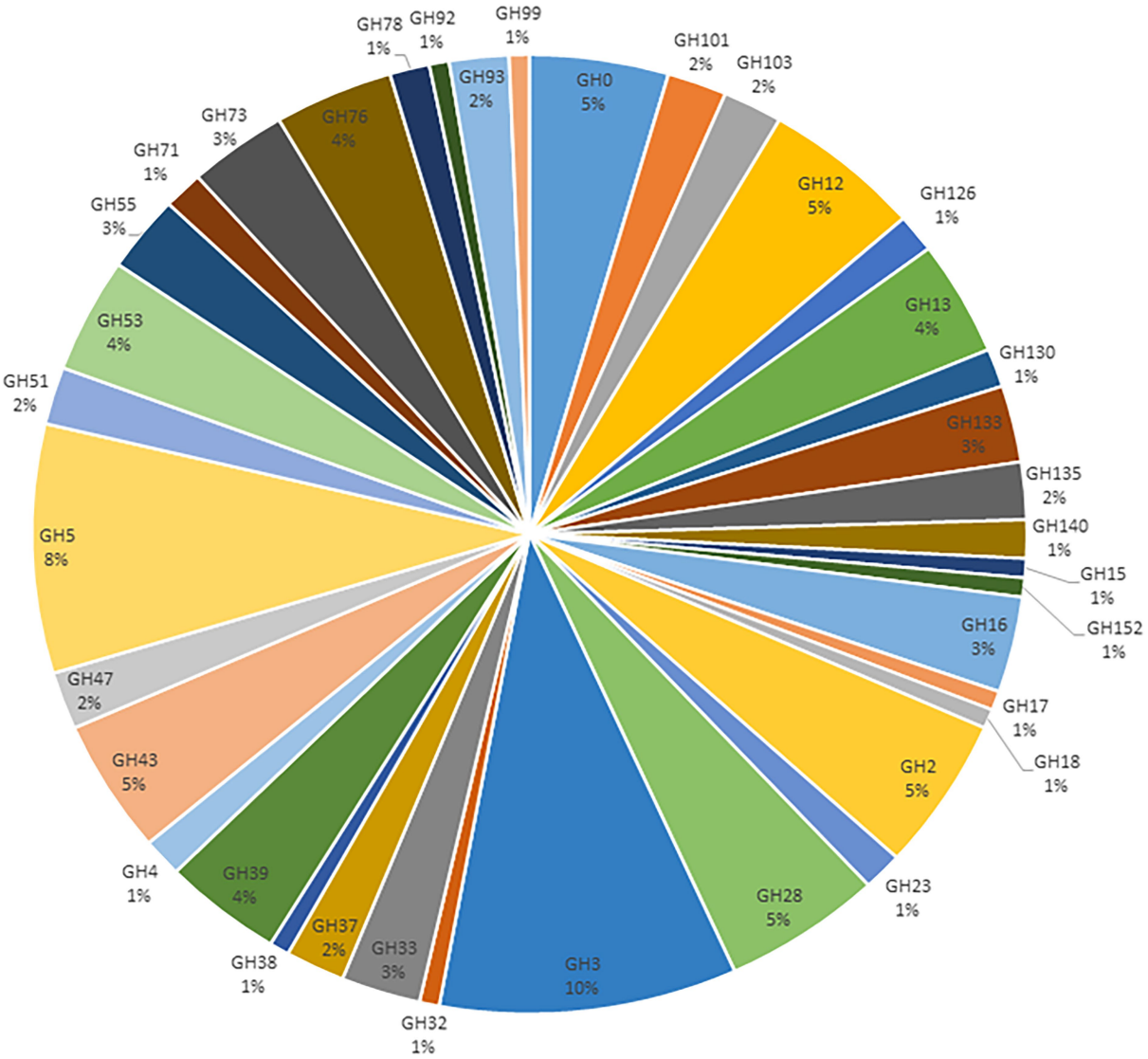

FIGURE 2
Classification of the annotated GH families from the metagenomics libraries of Ethiopian soda lakes.

metabolizable oligosaccharides produced are fed into the core carbohydrate metabolic pathways, providing energy and precursor metabolites for other pathways (Salam, 2018).

Among the components of lignocellulosic biomass, cellulose is the most prevalent biopolymer on the planet (Lakhundi et al., 2015). In nature, microorganisms involved in nutrient recycling in the ecosystem, including soda lakes, enzymatically hydrolyze cellulose to its monomeric unit and use it as a nutrient for growth. Different cellulase enzymes are required to achieve complete hydrolysis of cellulose, the main ones being endoglucanases and β-glucosidases (Tiwari et al., 2016). In this study, about 10 and 8% of the GHs families belonged to GH3 and GH5, respectively. The GH3 and GH5 families possess β-glucosidase (EC 3.2.1.21) and endo-1,4-glucanase (EC 3.2.1.4) activities, respectively. The GH5 enzymes are involved in the hydrolysis of cellulose into cellobiose (Wang et al., 2019), while GH3 enzymes break down cellobiose into glucose (Agirre et al., 2016). Members of the GH5 superfamily are extensively dispersed across archaea, bacteria, and eukaryotes, and various enzyme functions related to biomass conversion have been discovered in this superfamily (Mohammadi et al., 2022). In cellulose biomass degradation, β-glucosidase (GH3) activity is regarded as the rate-limiting factor, reducing cellobiose inhibition on endoglucanases and permitting more effective cellulolytic enzyme action (Tiwari et al., 2017; Zhang et al., 2017).

Among the hemicellulase enzymes, GH43 was the most abundant family in the present study. Previous studies have reported the enzyme activities of GH43 to be β-xylosidase (EC 3.2.1.37), xylanase (EC 3.2.1.8) and exo-β-1,3-galactanase (EC 3.2.1.145; (Shrivastava, 2020), which are enzymes contributing to

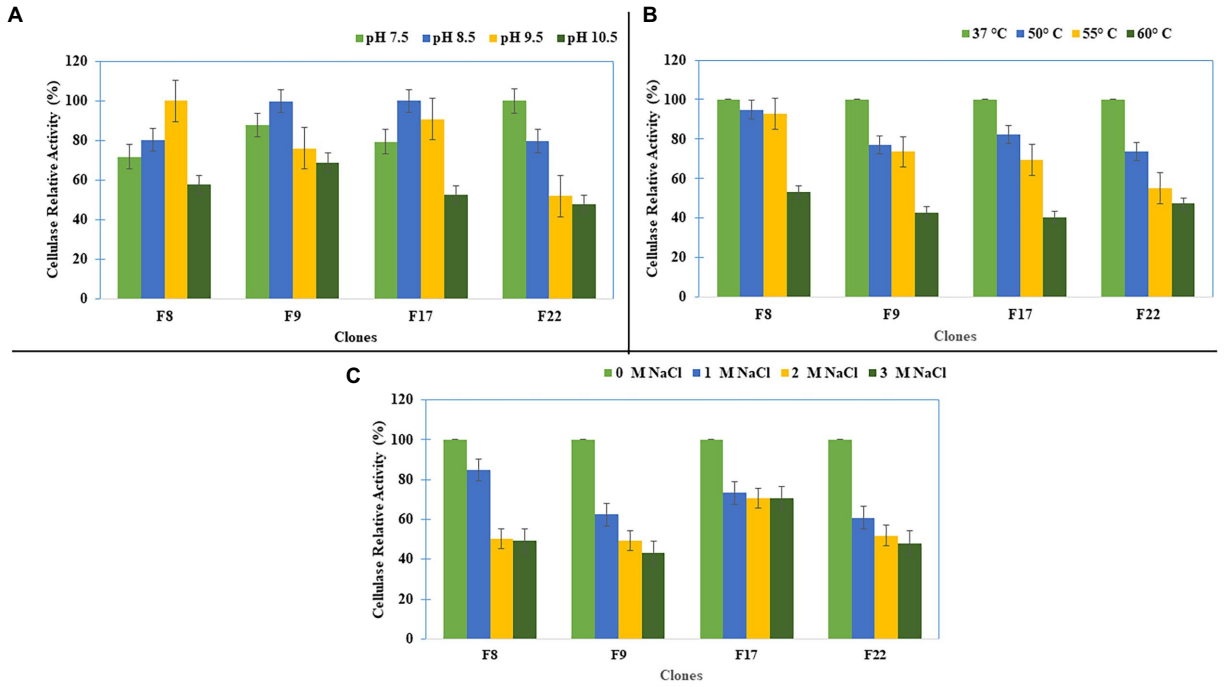

FIGURE 3
Cellulase Activity characterization of the clones for **(A)** pH, **(B)** Temperature, and **(C)** Salt concentration.

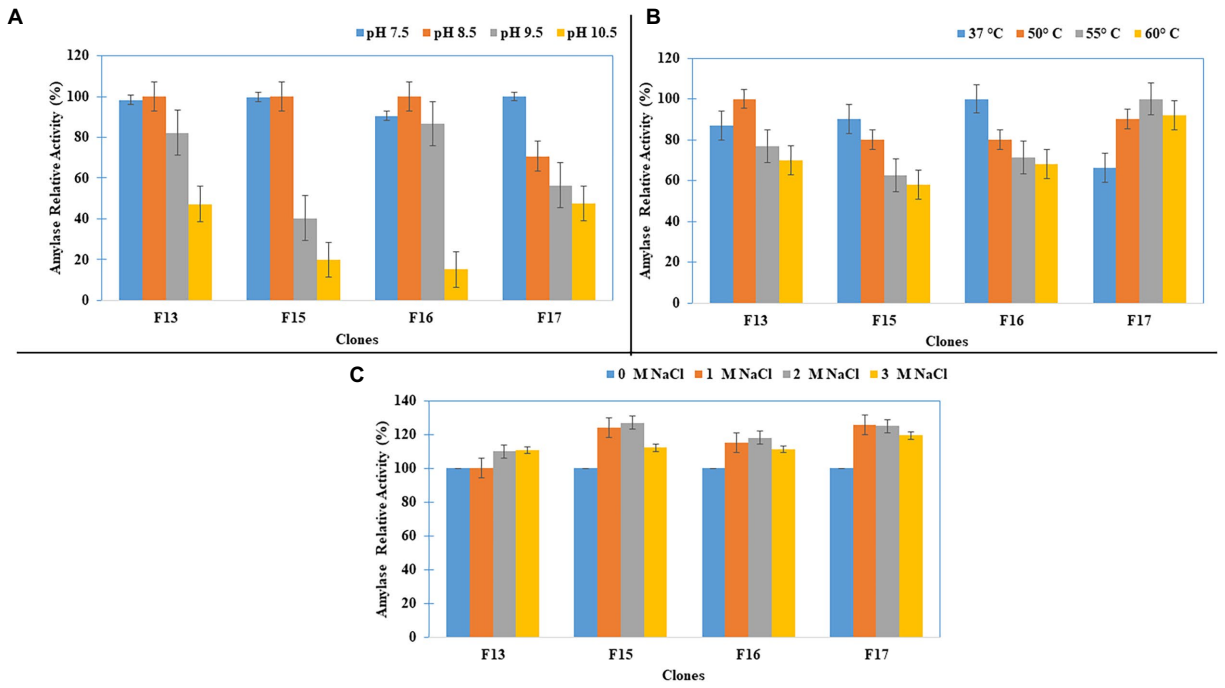

FIGURE 4
Amylase Activity characterization of the clones for **(A)** pH, **(B)** Temperature, and **(C)** Salt concentration.

the degradation of xylan (the main component of hemicellulose) to xylose monomers (Houfani et al., 2021). One major challenge in producing biofuels from lignocellulosic biomass by enzymatic hydrolysis is that hemicellulose and lignin create a protective barrier surrounding the cellulose. Furthermore, the crystalline form of cellulose renders it insoluble and resistant to enzyme

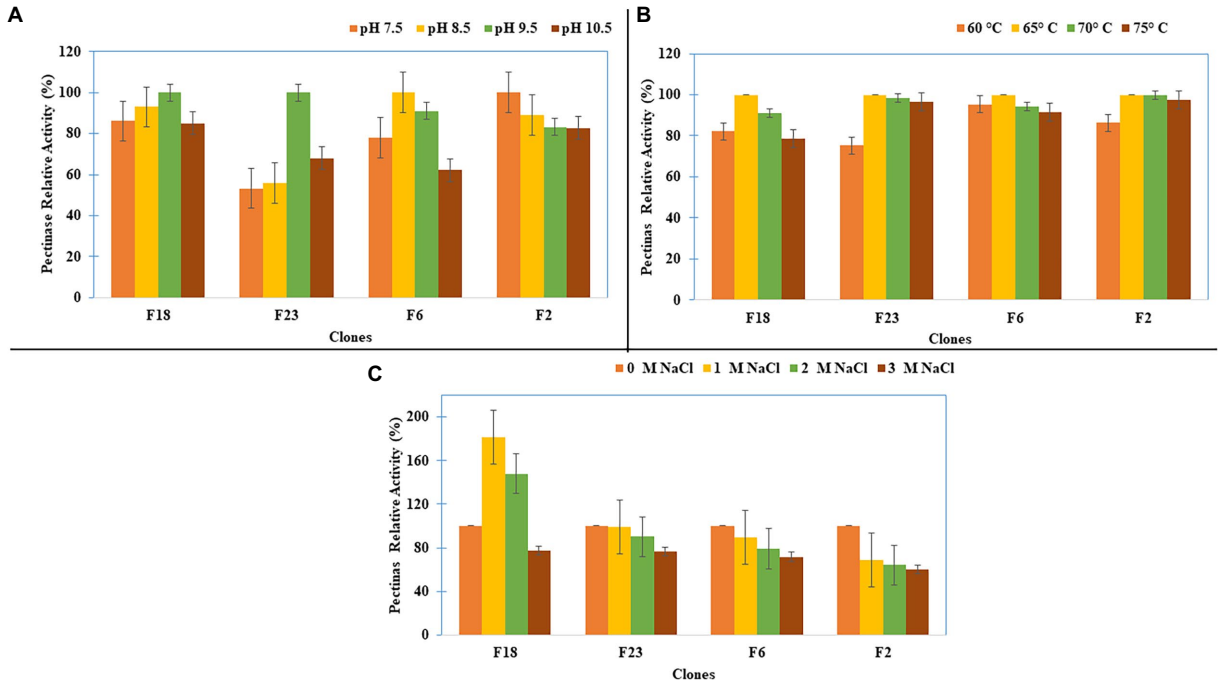

FIGURE 5
Pectinase Activity characterization of the clones for **(A)** pH, **(B)** Temperature, and **(C)** Salt concentration.

degradation (Zoghlami and Paës, 2019; Reichart et al., 2021). Thus, the removal of hemicellulose may result in increased access of cellulase to cellulose (Peng et al., 2015). Previous studies have shown that for hemicellulose degradation, the numerous GHs enzymes operating at various levels of the hemicellulolytic matrix are needed (Horn et al., 2012; Andlar et al., 2018). In this context, the breakdown of hemicelluloses by a monofunctional hemicellulase enzyme is uneconomical. However, the multifunctional hemicellulase activity of GH43 (primarily in the xylan component) can minimize enzyme costs and is essential for the complete hydrolysis of lignocellulosic biomass (Limsakul et al., 2021).

About 5% of GHs belonged to the family of GH28. The GH28 families have been shown to encode polygalacturonase, which acts on the 1,4-glycosidic bond, and plays a crucial part in pectin digestion (Zhao et al., 2014). The architectural characteristics of cell walls, which have been represented as a cellulose-hemicellulose network embedded in a pectin matrix, imply that pectins may hide cellulose and/or hemicellulose, preventing degradative enzymes from attacking them (Xiao and Anderson, 2013). Thus, pectin degradation is needed for the complete degradation of lignocellulose biomass. A recent study has shown that some haloalkaliphile *Bacteroidota* and *Clostridia* from soda lakes utilize pectin as a substrate (Sorokin et al., 2014).

Furthermore, approximately 4% of the GHs in this investigation belonged to GH13, which encodes amylases. The Ethiopian soda lakes are known to have one of the highest primary productivity of any natural habitat due to the thick biomass of cyanobacteria (Faris, 2017), which frequently accumulate starch (10–50%) as part of their biomass (Möllers et al., 2014). Therefore, these heterotrophic microorganisms are known to produce abundant hydrolytic enzymes, such as amylases, to allow the breakdown of starch (Sorokin et al., 2014).

Soda lakes are a unique source of microorganisms that thrive in high alkalinity and salinity (Sorokin et al., 2014). These microorganisms produce either haloalkaliphilic or haloalkali-tolerant hydrolytic enzymes. The haloalkaliphilic enzymes usually show optimal activity in high alkaline and saline ranges. On the other hand, the haloalkali-tolerant enzymes may work best at a neutral pH and without salt. Still, these enzymes are active and stable in the high alkalinity and salinity range (DasSarma and DasSarma, 2015). The cellulases obtained in this study were active and stable in alkaline conditions, high temperatures and salt concentrations, indicating these enzymes are haloalkali-tolerant. This is contrary to the majority of reported cellulases, which demonstrated limited activity in these multi-extreme circumstances, such as in the presence of alkaline and salinity, and just a few alkalophilic and halotolerant cellulases have been identified (Zhao et al., 2012; Garg et al., 2016). The conversion of lignocellulosic biomass usually occurs at high temperatures in the presence of alkaline conditions (Zhu et al., 2020). The production of salts arises from the neutralization of these alkalines. These salts must be eliminated, which consumes tons of water and energy, for subsequent processes to continue. However, these extreme

conditions affect the activity, and the stability of most known enzymes could be seriously affected (Sweeney and Xu, 2012). Therefore, enzymes that are stable in these extreme reaction conditions and in the presence of salts or tolerant to them are in great demand during downstream processes. Thus, the halo- and alkali-stable cellulases and hemicellulases identified in this study have the potential to hydrolyze lignocellulosic biomass for different industrial applications efficiently. In addition, the halotolerant nature of these enzymes offers an additional advantage because of their resistance to inactivation by salt residues that may result from pretreatment procedures (Zhang et al., 2011).

Furthermore, the biochemical characterization of the studied pectinase also showed high performance under alkaline, thermophilic, and halophilic conditions. There are several reports on alkaline and thermostable pectinase enzymes from various geographic locations and sources, particularly from agro- and industrial-wastes (Khatri et al., 2015; Oumer and Abate, 2017; Yu et al., 2017; Thakur et al., 2021). Regarding soda lakes, only two occurrences of pectin breakdown have thus far been described, both of which describe unique species of the phylum *Bacteroidota* belonging to the genera *Alkaliflexus* and *Natronoflexus* (Sorokin et al., 2014). At the same time, these microorganisms are low-salt tolerant saccharolytic fermentative alkaliphiles capable of hydrolyzing pectin. Thus, the poly-extreme nature of the pectinases in this study would make them ideal candidates for various industrial applications, particularly biomass degradation, retting and degumming of plant fibers, coffee and tea fermentation, and bio-scouring of cotton, all of which require extremes of temperature, pH, and ionic strength.

Halotolerant α-amylases have received considerably less consideration. However, most are thermostable and generate oligosaccharides in low-water or nonaqueous solvents, where hydrolytic processes are blocked (Masasa et al., 2022). This study's amylases had optimum activity in the alkalinity range and at high temperatures. In addition, salinity enhanced the amylase activity of some clones, suggesting that these amylases are poly-extremophilic. Previously, haloalkaliphilic amylases were reported from various environments (Chakraborty et al., 2011; Moshfegh et al., 2013), including soda lakes in Ethiopia (Martins et al., 2001); however, the vast majority of these studies were from bacterial origins. Polyextremophilic α-amylase are extremely useful for the textile, food, brewing, and distilling industries, as has been argued in previous publications (Patel and Saraf, 2015).

In this study, most of the GH genes identified were found to likely originate from bacteria belonging to the genus of *Halomonas,* which corresponds to *Halomonas* as one of the most abundant genera in our previous work on the microbial diversity of Ethiopian lakes using amplicon metagenomics (Jeilu et al., 2022). *Halomonas* have, in previous investigations, been reported to be one of the most abundant prokaryotes in soda lakes (Humayoun et al., 2003; Dimitriu et al., 2008; Asao et al., 2011; Lanzén et al., 2013; Sorokin et al., 2014), responsible for the biogeochemical cycling and the immediate degradation of organic matter produced by autotrophic bacteria like *cyanobacteria* (Jones and Grant, 1999; Sorokin et al., 2014). Thus, we anticipate that *Halomonas* would generate a variety of hydrolytic enzymes, such as those necessary for the hydrolysis of complex polysaccharides, including cellulose, hemicellulose, pectin, and starch, which has also been indicated in a previous study (Tahrioui et al., 2013).

This study identified novel halo-alkaline and thermostable carbohydrate-degrading enzymes with potential applications in lignocellulosic biomass degradation. In order to use these enzymes in biofuel industrial applications, additional extensive molecular cloning, purification, and characterization studies are needed.

Conclusion

Enzymes from halophiles and alkaliphiles are the most promising for biofuel generation and other industrial processes due to their inherent salt tolerance and thermal and alkaline stability. Soda lakes, in this aspect, are a one-of-a-kind source of extremophiles capable of harboring enzymes (extremozymes) that are active at both high pH and salinity. However, there is a scare of reports on searching CAZymes using culture-independent approaches from soda lakes. The present study has revealed the potential of functional metagenomics for exploiting the abundant genetic resources in uncultured microorganisms from extreme environments. Moreover, this study identified multiple families of GHs, indicating that the Ethiopian soda lakes constitute a unique biological niche for identifying novel CAZymes for applications in complete lignocellulose biomass degradations. Furthermore, many reported GH enzymes originated from mesophilic microorganisms where optimal activity and stability were around neutral pH and in the absence of salt. However, the biochemical characterization of the amylase, pectinase, and cellulase enzymes in this work shows that these enzymes are halo-alkaline and thermally stable. These properties strongly indicate the enzymes' potential for use in various industrial processes, particularly biorefinery for lignocellulose biomass conversion.

Data availability statement

The data presented in the study are deposited in the NCBI repository, accession number PRJNA799030. This data can be found at: https://www.ncbi.nlm.nih.gov/sra/PRJNA799030.

Author contributions

OJ, AS, EA, EJ, and AG: designed the experiment and contributed to the study's conception and design. OJ: data collection and analysis, wrote the first draft of the manuscript. All

authors contributed to the article and approved the submitted version.

Funding

This study was financed by the Swedish International Development Cooperation Agency (SIDA) through the research and training grant awarded to Addis Ababa University and the Swedish University of Agricultural Sciences (AAU-SLU Biotech; https://sida.aau.edu.et/index.php/biotechnology-phdprogram).

Acknowledgments

The authors thank the Ethiopian Wildlife Conservation Authority for providing an access permit to sample from the three soda lakes. We would also like to thank the Ethiopian Biodiversity Institute and National Soil Testing Center, Ministry of Agriculture of Ethiopia, for granting permission for genetic material transfer. We also thank Ganapathi Varma Saripella for cooperating in the bioinformatics analysis and designing the workflow.

Conflict of interest

The authors declare that the research was conducted in the absence of any commercial or financial relationships that could be construed as a potential conflict of interest.

Publisher's note

All claims expressed in this article are solely those of the authors and do not necessarily represent those of their affiliated organizations, or those of the publisher, the editors and the reviewers. Any product that may be evaluated in this article, or claim that may be made by its manufacturer, is not guaranteed or endorsed by the publisher.

Supplementary material

The Supplementary material for this article can be found online at: https://www.frontiersin.org/articles/10.3389/fmicb.2022.1059061/full#supplementary-material

References

Abdel-Hamid, A. M., Solbiati, J. O., and Cann, I. K. O. (2013). Insights into lignin degradation and its potential industrial applications. *Adv. Appl. Microbiol.* 82, 1–28. doi: 10.1016/B978-0-12-407679-2.00001-6

Agirre, J., Ariza, A., Offen, W. A., Turkenburg, J. P., Roberts, S. M., McNicholas, S., et al. (2016). Three-dimensional structures of two heavily N-glycosylated Aspergillus sp. family GH3 β-D-glucosidases. *Acta Crystallogr. Sect. D Struct. Biol.* 72, 254–265. doi: 10.1107/S2059798315024237

Andlar, M., Rezić, T., Marđetko, N., Kracher, D., Ludwig, R., and Šantek, B. (2018). Lignocellulose degradation: an overview of fungi and fungal enzymes involved in lignocellulose degradation. *Eng. Life Sci.* 18, 768–778. doi: 10.1002/elsc.201800039

Andrews, S. (2010). FastQC-A quality control tool for high throughput sequence data. Available at: http://www.bioinformatics.babraham.ac.uk/projects/fastqc/. BabrahamBioinforma (Accessed November 2021)

Antony, C. P., Kumaresan, D., Hunger, S., Drake, H. L., Murrell, J. C., and Shouche, Y. S. (2013). Microbiology of Lonar Lake and other soda lakes. *ISME J.* 7, 468–476. doi: 10.1038/ismej.2012.137

Anwar, Z., Gulfraz, M., and Irshad, M. (2014). Agro-industrial lignocellulosic biomass a key to unlock the future bio-energy: A brief review. *J. Radiat. Res. Appl. Sci.* 7, 163–173. doi: 10.1016/j.jrras.2014.02.003

Ariaeenejad, S., Abdollahzadeh Mamaghani, A. S., Maleki, M., Kavousi, K., Foroozandeh Shahraki, M., and Hosseini Salekdeh, G. (2020). A novel high performance in-silico screened metagenome-derived alkali-thermostable endo-β-1,4-glucanase for lignocellulosic biomass hydrolysis in the harsh conditions. *BMC Biotechnol.* 20:56. doi: 10.1186/s12896-020-00647-6

Asao, M., Pinkart, C. H., and Madigan, M. T. (2011). Diversity of extremophilic purple phototrophic bacteria in soap Lake, a Central Washington (USA) soda Lakee. *Environ. Microbiol.* 13, 2146–2157. doi: 10.1111/j.1462-2920.2011.02449.x

Bankevich, A., Nurk, S., Antipov, D., Gurevich, A. A., Dvorkin, M., Kulikov, A. S., et al. (2012). SPAdes: A new genome assembly algorithm and its applications to single-cell sequencing. *J. Comput. Biol.* 19, 455–477. doi: 10.1089/cmb.2012.0021

Baruah, J., Nath, B. K., Sharma, R., Kumar, S., Deka, R. C., Baruah, D. C., et al. (2018). Recent trends in the pretreatment of lignocellulosic biomass for value-added products. *Front. Energy Res.* 6, 1–19. doi: 10.3389/fenrg.2018.00141

Ben Hmad, I., and Gargouri, A. (2017). Neutral and alkaline cellulases: production, engineering, and applications. *J. Basic Microbiol.* 57, 653–658. doi: 10.1002/jobm.201700111

Berini, F., Casciello, C., Marcone, G. L., and Marinelli, F. (2017a). Metagenomics: novel enzymes from non-culturable microbes. *FEMS Microbiol. Lett.* 364, 1–19. doi: 10.1093/femsle/fnx211

Berini, F., Presti, I., Beltrametti, F., Pedroli, M., Vårum, K. M., Pollegioni, L., et al. (2017b). Production and characterization of a novel antifungal chitinase identified by functional screening of a suppressive-soil metagenome. *Microb. Cell Factories* 16:16. doi: 10.1186/s12934-017-0634-8

Berlemont, R., and Martiny, A. C. (2015). Genomic potential for polysaccharide deconstruction in bacteria. *Appl. Environ. Microbiol.* 81, 1513–1519. doi: 10.1128/AEM.03718-14

Bredon, M., Dittmer, J., Noël, C., Moumen, B., and Bouchon, D. (2018). Lignocellulose degradation at the holobiont level: teamwork in a keystone soil invertebrate 06 biological sciences 0605 microbiology. *Microbiome* 6, 1–19. doi: 10.1186/s40168-018-0536-y

Brettin, T., Davis, J. J., Disz, T., Edwards, R. A., Gerdes, S., Olsen, G. J., et al. (2015). RASTtk: A modular and extensible implementation of the RAST algorithm for building custom annotation pipelines and annotating batches of genomes. *Sci. Rep.* 5, 1–6. doi: 10.1038/srep08365

Cabrera, M. Á., and Blamey, J. M. (2018). Biotechnological applications of archaeal enzymes from extreme environments. *Biol. Res.* 51:37. doi: 10.1186/s40659-018-0186-3

Cantarel, B. I., Coutinho, P. M., Rancurel, C., Bernard, T., Lombard, V., and Henrissat, B. (2009). The carbohydrate-active EnZymes database (CAZy): an expert resource for glycogenomics. *Nucleic Acids Res.* 37, D233–D238. doi: 10.1093/nar/gkn663

Chakraborty, S., Khopade, A., Biao, R., Jian, W., Liu, X. Y., Mahadik, K., et al. (2011). Characterization and stability studies on surfactant, detergent and oxidant stable α-amylase from marine haloalkaliphilic *Saccharopolyspora* sp. A9. *J. Mol. Catal. B Enzym.* 68, 52–58. doi: 10.1016/j.molcatb.2010.09.009

Collins, T., Gerday, C., and Feller, G. (2005). Xylanases, xylanase families and extremophilic xylanases. *FEMS Microbiol. Rev.* 29, 3–23. doi: 10.1016/j.femsre.2004.06.005

Coughlan, L. M., Cotter, P. D., Hill, C., and Alvarez-Ordóñez, A. (2015). Biotechnological applications of functional metagenomics in the food and pharmaceutical industries. *Front. Microbiol.* 6:672. doi: 10.3389/fmicb.2015.00672

Culligan, E. P., Sleator, R. D., Marchesi, J. R., and Hill, C. (2014). Metagenomics and novel gene discovery: promise and potential for novel therapeutics. *Virulence* 5, 399–412. doi: 10.4161/viru.27208

Danecek, P., Bonfield, J. K., Liddle, J., Marshall, J., Ohan, V., Pollard, M. O., et al. (2021). Twelve years of SAMtools and BCFtools. *Gigascience* 10, 1–4. doi: 10.1093/gigascience/giab008

DasSarma, S., and DasSarma, P. (2015). Halophiles and their enzymes: negativity put to good use. *Curr. Opin. Microbiol.* 25, 120–126. doi: 10.1016/j.mib.2015.05.009

Dimitriu, P. A., Pinkart, H. C., Peyton, B. M., and Mormile, M. R. (2008). Spatial and temporal patterns in the microbial diversity of a meromictic soda Lake in Washington state †. *Appl. Environ. Microbiol.* 74, 4877–4888. doi: 10.1128/AEM.00455-08

Eberhart, B., Cross, D. F., and Chase, L. R. (1964). β-Glucosidase system of Neurospora crassa. I. BETA-Glucosidase and cellulase activities of mutant and wild-type strains. *J Bacteriol.* 87, 761–770. doi: 10.1128/jb.87.4.761-770.1964

Ellilä, S., Bromann, P., Nyyssönen, M., Itävaara, M., Koivula, A., Paulin, L., et al. (2019). Cloning of novel bacterial xylanases from lignocellulose-enriched compost metagenomic libraries. *AMB Express* 9:124. doi: 10.1186/s13568-019-0847-9

Ewels, P., Magnusson, M., Lundin, S., and Käller, M. (2016). MultiQC: summarize analysis results for multiple tools and samples in a single report. *Bioinformatics* 32, 3047–3048. doi: 10.1093/bioinformatics/btw354

Faris, G. (2017). Threats, use and management interventions for restoration of Lake Chitu west Arsi. *Ethiopia. Am. J. Biol. Environ. Stat.* 3:1. doi: 10.11648/j.ajbes.20170301.11

Ferrer, M., Ghazi, A., Beloqui, A., Vieites, J. M., López-Cortés, N., Marín-Navarro, J., et al. (2012). Functional metagenomics unveils a multifunctional glycosyl hydrolase from the family 43 catalysing the breakdown of plant polymers in the calf rumen. *PLoS One* 7:e38134. doi: 10.1371/journal.pone.0038134

Fongaro, G., Maia, G. A., Rogovski, P., Cadamuro, R. D., Lopes, J. C., Moreira, R. S., et al. (2020). Extremophile microbial communities and enzymes for bioenergetic application based on multi-Omics tools. *Curr. Genomics* 21, 240–252. doi: 10.2174/1389202921999200601144137

Garg, R., Srivastava, R., Brahma, V., Verma, L., Karthikeyan, S., and Sahni, G. (2016). Biochemical and structural characterization of a novel halotolerant cellulase from soil metagenome. *Sci. Rep.* 6, 1–15. doi: 10.1038/srep39634

Gessesse, A., and Mamo, G. (1998). Purification and characterization of an alkaline xylanase from alkaliphilic micrococcus sp AR-135. *J. Ind. Microbiol. Biotechnol.* 20, 210–214. doi: 10.1038/sj.jim.2900503

Grant, W. D., and Jones, B. E. (2016). "Bacteria, Archaea and viruses of Soda Lakes," in *Soda Lakes of East Africa*. ed. Schagerl, M. (Cham: Springer International Publishing), 97–147. doi: 10.1007/978-3-319-28622-8_5

Grant, W. D., and Sorokin, D. Y. (2011). "Distribution and diversity of soda Lake Alkaliphiles," in *Extremophiles Handbook* ed. Horikoshi, K. (Tokyo: Springer)

Horn, S. J., Vaaje-Kolstad, G., Westereng, B., and Eijsink, V. G. H. (2012). Novel enzymes for the degradation of cellulose. *Biotechnol. Biofuels* 5, 1–12. doi: 10.1186/1754-6834-5-45

Houfani, A. A., Anders, N., Loogen, J., Heyman, B., Azzouz, Z., Bettache, A., et al. (2021). Lignocellulosic biomass degradation enzymes and characterization of cellulase and xylanase from *Bosea* sp. FBZP-16. *Biomass. Convers. Biorefinery*. 11, 1–19. doi: 10.1007/s13399-021-02044-1

Humayoun, S. B., Bano, N., and Hollibaugh, J. T. (2003). Depth distribution of microbial diversity in mono Lake, a Meromictic soda Lake in California. *Appl. Environ. Microbiol.* 69, 1030–1042. doi: 10.1128/AEM.69.2.1030-1042.2003

Jeilu, O., Gessesse, A., Simachew, A., Johansson, E., and Alexandersson, E. (2022). Prokaryotic and eukaryotic microbial diversity from three soda lakes in the east African Rift Valley determined by amplicon metagenomics. *Front. Microbiol.* 13, 1–14. doi: 10.3389/fmicb.2022.999876

Jones, B. E., and Grant, W. D. (1999). "Microbial diversity and ecology of the Soda Lakes of East Africa," in *Proceedings of the 8th International Symposium on Microbial Ecology*.

Jönsson, L. J., and Martín, C. (2016). Pretreatment of lignocellulose: formation of inhibitory by-products and strategies for minimizing their effects. *Bioresour. Technol.* 199, 103–112. doi: 10.1016/j.biortech.2015.10.009

Kabeyi, M. J. B., and Olanrewaju, O. A. (2022). Sustainable energy transition for renewable and low carbon grid electricity generation and supply. *Front. Energy Res.* 9, 1–45. doi: 10.3389/fenrg.2021.743114

Kern, M., McGeehan, J. E., Streeter, S. D., Martin, R. N. A., Besser, K., Elias, L., et al. (2013). Structural characterization of a unique marine animal family 7 cellobiohydrolase suggests a mechanism of cellulase salt tolerance. *Proc. Natl. Acad. Sci. U. S. A.* 110, 10189–10194. doi: 10.1073/pnas.1301502110

Khatri, B. P., Bhattarai, T., Shrestha, S., and Maharjan, J. (2015). Alkaline thermostable pectinase enzyme from *Aspergillus niger* strain MCAS2 isolated from Manaslu conservation area, Gorkha, Nepal. *Springerplus* 4, 1–8. doi: 10.1186/s40064-015-1286-y

Lakhundi, S., Siddiqui, R., and Khan, N. A. (2015). Cellulose degradation: A therapeutic strategy in the improved treatment of Acanthamoeba infections. *Parasit. Vectors* 8:23. doi: 10.1186/s13071-015-0642-7

Lam, K. N., Cheng, J., Engel, K., Neufeld, J. D., and Charles, T. C. (2015). Current and future resources for functional metagenomics. *Front. Microbiol.* 6, 1–8. doi: 10.3389/fmicb.2015.01196

Langmead, B., and Salzberg, S. (2013). Fast gapped-read alignment with Bowtie 2. Nat Methods 9, 357–359. doi: 10.1038/nmeth.1923.

Lanzén, A., Simachew, A., Gessesse, A., Chmolowska, D., Jonassen, I., and Øvreås, L. (2013). Surprising prokaryotic and eukaryotic diversity, community structure and biogeography of Ethiopian soda lakes. *PLoS One* 8:e72577. doi: 10.1371/journal.pone.0072577

Liew, K. J., Liang, C. H., Lau, Y. T., Yaakop, A. S., Chan, K. G., Shahar, S., et al. (2022). Thermophiles and carbohydrate-active enzymes (CAZymes) in biofilm microbial consortia that decompose lignocellulosic plant litters at high temperatures. *Sci. Rep.* 12:2850. doi: 10.1038/s41598-022-06943-9

Limsakul, P., Phitsuwan, P., Waeonukul, R., Pason, P., Tachaapaikoon, C., Poomputsa, K., et al. (2021). A novel multifunctional arabinofuranosidase/endoxylanase/β-xylosidase gh43 enzyme from paenibacillus curdlanolyticus b-6 and its synergistic action to produce arabinose and xylose from cereal arabinoxylan. *Appl. Environ. Microbiol.* 87:e0173021. doi: 10.1128/AEM.01730-21

Liu, Z., Zhao, C., Deng, Y., Huang, Y., and Liu, B. (2015). Characterization of a thermostable recombinant β-galactosidase from a thermophilic anaerobic bacterial consortium YTY-70. *Biotechnol. Biotechnol. Equip.* 29, 547–554. doi: 10.1080/13102818.2015.1015244

López-Mondéjar, R., Tláskal, V., Větrovský, T., Štursová, M., Toscan, R., Nunes da Rocha, U., et al. (2020). Metagenomics and stable isotope probing reveal the complementary contribution of fungal and bacterial communities in the recycling of dead biomass in forest soil. *Soil Biol. Biochem.* 148:107875. doi: 10.1016/j.soilbio.2020.107875

Lu, Y., He, Q., Fan, G., Cheng, Q., and Song, G. (2021). Extraction and modification of hemicellulose from lignocellulosic biomass: a review. *Green Process. Synth.* 10, 779–804. doi: 10.1515/gps-2021-0065

Mamo, G. (2020). "Alkaline active Hemicellulases," in *Advances in Biochemical Engineering/Biotechnology* in, eds. G. Mamo and B. Mattiasson (Cham: Springer International Publishing), 245–291. doi: 10.1007/10_2019_101

Martin, M., and Vandenbol, M. (2016). The hunt for original microbial enzymes: an initiatory review on the construction and functional screening of (meta)genomic libraries. *BASE*, 20, 523–532. doi: 10.25518/1780-4507.13201

Martins, R. F., Davids, W., Abu Al-Soud, W., Levander, F., Rådström, P., and Hatti-Kaul, R. (2001). Starch-hydrolyzing bacteria from Ethiopian soda lakes. *Extremophiles* 5, 135–144. doi: 10.1007/s007920100183

Maruthamuthu, M., Jiménez, D. J., Stevens, P., and van Elsas, J. D. (2016). A multi-substrate approach for functional metagenomics-based screening for (hemi)cellulases in two wheat straw-degrading microbial consortia unveils novel thermoalkaliphilic enzymes. *BMC Genom.* 17:86. doi: 10.1186/s12864-016-2404-0

Masasa, M., Kushmaro, A., Chernova, H., Shashar, N., and Guttman, L. (2022). Carbohydrate-Active Enzymes of a Novel Halotolerant Alkalihalobacillus Species for Hydrolysis of Starch and Other Algal Polysaccharides. *Microbiol. Spectr.* 10:e0107822. doi: 10.1128/spectrum.01078-22

Miller, G. L. (1959). Use of Dinitrosalicylic acid reagent for determination of reducing sugar. *Anal. Chem.* 31, 426–428. doi: 10.1021/ac60147a030

Minig, M., Walker, D., Ledesma, P., Martínez, M. A., and Breccia, J. D. (2009). Bacterial isolates from ethiopian soda lake producers of alkaline-active β-glucanases resistant to chelating and surfactant compounds. *Res. J. Microbiol.* 4, 194–201. doi: 10.3923/jm.2009.194.201

Mohammadi, S., Tarrahimofrad, H., Arjmand, S., Zamani, J., Haghbeen, K., and Aminzadeh, S. (2022). Expression, characterization, and activity optimization of a novel cellulase from the thermophilic bacteria *Cohnella* sp. *A01. Sci Rep* 12:10301. doi: 10.1038/s41598-022-14651-7

Möllers, K. B., Cannella, D., Jørgensen, H., and Frigaard, N. U. (2014). Cyanobacterial biomass as carbohydrate and nutrient feedstock for bioethanol production by yeast fermentation. *Biotechnol. Biofuels* 7, 1–11. doi: 10.1186/1754-6834-7-64

Montella, S., Ventorino, V., Lombard, V., Henrissat, B., Pepe, O., and Faraco, V. (2017). Discovery of genes coding for carbohydrate-active enzyme by metagenomic analysis of lignocellulosic biomasses. *Sci. Rep.* 7, 1–15. doi: 10.1038/srep42623

Moshfegh, M., Shahverdi, A. R., Zarrini, G., and Faramarzi, M. A. (2013). Biochemical characterization of an extracellular polyextremophilic α-amylase from the halophilic archaeon Halorubrum xinjiangense. *Extremophiles* 17, 677–687. doi: 10.1007/s00792-013-0551-7

Ngara, T. R., and Zhang, H. (2018). Recent advances in function-based metagenomic screening. *Genom. Proteom. Bioinform.* 16, 405–415. doi: 10.1016/j.gpb.2018.01.002

Nguyen, N. H., Maruset, L., Uengwetwanit, T., Mhuantong, W., Harnpicharnchai, P., Champreda, V., et al. (2012). Identification and characterization of a cellulase-encoding gene from the buffalo rumen metagenomic library. *Biosci. Biotechnol. Biochem.* 76, 1075–1084. doi: 10.1271/bbb.110786

Ondov, B. D., Bergman, N. H., and Phillippy, A. M. (2011). Interactive metagenomic visualization in a web browser. *BMC Bioinform.* 12, 1–9. doi: 10.1186/1471-2105-12-385

Oriez, V., Peydecastaing, J., and Pontalier, P. Y. (2019). Lignocellulosic biomass fractionation by mineral acids and resulting extract purification processes: conditions, yields, and purities. *Molecules* 24, 1–21. doi: 10.3390/molecules24234273

Oumer, O. J., and Abate, D. (2017). Characterization of pectinase from *Bacillus subtilis* strain Btk 27 and its potential application in removal of mucilage from coffee beans. *Enzyme Res.* 2017, 1–7. doi: 10.1155/2017/7686904

Øvreås, L., Daae, F. L., Torsvik, V., and Rodríguez-Valera, F. (2003). Characterization of microbial diversity in hypersaline environments by melting profiles and reassociation kinetics in combination with terminal restriction fragment length polymorphism (T-RFLP). *Microb. Ecol.* 46, 291–301. doi: 10.1007/s00248-003-3006-3

Pabbathi, N. P. P., Velidandi, A., Tavarna, T., Gupta, S., Raj, R. S., Gandam, P. K., et al. (2021). Role of metagenomics in prospecting novel endoglucanases, accentuating functional metagenomics approach in second-generation biofuel production: a review. *Biomass Convers. Biorefinery.*, 11, 1–28. doi: 10.1007/s13399-020-01186-y

Patel, S., and Saraf, M. (2015). "Perspectives and application of halophilic enzymes," in *Halophiles: Biodiversity and Sustainable Exploitation*. vol 6. Springer, Cham. doi: 10.1007/978-3-319-14595-2_15

Peng, X., Qiao, W., Mi, S., Jia, X., Su, H., and Han, Y. (2015). Characterization of hemicellulase and cellulase from the extremely thermophilic bacterium Caldicellulosiruptor owensensis and their potential application for bioconversion of lignocellulosic biomass without pretreatment. *Biotechnol. Biofuels* 8:131. doi: 10.1186/s13068-015-0313-0

Privé, F., Newbold, C. J., Kaderbhai, N. N., Girdwood, S. G., Golyshina, O. V., Golyshin, P. N., et al. (2015). Isolation and characterization of novel lipases/esterases from a bovine rumen metagenome. *Appl. Microbiol. Biotechnol.* 99, 5475–5485. doi: 10.1007/s00253-014-6355-6

Rastogi, M., and Shrivastava, S. (2020). "Glycosyl hydrolases and biofuel," in *Industrial Applications of Glycoside Hydrolases* eds. Shrivastava, S. (Singapore: Springer) (Singapore: Springer). doi: 10.1007/978-981-15-4767-6_6

Reichart, N. J., Bowers, R. M., Woyke, T., and Hatzenpichler, R. (2021). High potential for biomass-degrading enzymes revealed by hot spring Metagenomics. *Front. Microbiol.* 12, 1–12. doi: 10.3389/fmicb.2021.668238

Salam, L. B. (2018). Detection of carbohydrate-active enzymes and genes in a spent engine oil-perturbed agricultural soil. *Bull. Natl. Res. Cent.* 42, 1–18. doi: 10.1186/s42269-018-0013-6

Schagerl, M. (2016). *Soda Lakes of East Africa*. New York, NY: Springer International Publishing. doi: 10.1007/978-3-319-28622-8

Sharma, S., Khan, F. G., and Qazi, G. N. (2010). Molecular cloning and characterization of amylase from soil metagenomic library derived from northwestern Himalayas. *Appl. Microbiol. Biotechnol.* 86, 1821–1828. doi: 10.1007/s00253-009-2404-y

Shen, J., Zheng, L., Chen, X., Han, X., Cao, Y., and Yao, J. (2020). Metagenomic analyses of microbial and carbohydrate-active enzymes in the rumen of dairy goats fed different rumen degradable starch. *Front. Microbiol.* 11. doi: 10.3389/fmicb.2020.01003

Shrivastava, S. (2020). "Introduction to glycoside hydrolases: Classification, identification and occurrence" in *Industrial Applications of Glycoside Hydrolases* (Singapore: Springer). doi: 10.1007/978-981-15-4767-6_1

Shuddhodana, S., Gupta, M. N., and Bisaria, V. S. (2018). Stable cellulolytic enzymes and their application in hydrolysis of Lignocellulosic biomass. *Biotechnol. J.* 13, 1–10. doi: 10.1002/biot.201700633

Simon, C., and Daniel, R. (2011). Metagenomic analyses: past and future trends. *Appl. Environ. Microbiol.* 77, 1153–1161. doi: 10.1128/AEM.02345-10

Sorokin, D. Y., Banciu, H. L., and Muyzer, G. (2015). Functional microbiology of soda lakes. *Curr. Opin. Microbiol.* 25, 88–96. doi: 10.1016/j.mib.2015.05.004

Sorokin, D. Y., Berben, T., Melton, E. D., Overmars, L., Vavourakis, C. D., and Muyzer, G. (2014). Microbial diversity and biogeochemical cycling in soda lakes. *Extremophiles* 18, 791–809. doi: 10.1007/s00792-014-0670-9

Sorokin, D. Y., and Kuenen, J. G. (2005). Chemolithotrophic haloalkaliphiles from soda lakes. *FEMS Microbiol. Ecol.* 52, 287–295. doi: 10.1016/j.femsec.2005.02.012

Stewart, R. D., Auffret, M. D., Warr, A., Wiser, A. H., Press, M. O., Langford, K. W., et al. (2018). Assembly of 913 microbial genomes from metagenomic sequencing of the cow rumen. *Nat. Commun.* 9:870. doi: 10.1038/s41467-018-03317-6

Sun, S. F., Yang, J., Wang, D. W., Yang, H. Y., Sun, S. N., and Shi, Z. J. (2021). Enzymatic response of ryegrass cellulose and hemicellulose valorization introduced by sequential alkaline extractions. *Biotechnol. Biofuels* 14:72. doi: 10.1186/s13068-021-01921-1

Sweeney, M. D., and Xu, F. (2012). Biomass converting enzymes as industrial biocatalysts for fuels and chemicals: recent developments. *Catalysts* 2, 244–263. doi: 10.3390/catal2020244

Sysoev, M., Grötzinger, S. W., Renn, D., Eppinger, J., Rueping, M., and Karan, R. (2021). Bioprospecting of novel Extremozymes from prokaryotes—the advent of culture-independent methods. *Front. Microbiol.* 12, 1–16. doi: 10.3389/fmicb.2021.630013

Tahrioui, A., Schwab, M., Quesada, E., and Llamas, I. (2013). Quorum sensing in some representative species of Halomonadaceae. *Life* 3, 260–275. doi: 10.3390/life3010260

Teather, R. M., and Wood, P. J. (1982). Use of Congo red-polysaccharide interactions in enumeration and characterization of cellulolytic bacteria from the bovine rumen. *Appl. Environ. Microbiol.* 43, 777–780. doi: 10.1128/aem.43.4.777-780.1982

Thakur, P., Singh, A. K., and Mukherjee, G. (2021). Isolation and characterization of alkaline pectinase productive Bacillus tropicus from fruit and vegetable waste dump soil. *Brazilian Arch. Biol. Technol.* 64, 1–14. doi: 10.1590/1678-4324-2021200319

Tiwari, R., Kumar, K., Singh, S., Nain, L., and Shukla, P. (2016). Molecular detection and environment-specific diversity of glycosyl hydrolase family 1 β-glucosidase in different habitats. *Front. Microbiol.* 7, 1–12. doi: 10.3389/fmicb.2016.01597

Tiwari, R., Singh, P. K., Singh, S., Nain, P. K. S., Nain, L., and Shukla, P. (2017). Bioprospecting of novel thermostable β-glucosidase from Bacillus subtilis RA10 and its application in biomass hydrolysis. *Biotechnol. Biofuels* 10:246. doi: 10.1186/s13068-017-0932-8

Verma, D. (2021). Extremophilic Prokaryotic Endoxylanases: Diversity, Applicability, and Molecular Insights. *Front Microbiol* 12, 1–21. doi: 10.3389/fmicb.2021.728475

Verma, D., and Satyanarayana, T. (2011). An improved protocol for DNA extraction from alkaline soil and sediment samples for constructing metagenomic libraries. *Appl. Biochem. Biotechnol.* 165, 454–464. doi: 10.1007/s12010-011-9264-5

Verma, D., and Satyanarayana, T. (2020). Xylanolytic Extremozymes Retrieved From Environmental Metagenomes: Characteristics, Genetic Engineering, and Applications. *Front. Microbiol.* 11, 1–18. doi: 10.3389/fmicb.2020.551109

Vester, J. K., Glaring, M. A., and Stougaard, P. (2015). An exceptionally cold-adapted alpha-amylase from a metagenomic library of a cold and alkaline environment. *Appl. Microbiol. Biotechnol.* 99, 717–727. doi: 10.1007/s00253-014-5931-0

Voget, S., Steele, H. L., and Streit, W. R. (2006). Characterization of a metagenome-derived halotolerant cellulase. *J. Biotechnol.* 126, 26–36. doi: 10.1016/j.jbiotec.2006.02.011

Wang, L., Hatem, A., Catalyurek, U. V., Morrison, M., and Yu, Z. (2013). Metagenomic insights into the carbohydrate-active enzymes carried by the microorganisms adhering to solid digesta in the rumen of cows. *PLoS One* 8, 1–11. doi: 10.1371/journal.pone.0078507

Wang, M., Lai, G. L., Nie, Y., Geng, S., Liu, L., Zhu, B., et al. (2015). Synergistic function of four novel thermostable glycoside hydrolases from a long-term enriched thermophilic methanogenic digester. *Front. Microbiol.* 6, 1–10. doi: 10.3389/fmicb.2015.00509

Wang, L., Zhang, G., Xu, H., Xin, H., and Zhang, Y. (2019). Metagenomic analyses of microbial and carbohydrate-active enzymes in the rumen of Holstein cows fed different forage-to-concentrate ratios. *Front. Microbiol.* 10, 1–14. doi: 10.3389/fmicb.2019.00649

Wood, R. B., Baxter, R. M., and Prosser, M. V. (1984). Seasonal and comparative aspects of chemical stratification in some tropical crater lakes. *Ethiopia. Freshw. Biol.* 14, 551–573. doi: 10.1111/j.1365-2427.1984.tb00176.x

Wood, D. E., Lu, J., and Langmead, B. (2019). Improved metagenomic analysis with kraken 2. *Genome Biol.* 20:257. doi: 10.1186/s13059-019-1891-0

Xiao, C., and Anderson, C. T. (2013). Roles of pectin in biomass yield and processing for biofuels. *Front. Plant Sci.* 4, 1–7. doi: 10.3389/fpls.2013.00067

Yu, P., Zhang, Y., and Gu, D. (2017). Production optimization of a heat-tolerant alkaline pectinase from Bacillus subtilis ZGL14 and its purification and characterization. *Bioengineered* 8, 613–623. doi: 10.1080/21655979.2017.1292188

Zhang, T., Datta, S., Eichler, J., Ivanova, N., Axen, S. D., Kerfeld, C. A., et al. (2011). Identification of a haloalkaliphilic and thermostable cellulase with improved ionic liquid tolerance. *Green Chem.* 13:2083. doi: 10.1039/c1gc15193b

Zhang, L., Fu, Q., Li, W., Wang, B., Yin, X., Liu, S., et al. (2017). Identification and characterization of a novel β-glucosidase via metagenomic analysis of *Bursaphelenchus xylophilus* and its microbial flora. *Sci. Rep.* 7:14850. doi: 10.1038/s41598-017-14073-w

Zhao, K., Guo, L. Z., and Lu, W. D. (2012). Extracellular production of novel halotolerant, thermostable, and alkali-stable carboxymethyl cellulase by marine bacterium Marinimicrobium sp. LS-A18. *Appl. Biochem. Biotechnol.* 168, 550–567. doi: 10.1007/s12010-012-9796-3

Zhao, Z., Liu, H., Wang, C., and Xu, J. R. (2014). Correction to comparative analysis of fungal genomes reveals different plant cell wall degrading capacity in fungi [BMC genomics 14(2013) 274]. *BMC Genom.* 15, 1–15. doi: 10.1186/1471-2164-15-6

Zhu, D., Adebisi, W. A., Ahmad, F., Sethupathy, S., Danso, B., and Sun, J. (2020). Recent development of extremophilic bacteria and their application in biorefinery. *Front. Bioeng. Biotechnol.* 8, 1–18. doi: 10.3389/fbioe.2020.00483

Zoghlami, A., and Paës, G. (2019). Lignocellulosic biomass: understanding recalcitrance and predicting hydrolysis. *Front. Chem.* 7, 1–11. doi: 10.3389/fchem.2019.00874

frontiers | Frontiers in Microbiology

TYPE Mini Review
PUBLISHED 02 February 2023
DOI 10.3389/fmicb.2023.1077561

OPEN ACCESS

EDITED BY
Furkan Orhan,
Ağri İbrahim Çeçen University, Türkiye

REVIEWED BY
Sandra Pucciarelli,
University of Camerino, Italy

*CORRESPONDENCE
Kesava Priyan Ramasamy
✉ kesava.ramasamy@umu.se

†These authors have contributed equally to this work

SPECIALTY SECTION
This article was submitted to Microbiotechnology, a section of the journal Frontiers in Microbiology

RECEIVED 23 October 2022
ACCEPTED 05 January 2023
PUBLISHED 02 February 2023

CITATION
Ramasamy KP and Mahawar L (2023) Coping with salt stress-interaction of halotolerant bacteria in crop plants: A mini review. *Front. Microbiol.* 14:1077561. doi: 10.3389/fmicb.2023.1077561

Coping with salt stress-interaction of halotolerant bacteria in crop plants: A mini review

Kesava Priyan Ramasamy[1*†] and Lovely Mahawar[2†]

[1]Department of Ecology and Environmental Science, Umeå University, Umeå, Sweden, [2]Department of Plant Physiology, Faculty of Agrobiology and Food resources, Slovak University of Agriculture, Nitra, Slovakia

Salinity is one of the major environmental abiotic stress factors that limit the growth and yield of crop plants worldwide. It is crucial to understand the importance of several adaptive mechanisms in plants toward salt stress so as to increase agricultural productivity. Plant resilience toward salinity stress is improved by cohabiting with diverse microorganisms, especially bacteria. In the last few decades, increasing attention of researchers has focused on bacterial communities for promoting plant growth and fitness. The biotechnological applications of salt-tolerant plant growth-promoting rhizobacteria (PGPR) gained widespread interest for their numerous metabolites. This review provides novel insights into the importance of halotolerant (HT) bacteria associated with crop plants in enhancing plant tolerance toward salinity stress. Furthermore, the present review highlights several challenges of using HT-PGPR in the agricultural field and possible solutions to overcome those challenges for sustainable agriculture development in the future.

KEYWORDS

salinity, halotolerant bacteria, crop plants, biotechnological applications, plant-microbe interaction

1. Introduction

Plants, due to their sessile nature, experience several environmental (abiotic and biotic) stresses during different developmental stages of their life cycle. The major abiotic stresses are drought, heavy metals, salinity, temperature, and ultraviolet (UV) light. Salinity is one of the extremely critical threats in the agricultural field, impacting one-fourth to one-third of crop production worldwide (Kumar et al., 2022). According to the Food and Agricultural Organization (FAO) report, over 424 million hectares (Mha) of topsoil (0–30 cm) (85% saline, 10% sodic, and 5% saline sodic) and 833 million hectares of subsoil (30–100 cm) (62% saline, 24% sodic, and 14% saline sodic) among 85% of the global land area are affected by salinity stress (Food Agriculture Organizations of the United Nations, 2022).

Soil salinity occurs mainly due to poor agricultural practices (high salt content water used for irrigation and fertilization) and the flow of saline water from the sea, rivers, etc., specifically in arid and semiarid regions (Zhang et al., 2021). Moreover, scarcity of rainfall and an increase in sea level due to climate change often cause the soil to become saline (Kumar et al., 2022). As a result, it produces hyperionic and hyperosmotic stresses in plant cells that impact the plant's growth (Kalaji et al., 2011) (Figure 1). Due to high osmotic stress, the uptake and transport of essential nutrients to a plant are affected highly (Farooq et al., 2015). Salinity stress affects the physiological development of plants (causes stomatal closure and premature senescence, reduces the rate of photosynthesis, and increases oxidative damage) (Mahawar and Shekhawat, 2019) and soil microbiota adversely, thus critically affecting complete soil health (Dubey et al., 2022) (Figure 1). However, plants must overcome salinity stress by modulating various morphophysiological and molecular responses (Zhao et al., 2020), such as improving the synthesis of phytohormones and osmoprotectants, upregulating antioxidant activities, and maintaining sodium ion (Na^+) homeostasis and compartmentalization (Arif et al., 2020).

Another strategy to overcome salinity stress in plants is to cohabit with diverse halotolerant (HT) microorganisms that enhance growth, stress tolerance, and nutrient uptake in plants, thus restoring the crop yield (Etesami and Beattie, 2018; Etesami and Glick, 2020; Orhan, 2021). Halotolerant (HT) microorganisms that interact with plants are (1) rhizosphere, (2) epiphytes, and (3) endophytes (Andrews and Harris, 2000; Hardoim et al., 2015). The rhizosphere region in plants serves as natural hotspots (reservoirs) for various microorganisms, especially bacteria (Ling et al., 2022). One among such bacteria pertains to plant growth-promoting rhizobacteria (PGPR) that colonize the rhizosphere of the plant species. Many studies have proven that salt-tolerant plant growth-promoting rhizobacteria (PGPR) are supplied by various mechanisms to plants (Mishra et al., 2021). The important function of PGPR is to boost key physiological processes in plants, including photosynthesis, source–sink relationships, mineral and water uptake (Ilangumaran and Smith, 2017), fixation of atmospheric nitrogen, prevention of phytopathogens, improvement in the production of metabolites and phytohormones, such as indole-3-acetic acid (IAA), gibberellic acid (GA3), and cytokinin, solubilization of phosphate, and production of siderophores (Kumar and Verma, 2018). However, numerous studies demonstrated that different plant species colonize their own microbial communities (Kuske et al., 2002). Isolation and identification of the specific plant-based microorganism using microbiological and molecular methods would promote research on the plant–microbe interactions. In recent decades, the use of "omics" technologies, such as transcriptomics, proteomics, and metabolomics, to study the regulatory networks of halotolerant plant–bacteria interaction has increased.

The present review focuses on recent advances in plant–bacteria interactions and the underlying mechanisms of rhizosphere-residing bacterial species in a plant's response under salinity stress at the physiological and molecular levels. Moreover, the application and biotechnological potential of salt-tolerant PGPR in saline conditions have been explored. The present review also aimed to explore the major challenges of using PGPR in the agricultural field and their possible scientific solutions.

2. Plant growth-promoting rhizobacteria in crop's adaptation toward salinity stress

Plants adopted three main strategies to overcome sodium chloride (NaCl) stress and survive in the saline environment–osmotic stress tolerance, Na^+/Cl^- exclusion, and tolerance to accumulate Na^+/Cl^-. Osmotic stress tolerance is mediated by a decrease in stomatal conductance, while the salinity stress-induced ionic response activates signal perception and transduction that limits the uptake, translocation, and accumulation of Na^+ in the cell (Rahman et al., 2021). The plant adaptation toward salinity stress is improved by cohabiting with diverse saline soil microbes known as halotolerant plant growth-promoting rhizobacteria (HT-PGPR) that not only allow plants to persist in salt habitat but also improve their growth and soil-related properties (Hidri et al., 2022). In recent years, the importance of halotolerant plant growth-promoting rhizobacteria (HT-PGPR) in alleviating salinity stress in crop plants has increased. HT-PGPR improve the productivity of the saline-agroecosystem, either directly by producing several beneficial metabolites, such as exopolysaccharides, siderophores, volatile organic compounds (VOCs), compatible osmolytes, and phytohormones (Bhat et al., 2020), or indirectly by regulating the expression of stress-related genes and inhibiting the phytopathogen effects (Prasad et al., 2019) (Figure 1). Several halotolerant bacteria, including *Rhizobium*, *Arthrobacter*, *Flavobacterium*, *Alcaligenes*, *Pseudomonas*, and *Azospirillum*, were found to improve crop salinity tolerance (Saghafi et al., 2019a; Kumar Arora et al., 2020).

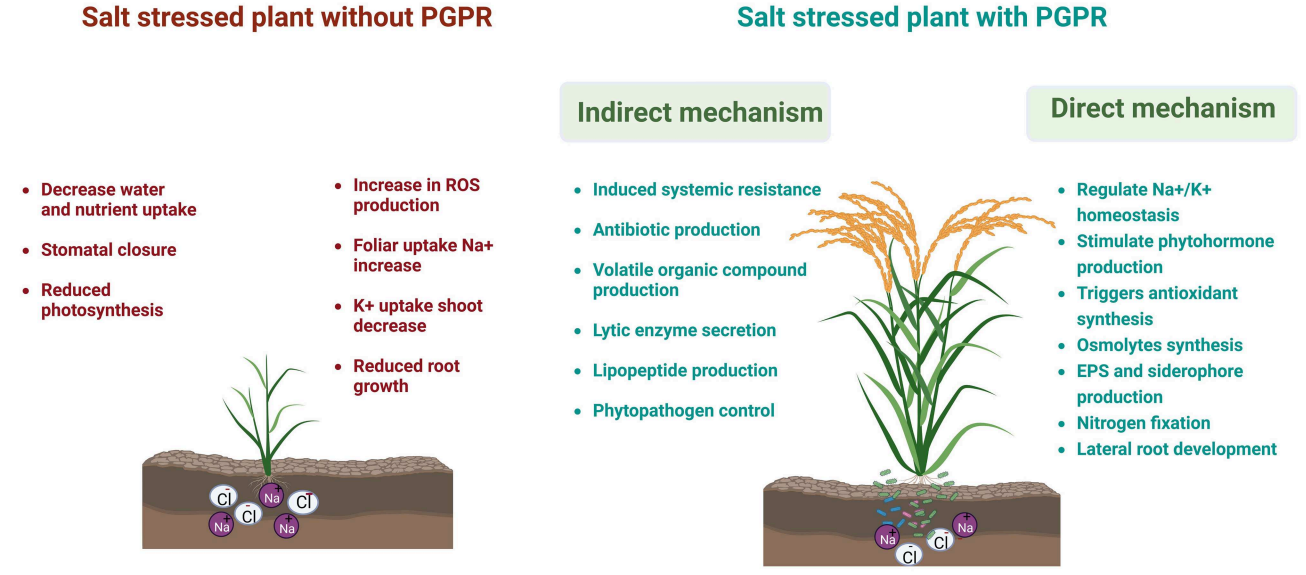

FIGURE 1
An underlying mechanism of halotolerant plant growth-promoting rhizobacteria (HT-PGPR) in alleviating salinity stress in crop plants. Licensed from biorender.

Halotolerant bacteria form biofilms and tend to produce extracellular polymeric substances/exopolysaccharides (EPSs) in a stressful environment (Haque et al., 2022). EPS production by HT-PGPR differs with the bacterial growth phase and external environment, such as nutrient medium composition, type of stress stimuli, pH, and temperature (Kumar Arora et al., 2020). Under a saline environment, EPS forms ∼40–90% of the bacterial weight (Sunita et al., 2020). EPS forms a nutrient-rich sheath around the plant's roots called the rhizosheath (which also serves as a carbon source), which improves the availability and uptake of nutrients and water from the rhizosphere and acts as a physical barrier against ionic salts and phytopathogens (Mishra and Arora, 2018; Kumar Arora et al., 2020). Previously, Mahmood et al. (2016) studied the role of EPS-producing halotolerant *Enterobacter cloacae* and *Bacillus drentensis* in improving the growth of salt-stressed mung bean by increasing the water uptake and nutrient availability in crop plants. EPS is also associated with soil aggregation, humification, water retention, nodulation, quorum sensing, and the establishment of microbial diversity that protects plant cells from desiccation in a saline environment (Kumar Arora et al., 2020). Furthermore, EPS possesses antioxidant properties that confer tolerance against salinity-induced oxidative damage (Sunita et al., 2020). Inoculation of *Pantoea alhagi* NX-11, an EPS-producing endophyte, alleviates salt stress damage and improves the growth of *Oryza sativa* by stimulating antioxidant activity (Sun et al., 2020). In another study, the combined effect of silicon dioxide (SiO_2) nanoparticles and exopolysaccharide (EPS)-producing bacterial inoculum on the upregulation of antioxidant activities in *Solanum lycopersicum* under salinity stress has been reported (Isfahani et al., 2019). Moreover, HT-PGPR in a stress environment produce low-molecular-weight, lipophilic metabolites known as volatile organic compounds (VOCs) (Sunita et al., 2020). The VOCs promote the growth and adaptability of stressed plants by stimulating the synthesis of siderophores, osmoprotectants, and phytohormones, triggering the expression of HKT1/K^+ transporters and regulating virulence factors and bacterial motility in the plant–microbe interaction (Bhat et al., 2020). The upregulation of HKT antiporters by VOC-producing HT-PGPR strains, such as *Dietzia natronolimnaea* (Bharti et al., 2016), *Arthrobacter nitroguajacolicus* (Safdarian et al., 2019) in *Triticum aestivum*, and *Bacillus amyloliquefaciens* SQR9 (Chen et al., 2016) in *Zea mays*, has been studied under salinity stress. Another major challenge for salinity-stressed crops is the low availability of soluble ferrous ions (Fe^{2+}) (iron form uptake by plants), which is determined primarily by the soil pH (available at acidic pH 6). Saline soils have alkaline pH (pH > 6.5) that causes the oxidation of ferrous ion (Fe^{2+}) to ferric ion (Fe^{3+}) and reduces the availability of iron to plants (Mahawar et al., 2022). The production of siderophores by HT-PGPR chelates Fe^{3+} and compensates the iron (Fe) requirement in salt-stressed crops (Kumar Arora et al., 2020). In this context, Mukherjee et al. (2019) studied the role of siderophores produced by the HT-PGPR strain, *Halomonas* sp., in promoting the growth and productivity of *Oryza sativa* growing in a saline environment.

Synthesis and accumulation of osmolytes/osmoprotectants are one of the earliest responses of plants to combat osmotic and oxidative damage imposed by salinity stress (Jogawat, 2019). HT-PGPR help plants to accumulate compatible osmolytes (amino acids, soluble sugars, and polyols) in a saline environment to minimize osmotic stress, maintain high turgor pressure, and sustain ion equilibrium in the cytoplasm. Moreover, HT-PGPR have been reported to upregulate osmolyte biosynthesis genes (mainly proline) and control stomatal conductance and transpiration rate (Saghafi et al., 2019b) to mitigate water stress in plants (Sunita et al., 2020). Bioinoculation of a halotolerant PGPR, *Bacillus fortis* SSB21, in capsicum, improved proline synthesis and expression of stress-related genes, namely, the pepper pathogen-induced protein gene (CAPIP2), a putative ketoacyl-ACP reductase (CaKR1), pepper osmotin-like protein 1 (CaOSM1), and pepper class II basic chitinase (CAChi2) during salinity stress (Yasin et al., 2018). Similarly, the inoculation of *Paenibacillus yonginensis* DCY84^T into *Panax ginseng* seeds subjected to salinity stress increases polyamine, total soluble sugar, chlorophyll and proline content, abscisic acid (ABA) synthesis, and the upregulation of stress-responsive genes in stressed plants (Sukweenadhi et al., 2018).

The modulation of phytohormone synthesis against stress environment is another important characteristic of HT-PGPR to confer symbiotic association and promote the growth and productivity of stressed plants (Kumar Arora et al., 2020). Recent studies reported that, under saline condition, phytohormone synthesis genes, mainly IAA, are upregulated in salt-tolerant PGPR that compensate for growth hormones' requirement in plants, alter plant root's morphology, and exclude excess ionic salts (Bhat et al., 2020). Several *in vitro* studies revealed that the improved IAA production by HT-PGPR in plants reduces tap root growth, promotes the elongation of root hairs, and increases the number and length of lateral roots. Thus, it improves crop growth by increasing the availability and uptake of water and nutrients (Nawaz et al., 2020; Grover et al., 2021; Sarker et al., 2022). Inoculation of *Pseudomonas putida*, *Pseudomonas stutzeri*, and *Stenotrophomonas maltophilia* in *Coleus forskohlii* enhanced the production of IAA, gibberellic acid, and cytokinin in plants (Patel and Saraf, 2017). Similarly, *Pseudomonas* sp. enhanced the production of gibberellins in *Glycine max* (Kang et al., 2014) and cytokinin in *Zea mays* (Sandhya et al., 2010) growing under sodium chloride (NaCl) stress. Apart from growth hormones, PGPR are capable of synthesizing and modulating the gene expression of stress hormones (abscisic acid (ABA) and ethylene) (Bhat et al., 2020). A study conducted by Bharti et al. (2016) demonstrated the role of halotolerant strain *Dietzia natronolimnaea* STR1 in upregulating the expression of ABA signaling cascade genes, such as ABA response elements (TaABARE) and 12-oxophytodienoate reductase 1 (TaOPR1), which stimulates the expression of the salt stress-induced gene, *TaST*, in *Triticum aestivum*. Ethylene, another stress hormone, promotes plant tolerance toward salinity stress but constrains their growth and productivity. HT-PGPR secrete 1-aminocyclopropane-1-carboxylase (ACC) deaminase that metabolizes ACC (ethylene precursor) into α-ketoglutarate and ammonia, thus hampering ethylene synthesis in plants (Bhat et al., 2020). Panwar et al. (2016) studied that ACC deaminase-producing strains of *Enterobacter* spp. and *Pseudomonas fluorescens* increased the growth and yield of *Zea mays* in a saline environment.

In addition to producing plant-beneficial metabolites, HT-PGPRs constrict the influx of Na^+ by regulating the Na^+/K^+ homeostasis and modulating the expression of different salt-tolerant genes, such as salt overly sensitive (SOS), high-affinity K^+ transporters (HKT),

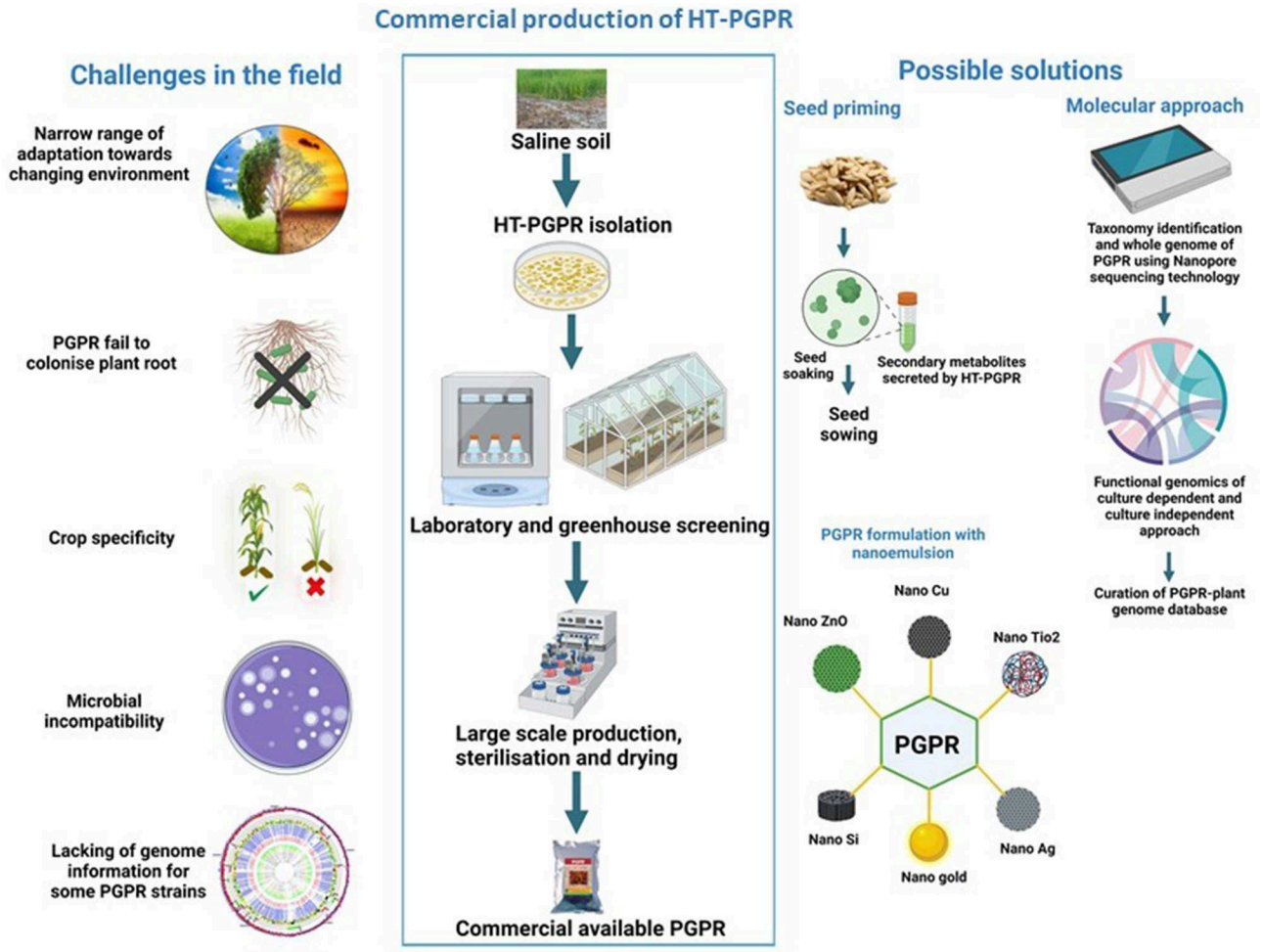

FIGURE 2
The major challenges of using halotolerant plant growth-promoting rhizobacteria (HT-PGPR) in the agricultural field and possible solutions to overcome them. The square box represents the steps involved in the commercial production of PGPR under controlled condition, while the **(left)** and **(right)** sides of the square explain the various problems involved in employing PGPR in the field and probable solutions to conquer them. Licensed from biorender.

Na^+/H^+ antiporter (NHX), aquaporins (AQPs), and antioxidants, thereby conferring plants resistance toward salinity stress. The treatment of HT-PGPR *Bacillus subtilis* (GB03) reduces Na^+ uptake in the halophyte grass *Puccinellia tenuiflora* by the upregulation of PtHKT1;5 and PtSOS1 and the downregulation of the PtHKT2;1 gene (Niu et al., 2016). A similar mechanism of *Bacillus subtilis* (GB03) was studied in *Triticum aestivum* growing under a saline environment (Zhang et al., 2014). Long-term exposure to a saline environment causes water deficiency in crops. Inoculation of HT-PGPR *Bacillus megaterium* upregulates the expression of the aquaporin genes ZmPIP1-1 and PIP2 in *Zea mays* that increase the water uptake in salt-stressed plants (Marulanda et al., 2010). Additionally, HT-PGPR augment salt tolerance in host plants by modulating the expression and activity of antioxidants (Kumar Arora et al., 2020). The priming of *Panax ginseng* seeds with salt-tolerant *Paenibacillus yonginensis* DCY84T improved the expression of *PgAPX* and *PgCAT* genes in salt-stressed plants (Sukweenadhi et al., 2018). In another study, HT-PGPR *Bradyrhizobium* and *Pseudomonas graminis* during a saline environment triggered the accumulation of ascorbate and glutathione in *Vigna unguiculata* (Santos et al., 2018). Similarly, inoculation of *B. megaterium* UPMR2 and *Enterobacter* sp. UPMR18 in *Abelmoschus esculentus* upregulates the expression of stress-related genes such as superoxide dismutase (SOD), ascorbate peroxidase (APX), catalase (CAT), glutathione reductase (GR), and dehydroascorbate reductase (DHAR) under NaCl stress (Habib et al., 2016). Supplementary Table 1 shows the list of bacterial species and their mechanisms in plant hosts to alleviate salinity stress.

3. The major challenges of HT-PGPRs in field conditions and their probable scientific solutions

The HT-PGPR is commercially used in agriculture due to its several advantages over synthetic agrochemicals in stimulating the growth and yield of economically important crops in both normal and stress conditions. Several PGPR-based bioformulations and products are available on the market and many of them are still in the development process. PGPR production from laboratory to field is a complex process that is completely based on laboratory screening assays and field trials (Figure 2) (Backer et al., 2018).

However, the commercial PGPR inoculants did not show similar promising effects in promoting crop growth in agricultural fields as those under controlled laboratory conditions. The major challenge in reducing the PGPR performance in field conditions is climate change. Considerable climate change not only impacts plant physiology but also affects the diversity, abundance, colonization, and activities of plant-associated microbial communities (Tabassum et al., 2017). Moreover, the climate in different ecological zones also affects the PGPR efficiency, as there is no potent commercial inoculant that has a similar response in all ecological zones (Liu et al., 2022). For an effective PGPR inoculum, the inoculated strains must colonize the plant roots and propagate into the rhizosphere. Certain bacterial strains fail to colonize the roots and are thus incompetent to promote plant growth in the field, as that under controlled conditions (Figure 2). Crop variety and PGPR strain are other important aspects that must be considered while using bioinoculants. The impact of specific PGPR strains or consortia on crop growth and yield varies with the crop cultivars (Figure 2). Furthermore, inoculation of defined microbial strain depends on crop necessity (pathogen resistance, stress tolerance, yield stimulation, etc.) (Tabassum et al., 2017). The carrier selection also plays a crucial role in PGPR performance. An inappropriate carrier reduces the survival and efficiency of bacteria in the rhizosphere. Moreover, the PGPR performance in a carrier material differs from strain to strain (Sohaib et al., 2020). The compatibility of microbes in consortia is another factor. Many bacterial species have antagonistic interactions with other strains, reducing PGPR efficiency in the field (Tabassum et al., 2017). Environmental safety associated with PGPR strain is an additional concern that cannot be neglected. Microbial inoculation triggers substantial changes at the level of native non-targeted microbial communities. Consortia/PGPR inoculants compete with the indigenous soil microbial population (for nutrients, habitat, trading metabolites, etc.) that results in changes to the community structure, loss of native diversity, and a rise in alien host diversity (Figure 2) (Thakur et al., 2019). Thus, all these aforementioned factors reshape the functionality of resident soil communities by provoking secondary succession (Liu et al., 2022).

The PGPR efficiency is dependent directly on soil properties, plant signaling molecules, and the surrounding environment. A careful selection of multipotent environment-friendly PGPR strains that can withstand a wide range of environments is the key to deploying a sustainable approach in crop improvement to the changing environment. In-depth studies on laboratory screening procedures are required for selecting suitable eco-friendly bioinoculants that favor the growth of crops under saline conditions (Figure 2). Recent advancements in "rhizosphere engineering" could mitigate salt stress by engineering the rhizosphere microbiome. For example, genome editing technology, such as Clustered Regularly Interspaced Short Palindromic Repeats (CRISPR)/CRISPR-associated protein 9 (Cas9), is a fast, eco-friendly, and effective way to understand the plant–PGPR interactions, in particular, to target pathways involved in various metabolites (Prabhukarthikeyan et al., 2020). Another approach is to unravel the "blackbox" of PGPRs using next-generation sequencing (NGS) to explore microbial diversity under salinity stress. In recent years, the culture-independent approach has been increased to configure the bacteriobiome complex associated with various plant species. Recently, Poncheewin et al. (2022) studied the plant-associated lifestyle of *Pseudomonas* strains using genome properties (GPs) of common biological pathways' annotation system and the machine learning (ML) approach to differentiate functional features. However, the 16S ribosomal RNA (16S rRNA) profiling of bacterial communities has a few limitations (such as the primer design, coverage, sequencing errors, and pipeline analysis from different sequencing platforms). To resolve these challenges in a culture-independent approach, the following strategies need to be included: (1) optimization of primer pairs, (2) sequencing depth and coverage, and (3) curated reference database. In addition, there is a need to develop a database to expand the knowledge of HT-PGPR—plant interaction for sustainable agriculture. In recent years, the increase in whole genome sequencing of PGPR and data availability has facilitated comparative genomics between host plants and endophytes. Moreover, the genome insights provide novel information about salinity-tolerant genes associated with specific interactions between host plants and PGPR. Seed priming with PGPR's secreted secondary metabolites is the other indirect approach to enhance crop productivity under salinity stress. The priming of seeds not only stimulates crop growth and yield in changing environments but also protects native soil microbial communities from direct exposure to PGPR. Moreover, the utilization of a nanoemulsion-based delivery system can improve PGPR performance. Nanoemulsion carriers can make PGPR more efficient in the agricultural field, due to their increase in solubility, stability, targeted delivery, controlled release, and cost-effectiveness (Ravichandran et al., 2022) (Figure 2).

4. Conclusion

Halotolerant plant growth-promoting rhizobacteria (HT-PGPR) are an excellent green alternative that facilitates crop plants to cope with increasing salinity stress. In recent years, the beneficial impact of PGPR on agriculture to yield economically important crops has increased. HT-PGPR promote crop production by several mechanisms (physiological and molecular level) in a saline environment. However, many molecular functions and signaling pathways of HT-PGPR used for promoting crop growth during the plant–microbe interaction are still unknown and need to be characterized. In addition, maintaining a similar efficiency of HT-PGPR in an agricultural field as that under controlled laboratory conditions is the other major field that needs to be focused on to accomplish sustainable agriculture. Isolation and genome sequencing of many unexplored novel PGPR strains could expand our knowledge by acquiring a better understanding of the PGPR-plant interaction with halophytes and for selecting specific multipotent broad ranges of strains or consortia. Moreover, biotechnological tools, such as rhizosphere engineering, next-generation sequencing, and a culture-independent approach, can be used to explore unidentified microbes in the complex bacteriobiome associated with plant species.

Author contributions

KPR and LM conceptualized the idea and constructed the figures and table. Both authors contributed equally to the writing of this review and approved the final version.

Conflict of interest

The authors declare that the research was conducted in the absence of any commercial or financial relationships that could be construed as a potential conflict of interest.

Publisher's note

All claims expressed in this article are solely those of the authors and do not necessarily represent those of their affiliatedorganizations, or those of the publisher, the editors and the reviewers. Any product that may be evaluated in this article, or claim that may be made by its manufacturer, is not guaranteed or endorsed by the publisher.

Supplementary material

The Supplementary Material for this article can be found online at: https://www.frontiersin.org/articles/10.3389/fmicb.2023.1077561/full#supplementary-material

References

Andrews, J. H., and Harris, R. F. (2000). The ecology and biogeography of microorganisms on plant surfaces. *Annu. Rev. Phytopathol.* 38, 145–180. doi: 10.1146/annurev.phyto.38.1.145

Arif, Y., Singh, P., Siddiqui, H., Bajguz, A., and Hayat, S. (2020). Salinity induced physiological and biochemical changes in plants: an omic approach towards salt stress tolerance. *Plant Physiol. Biochem.* 156, 64–77. doi: 10.1016/j.plaphy.2020.08.042

Backer, R., Rokem, J. S., Ilangumaran, G., Lamont, J., Praslickova, D., Ricci, E., et al. (2018). Plant growth-promoting rhizobacteria: context, mechanisms of action, and roadmap to commercialization of biostimulants for sustainable agriculture. *Front. Plant Sci.* 9, 1473. doi: 10.3389/fpls.2018.01473

Bharti, N., Pandey, S. S., Barnawal, D., Patel, V. K., and Kalra, A. (2016). Plant growth promoting rhizobacteria *Dietzia natronolimnaea* modulates the expression of stress responsive genes providing protection of wheat from salinity stress. *Sci. Rep.* 6, 34768. doi: 10.1038/srep34768

Bhat, M. A., Kumar, V., Bhat, M. A., Wani, I. A., Dar, F. L., Farooq, I., et al. (2020). Mechanistic insights of the interaction of plant growth-promoting rhizobacteria (PGPR) with plant roots toward enhancing plant productivity by alleviating salinity stress. *Front. Microbiol.* 11, 1952. doi: 10.3389/fmicb.2020.01952

Chen, L., Liu, Y., Wu, G., Njeri, K. V., Shen, Q., Zhang,. N., et al. (2016). Induced maize salt tolerance by rhizosphere inoculation of *Bacillus amyloliquefaciens* SQR9. *Physiol. Plant.* 158, 34–44. doi: 10.1111/ppl.12441

Dubey, S., Khatri, S., Bhattacharjee, A., and Sharma, S. (2022). Multiple passaging of rhizospheric microbiome enables mitigation of salinity stress in *Vigna radiata*. *Plant Growth Regul.* 97, 537–549. doi: 10.1007/s10725-022-00820-1

Etesami, H., and Beattie, G. A. (2018). Mining halophytes for plant growth promoting halotolerant bacteria to enhance the salinity tolerance of non-halophytic crops. *Front. Microbiol.* 9, 148. doi: 10.3389/fmicb.2018.00148

Etesami, H., and Glick, B. R. (2020). Halotolerant plant growth–promoting bacteria: prospects for alleviating salinity stress in plants. *Environ. Exp. Bot.* 178, 104124. doi: 10.1016/j.envexpbot.2020.104124

Farooq, M., Hussain, M., Wakeel, A., and Siddique, K. H. M. (2015). Salt stress in maize: effects, resistance mechanisms and management. A review. *Agron. Sustain. Dev.* 35, 461–481. doi: 10.1007/s13593-015-0287-0

Food and Agriculture Organizations of the United Nations (2022). Available online at: https://www.fao.org/soils-portal/data-hub/soil-maps-and-databases/global-map-of-salt-affected-soils/en/ (accessed July 23, 2022).

Grover, M., Bodhankar, S., Sharma, A., Sharma, P., Singh, J., and Nain, L. (2021). PGPR mediated alterations in root traits: way toward sustainable crop production. *Front. Sustain. Food Syst.* 4, 618230. doi: 10.3389/fsufs.2020.618230

Habib, S. H., Kausar, H., and Saud, H. M. (2016). Plant growth-promoting rhizobacteria enhance salinity stress tolerance in Okra through ROS-scavenging enzymes. *Biomed. Res. Int.* 2016, 6284547. doi: 10.1155/2016/6284547

Haque, M. M., Biswas, M. S., Mosharaf, M. K., Haque, M. A., Islam, M. S., Nahar, K., et al. (2022). Halotolerant biofilm-producing rhizobacteria mitigate seawater-induced salt stress and promote growth of tomato. *Sci. Rep.* 12, 5599. doi: 10.1038/s41598-022-09519-9

Hardoim, P. R., Van Overbeek, L. S., Berg, G., Pirttilä, A. M., Compant, S., Campisano, A., et al. (2015). The hidden world within plants: ecological and evolutionary considerations for defining functioning of microbial endophytes. *Microbiol. Mol. Biol. Rev.* 79, 293–320. doi: 10.1128/MMBR.00050-14

Hidri, R., Mahmoud, O. M.-B., Zorrig, W., Mahmoudi, H., Smaoui, A., Abdelly, C., et al. (2022). Plant growth-promoting rhizobacteria alleviate high salinity impact on the halophyte *Suaeda fruticosa* by modulating antioxidant defense and soil biological activity. *Front. Plant Sci.* 13, 821475. doi: 10.3389/fpls.2022.821475

Ilangumaran, G., and Smith, D. L. (2017). Plant growth promoting rhizobacteria in amelioration of salinity stress: a systems biology perspective. *Front. Plant Sci.* 8, 1768. doi: 10.3389/fpls.2017.01768

Isfahani, F. M., Tahmourespour, A., Hoodaji, M., Ataabadi, M., and Mohammadi, A. (2019). Influence of exopolysaccharide-producing bacteria and SiO_2 nanoparticles on proline content and antioxidant enzyme activities of tomato seedlings (*Solanum lycopersicum* L.) under salinity stress. *Pol. J. Environ. Stud.* 28, 153–163. doi: 10.15244/pjoes/81206

Jogawat, A. (2019). "Osmolytes and their role in abiotic stress tolerance in plants" in *Molecular Plant Abiotic Stress: Biology and Biotechnology*, eds A. Roychoudhury and D. Tripathi (New York, NY: John Wiley and Sons, Ltd.), 91–104.

Kalaji, H. M., Govindjee., Bosa, K., Kościelniak, J., and Zuk-Gołaszewska, K. (2011). Effects of salt stress on photosystem II efficiency and CO_2 assimilation of two Syrian barley landraces. *Environ. Exp. Bot.* 73, 64–72. doi: 10.1016/j.envexpbot.2010.10.009

Kang, S. M., Radhakrishnan, R., Khan, A. L., Kim, M. J., Park, J. M., Kim, B. R., et al. (2014). Gibberellin secreting rhizobacterium, *Pseudomonas putida* H-2-3 modulates the hormonal and stress physiology of soybean to improve the plant growth under saline and drought conditions. *Plant Physiol. Biochem.* 84, 115–124. doi: 10.1016/j.plaphy.2014.09.001

Kumar Arora, N., Fatima, T., Mishra, J., Mishra, I., Verma, S., Verma, R., et al. (2020). Halo-tolerant plant growth promoting rhizobacteria for improving productivity and remediation of saline soils. *J. Adv. Res.* 26, 69–82. doi: 10.1016/j.jare.2020.07.003

Kumar, A., and Verma, J. P. (2018). Does plant—microbe interaction confer stress tolerance in plants: a review? *Microbiol. Res.* 207, 41–52. doi: 10.1016/j.micres.2017.11.004

Kumar, P., Choudhary, M., Halder, T., Prakash, N. R., Singh, V., Vineeth, T. V., et al. (2022). Salinity stress tolerance and omics approaches: revisiting the progress and achievements in major cereal crops. *Heredity* 128, 497–518. doi: 10.1038/s41437-022-00516-2

Kuske, C. R., Ticknor, L. O., Miller, M. E., Dunbar, J. M., Davis, J. A., Barns, S. M., et al. (2002). Comparison of soil bacterial communities in rhizospheres of three plant species and the interspaces in an arid grassland. *App. Environ. Microbiol.* 68 , 1854–1863. doi: 10.1128/aem.68.4.1854-1863.2002

Ling, N., Wang, T., and Kuzyakov, Y. (2022). Rhizosphere bacteriome structure and functions. *Nat. Commun.* 13, 836. doi: 10.1038/s41467-022-28448-9

Liu, X., Roux, X. L., and Salles, J. , F. (2022). The legacy of microbial inoculants in agroecosystems and potential for tackling climate change challenges. *iScience* 25, 103821. doi: 10.1016/j.isci.2022.103821

Mahawar, L., Ramasamy, K. P., Pandey, A., and Prasad, S. M. (2022). Iron deficiency in plants: an update on homeostasis and its regulation by nitric oxide and phytohormones. *Plant Growth Regul.* 2022, 1–17. doi: 10.1007/s10725-022-00853-6

Mahawar, L., and Shekhawat, G. S. (2019). EsHO 1 mediated mitigation of NaCl induced oxidative stress and correlation between ROS, antioxidants and HO 1 in seedlings of *Eruca sativa*: underutilized oil yielding crop of arid region. *Physiol. Mol. Biol. Plants* 25, 895–904. doi: 10.1007/s12298-019-00663-7

Mahmood, S., Daur, I., Al-Solaimani, S. G., Ahmad, S., Madkour, M. H., Yasir, M., et al. (2016). Plant growth promoting rhizobacteria and silicon synergistically enhance salinity tolerance of mung bean. *Front. Plant. Sci.* 7, 876. doi: 10.3389/ fpls.2016.00876

Marulanda, A., Azcon, R., Chaumont, F., Ruiz-Lozano, J. M., and Aroca, R. (2010). Regulation of plasma membrane aquaporins by inoculation with a *Bacillus megaterium* strain in maize (*Zea mays* L.) plants under unstressed and salt-stressed conditions. *Planta* 232, 533–543. doi: 10.1007/s00425-010-1196-8

Mishra, J., and Arora, N. K. (2018). Secondary metabolites of fluorescent pseudomonads in biocontrol of phytopathogens for sustainable agriculture. *Appl. Soil Ecol.* 125, 35–45. doi: 10.1016/j.apsoil.2017.12.004

Mishra, P., Mishra, J., and Arora, N. K. (2021). Plant growth promoting bacteria for combating salinity stress in plants—recent developments and prospects: a review. *Microbiol. Res*. 252, 126861. doi: 10.1016/j.micres.2021.126861

Mukherjee, P., Mitra, A., and Roy, M. (2019). Halomonas rhizobacteria of *Avicennia marina* of indian sundarbans promote rice growth under saline and heavy metal stresses through exopolysaccharide production. *Front. Microbiol*. 10, 1207. doi: 10.3389/fmicb.2019.01207

Nawaz, A., Shahbaz, M., Asadullah., Imran, A., Marghoob, M. U., Imtiaz, M., et al. (2020). Potential of salt tolerant PGPR in growth and yield augmentation of wheat (*Triticum aestivum* L.) under saline conditions. *Front. Microbiol*. 11, 2019. doi: 10.3389/fmicb.2020.02019

Niu, S. Q., Li, H. R., Paré, P. W., Aziz, M., Wang, S. M., Shi, H., et al. (2016). Induced growth promotion and higher salt tolerance in the halophyte grass *Puccinellia tenuiflora* by beneficial rhizobacteria. *Plant Soil*. 407, 217–230. doi: 10.1007/s11104-015-2767-z

Orhan, F. (2021). Potential of halophilic/halotolerant bacteria in enhancing plant growth under salt stress. *Curr. Microbiol*. 78, 3708–3719. doi: 10.1007/s00284-021-02637-z

Panwar, M., Tewari, R., Gulati, A., and Nayyar, H. (2016). Indigenous salt-tolerant rhizobacterium *Pantoea dispersa* (PSB3) reduces sodium uptake and mitigates the effects of salt stress on growth and yield of chickpea. *Acta Physiol. Plant*. 38, 278. doi: 10.1007/s11738-016-2284-6

Patel, T., and Saraf, M. (2017). Biosynthesis of phytohormones from novel rhizobacterial isolates and their in vitro plant growth-promoting efficacy. *J. Plant Interact*. 12, 480–487. doi: 10.1080/17429145.2017.1392625

Poncheewin, W., van Diepeningen, A. D., van der Lee, T. A. J., et al. (2022). Classification of the plant-associated lifestyle of *Pseudomonas* strains using genome properties and machine learning. *Sci. Rep*. 12, 10857.

Prabhukarthikeyan, S. R., Parameswaran, C., Keerthana, U., Teli, B., Jagannadham, P. T., Cayalvizhi, B., et al. (2020). Understanding the plant-microbe interactions in CRISPR/cas9 era: indeed a sprinting start in Marathon. *Curr. Genom*. 21, 429–443. doi: 10.2174/1389202921999200716110853

Prasad, M., Ramakrishnan, S., Chaudhary, M., Choudhary, M., and Jat, L. K. (2019). "Plant growth promoting rhizobacteria (PGPR) for sustainable agriculture: perspectives and challenges" in *PGPR Amelioration in Sustainable Agriculture*, eds A. K. Singh, A. Kumar and P. K. Singh (Woodhead Publishing), 129–157. doi: 10.1016/B978-0-12-815879-1.00007-0

Rahman, M. M., Mostofa, M. G., Keya, S. S., Siddiqui, M. N., Ansary, M. M. U., Das, A. K., et al. (2021). Adaptive mechanisms of halophytes and their potential in improving salinity tolerance in plants. *Int. J. Mol. Sci*. 22, 10733. doi: 10.3390/ ijms221910733

Ravichandran, M., Samiappan, S. C., Rangaraj, S., Murugan, K., Al-Dhabi, N. A., and Karuppiah, P. (2022). "Nanoemulsion formulations with plant growth promoting rhizobacteria (PGPR) for sustainable agriculture" in *Nanobiotechnology for Plant Protection*, eds K. A. Abd-Elsalam and K. Murugan (Amsterdam: Elsevier) 207–223 doi: 10.1016/B978-0-323-89846-1.00017-6

Safdarian, M., Askari, H., Shariati, J. V., and Nematzadeh, G. (2019). Transcriptional responses of wheat roots inoculated with *Arthrobacter nitroguajacolicus* to salt stress. *Sci. Rep*. 9, 1792. doi: 10.1038/s41598-018-38398-2

Saghafi, D., Delangiz, N., Lajayer, B. A., and Ghorbanpour, M. (2019b). An overview on improvement of crop productivity in saline soils by halotolerant and halophilic PGPRs. *3 Biotech* 9, 261. doi: 10.1007/s13205-019-1799-0

Saghafi, D., Ghorbanpour, M., Ajirloo, H. S., and Lajayer, B. A. (2019a). Enhancement of growth and salt tolerance in *Brassica napus* L. seedlings by halotolerant Rhizobium strains containing ACC-deaminase activity. *Plant Physiol. Rep*. 24, 225–235. doi: 10.1007/s40502-019-00444-0

Sandhya, V., Ali, S. Z., Grover, M., Reddy, G., and Venkateswarlu, B. (2010). Effect of plant growth promoting *Pseudomonas* spp. on compatible solutes, antioxidant status and plant growth of maize under drought stress. *Plant Growth Regul*. 62, 21–30. doi: 10.1007/s10725-010-9479-4

Santos, A. D. A., Silveira, J. A. G. D., Bonifacio, A., Rodrigues, A. C., and Figueiredo, M. D. V. B. (2018). Antioxidant response of cowpea co-inoculated with plant growth-promoting bacteria under salt stress. *Braz. J. Microbiol*. 49, 513–521. doi: 10.1016/j.bjm.2017.12.003

Sarker, P. K., Karmoker, D., Shohan, M. U. S., Saha, A. K., Rima, F. S., Begum, R. A., et al. (2022). Effects of multiple halotolerant rhizobacteria on the tolerance, growth, and yield of rice plants under salt stress. *Folia Microbiol*. 2022, 1–18. doi: 10.1007/s12223-022-00997-y

Sohaib, M., Zahir, Z. A., Khan, M. Y., Ans, M., Asghar, H. N., Yasin, S., et al. (2020). Comparative evaluation of different carrier-based multi-strain bacterial formulations to mitigate the salt stress in wheat. *Saudi J. Biol. Sci*. 27,777–787. doi: 10.1016/j.sjbs.2019.12.034

Sukweenadhi, J., Balusamy, S. R., Kim, Y. J., Lee, C. H., Kim, Y. J., Koh, S. C., et al. (2018). A growth-promoting bacteria, *Paenibacillus yonginensis* DCY84T enhanced salt stress tolerance by activating defense-related systems in *Panax ginseng*. *Front. Plant. Sci*. 9, 813. doi: 10.3389/fpls.2018.00813

Sun, L., Lei, P., Wang, Q., Ma, J., Zhan, Y., Jiang, K., et al. (2020). The endophyte *Pantoea alhagi* NX-11 alleviates salt stress damage to rice seedlings by secreting exopolysaccharides. *Front. Microbiol*. 10, 3112. doi: 10.3389/fmicb.2019.03112

Sunita, K., Mishra, I., Mishra, J., Prakash, J., and Arora, N. K. (2020). Secondary metabolites from halotolerant plant growth promoting rhizobacteria for ameliorating salinity stress in plants. *Front. Microbiol*. 11, 567768. doi: 10.3389/fmicb.2020.567768

Tabassum, B., Khan, A., Tariq, M., Ramzan, M., Khan, M. S. I., Shahid, N., et al. (2017). Bottlenecks in commercialisation and future prospects of PGPR. *Appl. Soil Ecol*. 121, 102–117. doi: 10.1016/j.apsoil.2017.09.030

Thakur, M. P., Van der Putten, W. H., Cobben, M. M. P., Kleunen, M. V., and Geisen, S. (2019). Microbial invasions in terrestrial ecosystems. *Nat. Rev. Microbiol*. 17, 621–631. doi: 10.1038/s41579-019-0236-z

Yasin, N. A., Akram, W., Khan, W. U., Ahmad, S. R., Ahmad, A., and Ali, A. (2018). Halotolerant plant-growth promoting rhizobacteria modulate gene expression and osmolyte production to improve salinity tolerance and growth in *Capsicum annum* L. *Environ. Sci. Pollut. Res*. 25, 23236–23250. doi: 10.1007/s11356-018-2381-8

Zhang, J. L., Aziz, M., Qiao, Y., Han, Q. Q., Li, J., Wang, Y. Q., et al. (2014). Soil microbe *Bacillus subtilis* (GB03) induces biomass accumulation and salt tolerance with lower sodium accumulation in wheat. *Crop Pasture Sci*. 65, 423–427. doi: 10.1071/CP 13456

Zhang, X., Liu, P., Qing, C., Yang, C., Shen, Y., and Ma, L. (2021). Comparative transcriptome analyses of maize seedling root responses to salt stress. *Peer J*. 9, e10765. doi: 10.7717/peerj.10765

Zhao, C., Zhang, H., Song, C., Zhu, J.-K., and Shabala, S. (2020). Mechanisms of plant responses and adaptation to soil salinity. *Innovation* 1, 100017. doi: 10.1016/j.xinn.1 00017

frontiers | Frontiers in Microbiology

TYPE Original Research
PUBLISHED 14 February 2023
DOI 10.3389/fmicb.2023.1085787

OPEN ACCESS

EDITED BY
Sudhir K. Upadhyay,
Veer Bahadur Singh Purvanchal University, India

REVIEWED BY
Dilfuza Jabborova,
Academy of Sciences Republic of Uzbekistan (UzAS), Uzbekistan
Salma Mukhtar,
Connecticut Agricultural Experiment Station, United States

*CORRESPONDENCE
Joseph Ezra John
✉ ezrajohn4@gmail.com
Chidamparam Poornachandhra
✉ poorna155c@gmail.com

SPECIALTY SECTION
This article was submitted to Extreme Microbiology, a section of the journal Frontiers in Microbiology

RECEIVED 31 October 2022
ACCEPTED 16 January 2023
PUBLISHED 14 February 2023

CITATION
John JE, Maheswari M, Kalaiselvi T, Prasanthrajan M, Poornachandhra C, Rakesh SS, Gopalakrishnan B, Davamani V, Kokiladevi E and Ranjith S (2023) Biomining *Sesuvium portulacastrum* for halotolerant PGPR and endophytes for promotion of salt tolerance in *Vigna mungo* L. *Front. Microbiol.* 14:1085787. doi: 10.3389/fmicb.2023.1085787

Biomining *Sesuvium portulacastrum* for halotolerant PGPR and endophytes for promotion of salt tolerance in *Vigna mungo* L.

Joseph Ezra John[1]*, Muthunalliappan Maheswari[1], Thangavel Kalaiselvi[2], Mohan Prasanthrajan[1], Chidamparam Poornachandhra[1]*, Srirangarayan Subramanian Rakesh[1], Boopathi Gopalakrishnan[3], Veeraswamy Davamani[1], Eswaran Kokiladevi[4] and Sellappan Ranjith[2]

[1]Department of Environmental Sciences, AC&RI, Tamil Nadu Agricultural University, Coimbatore, India, [2]Department of Agricultural Microbiology, AC&RI, Tamil Nadu Agricultural University, Coimbatore, India, [3]ICAR-National Institute of Abiotic Stress Management, Baramati, India, [4]Department of Biotechnology, Agricultural College and Research Institute, Tamil Nadu Agricultural University, Coimbatore, India

Halophytic plants can tolerate a high level of salinity through several morphological and physiological adaptations along with the presence of salt tolerant rhizo-microbiome. These microbes release phytohormones which aid in alleviating salinity stress and improve nutrient availability. The isolation and identification of such halophilic PGPRs can be useful in developing bio-inoculants for improving the salt tolerance and productivity of non-halophytic plants under saline conditions. In this study, salt-tolerant bacteria with multiple plant growth promoting characteristics were isolated from the rhizosphere of a predominant halophyte, *Sesuvium portulacastrum* grown in the coastal and paper mill effluent irrigated soils. Among the isolates, nine halotolerant rhizobacterial strains that were able to grow profusely at a salinity level of 5% NaCl were screened. These isolates were found to have multiple plant growth promoting (PGP) traits, especially 1-aminocyclopropane-1-carboxylic acid deaminase activity (0.32–1.18 μM of α-ketobutyrate released mg^{-1} of protein h^{-1}) and indole acetic acid (9.4–22.8 μgmL^{-1}). The halotolerant PGPR inoculation had the potential to improve salt tolerance in *Vigna mungo* L. which was reflected in significantly ($p<0.05$) higher germination percentage (89%) compared to un-inoculated seeds (65%) under 2% NaCl. Similarly, shoot length (8.9–14.6cm) and vigor index (792–1785) were also higher in inoculated seeds. The strains compatible with each other were used for the preparation of two bioformulations and these microbial consortia were tested for their efficacy in salt stress alleviation of *Vigna mungo* L. under pot study. The inoculation improved the photosynthetic rate (12%), chlorophyll content (22%), shoot length (5.7%) and grain yield (33%) in *Vigna mungo* L. The enzymatic activity of catalase and superoxide dismutase were found to be lower (7.0 and 1.5%, respectively) in inoculated plants. These results revealed that halotolerant PGPR isolated from *S. portulacastrum* can be a cost-effective and ecologically sustainable method to improve crop productivity under high saline conditions.

KEYWORDS

Halophyte, rhizobacteria, endophytes, salt tolerance, crop improvement, ACC deaminase

1. Introduction

Agricultural productivity is very important to ensure food security in future with the ensuing population rise. As per the Global Agricultural Productivity (GAP) Index, the current growth rate of agricultural production is not enough to meet the projected food demand of 10 billion people in 2050 (Zeigler and Steensland, 2022). In addition to this, plants are confronted with various kinds of stresses such as drought, flooding, salinity, heat, cold, nutrient deficiency and exposure to heavy metals, phytopathogen, pest attack, etc. Among various environmental stressors, excessive presence of salts in soil (soil salinity) is one of the major problems responsible for the reduction of crop growth and productivity across the globe. It is reported that more than 1,000 million hectares of land are affected by salinity throughout the world (Negacz et al., 2022). Globally, about 10% of agricultural soils are under the threat of salinization due to continuous usage of fertilizer and poor-quality water for irrigation (Borsato et al., 2020; Kumar and Sharma, 2020). Salinity adversely affects crop productivity in arid and semi-arid areas around the world where it causes an annual loss of 1–2% of arable land (Shrivastava and Kumar, 2015). Soil salinity also induces biochemical changes in the salt sensitive crop owing to disturbance in osmotic potential, imbalance in ion concentration, and increased Reactive Oxygen Species (ROS) production (Singh et al., 2022). This leads to the break in electron transport chain and cleavage of hydrogen bond between the amino acids in the genetic material which has deleterious effect on crop (Ermakova et al., 2019). Furthermore, high concentration of salts in the plant cells were reported to induce oxidative stress and enhanced production of stress ethylene, which in turn affects the physiological processes like respiration, photosynthesis, nitrogen fixation, etc. (Gupta and Huang, 2014; Paul and Lade, 2014; Acosta-Motos et al., 2017).

Removal of salt from saline soil is an intensive process which is time consuming and requires financial investment (Qadir et al., 2014). However, for a long time, the reclamation of saline soils was carried out mainly by physical and chemical processes. In physical process, soluble salts in the root zone are removed by scraping, flushing and leaching methods, while the use of gypsum and lime as neutralizing agents in saline soils is employed in chemical method (Ayyam et al., 2019). But these methods are not sustainable when the salt concentration is too high in soils continuously irrigated with saline water. Unless these salts are leached from the soil, they accumulate to levels that are inhibitory to plant growth and may lead to soil salinity. In the long run, salinity causes the degradation of soil structure affecting water and root penetration along with other problems (Gul et al., 2014). In these cases, phytoremediation comes as a viable alternative to ensure soil productivity, preferably halophytes that have evolved to grow in saline soils and uptake salt (Flowers and Colmer, 2015). With considerable progress in understanding physiological and molecular mechanisms in salt tolerance of halophytes, some have been found to possess genes suitable for improving salt tolerance and phytoremediation potential (Shabala, 2013; Gul et al., 2014; Diray-Arce et al., 2015). Besides this, microbes associated with rhizosphere are known to promote the desired effect like, growth regulation, remediation potential, biotic and abiotic stress tolerance, etc. (Upadhyay et al., 2022a). Microbes found in the rhizosphere (rhizobacteria) or within plant tissues including roots (endophytes) have the potential to contribute significantly to the ability of plants to adapt to adverse conditions (Numan et al., 2018; Chauhan et al., 2022). However, the potential contribution of microorganisms associated with these plants in the soil, on plant surfaces, or within plant tissues is underutilized.

Exogenous compounds produced by microorganisms in the rhizosphere region promote nutrient uptake, control pathogens, and lessen the effects of salinity and sodicity (Damodaran et al., 2013). These include Indole Acetic Acid (IAA) production (Ahemad and Kibret, 2014), Hydrogen Cyanide (HCN) production, siderophore production, 1-Aminocyclopropane-1-carboxylate (ACC) deaminase production, nutrient solubilization and suppression of soil borne pathogens (Dimkpa et al., 2009). Furthermore, certain microorganisms promote the activity of plant anti-oxidants and osmolytes production (Etesami and Beattie, 2018). The direct and indirect mechanisms, metabolism and chemotaxis in promotion of growth in plants are interceded by gene cluster that activates host–PGPR interactions. In *Bacillus subtilis*-GB03, out of 38 genes, 30 genes responded to the change in the root structure of the host (*Arabidopsis* sp.) in addition to growth promotion (Ryu et al., 2003). The upsurge in nutrient availability and production of plant growth regulators (IAA, ACC deaminase, ethylene and gibberellic acid) are direct mechanisms through which microbes improve crop growth (Upadhyay et al., 2022b). The siderophore production is known to promote iron availability that has direct impact on crop growth. Siderophores also exert antimicrobial activity by limiting iron availability to the pathogens. The EPS, HCN and hydrolytic enzyme production has various indirect benefits to the crop such as antipathogenic potential, disease resistance and abiotic stress tolerance (Upadhyay et al., 2011, 2022b). Microbial isolates with PGP characteristics from rhizosphere regions of halophytes like *A. nummularia* (Da Silva et al., 2016) and *Salicornia* sp. (Mapelli et al., 2013) could provide an alternative option for chemical amendments. Characterizing these bacteria from saline environments may lead to the identification of beneficial microorganisms for use as inoculants to stimulate the growth of non-host plants under saline conditions.

In an earlier study with the halophyte *Sesuvium portulacastrum* collected from the coastal soils of Tamil Nadu, India, it was observed that *S. portulacastrum* had the potential to mitigate salination of soil irrigated with paper and pulp mill effluent containing high salt (John et al., 2022). This experiment was conducted in paper and pulp mill effluent irrigated area near Tamil Nadu Newsprint and Papers Limited (TNPL), Karur, Tamil Nadu, India and it is known as the Treated Effluent Water Lift Irrigation System area (TEWLIS). The current practice for managing saline soils among the farming community is flooding and leaching of salts with good quality water. However, the lack of good quality water, expertise in soil drainage and high-cost requirements discourage them from practicing it especially, where wastewater is the only source for irrigation. In this case, microbial assisted agriculture could improve the crop growth and yield which requires minimum skill and cost. Halophytes harbor salt tolerant microorganisms as endophytes and epiphytes which are also capable of growing in saline environment. These microorganisms have been reported to enhance biotic (Masum et al., 2018) and abiotic stress (Upadhyay et al., 2011) tolerance in many crops. However, endophytes of *Sesuvium portulacastrum* have not been reported yet. Due to its ability to grow in higher concentration of salt, it is felt that the culturable endo and epiphytic bacteria of *Sesuvium portulacastrum* could tolerate salinity and also trigger induced systemic tolerance against salinity stress in plant. Keeping this in view, the current study was conceived to isolate epiphytic and endophytic plant growth promoting bacterial flora from halophyte, *S. portulacastrum* grown in salt affected ecosystem. Further investigation was done to validate the potential of halotolerant plant

growth promoting bacterial effects on salt sensitive crop (*Vigna mungo* L.) grown in saline condition. A total of 31 isolates were obtained from rhizosphere of *S. portulacastrum* of which nine strains were found to be halotolerant. These isolates were evaluated for their PGP characteristics, tested under *in vitro* for their growth promotion in *Vigna mungo* L. at 2% NaCl and were identified through 16 s RNA sequencing. All the nine isolates had at least one PGP capability, hence two consortia with three strains in each were formulated based on the compatibility between the isolates. Microbial consortium I (MC I) had *Metabacillus indicus, Neobacillus niacini* and *Serratia marcescens*; while MC II (Microbial consortium II) was formulated with *Bacillus velezensis, Kocuria rhizophila*, and *Kosakonia radicincitans*. Consequently, their potential in growth promotion of salt sensitive glycophyte, *Vigno mungo* L. in paper and pulp mill effluent irrigated soil under pot culture experiment was confirmed.

2. Materials and methods

2.1. Collection of samples

The soil and plant samples were initially collected from the coastal area of Parangipettai, Tamil Nadu, India. The *S. portulacastrum* was mostly found on the sandy shores of the backwaters (Figure 1). The collected halophyte was successfully established in the soil salinized by paper and pulp mill effluent irrigation at Karur, Tamil Nadu, India. The rhizospheric soil from two soil series, Thulukanur and Vannapatti soil series in the paper mill effluent irrigated area was collected. The samples were collected in sterile plastic bags and transferred to laboratory for further analysis. The organic matter was analyzed by the Walkley-Black method while Electrical Conductivity (EC) and pH were analyzed by the saturated paste extract method (Murtaza et al., 2017). The physico chemical properties are tabulated in Supplementary Table S3. Soil samples required for the study were collected from the soils of long-term treated paper and pulp mill effluent irrigated area located at 11° 01′24.9″ N and 77° 59′59″ E. Adequate amount of soil was shade dried, large debris was removed and subsequently 10 kg of soil was transferred to perforated pots for secondary evaluation. The pH and EC of the experimental soil were found to be 8.18 and 2.62 dS m^{-1}, respectively (Supplementary Table S3). The Exchangeable Sodium Percentage (ESP) of the soil was 13.54 per cent with an organic carbon content of 0.63 per cent.

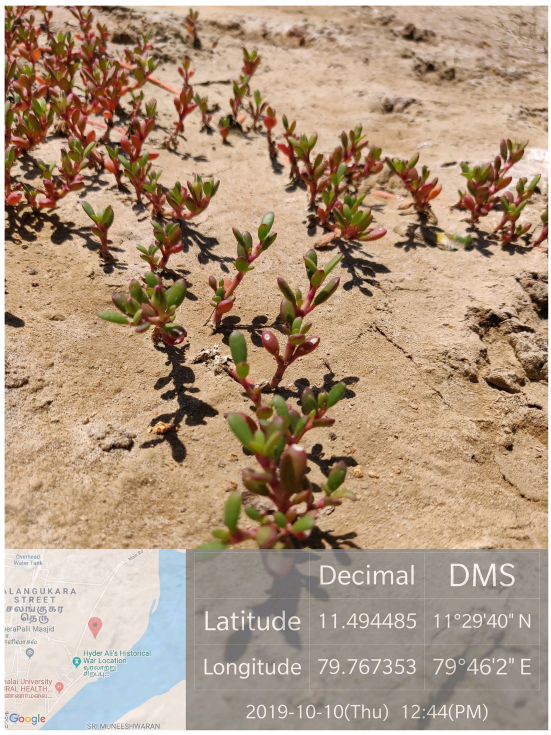

FIGURE 1
Collection of *Sesuvium portulacastrum* from the shores of backwaters at Parangipettai, Tamil Nadu, India.

2.2. Isolation and characterization of the halotolerant bacteria

To isolate rhizospheric bacteria, plant roots were gently shaken to remove the clumps of loosely adhering soil to the roots, leaving behind the root-firmly adhering soil particles (rhizospheric soil), which were then suspended and vortexed in 100 mL of sterile 1% NaCl solution. Thereafter, 10 folded serial dilutions (10×, 20×, 30×, 40×, and 50×) were prepared and 1 ml from each diluent was plated on nutrient agar (NA) medium (Supplementary Table S1) supplemented with 2% NaCl. The plates were incubated at 28°C and monitored for colony formation for up to 1 week (Fisher et al., 2007). For the isolation of endophytic bacteria, the roots of the collected samples were washed carefully under running tap water for 10 min to remove adhering soil particles. The roots were disinfected with 70% ethanol for 1 min, then rinsed three times with sterile distilled water. The roots were then surface sterilized with 3% sodium hypochlorite solution containing a few drops of Tween 20 R (Sigma-Aldrich, Steinheim, Germany) for 10 min followed by six rinses with sterile distilled water. To confirm root surface sterilization efficiency, an aliquot (100 mL) from the sixth wash solution was spread on NA medium and incubated at 28°C for 5 days. Thereafter, 1 g of the surface sterilized root tissue was macerated with a sterilized mortar and pestle in 10 mL distilled water and 1 mL from the tissue extracts and the serial diluents (10×, 20×, and 30×) were spread on NA medium supplemented with 2% NaCl. The plates were incubated at 28°C and monitored for up to 1 week for bacterial colony formation (Ramadoss et al., 2013).

The colonies of rhizospheric and endophytic bacterial isolates were examined morphologically for their shape, size, margin, elevation, appearance, texture, and pigmentation. In addition, cellular morphology, shape, Gram staining and biochemical characters were also examined (Sandhya and Ali, 2018; Supplementary Table S2). Colonies with distinct morphological characteristics were selected and purified by subculturing three times on NA media supplemented with 3% NaCl, before their storage in a 40% glycerol solution at −20°C till further use. Each sample was labeled representing the plant source (*Sesuvium portulacastrum*: SP) followed by the abbreviation of collection site (P: Parangipettai coastal soil; TV: TEWLIS area Vannapatti series and TT: TEWLIS area Thulukanur series), E in case of Endophytic, and the isolate number.

2.3. Halotolerant assay

Initially, all bacterial isolates were screened for halotolerance using NA media supplemented with 2 and 3% NaCl (14.7 and 21.6 dS m^{-1},

respectively). The cultures that were found to grow in 3% were selected for further evaluation with growth curve experiment. The 48 h old cultures of the isolates from the broth were transferred with an equal quantity of inoculum (Optical density of 660 nm = 0.10) to 100 mL NA broth supplemented with 3, 5 and 7% NaCl (21.6 dS m^{-1}, 32.3 dS m^{-1} and 41.1 dS m^{-1}, respectively). The OD 660 nm values were measured once in 4 h for all the isolates until the stationary phase is achieved. The OD 660 values were plotted against the time to obtain the growth curve under each level of NaCl.

2.4. Plant growth promotion assessment

Plant growth promoting traits of bacterial isolates were assessed for ammonia production, inorganic phosphate solubilization, siderophore production, IAA production and ACC deaminase activity. All assays were carried out in triplicates and the activity was assessed.

2.4.1. Ammonia production

The production of ammonia by rhizobacteria was tested in 10 mL of peptone water. After 48 h of incubation at 30°C, Nessler's reagent (0.5 mL) was added to each tube (Bhavani and Kumari, 2019). The development of brown to yellow color was quantified using spectrophotometer against standard graph (425 nm).

2.4.2. Phosphate solubilization assay

The ability of inorganic phosphate solubilization was conducted by spot inoculation of bacterial isolates on modified Pikovskayas agar plates using tricalcium phosphate as a substrate (Goswami et al., 2014). The formation of transparent halo zones around the bacterial colonies after 7 days of incubation at 28°C was considered an indication of phosphate solubilizing activity. The solubilization index was calculated by Equation 1.

$$\text{Solubilization index} = \frac{(\text{Colony diameter} + \text{Halo zone diameter})}{\text{Colony diameter}} \quad (1)$$

2.4.3. Siderophores production assay

The siderophore production was assayed by spot inoculation of selected bacterial isolates on Chrome Azurol S (CAS) blue agar plates as described by Schwyn and Neilands (1987). The cultures were incubated for 7 days at 28°C on CAS blue agar plates. The formation of orange zones around the growing colonies was monitored and bacterial isolates scored as siderophore producers.

$$\text{Siderophore production index} = \frac{(\text{Colony diameter} + \text{Orange zone diameter})}{\text{Colony diameter}} \quad (2)$$

2.4.4. Indole acetic acid production assay

Bacterial isolates were inoculated into 5 mL Luria-Bertani (LB) broth containing 0.2% L-tryptophan, pH 7.0 and incubated at 28°C with shaking at 125 rpm for 7 days. The cultures were centrifuged at 11,000 rpm for 15 min. One milliliter of the supernatant was mixed with 2 mL of Salkowski reagent and the appearance of a pink color indicated IAA production. OD was read at 530 nm using spectrophotometer. The level of IAA produced was estimated against a standard IAA (Shahzad et al., 2017).

2.4.5. ACC deaminase assay

The isolates were grown in 5 mL of LB broth at 28°C until they reached the stationary phase. To induce ACC deaminase activity, the cells were collected by centrifugation and washed twice with 0.1 M Tris–HCl (pH 7.5). Then the cells were suspended in 2 mL of modified DF minimal medium supplemented with 3 mM final concentration of ACC and incubated at 28°C with shaking for another 36–72 h. ACC deaminase activity was determined by measuring the cleavage of ACC into α-ketobutyrate and ammonia. The induced bacterial cells were harvested by centrifugation at 7,500 rpm for 5 min, washed twice with 0.1 M Tris–HCl (pH 7.5), and resuspended in 200 µL of 0.1 M Tris–HCl (pH 8.5). The cells were labialized by adding 5% toluene (v/v) and then vortexed at the highest speed for 30 s. 50 µL of labialized cell suspension was incubated with 5 µL of 0.3 M ACC in an Eppendorf tube at 28°C for 30 min. The negative control for this assay included 50 µL of labialized cell suspension without ACC, while the blank included 50 µL of 0.1 M Tris–HCl (pH 8.5) with 5 µL of 0.3 M ACC. The samples were then mixed thoroughly with 500 µL of 0.56 N HCl by vortexing and the cell debris was removed by centrifugation at 12,000 rpm for 5 min. A 500 µL aliquot of the supernatant was transferred to a glass test tube and mixed with 400 µL of 0.56 N HCl and 150 µL of DNF solution (0.1 g of 2,4-dinitrophenylhydrazine in 100 mL of 2 N HCl) and the mixture was incubated at 28°C for 30 min. One milliliter of 2 N NaOH was added to the sample before the absorbance at 540 nm was measured. The concentration of α-ketobutyrate in each sample was determined by comparison with a standard curve generated as follows: 500 µL α-ketobutyrate solutions of 0, 0.01, 0.05, 0.1, 0.2, 0.5, 0.75, and 1 mM were mixed, respectively, with 400 µL of 0.56 N HCl and 150 µL DNF solution. One milliliter of 2 N NaOH was added and the absorbance at 540 nm was determined as described above. The values for absorbance versus α-ketobutyrate concentration (mM) were used to construct a standard curve (Glick, 2014; Del Carmen Orozco-Mosqueda et al., 2019).

2.5. Identification through 16S rRNA sequencing

The bacterial isolates were confirmed by molecular analysis of the 16S rRNA gene for bacteria. DNA isolation from microbial samples was done using the EXpure Microbial DNA isolation kit developed by Bogar Bio Bee stores Pvt. Ltd. DNA concentrations were measured by Qubit fluorometer 3.0. The PCR amplification was done by adding 5 µL of isolated DNA in 25 µL of PCR reaction solution (1.5 µL of Forward Primer and Reverse Primer, 5 µL of deionized water, and 12 µL of Taq Master Mix). The DNA template is heated to 95°C for 2.5 min and cooled at 55°C for 30 s. Then it is heated to 72°C, the optimal temperature for DNA polymerization. The unincorporated primers and dNTPs from PCR products were removed by using Montage PCR Clean up kit (Millipore). Then the DNA sequencing was performed using an ABI PRISM® Big Dye™ Terminator Cycle Sequencing Kit with AmpliTaq® DNA polymerase (FS enzyme) (Applied Biosystems). Single-pass sequencing was performed using below 16 s rRNA universal primers. The samples were resuspended in distilled water and subjected to electrophoresis in an ABI 3730xl sequencer (Applied Biosystems).

The 16 s rRNA sequence was blasted using NCBI blast similarity search tool. The phylogeny analysis with the closely related sequence of blast results was performed by multiple sequence alignment. The MUSCLE 3.7 was used for multiple alignments of sequences (Edgar, 2004). Poorly aligned positions and divergent regions were cured using the program G blocks 0.91b (Talavera and Castresana, 2007). Finally, the program PhyML 3.0 aLRT was used for phylogeny analysis and HKY85 as substitution model. The program Tree Dyn 198.3 was used for tree rendering (Dereeper et al., 2008).

2.6. *In vivo* evaluation of the selected isolates on *Vigna mungo* L. under salinity

The salt tolerant isolates were evaluated for their effect on germination and growth attributes of *Vigna mungo* L. under salinity (2% NaCl). An initial standardization experiment was carried out to fix the level of initial tolerance of *Vigna mungo* L. Accordingly, germination and growth of *Vigna mungo* L. under three different salinity was evaluated (0.5, 1, 1.5, 2, 3% NaCl). As per ISTA (International Seed Testing Association), the NaCl concentration at which the germination percentage falls below 65% should be selected to observe the impact of microbial inoculation. Hence 2% NaCl concentration was selected for the *in vivo* evaluation of isolates. The *Vigna mungo* L. seeds were surface sterilized in 0.1% sodium hypochlorite for 3 min and repeatedly washed with distilled water. After this, the 28 h old inoculum of all the isolates was individually used for seed priming. The NA broth without isolate was used as a control. The microbial inoculum with an OD of 1 at 660 nm was used for seed priming. After which the seeds were grown in germination sheets placed in 2% NaCl solution. The germination percentage, root length, shoot length and total dry weight were measured after 20 days. The growth vigor was calculated using Equation 3.

$$\text{Vigor index} = \text{Germination percentage x Seedling length}\,(\text{mm}) \quad (3)$$

2.7. Compatibility evaluation among the isolates for developing consortium

The culture compatibility among the bacterial isolates was assessed by cross streaking method using NA medium. The bacterial strain was streaked at one end of the plate followed by streaking the other bacterial strains perpendicular to it and incubated at 30°C for 24–48 h. The inhibition in growth between the cultures was noted and the compatible microbes were selected for further confirmation. The selected compatible strains were streaked in a triangular pattern so that all the streaks overlap each other as a confirmation test. Any two perpendicular steaks that showed inhibition were incompatible and the absence of inhibition proved that the cultures were compatible (Thomloudi et al., 2019).

The elite compatible microbial isolates were mass multiplied as pure cultures in the NA media for further formulation of the microbial consortium. The mass culturing was carried out in 250 mL Erlenmeyer flask, which serves as seed culture for further multiplication. The culture broth was autoclaved in 15 lbs for 20 min and after cooling the microbial isolates were inoculated as loopful cultures in their respective broths prepared. The inoculated flasks were maintained as shake flask cultures by incubating them at room temperature at 120 rpm for 2 days for mass production. The 48 h old cultures were serially diluted and plated to count the population in the broth. To attain a uniform population in the consortium, 5 mL inoculum was centrifuged at 10,000 rpm for 15 min at 10°C and resuspended in 10 mL of deionized water to obtain 4×10^9 CFU (Jain and Srivastava, 2012). The OD 660 nm value was also recorded for the resuspended water used for consortium development. Talc was used as carrier material for the consortium due to its local availability and high Magnesium and Calcium content. Talc is a fine, light-weight powder that is easily soluble in water and has been shown to retain viable bio-inoculant propagules (Tripathi et al., 2015). A 100 g of talc was taken in autoclavable plastic bags and autoclaved. A 10 mL of the resuspended solution of each selected isolate was mixed to obtain the consortium. A total volume of 30 mL of the bacterial isolates was added to the carrier material and left for drying in shade (1 day), after which it was evaluated as a soil inoculant.

2.8. Evaluation of microbial consortium application on growth and yield of *Vigna mungo* L.

The potential of microbial consortium dosage on alleviation of salt stress in *Vigna mungo* L. was assessed through a pot culture experiment and the details of treatment are given in Table 1. The treated effluent with EC of 2.5 dS m^{-1} was used for irrigation. The pots were irrigated at an interval of 5–7 days based on the field capacity of the soil (22.5 per cent) which was estimated using pressure plate apparatus (Obi, 1974). After the application of amendments and microbial consortium, five seeds were sown in each 3 kg pot and irrigated with treated effluent. Thinning was carried out after 15 days to maintain a uniform population of 3 plants per pot. The morphological, physiological and biochemical parameters were recorded at three growth stages *viz*., vegetative (25th day), flowering (45th day) and harvest stage. The height of the plant from the ground level to the tip of the main stem was measured and expressed in centimeters. The physiological and biochemical parameters including chlorophyll content, leaf free proline content and catalase were carried out using standard procedures.

2.8.1. Morphological and physiological characterization of plant samples

The morphological and physiological characteristics of the plant were measured during the flowering stage of the crop (45 days after sowing). The Chlorophyll Content Meter (CCM-200+, United States) was used to assess chlorophyll content in the leaves. These measurements

TABLE 1 Details of treatment for assessing the salinity stress alleviation by microbial consortium.

Factor 1:	Microbial consortium
I_1 -	Control
I_2 -	Microbial consortium I (*M. indicus* + *N. niacini* + *S. marcescens*)
I_3 -	Microbial consortium II (*B. velezensis* + *K. radicincitans* + *K. rhizophila*)
Factor 2:	Dosage
D_1 -	2 kg ha^{-1} as soil application
D_2 -	4 kg ha^{-1} as soil application

were taken at three different points of young fully expanded leaves of each treatment during bright sunshine (Dhevagi et al., 2022). Similarly, photosynthetic rate and stomatal conductance were measured using a portable photosynthesis system (ADC BioScientific LCpro-SD System, United Kingdom) (Dhevagi et al., 2022).

2.8.2. Osmoregulatory metabolite and antioxidant enzymes analysis

The biochemical parameters like proline, catalase, and superoxide dismutase (SOD) were assessed during the flowering stage of the crop (45 days after sowing). For estimation of proline, 0.5 g of fresh leaf was homogenized in chilled 10 mL of 3% sulfosalicylic acid in precooled pestle and mortar. The homogenate was centrifuged at 12,000 rpm for 5 min at 4°C and 2 mL supernatant was transferred to test tube. Then 2 mL acid ninhydrin and 2 mL of glacial acetic acid were added and incubated in water bath (100°C) for 1 h. Then the test tubes were placed in ice bath to stop the reaction. Four mL of toluene was added and the tube was vortexed for 1 min. The extract was transferred to a cuvette to record the absorbance at 520 nm and plotted against standard graph of proline to express as µmol g^{-1} fresh weight (Bates et al., 1973). The catalase activity was estimated by following the methodology of Gopalachari (1963). Fresh plant tissue of 5 g was homogenized with ice-cold phosphate buffer (PB) 5 ml and centrifuged at 12,000 rpm for 10 min at 4°C to obtain the supernatant. One mL of supernatant was mixed with 1 mL of PB and 1 mL of 30 mM hydrogen peroxide and the absorbance of the supernatant was read at 240 nm. The decrease in absorbance was recorded every 30 s for 5 min. The absorbance was plotted against the standard graph of hydrogen peroxide to assess the catalase activity as the rate of oxidation of hydrogen peroxide per minute per gram. For SOD, one gram of fresh leaf was macerated in 10 ml of chilled 50 mM phosphate buffer in a prechilled mortar and pestle. The mixture was centrifuged at 12,000 rpm for 10 min at 4°C to collect the supernatant. A reaction mixture of 1.3 mL of sodium carbonate buffer, 500 µL of Nitroblue tetrazolium (NBT) and 100 µL EDTA was prepared. After which 100 µL of hydroxylamine hydrochloride was added and incubated for 2 min at room temperature to initiate the reaction. 100 µL of supernatant was added and the absorbance at 560 nm was recorded every 30 s for 1–2 min. The absorbance was plotted against the standard graph of NBT at 560 nm to obtain the superoxide dismutase activity per gram of sample (Dhindsa et al., 1981).

2.8.3. Assessing the quantity and quality of yield

The mature pods in *Vigna mungo* L. were harvested after the 65th day and expressed in g pot^{-1}. The harvest index used as a measure of reproductive efficiency was worked out by using Equation 4. The protein content in the seeds was assessed through Folin phenol reagent method (Lowry et al., 1951). About 250 mg of *Vigna mungo* L. pod sample was taken and macerated with 10 mL of phosphate buffer solution. Centrifuged the contents at 3,000 rpm for 10 min and the supernatant was collected and made up the volume to 25 mL with distilled water. To 1 mL of the supernatant taken in a test tube, 5 mL of Lowry reagent and 0.5 mL of Folin reagent were added and incubated for 30 min. The color development was measured at 660 nm in a UV–vis spectrophotometer and bovine serum albumin was used as standard.

$$\text{Harvest index} = \frac{\text{Economic yield}}{\text{Biological yield}} \quad (4)$$

2.9. Statistical analysis

The data on various characteristics studied during the investigation were statistically analyzed by the method given by Gomez and Gomez (1984) using SPSS Version 16.0. The critical difference was worked out at 5 per cent (0.05) probability levels.

3. Results and discussion

3.1. Isolation of halotolerant bacteria from rhizosphere and root endosphere of *Sesuvium portulacastrum*

A total of eight morphologically different bacterial strains were isolated from rhizospheric soil samples of *Sesuvium portulacastrum* collected from coastal areas of Parangipettai. Bacterial isolates were labeled as SPP 1 to SPP 8. The rhizosphere soil samples from paper and pulp mill effluent irrigated soil (TEWLIS area) were collected and 16 strains with varying morphology were isolated. Out of 16 isolates, 9 were from Thulukanur soil series (SPTT 1 – SPTT 9) and 7 were from Vannapatti soil series (SPTV 1 – SPTV 7). Similarly, eight endophytic bacterial isolates were obtained from roots of profusely grown *S. portulacastrum* cultivated in two soil series of paper and pulp mill effluent irrigated areas. Two strains from Thulukanur soil series were named SPTTE 1 and SPTTE 2. Similarly, five strains from Vannapatti soil series were isolated and named SPTVE 1 to SPTVE 5. The isolates were screened for salt tolerance in NA media supplemented with 3% NaCl, since identifying halotolerant PGPR with high tolerance potential is essential. The inoculated plates were observed for colony growth after 48 h of incubation. Among 31 bacterial isolates, profuse growth was observed in 9 isolates (SPP 2, SPP 5, SPP 6, SPTT 3, SPTT 7, SPPTT 8, SPTV 3, SPTVE 3, and SPTVE 4), whereas other strains failed to grow in NA media supplemented with 3% NaCl. Among the isolates, two (SPTVE 3 and SPTVE 4) were endophytes.

3.2. Morphological and biochemical characteristics of bacterial isolates

The selected 9 strains were characterized for cell morphology, Gram behavior, pigment production and motility (Supplementary Table S2). Out of 9 isolates, 6 tested positive in Gram test and the remaining were Gram negative. The isolate SPTT 8 was coccoid in shape and all others were rod shaped. The isolates SPP 2 and SPTT 8 exhibited orange and light green colonies, respectively, whereas no distinguishable colors were noticed in the other isolates. The orange or red pigmentation, due to carotenoids might help the bacteria against damaging UV radiation (Khaneja et al., 2010). Strains SPTT 3, SPTT 7, SPTVE 3, and SPTVE 4 were motile which has diffused zone of growth extended out from the line of inoculation. Both flagellar motility and citrate utilization are thought to be important in bacterial root colonization and maintenance (Weisskopf et al., 2011). Biochemical characters such as casein, starch hydrolysis, citrate, amylase, protease, urease, catalase and oxidase activities, indole production, nitrate reduction and Methyl Red test – Voges Proskauer (MR-VP) are given in Supplementary Table S2. Among these traits, protease, catalase and amylase were positive for all the isolates. MR-VP test was positive for all isolates except SPP 2, SPP 5 and SPTVE 3. Isolates SPP 6, SPTT 8 and SPTVE 3 tested positive for urease activity. The strains SPP 5, SPTT

3, SPTT 7 and SPTVE 3 had the ability to reduce nitrate to nitrite. All the isolates tested positive for catalase test which indicates all are aerobic bacteria and would neutralize hydrogen peroxide by producing catalase enzyme (Facklam and Elliott, 1995). Protease test was positive for all the isolates which indicates their ability to breakdown protein into amino acids.

3.3. Identification of PGPR isolates by 16S rRNA sequence analysis

The nine selected bacterial isolates were identified by 16S rRNA sequencing and blasting in the NCBI database. The isolate SPP 2 has a similarity (99.9%) with that of *Metabacillus indicus* and SPP 5 was 99.7% similar to *Neobacillus niacini*. The SPP 6 was 100% similar to *Staphylococcus warneri* and SPTT 3 was 99.8% similar to *Bacillus velezensis*. Similarly, SPTT 7, SPTT 8 and SPTV 3 were similar to *Bacillus circulans, Kocuria rhizophila* and *Bacillus oleronius*, respectively. The isolate SPTVE 3 had 99.9% similarity with *Serratia marcescens* and SPTVE 4 was 99.8% similar to *Kosakonia radicincitanas*. The phylogenetic tree of isolates used in microbial consortium II was obtained by the Neighbor Joining method with a boot strap value of 1,000 and depicted in Figure 2. The derived nucleotide sequence was submitted to NCBI database and the GenBank accession numbers are given in Table 2.

TABLE 2 16S rRNA identification of the halotolerant plant growth promoting bacterial isolates.

Strain	Best match	Accession number	Match index
SPP 2	*Metabacillus indicus*	OP836561.1	99.6%
SPP 5	*Neobacillus niacini*	OP836562.1	99.7%
SPP 6	*Staphylococcus warneri*	OP836563.1	100%
SPTT 3	*Bacillus velezensis*	OP836557.1	99.8%
SPTT 7	*Bacillus circulans*	OP836560.1	100%
SPTT 8	*Kocuria rhizophila*	OP836556.1	100%
SPTV 3	*Bacillus acidicola*	OP836559.1	99.2%
SPTVE 3	*Serratia marcescens*	OP836558.1	99.9%
SPTVE 4	*Kosakonia radicincitans*	OP836555.1	99.8%

3.4. Assay for *in vitro* plant growth promotion activity

3.4.1. Indole-3-acetic acid (IAA) production

The bacterial isolates were screened for their ability to produce auxin (IAA). IAA is a phytohormone that functions as a natural auxin in plants (Carmen and Roberto, 2011). By using L-tryptophan found in root exudates, several bacteria can produce IAA as a secondary metabolite. IAA-producing bacteria help plants maintain their growth under salt conditions by increasing root length. Except for *S. warneri*, all other isolates produced red color after the addition of Salkowski's reagent in the culture supernatant since IAA production was found very common in PGPR, as shown by similar studies (Galkovskyi et al., 2012; Zahid et al., 2015; Islam et al., 2016). However, the intensity of red color developed was very low without tryptophan in the isolates *N. niacini* and *B. olerenius*. With the addition of tryptophan in the broth, IAA production was enhanced. The isolate SPTVE 3 had the highest IAA production of 23.60 $\mu g\,mL^{-1}$ followed by SPP 2 (22.80 $\mu g\,mL^{-1}$). The lowest IAA production was recorded in isolate *B. olerenius* (9.41 $\mu g\,mL^{-1}$) in tryptophan supplemented medium (Table 3). Devi et al. (2016) reported that *Serratia marcescens* AL2-16 isolated from *Achyranthes aspera* L. produced 83.2 $\mu g\,mL^{-1}$ of IAA in the presence of 1% L-tryptophan after 24 h incubation. Similarly, *S. marcescens* isolated in this study also produced the highest IAA (23.60 $\mu g\,mL^{-1}$ in 0.2% L-tryptophan) among other isolates.

3.4.2. Phosphate solubilization

The presence of P-solubilizers in soils may be seen as positive signs of using microorganisms as biofertilizers to enhance crop yield and promote sustainable agriculture development. The production of

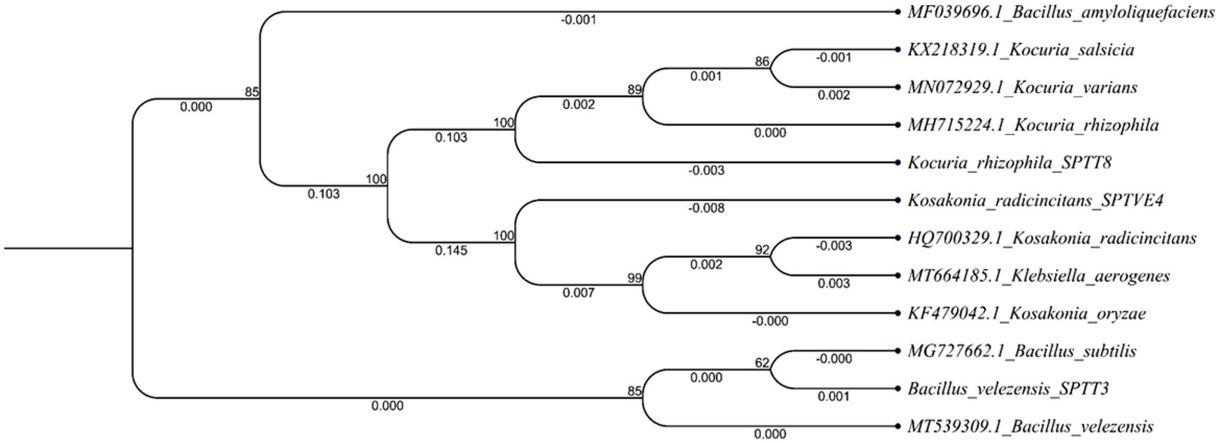

FIGURE 2
Phylogenetic tree of halotolerant isolates used for developing microbial consortium – II (*Bacillus velezensis*; *Kocuria rhizophila* and *Kosakonia radicincitans*). The 16S rRNA gene sequences of closely related species were retrieved from NCBI GenBank databases. The Neighbor joining phylogenetic tree was inferred using MEGA-7 software; evolutionary distance was computed using Maximum Composite Likelihood method at bootstrap value of 1,000.

TABLE 3 Plant growth promotion capabilities of the bacterial isolates from the rhizosphere and endosphere of *S. portulacastrum*.

Strains	Consortium	Phosphate solubilization index	Siderophore production index	IAA production ($\mu g mL^{-1}$)		Ammonia production ($\mu g mL^{-1}$)	ACC deaminase activity (μM of α-ketobutyrate released mg^{-1} protein h^{-1})
				2mg tryptophan g^{-1} broth	No tryptophan		
M. indicus	MC-I	2.44	–	22.81	4.20	3.86	0.603
N. niacini		–	2.88	10.40	1.70	–	–
S. marcescens		2.25	2.13	20.52	3.70	2.83	0.751
B. velezensis	MC-II	2.29	1.89	14.43	2.15	4.28	1.180
K. radicincitans		2.63	2.50	23.60	5.35	5.19	0.395
K. rhizophila		2.50	2.22	11.23	2.25	3.40	0.983
S. warneri	Non-compatible	2.00	1.70	–	–	–	–
B. acidicola		2.22	1.19	9.41	1.60	–	–
B. circulans		–	2.29	12.69	2.60	2.60	0.324

microbial metabolites such as organic acids, which lower the pH of the media, is primarily responsible for phosphate solubilization (Shahid et al., 2012). Phosphate solubilization by the isolates was visualized by the development of clear zones (Halo-zone) around the bacterial colonies after 3 days of incubation in Pikovskayas medium (Supplementary Figure S1). Out of 9, seven isolates were phosphate solubilizers indicated by the clear zones. The highest index was observed in the isolate *K. radicincitans* (2.63), followed by *K. rhizophila* at 2.50 (Table 3). The isolates *N. niacini* and *B. circulans* tested negative to solubilize phosphate. Shahid et al. (2015) stated that the most commonly exploited phosphate solubilizers are bacteria belonging to *Pseudomonas* sp., *Bacillus* sp., *Rhizobium* sp. and *Enterobacter* sp. Though *N. niacini* and *B. circulans* isolated in this study, belong to the bacillus genera they lack the ability to solubilize phosphate. *K. radicincitans* of Enterobacteriaceae family had the highest phosphate solubilization index (2.63) than the other isolates. Afridi et al. (2019) observed 16–17 mm halo zone around the colony of *Kocuria rhizophila*, whereas in the present study, 12 mm halo zone was formed in 48 h. Phosphate solubilizing bacteria have the ability to enhance phosphorus availability in the soil thereby promoting crop growth. In some cases, phosphate solubilization bacteria can promote plant growth both indirectly and directly by reducing phytopathogen growth and synthesizing phytohormones (Bhattacharjee, 2012).

3.4.3. Siderophore production

Siderophores are chemical compounds with iron-specific ligands that have low molecular weight (<10,000 Da). Various microorganisms synthesize it as an iron scavenging agent to maintain minimal iron stress. They are infinitesimal iron chelating compounds with a strong affinity for transporting ions across cell membranes and disease control (Pandey et al., 2017). Several studies have shown that the rhizosphere micro flora produces siderophores, which improve plant iron uptake (Kotasthane et al., 2017; Priyanka et al., 2020). Siderophore activity was absent in strain *M. indicus*, while all other isolates had production index in the range between 2.88 and 1.19 (Table 3). *Bacillus velezensis* NRRL B-41580 and *Bacillus siamensis* KCTC 13613 isolated from the rhizosphere of rice, respectively produced 69 and 55 per cent siderophore, according to Masum et al. (2018). Navarro-Torre et al. (2016) observed in their study that *S. warneri* isolated from the halophyte, *Arthrocnemum macrostachyum* had shown no siderophore activity. Contrastingly, in our study, the isolate *S. warneri* had a siderophore production index of 1.70. *Pantoea dispersa* isolated from mung bean rhizosphere had a 6–9 mm halo zone on Pikovskaya's agar medium indicating their ability to produce siderophore (Panwar et al., 2016; Supplementary Figure S2). The environmental conditions influence the production of bacterial siderophores and their efficacy in transferring iron (Singh et al., 2022). The siderophore increases the rate of phytoextraction of metals from rhizosphere. The production and transport of siderophore vary between Gram positive and Gram negative bacteria, since the outer membrane transporters are broadly absent in Gram positive bacteria. These transporters play a vital role in the transport of Fe-siderophore. RS-I (Reduction strategy) and CS-II (Chelation strategy) are two types of mechanism for Fe transport into the plant system. While, RS-I strategy is predominantly found in iron deficit soils, CS-II strategy is found in alkaline soil where bacteria are important agents for improving iron availability. This strategy (CS-II) is based on biosynthesis of siderophore that chelates Fe and transport it through TOM1 (Translocase of Outer Membrane) to the root (Dai et al., 2018).

3.4.4. Ammonia production

Ammonia production plays an important role in increasing plant growth by accumulating nitrogen, as well as assisting in root, shoot and biomass development (Dutta and Thakur, 2017). It also plays a vital role in remediation of polluted environment (Raklami et al., 2021), carbon sequestration (John and Lakshmanan, 2018) and various ecosystem services (Razzaghi Komaresofla et al., 2019). The highest value of 5.19 $\mu g mL^{-1}$ was recorded by isolate *K. radicincitans*, followed by *B. velezensis* (4.28 $\mu g mL^{-1}$). Ammonia production was absent in the isolates *N. niacini*, *S. warneri*, and *B. olernius*. Ammonia production in *K. rhizophila* isolated from *Oxalis corniculata* was reported to be 36 $\mu g mL^{-1}$ by Afridi et al. (2019), whereas in this study it was only 2.60 $\mu g mL^{-1}$ which is the lowest ammonia production among other isolates. The isolate *K. radicincitans* produced the highest ammonia (5.79 $\mu g mL^{-1}$), followed by *B. velezensis* (4.8 $\mu g mL^{-1}$) (Table 3). The accumulation of ammonia in soil disrupts the microbial community's homeostasis and prevents the germination of many fungal spores thereby adding many beneficial attributes (Gupta and Pandey, 2019).

3.4.5. ACC deaminase activity

Ethylene is produced in plant systems under stress conditions which have detrimental effects on crop growth. ACC deaminase produced by the bacterial isolates degrades ACC, a precursor of ethylene into α-ketobutyrate. Hence, they help plants to assuage the ethylene-induced effect on growth and development, particularly under salt stress (Arora, 2020). The highest activity was recorded in the isolate *B. velezensis* (1.180 μM mg^{-1} protein h^{-1}) and followed the order of *K. rhizophila* > *S. marcescens* > *M. indicus* > *K. radicincitans* > *B. circulans* (Table 3). The ACC deaminase activity was not recorded in the isolates *N. niacini*, *S. warneri* and *B. oleronius*. The breakdown products of ACC, notably α-ketobutyrate and ammonia, provide nitrogen and energy to the microorganisms that are involved in the degradation. The ACC deaminase activity of 853–2,107 nmol ketobutyrate mg $protein^{-1}$ h^{-1} was observed in PGPR strains belonging to *Pseudomonas* sp. and *Bacillus* sp. isolated from halophyte *Atriplex* sp. (Leontidou et al., 2020). They also suggested that plants thriving in extreme conditions like saline or drought stress environment might be the primary selectors of bacterial ACC deaminase activity.

3.5. Salinity tolerance of selected bacterial isolates under different salinity levels (0, 5 and 7% NaCl)

The salinity levels had a profound influence on the growth of isolates tested for tolerance (Figure 3). All the isolates had shown profound growth in control. The highest growth rate was observed in isolate SPTT 7. Including control, this isolate had grown well at both concentrations of NaCl (5 and 7%). In 7% NaCl, the stationary phase was attained at 52 h after inoculating. The isolates SPP 5 and SPTT 8 were unable to grow at 7% NaCl concentration and the growth rate slackened at 5% NaCl. *M. indicus* and *B. oleronius* had very slow growth rate at both the NaCl concentrations (5 and 7%) than the control. But the growth rate declined after 64 h in 5 and 7% NaCl. At 5% NaCl, *S. marcescens* had a slow and steady growth rate, while at 7% no growth was observed. In control, the lowest OD 660 nm value of 0.35 was recorded in the isolate *B. velezensis* at 60 h. The growth rate declined after 64 h at both NaCl concentrations (5 and 7%). The isolate *S. warneri* attained stationary phase after 40 and 60 h in control and 5% NaCl, respectively. High concentration of NaCl (7%) restricted the growth of the isolate. Isolates *S. warneri, K. rhizophila* and *S. marcescens* failed to grow at 7% NaCl, while they had a steady growth rate at 5%. Singh and Jha (2016b) also reported that *S. marcescens* grew well up to 6% NaCl. Similarly, *K. rhizophila* isolates had been reported to grow substantially in 5% salt medium, however, when salt concentration increased, the isolates showed a decreasing trend (Shi et al., 2021). *B. circulans* and *B. oleronius* had a shorter lag phase of 8 h than the other isolates, which indicated the potential of the microbe to grow under saline conditions (Finkel and Kolter, 1999). All the *Bacillus* genera (*B. oleronius*, *B. circulans*, *N. niacini*, and *M. indicus*) had long stationary phase that could be due to the synthesis of protective factors and adaptation of current environmental conditions at higher NaCl concentrations. In a study conducted by Duc et al. (2006), *B. indicus* tolerated higher levels of NaCl (8%), similarly *Metabacillus indicus* isolated in this study also tolerated 7% NaCl. Identifying halotolerant PGPR that could tolerate high levels of salinity is imperative for improving crop productivity under severe stress.

3.6. The modulation of metabolites and enzymes in plants under saline stress

High salt concentration in the rhizospheric zone leads to osmotic stress and disrupts cell ion homeostasis due to the accumulation of Na^+ and Cl^- ions (Paranychianakis and Chartzoulakis, 2005). This interferes with the uptake of essential nutrients and water thereby inhibiting plant growth. It affects shoot growth as well as xylem and root architecture. The root architecture in sense, the biomass, root network length and root length density are significantly altered, amplifying the impacts of salinity in the plants (Machado and Serralheiro, 2017). Plants cope with this by secretion of metabolites like proline and upregulation of potassium uptake that regulate homeostasis. The proline is synthesized from L-glutamate which requires ATP and NADH. Additionally, oxidative stress due to generation of ROS alters various biochemical pathways by inhibiting the binding of enzymes with substrate (Singh et al., 2022). Both osmotic stress and ionic stress result in oxidative damage to membrane components and cell organelles especially, chloroplasts. Owing to this the chlorophyll content in the plants under saline stress is reduced (Fatma et al., 2021). This inhibits photosynthetic activity and protein production, followed by inactivation of critical enzymes in the ATP synthesis (Singh et al., 2022). Nucleic acids, the structural component of proteins and DNA are impaired, leading to seizure of replication or transcription process (Hasanuzzaman et al., 2021). The chlorophyll degradation due to salinity is very high with the prolongation of stress (Hossain et al., 2017). In general, about 80% of the growth reduction at high salinity could be attributed to ethylene build up, resulting in reduction of leaf area, loss of chlorophyll content and decline in photosynthesis. The remaining 20% could be likely explained by a decrease in stomatal conductance and nutrient non-availability (Isayenkov and Maathuis, 2019). Ethylene is a plant hormone that regulates root hair, root growth, fruit ripening, leaf abscission, seed germination and ROS in the plant system (Fatma et al., 2021). Consequently, these changes in the plant's metabolism could reduce the growth and yield of crops. Hence, the alleviation of above impacts with the aid of microbiome could help the crop to tolerate the salinity and increase yield even under high saline environments.

3.7. Effect of isolated saline tolerant PGP bacterial strains on germination of *Vigna mungo* L. seeds under *in vitro* conditions (with 2% NaCl)

The results of *in vitro* experiment also revealed that when inoculated with the microbial isolates, the test plant's growth improved significantly even under salt stress (Table 4). Significant difference in germination percentage, root length, shoot length and vigor index of *Vigna mungo* L. seeds was noted. Each isolate showed varying degrees of enhancement in crop growth attributes. Among the treatments, the highest germination percentage (88.5%) of *Vigna mungo* L. seeds was reported in *S. marcescens* inoculated treatment (T_{10}) and the lowest was in (T_2) uninoculated control (2% NaCl) with 65.3%. Treatments inoculated with *N. niacini* (T_4) and *B. velezensis* (T_6) recorded 83.4 and 85.2% germination, respectively. Though germination percentage was high when inoculated with *S. marcescens* (T_{10}), root length was observed to be high (6.8 cm) when inoculated with *B. velezensis* (T_6). The highest vigor index of 1819 was recorded with *B. velezensis* (T_6), followed by *N. niacini* (T_4) inoculation (1785).

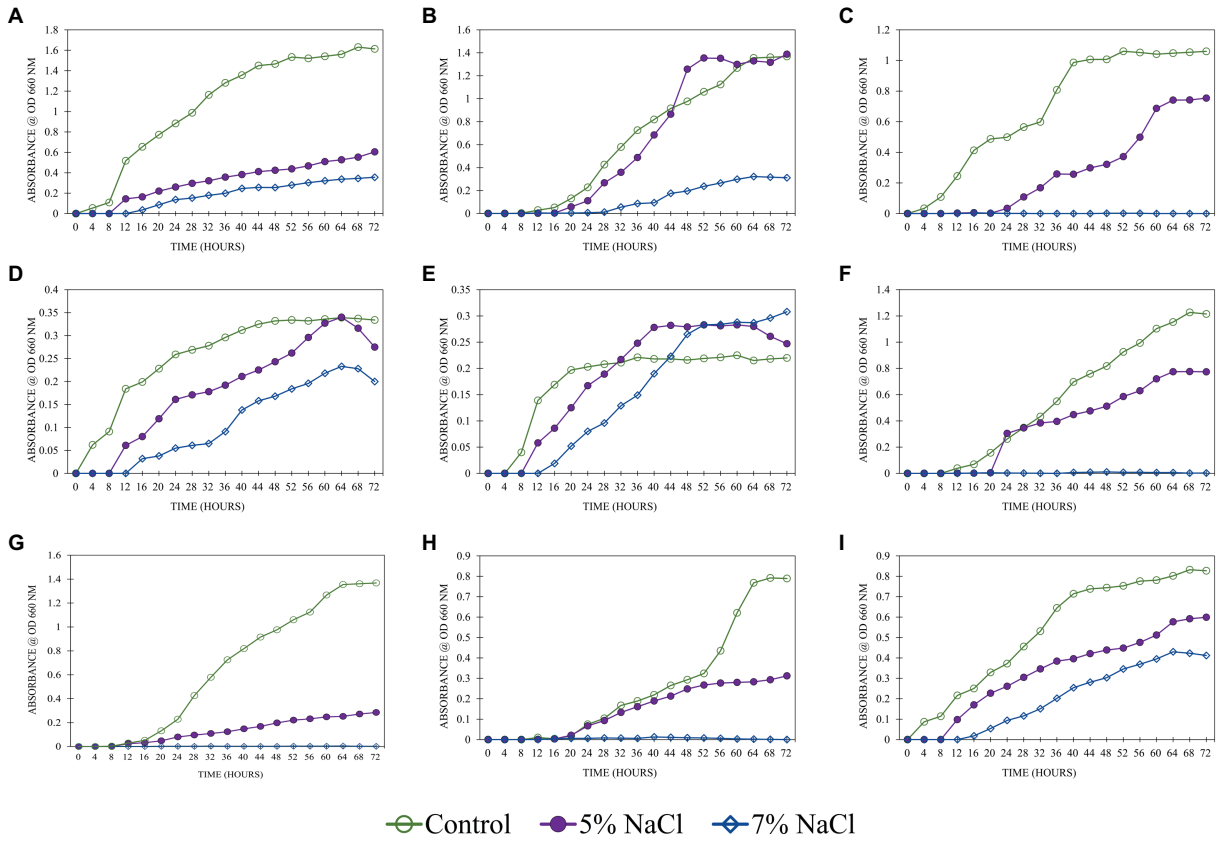

FIGURE 3
Salinity tolerance of the bacterial isolates under different levels of NaCl (0% -control, 5%, 7%) A: SPP 2 - *M. indicus*, B: SPP 5 - *N. niacini*, C: SPP 6 - *S. warneri*, D: SPTT 3 - *B. velezensis*, E: SPTT 7 - *B. circulans*, F: SPTT 8 - *K. rhizophila*, G: SPTV 3 - *B. oleronius*, H: SPTVE 3 - *S. marcescens* and I: SPTVE 4 - *K. radicincitans*.

The uninoculated control (2% NaCl) had the lowest vigor index of 780 followed by *S. warneri* (T_5) inoculation (792). In an experiment conducted by Singh and Jha (2016b), *S. marcescens* (T_{10}) inoculation improved wheat plant growth under salinity stress (150–200 mM) and effectively reduced the suppression of plant growth due to salt stresses. Under salt stress (2% NaCl), the lengths of shoots and roots in uninoculated plants were severely reduced, whereas their lengths increased significantly in the presence of PGPR. The availability of higher auxin concentrations as IAA by these inoculants is likely to be the cause of plants' increased root length (Rajkumar et al., 2005; Chakraborty et al., 2006). Shukla et al. (2012) also revealed that inoculation of halotolerant PGPR strains isolated from *Salicornia brachiata* improved the groundnut crop growth in hydroponics experiment with 100 mM NaCl than the control. The shoot length (14.6 cm) was observed to be higher in *S. marcescens* and *B. velezensis* inoculated plants, than in the uninoculated control (8.2 cm). Similarly, tomato seeds coated with *B. velezensis* strain had higher plant height and stem diameter at 100 mmol L^{-1} NaCl than the control (Medeiros and Bettiol, 2021). In this study, *K. radicincitans* inoculated treatment recorded high shoot and root growth of 62.2 and 79%, respectively, than the uninoculated control. Similarly, Berger et al. (2013) also reported 80 and 50% increase in root and shoot growth of 5 weeks old tomato plants, emphasizing *K. radicincitans* significance as a strong PGPR for variety of crops.

3.8. Compatibility and antagonistic activity among the bacterial strains

The bacterial isolate in the microbial consortium must be able to proliferate in the presence of each other without hindering the growth and development of other microorganisms. The phytohormone develops a signaling network which mutually regulates several metabolic systems between the microorganisms (Patel et al., 2016). When isolates in a consortium have antagonistic relationships with each other, it makes the consortium unstable, and the intended function is not attained (Sarkar and Chourasia, 2017). Compatibility analysis of different PGPR cultures with each other in line streak assay revealed the isolates antagonistic activity against each other. The absence of an inhibition zone indicated that the isolates were compatible with each other. A zone of inhibition was observed when isolates *B. circulans* and *B. oleronius* were streaked indicating their high antagonistic activity. Isolates *M. indicus*, *N. niacini*, and *S. marcescens* were compatible with each other, since there was no inhibition zone observed between these three isolates. Similarly, *B. velezensis*, *K. rhizophila*, *B. oleronius*, and *K. radicincitans* had compatibility with each other. In secondary confirmation study, *B. oleronius* had shown inhibition zone with *B. velezensis* and *K. radicincitans*. In this study, *B. circulans* had antagonistic effect with all the other isolates. Abada et al. (2014) noted the presence of Permetin A, an antibiotic chemical in *B. circulans* culture filtrate that had activity

against Gram negative bacteria. Hence, this could be the reason for incompatibility with other isolates. *M. indicus*, *N. niacin* and *S. marcescens* had synergism between them and were combined as Microbial consortium I. Similarly, Microbial consortium II was formed with *B. velezensis*, *K. rhizophila*, and *K. radicincitans*. These isolates were tested again for their compatibility by streaking them in triangular shape and no inhibition zone was observed between the isolates in both the consortia (Figure 4).

TABLE 4 *In vivo* evaluation of isolates for salinity stress alleviation in *Vigna mungo* L. under 2% NaCl.

Treatments	Germination percentage (%)	Shoot length (cm)	Root length (cm)	Vigor index
T_1 – Absolute control	98.3 ^{a*}	14.80 ^{a*}	7.90 ^{a*}	2,270 ^{a*}
T_2 – (2% NaCl)	65.3 ^{i*}	8.20 ^{h*}	3.80 ^{f*}	780 ^{h*}
T_3 – (*M. indicus* + 2% NaCl)	70.1 ^{g*}	12.60 ^{e*}	7.40 ^{a*}	1,225 ^{e*}
T_4 – (*N. niacini* + 2% NaCl)	83.4 ^{d*}	14.10 ^{b*}	4.90 ^{e*}	1785 ^{c*}
T_5 – (*S. warneri* + 2% NaCl)	66.0 ^{i*}	8.50 ^{g*}	3.50 ^{g*}	792 ^{h*}
T_6 – (*B. velezensis* + 2% NaCl)	85.2 ^{c*}	14.60 ^{a*}	6.80 ^{b*}	1819 ^{b*}
T_7 – (*B. circulans* + 2% NaCl)	78.0 ^{e*}	13.80 ^{c*}	3.20 ^{h*}	1,537 ^{d*}
T_8 – (*K. rhizophila* + 2% NaCl)	71.6 ^{f*}	11.08 ^{f*}	5.10 ^{d*}	1,158 ^{f*}
T_9 – (*B. acidicola* + 2% NaCl)	68.0 ^{h*}	8.90 ^{g*}	5.90 ^{c*}	823 ^{g*}
T_{10} – (*S. marcescens* + 2% NaCl)	88.5 ^{b*}	14.60 ^{a*}	5.30 ^{d*}	1751 ^{c*}
T_{11} – (*K. radicincitans* + 2% NaCl)	75.1 ^{e*}	13.30 ^{d*}	6.80 ^{b*}	1,508 ^{d*}
Mean	77.2	12.23	5.51	1,404

Values that do not share similar letters denote statistical significance; * denote significance at $p < 0.05$.

3.9. Effect of inoculation of microbial consortium on *Vigna mungo* L. under saline conditions

3.9.1. Inoculation of halotolerant microbial consortium on osmolytes and antioxidant enzymes in *Vigna mungo* L. leaves

The osmolyte, proline and stress enzymes such as catalase and SOD were lower in the microbial consortia inoculated treatments than the control. The lowest proline content of 10.45 µmol g^{-1} FW (I_3D_1) was recorded in the treatments inoculated with microbial consortium II (*B. velezensis*, *K. radicincitans* and *K. rhizophila*) at 2 kg ha^{-1} (Table 5). Concurrently, the control I_1D_1 followed by I_1D_2 had the highest proline contents with 13.86 and 12.87 µmol g^{-1} FW, respectively. The highest proline accumulation was observed in the uninoculated *Vigna mungo* L. seedlings, which was negated in treatments inoculated with the microbial consortium. The mean values ranged from 10.55 (I_3) to 13.36 µmol g^{-1} FW (I_1) which indicates a significant reduction in stress in crops inoculated with microbial consortium. Microbial consortia and dosage level were found to have a significant impact on the proline content of *Vigna mungo* L. Especially, the inoculation of MC-II at 2 kg ha^{-1} (24.6%) had the highest reduction in proline content than the MC-II at 4 kg ha^{-1} (17.2%). Plants generally accumulate osmoprotectants such as proline in response to salt stress, which aids in osmotic adjustment and prevents cellular oxidative damage (Shukla et al., 2012; Ilangumaran and Smith, 2017). The disruption in homeostasis under saline conditions could be caused by accumulation of sodium ions in large quantities. The siderophore producing potential of the MC-II is slightly higher than MC-I, which could have sequestered the sodium ions in the root surfaces similar to metals. In addition to that *B. velezensis* in MC-II was noted with high tendency to form mats of growth in the laboratory assays. This could have adsorbed the sodium ions there by reducing their availability around the root zone.

The control (I_1D_1) had higher catalase activity with 0.28 mM H_2O_2 oxidized min^{-1} g^{-1} followed by I_1D_2 at 0.27 mM H_2O_2 oxidized min^{-1} g^{-1}, compared to that of the other treatments (Table 5). This increase in the antioxidant enzymes could be due to the oxidative damage caused by ROS (Kang et al., 2014). The lower catalase activity of 0.25 mM H_2O_2 oxidized min^{-1} g^{-1} was recorded in I_3D_1 and I_3D_2 (inoculated with MC-II). There was no statistically significant difference in catalase activity due to the dosage of the microbial consortium. Remarkably, there is significant difference in the accumulation of SOD between

TABLE 5 Effect of halotolerant microbial consortia dosage on stress alleviation in *Vigna mungo* L. under salinity.

Treatments	Proline (µmolg^{-1} FW)			Catalase (mM H_2O_2 oxidized min^{-1} g^{-1})			Superoxide dismutase (Ug^{-1} FW)		
	D_1	D_2	Mean	D_1	D_2	Mean	D_1	D_2	Mean
I_1 (Control)	13.86 ^{d*}	12.87 ^{d*}	13.36	0.28 ^{c*}	0.27 ^{c*}	0.28	3.24 ^{b*}	3.25 ^{b*}	3.25
I_2 (MC-I)	12.48 ^{c*}	12.16 ^{b*}	12.32	0.26 ^{b*}	0.26 ^{b*}	0.26	3.22 ^{b*}	3.19 ^{a*}	3.21
I_3 (MC-II)	10.45 ^{a*}	10.65 ^{a*}	10.55	0.25 ^{a*}	0.25 ^{a*}	0.25	3.20 ^{a*}	3.17 ^{a*}	3.19
Mean	12.26	11.89	12.08	0.26	0.26	0.26	3.22	3.20	3.21

I_1 – Control; I_2 – Microbial consortium I; I_3 – Microbial consortium II and D1–2 kg of bioformulation per ha; D2–4 kg bioformulation per ha (Values that do not share similar letters denote statistical significance; * denote significance at $p < 0.05$).

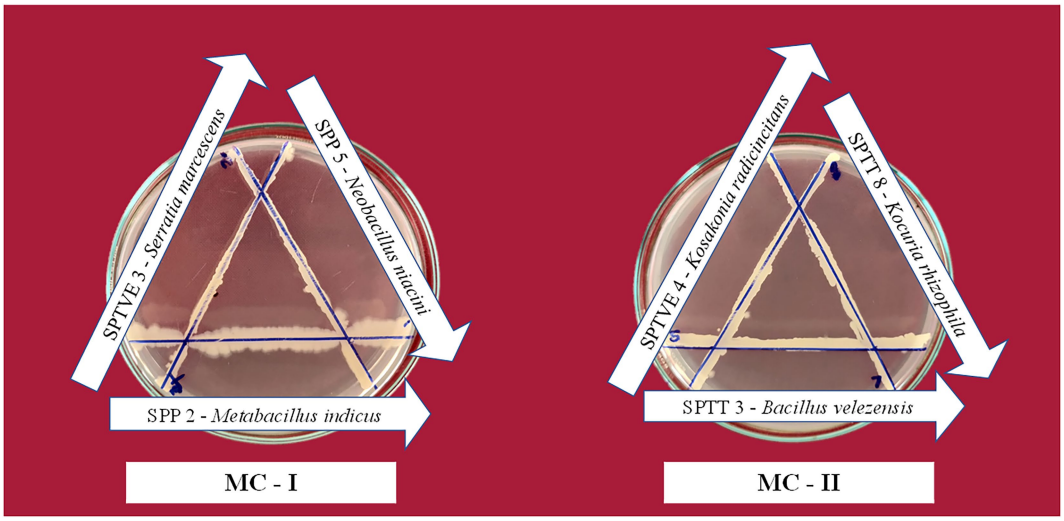

FIGURE 4
Compatibility assay between the bacterial isolates in the halotolerant microbial consortia. The lack of inhibition zone between two streaks indicate compatibility.

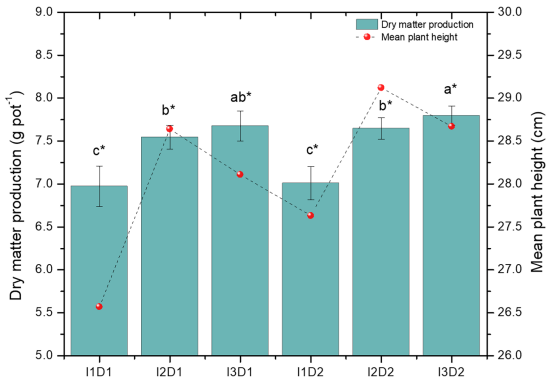

FIGURE 5
Effect of halotolerant microbial consortia dosage on growth of *Vigna mungo* L. under salinity. I_1 – Control; I_2 – Microbial consortium I; I_3 – Microbial consortium II and D_1-2kg of bioformulation per ha; D_2-4kg bioformulation per ha. Bars that do not share similar letters denote statistical significance. (*denote significance at $p<0.05$).

inoculated and uninoculated treatments. The lowest SOD content of 3.17 U g^{-1} FW was recorded in crops inoculated with MC-II (I_3D_2). The control I_1D_2 followed by I_1D_1 had higher SOD content with 3.25 and 3.24 U g^{-1} FW, respectively. Similar investigation by Chanratana et al. (2019) on salt stress alleviation in tomato using *Methylobacterium oryzae* recorded higher catalase and SOD activity in untreated plants than the inoculated. These antioxidants are either up-regulated or down-regulated to reduce abiotic stress depending on the plant and bacteria species. ROS (O_2^-, $^1O_2$, OH^- and H_2O_2) production was reported to be generated in plants under different types of environmental stresses, such as high or low temperature, salinity, drought, nutritional inadequacy, and pathogen attack (Singh et al., 2019). The ethylene signaling modulates salinity responses largely *via* regulation of ROS-generation in plant system (Zhang et al., 2016). The ACC deaminase activity by the microbial consortia reduces the percussor of ethylene leading to less ROS production. Owing to this the antioxidant enzymes, catalase and SOD activity have been reduced in crops inoculated with microbial consortia. Due to high ACC deaminase activity potential of MC-II (Table 2), the reduction of antioxidants in crops inoculated with MC-II is significantly lower than MC-I inoculated.

3.9.2. Effect on growth attributes of *Vigna mungo* L. due to inoculation of halotolerant microbial consortium under saline condition

Legume crops are sensitive to soil salinity, as the external NaCl salinity rises, their ability to prevent Na from entering the photosynthetically active leaves decreases rapidly (Arora et al., 2020). In the present study, all the growth traits increased significantly in the microbial consortium applied treatments than the control. The root biomass and shoot biomass of *Vigna mungo* L. were found to be the highest in the treatment I_3D_2 with the values of 9.09 and 23.39 g pot^{-1}, respectively (Figure 5). The least values for both the root (8.14 g pot^{-1}) and shoot biomass (20.92 g pot^{-1}) were recorded in I_1D_1. The presence of NaCl leads to specific ion toxicity that reduces the fresh and dry weight of control plants and is linked to reduced photosynthetic rate (Ambede et al., 2012). The plant height (29.10 cm) and dry matter production (7.80 g pot^{-1}) were the highest in I_2D_2 and I_3D_2, respectively. The mean values of the plant height in the treatments I_1, I_2, and I_3 were noted as 27.1, 28.9, and 28.4 cm, respectively. Growth attributes were significantly increased by the inoculation of microbial consortia. This increased shoot and root growth of inoculated plants could be attributed to phytohormone synthesis and bacterial N_2 fixation, which led to increased water and nutrient uptake (Shukla et al., 2012). The promotion of shoot length, root length and germination percentage under salinity were evident in the *in vivo* studies, where, *B. velezensis, S. marcescens, K. radicincitans, B. niacini, M. indicus*, and *K. rhizophila* had significantly higher potential compared to other strains. Owing to this, the microbial consortia with these strains could have resulted in better growth attributes than uninoculated control. Similarly, halotolerant PGPR consortia with *Pseudomonas fluorescens* and *Acinetobacter* sp. exhibited a substantial increase in plant height by 15.98 and 26.82 per cent, respectively, than uninoculated control (Yasin et al., 2018). The MC-II (*B. velezensis*, *K. radicincitans* and

K. rhizophila) inoculated at high dosage (4 kg ha^{-1}) had significantly higher dry matter production (11.3%) and mean plant height (4%) than the control (Figure 5). The high ammonia and IAA synthesis by MC-II have resulted in increment of the growth rate of *Vigna mungo* L. even under saline conditions. Significant reduction in shoot biomass of control plants due to retardation of plant growth in uninoculated treatments was also observed in earlier studies (Rahman et al., 2017; Borlu et al., 2018; Hassan et al., 2018). The ability *of B. velezensis* and *K. rhizophila* with high ACC deaminase activity may have supported root growth by lowering the ethylene level in plants under saline conditions.

3.9.3. Physiological parameters of *Vigna mungo* L.

The physiological parameters such as chlorophyll content, photosynthetic rate and stomatal conductance were found to be significantly higher in the MC inoculated treatments than the control (Figure 6). Treatment I_3D_2 followed by I_3D_1 had higher chlorophyll content of 26.95 and 26.10%, respectively compared to that of the control (I_1D_1 and I_1D_2). Subsequently, the lowest chlorophyll content of 19.88% was recorded in I_1D_2. Our findings are consistent with studies of Vimal and Singh (2019), who reported that PGPR inoculation increased chlorophyll content even under salinity stress. The prevention of nucleic acid damage in the chloroplast through reduction in ROS production by the inoculation of microbial consortium has led to increase in chlorophyll content in the active leaves. This in turn reflected in higher photosynthetic rate, since the amount of chlorophyll in a plant is directly proportional to its photosynthetic activity (Sapre et al., 2022). Treatment I_3D_1 followed by I_3D_2 had higher photosynthetic rate of 15.69 and 15.45 µmol CO_2 m^{-2} s^{-1}, respectively, compared to that of the control (I_1D_1 and I_1D_2). The least photosynthetic rate of 10.51 µmol CO_2 m^{-2} s^{-1} was recorded in I_1D_2. PGPR isolates with ACC deaminase activity (*M. indicus, S. marcescens, B. velezensis, K. radicincitans*, and *K. rhizophila*) has been found to prevent reduction in chlorophyll content, and there by maintaining the photosynthetic rate of plants under saline stress (Habib et al., 2016). However, treatment I_3D_1 followed by I_3D_2 had higher stomatal conductance with 0.85 and 0.74 µmol H_2O m^{-2} s^{-1}, respectively, compared to that of the control (I_1D_1 and I_1D_2). The higher stomatal conductance in active leaves is an adaptive mechanism of plants to overcome the salt stress. This could be made possible by maintaining the turgor pressure in the guard cells. The siderophore production by the halotolerant PGPR increases the iron and potassium availability which are key nutrients in photosynthetic activity (Chauhan et al., 2022). Owing to this the sodium and potassium balance is attained in the plants. The inoculation of MC- II at 2 kg ha^{-1} (*B. velezensis, K. radicincitans*, and *K. rhizophila*) increased photosynthetic rate and stomatal conductance by 0.3 and 1.3 times, respectively, as compared to the control. This was supported by the research conducted by Bayuelo-Jimenez et al. (2012), who found that neither stomatal conductance nor photosynthetic activity was affected by salt stress due to high IAA production when inoculated with salt tolerant PGPRs.

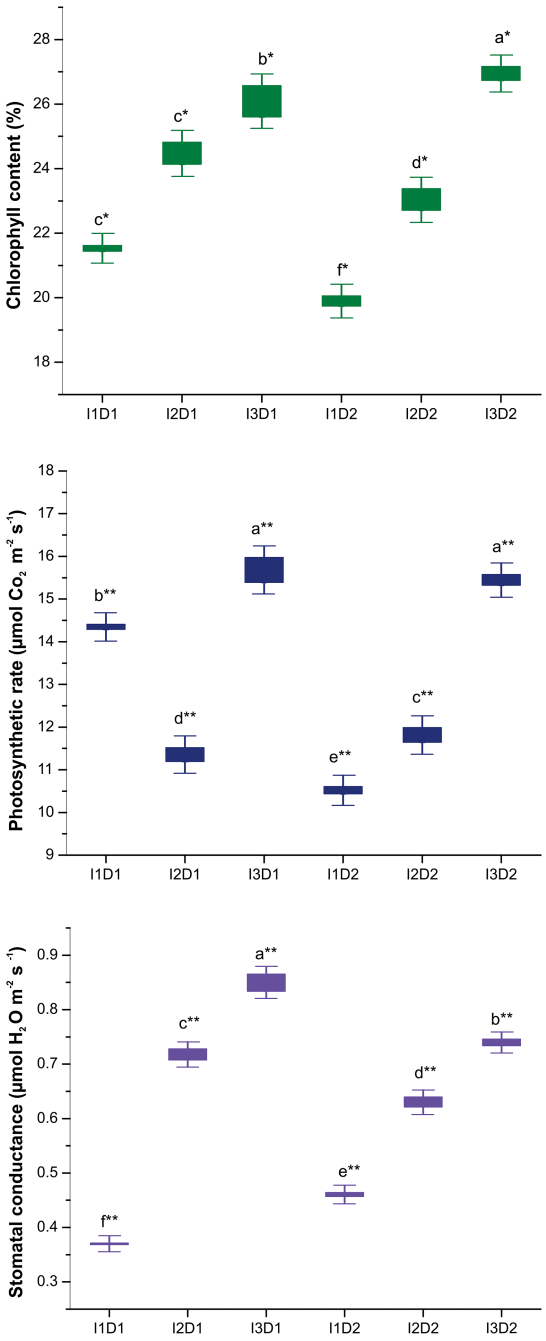

FIGURE 6
Effect of halotolerant microbial consortia dosage on physiological attributes of *Vigna mungo* L. under salinity. I_1 – Control; I_2 – Microbial consortium I; I_3 – Microbial consortium II and D_1-2kg of bioformulation per ha; D_2-4kg bioformulation per ha. Bars that do not share similar letters denote statistical significance. (* and ** denote significance at p<0.05 and p<0.01, respectively).

3.9.4. Yield attributes of *Vigna mungo* L.

The negative effects of salinity due to EC in soil (2.62 dS m^{-1}) and irrigation water (2.5 dS m^{-1}) have resulted in reduction of yield and protein quality in *Vigna mungo* L. The plant yield (3.87 g pot^{-1}) and pods per plant (11.55) were highest in I_3D_2 and I_3D_1, respectively. The treatments applied with MC-II had a significantly higher number of pods per plant (25.5%) and grain yield (45%) than the control (Figure 7). Similar results were obtained by Saravanakumar and Samiyappan (2007), where pods count and protein content in peanut crop was increased upon inoculation with *Pseudomonas fluorescens* under saline stress. The mean values of the yield in the treatments I_1, I_2, and I_3 were 2.60, 3.11, and 3.77 g pot^{-1}, respectively. This indicates a significant improvement in crop yield due to microbial consortium inoculation that alters the nutritional environment through production of plant growth regulators (Patel et al., 2021). Among the treatments inoculated with microbial consortium, MC-II inoculated (*B. velezensis,*

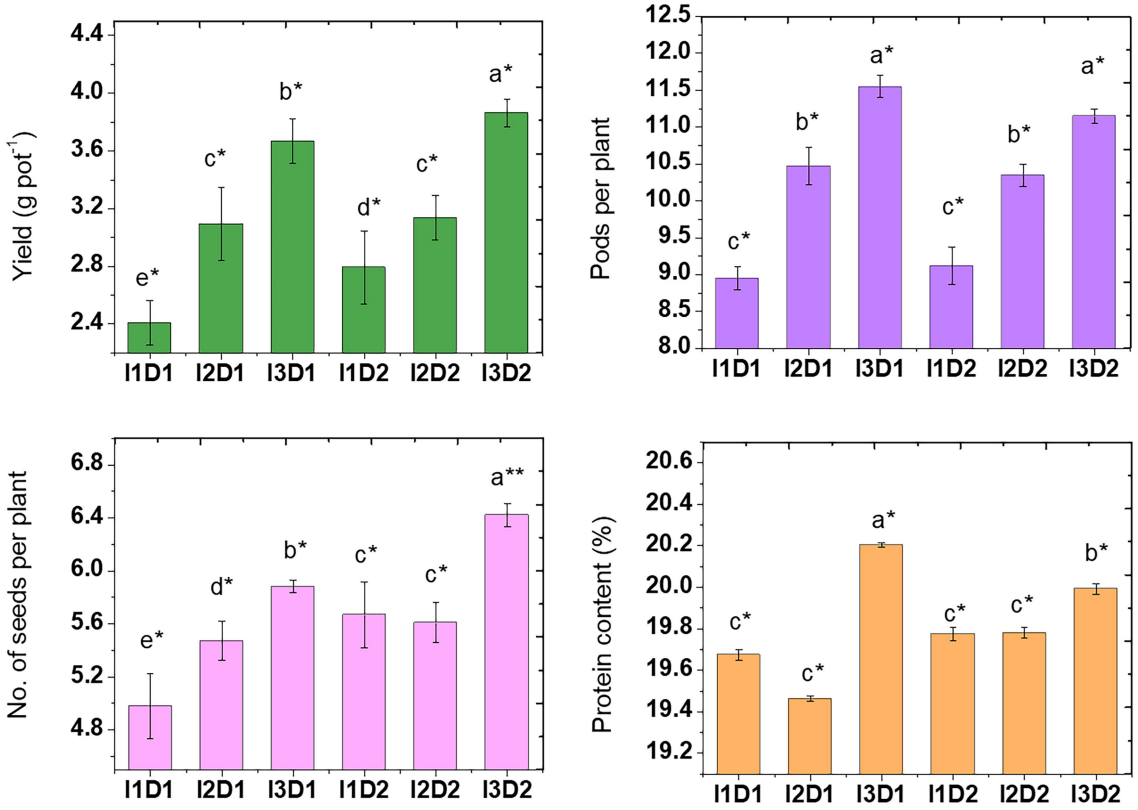

FIGURE 7
Effect of halotolerant microbial consortia dosage on yield quantity and quality of *Vigna mungo* L. under salinity. I_1 – Control; I_2 – Microbial consortium I; I_3 – Microbial consortium II and D_1-2kg of bioformulation per ha; D_2-4kg bioformulation per ha. Bars that do not share similar letters denote statistical significance. (* and ** denote significance at $p<0.05$ and $p<0.01$, respectively).

K. radicincitans, and *K. rhizophila*) had higher yield than MC-I (*M. indicus, S. marcescens*, and *N. Niacini*) inoculated. This is a direct indicator of high PGP potential of MC-II in comparison to MC-I.

Similarly, high protein content was recorded in I_3D_1 and I_3D_2 (MC-II inoculated treatments) with the corresponding values of 20.20 and 19.99%, respectively. Protein content in the seeds was significantly higher when inoculated with MC-II. The presence of more growth-promoting biochemicals in PGPR aids in the reduction of impacts caused by salt stress (Nadeem et al., 2016). Kavita and Alka (2010) stated that saline stress reduces N partitioning and fixation leading to lower protein accumulation in the seeds of legume plants. In line with this, seeds from the control treatment had low protein than microbial consortium inoculated treatments. The microbial consortia application improves nitrogen use efficiency, which in turn favored the accumulation of protein in seeds. Similarly, compared to the un-inoculated control, co-inoculation of *Bacillus* sp. and *Arthrobacter* sp. significantly increased protein content in the maize even under salt stress (100 mM NaCl; Hassan and Bano, 2015). The inoculation of PGPR with ACC deaminase activity on maize showed 3.3 folds increase in root length at EC 9 dS m^{-1} and shoot lengths increased by 2.3 folds over uninoculated control (Kausar and Shahzad, 2006). Inoculation of maize with salt tolerant PGPR and addition of organic amendments like poultry manure, cow dung and spent mushroom substrate has improved crop growth and fertility status of the soil in saline ecosystem. Further, the inoculation also reduced the sodium uptake by the crop thereby reducing the effect of salinity (Upadhyay and Chauhan, 2022).

3.10. Mechanism behind the improvement in crop growth through halotolerant PGPR inoculation and way forward

Several reports have shown that halotolerant PGPRs effectively improve the growth of various agricultural crops under salinity stress conditions (Qin et al., 2016; Singh and Jha, 2016a; Etesami and Noori, 2019; Orhan and Demirci, 2020). Mechanisms by which they impact growth are (i) triggering plant antioxidant defense by upregulating vital enzymes that scavenge excess ROS, (ii) alleviating nutrient deficiency by fixing atmospheric nitrogen and producing ammonia, solubilizing P, producing siderophores for Fe, Zn and Ln uptake, (iii) increasing the uptake of selected ions for maintaining a high K^+/Na^+ ratio (John and Lakshmanan, 2018), (iv) decreasing plant Na^+ accumulation by excreting exopolysaccharide to bind cations (especially Na^+) in roots and prevent their translocation to leaves, and (v) reduction in ROS production by counteracting ethylene synthesis (Figure 8). Probably, different mechanisms are involved in each interaction that leads to plant growth stimulation under saline conditions. The prevention of nucleic acid and chlorophyll damage by quenching the ROS plays a major role in improving the salt tolerance in the crops. Nevertheless, the variation in chloroplast structure and SOD activity among the different plants interferes with the PGPR ability in stress alleviation. Hence, a bacterial strain that stimulates the growth of a particular plant species in the presence of salt may not cause similar effect in

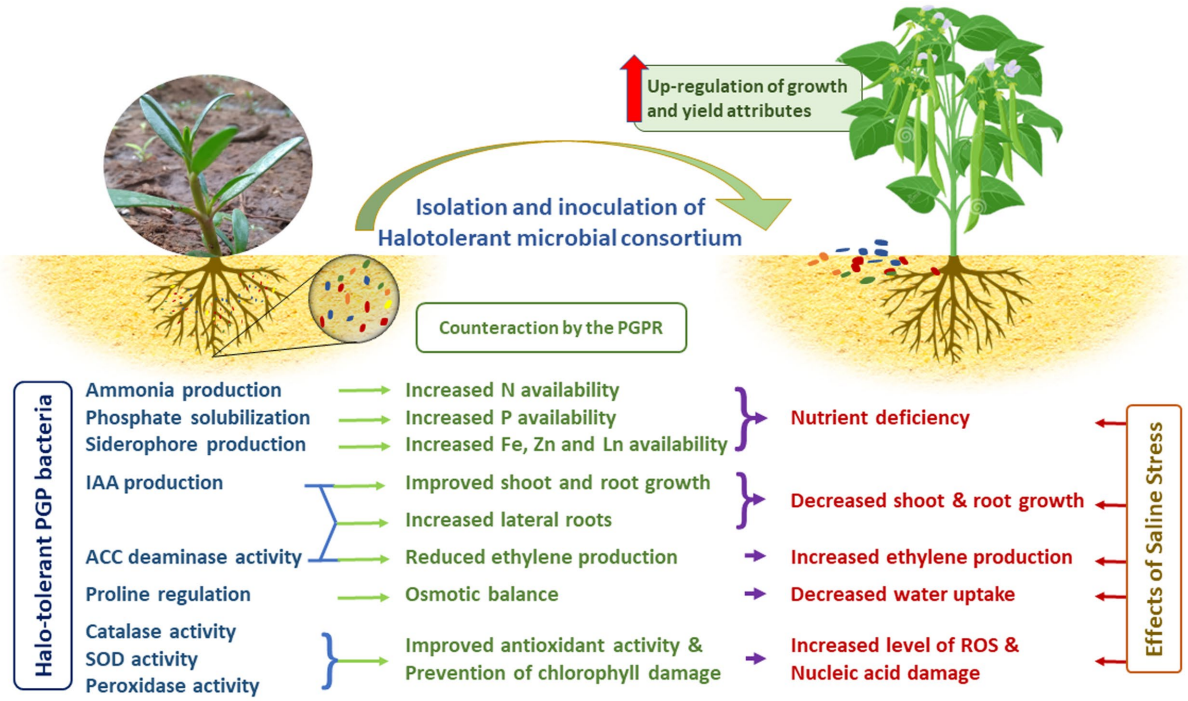

FIGURE 8
Prospects of halotolerant microbial consortia for alleviation of saline stress.

other plants. Furthermore, many intricate mechanisms are involved when endophytes come into the picture (Santoyo et al., 2016; Khan et al., 2017). The endophyte, *Burkholderia phytofirmans* enhanced the growth of six switchgrass cultivars out of the eight that were tested (Khan et al., 2017). Inoculation with this strain was found to induce wide-spread changes in gene expression in the host plant, including transcription factors that are known to regulate the expression of some plant stress factor genes (Lara-Chavez et al., 2015). It is likely that changes in plant gene expression could also be induced by the halotolerant consortium used in this study to inoculate *Vigna mungo* L. Hence further investigation of the genomic interaction with the plants is in process. This would have a significant influence in identifying microbial inoculums that guarantees the successful cultivation of crops under variety of stressful environments.

4. Conclusion

The current study revealed the plant growth-promoting attributes of halotolerant PGPR on *Vigna mungo* L., grown under saline conditions. Among the nine isolates, *S. marcescens, B. velezensis, K. rhizophila*, and *K. radicincitans* improved germination percentage, vigor index, shoot and root length of *Vigna mungo* L. In the pot study, *Vigna mungo* L. inoculated with microbial consortia (*K. rhizophila, B. velezensis*, and *K. radicincitanas* – MC-II) @ 4 kg ha^{-1} exhibited higher concentration of chlorophyll, photosynthetic rate and stomatal conductance. The poor leaf osmolyte (proline) content and antioxidant enzymes (catalase and superoxide dismutase) activities indicated lesser salt stress in inoculated plants over uninoculated control. Consequently, significant increase in growth and yield of *Vigna mungo* L. in soils salinized by long term irrigation of paper and pulp mill effluent was observed. Therefore, halotolerant microbial consortia, MC-II having the potential to induce salt stress tolerance can enhance crop growth. However, further research must be oriented towards improving the host plant-microbial compatibility to increase the salt tolerance and productivity of wide variety of crops. Utilization of biostimulants, nano-particles and bio-amendments along with PGPR is another emerging area of research which has the potential to improve the crop microbe association under saline conditions.

Data availability statement

The original contributions presented in the study are included in the article/Supplementary material, further inquiries can be directed to the corresponding authors.

Author contributions

JJ has conducted all the experiments under the guidance of MM and TK. JJ and CP completed the formal analysis and the first draft of the manuscript. BG, SSR, and SR participated in the analysis of experimental results. MP, EK, and VD directed the manuscript writing and revision of the manuscript. All authors have read and agreed on the final version of the text.

Funding

The financial assistance to carry out the research was provided by Tamil Nadu Newsprint and Papers Limited, Karur, India.

Acknowledgments

The authors are thankful to Tamil Nadu Newsprint and Papers Limited (TNPL), Karur, Tamil Nadu for providing financial assistance to carry out the research project. The authors are grateful to Dr. V. Prasath and Dr. R. Seenivasan for their technical assistance. The authors also thank the Tamil Nadu Agricultural University, Coimbatore for providing infrastructural support.

Conflict of interest

The authors declare that the research was conducted in the absence of any commercial or financial relationships that could be construed as a potential conflict of interest.

Publisher's note

All claims expressed in this article are solely those of the authors and do not necessarily represent those of their affiliated organizations, or those of the publisher, the editors and the reviewers. Any product that may be evaluated in this article, or claim that may be made by its manufacturer, is not guaranteed or endorsed by the publisher.

Supplementary material

The Supplementary material for this article can be found online at: https://www.frontiersin.org/articles/10.3389/fmicb.2023.1085787/full#supplementary-material

References

Abada, E. A., El-Hendawy, H. H., Osman, M. E., and Hafez, M. A. (2014). Antimicrobial activity of *Bacillus circulans* isolated from rhizosphere of *Medicago sativa*. *Life Sci. J.* 8, 711–719.

Acosta-Motos, J. R., Ortuño, M. F., Bernal-Vicente, A., Diaz-Vivancos, P., Sanchez-Blanco, M. J., and Hernandez, J. A. (2017). Plant responses to salt stress: adaptive mechanisms. *Agronomy* 7:18. doi: 10.3390/AGRONOMY7010018

Afridi, M. S., Mahmood, T., Salam, A., Mukhtar, T., Mehmood, S., Ali, J., et al. (2019). Induction of tolerance to salinity in wheat genotypes by plant growth promoting endophytes: involvement of ACC deaminase and antioxidant enzymes. *Plant Physiol. Biochem.* 139, 569–577. doi: 10.1016/j.plaphy.2019.03.041

Ahemad, M., and Kibret, M. (2014). Mechanisms and applications of plant growth promoting rhizobacteria: current perspective. *J. King Saud. Univ. Sci.* 26, 1–20. doi: 10.1016/J.JKSUS.2013.05.001

Ambede, J. G., Netondo, G. W., Mwai, G. N., and Musyimi, D. M. (2012). NaCl salinity affects germination, growth, physiology, and biochemistry of bambara groundnut. *Brazilian J. Plant Physiol.* 24, 151–160. doi: 10.1016/j.plaphy.2019.03.041

Arora, S. (2020). "Halotolerant microbes for amelioration of salt-affected soils for sustainable agriculture" in *Phyto-Microbiome in Stress Regulation*. eds. M. Kumar, V. Kumar and R. Prasad (Singapore: Springer), 323–343.

Arora, N. K., Fatima, T., Mishra, J., Mishra, I., Verma, S., Verma, R., et al. (2020). Halo-tolerant plant growth promoting rhizobacteria for improving productivity and remediation of saline soils. *J. Adv. Res.* 26, 69–82. doi: 10.1016/j.jare.2020.07.003

Ayyam, V., Palanivel, S., and Chandrakasan, S. (2019). "Biosaline agriculture" in *Coastal Ecosystems of the Tropics-Adaptive Management*. eds. V. Ayyam, S. Palanivel and S. Chandrakasan (Singapore: Springer), 493–510.

Bates, L. S., Waldren, R. P., and Teare, I. D. (1973). Rapid determination of free proline for water-stress studies. *Plant Soil* 39, 205–207. doi: 10.1007/BF00018060

Bayuelo-Jimenez, J. S., Jasso-Plata, N., and Ochoa, I. (2012). Growth and physiological responses of *Phaseolus* species to salinity stress. *Int. J. Agron.* 2012, 1–13. doi: 10.1155/2012/527673

Berger, B., Brock, A. K., and Ruppel, S. (2013). Nitrogen supply influences plant growth and transcriptional responses induced by *Enterobacter radicincitans* in *Solanum lycopersicum*. *Plant Soil* 370, 641–652. doi: 10.1007/s11104-013-1633-0

Bhattacharjee, S. (2012). The language of reactive oxygen species signaling in plants. *J. Bot.* 2012, 1–22. doi: 10.1155/2012/985298

Bhavani, D. G., and Kumari, A. M. (2019). Chick pea root endophytic bacteria and their plant growth promoting traits. *Indian J. Ecol.* 46, 72–76.

Borlu, H. O., Celiktas, V., Duzenli, S., Hossain, A., and El Sabagh, A. (2018). Germination and early seedling growth of five durum wheat cultivars (*Triticum durum* desf.) is affected by different levels of salinity. *Fresenius Environ. Bull.* 27, 7746–7757.

Borsato, E., Rosa, L., Marinello, F., Tarolli, P., and D'Odorico, P. (2020). Weak and strong sustainability of irrigation: A framework for irrigation practices under limited water availability. *Front. Sustain. Food Syst.* 4:17. doi: 10.3389/fsufs.2020.00017

Carmen, B., and Roberto, D. (2011). "Soil bacteria support and protect plants against abiotic stresses" in *Abiotic Stress in Plants: Mechanisms and Adaptations*. eds. A. K. Shanker and B. Venkateswarlu (London: InTech), 143–170.

Chakraborty, U., Chakraborty, B., and Basnet, M. (2006). Plant growth promotion and induction of resistance in *Camellia sinensis* by *Bacillus megaterium*. *J. Basic Microbiol.* 46, 186–195. doi: 10.1002/jobm.200510050

Chanratana, M., Joe, M. M., Roy Choudhury, A., Anandham, R., Krishnamoorthy, R., Kim, K., et al. (2019). Physiological response of tomato plant to chitosan-immobilized aggregated *Methylobacterium oryzae* CBMB20 inoculation under salinity stress. *3 Biotech* 9, 397–313. doi: 10.1007/s13205-019-1923-1

Chauhan, P. K., Upadhyay, S. K., Tripathi, M., Singh, R., Krishna, D., Singh, S. K., et al. (2022). Understanding the salinity stress on plant and developing sustainable management strategies mediated salt-tolerant plant growth-promoting rhizobacteria and CRISPR/Cas9. *Biotechnol. Genet. Eng. Rev.*, 1–37. doi: 10.1080/02648725.2022.2131958

Da Silva, F. G., Dos Santos, I. B., De Sousa, A. J., Raquel, A., Farias, B., Patrícia Da, W., et al. (2016). Bioprospecting and plant growth-promoting bacteria tolerant to salinity associated with *Atriplex nummularia* L. in saline soils. *African J. Microbiol. Res.* 10, 1203–1214. doi: 10.5897/AJMR2016.8202

Dai, J., Wang, N., Xiong, H., Qiu, W., Nakanishi, H., Kobayashi, T., et al. (2018). The Yellow Stripe-Like (YSL) gene functions in internal copper transport in Peanut. *Genes* 9:635. doi: 10.3390/genes9120635

Damodaran, T., Mishra, V. K., Sharma, D. K., Jha, S. K., Verma, C. L., Rai, R. B., et al. (2013). Management of sub-soil sodicity for sustainable banana production in sodic soil-an approach. *Int. J. Curr. Res.* 5, 1930–1934.

Del Carmen Orozco-Mosqueda, M., Duan, J., DiBernardo, M., Zetter, E., Campos-García, J., Glick, B. R., et al. (2019). The production of ACC deaminase and trehalose by the plant growth promoting bacterium *Pseudomonas* sp. UW4 synergistically protect tomato plants against salt stress. *Front. Microbiol.* 10:1392. doi: 10.3389/FMICB.2019.01392/FULL

Dereeper, A., Guignon, V., Blanc, G., Audic, S., Buffet, S., Chevenet, F., et al. (2008). Phylogeny.fr: robust phylogenetic analysis for the non-specialist. *Nucleic Acids Res.* 36, W465–W469. doi: 10.1093/NAR/GKN180

Devi, K. A., Pandey, P., and Sharma, G. D. (2016). Plant growth-promoting endophyte *Serratia marcescens* AL2-16 enhances the growth of *Achyranthes aspera* L., a medicinal plant. *HAYATI J. Biosci.* 23, 173–180. doi: 10.1016/j.hjb.2016.12.006

Dhevagi, P., Ramya, A., Priyatharshini, S., and Poornima, R. (2022). Effect of elevated tropospheric ozone on *Vigna Mungo* L. varieties. *Ozone Sci. Eng.* 44, 566–586. doi: 10.1080/01919512.2021.2009332

Dhindsa, R. S., Plumb-Dhindsa, P., and Thorpe, T. A. (1981). Leaf senescence: correlated with increased levels of membrane permeability and lipid peroxidation, and decreased levels of superoxide dismutase and catalase. *J. Exp. Bot.* 32, 93–101. doi: 10.1093/jxb/32.1.93

Dimkpa, C., Weinand, T., and Asch, F. (2009). Plant-rhizobacteria interactions alleviate abiotic stress conditions. *Plant Cell Environ.* 32, 1682–1694. doi: 10.1111/J.1365-3040.2009.02028.X

Diray-Arce, J., Clement, M., Gul, B., Khan, M. A., and Nielsen, B. L. (2015). Transcriptome assembly, profiling and differential gene expression analysis of the halophyte *Suaeda fruticosa* provides insights into salt tolerance. *BMC Genomics* 16, 353–324. doi: 10.1186/s12864-015-1553-x

Duc, L. H., Fraser, P. D., Tam, N. K. M., and Cutting, S. M. (2006). Carotenoids present in halotolerant *Bacillus* spore formers. *FEMS Microbiol. Lett.* 255, 215–224. doi: 10.1111/j.1574-6968.2005.00091.x

Dutta, J., and Thakur, D. (2017). Evaluation of multifarious plant growth promoting traits, antagonistic potential and phylogenetic affiliation of rhizobacteria associated with commercial tea plants grown in Darjeeling, India. *PLoS One* 12:e0182302. doi: 10.1371/journal.pone.0182302

Edgar, R. C. (2004). MUSCLE: multiple sequence alignment with high accuracy and high throughput. *Nucleic Acids Res.* 32, 1792–1797. doi: 10.1093/NAR/GKH340

Ermakova, M., Lopez-Calcagno, P. E., Raines, C. A., Furbank, R. T., and von Caemmerer, S. (2019). Overexpression of the Rieske FeS protein of the cytochrome b6f complex increases C4 photosynthesis in Setaria viridis. *Commun. Biol.* 2:314. doi: 10.1038/s42003-019-0561-9

Etesami, H., and Beattie, G. A. (2018). Mining halophytes for plant growth-promoting halotolerant bacteria to enhance the salinity tolerance of non-halophytic crops. *Front. Microbiol.* 9:148. doi: 10.3389/FMICB.2018.00148/BIBTEX

Etesami, H., and Noori, F. (2019). "Soil salinity as a challenge for sustainable agriculture and bacterial-mediated alleviation of salinity stress in crop plants" in *Saline Soil-Based Agriculture by Halotolerant Microorganisms*. eds. M. Kumar, H. Etesami and V. Kumar (Singapore: Springer), 1–22.

Facklam, R., and Elliott, J. A. (1995). Identification, classification, and clinical relevance of catalase-negative, gram-positive cocci, excluding the *Streptococci* and *Enterococci*. *Clin. Microbiol. Rev.* 8, 479–495. doi: 10.1128/cmr.8.4.479

Fatma, M., Iqbal, N., Gautam, H., Sehar, Z., Sofo, A., D'Ippolito, I., et al. (2021). Ethylene and sulfur coordinately modulate the antioxidant system and ABA accumulation in mustard plants under salt stress. *Plan. Theory* 10:180. doi: 10.1128/cmr.8.4.479

Finkel, S. E., and Kolter, R. (1999). Evolution of microbial diversity during prolonged starvation. *Proc. Natl. Acad. Sci.* 96, 4023–4027. doi: 10.1073/PNAS.96.7.4023

Fisher, T. S., Surdo, P. L., Pandit, S., Mattu, M., Santoro, J. C., Wisniewski, D., et al. (2007). Effects of pH and low density lipoprotein (LDL) on PCSK9-dependent LDL receptor regulation. *J. Biol. Chem.* 282, 20502–20512. doi: 10.1074/jbc.M701634200

Flowers, T. J., and Colmer, T. D. (2015). Plant salt tolerance: adaptations in halophytes. *Ann. Bot.* 115, 327–331. doi: 10.1093/aob/mcu267

Galkovskyi, T., Mileyko, Y., Bucksch, A., Moore, B., Symonova, O., Price, C. A., et al. (2012). GiA roots: software for the high throughput analysis of plant root system architecture. *BMC Plant Biol.* 12, 1–12. doi: 10.1186/1471-2229-12-116

Glick, B. R. (2014). Bacteria with ACC deaminase can promote plant growth and help to feed the world. *Microbiol. Res.* 169, 30–39. doi: 10.1016/j.micres.2013.09.009

Gomez, K. A., and Gomez, A. A. (1984). *Statistical Procedures for Agricultural Research*. NewYork: John Wiley and Sons.

Gopalachari, N. C. (1963). Changes in the activities of certain oxidizing enzymes during germination and seedling development of *Phaseolus mungo* and *Sorghum vulgare*. *Indian J. Exp. Biol.* 1, 98–100.

Goswami, D., Dhandhukia, P., Patel, P., and Thakker, J. N. (2014). Screening of PGPR from saline desert of Kutch: growth promotion in *Arachis hypogea* by *Bacillus licheniformis* A2. *Microbiol. Res.* 169, 66–75. doi: 10.1016/j.micres.2013.07.004

Gul, B., Ansari, R., Ali, H., Adnan, M. Y., Weber, D. J., Nielsen, B. L., et al. (2014). The sustainable utilization of saline resources for livestock feed production in arid and semi-arid regions: A model from Pakistan. *Emirates J. Food Agric.* 26, 1032–1045. doi: 10.9755/ejfa.xxx.xxx

Gupta, B., and Huang, B. (2014). Mechanism of salinity tolerance in plants: physiological, biochemical, and molecular characterization. *Int. J. Genomics* 2014, 1–18. doi: 10.1155/2014/701596

Gupta, S., and Pandey, S. (2019). ACC deaminase producing bacteria with multifarious plant growth promoting traits alleviates salinity stress in French Bean (*Phaseolus vulgaris*) plants. *Front. Microbiol.* 10:1506. doi: 10.3389/FMICB.2019.01506/BIBTEX

Habib, S. H., Kausar, H., and Saud, H. M. (2016). Plant growth-promoting rhizobacteria enhance salinity stress tolerance in okra through ROS-scavenging enzymes. *Biomed. Res. Int.* 2016, 1–10. doi: 10.1155/2016/6284547

Hasanuzzaman, M., Raihan, M. R. H., Masud, A. A. C., Rahman, K., Nowroz, F., Rahman, M., et al. (2021). Regulation of reactive oxygen species and antioxidant defense in plants under salinity. *Int. J. Mol. Sci.* 22:9326. doi: 10.3390/ijms22179326

Hassan, T. U., and Bano, A. (2015). Role of carrier-based biofertilizer in reclamation of saline soil and wheat growth. *Arch. Agron. Soil Sci.* 61, 1719–1731. doi: 10.1080/03650340.2015.1036045

Hassan, N., Hasan, M. K., Shaddam, M. O., Islam, M. S., Barutçular, C., Sabagh, E. L., et al. (2018). Responses of maize varieties to salt stress in relation to germination and seedling growth. *Int. Lett. Nat. Sci.* 69, 1–11. doi: 10.18052/www.scipress.com/ilns.69.1

Hossain, M. S., Alam, M. U., Rahman, A., Hasanuzzaman, M., Nahar, K., Al Mahmud, J., et al. (2017). Use of iso-osmotic solution to understand salt stress responses in lentil (*Lens culinaris* Medik.). *South African J. Bot.* 113, 346–354. doi: 10.1016/j.sajb.2017.09.007

Ilangumaran, G., and Smith, D. L. (2017). Plant growth promoting rhizobacteria in amelioration of salinity stress: a systems biology perspective. *Front. Plant Sci.* 8:1768. doi: 10.3389/fpls.2017.01768

Isayenkov, S. V., and Maathuis, F. J. M. (2019). Plant salinity stress: many unanswered questions remain. *Front. Plant Sci.* 10:80. doi: 10.3389/fpls.2019.00080

Islam, S., Akanda, A. M., Prova, A., Islam, M. T., and Hossain, M. M. (2016). Isolation and identification of plant growth promoting rhizobacteria from cucumber rhizosphere and their effect on plant growth promotion and disease suppression. *Front. Microbiol.* 6:1360. doi: 10.3389/fmicb.2015.01360

Jain, R., and Srivastava, S. (2012). Nutrient composition of spent wash and its impact on sugarcane growth and biochemical attributes. *Physiol. Mol. Biol. Plants* 18, 95–99. doi: 10.1007/s12298-011-0087-1

John, J. E., and Lakshmanan, A. (2018). Carbon sequestration as biomass carbon and mineral carbonates by cyanobacterial systems in rice soil. *Trends Biosci.* 11, 3478–3484.

John, J. E., Thangavel, P., Maheswari, M., Balasubramanian, G., Kalaiselvi, T., Kokiladevi, E., et al. (2022). *Sesuvium portulacastrum* mitigates salinity induced by irrigation with paper and pulp mill effluent. *Int. J. Environ. Stud.* 1-13, 1–13. doi: 10.1080/00207233.2022.2055346

Kang, G., Li, G., and Guo, T. (2014). Molecular mechanism of salicylic acid-induced abiotic stress tolerance in higher plants. *Acta Physiol. Plant.* 36, 2287–2297.

Kausar, R., and Shahzad, S. M. (2006). Effect of ACC-deaminase containing rhizobacteria on growth promotion of maize under salinity stress. *J. Agric. Soc. Sci.* 2, 216–218.

Kavita, K., and Alka, S. (2010). Assessment of salinity tolerance of *Vigna mungo* var. Pu-19 using ex vitro and in vitro methods. *Asian J. Biotechnol.* 2, 73–85. doi: 10.3923/ajbkr.2010.73.85

Khan, A. L., Waqas, M., Asaf, S., Kamran, M., Shahzad, R., Bilal, S., et al. (2017). Plant growth-promoting endophyte *Sphingomonas* sp. LK11 alleviates salinity stress in *Solanum pimpinellifolium*. *Environ. Exp. Bot.* 133, 58–69. doi: 10.1016/j.envexpbot.2016.09.009

Khaneja, R., Perez-Fons, L., Fakhry, S., Baccigalupi, L., Steiger, S., To, E., et al. (2010). Carotenoids found in *Bacillus*. *J. Appl. Microbiol.* 108, 1889–1902. doi: 10.1111/j.1365-2672.2009.04590.x

Kotasthane, A. S., Agrawal, T., Zaidi, N. W., and Singh, U. S. (2017). Identification of siderophore producing and cynogenic fluorescent *Pseudomonas* and a simple confrontation assay to identify potential bio-control agent for collar rot of chickpea. *3 Biotech* 7, 1–8. doi: 10.1111/j.1365-2672.2009.04590.x

Kumar, P., and Sharma, P. K. (2020). Soil salinity and food security in India. *Front. Sustain. Food Syst.* 4:174. doi: 10.3389/FSUFS.2020.533781/BIBTEX

Lara-Chavez, A., Lowman, S., Kim, S., Tang, Y., Zhang, J., Udvardi, M., et al. (2015). Global gene expression profiling of two switchgrass cultivars following inoculation with *Burkholderia phytofirmans* strain PsJN. *J. Exp. Bot.* 66, 4337–4350. doi: 10.1093/jxb/erv096

Leontidou, K., Genitsaris, S., Papadopoulou, A., Kamou, N., Bosmali, I., Matsi, T., et al. (2020). Plant growth promoting rhizobacteria isolated from halophytes and drought-tolerant plants: genomic characterisation and exploration of phyto-beneficial traits. *Sci. Rep.* 10, 1–15. doi: 10.1038/s41598-020-71652-0

Lowry, O. H., Rosenbrough, N. J., Farr, A. L., and Randall, R. J. (1951). Protein measurment with Folin phenol reagent. *J. Biol. Chem.* 193, 265–275.

Machado, R. M. A., and Serralheiro, R. P. (2017). Soil salinity: effect on vegetable crop growth. Management practices to prevent and mitigate soil salinization. *Horticulturae* 3:30. doi: 10.3390/horticulturae3020030

Mapelli, F., Marasco, R., Rolli, E., Barbato, M., Cherif, H., Guesmi, A., et al. (2013). Potential for plant growth promotion of rhizobacteria associated with *Salicornia* growing in Tunisian hypersaline soils. *Biomed. Res. Int.* 2013, 1–13. doi: 10.1155/2013/248078

Masum, M. M. I., Liu, L., Yang, M., Hossain, M. M., Siddiqa, M. M., Supty, M. E., et al. (2018). Halotolerant bacteria belonging to operational group *Bacillus amyloliquefaciens* in biocontrol of the rice brown stripe pathogen *Acidovorax oryzae*. *J. Appl. Microbiol.* 125, 1852–1867. doi: 10.1111/jam.14088

Medeiros, C. A. A., and Bettiol, W. (2021). Multifaceted intervention of *Bacillus* spp. against salinity stress and Fusarium wilt in tomato. *J. Appl. Microbiol.* 131, 2387–2401. doi: 10.1111/jam.15095

Murtaza, B., Murtaza, G., Sabir, M., Owens, G., Abbas, G., Imran, M., et al. (2017). Amelioration of saline–sodic soil with gypsum can increase yield and nitrogen use efficiency in rice–wheat cropping system. *Arch. Agron. Soil Sci.* 63, 1267–1280. doi: 10.1080/03650340.2016.1276285

Nadeem, S. M., Ahmad, M., Naveed, M., Imran, M., Zahir, Z. A., and Crowley, D. E. (2016). Relationship between in vitro characterization and comparative efficacy of plant growth-promoting rhizobacteria for improving cucumber salt tolerance. *Arch. Microbiol.* 198, 379–387. doi: 10.1007/S00203-016-1197-5

Navarro-Torre, S., Mateos-Naranjo, E., Caviedes, M. A., Pajuelo, E., and Rodríguez-Llorente, I. D. (2016). Isolation of plant-growth-promoting and metal-resistant cultivable bacteria from *Arthrocnemum macrostachyum* in the Odiel marshes with potential use in phytoremediation. *Mar. Pollut. Bull.* 110, 133–142. doi: 10.1016/j.marpolbul.2016.06.070

Negacz, K., Malek, Ž., de Vos, A., and Vellinga, P. (2022). Saline soils worldwide: identifying the most promising areas for saline agriculture. *J. Arid Environ.* 203:104775. doi: 10.1016/j.jaridenv.2022.104775

Numan, M., Bashir, S., Khan, Y., Mumtaz, R., Shinwari, Z. K., Khan, A. L., et al. (2018). Plant growth promoting bacteria as an alternative strategy for salt tolerance in plants: A review. *Microbiol. Res.* 209, 21–32. doi: 10.1016/J.MICRES.2018.02.003

Obi, A. O. (1974). The wilting point and available moisture in tropical forest soils of Nigeria. *Exp. Agric.* 10, 305–312. doi: 10.1017/S0014479700006098

Orhan, F., and Demirci, A. (2020). Salt stress mitigating potential of halotolerant/halophilic plant growth promoting. *Geomicrobiol J.* 37, 663–669. doi: 10.1080/01490451.2020.1761911

Pandey, S. S., Patnana, P. K., Rai, R., and Chatterjee, S. (2017). Xanthoferrin, the α-hydroxycarboxylate-type siderophore of *Xanthomonas campestris* pv. campestris, is required for optimum virulence and growth inside cabbage. *Mol. Plant Pathol.* 18, 949–962. doi: 10.1111/mpp.12451

Panwar, M., Tewari, R., Gulati, A., and Nayyar, H. (2016). Indigenous salt-tolerant rhizobacterium *Pantoea dispersa* (PSB3) reduces sodium uptake and mitigates the effects of salt stress on growth and yield of chickpea. *Acta Physiol. Plant.* 38, 1–12. doi: 10.1007/s11738-016-2284-6

Paranychianakis, N. V., and Chartzoulakis, K. S. (2005). Irrigation of mediterranean crops with saline water: from physiology to management practices. *Agric. Ecosyst. Environ.* 106, 171–187. doi: 10.1016/j.agee.2004.10.006

Patel, R. R., Patel, D. D., Bhatt, J., Thakor, P., Triplett, L. R., and Thakkar, V. R. (2021). Induction of pre-chorismate, jasmonate and salicylate pathways by *Burkholderia* sp. RR18 in peanut seedlings. *J. Appl. Microbiol.* 131, 1417–1430. doi: 10.1111/JAM.15019

Patel, R. R., Thakkar, V. R., and Subramanian, R. B. (2016). Simultaneous detection and quantification of phytohormones by a sensitive method of separation in culture of *Pseudomonas* sp. *Curr. Microbiol.* 72, 744–751. doi: 10.1007/S00284-016-1012-1/TABLES/3

Paul, D., and Lade, H. (2014). Plant-growth-promoting rhizobacteria to improve crop growth in saline soils: a review. *Agron. Sustain. Dev.* 34, 737–752. doi: 10.1007/s13593-014-0233-6

Priyanka, A., Akshatha, K., Deekshit, V. K., Prarthana, J., and Akhila, D. S. (2020). "*Klebsiella pneumoniae* infections and antimicrobial drug resistance" in *Model Organisms for Microbial Pathogenesis, Biofilm Formation and Antimicrobial Drug Discovery*. eds. B. Siddhardha, M. Dyavaiah and A. Syed (Singapore: Springer), 195–225.

Qadir, M., Quillérou, E., Nangia, V., Murtaza, G., Singh, M., Thomas, R. J., et al. (2014). Economics of salt-induced land degradation and restoration. *Nat. Resour. Forum* 38, 282–295. doi: 10.1111/1477-8947.12054

Qin, Y., Druzhinina, I. S., Pan, X., and Yuan, Z. (2016). Microbially mediated plant salt tolerance and microbiome-based solutions for saline agriculture. *Biotechnol. Adv.* 34, 1245–1259. doi: 10.1016/j.biotechadv.2016.08.005

Rahman, S. S., Siddique, R., and Tabassum, N. (2017). Isolation and identification of halotolerant soil bacteria from coastal Patenga area. *BMC. Res. Notes* 10, 531–536. doi: 10.1186/s13104-017-2855-7

Rajkumar, M., Lee, K. J., Lee, W. H., and Banu, J. R. (2005). Growth of *Brassica juncea* under chromium stress: influence of siderophores and indole 3 acetic acid producing rhizosphere bacteria. *J. Environ. Biol.* 26, 693–699.

Raklami, A., Tahiri, A. I., Bechtaoui, N., Abdelhay, E. G., Pajuelo, E., Baslam, M., et al. (2021). Restoring the plant productivity of heavy metal-contaminated soil using phosphate sludge, marble waste, and beneficial microorganisms. *J. Environ. Sci.* 99, 210–221. doi: 10.1016/J.JES.2020.06.032

Ramadoss, D., Lakkineni, V. K., Bose, P., Ali, S., and Annapurna, K. (2013). Mitigation of salt stress in wheat seedlings by halotolerant bacteria isolated from saline habitats. *Springerplus* 2, 1–7. doi: 10.1186/2193-1801-2-6

Razzaghi Komaresofla, B., Alikhani, H. A., Etesami, H., and Khoshkholgh-Sima, N. A. (2019). Improved growth and salinity tolerance of the halophyte *Salicornia* sp. by co–inoculation with endophytic and rhizosphere bacteria. *Appl. Soil Ecol.* 138, 160–170. doi: 10.1016/J.APSOIL.2019.02.022

Ryu, C.-M., Farag, M. A., Hu, C.-H., Reddy, M. S., Wei, H.-X., Paré, P. W., et al. (2003). Bacterial volatiles promote growth in Arabidopsis. *Proc. Natl. Acad. Sci.* 100, 4927–4932. doi: 10.1073/pnas.0730845100

Sandhya, V., and Ali, S. Z. (2018). Quantitative mRNA analysis of induced genes in maize inoculated with *Acinetobacter baumannii* strain MZ30V92. *Curr. Biotechnol.* 7, 438–452. doi: 10.2174/2211550108666190125114821

Santoyo, G., Moreno-Hagelsieb, G., del Carmen Orozco-Mosqueda, M., and Glick, B. R. (2016). Plant growth-promoting bacterial endophytes. *Microbiol. Res.* 183, 92–99. doi: 10.1016/j.micres.2015.11.008

Sapre, S., Gontia-Mishra, I., and Tiwari, S. (2022). Plant growth-promoting rhizobacteria ameliorates salinity stress in pea (*Pisum sativum*). *J. Plant Growth Regul.* 41, 647–656. doi: 10.1007/s00344-021-10329-y

Saravanakumar, D., and Samiyappan, R. (2007). ACC deaminase from *Pseudomonas fluorescens* mediated saline resistance in groundnut (*Arachis hypogea*) plants. *J. Appl. Microbiol.* 102, 1283–1292. doi: 10.1111/j.1365-2672.2006.03179.x

Sarkar, P., and Chourasia, R. (2017). Bioconversion of organic solid wastes into biofortified compost using a microbial consortium. *Int. J. Recycl. Org. Waste Agric.* 6, 321–334. doi: 10.1007/s40093-017-0180-8

Schwyn, B., and Neilands, J. B. (1987). Universal chemical assay for the detection and determination of siderophores. *Anal. Biochem.* 160, 47–56. doi: 10.1016/0003-2697(87)90612-9

Shabala, S. (2013). Learning from halophytes: physiological basis and strategies to improve abiotic stress tolerance in crops. *Ann. Bot.* 112, 1209–1221. doi: 10.1093/aob/mct205

Shahid, M., Hameed, S., Imran, A., Ali, S., and van Elsas, J. D. (2012). Root colonization and growth promotion of sunflower (*Helianthus annuus* L.) by phosphate solubilizing *Enterobacter* sp. Fs-11. *World J. Microbiol. Biotechnol.* 28, 2749–2758. doi: 10.1007/s11274-012-1086-2

Shahid, M., Hameed, S., Tariq, M., Zafar, M., Ali, A., and Ahmad, N. (2015). Characterization of mineral phosphate-solubilizing bacteria for enhanced sunflower growth and yield-attributing traits. *Ann. Microbiol.* 65, 1525–1536. doi: 10.1007/s13213-014-0991-z

Shahzad, R., Waqas, M., Latif Khan, A., Al-Hosni, K., Kang, S.-M., Seo, C.-W., et al. (2017). Indoleacetic acid production and plant growth promoting potential of bacterial endophytes isolated from rice (*Oryza sativa* L.) seeds. *Acta Biol. Hung.* 68, 175–186. doi: 10.1556/018.68.2017.2.5

Shi, Q., Wang, X., Ju, Z., Liu, B., Lei, C., Wang, H., et al. (2021). Technological and safety characterization of *Kocuria rhizophila* isolates from traditional ethnic dry-cured ham of Nuodeng, Southwest China. *Front. Microbiol.* 12:761019. doi: 10.3389/fmicb.2021.761019

Shrivastava, P., and Kumar, R. (2015). Soil salinity: a serious environmental issue and plant growth promoting bacteria as one of the tools for its alleviation. *Saudi J. Biol. Sci.* 22, 123–131. doi: 10.1016/j.sjbs.2014.12.001

Shukla, P. S., Agarwal, P. K., and Jha, B. (2012). Improved salinity tolerance of *Arachis hypogaea* (L.) by the interaction of halotolerant plant-growth-promoting rhizobacteria. *J. Plant Growth Regul.* 31, 195–206. doi: 10.1007/s00344-011-9231-y

Singh, P., Chauhan, P. K., Upadhyay, S. K., Singh, R. K., Dwivedi, P., Wang, J., et al. (2022). Mechanistic insights and potential use of siderophores producing microbes in rhizosphere for mitigation of stress in plants grown in degraded land. *Front. Microbiol.* 13:898979. doi: 10.3389/fmicb.2022.898979

Singh, R. P., and Jha, P. N. (2016a). A halotolerant bacterium *Bacillus licheniformis* HSW-16 augments induced systemic tolerance to salt stress in wheat plant (*Triticum aestivum*). *Front. Plant Sci.* 7:1890. doi: 10.3389/fpls.2016.01890

Singh, R. P., and Jha, P. N. (2016b). The multifarious PGPR *Serratia marcescens* CDP-13 augments induced systemic resistance and enhanced salinity tolerance of wheat (*Triticum aestivum* L.). *PLoS One* 11:e0155026. doi: 10.1371/journal.pone.0155026

Singh, A., Kumar, A., Yadav, S., and Singh, I. K. (2019). Reactive oxygen species-mediated signaling during abiotic stress. *Plant Gene* 18:100173. doi: 10.1007/s00344-011-9231-y

Talavera, G., and Castresana, J. (2007). Improvement of phylogenies after removing divergent and ambiguously aligned blocks from protein sequence alignments. *Syst. Biol.* 56, 564–577. doi: 10.1080/10635150701472164

Thomloudi, E.-E., Tsalgatidou, P. C., Douka, D., Spantidos, T.-N., Dimou, M., Venieraki, A., et al. (2019). Multistrain versus single-strain plant growth promoting microbial inoculants-the compatibility issue. *Hell. Plant Prot. J.* 12, 61–77. doi: 10.2478/hppj-2019-0007

Tripathi, S., Das, A., Chandra, A., and Varma, A. (2015). Development of carrier-based formulation of root endophyte *Piriformospora indica* and its evaluation on *Phaseolus vulgaris* L. *World J. Microbiol. Biotechnol.* 31, 337–344. doi: 10.1007/s11274-014-1785-y

Upadhyay, S. K., and Chauhan, P. K. (2022). Optimization of eco-friendly amendments as sustainable asset for salt-tolerant plant growth-promoting bacteria mediated maize (*Zea Mays* L.) plant growth, Na uptake reduction and saline soil restoration. *Environ. Res.* 211:113081. doi: 10.1016/j.envres.2022.113081

Upadhyay, S. K., Rajput, V. D., Kumari, A., Espinosa-Saiz, D., Menendez, E., Minkina, T., et al. (2022a). Plant growth-promoting rhizobacteria: a potential bio-asset for restoration of degraded soil and crop productivity with sustainable emerging techniques. *Environ. Geochem. Health* 1–24. doi: 10.1007/s10653-022-01433-3

Upadhyay, S. K., Singh, J. S., and Singh, D. P. (2011). Exopolysaccharide-producing plant growth-promoting rhizobacteria under salinity condition. *Pedosphere* 21, 214–222. doi: 10.1016/S1002-0160(11)60120-3

Upadhyay, S. K., Srivastava, A. K., Rajput, V. D., Chauhan, P. K., Bhojiya, A. A., Jain, D., et al. (2022b). Root exudates: mechanistic insight of plant growth promoting Rhizobacteria for sustainable crop production. *Front. Microbiol.* 13:916488. doi: 10.3389/FMICB.2022.916488

Vimal, S. R., and Singh, J. S. (2019). Salt tolerant PGPR and FYM application in saline soil paddy agriculture sustainability. *Clim. Chang. Environ. Sustain.* 7, 61–71. doi: 10.5958/2320-642X.2019.00008.5

Weisskopf, L., Heller, S., and Eberl, L. (2011). *Burkholderia* species are major inhabitants of white lupin cluster roots. *Appl. Environ. Microbiol.* 77, 7715–7720. doi: 10.1128/AEM.05845-11

Yasin, N. A., Khan, W. U., Ahmad, S. R., Ali, A., Ahmad, A., and Akram, W. (2018). Imperative roles of halotolerant plant growth-promoting rhizobacteria and kinetin in improving salt tolerance and growth of black gram (*Phaseolus mungo*). *Environ. Sci. Pollut. Res.* 25, 4491–4505. doi: 10.1007/s11356-017-0761-0

Zahid, M., Abbasi, M. K., Hameed, S., and Rahim, N. (2015). Isolation and identification of indigenous plant growth promoting rhizobacteria from Himalayan region of Kashmir and their effect on improving growth and nutrient contents of maize (*Zea mays* L.). *Front. Microbiol.* 6:207. doi: 10.3389/fmicb.2015.00207

Zeigler, M. M., and Steensland, A. (2022). Participatory farmer research and exploring the phytobiome: next steps for agricultural productivity growth. *Russ. J. Econ.* 8, 16–28. doi: 10.32609/j.ruje.8.80597

Zhang, M., Smith, J. A. C., Harberd, N. P., and Jiang, C. (2016). The regulatory roles of ethylene and reactive oxygen species (ROS) in plant salt stress responses. *Plant Mol. Biol.* 91, 651–659. doi: 10.1007/s11103-016-0488-1

frontiers | Frontiers in Microbiology

TYPE Original Research
PUBLISHED 17 February 2023
DOI 10.3389/fmicb.2023.1096826

OPEN ACCESS

EDITED BY
Sumit Kumar,
Amity University,
India

REVIEWED BY
Amr Shehabeldine,
Al-Azhar University,
Egypt
Salma Mukhtar,
Connecticut Agricultural Experiment Station,
United States

*CORRESPONDENCE
Manjula Ishwara Kalyani
✉ manjuganesh7176@gmail.com
Muntazir Mushtaq
✉ muntazirhuda@gmail.com

SPECIALTY SECTION
This article was submitted to Extreme Microbiology, a section of the journal Frontiers in Microbiology

RECEIVED 12 November 2022
ACCEPTED 26 January 2023
PUBLISHED 17 February 2023

CITATION
Karthik Y, Ishwara Kalyani M, Krishnappa S, Devappa R, Anjali Goud C, Ramakrishna K, Wani MA, Alkafafy M, Hussen Abduljabbar M, Alswat AS, Sayed SM and Mushtaq M (2023) Antiproliferative activity of antimicrobial peptides and bioactive compounds from the mangrove *Glutamicibacter mysorens*. *Front. Microbiol.* 14:1096826. doi: 10.3389/fmicb.2023.1096826

Antiproliferative activity of antimicrobial peptides and bioactive compounds from the mangrove *Glutamicibacter mysorens*

Yalpi Karthik[1], Manjula Ishwara Kalyani[1]*, Srinivasa Krishnappa[2], Ramakrishna Devappa[3], Chengeshpur Anjali Goud[4], Krishnaveni Ramakrishna[5], Muneeb Ahmad Wani[6], Mohamed Alkafafy[7], Maram Hussen Abduljabbar[8], Amal S. Alswat[9], Samy M. Sayed[10] and Muntazir Mushtaq[11,12]*

[1]Department of Studies and Research in Microbiology, Mangalore University, Mangalore, Karnataka, India, [2]Department of Studies and Research in Biochemistry, Mangalore University, Mangalore, Karnataka, India, [3]Dr. C.D Sagar Centre for Life Sciences, Biotechnology Department, Dayananda Sagar College of Engineering, Dayananda Sagar Institutions, Bengaluru, India, [4]Department of Plant Biotechnology, School of Agricultural Sciences, Malla Reddy University, Hyderabad, India, [5]Department of Studies and Research in Microbiology, Vijayanagara Sri Krishnadevaraya University, Ballari, Karnataka, India, [6]Division of Floriculture, Sher-e-Kashmir University of Agricultural Sciences and Technology, Srinagar, Jammu and Kashmir, India, [7]Department of Cytology and Histology, Faculty of Veterinary Medicine, University of Sadat City, Sadat City, Egypt, [8]Department of Pharmacology and Toxicology, College of Pharmacy, Taif University, Taif, Saudi Arabia, [9]Department of Biotechnology, College of Science, Taif University, Taif, Saudi Arabia, [10]Department of Economic Entomology and Pesticides, Faculty of Agriculture, Cairo University, Giza, Egypt, [11]ICAR-National Bureau of Plant Genetic Resources, Division of Germplasm Evaluation, New Delhi, India, [12]MS Swaminathan School of Agriculture, Shoolini University of Biotechnology and Management, Bajhol, Himachal Pradesh, India

The *Glutamicibacter* group of microbes is known for antibiotic and enzyme production. Antibiotics and enzymes produced by them are important in the control, protection, and treatment of chronic human diseases. In this study, the *Glutamicibacter mysorens* (*G. mysorens*) strain MW647910.1 was isolated from mangrove soil in the Mangalore region of India. After optimization of growth conditions for *G. mysorens* on starch casein agar media, the micromorphology of *G. mysorens* was found to be spirally coiled spore chain, each spore visualized as an elongated cylindrical hairy appearance with curved edges visualized through Field Emission Scanning Electron Microscopy (FESEM) analysis. The culture phenotype with filamentous mycelia, brown pigmentation, and ash–colored spore production was observed. The intracellular extract of *G. mysorens* characterized through GCMS analysis detected bioactive compounds reported for pharmacological applications. The majority of bioactive compounds identified in intracellular extract when compared to the NIST library revealed molecular weight ranging below 1kgmole^{-1}. The Sephadex G-10 could result in 10.66 fold purification and eluted peak protein fraction showed significant anticancer activity on the prostate cancer cell line. Liquid Chromatography–Mass Spectrometry (LC–MS) analysis revealed Kinetin-9-ribose and Embinin with a molecular weight below 1kDa. This study showed small molecular weight bioactive compounds produced from microbial origin possess dual roles, acting as antimicrobial peptides (AMPs) and anticancer peptides (ACPs). Hence, the bioactive compounds produced from microbial origin are a promising source of future therapeutics.

KEYWORDS

anticancer, chromatography, FESEM, *Glutamicibacter mysorens*, mangrove soil, microbial peptides

Introduction

The environmental conditions in a particular ecosystem play an important role in determining biodiversity composition. High tides, hypersaline water, significant temperature fluctuations, and optimal flora and fauna diversity are just a few of the distinctive environmental characteristics of the mangrove ecosystem (Karthik et al., 2020). Microbes can better adapt to any extreme environment in these vulnerable situations. The isolation of bioactive chemicals will be greatly aided by this habitat (Alongi, 2015).

Actinomyces word derived from the words "atkis" which means "a ray" and "mykes" which means "fungi" are filamentous, Gram–positive bacteria distinguished by different coloration and spore production at maturity (Chater, 2006). *Actinomyces* share the characteristics of bacteria and fungi. The *Actinomyces* group's genetic and environmental flexibility facilitates the development of worthwhile bioactive substances. *Actinomyces* contribute more in enzyme production to pharmacological industries for the treatment, and prevention of various ailments (Chater, 2013).

The pharmaceutical industry is constantly looking for drugs with innovative structures and new modes of action as a result of the rise in antibiotic resistance. There are still many environmental niches to investigate as potential sources of antibiotics (Karthik and Kalyani, 2021, 2022). One such *Actinomyces* group *Glutamicibacter* genus is broadly utilized in the control, treatment, and prevention of diseases through the production of bioactive compounds, widely used as antibiotics (Phuong and Diep, 2020), anti-tumor, anti-tubercular (Khusro et al., 2020), anti-helminthic, anti-diabetic, anti-oxidant from an exo-polysaccharide (Xiong et al., 2020; Fukuda and Kono, 2021; Hidri et al., 2022), anti-angiogenic, growth hormones (Qin et al., 2018; Hidri et al., 2022), immuno-suppressors, neuritogenic (Tang et al., 2021), anti-inflammatory (Hui et al., 2021), anti-algal (Agamennone et al., 2018), anti-fungal with enzymatic source (Mihooliya et al., 2017; Asif et al., 2020), anti-proliferative (Baig et al., 2021), anti-parasitic, anti-malarial, anti-viral, anti-bacterial and many more biological applications (Nishioka and Katayama, 1978; Renner et al., 1999; Fernebro, 2011; Janardhan et al., 2014; Desouky et al., 2015; Abd-Elnaby et al., 2016).

The various species of genus *Glutamicibacter* shown huge biological importance as detailed above. Whereas *G. creatinolyticus* shown resistance to antibiotics as well as heavy metals (copper, arsenic, cadmium, cobalt, zinc, and chromium; Santos et al., 2020). The *G. arilaitensis* produced pink colored pigment and coprophorphyrin binds zinc and regulates in cheese rinds (Cleary et al., 2018). Another *Gluamicibacter sps.* Possessing genes that regulates the growth of plant under saline conditions, cold adaptation, efficient degradation and chitinase enzyme producing genes which help in control the growth of pathogenic bacteria (Borker et al., 2021; Fu et al., 2021). While *G. nicotianae* involved in heavy metals degradation (Wang et al., 2021). The *G. mishrai* and *halophytocola* isolated from Andaman sea sample. Genes involved in cell wall biogenesis, replication, recombination, repair mechanism and amino acid metabolism along possess important role in physiology and behavior of insects (Qin et al., 2018; Das et al., 2020; Wang W, et al., 2022).

Antimicrobial peptides (AMPs) are peptides with antimicrobial properties. In multicellular organisms, these positively charged host defense molecules, or AMPs, serve as the initial line of protection. Many AMP's from both prokaryotes and eukaryotes have been categorized (Brandenburg et al., 2012; Desriac et al., 2013). Several genera of AMP's -producing microorganisms have been discovered, including bacteriocins produced by *Leuconostoc gelidum*, *Enterococcus faecium*, and other species (Juturu and Wu, 2018; Khodaei and Sh, 2018). Microcins A and B, antimicrobial bacteriocins derived from *Streptomyces pluripotens*, have been shown to be effective against *Escherichia coli, Salmonella typhimurium, Staphylococcus aureus,* and *Listeria monocytogenes* (Collin and Maxwell, 2019; Kurnianto et al., 2021).These AMPs have been found to be effective in the treatment of a broad range of ailments (Sugrue et al., 2019; Karthik et al., 2020; Khadayat et al., 2020; Zhang et al., 2020). AMP's are peptides derived from microbes that exhibit antimicrobial activity. AMPs have been shown to target cell walls or cell membranes, permitting them to penetrate cells and affect vital components while inhibiting growth (Desriac et al., 2013; Wang et al., 2020). As a result of their target-specific activity against resistant microbial species, AMPs are thought to be anti–microbial compounds.

Peptides with selective action and non-selective activity, i.e., those that have activity against bacteria, cancer cells, and healthy cells, can be categorized as having antitumor activity in Hoskin and Ramamoorthy's investigations (Hoskin and Ramamoorthy, 2008).The peptides have antibacterial and anticancer properties, but not against normal cells. Cecropins, buforins, and magainins, among other peptides, have demonstrated anticancer effects without harming normal eukaryotic cells (Cruciani et al., 1991; Cho et al., 2009). These studies go into great detail and provide a compelling case for the fact that many peptides have biological activity in a variety of dimensions and properties and can possess dual activity as AMPs and ACPs. Therefore, we are searching for mangrove soil *Actinomyces* in the Mangalore region to isolate and characterize bioactive peptides that can function as both AMPs and ACPs.

In our previous study, we reported the detailed procedures for isolation, microscopic and macroscopic characters, identified as *Glutamicibacter mysorens* with GenBank accession number MW647910.1, the intracellular protein; extraction, estimation, along with their potential antimicrobial activity was observed against test pathogens *Salmonella typhimurium* (ATCC23564), *Staphylococcus aureus* (ATCC6538P),*Bacillus cereus* (ATCC10876), *Proteus vulgaris* (ATCC13315), and *Pseudomonas aeruginosa* (ATCC9027) cultures. The protein was characterized through LCMS and SDS PAGE techniques and small peptides were detected (Karthik and Kalyani, 2021).

In this study, the optimization of suitable growth media for *G. mysorens* and its micromorphology were analyzed using FESEM. The isolation of intracellular extract of *G. mysorens* was characterized through GCMS and LCMS. These GCMS studies revealed a large number of small bioactive compounds that possess significant biological activities are discussed. Whereas the LCMS studies resulted in the detection of low molecular weight Kinetin-9-ribose and Embinin showed significant anti-tumor potential against PC3 cell line in comparison to standard cisplatin drug.

Materials and methods

Mangrove soil collection

Soil samples were collected from Mangroves soil in Mangalore, Dakshina Kannada. Jeppinamogaru (JPMU) is located at 12°50′31.4"N 74°51′36.4"E. At the collecting site, the soil was brown with a powdery

texture, and environmental parameters; the temperature of 21°C and pH of 7.2 was recorded. The collected samples were shifted to the Molecular Research Laboratory (MRL), Department of Microbiology, Jnana Kaveri, Mangalore University, India, in aseptic containers. To prevent fungal and bacterial growth, the soil sample was pre-heated for 2 h at 60°C prior to serial dilution and isolation (Mohan et al., 2013; Sridevi et al., 2015; Sapkota et al., 2020).

Cultural characteristics

The isolated *G. mysorens* strain was subjected to FESEM analysis at different objectives distances; spore structure (1 and 2 µm) mycelial structure (10 and 20 µm) to visualize the complete micromorphological structures. The sequencing and identification of *G. mysorens* are reported by Karthik and Kalyani (2021).

Intracellular extract

The *G. mysorens* strain was grown in SCN broth for 7 days at 30 ± 2°C with continuous shaking at 100 rpm. Centrifugation at 7000 rpm for 8 min separated the cultured biomass cells, which were then washed twice using phosphate-buffered saline devoid of Mg^{2+} and Ca^{2+} and centrifuged again. The cells were then re-suspended in 10 ml of chilled acetone for 5 min before being centrifuged at 7,000 rpm for 8 min. The intracellular extract was incubated for 2 min with 1.0 ml of 1% SDS after the traces of acetone was removed with a nitrogen stream (Bhaduri and Demchick, 1983). This intracellular extract was characterized using spectrometric (LCMS, GCMS) tools along with a comparison to the NIST library.

Gas chromatography-mass spectroscopic analysis

The following equipment was assessed for the GC–MS studies of *G. mysorens* intracellular extract: a PerkinElmer Clarus 680 Gas Chromatograph and a PerkinElmer Clarus SQ 8C Mass Spectrometer. A PerkinElmer Elite-5MS standard column with dimensions of 30 m long x 0.250 mm inner diameter x 1 micron (60–350°C) is utilized in the equipment. With an equivalence ratio of 10:1, the injected volume of 2 µl was completely run for 26.6 min. Helium is used as the carrier gas, with a flow rate of 2 ml/min. The source temperature was set to 230 degrees Celsius, and the inlet temperature was set to 250 degrees Celsius. The oven temperature was initially set to 80°C with a hold time of 2.0 min; ramp1 was set to 10.0 /min to 150°C with a hold time of 1.0 min; and ramp2 was set to 15.0 /min to 250°C with a hold time of 10.0 min. The components were identified by comparing them to those contained in the NIST computer library, which was linked to the GC–MS apparatus, and the results were published.

Gel filtration

The microbial proteins were purified using SephadexG-10. For 5 h, the Sephadex G-10 was allowed to swell in excess of dH_2O in a boiling water bath. After decanting the gel to remove fines, it was equilibrated with 0.05 M sodium phosphate buffer, pH 7.0. Under gravity, the gel was packed into a 1.0 cm × 110.0 cm column. At a flow rate of 10 ml/h, the column was standardized with two-bed volumes of phosphate buffer of concentration 0.05 M, pH 7.0. The 20 mg of isolate protein sample was loaded onto the gel, eluted with 0.05 M sodium phosphate buffer, pH 7.0, and 2.0 ml fractions were collected and further analyzed (Bharadwaj et al., 2018).

Liquid chromatography-mass spectrophotometer

The Sephadex G-10 peak fraction was analyzed using LC–MS, model Synapt G2, an analytical chemistry technique that combines the physical separation capabilities of liquid chromatography with mobile phases A: 0.1% Formic acid in Water and mobile phase B: 0.1% Formic acid in Acetonitrile with the mass analysis capabilities of mass spectrometry (MS) an Agilent 1100 LC system with a vacuum degasser, A BEH C18, 50 mm × 1.0 mm, 1.7 µm C18 column (Waters, United States) was used to achieve chromatographic separation in comparison to the NIST computer library.

MTT assay

Prostate cancer cells (PC3) procured from NCCS Pune; were harvested in T-25 flasks for the *in vitro* studies. PC3 cells were trypsinized and aspirated into a 5 ml centrifuge tube. After centrifugation at 300 rpm for 10 min, the cell pellet was separated. The cell count was adjusted using DMEM HG medium so that 200 µl of suspension contained approximately 10,000 cells. In an ESCO model CLM170B-8-UV CO_2 incubator, a 200 µl cell suspension was added to each well of the 96-well microtiter plate, and the plate was incubated for 24 h at 37°C and 5% CO_2 atmosphere. After 24 h, the spent medium was aspirated. In each well, 200 µl of various test drug concentrations and the standard drug cisplatin were added. After that, the plates were incubated for 24 h at 37°C and 5% CO_2. The drug-containing media was aspirated after the plate was removed from the incubator. The plate was then incubated for 3 h at 37\u00B0C and 5% CO_2 atmosphere with 200 µl of medium containing 10% MTT reagent in each well to achieve a final concentration of 0.5 mg/ml. The culture medium was completely removed without disturbing the formed crystals. To solubilize the formed formazan, the plate was gently shaken in a gyrator shaker with 100 µl of solubilization solution (DMSO). The absorbance was read at 570 and 630 nm using the microplate reader of a Multiskan sky ELISA spectrophotometer.

Results and discussion

The Mangrove region in Jeppinamogaru located at Mangalore, India, served as a suitable source for isolating *G. mysorens* strain. The *G. mysorens* strain received a GenBank accession number MW647910.1 and was isolated and their biological activities were reported by Karthik and Kalyani (2021). In continuation to previous work; initially, the *G. mysorens* strain was observed for morphological characteristics after performing FESEM analysis. Also, biologically important chemical components present in the intracellular extract of the *G. mysorens* strain were characterized using GCMS and a partially purified protein sample

was characterized using LCMS and have a shown significant number of bioactive compounds.

The cultural characteristics of mangrove adapted *G. mysorens* strain upon growth on starch casein nitrate agar medium exhibited as white colored filamentous mycelia and at maturity showed ash-colored spores. Production of brown pigmentation on SCNA media was observed. Further microscopic analysis showed Gram staining positive. The isolate when further subjected to FESEM microscopic studies revealed mycelial morphological characteristics of the genus *Glutamicibacter.* Further, the culture showed filamentous mycelia possessing spirally coiled spore chains. Each spore is visualized as an elongated cylindrical hairy appearance with curved edges as shown in Figure 1. The *G. mysorens* when grown on different *Actinomyces*-specific media have shown distinctive phenotypic characteristics as listed in Table 1. Excellent growth was achieved on starch casein nitrate agar, whereas good growth was seen on, glucose leucine agar, yeast extract agar, and nutrient agar media. Moderate growth was seen on sucrose peptone agar, and malt extract agar. Whereas in another study, lysogeny agar was chosen as the best growth media for *G. mysorens* according to Wang Y. et al. (2022) and Deb et al. (2020).

In our previous report, the *G. mysorens* strain when subjected to simple and rapid disruption followed according to the method of Bhaduri yielded significant intracellular extraction in buffer (Bhaduri and Demchick, 1983). A 20 mg of protein was loaded on top of the column and 2 ml fractions were collected and about 2.5 times (216 ml) bed volumes of protein elutions were collected. The absorbance of protein fractions was checked at 280 nm and graphs were plotted. The

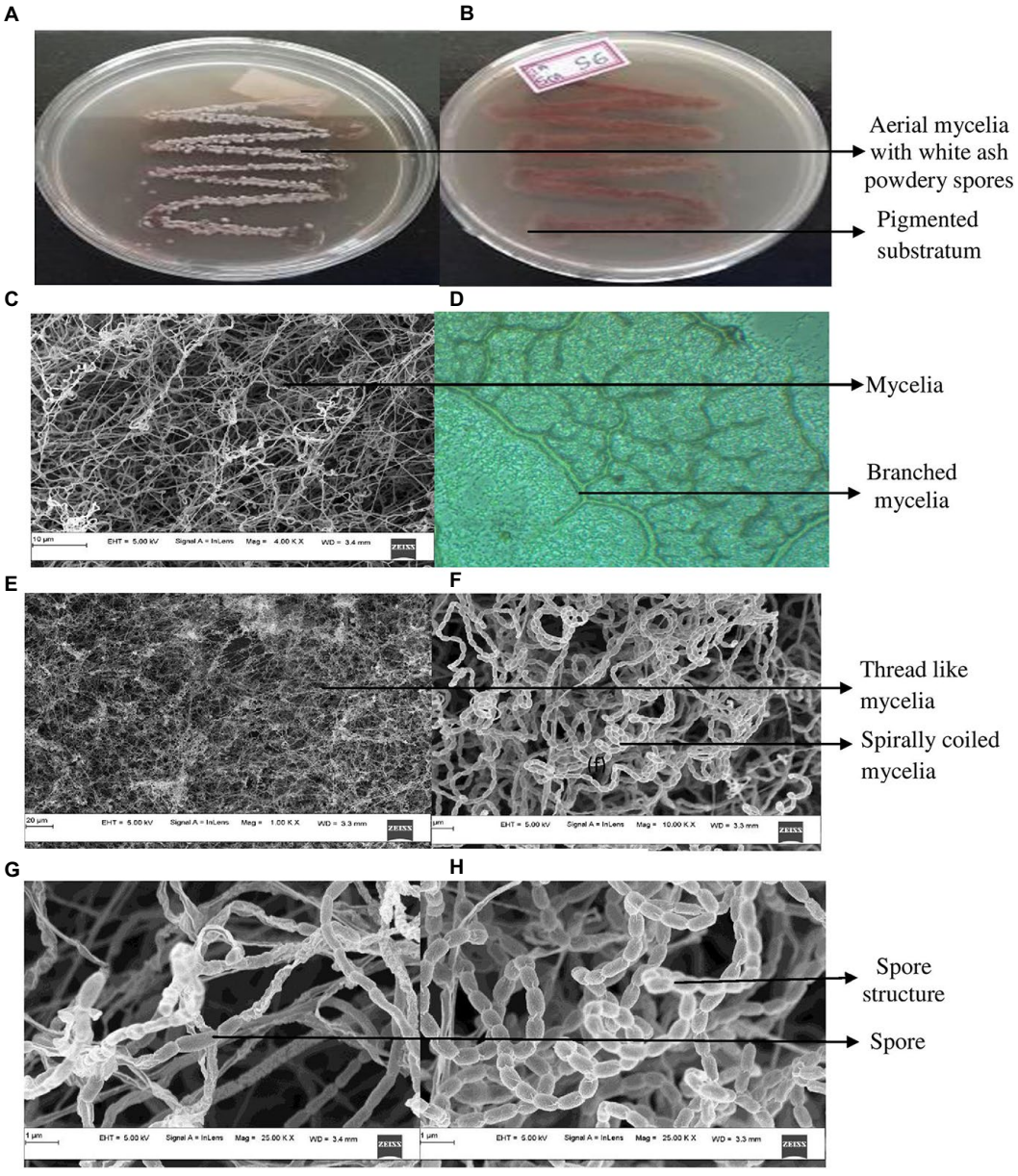

FIGURE 1
Cultural characteristics of *Glutamicibacter mysorens*. **(A)** Front view of isolate. **(B)** Rear view of isolate. **(C)** Mycelia observations under FESEM. **(D)** Phase contrast microscopic analysis. **(E,F)** Mycelia along with spore analysis under FESEM. **(G,H)** Spore structure analysis using FESEM.

X-axis indicates fraction numbers and absorbance plotted on Y-axis for each fraction collected from Sephadex G-10 column chromatography as showed in Figure 2. This column separation chromatography purifies 10.66 folds as detailed in Table 2. The GCMS studies depicted the presence of 155 bioactive molecules present in the intracellular extract of *G. mysorens* and the obtained elution profile is as shown in Figure 3. Whereas GCMS analysis depicted the highest probable compounds such as Cyclopentane undecanoic acid, methyl ester 22.7% and Glutaric acid, 2,2-dichloroethyl 3-fluorophenyl ester 34% probability as shown in Figure 4. All the compounds detected through GCMS showed low molecular weight below 1Kgmol^{-1}with various pharmacological applications. The majority of bioactive compounds have shown antimicrobial, enzyme inhibitors, activators, antioxidants, anti-inflammatory, anticancer, agrochemical, insecticide, anti-obese, and many other applications as listed in Table 3. The intracellular extract of *G. mysorens* had shown potent antimicrobial activity to a broad spectrum of test pathogens such as *Salmonella typhimurium* (ATCC23564), *Staphylococcus aureus* (ATCC6538P), *Pseudomonas aeruginosa* (ATCC9027), *Proteus vulgaris* (ATCC13315), and *Bacillus cereus* (ATCC10876) cultures. In order to focus further on prominent bioactive compounds the intracellular extract was partially purified using a Sephadex G-10 column. The eluted peak fraction upon spectrophotometry and electrophoretic analysis revealed the presence of peptide and is reported in our previous article (Karthik and Kalyani, 2021). A similar study was illustrated on 41 different *Actinomyces* species and majority isolates shown antagonist activity against *Staphylococcus aureus, Escherichia coli* and *Klebsiella pneumoniae* (Sapkota et al., 2020).

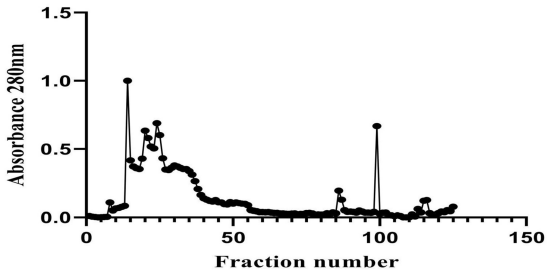

FIGURE 2
Elution profile of *Glutamicibacter mysorens* by using Sephadex G-10 column chromatography.

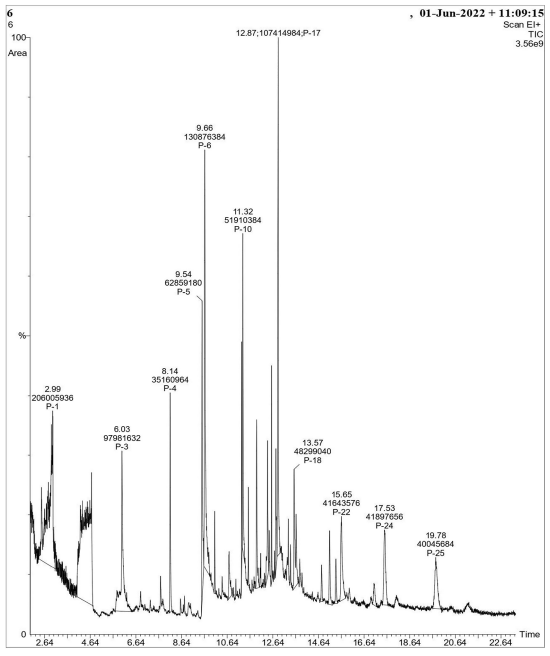

FIGURE 3
Elution profile of GCMS analysis for *Glutamicibacter mysorens* intracellular extract.

One of the previous study; extracellular protein of *Actinomyces* are actively producers for enzyme ligno cellulase (Clark Mason et al., 1988). The eluted peak fraction for proteins of *G. mysorens* has shown significant activity for different concentrations 50 µg of protein fraction showed 24% antiproliferative activity against prostate cancer PC3 cell line, for 100 µg 35% antiproliferative activity was observed, for 150 µg 47% antiproliferative activity was observed and for 200 µg 56% antiproliferative activity was observed in comparison with standard drug cisplatin at 5 µg showed 47% antiproliferative activity as showed in Figure 5.

Similar studies reported that other bioactive compounds isolated from the genus *Glutamicibacter* have been characterized for antimicrobial activity (Phuong and Diep, 2020; Xiong et al., 2020). In another study reported that plant-growth promoting bioactive

TABLE 1 Phenotypic characteristics of *Glutamicibacter mysorens* on different media.

Media	Growth	Front view	Rear view	Pigment	Spores
Sucrose peptone agar	Moderate	Cream	Creamish white	–	No
Glucose luecine agar	Good	Cream	White	–	Black
Nutrient agar	Good	Creamish	Creamish	–	–
Malt extract agar	Moderate	Creamish white	Creamish white	–	No
Yeast extract agar	Good	Cream	Cream	–	White
Starch casein nitrate agar	Excellent	White ash	Brown	+	Grey

TABLE 2 Purification chart of *Glutamicibacter mysorens* intracellular protein.

Sample	Protein (mg/ml)	Fold purification	% yield
Crude protein	2.0	1	100
Gel filtration (Sephadex G-10)	0.1875	10.66	9.38

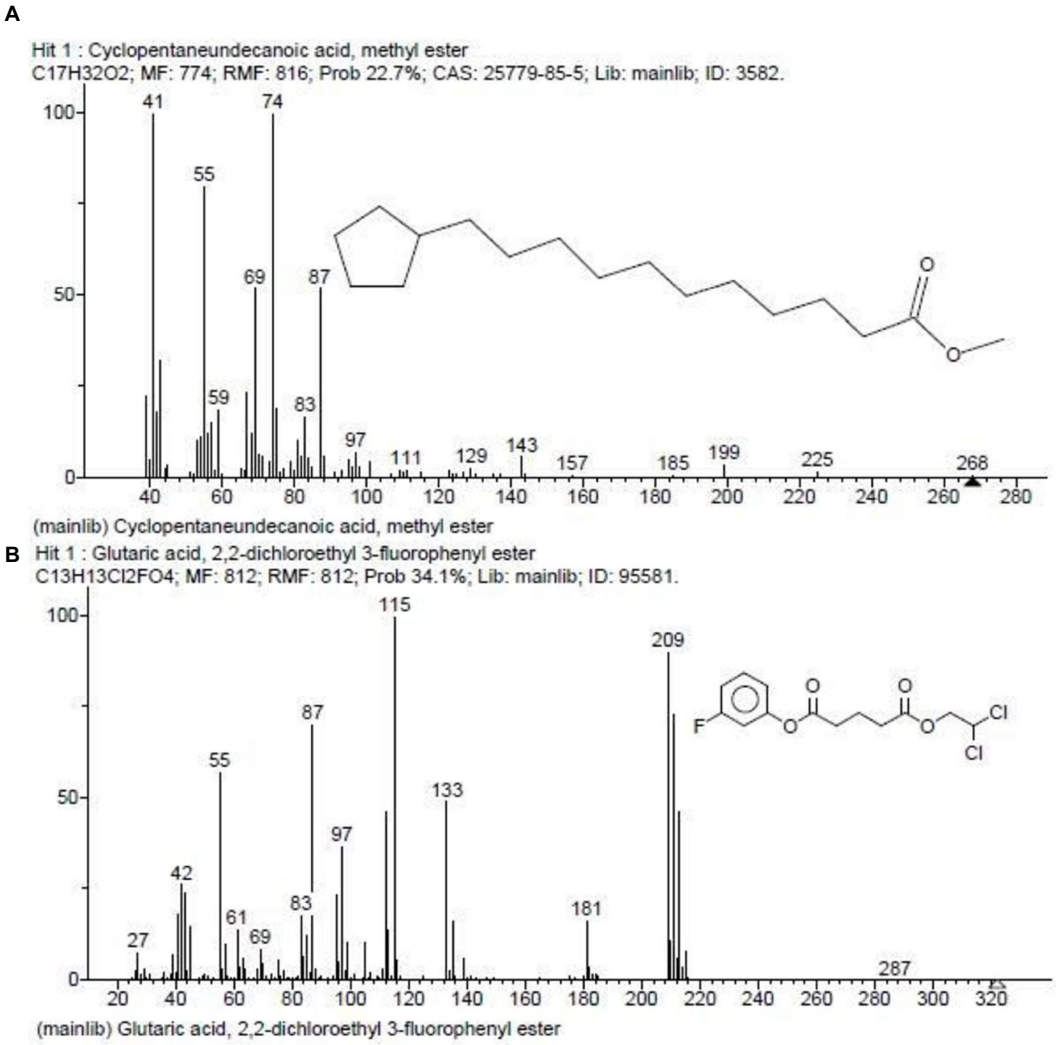

FIGURE 4
GCMS depicted highest probable compounds. **(A)** Cyclopentaneundecanoic acid, methyl ester 22.7%. **(B)** Glutaric acid, 2,2-dichloroethyl 3-fluorophenyl ester 34% probability.

compounds was produced by *Glutamicibacter halophytocola* coastal region of China (Qin et al., 2018). Whereas another study describes the anti-fungal efficiency of the *Glutamicibacter* genus with chitin hydrolyzing activity (Asif et al., 2020). The intracellular protein extraction already reported in our previous studies characterized for an antimicrobial activity that can be considered as antimicrobial peptides (AMPs) from the microbial origin (Karthik and Kalyani, 2021). In the present work the *G. mysorens* protein fraction is also exhibiting antiproliferative activity against cancerous cells acting also as anticancer peptides (ACP's) and the protein molecules detected and characterized by LC–MS analysis. We are also reporting GCMS analysis and detected bioactive compounds from *G. mysorens*.

As discussed above the Sephadex G-10 eluted peak protein fraction was further subjected to LCMS analysis. The LCMS analysis and elution profile as shown in Figure 6, revealed the detection of pharmacologically applicable bioactive peptide compounds. With respect to elution peak from LCMS analysis and detection through the NIST, the computer library resulted in the identification of Kinetin-9-riboside and Embinin. The detected Kinetin-9-riboside with 347 Da molecular weight structure and mass confirmation are shown in Figure 7. The mass confirmation and structure of Embinin with a molecular weight of 606 Da showed in Figure 8. These bioactive molecules are well-known for their effective activity in various biological applications.

In a previous study, the therapeutic and biological studies of Kinetin-9-riboside as an immuno-stimulant; immuno-stimulatory activities, and their uses as an adjuvant were reported. Because mutations in induced putative kinase 1 (PINK1) induce severe Parkinson's disease, there's a lot of interest in finding small molecules that boost PINK1's kinase activity. Several studies on the design, synthesis, serum stability and hydrolysis of four kinetin riboside ProTides have been published. These ProTides, in combination with kinetin riboside, activated PINK1 in cells that had not been depolarized by mitochondria. This demonstrates the therapeutic potential of modified nucleosides and their phosphate prodrugs for Parkinson's disease, the second most common neurodegenerative disease (Osgerby et al., 2017).

10.3389/fmicb.2023.1096826

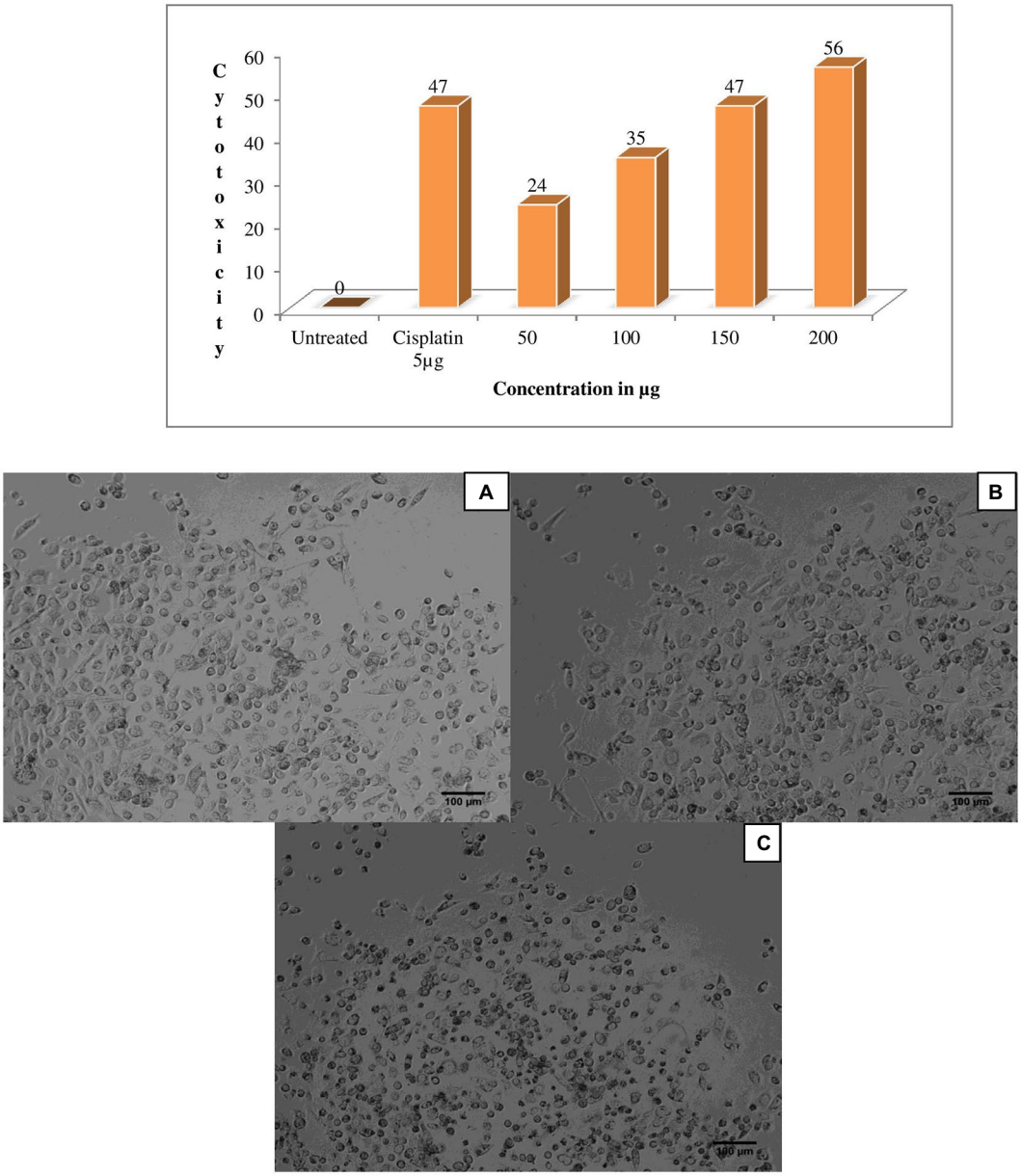

FIGURE 5
Anticancer activity of *Glutamicibacter mysorens* strain protein. MTT assay performed by using prostate cancer PC3 cell line. **(A)** Untreated cells of PC3 cell line, **(B)** Standard cisplatin at 5µg/ml, **(C)** 56% Anticancer activity of *Glutamicibacter mysorens* protein at 200µg/ml.

Another study found that the epithelial-mesenchymal transition (EMT) is a molecular phenomenon associated with increased vimentin expression and raised activity of transcriptional factors (Snail, Twist) that inhibit E-cadherin. EMT has been linked to prostate cancer metastatic potential, therapy resistance, and poor outcomes. Kinetin riboside (KR) is a naturally occurring cytokinin with effective anticancer activity against several human cancer cell lines. mRNA and protein levels of AR, E-, N-cadherins, Vimentin, Snail, Twist, and MMPs were measured using Western Blot and RT-PCR or RQ-PCR techniques to determine the effect of KR on human prostate cell lines.KR inhibited the growth of human prostate cancer cells and, to a lesser extent, normal cells. The cell type and androgen sensitivity determined this effect. KR also decreased the level of p-Akt, which is involved in androgen signaling modulation. When cancer cell lines are exposed to KR, the anti-apoptotic Bcl-2 protein is down-regulated, whereas the Bax protein is up-regulated. KR was involved in E-cadherin re-expression as well as pivotal changes in cell migration. Taken together, the findings suggest that, for the first time, KR can be anticipated as a factor for signaling pathway regulation that involves the inhibition of the development of aggressive forms of prostate cancer, potentially leading to future therapeutic interventions. As a result, research indicates that KR is an effective inhibitor of EMT in human prostate cells (Thakor et al., 2016; Dulińska-Litewka et al., 2020).

Whereas Embinin is a C-Glycosyl flavone and has a wide therapeutic applications in cardiovascular diseases (Ivkin et al.,

TABLE 3 List of GC–MS analysis of bioactive compounds from *Glutamicibacter mysorens* intracellular extract.

Sl. No.	R.T (min)	Compound name	Activity/ Applications	Molecular formula	Molecular weight (g/mol)	Area percentage	References
1	4.5	2-Pentanone, 4-hydroxy-4-methyl-	Photolysis	$C_6H_{12}O_2$	116	0.9	Qiu et al. (2019)
2		Tert-Butyl Hydroperoxide	Oxidant	$C_4H_{10}O_2$	90		Gad (2014)
3		1,3-Dioxolane-2-methanol, 2,4-dimethyl-	Chlorinating agent	$C_6H_{12}O_3$	132		Simon and Losada (2008), Fuentes et al. (2016)
4		2-Propanol, 2-nitroso-, acetate	Cosmetics	$C_5H_9NO_3$	131		Lemieux and Nagabhushan (1968)
5		2-Hexanone, 4-methyl-	Paints	$C_7H_{14}O$	114		Rebbert and Ausloos (1962)
6		2-Acetoxyisobutyryl chloride	Epoxides synthesis	$C_6H_9ClO_3$	164		Zibuck (2001)
7	6.0	Octanoic acid, methyl ester	Oxidation	$C_9H_{18}O_2$	158	8.6	Schwabe et al. (1964)
8		Undecanoic acid, 2-methyl-	Antifungal	$C_{12}H_{24}O_2$	200		Rossi et al. (2021)
9		Methyl 6-methyl heptanoate	Biomolecule synthesis	$C_9H_{18}O_2$	158		Kroumova and Wagner (2003)
10		Decanoic acid, methyl ester	Antibacterial	$C_{11}H_{22}O_2$	186		Damiano et al. (2020)
11	6.8	Dodecanoic acid, 3-hydroxy-	Cytotoxic	$C_{12}H_{24}O_3$	216	5.3	Viegas et al. (1989)
12		Oleic Acid	Anti-tumor	$C_{18}H_{34}O_2$	282		Carrillo Perez et al. (2012)
13		12-Methyl-E,E-2,13-octadecadien-1-ol	Antioxidant	$C_{19}H_{36}O$	280		Salem et al. (2016)
14		Z-8-Methyl-9-tetradecenoic acid	Antibacterial	$C_{15}H_{28}O_2$	240		Jawad et al. (2016)
15		Z-(13,14-Epoxy)tetradec-11-en-1-ol acetate	Anti-inflammatory	$C_{16}H_{28}O_3$	268		Abdul et al. (2020)
16		trans-13-Octadecenoic acid/ cis-Vaccenic acid	Anti-protozoal/ Protects from Heart failure	$C_{18}H_{34}O_2$	282		Carballeira et al. (2009), Djoussé et al. (2014)
17		7-Hexadecenoic acid, methyl ester, (Z)-	Antioxidant	$C_{17}H_{32}O_2$	268		Reza et al. (2021)
18		1-Octanol, 2,7-dimethyl-	Antioxidant, hepatoprotective and anti-inflammatory	$C_{10}H_{22}O$	158		Bentley et al. (2002)
19		Carbonic acid, prop-1-en-2-yl undecyl ester	Beverages production	$C_{15}H_{28}O_3$	256		Millero et al. (2006)
20		1-Decanol, 2-ethyl-	Surfactant	$C_{12}H_{26}O$	186		Achimon et al., 2022
21		1-Decanol, 2-methyl-	Lubricants, Plasticizers	$C_{11}H_{24}O$	172		Halling et al. (1998)
22		Trichloroacetic acid, decyl ester	Disinfectant	$C_{12}H_{21}Cl_3O_2$	302		Anand et al. (2014)
23		1-Heptanol, 2-propyl-	Pheromone	$C_{10}H_{22}O$	158		Francke and Schulz (1999)
24		1-Octanol, 2-butyl-	Antioxidant	$C_{12}H_{26}O$	186		Abdillah et al. (2015)
25		Carbonic acid, decyl prop-1-en-2-yl ester	Beverages production	$C_{14}H_{26}O_3$	242		Millero et al. (2006)
26	7.2	1,7-Octanediol, 3,7-dimethyl-	Polymer	$C_{10}H_{22}O_2$	174	8.6	Reddy and Ananthaprasad (2021)
27		Octanoic acid, 7-oxo–/ Methyl 6-oxoheptanoate	Antibacterial	$C_8H_{14}O_3$	158		Schwabe et al. (1964)
28		1,8-Nonanediol, 8-methyl-	Agrochemicals	$C_{10}H_{22}O2$	174		Kula et al. (2001)
29		7-Octen-2-ol, 2,6-dimethyl-	Cosmetics	$C_{10}H_{20}O$	156		Ham and Raymond Wells (2009)
30		3-Heptanol, 4-methyl-	Therapeutics	$C_8H_{18}O$	130		Ley and Madin (1991)

(Continued)

TABLE 3 (Continued)

Sl. No.	R.T (min)	Compound name	Activity/ Applications	Molecular formula	Molecular weight (g/mol)	Area percentage	References
31		4-Heptanone, 2,3:5,6-diepoxy-2,6-dimethyl-	Oxidant	$C_9H_{14}O_3$	170		Ley and Madin (1991)
32		3-Tridecanol	Lubricant	$C_{13}H_{28}O$	200		Chagnes et al. (2010)
33		2-Dodecanone	Insecticide	$C_{12}H_{24}O$	184		Wang et al. (2019)
34	7.7	3-(Prop-2-enoyloxy)dodecane	Antibiotics	C15H28O2	240	5.3	Fadhil et al. (2018)
35		3-(Prop-2-enoyloxy)tetradecane	Phyto-constituent	$C_{17}H_{32}O_2$	268		Ezekwe et al. (2020)
36		2-Propenoic acid, 1-methylundecyl ester	Antibacterial	C15H28O2	240		Deryabin and Tolmacheva (2015)
37		5-(Prop-2-enoyloxy)pentadecane	Antimicrobial	$C_{18}H_{34}O_2$	282		Xue et al. (2017), Gadhi et al. (2019)
38		3-Cyclopropylcarbonyloxydodecane	Reducing Agent	$C_{16}H_{30}O_2$	254		Bolade et al. (2018)
39		9-Methyl-Z-10-pentadecen-1-ol	Antioxidant	$C_{16}H_{32}O$	240		Soleha et al. (2020)
40		Octadecane, 1-(ethenyloxy)-	Anti-corrosion	$C_{20}H_{40}O$	296		Zeitoun et al. (2021)
41		Dodecyl acrylate	Polyemerization	$C_{15}H_{28}O_2$	240		Buback and Kowollik (1999)
42		Octanoic acid, 2-propenyl ester	Antioxidant	$C_{11}H_{20}O_2$	184		Windey et al. (2012)
43	8.7	Octadecane, 6-methyl-	Enzymatic	$C_{19}H_{40}$	268	4.1	Holman et al. (1966)
44		Hydroxylamine, O-decyl-	Reducing agent	$C_{10}H_{23}NO$	173		(Gad, 2014)
45		Tetradecane, 2,6,10-trimethyl-	Hydrocarbon	$C_{17}H_{36}$	240		McCarthy and Calvin (1967)
46		Silane, trichlorodocosyl-	Surfactant	$C_{22}H_{45}Cl_3Si$	442		Janneck et al. (2018)
47		Nonadecane	Binding material	$C_{19}H_{40}$	268		Li et al. (2010)
48		Oxirane, [(hexadecyloxy)methyl]-	Antibacterial	$C_{19}H_{38}O_2$	298		Es (2014)
49		Decane, 1,1′-oxybis-	Antimicrobial	$C_{20}H_{42}O$	298		Fauzi et al. (2017)
50		1-Hexadecanol, 2-methyl-	Antioxidant	$C_{17}H_{36}O$	256		Hussein et al. (2015)
51		4-Hydroxy-4-methylhex-5-enoic acid, tert.-butyl ester	Hydrocarbon	$C_{11}H_{20}O_3$	200		Ming Miao and Zhi (2018)
52		Z,Z-2,5-Pentadecadien-1-ol	Pharmacological	$C_{15}H_{28}O$	224		Millero et al. (2006)
53		l-Gala-l-ido-octose	Neuritogenic, Anti-hyper cholesteromia	$C_8H_{16}O_8$	240		Jahan et al. (2020)
54		2-Cyclopropylcarbonyloxytridecane	aphrodisiac, anti-inflammatory, antihypertensive	$C_{17}H_{32}O_2$	268		Sridhar et al. (2016)
55		Imidazole, 2-amino-5-[(2-carboxy) vinyl]-	Therapeutic	$C_6H_7N_3O_2$	153		Shalini et al. (2010)
56	9.5	4-Ethylacridine/3H-indole, 2-methyl-3-phenyl-	Antioxidant	$C_{15}H_{13}N$	207	4.2	Hosseini Hashemi et al. (2015)), Britten and Smith (1972)
57							
58		4-Pyridinol 3,5-dichloro-2-ethyl-6-methyl-	Herbicide	$C_8H_9Cl_2NO$	205		Ransom et al. (2012)
59		5-Methyl-2-phenylindolizine/3-Methyl-2-phenylindole/2-Methyl-7-phenylindole	Antimicrobial, Antioxidant	$C_{15}H_{13}N$	207		Onocha et al. (2011)
60		Pyridine, 2,4-dichloro-5-thiocyanato-	Antimicrobial	$C_6H_2Cl_2N_2S$	204		Al-Salahi et al. (2010)

(Continued)

TABLE 3 (Continued)

Sl. No.	R.T (min)	Compound name	Activity/ Applications	Molecular formula	Molecular weight (g/mol)	Area percentage	References
61		Dichloroacetic acid, phenyl ester/ Benzoic acid, 2,5-dichloro-, methyl ester	Therapeutic	$C_8H_6Cl_2O_2$	204		Babar et al. (2008)
62		3,5-Dichloro-2,4-dimethyl-1-methoxybenzene	Anticancer	$C_9H_{10}Cl_2O$	204		Dhakal et al. (2020)
63		1-Chloroundecane	Precursor for fatty acid synthesis	$C_{11}H_{23}Cl$	190		Gensler and Thomas (1952)
64		Dodecane, 1-chloro-	Hydrocarbon	$C_{12}H_{25}Cl$	204		Moldoveanu (2019)
65		Tetradecane, 1-chloro-	Chlorination	$C_{14}H_{29}Cl$	232		Assassi et al. (2005)
66		Nonane, 1-chloro-	Hydrocarbon	$C_9H_{19}Cl$	162		Moldoveanu (2019)
67	10.0	Benzene, 1,4-bis(trifluoromethyl)-	Flurochrome	$C_8H_4F_6$	214		Skhirtladze et al. (2022)
68		Pyrimidine, 4,5-diamino-6-chloro-2-(trifluoromethyl)-	Transcriptional activator	$C_5H_4ClF_3N_4$	212		Palanki et al. (2000)
69		1H-Imidazole, 1-(2,2,3,3,3-pentafluoro-1-oxopropyl)-	Anticancer	$C_6H_3F_5N_2O$	214		Zhang et al. (2014)
70		Sulfaguanidine	Enzyme inhibitor	$C_7H_{10}N_4O_2S$	214		Akocak et al. (2021)
71		Anthracene, 2-chloro-	Antibacterial	$C_{14}H_9Cl$	212		de Bony et al. (1984)
72		Ethyl iodoacetate	Enzyme activator	$C_4H_7IO_2$	214		Tanaka and Hayashi (2008)
73		8-Methyl-4-(1-pyrrolidinyl) pyrido[3,2-c]pyridazine	Cancer therapies	$C_{12}H_{14}N_4$	214		Jubete et al. (2019)
74		[1,1'-Biphenyl]-4-carboxylic acid, 4′-hydroxy-	Precursor for synthesis of bioactive molecules	$C_{13}H_{10}O_3$	214		Patel et al. (2004)
75		Benzoic acid, 2-(1,2,4-triazol-3-yl-aminocarbonyl)-	Breast and prostate cancer therapy	$C_{10}H_8N_4O_3$	232		Jamieson et al. (2012)
76		Succinic acid, 2-methylpent-3-yl pentafluorobenzyl ester	Antioxidant	$C_{17}H_{19}F_5O_4$	382		Cullere et al. (2004)
77		1,1'-Biphenyl, 2-iodo-	Substrate	$C_{12}H_9I$	280		Fang et al. (2017)
78		Benzamide, N-(1,4,6-trimethyl-1H-pyrazolo[3,4-b]pyridin-3-yl)-	Substrate	$C_{16}H_{16}N_4O$	280		Jachak et al. (2006)
79		4-[N′-(4-Methoxy-benzoyl)-hydrazino]-4-oxo-butyric acid methyl ester	Antibacterial	$C_{13}H_{16}N_2O_5$	280		EL-Hashash et al. (2014)
80		Dibenzo[a,c]phenazine	Flurochrome	$C_{20}H_{12}N_2$	280		Xie et al. (2019)
81		Benzofuro[3,2-d]pyrimidine, 4-(2-pyridylthio)-	Therapeutic	$C_{15}H_9N_3OS$	279		Campos et al. (2022)
82		(9E)-Styrylanthracene	Luminophore	$C_{22}H_{16}$	280		Zhang et al. (2017)
83		1H-Purine-2,6-dione,3,7-dihydro-3-methyl-7-carboxymethyl-8-n-butyl	Anti-inflammatory	$C_{12}H_{16}N_4O_4$	280		Abou-Ghadir et al. (2014)
84		Methyl 2-phenyl-2,3-epoxyindan-1-one-3-carboxylate	Catalyst	$C_{17}H_{12}O_4$	280		Godwin et al. (2012)
85		Propyl N-(heptafluorobutyryl) pyroglutamate	Metabolite	$C_{12}H_{12}F_7NO_4$	367		Hušek et al. (2016)

(Continued)

TABLE 3 (Continued)

Sl. No.	R.T (min)	Compound name	Activity/ Applications	Molecular formula	Molecular weight (g/mol)	Area percentage	References
86	10.4	3-Trifluoroacetoxypentadecane	Antimicrobial	$C_{17}H_{31}F_3O_2$	324	1.3	Hussein et al. (2015)
87		3-Cyclopropylcarbonyloxytetradecane	Antioxidant, Cytotoxic and Antibacterial	$C_{18}H_{34}O_2$	282		Upgade and Bhaskar (2013)
88		10-Undecenoic acid, octyl ester	Antimicrobial	$C_{19}H_{36}O_2$	296		Van der Steen and Stevens (2009)
89		3-(Prop-2-enoyloxy)tetradecane	Antioxidant	C17H32O2	268		Ezekwe et al. (2020)
90		Z-10-Tetradecen-1-ol acetate	Pharmaceutical	$C_{16}H_{30}O_2$	254		Bolade et al. (2018)
91		5-Amino-2-methoxy-4-(1H-1,2,3,4-tetrazol-5-yl)phenol	Antimicrobial	$C_8H_9N_5O_2$	207		Arulmurugan and Kavitha (2010)
92		4H-Pyrido[1,2-a]pyrimidine-3-carboxamide, 6,7,8,9-tetrahydro-6-methyl-4-oxo-	Antimicrobial and antitumor	$C_{10}H_{13}N_3O_2$	207		Al-Taisan et al. (2010)
93		1-Adamantanecarboxamide, N,N-dimethyl—/ Pent-3-yn-2-ol, 2-cyclopropyl-5-(1-piperidyl)	Anticancer	$C_{13}H_{21}NO$	207		Su et al. (2012)
94		trans-4-Ethoxy-β-methyl-β-nitrostyrene/ Carbamic acid, 4-methoxyphenyl-, allyl ester	Cardiovascular therapy	$C_{11}H_{13}NO_3$	207		Alves-Santos et al. (2019)
95		Thiophen-2-methylamine, N-(2-fluorophenyl)-	Catalytic activity	$C_{11}H_{10}FNS$	207		Tanak et al. (2020)
96		2-(1-Piperidino)-3-nitropyridine	Antimicrobial	$C_{10}H_{13}N_3O_2$	207		Sivaprakash et al. (2019)
97		Benzoic acid, 4-amino-, pentyl ester	Cytotoxicity	$C_{12}H_{17}NO_2$	207		Kratky et al. (2019)
98	10.5	Cyclopentaneundecanoic acid, methyl ester	Antioxidant and Antibacterial	$C_{17}H_{32}O_2$	268	1.3	Daniels and Temikotan (2021)
99		Undecanoic acid, 10-methyl-, methyl ester	Antioxidant	$C_{13}H_{26}O_2$	214		Narra et al. (2017)
100		Methyl 8-methyl-nonanoate	Antimicrobial and Anti-inflammatory	$C_{11}H_{22}O_2$	186		Kaur et al. (2022)
101		Tetradecanoic acid, 12-methyl-, methyl ester	Larvicidial	$C_{16}H_{32}O_2$	256		Xu et al. (2008)
102		Cyclopentanetridecanoic acid, methyl ester	Cytotoxic	$C_{19}H_{36}O_2$	296		Joshi et al. (2020)
103	10.7	Glutaric acid, 2,2-dichloroethyl 3-fluorophenyl ester	Anti-angiogenic	$C_{13}H_{13}Cl_2FO_4$	322	1.0	Amaral et al. (2021)
104		Triethylgermanium bromide	Oxidant	$C_6H_{15}BrGe$	240		Satgé et al. (1973)
105		2,5-Cyclohexadien-1-one, 2,6-dichloro-4-(chloroimino)—/ benzene, 1,3,5-trichloro-2-nitroso-	Surfactant	$C_6H_2Cl_3NO$	209		Yamamoto (2002)
106		Pyridine, 3,4,5-trichloro-2,6-dimethyl-	Antimicrobial	$C_7H_6Cl_3N$	209		Khidre et al. (2011)
107		Ethaneselenoamide, N-(4-methylphenyl)-	Anticancer	$C_9H_{11}NSe$	213		Watanabe et al. (1997)
108		Stannane, chlorotriethyl-	Polymerization	$C_6H_{15}ClSn$	242		Qiu et al. (2013)
109		1-(2,4,5-Trichlorophenyl)ethanol	Cytotoxic	$C_8H_7Cl_3O$	224		Shawky et al. (2021)
110		1,3-Dioxolane, 2-(5,5,5-trichloro-3-penten-1-yl)-, (E)-	Flavoring agent	$C_8H_{11}Cl_3O_2$	244		Ivankin (2017)
111		benzene, 1,1′-[oxybis(methyleneoxy)] bis[2,4,6-trichloro-	Toxic agent	$C_{14}H_8Cl_6O_3$	434		Holman et al. (1966)

(Continued)

TABLE 3 (Continued)

Sl. No.	R.T (min)	Compound name	Activity/ Applications	Molecular formula	Molecular weight (g/mol)	Area percentage	References
112	11.5	Undecanoic acid	Antifungal	$C_{11}H_{22}O_2$	186	0.9	Rossi et al. (2021)
113		n-Decanoic acid	Beverage production	$C_{10}H_{20}O_2$	172		Viegas et al. (1989)
114		n-Hexadecanoic acid	Anti-inflammatory	$C_{16}H_{32}O_2$	256		Aparna et al. (2012)
115		4-(Benzoylmethyl)-6-methyl-2H-1,4-benzoxazin-3-one	Antimicrobial	$C_{17}H_{15}NO_3$	281		Ozden et al. (2000)
116		Adenine, N4-pentafluoropropionyl-	Oxidization	$C_8H_4F_5N_5O$	281		Tsunoda et al. (2011)
117		2-Furancarboxylic acid, N′-[(8-hydroxy-5-quinolinyl)methylidene] hydrazide	Antioxidant	$C_{15}H_{11}N_3O_3$	281		Gülerman et al. (2000)
118		1-Phenyl-4-(trifluoromethyl)-1H,4H,5H,6H,7H-pyrazolo[3,4-b] pyridin-6-one	Antiproliferative	$C_{13}H_{10}F_3N_3O$	281		Martín-Acosta et al. (2021)
119		Acetamide, 2-(2,4-difluorophenoxy)-N-(4-fluorophenyl)-	Inhibitor	$C_{14}H_{10}F_3NO_2$	281		Williams et al. (2015)
120		Succinic acid, 3,5-dinitrobenzyl 2-methylhex-3-yl ester	Enzyme activator	$C_{18}H_{24}N_2O_8$	396		Martinez et al. (2008)
121		Oxalic acid, monoamide, N-(2-fluorophenyl)-, heptyl ester	Antioxidant	$C_{15}H_{20}FNO_3$	281		Ganyam et al. (2019)
122		Propanamide, 2,2,3,3,3-pentafluoro-N-(2,4,6-trimethylphenyl)-	Inhibitor	$C_{12}H_{12}F_5NO$	281		Talley et al. (2000)
123	12.3	3-Trifluoroacetoxydodecane	Antioxidant	$C_{14}H_{25}F_3O_2$	282		Zagulyaeva et al. (2010)
124	12.5	Cyclopropanepentanoic acid, 2-undecyl-, methyl ester, trans-	Anti-mycobacterial	$C_{20}H_{38}O_2$	310	1.5	Carballeira et al. (2007)
125		13,16-Octadecadiynoic acid, methyl ester	Antioxidant	$C_{19}H_{30}O_2$	290		Hamalainen et al. (2001)
126		13-Tetradecynoic acid, methyl ester	Anti-inflammatory	$C_{15}H_{26}O_2$	238		James and Martin (1956)
127		Oxiraneundecanoic acid, 3-pentyl-, methyl ester, cis-	Antimicrobial	$C_{19}H_{36}O_3$	312		Al-Marzoqi et al. (2016)
128		9-Octadecenoic acid (Z)-, methyl ester/11-Octadecenoic acid, methyl ester	Food and Pharmacological	$C_{19}H_{36}O_2$	296		Jiang and Jia (2015)
129		13-Docosenoic acid, methyl ester	Food industires	$C_{23}H_{44}O_2$	352		Beare-Rogers (1977)
130	13.2	Z-(13,14-Epoxy)tetradec-11-en-1-ol acetate	Anti-inflammatory	$C_{16}H_{28}O_3$	268	2.0	Abdul et al. (2020)
131		12-Methyl-E,E-2,13-octadecadien-1-ol/2-Methyl-Z,Z-3,13-octadecadienol	Therapeutic	$C_{19}H_{36}O$	280		Adeyemi (2017)
132		Z-8-Methyl-9-tetradecenoic acid	Antimicrobial	$C_{15}H_{28}O_2$	240		Jawad et al. (2016)
133		Oxiraneoctanoic acid, 3-octyl-, cis-	Antimicrobial	$C_{18}H_{34}O_3$	298		Hussein et al., 2016
134		Pentadecanoic acid	Oxidation	$C_{15}H_{30}O_2$	242		Jenkins et al. (2015)
135		Heptadecanoic acid, heptadecyl ester	Antimicrobial	$C_{34}H_{68}O_2$	508		Gautam et al. (2016)
136		2-Myristynoyl pantetheine	Antimicrobial	$C_{25}H_{44}N_2O_5S$	484		Srivastava et al. (2015)
137		9-Octadecenoic acid, (E)-	Inhibitor	$C_{18}H_{34}O_2$	282		Carrillo Perez et al. (2012)
138		9-Hexadecenoic acid/1,2-15,16-Diepoxyhexadecane	Cosmetics	$C_{16}H_{30}O_2$	254		Takigawa et al. (2005)
139		cis-13-Eicosenoic acid	Anti-obesity	$C_{20}H_{38}O_2$	310		Senarath et al. (2018)
140		3-Heptafluorobutyroxytetradecane	Polymerization	$C_{18}H_{29}F_7O_2$	410		MacKenzie and Tenaschuk (1979)
141		n-Nonadecanol-1	Antifeedant	$C_{19}H_{40}O$	284		Aznar-Fernandez et al. (2019)

(Continued)

10.3389/fmicb.2023.1096826

TABLE 3 (Continued)

Sl. No.	R.T (min)	Compound name	Activity/ Applications	Molecular formula	Molecular weight (g/mol)	Area percentage	References
142	14.7	Hexanedioic acid, mono(2-ethylhexyl) ester	Antibacterial	$C_{14}H_{26}O_4$	258	0.4	Choi and Jiang (2014)
143		Hexanedioic acid, dioctyl ester	Inhibitor	$C_{22}H_{42}O_4$	370		Chaler et al. (2004)
144		Cyclohexanecarboxylic acid, octyl ester		$C_{15}H_{28}O_2$	240		Andersson et al. (1965)
145		1-Dodecanol, 3,7,11-trimethyl-	Cytotoxic	$C_{15}H_{32}O$	228		Fahem et al. (2020)
146		Cyclohexanecarboxylic acid, decyl ester/2-Propenoic acid, tetradecyl ester	Antioxidant	$C_{17}H_{32}O_2$	268		Matthew et al. (2022)
147		Hexanedioic acid, bis(2-ethylhexyl) ester	Biomarker	$C_{22}H_{42}O_4$	370		Silva et al. (2013)
148	15.3	10-Octadecenal/4-Octadecenal	Adjuvant/ pheromones	$C_{18}H_{34}O$	266	0.4	Gil et al. (1995)
149		Cyclopropanetetradecanoic acid, 2-octyl-, methyl ester	Pharmacological	$C_{26}H_{50}O_2$	394		Srivastava et al. (2015)
150		9-Methyl-Z-10-pentadecen-1-ol	Antioxidant	$C_{16}H_{32}O$	240		Soleha et al. (2020)
151		Hexadecane, 1,1-bis(dodecyloxy)-		$C_{40}H_{82}O_2$	594		Ser et al. (2015)
152		3-Chloropropionic acid, heptadecyl ester	Antibiotic	$C_{20}H_{39}ClO_2$	346		Ikhsanov et al. (2018)
153		2-Tridecenoic acid, (E)-	Antimicrobial	$C_{13}H_{24}O_2$	212		Chowdhury et al. (2021)
154		trans-2-undecenoic acid	Larvicidal	$C_{11}H_{20}O_2$	184		Saxena and Stotzky (2001)
155		Ethanol, 2-(octadecyloxy)-	Antimicrobial	$C_{20}H_{42}O_2$	314		Jaffar et al. (2015)

*R.T (min): Retention Time.

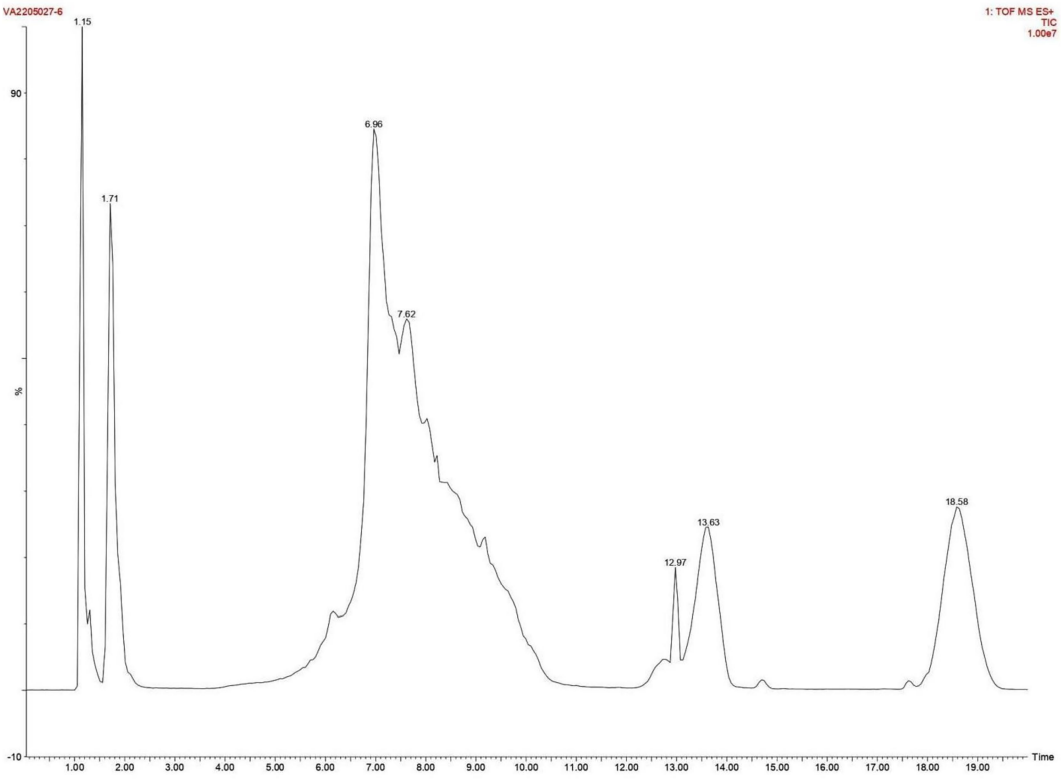

FIGURE 6
Elution profile of intracellular protein extract from *Glutamicibacter mysorens* by LCMS.

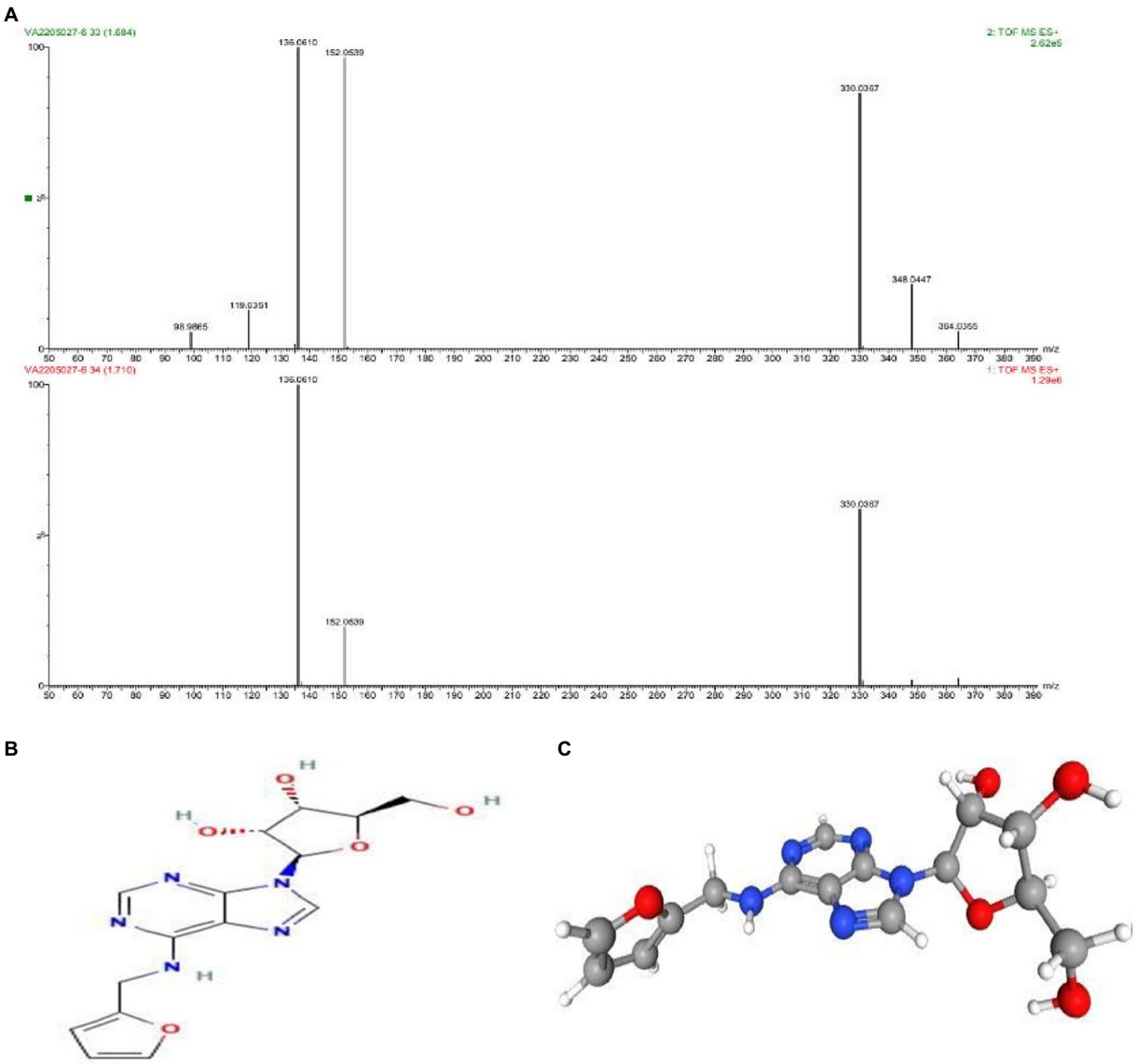

FIGURE 7
(A) Mass confirmation and analysis record. **(B)** 2D structure of kinetin-9-ribose, **(C)** 3D structure of kinetin-9-ribose molecule.

2018). Another study reports the production of Embinin frompetals of *Iris germanica* Linnaeus and *Iris lactea* Leaves (Kawase and Yagishita, 1968; Chen et al., 2018). Our study elucidates the cytotoxicity activity of *G. mysorens* bioactive peptide as characterized by LCMS/MS revealed the presence of Kinetin-9-Riboside and Embininin the peptide fraction showing its antiproliferative effect on the prostate cancer cell line. Thus microbial-originated intracellular peptides have potential antimicrobial (AMPs) and anticancer (ACPs) have been significantly substantiated in our studies.

Conclusion

The present study is illustrative for exploring untapped mangrove habitat in the Mangalore region of Karnataka. In our study, we could demonstrate that mangrove *G. mysorens* is an efficient microbe to produce bioactive compounds and enzymes responsible for both antimicrobial and anticancer activity. The antimicrobial potentiality was detailed in our previous article. In this present study; anticancer activity on prostate cancer cell lines and to treat various other related ailments. Peptides from reliable sources such as *Actinomyces* could be demonstrated as having dual roles as AMPs as well as ACPs. Hence, this study supports and proves that the genus *Glutamicibacter* is an effective microbial group for the isolation of peptides to treat multidrug-resistant pathogens.

Data availability statement

The datasets presented in this study can be found in online repositories. The names of the repository/repositories and accession number(s) can be found at: NCBI - MW647910.

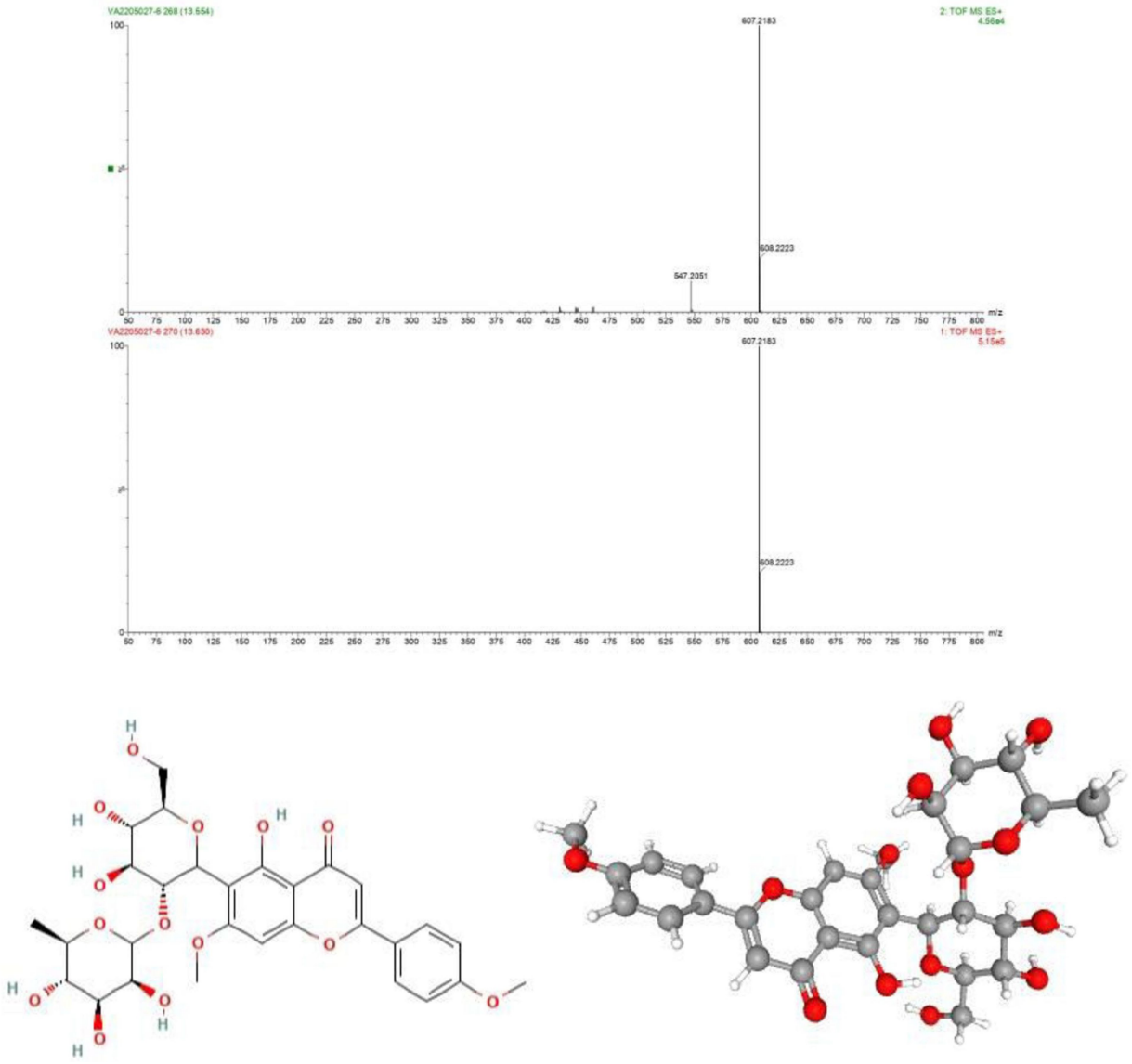

FIGURE 8
(A) Mass confirmation of Embinin, **(B)** 2D structure of Embinin, **(C)** 3D structure of Embinin.

Author contributions

YK conducted the research and wrote the manuscript. MI, SK, RD, and CA performed the data analyses and reviewed the manuscript. SK, YK, KR, MAh, MAl, MH, AA, SS, and MM edited and reviewed the manuscript. MI provided experimental support, planned, supervised, and organized the experiment, and wrote and reviewed the manuscript. All authors contributed to the article and approved the submitted version.

Funding

This work is supported by Science & Engineering Research Board, DST, Govt. of India and Vision Group of Science and Technology Govt. of Karnataka by providing financial and equipment grants.

Conflict of interest

The authors declare that the research was conducted in the absence of any commercial or financial relationships that could be construed as a potential conflict of interest.

Publisher's note

All claims expressed in this article are solely those of the authors and do not necessarily represent those of their affiliated organizations, or those of the publisher, the editors and the reviewers. Any product that may be evaluated in this article, or claim that may be made by its manufacturer, is not guaranteed or endorsed by the publisher.

References

Abd-Elnaby, H., Abo-Elala, G., Abdel-Raouf, U., Abd-elwahab, A., and Hamed, M. (2016). Antibacterial and anticancer activity of marine Streptomyces parvus: optimization and application. *Biotechnol. Biotechnol. Equip.* 30, 180–191. doi: 10.1080/13102818.2015.1086280

Abdillah, S., Tambunan, R. M., Farida, Y., Sandhiutami, N. M. D., and Dewi, R. M. (2015). Phytochemical screening and antimalarial activity of some plants traditionally used in Indonesia. *Asian Pac. J. Trop. Dis.* 5, 454–457. doi: 10.1016/S2222-1808(15)60814-3

Abdul, K., Shaheed, A., Imtair, N., Awi, A. N., Kariem, A., Abbas, Z., et al. (2020). Analysis of bioactive phytochemical compound of (*Cyperus iria* L.) by using gas chromatography -mass spectrometry.

Abou-Ghadir, O., Alaa, M. H., Abdel-Moty, S., and Hussein, M. (2014). Design and synthesis of some new purine-dione derivatives of potential anti-inflammatory activity. *Der Pharma Chem.* 6, 199–211.

Achimon, F., Brito, V. D., Pizzolitto, R. P., and Zygadlo, J. A. (2022). Effect of carbon sources on the production of volatile organic compounds by Fusarium verticillioides. *J. Fungi* 8:158. doi: 10.3390/jof8020158

Adeyemi, M. (2017). Phytochemical analysis and GC-MS determination of Lagenaria breviflora R. Fruit. *Int. J. Pharmacogn. Phytochem. Res.* 9, 1045–1050. doi: 10.25258/phyto.v9i07.11178

Agamennone, V., Roelofs, D., van Straalen, N., and Janssens, T. K. S. (2018). Antimicrobial activity in culturable gut microbial communities of springtails. *J. Appl. Microbiol.* 125, 740–752. doi: 10.1111/jam.13899

Akocak, S., Taslimi, P., Lolak, N., Işık, M., Durgun, M., Budak, Y., et al. (2021). Synthesis, characterization, and inhibition study of novel substituted Phenylureido Sulfaguanidine derivatives as α-glycosidase and cholinesterase inhibitors. *Chem. Biodivers.* 18:e2000958. doi: 10.1002/cbdv.202000958

Al-Marzoqi, A., Hadi, M., and Hameed, I. (2016). Determination of metabolites products by Cassia angustifolia and evaluate antimicobial activity. *J. Pharmacogn. Phytother.* 8, 25–48. doi: 10.5897/JPP2015.0367

Alongi, D. M. (2015). The impact of climate change on mangrove forests. *Curr. Clim. Change Rep.* 1, 30–39. doi: 10.1007/s40641-015-0002-x

Al-Salahi, R. A., Al-Omar, M. A., and Amr, A. E.-G. E. (2010). Synthesis of chiral macrocyclic or linear pyridine carboxamides from pyridine-2,6-dicarbonyl dichloride as antimicrobial agents. *Molecules* 15, 6588–6597. doi: 10.3390/molecules15096588

Al-Taisan, K. M., Al-Hazimi, H. M. A., and Al-Shihry, S. S. (2010). Synthesis, characterization and biological studies of some novel thieno[2,3-d]pyrimidines. *Molecules* 15, 3932–3957. doi: 10.3390/molecules15063932

Alves-Santos, T. R., Silva, O. A., Moreira, H. S., Borges, R. S., Duarte, G. P., Magalhães, P. J. C., et al. (2019). Cardiovascular effects of trans-4-Methoxy-β-nitrostyrene in spontaneously hypertensive rats: comparison with its parent drug β-nitrostyrene. *Front. Pharmacol.* 10:1407. doi: 10.3389/fphar.2019.01407

Amaral, A. U., Ferreira, G. C., Seminotti, B., Leipnitz, G., and Wajner, M. (2021). "Glutaric acid neurotoxicity: mechanisms and actions" in *Handbook of neurotoxicity*. ed. R. M. Kostrzewa (Cham: Springer International Publishing), 1–35.

Anand, S. S., Philip, B. K., and Mehendale, H. M. (2014). "Chlorination byproducts" in *Encyclopedia of toxicology*. ed. P. Wexler. *Third* ed (Oxford: Academic Press), 855–859.

Andersson, L., Nilsson, I. M., Niléhn, J.-E., Hedner, U., Granstrand, B., and Melander, B. (1965). Experimental and clinical studies on AMCA, the antifibrinolytically active isomer of p-Aminomethyl cyclohexane carboxylic acid. *Scand. J. Haematol.* 2, 230–247. doi: 10.1111/j.1600-0609.1965.tb01300.x

Aparna, V., Dileep, K. V., Mandal, P. K., Karthe, P., Sadasivan, C., and Haridas, M. (2012). Anti-inflammatory property of n-hexadecanoic acid: structural evidence and kinetic assessment. *Chem. Biol. Drug Des.* 80, 434–439. doi: 10.1111/j.1747-0285.2012.01418.x

Arulmurugan, S., and Kavitha, H. (2010). 2-Methyl-3-{4-[2-(1H-tetrazol-5-yl) ethylamino]phenyl}-3H-quinazolin-4-one. *Mol. Ther.* 2010, 1–5. doi: 10.3390/M695

Asif, T., Javed, U., Zafar, S. B., Ansari, A., Ul Qader, S. A., and Aman, A. (2020). Bioconversion of colloidal chitin using novel Chitinase from *Glutamicibacter uratoxydans* exhibiting anti-fungal potential by hydrolyzing chitin within fungal Cell Wall. *Waste Biomass Valor* 11, 4129–4143. doi: 10.1007/s12649-019-00746-2

Assassi, N., Tazerouti, A., and Canselier, J. (2005). Analysis of chlorinated, sulfochlorinated and sulfonamide derivatives of n-tetradecane by gas chromatography/mass spectrometry. *J. Chromatogr. A* 1071, 71–80. doi: 10.1016/j.chroma.2005.01.102

Aznar-Fernandez, T., Cimmino, A., Masi, M., Rubiales, D., and Evidente, A. (2019). Antifeedant activity of long-chain alcohols, and fungal and plant metabolites against pea aphid (*Acyrthosiphon pisum*) as potential biocontrol strategy. *Nat. Prod. Res.* 33, 2471–2479. doi: 10.1080/14786419.2018.1452013

Babar, T., Qadeer, G., Rama, N., Ruzicka, A., and Padelkova, Z. (2008). Methyl 2,5-dichlorobenzoate. *Acta Crystallogr. Sect. E: Struct. Rep. Online* 64:o1970. doi: 10.1107/S1600536808029541

Baig, U., Dahanukar, N., Shintre, N., Holkar, K., Pund, A., Lele, U., et al. (2021). Phylogenetic diversity and activity screening of cultivable actinobacteria isolated from marine sponges and associated environments from the western coast of India. *Access Microbiol.* 3:000242. doi: 10.1099/acmi.0.000242

Beare-Rogers, J. L. (1977). Docosenoic acids in dietary fats. *Prog. Chem. Fats Other Lipids* 15, 29–56. doi: 10.1016/0079-6832(77)90006-4

Bentley, S. D., Chater, K. F., Cerdeño-Tárraga, A.-M., Challis, G. L., Thomson, N. R., James, K. D., et al. (2002). Complete genome sequence of the model actinomycete Streptomyces coelicolor A3(2). *Nature* 417, 141–147. doi: 10.1038/417141a

Bhaduri, S., and Demchick, P. H. (1983). Simple and rapid method for disruption of bacteria for protein studies. *Appl. Environ. Microbiol.* 46, 941–943. doi: 10.1128/aem.46.4.941-943.1983

Bharadwaj, R. P., Raju, N. G., and Chandrashekharaiah, K. S. (2018). Purification and characterization of alpha-amylase inhibitor from the seeds of underutilized legume, *Mucuna pruriens*. *J. Food Biochem.* 42:e12686. doi: 10.1111/jfbc.12686

Bolade, O. P., Akinsiku, A. A., Adeyemi, A. O., Williams, A. B., and Benson, N. U. (2018). Dataset on phytochemical screening, FTIR and GC–MS characterisation of *Azadirachta indica* and *Cymbopogon citratus* as reducing and stabilising agents for nanoparticles synthesis. *Data Brief* 20, 917–926. doi: 10.1016/j.dib.2018.08.133

Borker, S. S., Thakur, A., Kumar, S., Kumari, S., Kumar, R., and Kumar, S. (2021). Comparative genomics and physiological investigation supported safety, cold adaptation, efficient hydrolytic and plant growth-promoting potential of psychrotrophic *Glutamicibacter arilaitensis* LJH19, isolated from night-soil compost. *BMC Genomics* 22:307. doi: 10.1186/s12864-021-07632-z

Brandenburg, L.-O., Merres, J., Albrecht, L.-J., Varoga, D., and Pufe, T. (2012). Antimicrobial peptides: multifunctional drugs for different applications. *Polymers* 4, 539–560. doi: 10.3390/polym4010539

Britten, A. Z., and Smith, G. F. (1972). Autoxidation of 3,3′-dimethyl-2,2′-bi-indolyl. *J. Chem. Soc. Perkin Trans.* 1, 418–420. doi: 10.1039/P19720000418

Buback, M., and Kowollik, C. (1999). Termination kinetics in free-radical bulk copolymerization: the systems dodecyl acrylate−dodecyl methacrylate and dodecyl acrylate−methyl acrylate. *Macromolecules* 32, 1445–1452. doi: 10.1021/ma9814806

Campos, J. F., Besson, T., and Berteina-Raboin, S. (2022). Review on the synthesis and therapeutic potential of pyrido[2,3-d], [3,2-d], [3,4-d] and [4,3-d]pyrimidine derivatives. *Pharmaceuticals* 15:352. doi: 10.3390/ph15030352

Carballeira, N. M., Montano, N., Balaña-Fouce, R., and Prada, C. F. (2009). First total synthesis and antiprotozoal activity of (Z)-17-methyl-13-octadecenoic acid, a new marine fatty acid from the sponge *Polymastia penicillus*. *Chem. Phys. Lipids* 161, 38–43. doi: 10.1016/j.chemphyslip.2009.06.140

Carballeira, N. M., Montano, N., Vicente, J., and Rodriguez, A. D. (2007). Novel cyclopropane fatty acids from the phospholipids of the Caribbean sponge *Pseudospongosorites suberitoides*. *Lipids* 42, 519–524. doi: 10.1007/s11745-007-3047-3

Carrillo Perez, C., Del, C. C. M., and Alonso De La Torre, S. (2012). Antitumor effect of oleic acid; mechanisms of action. A review. *Nutr. Hosp.* 27, 1860–1865. doi: 10.3305/nh.2012.27.6.6010

Chagnes, A., Rager, M.-N., Courtaud, B., Thiry, J., and Cote, G. (2010). Speciation of vanadium (V) extracted from acidic sulfate media by trioctylamine in n-dodecane modified with 1-tridecanol. *Hydrometallurgy* 104, 20–24. doi: 10.1016/j.hydromet.2010.04.004

Chaler, R., Canton, L., Vaquero, M., and Grimalt, J. O. (2004). Identification and quantification of n-octyl esters of alkanoic and hexanedioic acids and phthalates as urban wastewater markers in biota and sediments from estuarine areas. *J. Chromatogr. A* 1046, 203–210.

Chater, K. F. (2006). Streptomyces inside-out: a new perspective on the bacteria that provide us with antibiotics. *Philos. Trans. R. Soc. Lond., B, Biol. Sci.* 361, 761–768. doi: 10.1098/rstb.2005.1758

Chater, K. F. (2013). "Streptomyces," in *Brenner's encyclopedia of genetics*. eds. S. Maloy and K. Hughes (Cambridge, Massachusetts, United States: Elsevier), 565–567.

Chen, D., Meng, Y., Zhu, Y., Wu, G., Yuan, J., Qin, M., et al. (2018). Qualitative and quantitative analysis of C-glycosyl-flavones of Iris lactea leaves by liquid chromatography/tandem mass spectrometry. *Molecules* 23:3359. doi: 10.3390/molecules23123359

Cho, J. H., Sung, B. H., and Kim, S. C. (2009). Buforins: histone H2A-derived antimicrobial peptides from toad stomach. *Biochim. Biophys. Acta Biomembr.* 1788, 1564–1569. doi: 10.1016/j.bbamem.2008.10.025

Choi, W. H., and Jiang, M. (2014). Evaluation of antibacterial activity of hexanedioic acid isolated from *Hermetia illucens* larvae. *J. Appl. Biomed.* 12, 179–189. doi: 10.1016/j.jab.2014.01.003

Chowdhury, S. K., Dutta, T., Chattopadhyay, A. P., Ghosh, N. N., Chowdhury, S., and Mandal, V. (2021). Isolation of antimicrobial tridecanoic acid from *Bacillus* sp. LBF-01 and its potentialization through silver nanoparticles synthesis: a combined experimental and theoretical studies. *J. Nanostruct. Chem.* 11, 573–587. doi: 10.1007/s40097-020-00385-3

Clark Mason, J., Richards, M., Zimmermann, W., and Broda, P. (1988). Identification of extracellular proteins from actinomycetes responsible for the solubilisation of lignocellulose. *Appl. Microbiol. Biotechnol.* 28, 276–280. doi: 10.1007/BF00250455

Cleary, J. L., Kolachina, S., Wolfe, B. E., and Sanchez, L. M. (2018). Coproporphyrin III produced by the bacterium *Glutamicibacter arilaitensis* binds zinc and is upregulated by fungi in cheese rinds. *mSystems* 3, e00036–e00018. doi: 10.1128/mSystems.00036-18

Collin, F., and Maxwell, A. (2019). The microbial toxin microcin B17: prospects for the development of new antibacterial agents. *J. Mol. Biol.* 431, 3400–3426. doi: 10.1016/j.jmb.2019.05.050

Cruciani, R. A., Barker, J. L., Zasloff, M., Chen, H. C., and Colamonici, O. (1991). Antibiotic magainins exert cytolytic activity against transformed cell lines through channel formation. *Proc. Natl. Acad. Sci. U. S. A.* 88, 3792–3796. doi: 10.1073/pnas.88.9.3792

Cullere, L., Cacho, J., and Ferreira, V. (2004). Analysis for wine C5–C8 aldehydes through the determination of their O-(2,3,4,5,6-pentafluorobenzyl)oximes formed directly in the solid phase extraction cartridge. *Anal. Chim. Acta* 524, 201–206. doi: 10.1016/j.aca.2004.03.025

Damiano, F., De Benedetto, G. E., Longo, S., Giannotti, L., Fico, D., Siculella, L., et al. (2020). Decanoic acid and not octanoic acid stimulates fatty acid synthesis in U87MG glioblastoma cells: a metabolomics study. *Front. Neurosci.* 14:783. doi: 10.3389/fnins.2020.00783

Daniels, A., and Temikotan, T. (2021). Fatty acid profile, antioxidant and antibacterial effect of the ethyl acatate extract of cleistopholis patens. *Bull. Sci. Res.* 3, 21–31. doi: 10.34256/bsr2113

Das, L., Deb, S., and Das, S. (2020). *Glutamicibacter mishrai* sp. nov., isolated from the coral *Favia veroni* from Andaman Sea. *Arch. Microbiol.* 202, 1–13. doi: 10.1007/s00203-019-01783-0

de Bony, J., Martin, G., Welby, M., and Tocanne, J. F. (1984). Evidence for a homogeneous lateral distribution of lipids in a bacterial membrane: a photo cross-linking approach using anthracene as a photoactivable group. *FEBS Lett.* 174, 1–6. doi: 10.1016/0014-5793(84)81065-0

Deb, S., Das, L., and Das, S. K. (2020). Phylogenomic analysis reveals that *Arthrobacter mysorens* Nand and Rao 1972 (approved lists 1980) and *Glutamicibacter mysorens* Busse 2016 are later heterotypic synonyms of *Arthrobacter nicotianae* Giovannozzi-Sermanni 1959 (approved lists 1980) and Glutamicibacter nicotianae Busse 2016. *Curr. Microbiol.* 77, 3793–3798. doi: 10.1007/s00284-020-02176-z

Deryabin, D. G., and Tolmacheva, A. A. (2015). Antibacterial and anti-quorum sensing molecular composition derived from Quercus cortex (oak bark) extract. *Molecules* 20, 17093–17108. doi: 10.3390/molecules200917093

Desouky, S. E., Shojima, A., Singh, R. P., Matsufuji, T., Igarashi, Y., Suzuki, T., et al. (2015). Cyclodepsipeptides produced by actinomycetes inhibit cyclic-peptide-mediated quorum sensing in Gram-positive bacteria. *FEMS Microbiol. Lett.* 362:fnv109. doi: 10.1093/femsle/fnv109

Desriac, F., Jegou, C., Balnois, E., Brillet, B., Chevalier, P. L., and Fleury, Y. (2013). Antimicrobial peptides from marine proteobacteria. *Mar. Drugs* 11, 3632–3660. doi: 10.3390/md11103632

Dhakal, R., Li, X., Parkin, S. R., and Lehmler, H.-J. (2020). Synthesis of mono- and dimethoxylated polychlorinated biphenyl derivatives starting from fluoroarene derivatives. *Environ. Sci. Pollut. Res. Int.* 27, 8905–8925. doi: 10.1007/s11356-019-07133-3

Djoussé, L., Matsumoto, C., Hanson, N. Q., Weir, N. L., Tsai, M. Y., and Gaziano, J. M. (2014). Plasma cis-vaccenic acid and risk of heart failure with antecedent coronary heart disease in male physicians. *Clin. Nutr.* 33, 478–482. doi: 10.1016/j.clnu.2013.07.001

Dulińska-Litewka, J., Gąsiorkiewicz, B., Litewka, A., Gil, D., Gołąbek, T., and Okoń, K. (2020). Could the kinetin riboside be used to inhibit human prostate cell epithelial–mesenchymal transition? *Med. Oncol.* 37:17. doi: 10.1007/s12032-020-1338-1

EL-Hashash, M. A., Essawy, A., and Sobhy Fawzy, A. (2014). Synthesis and antimicrobial activity of some novel heterocyclic candidates via Michael addition involving 4-(4-Acetamidophenyl)-4-oxobut-2-enoic acid. *Adv. Chem.* 2014:e619749, 1–10. doi: 10.1155/2014/619749

Es, B. (2014). Antibacterial potential of Luprops tristis - the nuisance rubber plantation Pest from Western Ghats of India. *IJAIR* 3

Ezekwe, S., Rizwan, A., Rabiu, K., and Ogbonnaya, E. (2020). Qualitative phytochemical and GC-MS analysis of some commonly consumed vegetables. *GSC Biol. Pharm. Sci.* 12, 208–214. doi: 10.30574/gscbps.2020.12.3.0299

Fadhil, L., Kadhim, S., and Hameed, I. (2018). Detection of bioactive secondary metabolites produced by *Bacillus subtilis* using gas chromatography-mass spectrometry technique. *Indian J. Public Health Res. Dev.* 9:1097. doi: 10.5958/0976-5506.2018.00877.X

Fahem, N., Djellouli, A. S., and Bahri, S. (2020). Cytotoxic activity assessment and GC-MS screening of two codium species extracts. *Pharm. Chem. J.* 54, 755–760. doi: 10.1007/s11094-020-02266-z

Fang, B.-Z., Salam, N., Han, M.-X., Jiao, J.-Y., Cheng, J., Wei, D.-Q., et al. (2017). Insights on the effects of heat pretreatment, pH, and calcium salts on isolation of rare actinobacteria from Karstic caves. *Front. Microbiol.* 8:1535. doi: 10.3389/fmicb.2017.01535

Fauzi, A., Jawad, M., and Hameed, I. (2017). Phytochemical profiles of methanolic seeds extract of Cuminum cyminum using GC-MS technique. *Int. J. Curr. Pharm. Rev. Res.* 8, 1–9. doi: 10.25258/ijcprr.v8i02.9194

Fernebro, J. (2011). Fighting bacterial infections-future treatment options. *Drug Resist. Updat.* 14, 125–139. doi: 10.1016/j.drup.2011.02.001

Francke, W., and Schulz, S. (1999). "8.04 - pheromones" in *Comprehensive natural products chemistry*. eds. S. D. Barton, K. Nakanishi and O. Meth-Cohn (Oxford: Pergamon), 197–261.

Fu, B., Olawole, O., and Beattie, G. A. (2021). Biological control and microbial ecology draft genome sequence data of *Glutamicibacter* sp. FBE-19, a bacterium antagonistic to the plant pathogen *Erwinia tracheiphila*. *Phytopathology* 111, 765–768. doi: 10.1094/PHYTO-09-20-0380-A

Fuentes, A. S., del Pozo Losada, C., and Vora, H. U. (2016). "(−)-(4R,5R)-4,5-Bis[hydroxy(diphenyl)methyl]-2,2-dimethyl-1,3-dioxolane" in *Encyclopedia of reagents for organic synthesis*. eds. A. Charette, J. Bode, T, Rovis, and R. Shenvi (Hoboken, New Jersey, United States: John Wiley & Sons, Ltd), 1–9.

Fukuda, K., and Kono, H. (2021). "Cost-benefit analysis and industrial potential of exopolysaccharides," in *Microbial exopolysaccharides as novel and significant biomaterials*. eds. A. K. Nadda, K. V. Sajna and S. Sharma (Cham: Springer), 303–339.

Gad, S. E. (2014). "Hydroperoxide, tert-Butyl" in *Encyclopedia of toxicology*. ed. P. Wexler. *Third* ed (Oxford: Academic Press), 977–978.

Gadhi, A., El-Sherbiny, M., Al-Sofynai, A., Baakdah, M., and Sathianeson, S. (2019). Antimicrofouling activities of marine macroalga Dictyota dichotoma from the Red Sea. *J. Agric. Mar. Sci.* 23:58. doi: 10.24200/jams.vol23iss0pp58-67

Ganyam, M., Anaduaka, E., Gabriel, F., Sani, S., and Fedilis, I. (2019). Effects of methanol extract of toasted african yam bean seeds (*Sphenostylis stenocarpa*) on anti-inflammatory properties. *Pharmacol. Online* 3, 100–113.

Gautam, V., Sharma, A., Arora, S., and Bhardwaj, R. (2016). Bioactive compounds in the different extracts of flowers of *Rhododendron arboreum Sm*. *J. Chem. Pharm. Res.* 2016, 439–444.

Gensler, W. J., and Thomas, G. R. (1952). Synthesis of unsaturated fatty acids: vaccenic acid. *J. Am. Chem. Soc.* 74, 3942–3943. doi: 10.1021/ja01135a511

Gil, S., Lázaro, M. A., Mestres, R., Millan, F., and Parra, M. (1995). Components of the sex pheromone of chilo supressalis: efficient syntheses of (Z)-11-hexadecenal and (Z)-13-Octadecenal. *Synth. Commun.* 25, 351–361. doi: 10.1080/00397919508011366

Godwin, J., Chukwu, U. J., and Gad, T. (2012). Distribution of iron (ii) between buffered aqueous solutions and chloroform solution of N, N'-ethylenebis(4-butanoyl-2,4-dihydro-5-methyl-2-phenyl-3h-pyrazol-3-oneimine). *J. Adv. Chem.* 8, 1581–1589. doi: 10.24297/jac.v8i2.4039

Gülerman, N., Oruç-Emre, E., Kartal, F., and Rollas, S. (2000). In vivo metabolism of 4-fluorobenzoic acid [(5-nitro-2-furanyl)methylene] hydrazide in rats. *Eur. J. Drug Metab. Pharmacokinet.* 25, 103–108. doi: 10.1007/BF03190075

Halling, P. J., Ross, A. C., and Bell, G. (1998). "Inactivation of enzymes at the aqueous-organic interface" in *Progress in biotechnology stability and stabilization of biocatalysts*. eds. A. Ballesteros, F. J. Plou, J. L. Iborra and P. J. Halling (Amsterdam, Netherlands: Elsevier), 365–372.

Ham, J. E., and Raymond Wells, J. (2009). Surface chemistry of dihydromyrcenol (2,6-dimethyl-7-octen-2-ol) with ozone on silanized glass, glass, and vinyl flooring tiles. *Atmos. Environ.* 43, 4023–4032. doi: 10.1016/j.atmosenv.2009.05.007

Hamalainen, T. I., Sundberg, S., Makinen, M., Kaltia, S., Hase, T., and Hopia, A. (2001). Hydroperoxide formation during autoxidation of conjugated linoleic acid methyl ester. *Eur. J. Lipid Sci. Technol.* 103, 588–593. doi: 10.1002/1438-9312(200109)103:9<588::AID-EJLT5880>3.0.CO;2-L

Hidri, R., Mahmoud, O. M.-B., Zorrig, W., Mahmoudi, H., Smaoui, A., Abdelly, C., et al. (2022). Plant growth-promoting rhizobacteria alleviate high salinity impact on the halophyte *Suaeda fruticosa* by modulating antioxidant defense and soil biological activity. *Front. Plant Sci.* 13:821475. doi: 10.3389/fpls.2022.821475

Holman, R. T., Deubig, M., and Hayes, H. (1966). Pyrolysis chromatography of lipids. I. Mass spectrometric identification of pyrolysis products of hydrocarbons. *Lipids* 1, 247–253. doi: 10.1007/BF02531610

Hoskin, D. W., and Ramamoorthy, A. (2008). Studies on anticancer activities of antimicrobial peptides. *Biochim. Biophys. Acta - Biomembr.* 1778, 357–375. doi: 10.1016/j.bbamem.2007.11.008

Hosseini Hashemi, S. K., Anooshei, H., Aghajani, H., and Salem, M. (2015). Chemical composition and antioxidant activity of extracts from the inner bark of *Berberis vulgaris* stem. *Bioresources* 10, 7958–7969. doi: 10.15376/biores.10.4.7958-7969

Hui, M. L.-Y., Tan, L. T.-H., Letchumanan, V., He, Y.-W., Fang, C.-M., Chan, K.-G., et al. (2021). The extremophilic actinobacteria: from microbes to medicine. *Antibiotics* 10:682. doi: 10.3390/antibiotics10060682

Hušek, P., Švagera, Z., Hanzlíková, D., Řimnáčová, L., Zahradníčková, H., Opekarová, I., et al. (2016). Profiling of urinary amino-carboxylic metabolites by in-situ heptafluorobutyl chloroformate mediated sample preparation and gas chromatography–mass spectrometry. *J. Chromatogr. A* 1443, 211–232. doi: 10.1016/j.chroma.2016.03.019

Hussein, A. O., Hameed, I. H., Jasim, H., and Kareem, M. A. (2015). Determination of alkaloid compounds of *Ricinus communis* by using gas chromatography- mass spectroscopy (GC-MS). *JMPR* 9, 349–359. doi: 10.5897/JMPR2015.5750

Hussein, J., Mohammed, Y. H., and Imad, H. H. (2016). Study of chemical composition of Foeniculum vulgare using Fourier transform infrared spectrophotometer and gas chromatography -mass spectrometry. *J. Pharmacogn. Phytother.* 8, 60–89. doi: 10.5897/JPP2015.0372

Ikhsanov, Y. S., Abilov Zh, A., Choudhary, M. I., and Sultanova, N. A. (2018). Study of the chemical composition of dichloromethane extract Tamarix hispida. Bulletin of the Karaganda University. Chemistry Series.

Ivankin, A. (2017). Biotechnology for formation of aromatic properties of National-Foodstuffs on the basis of meat raw material under influence of bacterial crops and Chromato-mass-spectrometric analysis of the flavoring components. *J. Appl. Biotechnol. Bioeng.* 3, 366–372. doi: 10.15406/jabb.2017.03.00072

Ivkin, D. Y., Luzhanin, V. G., Karpov, A. A., Minasyan, S. M., Poleshchenko, Y. I., Mamedov, A. E., et al. (2018). Embinin is a perspective cardiotonic mean for natural origin. *Drug Dev. Regist.* 0, 166–170.

Jachak, M., Bhusnar, A., Medhane, V., and Toche, R. (2006). A convenient route for the synthesis of pyrazolo[3,4-d]pyrimidine, pyrazolo[3,4-b][1,6]naphthyridine and pyrazolo[3,4-b]quinoline derivatives. *J. Heterocyclic Chem.* 43, 1169–1175. doi: 10.1002/jhet.5570430506

Jaffar, A., Somanath, B., and Karthi, S. (2015). Efficacy of methanolic extract of a marine ascidian, *Lissoclinum bistratum* for antimicrobial activity. *J. Chem. Biol. Phys. Sci.* 5:4119.

Jahan, I., Tona, M. R., Sharmin, S., Sayeed, M. A., Tania, F. Z., Paul, A., et al. (2020). GC-MS phytochemical profiling, pharmacological properties, and in Silico studies of *Chukrasia velutina* leaves: a novel source for bioactive agents. *Molecules* 25:3536. doi: 10.3390/molecules25153536

James, A. T., and Martin, A. J. P. (1956). Gas–liquid chromatography: the separation and identification of the methyl esters of saturated and unsaturated acids from formic acid to n-octadecanoic acid. *Biochem. J.* 63, 144–152. doi: 10.1042/bj0630144

Jamieson, S. M. F., Brooke, D. G., Heinrich, D., Atwell, G. J., Silva, S., Hamilton, E. J., et al. (2012). 3-(3,4-Dihydroisoquinolin-2(1H)-ylsulfonyl)benzoic acids: highly potent and selective inhibitors of the type 5 17-β-hydroxysteroid dehydrogenase AKR1C3. *J. Med. Chem.* 55, 7746–7758. doi: 10.1021/jm3007867

Janardhan, A., Kumar, A. P., Viswanath, B., Saigopal, D. V. R., and Narasimha, G. (2014). Production of bioactive compounds by actinomycetes and their antioxidant properties. *Biotechnol. Res. Int.* 2014, 1–9. doi: 10.1155/2014/217030

Janneck, R., Heremans, P., Genoe, J., and Rolin, C. (2018). Influence of the surface treatment on the solution coating of single-crystalline organic thin-films. *Adv. Mater. Interfaces* 5:1800147. doi: 10.1002/admi.201800147

Jawad, M., Mohammad, G., and Hussein, H. (2016). Analysis of bioactive metabolites from Candida albicans using (GC-MS) and evaluation of antibacterial activity 8, 655–670.

Jenkins, B., West, J. A., and Koulman, A. (2015). A review of odd-chain fatty acid metabolism and the role of pentadecanoic acid (C15:0) and heptadecanoic acid (C17:0) in health and disease. *Molecules* 20, 2425–2444. doi: 10.3390/molecules20022425

Jiang, J., and Jia, X. (2015). Profiling of fatty acids composition in suet oil based on GC–EI-qMS and chemometrics analysis. *Int. J. Mol. Sci.* 16, 2864–2878. doi: 10.3390/ijms16022864

Joshi, P. R., Paudel, M. R., Chand, M. B., Pradhan, S., Pant, K. K., Joshi, G. P., et al. (2020). Cytotoxic effect of selected wild orchids on two different human cancer cell lines. *Heliyon* 6:e03991. doi: 10.1016/j.heliyon.2020.e03991

Jubete, G., Puig de la Bellacasa, R., Estrada-Tejedor, R., Teixidó, J., and Borrell, J. I. (2019). Pyrido[2,3-d]pyrimidin-7(8H)-ones: synthesis and biomedical applications. *Molecules* 24:4161. doi: 10.3390/molecules24224161

Juturu, V., and Wu, J. C. (2018). Microbial production of bacteriocins: latest research development and applications. *Biotechnol. Adv.* 36, 2187–2200. doi: 10.1016/j.biotechadv.2018.10.007

Karthik, Y., and Kalyani, M. I. (2021). Molecular profiling of Glutamicibacter Mysorens strain YKIKM.MU and bioactive peptides characterization for antibacterial activity. *Int. J. Pharm. Clin. Res.* 13:15.

Karthik, Y., and Kalyani, M. I. (2022). Occurrence of Streptomyces tauricus in mangrove soil of Mangalore region in Dakshina Kannada as a source for antimicrobial peptide. *J. Basic Microbiol.* 62, 1–15. doi: 10.1002/jobm.202200108

Karthik, Y., Kalyani, M. I., Sheetal, K., Rakshitha, D., and Bineesha, B. K. (2020). Cytotoxic and antimicrobial activities of microbial proteins from mangrove soil actinomycetes of Mangalore, Dakshina Kannada. *Biomedicine* 40, 59–67. doi: 10.51248/.v40i1.104

Kaur, S., Sharma, P., Bains, A., Chawla, P., Sridhar, K., Sharma, M., et al. (2022). Antimicrobial and anti-inflammatory activity of low-energy assisted nanohydrogel of *Azadirachta indica* oil. *Gels* 8:434. doi: 10.3390/gels8070434

Kawase, A., and Yagishita, K. (1968). On the structure of a new C-glycosyl flavone, embinin, isolated from the petals of Iris germanica Linnaeous*1. *Agric. Biol. Chem.* 32, 537–538. doi: 10.1080/00021369.1968.10859095

Khadayat, K., Sherpa, D. D., Malla, K. P., Shrestha, S., Rana, N., Marasini, B. P., et al. (2020). Molecular identification and antimicrobial potential of *Streptomyces* species from nepalese soil. *Int. J. Microbiol.* 2020:e8817467. doi: 10.1155/2020/8817467

Khidre, R., Abuhashem, A., and El-Shazly, M. (2011). Synthesis and anti-microbial activity of some 1-substituted amino-4, 6-dimethyl-2-oxo-pyridine-3-carbonitrile derivatives. *Eur. J. Med. Chem.* 46, 5057–5064. doi: 10.1016/j.ejmech.2011.08.018

Khodaei, M., and Sh, S. N. (2018). Isolation and molecular identification of Bacteriocin-producing enterococci with broad antibacterial activity from traditional dairy products in Kerman Province of Iran. *Korean J. Food Sci. Anim. Resour.* 38, 172–179. doi: 10.5851/kosfa.2018.38.1.172

Khusro, A., Aarti, C., and Agastian, P. (2020). Microwave irradiation-based synthesis of anisotropic gold nanoplates using *Staphylococcus hominis* as reductant and its optimization for therapeutic applications. *J. Environ. Chem. Eng.* 8:104526. doi: 10.1016/j.jece.2020.104526

Kratky, M., Konečná, K., Janoušek, J., Brablíková, M., Janďourek, O., Trejtnar, F., et al. (2019). 4-Aminobenzoic acid derivatives: converting folate precursor to antimicrobial and cytotoxic agents. *Biomol. Ther.* 10:9. doi: 10.3390/biom10010009

Kroumova, A. B., and Wagner, G. J. (2003). Different elongation pathways in the biosynthesis of acyl groups of trichome exudate sugar esters from various solanaceous plants. *Planta* 216, 1013–1021. doi: 10.1007/s00425-002-0954-7

Kula, J., Quang, T. B., and Smigielski, K. (2001). Convenient synthesis of (r)-1,3-nonanediol. *Synth. Commun.* 31, 463–467. doi: 10.1081/SCC-100000540

Kurnianto, M. A., Kusumaningrum, H. D., Lioe, H. N., and Chasanah, E. (2021). Partial purification and characterization of bacteriocin-like inhibitory substances produced by *Streptomyces* sp. isolated from the gut of Chanos chanos. *Biomed. Res. Int.* 2021:7190152. doi: 10.1155/2021/7190152

Lemieux, R. U., and Nagabhushan, T. L. (1968). The synthesis of 2-amino-2-deoxyhexoses: D-glucosamine, D-mannosamine, D-galactosamine, and D-talosamine. *Can. J. Chem.* 46, 401–403. doi: 10.1139/v68-064

Ley, S. V., and Madin, A. (1991). "2.7 - oxidation adjacent to oxygen of alcohols by chromium reagents" in *Comprehensive organic synthesis*. eds. B. M. Trost and I. Fleming (Oxford: Pergamon), 251–289.

Li, H., Liu, X., and Fang, G. (2010). Preparation and characteristics of n-nonadecane/cement composites as thermal energy storage materials in buildings. *Energ. Buildings* 42, 1661–1665. doi: 10.1016/j.enbuild.2010.04.009

MacKenzie, S. L., and Tenaschuk, D. (1979). Quantitative fromation of N(O,S)-heptafluorobutyryl isobutyl amino acids for gas chromatographic analysis: I. Esterification. *J. Chromatogr. A* 171, 195–208. doi: 10.1016/S0021-9673(01)95299-9

Martín-Acosta, P., Amesty, A., Guerra-Rodríguez, M., Guerra, B., Fernández-Pérez, L., and Estévez-Braun, A. (2021). Modular synthesis and antiproliferative activity of new dihydro-1H-pyrazolo[1,3-b]pyridine embelin derivatives. *Pharmaceuticals (Basel)* 14:1026. doi: 10.3390/ph14101026

Martinez, C., Hu, S., Dumond, Y., Tao, J., Kelleher, P., and Tully, L. (2008). Development of a Chemoenzymatic manufacturing process for pregabalin. *Org. Process Res. Dev.* 12, 392–398. doi: 10.1021/op7002248

Matthew, O., James, A., Akogwu, I., Fabunmi, T., Godwin, I., Ebun, B., et al. (2022). The reference colored blue in the reference section should be cited in the body of the work evaluation of in vitro antioxidant, phytochemical and Gc- Ms analysis of aqueous extract of Solanum Dasyphyllum fruits.

McCarthy, E. D., and Calvin, M. (1967). The isolation and identification of the C17 saturated isoprenoid hydrocarbon 2,6,10-trimethyltetradecane from a Devonian shale: the role of squalane as a possible precursor. *Tetrahedron* 23, 2609–2619. doi: 10.1016/0040-4020(67)85125-1

Mihooliya, K. N., Nandal, J., Swami, L., Verma, H., Chopra, L., and Sahoo, D. K. (2017). A new pH indicator dye-based method for rapid and efficient screening of l-asparaginase producing microorganisms. *Enzym. Microb. Technol.* 107, 72–81. doi: 10.1016/j.enzmictec.2017.08.004

Millero, F. J., Graham, T. B., Huang, F., Bustos-Serrano, H., and Pierrot, D. (2006). Dissociation constants of carbonic acid in seawater as a function of salinity and temperature. *Mar. Chem.* 100, 80–94. doi: 10.1016/j.marchem.2005.12.001

Ming Miao, Y., and Zhi, Y. (2018). Mass spectrum of acids, alcohols, esters and amines of coffee hull (Typical.Arabica).

Mohan, Y., Sirisha, B., Haritha, R., and Ramana, T. (2013). Selective screening, isolation and characterization of antimicrobial agents from marine actinomycetes. *Int J Pharm Pharm Sci* 5, 443–449.

Moldoveanu, S. C. (2019). "Chapter 2 - pyrolysis of hydrocarbons," in *Pyrolysis of organic molecules*. ed. S. C. Moldoveanu. *Second* ed (Amsterdam, Netherlands: Elsevier), 35–161.

Narra, N., Kaki, S. S., Badari, R., Prasad, R. B. N., Misra, S., Koude, D., et al. (2017). Synthesis and evaluation of anti-oxidant and cytotoxic activities of novel 10-undecenoic acid methyl ester based lipoconjugates of phenolic acids. *Beilstein J. Org. Chem.* 2017, 26–32. doi: 10.3762/bjoc.13.4

Nishioka, K., and Katayama, I. (1978). Angiogenic activity in culture supernatant of antigen-stimulated lymph node cells. *J. Pathol.* 126, 63–69. doi: 10.1002/path.1711260202

Onocha, A., Abimbade, S., and Oloyede, G. (2011). Chemical composition, toxicity, antimicrobial and antioxidant activities of leaf and stem essential oils of *Dieffenbachia picta* (Araceae). *Eur. J. Sci. Res.* 49, 567–580.

Osgerby, L., Lai, Y.-C., Thornton, P. J., Amalfitano, J., Le Duff, C. S., Jabeen, I., et al. (2017). Kinetin riboside and its ProTides activate the Parkinson's disease associated PTEN-induced putative kinase 1 (PINK1) independent of mitochondrial depolarization. *J. Med. Chem.* 60, 3518–3524. doi: 10.1021/acs.jmedchem.6b01897

Ozden, S., Oztürk, A., Goker, H., and Altanlar, N. (2000). Synthesis and antimicrobial activity of some new 4-hydroxy-2H-1,4-benzoxazin-3(4H)-ones. *Farmaco* 55, 715–718. doi: 10.1016/S0014-827X(00)00098-7

Palanki, M., Erdman, P. E., Goldman, M. E., Suto, C., and Suto, M. J. (2000). Synthesis and structure-activity relationship studies of conformationally restricted, analogs of 2-chloro-4-trifluoromethylpyrimidine- 5-[N-(3′,5′-bis(trifluoromethyl)phenyl)] carboxamide. *Med. Chem. Res.* 10, 19–29.

Patel, K., Piagentini, M., Rascher, A., Tian, Z.-Q., Buchanan, G. O., Regentin, R., et al. (2004). Engineered biosynthesis of geldanamycin analogs for Hsp90 inhibition. *Chem. Biol.* 11, 1625–1633. doi: 10.1016/j.chembiol.2004.09.012

Phuong, T. V., and Diep, C. N. (2020). Isolation and selection of actinobacteria against pathogenic bacteria from shrimp pond water on Duyen Hai District, Tra Vinh Province, Vietnam. *Int. J. Environ. Agric. Res.* 6:8.

Qin, S., Feng, W.-W., Zhang, Y.-J., Wang, T.-T., Xiong, Y.-W., and Xing, K. (2018). Diversity of bacterial microbiota of coastal halophyte *Limonium sinense* and amelioration of salinity stress damage by symbiotic plant growth-promoting actinobacterium *Glutamicibacter halophytocola* KLBMP 5180. *Appl. Environ. Microbiol.* 84, e01533–e01518. doi: 10.1128/AEM.01533-18

Qiu, H., Liu, R., and Long, L. (2019). Analysis of chemical composition of extractives by acetone and the chromatic aberration of teak (Tectona Grandis L.F.) from China. *Molecules* 24, 1–10. doi: 10.3390/molecules24101989.

Qiu, D., Meng, H., Jin, L., Wang, S., Tang, S., Wang, X., et al. (2013). ChemInform abstract: synthesis of aryl trimethylstannanes from aryl amines: a sandmeyer-type stannylation reaction. *Angew. Chem. Int. Ed. Eng.* 125, 11581–11584. doi: 10.1002/anie.201304579

Ransom, C., Grey, T., Howatt, K., Johnson, E., Keese, R., Nurse, R., et al. (2012). Common and chemical names of herbicides approved by the weed science Society of America. *Weed Sci.* 60, 650–657.

Rebbert, R. E., and Ausloos, P. (1962). Intramolecular rearrangements in the solid phase photolysis of 4-methyl-2-hexanone and sec-butyl acetate. *J. Chem. Phys.* 37, 1158–1159. doi: 10.1063/1.1733239

Reddy, N., and Ananthaprasad, M. G. (2021). "Chapter 11 - polymeric materials for three-dimensional printing" in *Additive manufacturing Woodhead publishing reviews: Mechanical engineering series*. eds. M. Manjaiah, K. Raghavendra, N. Balashanmugam and J. P. Davim (Darya Ganj, Delhi, India: Woodhead Publishing), 233–274.

Renner, M. K., Shen, Y.-C., Cheng, X.-C., Jensen, P. R., Frankmoelle, W., Kauffman, C. A., et al. (1999). Cyclomarins a–C, new antiinflammatory cyclic peptides produced by a marine bacterium (*Streptomyces* sp.). *J. Am. Chem. Soc.* 121, 11273–11276. doi: 10.1021/ja992482o

Reza, A. S. M. A., Haque, M. A., Sarker, J., Nasrin Mst, S., Rahman, M. M., Tareq, A. M., et al. (2021). Antiproliferative and antioxidant potentials of bioactive edible vegetable fraction of *Achyranthes ferruginea* Roxb. In cancer cell line. *Food Sci. Nutr.* 9, 3777–3805. doi: 10.1002/fsn3.2343

Rossi, A., Martins, M. P., Bitencourt, T. A., Peres, N. T. A., Rocha, C. H. L., Rocha, F. M. G., et al. (2021). Reassessing the use of undecanoic acid as a therapeutic strategy for treating fungal infections. *Mycopathologia* 186, 327–340. doi: 10.1007/s11046-021-00550-4

Salem, M. Z. M., Zayed, M. Z., Ali, H. M., and Abd El-Kareem, M. S. M. (2016). Chemical composition, antioxidant and antibacterial activities of extracts from *Schinus molle* wood branch growing in Egypt. *J. Wood Sci.* 62, 548–561. doi: 10.1007/s10086-016-1583-2

Santos, R. G., Hurtado, R., Gomes, L. G. R., Profeta, R., Rifici, C., Attili, A. R., et al. (2020). Complete genome analysis of *Glutamicibacter creatinolyticus* from mare abscess and comparative genomics provide insight of diversity and adaptation for Glutamicibacter. *Gene* 741:144566. doi: 10.1016/j.gene.2020.144566

Sapkota, A., Thapa, A., Budhathoki, A., Sainju, M., Shrestha, P., and Aryal, S. (2020). Isolation, characterization, and screening of antimicrobial-producing actinomycetes from soil samples. *Int. J. Microbiol.* 2020, 1–7. doi: 10.1155/2020/2716584

Satgé, J., Massol, M., and Rivière, P. (1973). Divalent germanium species as starting materials and intermediates in organo germanium chemistry. *J. Organomet. Chem.* 56, 1–39. doi: 10.1016/S0022-328X(00)89951-9

Saxena, D., and Stotzky, G. (2001). Bacillus thuringiensis (Bt) toxin released from root exudates and biomass of Bt corn has no apparent effect on earthworms, nematodes, protozoa, bacteria, and fungi in soil. *Soil Biol. Biochem.* 33, 1225–1230. doi: 10.1016/S0038-0717(01)00027-X

Schwabe, A. D., Bennett, L. R., and Bowman, L. P. (1964). Octanoic acid absorption and oxidation in humans. *J. Appl. Physiol.* 19, 335–337. doi: 10.1152/jappl.1964.19.2.335

Senarath, S., Yoshinaga, K., Nagai, T., Yoshida, A., Beppu, F., and Gotoh, N. (2018). Differential effect of cis-eicosenoic acid positional isomers on adipogenesis and lipid accumulation in 3T3-L1 cells. *Eur. J. Lipid Sci. Technol.* 120:1700512. doi: 10.1002/ejlt.201700512

Ser, H. L., Palanisamy, U., Yin, W.-F., Abd Malek, N., Chan, K.-G., Goh, B. H., et al. (2015). Presence of antioxidative agent, pyrrolo[1,2-a]pyrazine-1,4-dione, hexahydro- in newly isolated *Streptomyces mangrovisoli* sp. nov. *Front. Microbiol.* 6:854. doi: 10.3389/fmicb.2015.00854

Shalini, K., Sharma, P. K., and Kumar, N. (2010). Imidazole and its biological activities: a review 13, 36–47.

Shawky, A. M., Ibrahim, N. A., Abdalla, A. N., Abourehab, M. A. S., and Gouda, A. M. (2021). Novel pyrrolizines bearing 3,4,5-trimethoxyphenyl moiety: design, synthesis, molecular docking, and biological evaluation as potential multi-target cytotoxic agents. *J. Enzyme Inhib. Med. Chem.* 36, 1312–1332. doi: 10.1080/14756366.2021.1937618

Silva, M. J., Samandar, E., Ye, X., and Calafat, A. M. (2013). In vitro metabolites of Di-2-ethylhexyl adipate (DEHA) as biomarkers of exposure in human biomonitoring applications. *Chem. Res. Toxicol.* 26, 1498–1502. doi: 10.1021/tx400215z

Simon, A., and Losada, C. (2008). (−)-(4 R,5 R)-4,5-Bis[hydroxy(diphenyl)methyl]-2,2-dimethyl-1,3-dioxolane.

Sivaprakash, S., Prakash, S., Mohan, S., and Jose, S. P. (2019). Quantum chemical studies and spectroscopic investigations on 2-amino-3-methyl-5-nitropyridine by density functional theory. *Heliyon* 5:e02149. doi: 10.1016/j.heliyon.2019.e02149

Skhirtladze, L., Leitonas, K., Bucinskas, A., Volyniuk, D., Mahmoudi, M., Mukbaniani, O., et al. (2022). 1,4-Bis(trifluoromethyl)benzene as a new acceptor for the design and synthesis of emitters exhibiting efficient thermally activated delayed fluorescence and electroluminescence: experimental and computational guiding. *J. Mater. Chem. C* 10, 4929–4940. doi: 10.1039/D1TC05420A

Soleha, M., Pratiwi, D., Sari, I., Hermiyanti, E., Yunarto, N., and Setyorini, H. (2020). Antioxidant activity of methanol extract *Tetracera scanden* L Merr predicted active compound of methanol extract with GCMS NIST library. *J. Phys. Conf. Ser.* 1665:012028. doi: 10.1088/1742-6596/1665/1/012028

Sridevi, V., Priyadarshini, P. S., and Gautam, Y. A. (2015). Selection of marine actinomycetes with bioactive potential isolated from sediments of Bay of Bengal and characterization of promising isolate, ABT-103. *Microbiol. Res. J. Int.* 10, 1–9. doi: 10.9734/BMRJ/2015/20132

Sridhar, K., Bhargavan, R., and Kasinathan, S. (2016). Phytochemical screening and gc-ms analysis of ethanolic extract of *Tribulus terrestris*. *Int. J. Pharmacol. Res.* 6, 44–50.

Srivastava, R., Mukerjee, A., and Verma, A. (2015). GC-MS analysis of Phytocomponents in, pet ether fraction of *Wrightia tinctoria* seed. *Pharm. J.* 7, 249–253. doi: 10.5530/pj.2015.4.7

Su, X., Halem, H. A., Thomas, M. P., Moutrille, C., Culler, M. D., Vicker, N., et al. (2012). Adamantyl carboxamides and acetamides as potent human 11β-hydroxysteroid dehydrogenase type 1 inhibitors. *Bioorg. Med. Chem.* 20, 6394–6402. doi: 10.1016/j.bmc.2012.08.056

Sugrue, I., O'Connor, P. M., Hill, C., Stanton, C., and Ross, R. P. (2019). Actinomyces produces defensin-like bacteriocins (Actifensins) with a highly degenerate structure and broad antimicrobial activity. *J. Bacteriol.* 202, 1–15. doi: 10.1128/JB.00529-19

Takigawa, H., Nakagawa, H., Kuzukawa, M., Mori, H., and Imokawa, G. (2005). Deficient production of hexadecenoic acid in the skin is associated in part with the vulnerability of atopic dermatitis patients to colonization by *Staphylococcus aureus*. *DRM* 211, 240–248. doi: 10.1159/000087018

Talley, J. J., Bertenshaw, S. R., Brown, D. L., Carter, J. S., Graneto, M. J., Kellogg, M. S., et al. (2000). N-[[(5-methyl-3-phenylisoxazol-4-yl)- phenyl]sulfonyl]propanamide, sodium salt, parecoxib sodium: a potent and selective inhibitor of COX-2 for parenteral administration. *J. Med. Chem.* 43, 1661–1663. doi: 10.1021/jm000069h

Tanak, H., Karataş, Ş., Meral, S., and Agar, A. A. (2020). Synthesis, molecular structure and quantum chemical studies of N-(2-fluorophenyl)-1-(5-nitrothiophen-2-yl) methanimine. *Crystallogr. Rep.* 65, 1212–1216. doi: 10.1134/S106377452007024X

Tanaka, T., and Hayashi, M. (2008). Catalytic enantioselective reformatsky reaction of alkyl iodoacetate with aldehydes catalyzed by chiral Schiff Base. *Chem. Lett.* 37, 1298–1299. doi: 10.1246/cl.2008.1298

Tang, W., Meng, Z., Li, N., Liu, Y., Li, L., Chen, D., et al. (2021). Roles of gut microbiota in the regulation of hippocampal plasticity, inflammation, and hippocampus-dependent behaviors. *Front. Cell. Infect. Microbiol.* 10, 1–15. doi: 10.3389/fcimb.2020.611014

Thakor, P., Mehta, J. B., Patel, R. R., Patel, D. D., Subramanian, R. B., and Thakkar, V. R. (2016). Extraction and purification of phytol from *Abutilon indicum*: cytotoxic and apoptotic activity. *RSC Adv.* 6, 48336–48345. doi: 10.1039/C5RA24464A

Tsunoda, H., Kudo, T., Masaki, Y., Ohkubo, A., Seio, K., and Sekine, M. (2011). Biochemical behavior of N-oxidized cytosine and adenine bases in DNA polymerase-mediated primer extension reactions. *Nucleic Acids Res.* 39, 2995–3004. doi: 10.1093/nar/gkq914

Upgade, A., and Bhaskar, A. (2013). Characterization and medicinal importance of phytoconstituents of *C. Papaya* from down south Indian region using gas chromatography and mass spectroscopy. *Asian J. Pharm. Clin. Res.* 6, 101–106.

Van der Steen, M., and Stevens, C. V. (2009). Undecylenic acid: a valuable and physiologically active renewable building block from castor oil. *ChemSusChem* 2, 692–713. doi: 10.1002/cssc.200900075

Viegas, C. A., Rosa, M. F., Sa-Correia, I., and Novais, J. M. (1989). Inhibition of yeast growth by octanoic and decanoic acids produced during ETHANOLIC fermentation. *Appl. Environ. Microbiol.* 55, 21–28. doi: 10.1128/aem.55.1.21-28.1989

Wang, C., Lu, Y., and Cao, S. (2020). Antimicrobial compounds from marine actinomycetes. *Arch. Pharm. Res.* 43, 677–704. doi: 10.1007/s12272-020-01251-0

Wang, X., Shen, S., Wu, H., Wang, H., Wang, L., and Lu, Z. (2021). *Acinetobacter tandoii* ZM06 assists *Glutamicibacter nicotianae* ZM05 in resisting cadmium pressure to preserve dipropyl phthalate biodegradation. *Microorganisms* 9:1417. doi: 10.3390/microorganisms9071417

Wang, Y., Su, X., Liu, J., Fang, W., and Zhu, L. (2022). Complete genome sequence of *Glutamicibacter mysorens* NBNZ-009, isolated from Jin Lake sediment. *Microbiol. Resour. Announc.* 0, e00762–e00722. doi: 10.1128/mra.00762-22

Wang, W., Xiao, G., Du, G., Chang, L., Yang, Y., Ye, J., et al. (2022). Glutamicibacter halophytocola-mediated host fitness of potato tuber moth on *Solanaceae* crops. *Pest Manag. Sci.* 78, 3920–3930. doi: 10.1002/ps.6955

Wang, Y., Zhang, L.-T., Feng, Y.-X., Guo, S.-S., Pang, X., Zhang, D., et al. (2019). Insecticidal and repellent efficacy against stored-product insects of oxygenated monoterpenes and 2-dodecanone of the essential oil from *Zanthoxylum planispinum* var. dintanensis. *Environ. Sci. Pollut. Res.* 26, 24988–24997. doi: 10.1007/s11356-019-05765-z

Watanabe, M., Koike, H., Ishiba, T., Okada, T., Seo, S., and Hirai, K. (1997). Synthesis and biological activity of methanesulfonamide pyrimidine- and N-methanesulfonyl pyrrole-substituted 3,5-dihydroxy-6-heptenoates, a novel series of HMG-CoA reductase inhibitors. *Bioorg. Med. Chem.* 5, 437–444. doi: 10.1016/S0968-0896(96)00248-9

Williams, J. D., Torhan, M. C., Neelagiri, V., Brown, C., Bowlin, N. O., Di, M., et al. (2015). Synthesis and structure-activity relationships of novel phenoxyacetamide inhibitors of the Pseudomonas aeruginosa type III secretion system (T3SS). *Bioorg. Med. Chem.* 23, 1027–1043. doi: 10.1016/j.bmc.2015.01.011

Windey, K., De Preter, V., Louat, T., Schuit, F., Herman, J., Vansant, G., et al. (2012). Modulation of protein fermentation does not affect fecal water toxicity: a randomized cross-over study in healthy subjects. *PLoS One* 7:e52387. doi: 10.1371/journal.pone.0052387

Xie, F.-M., Li, H.-Z., Dai, G.-L., Li, Y.-Q., Cheng, T., Xie, M., et al. (2019). Rational molecular design of dibenzo[a,c]phenazine-based thermally activated delayed fluorescence emitters for orange-red OLEDs with EQE up to 22.0%. *ACS Appl. Mater. Interfaces* 11, 26144–26151. doi: 10.1021/acsami.9b06401

Xiong, Y.-W., Ju, X.-Y., Li, X.-W., Gong, Y., Xu, M.-J., Zhang, C.-M., et al. (2020). Fermentation conditions optimization, purification, and antioxidant activity of exopolysaccharides obtained from the plant growth-promoting endophytic actinobacterium *Glutamicibacter halophytocola* KLBMP 5180. *Int. J. Biol. Macromol.* 153, 1176–1185. doi: 10.1016/j.ijbiomac.2019.10.247

Xu, Y., Li, H., Li, X., Xiao, X., and Qian, P.-Y. (2008). Inhibitory effects of a branched-chain fatty acid on larval settlement of the polychaete hydroides elegans. *Mar. Biotechnol.* 11, 495–504. doi: 10.1007/s10126-008-9161-2

Xue, J., Zhuo, J., Liu, M., Chi, Y., Zhang, D., and Yao, Q. (2017). Synergetic effect of co-pyrolysis of cellulose and polypropylene over an all-silica mesoporous catalyst MCM-41 using Thermogravimetry–Fourier transform infrared spectroscopy and pyrolysis–gas chromatography–mass spectrometry. *Energy Fuel* 31, 9576–9584. doi: 10.1021/acs.energyfuels.7b01651

Yamamoto, T. (2002). Chlorination of bisphenol a in aqueous media: formation of chlorinated bisphenol a congeners and degradation to chlorinated phenolic compounds. *Chemosphere* 46, 1215–1223. doi: 10.1016/S0045-6535(01)00198-9

Zagulyaeva, A. A., Yusubov, M. S., and Zhdankin, V. V. (2010). A general and convenient preparation of [bis(trifluoroacetoxy)iodo]perfluoroalkanes and [bis(trifluoroacetoxy)iodo] arenes by oxidation of organic iodides using oxone and trifluoroacetic acid. *J. Organomet. Chem.* 75, 2119–2122. doi: 10.1021/jo902733f

Zeitoun, M., Adel, M., Abulfotouh, F., and Ebrahim, S. (2021). Thermophysical properties enhancement of octadecane using reduced graphene oxide and graphene oxide nanoplatelets. *J. Energy Storage* 38:102512. doi: 10.1016/j.est.2021.102512

Zhang, D., Lu, Y., Chen, H., Wu, C., Zhang, H., Chen, L., et al. (2020). Antifungal peptides produced by actinomycetes and their biological activities against plant diseases. *J. Antibiot.* 73, 265–282. doi: 10.1038/s41429-020-0287-4

Zhang, L., Peng, X.-M., Damu, G. L. V., Geng, R.-X., and Zhou, C.-H. (2014). Comprehensive review in current developments of imidazole-based medicinal chemistry. *Med. Res. Rev.* 34, 340–437. doi: 10.1002/med.21290

Zhang, X., Wang, Y.-X., Zhao, J., Duan, P., Chen, Y., and Chen, L. (2017). Structural insights into 9-Styrylanthracene-based luminophores: geometry control versus mechanofluorochromism and sensing properties. *Chem. Asian J.* 12, 830–834. doi: 10.1002/asia.201700183

Zibuck, R. (2001). "2-Acetoxyisobutyryl chloride" in *Encyclopedia of reagents for organic synthesis*. eds. A. Charette, J. Bode, T. Rovis, and R. Shenvi (Hoboken, New Jersey, United States: John Wiley & Sons, Ltd)

frontiers | Frontiers in Microbiology

TYPE Perspective
PUBLISHED 13 March 2023
DOI 10.3389/fmicb.2023.1111472

OPEN ACCESS

EDITED BY
Rosa María Martínez-Espinosa,
University of Alicante,
Spain

REVIEWED BY
Kesava Priyan Ramasamy,
Nanyang Technological University,
Singapore

*CORRESPONDENCE
Peng Zhou
✉ zhoupeng@sio.org.cn

SPECIALTY SECTION
This article was submitted to Extreme Microbiology, a section of the journal Frontiers in Microbiology

RECEIVED 29 November 2022
ACCEPTED 16 February 2023
PUBLISHED 13 March 2023

CITATION
Zhou P, Bu Y-X, Xu L, Xu X-W and Shen H-B (2023) Understanding the mechanisms of halotolerance in members of *Pontixanthobacter* and *Allopontixanthobacter* by comparative genome analysis. *Front. Microbiol.* 14:1111472. doi: 10.3389/fmicb.2023.1111472

Understanding the mechanisms of halotolerance in members of *Pontixanthobacter* and *Allopontixanthobacter* by comparative genome analysis

Peng Zhou[1]*, Yu-Xin Bu[1], Lin Xu[1,2], Xue-Wei Xu[1,3] and Hong-Bin Shen[4]

[1]Key Laboratory of Marine Ecosystem Dynamics, Ministry of Natural Resources and Second Institute of Oceanography, Ministry of Natural Resources, Hangzhou, China, [2]College of Life Sciences and Medicine, Zhejiang Sci-Tech University, Hangzhou, China, [3]School of Oceanography, Shanghai Jiao Tong University, Shanghai, China, [4]Institute of Image Processing and Pattern Recognition, Shanghai Jiao Tong University, and Key Laboratory of System Control and Information Processing, Ministry of Education of China, Shanghai, China

Halotolerant microorganisms have developed versatile mechanisms for coping with saline stress. With the increasing number of isolated halotolerant strains and their genomes being sequenced, comparative genome analysis would help understand the mechanisms of salt tolerance. Six type strains of *Pontixanthobacter* and *Allopontixanthobacter*, two phylogenetically close genera, were isolated from diverse salty environments and showed different NaCl tolerances, from 3 to 10% (w/v). Based on the co-occurrence greater than 0.8 between halotolerance and open reading frame (ORF) among the six strains, possible explanations for halotolerance were discussed regarding osmolyte, membrane permeability, transportation, intracellular signaling, polysaccharide biosynthesis, and SOS response, which provided hypotheses for further investigations. The strategy of analyzing genome-wide co-occurrence between genetic diversity and physiological characteristics sheds light on how microorganisms adapt to the environment.

KEYWORDS

halotolerance, co-occurrence, comparative genomics, *Erythrobacteraceae*, adaptation

Introduction

Halotolerance is a relative term that refers to the ability to tolerate salt concentrations higher than those necessary for growth, and microorganisms are considered halotolerant if they survive at high salt concentrations but do not require these conditions for growth (Anton, 2014). With advances in technology, halotolerance mechanisms have been investigated using omics approaches. For instance, comparative transcriptomic and physiological analysis revealed that the halotolerant bacterium *Egicoccus halophilus* EGI 80432^T increased inorganic ions uptake and accumulated trehalose and glutamate in response to moderate salinity condition, while the high salt condition led to up-regulated transcription of genes required for the synthesis of compatible solutes, such as glutamate, histidine, threonine, proline, and ectoine (Chen et al., 2021). The role of glutamate as a key compatible solute for halotolerance was also reported in a halotolerant strain of *Staphylococcus saprophyticus* based on transcriptome comparison of cells cultivated in media containing different concentrations of NaCl (0, 10, and 20%; Jo et al., 2022). In the

exoproteome of the halotolerant bacterium *Tistlia consotensis* grown at high salinity, proteins associated with osmosensing, exclusion of Na^+ and transport of compatible solutes, such as glycine betaine or proline are abundant (Rubiano-Labrador et al., 2015). Similarly, the proteomic analysis of halotolerant nodule endophytes, *Rahnella aquatilis* strain Ra4 and *Serratia plymuthica* strain Sp2 identified that different trans-membrane ABC transporters (ATP-binding cassettes) were the most represented among the up-regulated proteins in response to salt stress (Novello et al., 2022). Moreover, the proteome comparison of halotolerant bacterium *Staphylococcus aureus* under different osmotic stress conditions revealed the differentially expressed proteins (DEPs) involved in fatty acid synthesis, proline/glycine betaine biosynthesis and transportation, stress tolerance, cell wall biosynthesis, and the TCA cycle, which may contribute to the osmotic stress tolerance of *S. aureus* (Ming et al., 2019). These findings shed light on halotolerance mechanisms. However, halotolerance-related genes may be ignored in transcriptomic and proteomic comparison if there is no significant change in their expression under the experimental conditions.

Genomic comparisons

Genomic comparisons of closely related halotolerant microorganisms can identify genes conserved among species as well as genes that may give an organism its unique characteristics, which helps to understand the mechanisms of salt tolerance. For example, through comparative genome analysis it was uncovered that the members of *Acidihalobacter* genus contained similar genes for the synthesis and transport of ectoine, as well as genes encoding low affinity potassium pumps. Variations were observed in genes encoding high affinity potassium pumps and proteins involved in the synthesis and/or transport of periplasmic glucans, sucrose, proline, taurine, and glycine betaine (Khaleque et al., 2019). To elucidate salt adaptation strategies in *Nitriliruptoria*, the genomes of five members from group *Nitriliruptoria* were analyzed. The results showed that *Nitriliruptoria* harbor similar synthesis systems of solutes, such as trehalose, glutamine, glutamate, and proline, and on the other hand each member of *Nitriliruptoria* species possesses specific mechanisms, K^+ influx and efflux, betaine and ectoine synthesis, and compatible solutes transport (Chen et al., 2020). Using whole-genome analysis, the halotolerant strains of *Martelella soudanensis*, NC18^T and NC20, were predicted to harbor various halotolerant-associated genes, including K^+ uptake protein, K^+ transport system, ectoine transport system, glycine betaine transport system, and glycine betaine uptake protein, indicating that strains NC18^T and NC20 might tolerate high salinity through the accumulation of potassium ions, ectoine, glycine betaine (Lee and Kim, 2022). Although these findings help to understand the versatile mechanisms of halotolerance existing in halotolerant microbes, genomic comparisons are usually based on genome-wide searches for homologs of known halotolerance-related genes, such as those involved in K^+ and Na^+ influx and efflux and the synthesis and transport of compatible solutes.

The aim of this perspective is to provide new insights into the development of novel hypotheses and promote further studies on the halotolerance mechanisms. Therefore, co-occurrence analysis between halotolerance and open reading frames (ORFs) was performed to provide intuitive information on halotolerance.

Strains used for analysis

Microorganisms develop abilities that enable them to deal with evolutionary pressure from the environment, such as salinity, temperature, and the power of hydrogen (pH). The phylogenetically closely related strains, which showed similar growth temperature and pH range but different halotolerance, would simplify the analysis. Furthermore, considering the ionic strength of different media may affect the cell growth, the tolerance to NaCl used for co-occurrence analysis should be determined by using same medium. Herein six type strains from two phylogenetically close genera, *Pontixanthobacter* and *Allopontixanthobacter*, were chosen for this study. Because of their close phylogenetic relationship, *Allopontixanthobacter sediminis* and *Allopontixanthobacter confluentis* have been previously classified as *Pontixanthobacter* species (Xu et al., 2020; Liu et al., 2021b), and later were reclassified as *Allopontixanthobacter* species (Xu et al., 2020; Liu et al., 2021a,b). Notably, all the type strains belonging to the two genera were isolated from the Yellow Sea and surrounding areas, but from diverse salty environments, such as *Pontixanthobacter aestiaquae* KCTC 42006^T and *Pontixanthobacter rizhaonensis* KCTC 62828^T from seawater (Jung et al., 2014; Liu et al., 2021b), *Pontixanthobacter gangjinensis* JCM 17802^T and *Pontixanthobacter luteolus* KCTC 12311^T from tidal flat (Yoon et al., 2005; Jeong et al., 2013), *Pontixanthobacter aquaemixtae* KCTC 52763^T from the junction between ocean and fresh spring (Park et al., 2017), *A. sediminis* KCTC 42453^T from lagoon sediments (Kim et al., 2016), and *A. confluentis* KCTC 52259^T from water of estuary environment (Park et al., 2017). These strains showed similar optimum NaCl concentrations for growth (1–3%, w/v), but displayed different halotolerances, from 3 to 10% (w/v; Table 1), indicating that these strains adapt to their diverse habitats, including lagoon, junction between ocean and fresh spring, tidal flat, and seawater. The availability of their genomes provides remarkable opportunity to understand their different halotolerances by comparative genome analysis. Here, co-occurrence between halotolerance and the open reading frames (ORFs) was calculated among six strains of *Pontixanthobacter* and *Allopontixanthobacter*, and the ORFs showing high co-occurrence were discussed for possible contribution to halotolerance.

Clusters highly co-occurred with halotolerance

Open reading frames in the six genomes were predicted and clustered based on similarity using R package micropan (Snipen and Liland, 2015). Analysis of co-occurrence between ORFs and the maximum NaCl concentration tolerated among the six strains was conducted, and 113 clusters of ORFs were identified with co-occurrence greater than 0.8 (Table 2). The co-occurrence for the remaining clusters is listed in Supplementary material, as well as ORFs predicted in the six genomes and the index for clusters and ORFs. ORFs were annotated by searching standard database using protein–protein BLAST.[1]

1 https://blast.ncbi.nlm.nih.gov

TABLE 1 Strains used for analysis in this study.

Species	Strain	Maximum NaCl (%, w/v)	Optimum NaCl (%, w/v)	Habitat	GenBank accession number
Pontixanthobacter aestiaquae	KCTC 42006	10	2–3	Seawater	GCF_009827455.1_ASM982745v1
Pontixanthobacter gangjinensis	JCM 17802	9	2	Tidal flat	GCF_009827545.1_ASM982754v1
Pontixanthobacter luteolus	KCTC 12311	9	2	Tidal flat	GCF_009828095.1_ASM982809v1
Pontixanthobacter aquaemixtae	KCTC 52763	5	2	Junction between ocean and fresh spring	GCF_009827395.1_ASM982739v1
Allopontixanthobacter sediminis	KCTC 42453	4	1	Lagoon sediments	GCF_009828115.1_ASM982811v1
Allopontixanthobacter confluentis	KCTC 52259	3	1–2	Water of estuary environment	GCF_009827615.1_ASM982761v1

The tolerance of NaCl for all the six strains were investigated based on marine broth (MB). The strain *Pontixanthobacter rizhaonensis* KCTC 62828^T was excluded from this study, because it is tested on different medium (Liu et al., 2020, 2021b).

Osmolyte

The ORFs of Cluster_111 (co-occurrence of 0.97, Table 2) were annotated as TauD/TfdA family dioxygenase. TauD is involved in the utilization of taurine (VanderPloeg et al., 1996), an organic osmolyte involved in cell volume regulation (Harris and Wen, 2012). Taurine is used as an osmoprotectant, such as in *Escherichia coli* at high osmolarity (McLaggan and Epstein, 1991) and in microbial communities from biofilms in metal-rich environment (Mosier et al., 2013). The ORFs of Cluster_111 only exist in three halotolerant strains, suggesting that taurine may be accumulated as an osmoprotectant. Interestingly, halotolerant strains harbor genes involved in various pathways related to glutamate generation. For instance, according to annotation, ORFs of Cluster_113 (co-occurrence of 0.81, Table 2) belong to the hydantoinase B/oxoprolinase family, which includes 5-oxoprolinase, catalyzing the formation of L-glutamate from 5-oxo-L-proline (Niehaus et al., 2017). Besides, ORFs of Cluster_1328 (co-occurrence of 0.81, Table 2) possess similarity to *p*-aminobenzoyl-glutamate (PABA-GLU) hydrolase subunit from *Altererythrobacter insulae* (GenBank Accession Number: RGP41665.1). PABA-GLU is a folate catabolite found in bacteria, and the enzyme PABA-GLU hydrolase breaks down PABA-GLU by cleaving glutamate (Larimer et al., 2014). Additionally, ORFs of Cluster_1747 (co-occurrence of 0.81 Table 2) showed similarity to asparagine synthase from *Salinigranum halophilum* (GenBank Accession Number: WP_136601134.1). Asparagine synthetase catalyzes an ATP-dependent amidotransferase reaction between aspartate and glutamine, which produces asparagine and glutamate (Richards and Kilberg, 2006).

Permeability

To ensure a physiologically acceptable level of cellular hydration and turgor at high osmolarity, many bacteria accumulate compatible solutes as osmoprotectants (Ziegler et al., 2010). ORFs of Cluster_875 (co-occurrence of 0.81, Table 2) were annotated as proteins of Betaine/Carnitine/Choline Transporter (BCCT) family. The BCCT family includes transporters for carnitine, choline and glycine betaine, and some of which exhibit osmosensory and osmoregulatory properties (Ziegler et al., 2010). Furthermore, the ORFs of Cluster_1740, annotated as ABC transporter ATP-binding proteins, were present only in these three halotolerant strains. The salt-induced ABC transporter Ota from *Methanosarcina mazei* Gö1 acts as a glycine betaine transporter (Schmidt et al., 2007). Another ABC transporter in *Listeria*, OpuC, is shown to be necessary for glycine betaine and choline chloride uptake (Verheul et al., 1997). Compared to the wild type of *S. aureus*, mutating OpuC did reduce their ability to grow under osmotic stress (10% NaCl; Kiran et al., 2009). The function of ORFs of Cluster_1740 and their contribution to halotolerance can be further characterized. Additionally, previous studies have shown that water permeability is clearly affected by the number of double bonds in the fatty acid conjugates of lipids, the higher the degree of unsaturation, the greater the water permeability (Graziani and Livne, 1972), and sterol type is one of the determining factors in the permeability of membranes to small solutes (Fralliciardi et al., 2022). The genomes of three halotolerant strains contain ORFs of Cluster_1548, annotated as sterol desaturase family proteins, indicating that sterols might be used to change permeability.

Cell signaling

Cluster_1549 also consists of three ORFs present in the three halotolerant strains, which showed similarity to the domain superfamily found in a large number of proteins including magnesium dependent endonucleases and phosphatases involved in intracellular signaling (Dlakic, 2000). Its role in the regulation of gene expression, such as triggering the salt-stress response, is worth of further study.

Polysaccharide

It has been reported that extracellular polysaccharides (EPS) may influence the salt tolerance of certain rhizobial strains (Samir and Kanak, 1997) and the lipopolysaccharide pattern could alter according to different salinities in a salt-tolerant strain of *Mesorhizobium cicero* (Soussi et al., 2001). All three halotolerant strains harbor ORFs annotated with polysaccharide/lipopolysaccharide biosynthesis (Cluster_2062, 2065, 2067, 2069, 2071, 2074, and 2076 in Table 2), such as 3-deoxy-d-manno-octulosonate cytidylyltransferase, a key enzyme in the biosynthesis of lipopolysaccharide (LPS) in Gram-negative organisms (Yi et al., 2011). Furthermore, ORFs of Cluster_2473 (co-occurrence as 0.81 Table 2) were annotated to

TABLE 2 Clusters highly co-occurred with halotolerance.

Cluster	Co-occurrence	Annotation
Cluster_111	0.97	TauD/TfdA family dioxygenase
Cluster_229	0.97	Hypothetical protein
Cluster_593	0.97	Metal-dependent hydrolase
Cluster_762	0.97	TonB-dependent receptor
Cluster_1374	0.97	Carbon-nitrogen hydrolase family protein
Cluster_1548	0.97	Sterol desaturase family protein
Cluster_1549	0.97	Endonuclease/exonuclease/phosphatase family protein
Cluster_1706	0.97	Hypothetical protein
Cluster_1740	0.97	ABC transporter ATP-binding protein
Cluster_1899	0.97	VirB4 family type IV secretion/conjugal transfer ATPase
Cluster_2062	0.97	Polysaccharide pyruvyl transferase family protein
Cluster_2063	0.97	Hypothetical protein
Cluster_2065	0.97	EpsG family protein
Cluster_2067	0.97	Glycosyltransferase
Cluster_2069	0.97	Polysaccharide biosynthesis C-terminal domain-containing protein
Cluster_2071	0.97	KpsF/GutQ family sugar-phosphate isomerase
Cluster_2074	0.97	3-Deoxy-manno-octulosonate cytidylyltransferase
Cluster_2076	0.97	3-Deoxy-8-phosphooctulonate synthase
Cluster_2401	0.97	Hypothetical protein
Cluster_2536	0.97	Histone deacetylase
Cluster_2670	0.97	Hypothetical protein
Cluster_2677	0.97	SOS response-associated peptidase family protein
Cluster_614	0.87	Putative quinol monooxygenase
Cluster_1440	0.86	Tail fiber protein
Cluster_1633	0.84	2OG-Fe(II) oxygenase
Cluster_11	0.81	Hypothetical protein
Cluster_12	0.81	DUF885 domain-containing protein
Cluster_59	0.81	PspA/IM30 family protein
Cluster_113	0.81	Hydantoinase B/oxoprolinase family protein
Cluster_115	0.81	DUF969 domain-containing protein
Cluster_116	0.81	DUF979 domain-containing protein
Cluster_117	0.81	DUF2891 domain-containing protein
Cluster_151	0.81	Aldolase/citrate lyase family protein
Cluster_155	0.81	Methyltransferase domain-containing protein
Cluster_166	0.81	Hypothetical protein
Cluster_208	0.81	Trigger factor
Cluster_294	0.81	Enoyl-CoA hydratase-related protein
Cluster_336	0.81	Aspartyl/asparaginyl beta-hydroxylase domain-containing protein
Cluster_395	0.81	Hypothetical protein
Cluster_551	0.81	Hypothetical protein
Cluster_595	0.81	DUF4167 domain-containing protein
Cluster_687	0.81	Amidohydrolase family protein
Cluster_712	0.81	TonB-dependent receptor
Cluster_729	0.81	OmpH family outer membrane protein
Cluster_752	0.81	PilZ domain-containing protein

(Continued)

TABLE 2 (Continued)

Cluster	Co-occurrence	Annotation
Cluster_875	0.81	BCCT family transporter
Cluster_879	0.81	Cell division protein ZapA
Cluster_895	0.81	Hypothetical protein
Cluster_983	0.81	GNAT family N-acetyltransferase
Cluster_1081	0.81	DUF805 domain-containing protein
Cluster_1089	0.81	Aminotransferase class IV
Cluster_1090	0.81	Sulfotransferase
Cluster_1132	0.81	Pilus assembly protein TadG-related protein
Cluster_1282	0.81	Hypothetical protein
Cluster_1289	0.81	SDR family oxidoreductase
Cluster_1315	0.81	CinA family protein
Cluster_1328	0.81	Amidohydrolase
Cluster_1340	0.81	Glutathione S-transferase family protein
Cluster_1364	0.81	M2 family metallopeptidase
Cluster_1465	0.81	Hypothetical protein
Cluster_1491	0.81	Hypothetical protein
Cluster_1495	0.81	Serine hydrolase
Cluster_1499	0.81	MarR family transcriptional regulator
Cluster_1565	0.81	Thioesterase family protein
Cluster_1575	0.81	LysR family transcriptional regulator
Cluster_1578	0.81	NAD(P)H-dependent oxidoreductase
Cluster_1663	0.81	Prolyl oligopeptidase family serine peptidase
Cluster_1738	0.81	Lasso peptide biosynthesis B2 protein
Cluster_1739	0.81	Nucleotidyltransferase family protein
Cluster_1741	0.81	Sulfotransferase
Cluster_1742	0.81	Aspartyl beta-hydroxylase
Cluster_1743	0.81	Hypothetical protein
Cluster_1744	0.81	Sulfotransferase domain-containing protein
Cluster_1746	0.81	PqqD family protein
Cluster_1747	0.81	Asparagine synthase-related protein
Cluster_1748	0.81	Glycosyltransferase
Cluster_1838	0.81	DUF3142 domain-containing protein
Cluster_1839	0.81	Hypothetical protein
Cluster_1862	0.81	Hypothetical protein
Cluster_1883	0.81	Isopropylmalate isomerase
Cluster_1896	0.81	Conjugal transfer protein TrbI
Cluster_1901	0.81	VirB3 family type IV secretion system protein
Cluster_1954	0.81	TrbG/VirB9 family P-type conjugative transfer protein
Cluster_1955	0.81	VirB8/TrbF family protein
Cluster_1956	0.81	Type IV secretion system protein
Cluster_2019	0.81	Dipeptidase
Cluster_2022	0.81	Glycerophosphodiester phosphodiesterase family protein
Cluster_2052	0.81	Hypothetical protein
Cluster_2059	0.81	O-antigen ligase family protein

(Continued)

TABLE 2 (Continued)

Cluster	Co-occurrence	Annotation
Cluster_2105	0.81	GNAT family N-acetyltransferase
Cluster_2171	0.81	Divalent-cation tolerance protein CutA
Cluster_2209	0.81	DUF2183 domain-containing protein
Cluster_2241	0.81	FKBP-type peptidyl-prolyl cis-trans isomerase
Cluster_2302	0.81	Carbohydrate porin
Cluster_2329	0.81	N-acetyltransferase
Cluster_2345	0.81	NADH:flavin oxidoreductase/NADH oxidase family protein
Cluster_2374	0.81	AI-2E family transporter
Cluster_2384	0.81	Endonuclease III
Cluster_2402	0.81	RNA polymerase sigma factor
Cluster_2408	0.81	GntP family permease
Cluster_2420	0.81	Hypothetical protein
Cluster_2425	0.81	Hypothetical protein
Cluster_2473	0.81	GtrA family protein
Cluster_2474	0.81	Ferritin-like domain-containing protein
Cluster_2475	0.81	Peroxide stress protein YaaA
Cluster_2520	0.81	DsrE family protein
Cluster_2544	0.81	Hypothetical protein
Cluster_2545	0.81	DNA-binding domain-containing protein
Cluster_2546	0.81	Alpha/beta hydrolase
Cluster_2562	0.81	LytTR family DNA-binding domain-containing protein
Cluster_2573	0.81	DUF2306 domain-containing protein
Cluster_2644	0.81	DUF6356 family protein
Cluster_2671	0.81	DUF1295 domain-containing protein

encode proteins of the GtrA family, whose members are often involved in the synthesis of cell surface polysaccharides (Kolly et al., 2015).

DNA repair

Open reading frames of Cluster_2677 are annotated encoding SOS response-associated peptidase family protein. The bacterial SOS response induced under stress conditions is recruited to DNA repair and adaptive mutagenesis (Shinagawa, 1996; Aravind et al., 2013). Hence, ORFs of Cluster_2677 could be further investigated for its importance to halotolerance.

Discussion

Salinity is one of the most important environmental factors for aquatic microorganisms and varies among habitats. Therefore, halotolerant microorganisms have developed versatile strategies to cope with saline stress. Based on the findings of co-occurrence analysis, possible explanations for mechanisms resulting in different salt tolerances among six strains are discussed above, which provided hypotheses for further investigations. Moreover, among the highly co-occurred clusters, there are several uncharacterized or hypothetical proteins (Table 2), which may contribute to halotolerance. It should be noted that the genes related to resistance to salts other than sodium chloride could also be discovered by co-occurrence analysis, since various salts co-exist in high ionic environments. For instance, ORFs of Cluster_2171 (co-occurrence as 0.81, Table 2) were annotated as divalent-cation tolerance protein CutA, which is required for copper tolerance in *E. coli* and affects tolerance levels to zinc, nickel, cobalt, and cadmium salts (Fong et al., 1995). This study sheds light on the mechanisms through which microorganisms cope with environmental stress. With the increasing number of isolated halotolerant strains and their genomes being sequenced, analyzing genome-wide co-occurrence between genetic diversity and physiological characteristics would expand the knowledge of the salinity adaptation strategies and provide comprehensive information on how microorganisms adapt to the environment, together with findings at the transcriptomic and proteomic levels.

Data availability statement

Publicly available datasets were analyzed in this study. This data can be found here: https://www.ncbi.nlm.nih.gov. Accession Numbers are as follows: GCF_009827455.1_ASM982745v1, GCF_009827545.1_ASM982754v1, GCF_009828095.1_ASM982809v1,

GCF_009827395.1_ASM982739v1, GCF_009828115.1_ASM982811v1, and GCF_009827615.1_ASM982761v1.

Author contributions

PZ contributed to study concept and design and performed data acquisition, analysis and visualization, and interpretation of results. PZ and Y-XB drafted the manuscript. LX, X-WX, and H-BS revised the manuscript. All authors contributed to the article and approved the submitted version.

Funding

This work was supported by grants from the National Science and Technology Fundamental Resources Investigation Program of China (2021FY100900), the Scientific Research Fund of the Second Institute of Oceanography, MNR (No. JZ1901 and JB2003), Natural Science Foundation of China (32000001), and the Oceanic Interdisciplinary Program of Shanghai Jiao Tong University (SL2022ZD108).

Conflict of interest

The authors declare that the research was conducted in the absence of any commercial or financial relationships that could be construed as a potential conflict of interest.

Publisher's note

All claims expressed in this article are solely those of the authors and do not necessarily represent those of their affiliated organizations, or those of the publisher, the editors and the reviewers. Any product that may be evaluated in this article, or claim that may be made by its manufacturer, is not guaranteed or endorsed by the publisher.

Supplementary material

The Supplementary material for this article can be found online at: https://www.frontiersin.org/articles/10.3389/fmicb.2023.1111472/full#supplementary-material

References

Anton, J. (2014). "Halotolerance" in *Encyclopedia of Astrobiology*. eds. R. Amils, M. Gargaud, J. C. Quintanilla, H. J. Cleaves, W. M. Irvine and D. Pintiet al. (Berlin, Heidelberg: Springer Berlin Heidelberg), 1–2.

Aravind, L., Anand, S., and Iyer, L. M. (2013). Novel autoproteolytic and DNA-damage sensing components in the bacterial SOS response and oxidized methylcytosine-induced eukaryotic DNA demethylation systems. *Biol. Direct* 8:20. doi: 10.1186/1745-6150-8-20

Chen, D. D., Fang, B. Z., Manzoor, A., Liu, Y. H., Li, L., Mohamad, O. A. A., et al. (2021). Revealing the salinity adaptation mechanism in halotolerant bacterium *Egicoccus halophilus* EGI 80432(T) by physiological analysis and comparative transcriptomics. *Appl. Microbiol. Biotechnol.* 105, 2497–2511. doi: 10.1007/s00253-021-11190-5

Chen, D. D., Tian, Y., Jiao, J. Y., Zhang, X. T., Zhang, Y. G., Dong, Z. Y., et al. (2020). Comparative genomics analysis of Nitriliruptoria reveals the genomic differences and salt adaptation strategies. *Extremophiles* 24, 249–264. doi: 10.1007/s00792-019-01150-3

Dlakic, M. (2000). Functionally unrelated signalling proteins contain a fold similar to Mg^{2+}–dependent endonucleases. *Trends Biochem. Sci.* 25, 272–273. doi: 10.1016/s0968-0004(00)01582-6

Fong, S.-T., Camakaris, J., and Lee, B. T. O. (1995). Molecular genetics of a chromosomal locus involved in copper tolerance in *Escherichia coli* K-12. *Mol. Microbiol.* 15, 1127–1137. doi: 10.1111/j.1365-2958.1995.tb02286.x

Fralliciardi, J., Melcr, J., Siginou, P., Marrink, S. J., and Poolman, B. (2022). Membrane thickness, lipid phase and sterol type are determining factors in the permeability of membranes to small solutes. *Nat. Commun.* 13:1605. doi: 10.1038/s41467-022-29272-x

Graziani, Y., and Livne, A. (1972). Water permeability of bilayer lipid membranes: sterol-lipid interaction. *J. Membr. Biol.* 7, 275–284. doi: 10.1007/BF01867920

Harris, R., and Wen, S. (2012). Review: Taurine: A "very essential" amino acid. *Mol Vis.* 18, 2673–2686.

Jeong, S. H., Jin, H. M., Lee, H. J., and Jeon, C. O. (2013). *Altererythrobacter gangjinensis* sp. nov., a marine bacterium isolated from a tidal flat. *Int. J. Syst. Evol. Microbiol.* 63, 971–976. doi: 10.1099/ijs.0.039024-0

Jo, E., Hwang, S., and Cha, J. (2022). Transcriptome analysis of Halotolerant *Staphylococcus saprophyticus* isolated from Korean fermented shrimp. *Foods* 11:524. doi: 10.3390/foods11040524

Jung, Y. T., Park, S., Lee, J. S., and Yoon, J. H. (2014). *Altererythrobacter aestiaquae* sp. nov., isolated from seawater. *Int. J. Syst. Evol. Microbiol.* 64, 3943–3949. doi: 10.1099/ijs.0.066639-0

Khaleque, H. N., Gonzalez, C., Shafique, R., Kaksonen, A. H., Holmes, D. S., and Watkin, E. L. J. (2019). Uncovering the mechanisms of Halotolerance in the extremely acidophilic members of the *Acidihalobacter* genus through comparative genome analysis. *Front. Microbiol.* 10:155. doi: 10.3389/fmicb.2019.00155

Kim, J. H., Yoon, J. H., and Kim, W. (2016). *Altererythrobacter sediminis* sp. nov., isolated from lagoon sediments. *Int. J. Syst. Evol. Microbiol.* 66, 5424–5429. doi: 10.1099/ijsem.0.001535

Kiran, M. D., Akiyoshi, D. E., Giacometti, A., Cirioni, O., Scalise, G., and Balaban, N. (2009). OpuC—an ABC transporter that is associated with *Staphylococcus aureus* pathogenesis. *Int. J. Artif. Organs* 32, 600–610. doi: 10.1177/039139880903200909

Kolly, G. S., Mukherjee, R., Kilacskova, E., Abriata, L. A., Raccaud, M., Blasko, J., et al. (2015). GtrA protein Rv3789 is required for Arabinosylation of Arabinogalactan in *Mycobacterium tuberculosis*. *J. Bacteriol.* 197, 3686–3697. doi: 10.1128/JB.00628-15

Larimer, C. M., Slavnic, D., Pitstick, L. D., and Green, J. M. (2014). Comparison of substrate specificity of *Escherichia coli* p-Aminobenzoyl-glutamate hydrolase with *Pseudomonas* Carboxypeptidase G. *Adv. Enzyme Res.* 2, 39–48. doi: 10.4236/aer.2014.21004

Lee, J. Y., and Kim, D. H. (2022). Genomic analysis of Halotolerant bacterial strains *Martelella soudanensis* NC18(T) and NC20. *J. Microbiol. Biotechnol.* 32, 1427–1434. doi: 10.4014/jmb.2208.08011

Liu, A., Xue, Q. J., Li, S. G., and Zhang, Y. J. (2021a). Corrigendum: *Pontixanthobacter rizhaonensis* sp. nov., a marine bacterium isolated from surface seawater of the Yellow Sea, and the proposal of *Pseudopontixanthobacter* gen. Nov., *Pseudopontixanthobacter confluentis* comb. nov. and *Pseudopontixanthobacter sediminis* comb. nov. *Int. J. Syst. Evol. Microbiol.* 71:004931. doi: 10.1099/ijsem.0.004931

Liu, A., Xue, Q. J., Li, S. G., and Zhang, Y. J. (2021b). *Pontixanthobacter rizhaonensis* sp. nov., a marine bacterium isolated from surface seawater of the Yellow Sea, and proposal of *Pseudopontixanthobacter* gen. Nov., *Pseudopontixanthobacter confluentis* comb. nov. and *Pseudopontixanthobacter sediminis* comb. nov. *Int. J. Syst. Evol. Microbiol.* 71:004780. doi: 10.1099/ijsem.0.004780

Liu, A., Zhang, Y. J., Xue, Q. J., Wang, H., Yang, Y. Y., Du, F., et al. (2020). *Litorilituus lipolyticus* sp. nov., isolated from intertidal sand of the Yellow Sea in China, and emended description of *Colwellia asteriadis*. *Antonie Van Leeuwenhoek* 113, 449–458. doi: 10.1007/s10482-019-01355-8

McLaggan, D., and Epstein, W. (1991). *Escherichia coli* accumulates the eukaryotic osmolyte taurine at high osmolarity. *FEMS Microbiol. Lett.* 81, 209–213. doi: 10.1016/0378-1097(91)90304-s

Ming, T., Geng, L., Feng, Y., Lu, C., Zhou, J., Li, Y., et al. (2019). iTRAQ-based quantitative proteomic profiling of *Staphylococcus aureus* under different osmotic stress conditions. *Front. Microbiol.* 10:1082. doi: 10.3389/fmicb.2019.01082

Mosier, A. C., Justice, N. B., Bowen, B. P., Baran, R., Thomas, B. C., Northen, T. R., et al. (2013). Metabolites associated with adaptation of microorganisms to an acidophilic, metal-rich environment identified by stable-isotope-enabled metabolomics. *MBio* 4, e00484–e00412. doi: 10.1128/mBio.00484-12

Niehaus, T. D., Elbadawi-Sidhu, M., de Crecy-Lagard, V., Fiehn, O., and Hanson, A. D. (2017). Discovery of a widespread prokaryotic 5-oxoprolinase that was hiding in plain sight. *J. Biol. Chem.* 292, 16360–16367. doi: 10.1074/jbc.M117.805028

Novello, G., Gamalero, E., Massa, N., Cesaro, P., Lingua, G., Todeschini, V., et al. (2022). Proteome and physiological characterization of Halotolerant nodule Endophytes: the case of *Rahnella aquatilis* and *Serratia plymuthica*. *Microorganisms* 10:890. doi: 10.3390/microorganisms10050890

Park, S., Jung, Y. T., Choi, S. J., and Yoon, J. H. (2017). *Altererythrobacter aquaemixtae* sp. nov., isolated from the junction between the ocean and a freshwater spring. *Int. J. Syst. Evol. Microbiol.* 67, 3446–3451. doi: 10.1099/ijsem.0.002136

Richards, N. G., and Kilberg, M. S. (2006). Asparagine synthetase chemotherapy. *Annu. Rev. Biochem.* 75, 629–654. doi: 10.1146/annurev.biochem.75.103004.142520

Rubiano-Labrador, C., Bland, C., Miotello, G., Armengaud, J., and Baena, S. (2015). Salt stress induced changes in the exoproteome of the Halotolerant bacterium *Tistlia consotensis* deciphered by Proteogenomics. *PLoS One* 10:e0135065. doi: 10.1371/journal.pone.0135065

Samir, K. M., and Kanak, R. S. (1997). The correlation between salt tolerance and extracellular Polysaccharid. *Microbes Environ.* 12, 9–13.

Schmidt, S., Pfluger, K., Kogl, S., Spanheimer, R., and Muller, V. (2007). The salt-induced ABC transporter Ota of the methanogenic archaeon *Methanosarcina mazei* Go1 is a glycine betaine transporter. *FEMS Microbiol. Lett.* 277, 44–49. doi: 10.1111/j.1574-6968.2007.00938.x

Shinagawa, H. (1996). SOS response as an adaptive response to DNA damage in prokaryotes. *EXS* 77, 221–235. doi: 10.1007/978-3-0348-9088-5_14

Snipen, L., and Liland, K. H. (2015). Micropan: an R-package for microbial pan-genomics. *BMC Bioinf.* 16:79. doi: 10.1186/s12859-015-0517-0

Soussi, M., Santamaria, M., Ocana, A., and Lluch, C. (2001). Effects of salinity on protein and lipopolysaccharide pattern in a salt-tolerant strain of *Mesorhizobium ciceri*. *J. Appl. Microbiol.* 90, 476–481. doi: 10.1046/j.1365-2672.2001.01269.x

VanderPloeg, J. R., Weiss, M. A., Saller, E., Nashimoto, H., Saito, N., Kertesz, M. A., et al. (1996). Identification of sulfate starvation-regulated genes in *Escherichia coli*: a gene cluster involved in the utilization of taurine as a sulfur source. *J. Bacteriol.* 178, 5438–5446. doi: 10.1128/jb.178.18.5438-5446.1996

Verheul, A., Glaasker, E., Poolman, B., and Abee, T. (1997). Betaine and L-carnitine transport by *Listeria monocytogenes* Scott a in response to osmotic signals. *J. Bacteriol.* 179, 6979–6985. doi: 10.1128/jb.179.22.6979-6985.1997

Xu, L., Sun, C., Fang, C., Oren, A., and Xu, X. W. (2020). Genomic-based taxonomic classification of the family *Erythrobacteraceae*. *Int. J. Syst. Evol. Microbiol.* 70, 4470–4495. doi: 10.1099/ijsem.0.004293

Yi, L., Velasquez, M. S., Holler, T. P., and Woodard, R. W. (2011). A simple assay for 3-deoxy-d-manno-octulosonate cytidylyltransferase and its use as a pathway screen. *Anal. Biochem.* 416, 152–158. doi: 10.1016/j.ab.2011.05.022

Yoon, J. H., Kang, K. H., Yeo, S. H., and Oh, T. K. (2005). *Erythrobacter luteolus* sp. nov., isolated from a tidal flat of the Yellow Sea in Korea. *Int. J. Syst. Evol. Microbiol.* 55, 1167–1170. doi: 10.1099/ijs.0.63522-0

Ziegler, C., Bremer, E., and Kramer, R. (2010). The BCCT family of carriers: from physiology to crystal structure. *Mol. Microbiol.* 78, 13–34. doi: 10.1111/j.1365-2958.2010.07332.x

frontiers | Frontiers in Microbiology

TYPE Review
PUBLISHED 31 March 2023
DOI 10.3389/fmicb.2023.1113540

OPEN ACCESS

EDITED BY
Philippe M. Oger,
UMR 5240 Microbiologie, Adaptation et Pathogenie (MAP), France

REVIEWED BY
Salma Mukhtar,
The Connecticut Agricultural Experiment Station, United States
Judith Maria Braganca,
Birla Institute of Technology and Science, India

*CORRESPONDENCE
Ranjith Kumavath
✉ rnkumavath@gmail.com;
✉ rnkumavath@pondiuni.ac.in
Rosa María Martínez-Espinosa
✉ rosa.martinez@ua.es

†These authors have contributed equally to this work

SPECIALTY SECTION
This article was submitted to Extreme Microbiology, a section of the journal Frontiers in Microbiology

RECEIVED 01 December 2022
ACCEPTED 14 March 2023
PUBLISHED 31 March 2023

CITATION
Moopantakath J, Imchen M, Anju VT, Busi S, Dyavaiah M, Martínez-Espinosa RM and Kumavath R (2023) Bioactive molecules from haloarchaea: Scope and prospects for industrial and therapeutic applications. *Front. Microbiol.* 14:1113540. doi: 10.3389/fmicb.2023.1113540

Bioactive molecules from haloarchaea: Scope and prospects for industrial and therapeutic applications

Jamseel Moopantakath[1†], Madangchanok Imchen[2], V. T. Anju[3†], Siddhardha Busi[2], Madhu Dyavaiah[3], Rosa María Martínez-Espinosa[4,5*] and Ranjith Kumavath[1,6*]

[1]Department of Genomic Science, School of Biological Sciences, Central University of Kerala, Kerala, India, [2]Department of Microbiology, School of Life Sciences, Pondicherry University, Puducherry, India, [3]Department of Biochemistry and Molecular Biology, School of Life Sciences, Pondicherry University, Puducherry, India, [4]Biochemistry, Molecular Biology, Edaphology and Agricultural Chemistry Department, Faculty of Sciences, University of Alicante, Alicante, Spain, [5]Multidisciplinary Institute for Environmental Studies "Ramón Margalef", University of Alicante, Alicante, Spain, [6]Department of Biotechnology, School of Life Sciences, Pondicherry University, Puducherry, India

Marine environments and salty inland ecosystems encompass various environmental conditions, such as extremes of temperature, salinity, pH, pressure, altitude, dry conditions, and nutrient scarcity. The extremely halophilic archaea (also called haloarchaea) are a group of microorganisms requiring high salt concentrations (2–6 M NaCl) for optimal growth. Haloarchaea have different metabolic adaptations to withstand these extreme conditions. Among the adaptations, several vesicles, granules, primary and secondary metabolites are produced that are highly significant in biotechnology, such as carotenoids, halocins, enzymes, and granules of polyhydroxyalkanoates (PHAs). Among halophilic enzymes, reductases play a significant role in the textile industry and the degradation of hydrocarbon compounds. Enzymes like dehydrogenases, glycosyl hydrolases, lipases, esterases, and proteases can also be used in several industrial procedures. More recently, several studies stated that carotenoids, gas vacuoles, and liposomes produced by haloarchaea have specific applications in medicine and pharmacy. Additionally, the production of biodegradable and biocompatible polymers by haloarchaea to store carbon makes them potent candidates to be used as cell factories in the industrial production of bioplastics. Furthermore, some haloarchaeal species can synthesize nanoparticles during heavy metal detoxification, thus shedding light on a new approach to producing nanoparticles on a large scale. Recent studies also highlight that exopolysaccharides from haloarchaea can bind the SARS-CoV-2 spike protein. This review explores the potential of haloarchaea in the industry and biotechnology as cellular factories to upscale the production of diverse bioactive compounds.

KEYWORDS

haloarchaea, nanoparticles, antimicrobial compound, anticancer, antioxidants, carotenoids, halocins

1. Introduction: Haloarchaeal diversity and ecology

Microorganisms possess several mechanisms to acclimatize to stress conditions that influence growth and survival in saline environments. Halophiles are microbes that can survive such saline conditions from low to high saturation points. There are different stress proteins and strategies that halophiles adapt to counteract stressful factors such as ions, temperature, pH, and UV radiation. Prokaryotic halophiles have attracted the attention of researchers worldwide because of their distinctive features, ease of manipulation, lesser space requirements for cultivation, and the production of diverse metabolites compared to plants or eukaryotic algae (Torregrosa-Crespo et al., 2017; Dutta and Bandopadhyay, 2022). A significant group of halophilic archaea, represented under the halobacteria class, are tolerant to extreme saline environments. These environments include salt lakes, estuaries, rivers, mangrove swamps, open seawater, coastal waters, salt lakes, estuaries, and salt deserts. Halobacterial class constitutes a wide range of genera (**Figure 1**) – *Salarchaeum, Halobiforma, Natronolimnobius, Halopelagius, Halogranum, Halonotius, Haladaptatus, Natronococcus, Haloferax, Halococcus, Haloalcalophilium, Halorubrum, Halorhabdus, Halorussus, Halopiger, Halomarina, Natronoarchaeum, Halobellus*, *Natrialba Halobaculum, Haloplanus, Halostagnicola, Halorientalis, Natronomonas, Natrialba, Natronobacterium, Natronorubrum, Haloarcula, Halobacterium, Haloterrigena, Natrinema, Halogeometricum, Halalkalicoccus, Haloquadratum, Halogeometricum, Natronorubrum, Halomicrobium, Halolamina, Halovivax, Halarchaeum,* and *Halosimplex* (Cui and Dyall-Smith, 2021).

Considering the difficulties found by researchers to obtain pure cultures of extremophilic microorganisms (including halophilic archaea) from environmental samples, and consequently to know the microbial biodiversity in those samples, recent advances in omic-based approaches have contributed to a better understanding of haloarchaeal biodiversity. Particularly, metagenomic analysis has been used to overcome this limitation. Metagenomic analysis of environmental samples from the Dead Sea, RedSea, Gulf of Cambay, Mediterranean Sea, Sundarbans mangrove forest, Karak Salt Mine, and Pannonian Steppe, revealed the predominance of haloarchaeal genera in the natural environment, including *Haloarcula*, *Halorubrum*, and *Halorhabdus* (Oh et al., 2010; Rhodes et al., 2012; Somboonna et al., 2012; Fernández et al., 2014; Bhattacharyya et al., 2015; Keshri et al., 2015; Behzad et al., 2016; Szabó et al., 2017; Haldar and Nazareth, 2018; Osman et al., 2019; Cecil et al., 2020). Similarly, a global metagenomic meta-analysis revealed the dominance of *Haloarcula* and *Haloquandratum* sp., in the seacoast (Moopantakath et al., 2021). The biogeography of haloarchaea also varies based on the biosystems. For instance, the *Haloferax* genus is highly dominant in seashores and island samples and estuaries, while the *Natrialba* genus is predominant in rivers, mangroves, and lakes (Hegazy et al., 2020; Moopantakath et al., 2020; Cho et al., 2021). Thus, the prevalence of halophilic microorganisms in general, and particularly of haloarchaea, is highly dependent on the environment, geography, and physicochemical parameters like salinity, pH, oxygen availability and sun radiation, among other factors (Ventosa, 2006; Mani et al., 2020). As an example, recent whole genome sequencing studies revealed that autotrophic haloarchaea are highly abundant in coastal environments, probably due to salinity and direct sunlight exposure (Moopantakath et al., 2021). These environments display unique features and salt deposition phenomena that contribute to the increase of some haloarchaeal populations requiring extremely high concentrations for optimal growth.

Environmental degradation, such as the release of industrial chemicals into the coastal environment, is also a major factor in pollution and shoreline contamination (Lu et al., 2018) and in microbial biodiversity. Nonetheless, the microbial community plays a significant role in the polluted site, and the unique metabolic features of haloarchaea contribute to the homeostasis of these environments. *Halorhabdus* and *Natrinema* sp., have been reported to degrade xylan and produce halocin (antimicrobial peptide), respectively (Begemann et al., 2011; Besse et al., 2017). Similarly, recent advances in the metagenomic analysis have revealed that haloarchaea, such as *Haloferax*, *Haladaptatus*, *Natrialba,* etc., participate in maintaining the biogeochemical processes in coastal ecosystems (Osman et al., 2019). Some haloarchaea can carry out interesting metabolic processes from an industrial point of view; examples: sulfur reduction by *Natranaeroarchaeum sulfidigenes* (Sorokin et al., 2022), nitrification by *Haloarcula, Halolamina*, and *Halobacterium* (Wei et al., 2022), phosphorus solubilization by *Haloarcula*, *Halobacterium, Halococcus*, and *Haloferax* (Yadav et al., 2015) or denitrification by *Haloarcula* or *Haloferax* (Miralles-Robledillo et al., 2021).

In summary, haloarchaea exhibit diverse metabolic pathways and biological activities of interest for biotechnological purposes. They constitute predominant microbial communities in salty ecosystems, which are widespread worldwide. For example, *Haloarcula*, *Haloferax*, *and Halogeometricum* sp., can be isolated from saline sediments across the world, such as from Spanish coastal and inland salted ponds (Martínez et al., 2022), Algerian salt lakes, Indian salt pans, Verkhnekamsk deposit etc., and exhibit several biological activities, including the production of carotenoid pigments (Das et al., 2019; Sahli et al., 2022). Besides, many more ecosystems characterized by their high salt concentrations are far from known from a microbiological point of view (i.e., saline mines in Senegal). This review aims to summarize new advances in the knowledge of biological applications of halophilic archaea and the synthesis of secondary metabolites thus contributing to the design of new biotech processes low cost and environmentally friendly based on the use of haloarchaea as cellular factories.

1.1. Haloarchaeal strategies to cope with stress

Haloarchaea can survive in stress conditions such as salinity, ultraviolet (UV), high concentration of ions, high temperature, and extreme pH values. In addition, continuous heavy rain or change in temperature can lead to a dramatic shift in the salinity, causing significant pressure on haloarchaea and promoting the switching on of molecular machinery to be better adapted to these environmental changes (Griffiths and Philippot, 2013; Thombre et al., 2016). Halophiles inhabiting saline environments can exist at different salt concentrations, mainly above 1 M. Based on

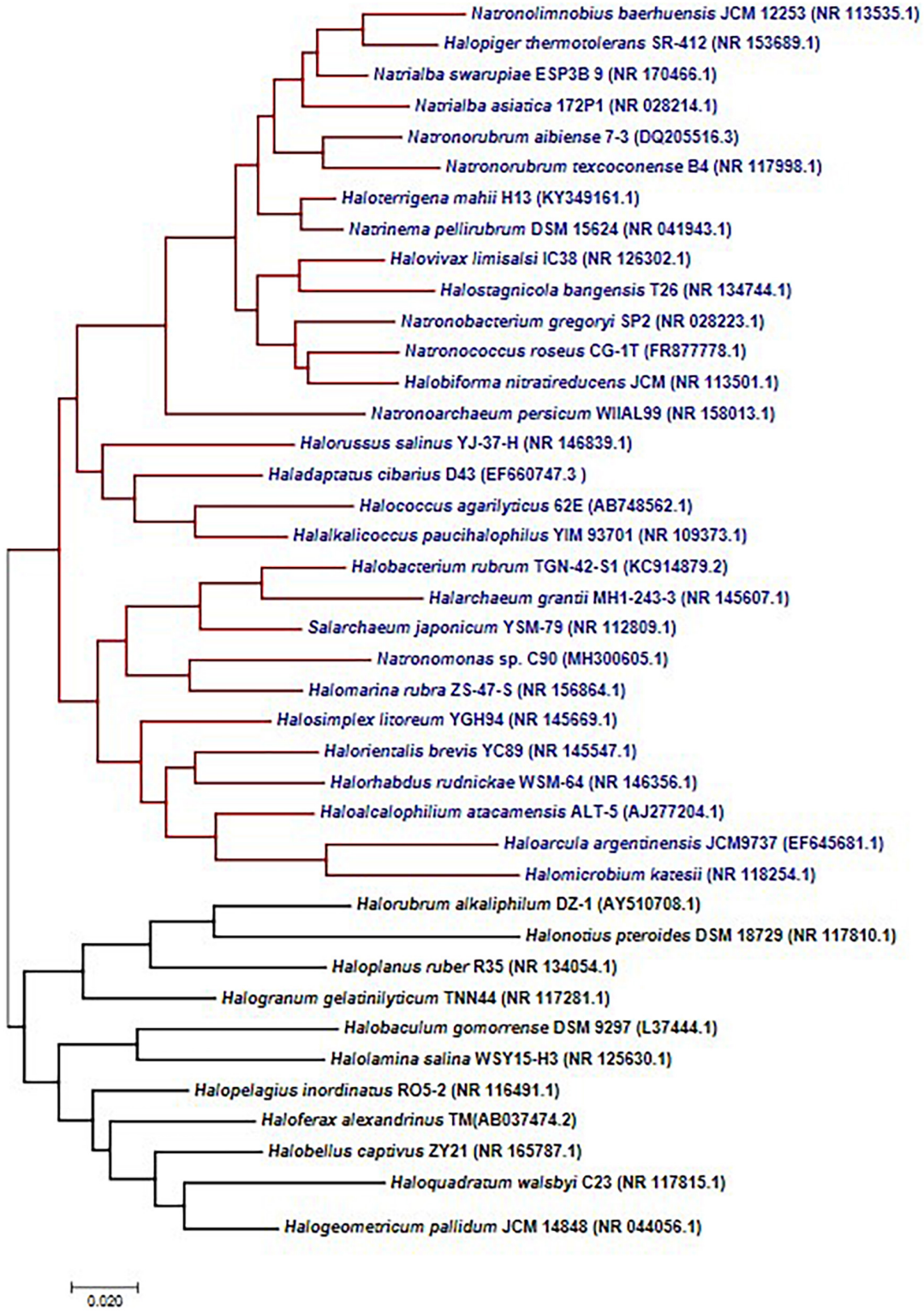

FIGURE 1
Haloarchaeal 16s RNA gene diversity. Phylogenetic tree constructed using the maximum likelihood methods suggests two separate clades, and most of the organisms are represented under a single clade.

the optimum salinity requirements, halophiles can be classified into slight halophiles (0.34 to 0.85 M), moderate halophiles (0.85 to 3.4 M), and extreme halophiles (3.4 M to saturation point) (Abaramak et al., 2020). Haloarchaea requires ~10 to 35% w/v (1.71 to 6 M) of salt concentration for optimum growth. Interestingly, haloarchaea are the dominant class of microbes when the salt concentration increases above 16% w/v (2.74 M) (Oren, 2002b; Andrei et al., 2012).

Haloarchaea evolved with several metabolic adaptations to survive different stresses among which salt stress is one of the most significant affecting the protein structures and therefore, their biological activities (Britton et al., 2006). Thus, most of their proteins are salt dependent for optimal enzymatic activity and stability. The unique feature of these proteins is due to the presence of acidic amino acids on the surface (Esclapez et al., 2007). The negatively charged acidic amino acids on the surface develop into a cluster form and interact with networks of hydrated ions. Consequently, this feature avoids the precipitation of haloarchaeal proteins under high KCl/NaCl concentrations. Also, proteins exhibit less hydrophobic interactions owing to the limited content of hydrophilic amino acids such as lysine. Hence, a lack of optimum salt concentration may cause the unfolding of proteins owing to the presence of negatively charged amino acids (Kennedy et al., 2001; Oren, 2002a; Zafrilla et al., 2010; Andrei et al., 2012).

Some haloarchaea are called polyextremophiles owing to their ability to respond to multiple extreme conditions (Das and Dash, 2018). They can adjust to osmotic stress and survive at low water activity and desiccation. The presence of high salt concentrations may reduce water activity from 1 to 0.75. Further, salt-in and low-salt-in are the two methods adopted by haloarchaea to resist osmotic stress. In the salt-in method, K^+ is accumulated inside cells with the help of protein transport and ion pumps (Schäfer et al., 1996; Oren, 2013). *Halobacterium* sp., NRC-1 utilizes the salt-in strategy with the help of potassium transporters and sodium efflux pumps (Ng et al., 2000).

In the low-salt-in method, some organisms produce compatible and low molecular-weight solutes to adapt to osmotic stress (Grant et al., 2004). The compatible solutes such as amino acids, ectoines, thetines, polyols, betaines, derivatives of sugar, and glutamine amide are accumulated in low concentration in the cytoplasm to tolerate osmotic stress (Matarredona et al., 2020). For instance, solutes like 2-sulphotrehalose, and glycine produced by *Natronobacterium* and *Natronococcus*, respectively, help in the low-salt process (Grant et al., 2004; Matarredona et al., 2020). The square-shaped haloarchaea, *Haloquadratum walsbyi*, carries a unique protein, halomucin, which helps to survive desiccation. The protein is glycosylated and sulfated to develop as a water-rich capsule around the archaea. The water-rich cloud formed around the cell protects it from surrounding desiccation or the presence of low water activity (Bolhuis et al., 2006; Dyall-Smith et al., 2011; Zenke et al., 2015).

Regarding stress due to temperature changes, haloarchaea can tolerate different temperature variations in saline environments thanks to the presence of heat shock proteins (e.g., chaperones and chaperonins). The molecular chaperones are involved in the folding or unfolding of proteins at extreme temperatures (Fenderson, 2006; Shukla, 2006; Coker et al., 2007). The most common heat shock proteins observed in haloarchaea are Hsp60 and 70 (Macario et al., 1999). The expression and synthesis of cold shock proteins, polar lipids, and gas vesicles in cold temperatures help to maintain homeostasis (Coker et al., 2007). Some haloarchaea, for example, *Haloferax,* produce thermoprotectans, such as glycoside hydrolases, to withstand high temperatures by promoting protein stabilization (Amin et al., 2021).

The ecosystems inhabited by haloarchaea are exposed to high sun radiation doses that cause UV irradiation and the formation of photoproducts and pyrimidine dimers in DNA. The photoreactivation process can remove these lesions with the help of photolyase expressed by haloarchaea. Haloarchaea has unique compounds that include rhodopsin which has a phototaxis mechanism. On the other hand, gas vesicles play a crucial role in light regulation and responses to oxygen availability changes (Jones and Baxter, 2017; Miralles-Robledillo et al., 2021). Response to UV irradiation also includes the downregulation of genes involved in the gas vesicle production to sink the cells below the water surface (Kottemann et al., 2005). Some haloarchaea, such as *Halorubrum lacusprofundi* and *Haloferax volcanii,* can withstand a wide range of pH. They can exist in both low-pH environments like acidic lakes and alkaline lakes (Mormile et al., 2009). In the case of *Halorubrum lacusprofundi*, *Haloferax volcanii*, and *Halobacterium* sp., residing in alkaline pH conditions, it has been described that several stress genes such as *hsp20* family, universal stress protein *uspA*, or *groEL* chaperone are upregulated. In contrast, *H. lacusprofundi* exhibited upregulation of *hlac3059* and *hlac3556* gene expression in acidic pH. Besides, they display dormancy-specific responses at acidic pH to survive in the environment (Moran-Reyna and Coker, 2014).

2. Biotechnological significance of haloarchaea

Several biotechnological-based processes can be benefited from the use of haloarchaea. Thus, the use of whole cells in wastewater treatments and bioremediation of brines and salty soils has been recently revealed as a promising tool. Hypersaline wastewater is a common byproduct of industrial processes. Hence, cost-effective treatment of hypersaline wastewater is necessary for sustainable development. Biological wastewater treatment has been considered a more economical approach, but mesophilic microorganisms used so far for this purpose can not be used in the biological treatment of polluted brines of wastewater containing high salt concentration. In this context, recent research findings revealed the role of haloarchaea in the treatment of salty wastewater and brine generated as final residues in water desalination plants (Li et al., 2021; Martínez et al., 2022). Haloarchaea can also degrade hydrocarbons; however, their degradation is more efficient for low molecular-weight hydrocarbons. The degradation of naphthalene, phenol, p-hydroxybenzoic acid, and 3-phenyl propionic acid, and oxychlorides like perchlorate or chlorate by haloarchaea also make it an attractive choice for wastewater treatment (Martínez-Espinosa et al., 2015; Mukherji et al., 2020; Li et al., 2021). Another interesting approach related to wastewater treatments is the removal of nitrogen to avoid eutrophication in the receiving water bodies and heavy metals to avoid global toxicity. Haloarchaea, such as *Haloferax mediterranei*, can use NO_3^- and NO_2^- as nitrogen sources for growth or as final electron acceptors instead of oxygen in an anaerobic respiratory process (denitrification). For example, *Haloferax mediterranei* encodes nitrate reductase (*nas*) and nitrite reductase (*nir*) that can perform assimilatory nitrate/nitrite reduction (Martínez-Espinosa et al., 2007), whilst Nar, NirK, Nor, and Nos encodes key enzymes in catalyzing the reactions involved in the process of denitrification (Bernabeu et al., 2021). Regarding heavy metals, several recent studies have demonstrated that some haloarchaeal species can grow in the presence of heavy metals at concentrations that are

toxic for most living beings. In some cases, because of cellular growth, heavy metals are accumulated, modified or bioassimilated. Molecular machinery for the potential removal of cooper and cadmium has also been identified from many haloarchaeal species (Vera-Bernal and Martínez-Espinosa, 2021; Llorca and Martínez-Espinosa, 2022). In other cases, haloarchaea growing in the presence of heavy metals can also synthesize nanoparticles (NPs) from wastewater polluted with cadmium, arsenic, and zinc (Taran et al., 2017; Li et al., 2021; Gaonkar and Furtado, 2022). Haloarchaea have various mechanisms to tolerate the arsenate metals using minichromosomes/megaplasmids (*arsADRC* gene cluster) in the *Halobacterium* species (Wang et al., 2004; Voica et al., 2016). The zinc tolerance mechanism was found due to the presence of physical bioabsorption, ion exchange and intracellular accumulation which can be used for the various biological process inside the cell (Popescu and Dumitru, 2009; Williams et al., 2013; Salgaonkar et al., 2016). Similarly, cadmium also plays a crucial aid in intracellular metabolic functions so cadmium can be tolerated inside the cell without stress (Vera-Bernal and Martínez-Espinosa, 2021).

Another interesting biotechnological application is related to the enzymes from haloarchaea. They exhibit increased tolerance, not only to salinity but also to pH, pressure, temperature, etc. Haloenzymes have several advantages, such as minimum steps in purification, sterilization, and cost-effectiveness (Amoozegar et al., 2017). Haloenzymes such as lipase and alcohol dehydrogenase from *Haloferax volcanii* and *Haloarcula* sp., G41, respectively, have been immobilized successfully for increased activity (Alsafadi and Paradisi, 2014; Li and Yu, 2014). Saline-tolerant lipases and esterases like those described from *Haloarcula marismortui* and *Natronococcus* sp., TC6 are essential enzymes in several biotechnological applications such as biofuel, detergent, textile, etc (Camacho et al., 2009; Del Campo et al., 2015).

The haloarchaeal membrane protein bacteriorhodopsin, initially discovered from *Halobacterium salinarum*, is highly stable to thermal and photochemical stress. Bacteriorhodopsin can sense light and convert it into electrical signals (Singh and Singh, 2017). Bacteriorhodopsin from haloarchaea has also found applications in biosensors and artificial retinas (**Figure 2**; Amoozegar et al., 2017). The gas vesicles mentioned in section "1. Introduction: haloarchaeal diversity and ecology" have applications in drug delivery systems and vaccine development (Cánovas et al., 2021). Meanwhile, poly-β-hydroxy-alkanoates (PHAs) produced by haloarchaea, such as *Haloferax mediterranei*, are considered an alternative to plastics produced from petroleum and in medical applications owing to their biocompatibility (Salgaonkar et al., 2013; Li et al., 2021). Thus, PHA can be synthesized using these microorganisms as biofactories thanks to cheaper procedures in which the biomass downstream process as well as the purification process of the biopolymer can be done with single steps (Simó-Cabrera et al., 2021). PHA produced by various materials such as residues from food and agriculture products can be synthesized into PHA with a help of haloarchaea (Quillaguamán et al., 2010). Genomic insights of halophiles such as *Halonotius terrestris* sp., nov. and *Halonotius roseus* sp., nov. have been recently delineated and found to encode the complete biosynthetic genes for the biosynthesis of cobalamin (vitamin B12) (Durán-Viseras et al., 2019).

Halophiles produce saline-tolerant proteins and metabolites, such as carotenoids, which assist in tolerance toward salinity. Haloarchaeal carotenoids have industrial interest due to their antioxidant, anticancer, antimicrobial, anti-inflammatory, food colorant, and several other biomedical applications (Verma et al., 2020). Bacterioruberin is also commonly used in cosmetics and drug encapsulation (Serrano et al., 2022). Haloarchaea have been extensively explored for bioactive metabolites with anticancer, antimicrobial, and antioxidant activities (**Table 1**). Among the several haloarchaeal secondary metabolites, carotenoids gained attention due to their multi-faced applications in cosmetics, food, and biomedical sectors (Serrano et al., 2022). Carotenoids have multiple roles in bacteria, plants, and archaea. Carotenoid helps photosynthetic plants and microbes to increase light absorption in the blue-green region through the singlet-singlet energy transfer (Hashimoto et al., 2015). It also has photoprotective effects against excessive light and reactive oxygen species through the triplet energy transfer of chlorophylls to carotenoids (Maoka, 2020). They are crucial in structural stabilization and render tolerance to hypersalinity.

Due to the advancements in culture-based methods and metagenomics, the identification and discovery of novel species of haloarchaea become a continuous process. Recently, 12 haloarchaeal isolates were isolated from Tamil Nadu (India), out of which nine isolates were novel. Interestingly, all of the isolates produced carotenoids (Verma et al., 2020). Haloarchaea has an inherent molecule known as bacterioruberin, which is found in most haloarchaea (Nagar et al., 2022). Similarly, novel species under the genus *Halorubrum*, isolated from South Korea, produced C_{50} carotenoid (bacterioruberin), having a strong antioxidant activity (Hwang et al., 2022). Likewise, carotenoids from novel *Haloarcula* sp., and *Halorubrum* sp., strains were isolated from the Atacama Desert (Lizama et al., 2021). Large-scale whole genome ($n = 68$) analysis suggested that haloarchaea has a wide diversity of carotenoid biosynthetic genes (Serrano et al., 2022), suggesting that haloarchaeal species could be a reservoir of carotenoid derivatives.

2.1. Anticancer compounds

Haloarchaea and their metabolic products are getting more attention for the treatment of several cancers. Carotenoid pigment from *Halobacterium halobium,* isolated from a saltern in Tunisia, exhibited anticancer activity against the HepG2 cell line (Abbes et al., 2013). In addition, the carotenoid pigment of *Halogeometricum limi*, at a concentration of 720 μg/l, exhibited ~23% anticancer activity against HepG2 cells (Hou and Cui, 2018). Similarly, high carotenoid-producing (0.98 g/l) haloarchaea i.e., *Natrialba* sp., M6, which thrives at 25% NaCl and a pH of 10.0, exhibited 50% anticancer activity against MCF-7, HepG2, and HeLa cells at low concentrations (<39 μg/ml) (Hegazy et al., 2020).

Compared to β-carotene, bacterioruberin has a superior antihemolytic and cytotoxic effect against HepG2 cells (Hou and Cui, 2018). *Natrialba* sp., M6, under the phylum Euryarchaeota, isolated from Egypt, produced C_{50} carotenoid as the predominant compound (Hegazy et al., 2020). The pigment had a higher selectivity toward cancer cells than the standard chemotherapeutic agent 5-fluorouracil. It is active against breast, liver, and colon

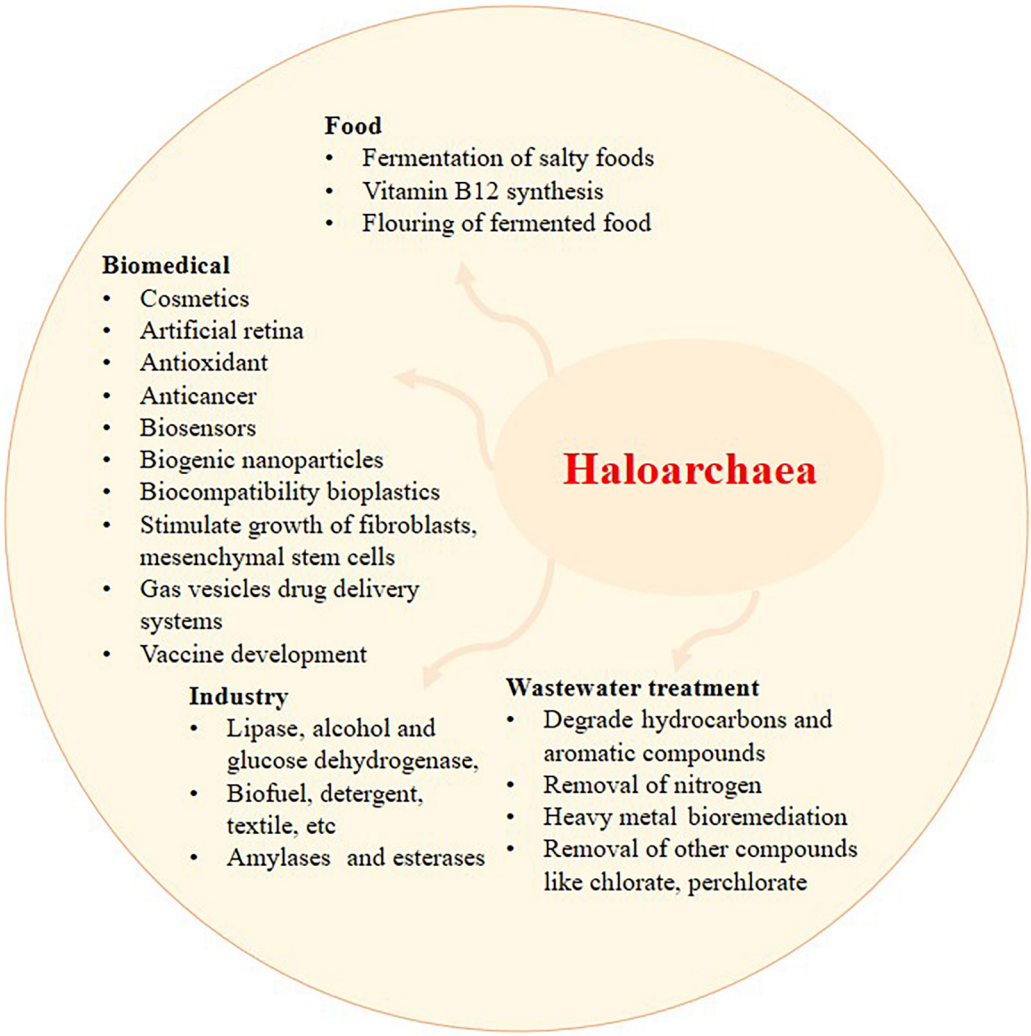

FIGURE 2
The application of haloarchaea and its metabolites. Recent exploration of haloarchaea and its metabolites has shed light on their potential applications in wastewater treatment, biomedical, food, and industrial sectors. Haloarchaea is a preferred source of haloenzymes since the growth and purification of enzymes involve minimal steps and are prone to less contamination.

cancer cells. On the other hand, C_{50} carotenoid bacterioruberin with dexamethasone reduced the release of TNF-α and IL-8, reversed the inflammation-induced morphological changes of macrophage, and had a potential role as an intestinal barrier repairing agent (Higa et al., 2020).

2.2. Antimicrobial compounds

Microorganisms causing infectious diseases evolve and acquire antimicrobial resistance continuously. Thus, alternative antimicrobials are required to meet emerging health challenges. Haloarchaeal carotenoids as antimicrobials have been explored less compared to other carotenoids. However, the potential of haloarchaeal carotenoids as antimicrobials was demonstrated against several pathogens (Gómez-Villegas et al., 2020). Recent reports have shown that carotenoids from *Halogeometricum* sp., ME3, *Haloarcula* sp., BT9 and *Haloferax* sp., ME16 have antimicrobial activity against *Vibrio anguillarum*, *Pseudomonas aeruginosa,* and *Pseudomonas anguilliseptica,* respectively (Sahli et al., 2022).

Haloarchaea produce halocins with potent antimicrobial activity. Halocin from the supernatant of *Haloferax larsenii* HA1 exhibits potent antimicrobial activity (Kumar and Tiwari, 2017). Previous works on halocines from haloarchaea suggested that the antimicrobial action of halocins could be related to processes of competition between different species for niche, food, or space. For instance, *Halobacterium salinarum* ETD5, isolated from the solar saltern of Sfax, Tunisia, exhibited antagonistic activity against haloarchaea of similar niches such as *Halorubrum* sp (strain ETD1, ETD2, ETD6, ETR7), *Halorubrum chaoviator* sp (strains ETD3, ETR14, and SS1R17), and *Halobacterium salinarum* ETD19 (Ghanmi et al., 2016). Furthermore, the C50 carotenoid pigment from *Natrialba* sp., M6 also exhibited promising potential in the elimination of hepatitis C virus (HCV) and hepatitis B virus (HBV) from human blood mononuclear cells suggesting its strong antiviral activity (Hegazy et al., 2020).

TABLE 1 Overview of the biological application of haloarchaea and their compounds: anticancer, antioxidant and antimicrobial activities of the metabolites derived from haloarchaea.

Haloarchaea	Compounds	Complementary information	References
Anticancer activity			
Halobacterium halobium	Carotenoid	Antiproliferative activities (>0.5 μm)	Abbes et al., 2013
Halogeometricum. limi	Carotenoid	HepG2 cells, 23% at a high concentration of 720 μg/L (~1 μm)	Hou and Cui, 2018
Halobiforma sp.,	Superparamagnetic iron oxide nanoparticles	Localized hyperthermia cancer therapy	Salem et al., 2020
Haloferax mediterranei	Carotenoid	HER2-positive or triple-negative breast cancer (TNBC)	Giani and Martínez-Espinosa, 2020
Natrialba sp., M6	Carotenoid	Normal human lung fibroblast cells (Wi-38) 50 and 100% cell viability.	Hegazy et al., 2020
		50% cell death for Caco-2 (colon cancer line),	
		MCF7 (breast cancer cell line)	
		HepG2 (liver cancer line)	
		HeLa (cervical cancer cell line)	
Antioxidant activities			
Haloferax	Carotenoid	DPPH:IC_{50} = 56.69 μg/ml,	Sahli et al., 2022
		ABTS:IC_{50} = 39.66 μg/ml	
Halogeometricum	Carotenoid	DPPH:IC_{50} = 170.4 μg/ml,	
		ABTS:IC_{50} = 136.43 μg/ml	
Genetically modified *Haloferax volcanii* strain (HVLON3)	Bacterioruberin	EC_{50} yielded 4.5 × 10^{-5} mol/l	Zalazar et al., 2019
H. Hispanica hm1	Carotenoid	ABTS (88%; IC_{50} = 3.89 μg/ml), FRP assay (82%; EC_{50} = 3.12 μg/ml)	Gómez-Villegas et al., 2020
Hfx. Volcanic, Hgn. rubrum, and Hpl. coordinates	Carotenoid	DPPH radical scavenging activity > 80% at 10 ug/ml	Hou and Cui, 2018
Haloferax mediterranei	Carotenoid	Oxidative stress	Giani et al., 2021
Haloferax mediterranei	Carotenoid	Antioxidant, antiglycemic, and antilipidemic activities	Giani et al., 2022
Antimicrobial activities			
Halogeometricum sp., ME3, *Haloarcula* sp., BT9, *Haloferax* sp., ME16	Carotenoid	*Vibrio anguillarum*, *Pseudomonas aeruginosa*, *Pseudomonas anguilliseptica*	Sahli et al., 2022
Haloferax alexandrinus	AgNPS	*Pseudomonas aeruginosa* ATCC 9027, *Bordetellabronchiseptica* ATCC 4617, *Staphylococcusaureus* ATCC 6538P	Patil et al., 2014
Haloferax alexandrinus and *Haloferax lucentense*	AgCl-NPS	*Pseudomonas aeruginosa* and *Bacillus* sp	Moopantakath et al., 2022

2.3. Antioxidant compounds

The human body produces free radicals during metabolic processes, which create oxidative stress and contribute to inflammation and lifestyle diseases. At present, haloarchaeal compounds have received significant attention due to their free radical scavenging properties at lower concentrations which are considerably more effective than the standard reference compounds like ascorbic acids. Bacterioruberin has a conjugated structure containing 13 C-C units and has a high free radical scavenging activity. The carotenoid from *Haloferax* sp., exhibited high antioxidative activity, confirmed with DPPH (2,2-diphenylpicrylhydrazyl) and ABTS (2,2'-azino-bis(3-ethylbenzothiazoline-6-sulfonic acid) assay. The IC_{50} values for the carotenoid compound were 56.69 and 39.66 μg/ml in DPPH and ABTS assay, respectively (Sahli et al., 2022). In contrast, carotenoid pigments isolated from the *Halogeometricum* sp., exhibited antioxidative activity with an IC_{50}?170.4 μg/ml (DPPH assay) (Sahli et al., 2022). Similarly, acetone extracts from the *H. hispanica* HM1 showed 88% (ABTS) and 82% (Ferric ion reducing power) activity (Gómez-Villegas et al., 2020). Similarly, carotenoids from *H. volcanii*, *Hgn. rubrum*, and *Hpl. Inordinat*ehave highlighted higher (80%) free radical scavenging properties at a concentration of 10 μg/ml (Hou and Cui, 2018). Zalazar et al. (2019) reported a genetically modified *Haloferax volcanii* strain (HVLON3) with high antioxidative activities (EC_{50} = 4.5 × 10^{-5} mol/l). Thus, haloarchaeal compounds can serve as a prominent source of antioxidant molecules in the future.

Bacterioruberin and β-carotene are the most desirable carotenoids for biological applications. Bacterioruberin, as an antioxidant molecule, can capture reactive oxygen species. Its exhibits antioxidant activity higher than the standard ascorbic acid (Sahli et al., 2022). Bacterioruberin has superior antioxidant properties compared to the β-carotene (Zalazar et al., 2019). Oxidative stress in the form of H_2O_2 increases the bacterioruberin

production in *Haloferax mediterranei* strain R-4 up to 78% (Giani and Martínez-Espinosa, 2020). Furthermore, the antioxidant activity of haloarchaea varies between species. For instance, carotenoids from *Haloferax* sp., ME16 have a higher antioxidant activity than *Halogeometricum* and *Haloarcula* (Sahli et al., 2022).

3. Hydrolytic enzymes from haloarchaea

The wide range of enzymes produced by halophiles plays a vital role in biotechnology, including biosynthesis, food processing industries, and bioremediation methods. As the enzymes produced by haloarchaea are stable at high salt concentrations they can be utilized in several processes related to food or leather tanning. The most important hydrolytic enzymes produced by haloarchaea are proteases and lipases (Modern et al., 2000). The first hydrolase enzyme, a serine protease, was purified and studied from *Halobacterium salinarum*. This enzyme was active only at a high concentration of NaCl (more than 2 M), being an enzyme rich in negatively charged amino acids (Ventosa et al., 2005). Starch-degrading alpha-amylases are synthesized by halophiles such as *Halobacterium salinarum*, *Haloferax mediterranei*, *Halomonas meridiana*, and *Natronococcus amylolyticus* (Kumar et al., 2016). Besides amylases, pullulanase is produced by different archaea, such as *Halorubrum* sp., Ha25, which is already used in the starch industry (Siroosi et al., 2014). Cellulase-degrading cellulases and glycoside hydrolase gene homologs are present in *Halorhabdus utahensis* (Zhang et al., 2011), *Haloarcula* sp., (Ogan et al., 2012), *Halorubrum lacusprofundi* (Karan et al., 2013), *Haloarcula vallismortis* (Nercessian et al., 2015), *Natronobiforma cellulositropha* (Sorokin et al., 2018), *Halalkalicoccus jeotgali* (Anderson et al., 2011), and *Haloferax sulfurifontis* (Malik and Furtado, 2019). **Table 2** displays different intracellular or extracellular hydrolytic enzymes produced by haloarchaea.

Amylase, one of the important industrial enzymes, was reported to synthesize by a new haloarchaeal strain isolated from salterns. High amylase activity was exhibited by the new strain *Haloarcula* sp., HS and found to be poly extremotolerant. The optimum enzyme yield was obtained at high salt concentrations (25%), 60°C, and was calcium-dependent. Amylases were found to be synthesized in extracellular and intracellular fractions and observed as 3 different types of enzymes. The extracted enzymes were tested on bakery waste. It was found that amylases degraded bakery waste efficiently at high salt concentrations (Gómez-Villegas et al., 2021). Interestingly, extracellular hydrolytic enzymes were produced by haloarchaeal strains obtained from hypersaline lakes. The two most abundant archaeal species, *Natrinema* and *Halorubrum*, produced cellulase, pectinase, amylase, lipase, and xylanase but not protease (Karray et al., 2018). In the study, alpha-amylase obtained from *H. salinarum* was immobilized in calcium alginate to enhance its stability (Patel et al., 1996). In another study, the tolerance of alcohol dehydrogenase enzyme, obtained from *Haloferax volcanii,* to organic solvents was reported to improve upon immobilization with sepabeads (Alsafadi and Paradisi, 2014). Immobilized lipase enzyme on anionic resin obtained from *Haloarcula* sp., was used to produce biodiesel (Li and Yu, 2014). *Halobacterium salinarum* NRC-1, *Haloarcula japonica*, *H. salinarum* CECT 395, and *H. mediterranei* can grow on chitin thanks to chitinases (García-Fraga et al., 2014; Hou et al., 2014). Haloarchaea degrades lignin through laccase and peroxidase enzymes. Some haloarchaea produces enzymes like esterases and lipases to degrade ester, ether, and glycosidic linkages. Menasria et al. (2018) have reported extensive bioprospecting of salt-stable and active hydrolytic enzymes from haloarchaea of arid and semi-arid wetlands. The major haloarchaea identified were from the class halobacteria such as *Haloarcula*, *Halogeometricum*, *Halococcus*, *Haloterrigena*, etc. Among the 68 isolates screened, 89.7% of isolates produced 2 halophilic enzymes, whereas 52.9% produced 3 hydrolytic enzymes. These isolates produced gelatinase, cellulase, esterase, and inulinase. Secondly, some isolates were profound in producing xylanase, pectinase, and nuclease. The study also reported that the high cellulase activity (35%) makes it a potential candidate in the food and textile industries (Menasria et al., 2018). Likewise, out of 300 isolates from a salt lake, 293 haloarchaea isolates were selected and studied for active hydrophilic hydrolytic enzymes.

The cellulase, xylanase, amylase, DNase, lipase, protease, pullulanase, chitinase, and inulinase were observed in 9 potential isolates. The most abundant enzymes produced by haloarchaeal isolates (*Halorubrum* and *Haloarcula*) were lipase, DNase, and amylase (Makhdoumi Kakhki et al., 2011).

4. Biodegradable and biocompatible polymers by haloarchaea

Search for eco-friendly biopolymers is one of the important research objectives worldwide to reduce global plastic pollution and in the production of biomedical devices (Simó-Cabrera et al., 2021). Regarding biomedicine, the desirable properties of biodegradable polymers vary based on their application, such as the high degradative potential for surgical mesh and low degradative potential for bioengineered skin. For such applications, biopolymers can be synthetically prepared, such as polylactic acid (PLA) and polyglycolic acid (PGA) (Han et al., 2015). Yet such synthetically prepared biopolymers are associated with setbacks such as biocompatibility and inflammation. Among natural biopolymers with interesting physicochemical properties to be used as bioplastic for packaging or biomedical applications, polyhydroxyalkanoates (PHAs) from haloarchaea are of research interest. The advantages of PHAs include their ease of mechanical customization, biodegradability, and biocompatibility (Han et al., 2015). Hence, PHAs have been under extensive research for application in medical implants, drug delivery, tissue replacement, etc. PHAs, composed of hydroxyalkanoate monomers, are stored as a source of carbon and energy under stress conditions in archaea and bacteria. The type of hydroxyalkanoate monomers determines the physical properties (rigid or elastic) of the PHAs. Among the PHAs, the most common ones are poly-3-hydroxybutyrate (PHB) and poly(3-hydroxybutyrate-co-3-hydroxyvalerate) (PHBHV). PHBHV comprises PHB and 3-hydroxyvalerate (3HV) monomer. PHBHV, upon degradation in the body, does not release toxic byproducts, has more outstanding biocompatibility and biodegradation, and helps in the growth of fibroblasts, mesenchymal stem cells, etc (Ahmed et al., 2010).

TABLE 2 Hydrolytic enzymes produced by haloarchaea and their biosynthesis mode.

Haloarchaea	Hydrolytic enzymes	Location	References
Haloterrigenaturkmenica	α-amylase	Extracellular	Santorelli et al., 2016
Haloferax mediterranei	Monomeric α-amylase	Extracellular	Pérez-Pomares et al., 2003
Haloarcula sp., strain S-1	Organic solvent tolerant α-amylase	Extracellular	Fukushima et al., 2005
Haloarculahispanica	Highly stable α-amylase	Extracellular	Hutcheon et al., 2005
Haloarcula sp., HS	Poly-extremotolerant α-amylase	Intracellular and extracellular	Gómez-Villegas et al., 2021
Haloarcula sp., LLSG7	Organic solvent-tolerant cellulase	Extracellular	Li and Yu, 2013
Halorhabdus utahensis	Heat and ionic liquid-tolerant cellulase	Extracellular	Zhang et al., 2011
Halomicrobium and *Salinarchaeum*	Chitinase	Extracellular	Sorokin et al., 2015
Haloterrigena	Chitinase	Intracellular	Sorokin et al., 2015
Halobacterium salinarum NRC-1	Chitinase	Extracellular	Yatsunami et al., 2010
Haloferax mediterranei S1	Lipase	Extracellular	Akmoussi-Toumi et al., 2018
Haloarcula sp., G41	Organic solvent tolerant lipase	Extracellular	Li and Yu, 2014
Natrialba asiatica 172 P1	Protease	Extracellular	De Castro et al., 2006
Halobacterium salinarum I and IM	Protease	Extracellular	De Castro et al., 2006
Natronococcus sp., TC6	Esterase	Extracellular	Martin del Campo et al., 2015
H. marismortui	Esterase and lipase	Intracellular	Camacho et al., 2009
Haloferax volcanii	Laccase	Extracellular	Uthandi et al., 2010

TABLE 3 Different types of nanoparticles synthesized using haloarchaea and their biological activities.

Haloarchaea	Nanoparticles	Applications	References
H. salifodinae BK3 and BK6	Intracellular silver	Antibacterial activity (gram-positive and negative)	Tiquia-Arashiro and Rodrigues, 2016
Haloferax sp	Intracellular silver	Antibacterial activity against pathogenic bacteria	Abdollahnia et al., 2020
Halogeometricum sp	Intracellular selenium	Antibacterial activity against pathogenic bacteria	Abdollahnia et al., 2020
Haloferax alexandrinus RK_AK2 and *Haloferax lucentense* RK_MY6	Silver chloride	Anti-inflammatory, antioxidant, and antibacterial activity	Moopantakath et al., 2022
Haloferax sp., NRS1	Intracellular silver	Non-hemolytic (non-toxic) activity	Tag et al., 2021
Halobacterium sp., NRC-1	Self-adjuvant gas vesicle nanoparticles	Antigen delivery and development of salmonella vaccines	DasSarma et al., 2015
Halomonas elongata IBRCM	Zinc oxide	Antibacterial activity (*E. coli* and methicillin-resistant *S. aureus*)	Taran et al., 2018
Halococcussalifodinae BK3	Needle shape tellurium NPs	Antibacterial activity (gram-positive and negative)	Srivastava et al., 2015
Halobiforma sp., N1	Superparamagnetic iron oxide NPs	Hyperthermia treatment of cancer	Salem et al., 2020

Archaea are considered promising cell factories and more cost-effective than bacteria for PHBHV production. For instance, *Haloferax mediterranei* produces PHBHV with a lower melting point than *Hydrogenophaga pseudoflava* (Koller et al., 2007). PHBHV produced by *Halogranum amylolyticum* has a higher hemocompatibility than *Ralstonia eutropha* (Zhao Y. et al., 2015). Furthermore, the entire process of biosynthesis is within the cell. PHAs are water-insoluble, degradable without oxygen, and increase their solubility in chlorinated solvents (Simó-Cabrera et al., 2021). Based on the monomers, PHAs are classified as homopolymers consisting of the same type of monomers (P4HB, P3HP, P3H4P, etc.), random copolymers consisting of multiple monomer types distributed random, and block copolymers where the distinct polymers are distributed in discrete blocks (Simó-Cabrera et al., 2021). *Haloferax mediterranei* can also produce varying types of PHBHV based on the concentration of valerate being fed (Han et al., 2015). These variations are of two main types, higher-order copolymers (O-PHBHV) composed of PHB and PHV with random PHBHV segments. R-PHBHV comprises random copolymers 3HB and 3HV (Han et al., 2015). PHAs are also produced by *Halogranum amylolyticum* TNN58 with poly (3-hydroxybutyrate-co-3-hydroxyvalerate) (PHBV) and 3-hydroxyvalerate (3HV) fraction when the carbon source is glucose (Zhao Y. X. et al., 2015). Genetic engineering, such as CRISPR-Cas technology, can enhance gene expression for PHAs production. A recent study showed a ∼165% increase in the output of PHA when *citZ* and *gltA* genes were downregulated by CRISPRi (Lin et al., 2021). Recently, robust methods have been developed for monitoring PHA granules in *Haloferax mediterranei,* such as through confocal

fluorescence microscopy stained with Nile red and SYBR Green (Cánovas et al., 2021).

5. Synthesis and application of bioactive nanoparticles from haloarchaea

Nanobiotechnology is a boon to the field of medicine, which deals with the synthesis and application of a wide range of NPs for the treatment of diseases and targeted delivery of drugs (Patra et al., 2018; Dash et al., 2020). Synthesis of NPs using biological entities is always important due to their ease of production, eco-friendly approach, and bioavailability. The green approach in nanotechnology involves producing stable NPs capped with metabolites employed by organisms or plants (Singh et al., 2018). Several works have demonstrated that some haloarchaea can synthesize nanoparticles. However, the synthesis of NPs using haloarchaea needs to be better explored.

Recently, haloarchaea has been explored due to its ability to produce several NPs by detoxifying heavy metals. These organisms survive in the presence of heavy metals by employing enzymatic reduction of metals and sequestration methods to detoxify them (Voica et al., 2016). **Table 3** shows different NPs synthesized using haloarchaea as well as their potential biological applications (**Table 3**). Additional factors such as salt, pH, temperature, and size affect the stability and efficiency of NPs (Dutta and Bandopadhyay, 2022).

Abdollahnia et al. (2020) studied the synthesis of silver and selenium nanoparticles by haloarchaea isolated from solar salterns. Intracellular production of silver and selenium NPs were reported by *Haloferax* sp., and *Halogeometricum* sp., respectively (Abdollahnia et al., 2020; Nagar et al., 2022). The biosynthesized nanoparticles exhibited antibacterial activity against *S. aureus, E. coli*, *B. subtilis*, and *P. aeruginosa* (Abdollahnia et al., 2020). A haloarchaea, *Haloferax* sp., NRS1 screened from solar saltern found in Saudi Arabia showed promising potential in synthesizing silver NPs. The biogenic silver NPs showed non-hemolytic activity below 12.5 μg/ml concentration suggesting their thrombolysis property. The non-toxic/hemolytic property of synthesized NPs potentiates their application as nano drug carriers (Tag et al., 2021).

Similarly, silver NPs synthesized by another group exhibited broad antimicrobial activity. The archaea *Halococcus salifodinae* BK6, mediated synthesis of silver NPs, employs NADH-dependent nitro reductases to reduce metal to nanoparticles. They showed promising antibacterial activity against *S. aureus* and *M. luteus* (Gram-positive) and *E. coli* and *P. aeruginosa* (Gram-negative) (Srivastava et al., 2014b).

Srivastava et al. (2014a) discussed the synthesis of selenium NPs using *H. salifodinae* BK18. Similar to their previous work, nitro reductases reduced sodium selenite to NPs. The intracellular synthesized NPs exhibited antiproliferative properties against HeLa cancer cell lines. Also, the NPs were found to be non-toxic against normal cells suggesting their application as an anticancer agent (Srivastava et al., 2014a). Bioactive gold and silver NPs were synthesized using *Haloferax volcanii*. Significant antibacterial activities were observed with synthesized silver NPs against *E. coli* and *P. putida* (Costa et al., 2020). In addition, haloarchaeal nanoparticles hold promising antibacterial properties. *Haloferax alexandrinus* was used to synthesize silver nanoparticles with an average size of 18 nm and with an amide carbonyl group on the surface. This synthesized nanoparticle has shown antimicrobial activity against *P. aeruginosa, Bordetella bronchiseptica,* and *S. aureus* at 5 μg concentrations (Patil et al., 2014). Another study also highlights the synthesis of spherical-shaped silver chloride nanoparticles (MY6-NP and AK2-NPs) with a size of 30–50 nm using *Haloferax Alexandrinus* and *Haloferax lucentense* at high salt-saturated conditions. According to a study by Salem et al. (2020), hyperthermia therapy can be employed with the help of superparamagnetic iron oxide nanoparticles synthesized using *Halobiforma* sp., N1. The nanoparticles were monodispersed and presented growth inhibition activity against *P. aeruginosa* PAO1 and *Bacillus* sp., at 200 μg/ml concentration (Moopantakath et al., 2022).

6. Conclusion

Haloarchaea, or extremely halophilic archaea, are a group of microbes with genuine metabolic features. They inhabit and even predominate in various extreme geographical and ecological/environmental conditions, The number of new haloarchaeon discovered through culturable and non-culturable methods and techniques is increasing during the last decades. Metabolites synthesized by several haloarchaeal species are of high interest due to their potential applications in biotechnology Thus, carotenoids are highly efficient as antimicrobials, antioxidants, and food colorants. They have been reported to have diverse biological activities, including anticancer and antimicrobial activities. Among carotenoids, bacterioruberin, carotenoids almost produce by haloarchaea show higher antioxidant activity than most of the referenced carotenoids from plants, yeast or algae. Haloarchaea are also implemented in hypersaline wastewater treatment to degrade hydrocarbons, nitrogen removal, and heavy metal bioremediation and nanoparticle (NP) biosynthesis. On the other hand, enzymes from haloarchaea like amylase, chitinase, lipase, protease, and esterase show high activity at extreme conditions (in terms of pH, temperature etc.) which are of interest for industrial processes. The biosynthesis of nanoparticles by haloarchaea has also described being many of those nanoparticles effective against drug-resistant microbes. The haloarchaea, haloenzymes, and pigments are also widely used in the fermentation of salty foods, cosmetics, food, biomedical sectors, biocompatible bioplastics, and biosensors. Despite such an array of applications, their roles within the cells in natural environments as well as in industrial processes remain unexplored consequently, the research on the metabolites synthesized by these microorganisms must continue through more specialized approaches using high-tech equipments.

Author contributions

RK and SB designed the study. JM and VA prepared the figures. RK, SB, MI, JM, and VA wrote the manuscript. RK, SB, RM-E, and MD critically revised the manuscript. All authors have read and agreed to the submitted version of the manuscript.

Funding

This study was supported by the Science and Engineering Research Board (SERB) Government of India funds through the EEQ (EEQ/2018/001085) scheme. This study was also supported by Generalitat Valenciana, Spain (PROMETEO/2021/055), and VIGROB-309 (University of Alicante) to RM-E.

Acknowledgments

We thank the research facilities supported by the Pondicherry University and the Central University of Kerala. RK thanks SERB-EEQ (EEQ/2018/001085), Government of India. JM thanks ICMR-SRF, the Government of India. Financial support from the DBT-RA Programme in Biotechnology and Life Sciences is gratefully acknowledged by MI.

Conflict of interest

The authors declare that the research was conducted in the absence of any commercial or financial relationships that could be construed as a potential conflict of interest.

Publisher's note

References

Abaramak, G., Kırtel, O., and Öner, E. T. (2020). "Fructanogenic halophiles: a new perspective on extremophiles," in *Physiological and Biotechnological Aspects of Extremophiles*, eds. R. Salwan and V. Sharma (London: Elsevier, Academic Press), 123–130. doi: 10.1016/B978-0-12-818322-9.00009-5

Abbes, M., Baati, H., Guermazi, S., Messina, C., Santulli, A., Gharsallah, N., et al. (2013). Biological properties of carotenoids extracted from *Halobacterium halobium* isolated from a Tunisian solar saltern. *BMC Complement Altern. Med.* 13:255. doi: 10.1186/1472-6882-13-255

Abdollahnia, M., Makhdoumi, A., Mashreghi, M., and Eshghi, H. (2020). Exploring the potentials of halophilic prokaryotes from a solar saltern for synthesizing nanoparticles: The case of silver and selenium. *PLoS One* 15:e0229886. doi: 10.1371/journal.pone.0229886

Ahmed, T., Marçal, H., Lawless, M., Wanandy, N. S., Chiu, A., and Foster, L. J. (2010). Polyhydroxybutyrate and its copolymer with polyhydroxy valerate as biomaterials: Influence on progression of stem cell cycle. *Biomacromolecules* 11, 2707–2715. doi: 10.1021/bm1007579

Akmoussi-Toumi, S., Khemili-Talbi, S., Ferioune, I., and Kebbouche-Gana, S. (2018). Purification and characterization of an organic solvent-tolerant and detergent-stable lipase from *Haloferax mediterranei* CNCMM 50101. *Int. J. Biol. Macromol.* 116, 817–830. doi: 10.1016/j.ijbiomac.2018.05.087

Alsafadi, D., and Paradisi, F. (2014). Covalent immobilization of alcohol dehydrogenase (ADH2) from *Haloferax volcanii*: How to maximize activity and optimize performance of halophilic enzymes. *Mol. Biotechnol.* 56, 240–247. doi: 10.1007/s12033-013-9701-5

Amin, K., Tranchimand, S., Benvegnu, T., Abdel-Razzak, Z., and Chamieh, H. (2021). Glycoside hydrolases and glycosyltransferases from hyperthermophilic archaea: Insights on their characteristics and applications in biotechnology. *Biomolecules* 11:1557. doi: 10.3390/biom11111557

Amoozegar, M. A., Siroosi, M., Atashgahi, S., Smidt, H., and Ventosa, A. (2017). Systematics of haloarchaea and biotechnological potential of their hydrolytic enzymes. *Microbiology* 163, 623–645. doi: 10.1099/mic.0.000463

Anderson, I., Scheuner, C., Göker, M., Mavromatis, K., Hooper, S. D., Porat, I., et al. (2011). Novel insights into the diversity of catabolic metabolism from ten haloarchaeal genomes. *PLoS One* 6:e20237. doi: 10.1371/journal.pone.0020237

Andrei, A. Ş, Banciu, H. L., and Oren, A. (2012). Living with salt: Metabolic and phylogenetic diversity of archaea inhabiting saline ecosystems. *FEMS Microbiol. Lett.* 330, 1–9. doi: 10.1111/j.1574-6968.2012.02526.x

Begemann, M. B., Mormile, M. R., Paul, V. G., and Vidt, D. J. (2011). "Potential enhancement of biofuel production through enzymatic biomass degradation activity and biodiesel production by halophilic microorganisms," in *Halophiles and hypersaline environments*, eds A. Ventosa, A. Oren, and Y. Ma (Berlin: Springer), 341–357. doi: 10.1007/978-3-642-20198-1_18

Behzad, H., Ibarra, M. A., Mineta, K., and Gojobori, T. (2016). Metagenomic studies of the Red Sea. *Gene* 576, 717–723. doi: 10.1016/j.gene.2015.10.034

Bernabeu, E., Miralles-Robledillo, J., Giani, M., Valdés, E., Martínez-Espinosa, R., and Pire, C. (2021). In silico analysis of the enzymes involved in haloarchaeal denitrification. *Biomolecules* 11:1043. doi: 10.3390/biom11071043

Besse, A., Vandervennet, M., Goulard, C., Peduzzi, J., Isaac, S., Rebuffat, S., et al. (2017). Halocin C8: An antimicrobial peptide distributed among four halophilic archaeal genera: *Natrinema*, *Haloterrigena*, *Haloferax*, and *Halobacterium*. *Extremophiles* 21, 623–638. doi: 10.1007/s00792-017-0931-5

Bhattacharyya, A., Majumder, N. S., Basak, P., Mukherji, S., Roy, D., Nag, S., et al. (2015). Diversity and distribution of Archaea in the mangrove sediment of Sundarbans. *Archaea* 2015:968582. doi: 10.1155/2015/968582

Bolhuis, H., Palm, P., Wende, A., Falb, M., Rampp, M., Rodriguez-Valera, F., et al. (2006). The genome of the square archaeon *Haloquadratum walsbyi*: Life at the limits of water activity. *BMC Genomics* 7:169. doi: 10.1186/1471-2164-7-169

Britton, K. L., Baker, P. J., Fisher, M., Ruzheinikov, S., Gilmour, D. J., Bonete, M. J., et al. (2006). Analysis of protein solvent interactions in glucose dehydrogenase from the extreme halophile *Haloferax mediterranei*. *Proc. Natl. Acad. Sci. U.S.A.* 103, 4846–4851. doi: 10.1073/pnas.0508854103

Camacho, R. M., Mateos, J. C., González-Reynoso, O., Prado, L. A., and Córdova, J. (2009). Production and characterization of esterase and lipase from *Haloarcula marismortui*. *J. Ind. Microbiol. Biotechnol.* 36, 901–909. doi: 10.1007/s10295-009-0568-1

Cánovas, V., Garcia-Chumillas, S., Monzó, F., Simó-Cabrera, L., Fernández-Ayuso, C., Pire, C., et al. (2021). Analysis of polyhydroxyalkanoates granules in *Haloferax mediterranei* by double-fluorescence staining with Nile Red and SYBR Green by confocal fluorescence microscopy. *Polymers* 13:1582. doi: 10.3390/polym13101582

Cecil, L. M., DasSarma, S., Pecher, W., McDonald, R., AbdulSalam, M., and Hasan, F. (2020). Metagenomic insights into the diversity of halophilic microorganisms indigenous to the Karak Salt Mine. *Pak. Front. Microbiol.* 11:1567. doi: 10.3389/fmicb.2020.01567

Cho, E. S., Cha, I. T., Roh, S. W., and Seo, M. J. (2021). *Haloferax litoreum* sp. nov., *Haloferax marinisediminis* sp. nov., and *Haloferax marinum* sp. nov., low salt-tolerant haloarchaea isolated from seawater and sediment. *Antonie van Leeuwenhoek* 114, 2065–2082. doi: 10.1007/s10482-021-01661-0

Coker, J. A., DasSarma, P., Kumar, J., Müller, J. A., and DasSarma, S. (2007). Transcriptional profiling of the model Archaeon *Halobacterium* sp. NRC-1: Responses to changes in salinity and temperature. *Saline Syst.* 3:6. doi: 10.1186/1746-1448-3-6

Costa, M. I., Álvarez-Cerimedo, M. S., Urquiza, D., Ayude, M. A., Hoppe, C. E., Fasce, D. P., et al. (2020). Synthesis, characterization and kinetic study of silver and gold nanoparticles produced by the archaeon *Haloferax volcanii*. *J. Appl. Microbiol.* 129, 1297–1308. doi: 10.1111/jam.14726

Cui, H.-L., and Dyall-Smith, M. L. (2021). Cultivation of halophilic Archaea (class Halobacteria) from thalassohaline and athalassohaline environments. *Mar. Life Sci. Technol.* 3, 243–251. doi: 10.1007/s42995-020-00087-3

Das, D., Kalra, I., Mani, K., Salgaonkar, B. B., and Braganca, J. M. (2019). Characterization of extremely halophilic archaeal isolates from Indian salt pans and

their screening for production of hydrolytic enzymes. *Environ. Sustain.* 2, 227–239. doi: 10.1007/s42398-019-00077-x

Das, S., and Dash, H. R. (2018). *Microbial diversity in the genomic era*. Cambridge, MA: Academic Press, doi: 10.1016/c2017-0-01759-7

Dash, D. K., Panik, R. K., Sahu, A. K., and Tripathi, V. (2020). "Role of nanobiotechnology in drug discovery, development and molecular diagnostic," in *Applications of nanobiotechnology*, eds M. Stoytcheva and R. Zlatev (London: IntechOpen), 225–240. doi: 10.5772/intechopen.92796

DasSarma, P., Negi, V. D., Balakrishnan, A., Kim, J.-M., Karan, R., Chakravortty, D., et al. (2015). Haloarchaeal gas vesicle nanoparticles displaying *Salmonella* antigens as a novel approach to vaccine development. *Procedia Vaccinol.* 9, 16–23. doi: 10.1016/j.provac.2015.05.003

De Castro, R. E., Maupin-Furlow, J. A., Giménez, M. I., Herrera Seitz, M. K., and Sánchez, J. J. (2006). Haloarchaeal proteases and proteolytic systems. *FEMS Microbiol. Rev.* 30, 17–35. doi: 10.1111/j.1574-6976.2005.00003.x

Del Campo, M. M., Camacho, R. M., Mateos-Díaz, J. C., Müller-Santos, M., Córdova, J., and Rodríguez, J. A. (2015). Solid-state fermentation as a potential technique for esterase/lipase production by halophilic archaea. *Extremophiles* 19, 1121–1132.

Durán-Viseras, A., Andrei, A. S., Ghai, R., Sánchez-Porro, C., and Ventosa, A. (2019). New Halonotius species provide genomics-based insights into cobalamin synthesis in haloarchaea. *Front. Microbiol.* 27:1928. doi: 10.3389/fmicb.2019.01928

Dutta, B., and Bandopadhyay, R. (2022). Biotechnological potentials of halophilic microorganisms and their impact on mankind. *Beni Suef Univ. J. Basic Appl. Sci.* 11:75. doi: 10.1186/s43088-022-00252-w

Dyall-Smith, M. L., Pfeiffer, F., Klee, K., Palm, P., Gross, K., Schuster, S. C., et al. (2011). *Haloquadratum walsbyi*: Limited diversity in a global pond. *PLoS One* 6:e20968. doi: 10.1371/journal.pone.0020968

Esclapez, J., Pire, C., Bautista, V., Martínez-Espinosa, R. M., Ferrer, J., and Bonete, M. J. (2007). Analysis of acidic surface of *Haloferax mediterranei* glucose dehydrogenase by site-directed mutagenesis. *FEBS Lett.* 581, 837–842. doi: 10.1016/j.febslet.2007.01.054

Fenderson, B. A. (2006). Molecular chaperones and cell signalling. *Shock* 25:426. doi: 10.1097/01.shk.0000215322.52607.c3

Fernández, A. B., Vera-Gargallo, B., Sánchez-Porro, C., Ghai, R., Papke, R. T., Rodriguez-Valera, F., et al. (2014). Comparison of prokaryotic community structure from Mediterranean and Atlantic saltern concentrator ponds by a metagenomic approach. *Front. Microbiol.* 5:196. doi: 10.3389/fmicb.2014.00196

Fukushima, T., Mizuki, T., Echigo, A., Inoue, A., and Usami, R. (2005). Organic solvent tolerance of halophilic α-amylase from a Haloarchaeon, *Haloarcula* sp. strain S-1. *Extremophiles* 9, 85–89. doi: 10.1007/s00792-004-0423-2

Gaonkar, S. K., and Furtado, I. J. (2022). Biorefinery-fermentation of agro-wastes by *Haloferax lucentensis* GUBF-2 MG076878 to haloextremozymes for use as biofertilizer and biosynthesizer of AgNPs. *Waste Biomass Valorization* 13, 1117–1133. doi: 10.1007/S12649-021-01556-1/FIGURES/6

García-Fraga, B., Da Silva, A. F., López-Seijas, J., and Sieiro, C. (2014). Functional expression and characterization of a chitinase from the marine archaeon *Halobacterium salinarum* CECT 395 in *Escherichia coli*. *Appl. Microbiol. Biotechnol.* 98, 2133–2143. doi: 10.1007/s00253-013-5124-2

Ghanmi, F., Carré-Mlouka, A., Vandervennet, M., Boujelben, I., Frikha, D., Ayadi, H., et al. (2016). Antagonistic interactions and production of halocin antimicrobial peptides among extremely halophilic prokaryotes isolated from the solar saltern of Sfax, Tunisia. *Extremophiles* 20, 363–374. doi: 10.1007/s00792-016-0827-9

Giani, M., Gervasi, L., Loizzo, M., and Martínez-Espinosa, R. (2022). Carbon source influences antioxidant, antiglycemic, and antilipidemic activities of *Haloferax mediterranei* carotenoid extracts. *Mar. Drugs* 20:659. doi: 10.3390/md20110659

Giani, M., and Martínez-Espinosa, R. (2020). Carotenoids as a protection mechanism against oxidative stress in *Haloferax mediterranei*. *Antioxidants* 9:1060. doi: 10.3390/antiox9111060

Giani, M., Montoyo-Pujol, Y., Peiró, G., and Martínez-Espinosa, R. (2021). Halophilic carotenoids and breast cancer: From salt marshes to biomedicine. *Mar. Drugs* 19:594. doi: 10.3390/md19110594

Gómez-Villegas, P., Vigara, J., Romero, L., Gotor, C., Raposo, S., Gonçalves, B., et al. (2021). Biochemical characterization of the amylase activity from the new haloarchaeal strain *Haloarcula* sp. HS isolated in the Odiel Marshlands. *Biology* 10:337. doi: 10.3390/biology10040337

Gómez-Villegas, P., Vigara, J., Vila, M., Varela, J., Barreira, L., and Léon, R. (2020). Antioxidant, antimicrobial, and bioactive potential of two new haloarchaeal strains isolated from odiel salterns (Southwest Spain). *Biology* 9:298. doi: 10.3390/biology9090298

Grant, W. D., Danson, M. J., Scott, D. J., Halling, P. J., Engberts, J. B. F. N., Ho, M. W., et al. (2004). Life at low water activity. *Philos. Trans. R. Soc. Lond. B Biol. Sci.* 359, 1249–1267. doi: 10.1098/rstb.2004.1502

Griffiths, B. S., and Philippot, L. (2013). Insights into the resistance and resilience of the soil microbial community. *FEMS Microbiol. Rev.* 37, 112–129. doi: 10.1111/j.1574-6976.2012.00343.x

Haldar, S., and Nazareth, S. W. (2018). Taxonomic diversity of bacteria from mangrove sediments of Goa: Metagenomic and functional analysis. *3 Biotech* 8:436. doi: 10.1007/s13205-018-1441-6

Han, J., Wu, L. P., Hou, J., Zhao, D., and Xiang, H. (2015). Biosynthesis, characterization, and hemostasis potential of tailor-made poly (3-hydroxybutyrate-co-3-hydroxyvalerate) produced by *Haloferax mediterranei*. *Biomacromolecules* 16, 578–588. doi: 10.1021/bm5016267

Hashimoto, H., Sugai, Y., Uragami, C., Gardiner, A. T., and Cogdell, R. J. (2015). Natural and artificial light-harvesting systems utilizing the functions of carotenoids. *J. Photochem. Photobiol. C.* 25, 46–70. doi: 10.1016/j.jphotochemrev.2015.07.004

Hegazy, G. E., Abu-Serie, M. M., Abo-Elela, G. M., Ghozlan, H., Sabry, S. A., Soliman, N. A., et al. (2020). *In vitro* dual (anticancer and antiviral) activity of the carotenoids produced by haloalkaliphilic archaeon Natrialba sp. M6. *Sci. Rep.* 10:5986. doi: 10.1038/s41598-020-62663-y

Higa, L. H., Schilrreff, P., Briski, A. M., Jerez, H. E., de Farias, M. A., Portugal, R. V., et al. (2020). Bacterioruberin from Haloarchaea plus dexamethasone in ultra-small macrophage-targeted nanoparticles as potential intestinal repairing agent. *Colloids Surf. B.* 191:110961. doi: 10.1016/j.colsurfb.2020.110961

Hou, J., and Cui, H. L. (2018). In vitro antioxidant, antihemolytic, and anticancer activity of the carotenoids from halophilic archaea. *Curr. Microbiol.* 75, 266–271. doi: 10.1007/s00284-017-1374-z

Hou, J., Han, J., Cai, L., Zhou, J., Lü, Y., Jin, C., et al. (2014). Characterization of genes for chitin catabolism in *Haloferax mediterranei*. *Appl. Microbiol. Biotechnol.* 8, 1185–1194. doi: 10.1007/s00253-013-4969-8

Hutcheon, G. W., Vasisht, N., and Bolhuis, A. (2005). Characterisation characterization of a highly stable α-amylase from the halophilic archaeon *Haloarcula hispanica*. *Extremophiles* 9, 487–495. doi: 10.1007/s00792-005-0471-2

Hwang, C. Y., Cho, E. S., Rhee, W. J., Kim, E., and Seo, M. J. (2022). Genomic and physiological analysis of C_{50} carotenoid-producing novel *Halorubrumruber* sp. nov. *J. Microbiol.* 26, 1007–1020. doi: 10.1007/s12275-022-2173-1

Jones, D. L., and Baxter, B. K. (2017). DNA repair and photoprotection: Mechanisms of overcoming environmental ultraviolet radiation exposure in halophilic archaea. *Front. Microbiol.* 8:1882. doi: 10.3389/fmicb.2017.01882

Karan, R., Capes, M. D., DasSarma, P., and DasSarma, S. (2013). Cloning, overexpression, purification, and characterization of a polyextremophilic β-galactosidase from the Antarctic haloarchaeon *Halorubrum lacusprofundi*. *BMC Biotechnol.* 13:3. doi: 10.1186/1472-6750-13-3

Karray, F., Ben Abdallah, M., Kallel, N., Hamza, M., Fakhfakh, M., and Sayadi, S. (2018). Extracellular hydrolytic enzymes produced by halophilic bacteria and archaea isolated from hypersaline lake. *Mol. Biol. Rep.* 45, 1297–1309. doi: 10.1007/s11033-018-4286-5

Kennedy, S. P., Ng, W. V., Salzberg, S. L., Hood, L., and DasSarma, S. (2001). Understanding the adaptation of *Halobacterium* species NRC-1 to its extreme environment through computational analysis of its genome sequence. *Genome Res.* 11, 1641–1650. doi: 10.1101/gr.190201

Keshri, J., Yousuf, B., Mishra, A., and Jha, B. (2015). The abundance of functional genes, *cbbL, nifH, amoA* and *apsA*, and bacterial community structure of intertidal soil from Arabian Sea. *Microbiol. Res.* 175, 57–66. doi: 10.1016/j.micres.2015.02.007

Koller, M., Hesse, P., Bona, R., Kutschera, C., Atliæ, A., and Braunegg, G. (2007). Potential of various archaea and eubacterial strains as industrial polyhydroxyalkanoate producers from whey. *Macromol. Biosci.* 7, 218–226. doi: 10.1002/mabi.200600211

Kottemann, M., Kish, A., Iloanusi, C., Bjork, S., and DiRuggiero, J. (2005). Physiological responses of the halophilic archaeon *Halobacterium* sp. strain NRC1 to desiccation and gamma irradiation. *Extremophiles* 9, 219–227. doi: 10.1007/s00792-005-0437-4

Kumar, S., Grewal, J., Sadaf, A., Hemamalini, R., and Khare, S. K. (2016). Halophiles as a source of polyextremophilic α-amylase for industrial applications. *AIMS Microbiol.* 2, 1–26. doi: 10.3934/Microbiol.2016.1.1

Kumar, V., and Tiwari, S. K. (2017). Halocin HA1: An archaeocin produced by the haloarchaeon *Haloferax larsenii* HA1. *Process Biochem.* 61, 202–208. doi: 10.1016/j.procbio.2017.06.010

Li, J., Gao, Y., Dong, H., and Sheng, G. P. (2021). Haloarchaea, excellent candidates for removing pollutants from hypersaline wastewater. *Trends Biotechnol.* 40, 226–239. doi: 10.1016/j.tisbtech.2021.06.006

Li, X., and Yu, H. Y. (2013). Halostable cellulase with organic solvent tolerance from *Haloarcula* sp. LLSG7 and its application in bioethanol fermentation using agricultural wastes. *J. Ind. Microbiol. Biotechnol.* 40, 1357–1365. doi: 10.1007/s10295-013-1340-0

Li, X., and Yu, H. Y. (2014). Characterization of an organic solvent-tolerant lipase from *Haloarcula* sp. G41 and its application for biodiesel production. *Folia Microbiol.* 59, 455–463. doi: 10.1007/s12223-014-0320-8

Lin, L., Chen, J., Mitra, R., Gao, Q., Cheng, F., Xu, T., et al. (2021). Optimising optimizing PHBV biopolymer production in haloarchaea via CRISPRi-mediated redirection of carbon flux. *Commun. Biol.* 4:1007. doi: 10.1038/s42003-021-02541-z

Lizama, C., Romero-Parra, J., Andrade, D., Riveros, F., Bórquez, J., Ahmed, S., et al. (2021). Analysis of carotenoids in haloarchaea species from atacama saline lakes

by high resolution UHPLC-Q-orbitrap-mass spectrometry: Antioxidant potential and biological effect on cell viability. *Antioxidants* 10:1230. doi: 10.3390/antiox10081230

Llorca, M., and Martínez-Espinosa, R. (2022). Assessment of *Haloferax mediterranei* genome in search of copper-molecular machinery with potential applications for bioremediation. *Front. Microbiol.* 13:895296. doi: 10.3389/fmicb.2022.895296

Lu, Y., Yuan, J., Lu, X., Su, C., Zhang, Y., Wang, C., et al. (2018). Major threats of pollution and climate change to global coastal ecosystems and enhanced management for sustainability. *Environ. Pollut.* 239, 670–680. doi: 10.1016/j.envpol.2018.04.016

Macario, A. J. L., Lange, M., Ahring, B. K., and De Macario, E. C. (1999). Stress genes and proteins in the Archaea. *Microbiol. Mol. Biol. Rev.* 63, 923–967. doi: 10.1128/MMBR.63.4.923-967.1999

Makhdoumi Kakhki, A., Amoozegar, M. A., and Mahmodi Khaledi, E. (2011). Diversity of hydrolytic enzymes in haloarchaeal strains isolated from salt lake. *Int. J. Environ. Sci. Technol.* 8, 705–714. doi: 10.1007/bf03326255

Malik, A. D., and Furtado, I. J. (2019). *Haloferax sulfurifontis* GUMFAZ2 producing xylanase-free cellulase retrieved from *Haliclona* sp. inhabiting rocky shore of Anjuna, Goa-India. *J. Basic Microbiol.* 59, 692–700. doi: 10.1002/jobm.201800672

Mani, K., Taib, N., Hugoni, M., Bronner, G., Bragança, J. M., and Debroas, D. (2020). Transient dynamics of archaea and bacteria in sediments and brine across a salinity gradient in a solar saltern of Goa, India. *Front. Microbiol.* 11:1891. doi: 10.3389/fmicb.2020.01891

Maoka, T. (2020). Carotenoids as natural functional pigments. *J. Nat. Med.* 74, 1–6. doi: 10.1007/s11418-019-01364-x

Martin del Campo, M., Camacho, R. M., Mateos-Díaz, J. C., Müller-Santos, M., Córdova, J., and Rodríguez, J. A. (2015). Solid-state fermentation as a potential technique for esterase/lipase production by halophilic archaea. *Extremophiles* 19, 1121–1132. doi: 10.1007/s00792-015-0784-8

Martínez, G., Pire, C., and Martínez-Espinosa, R. (2022). Hypersaline environments as natural sources of microbes with potential applications in biotechnology: The case of solar evaporation systems to produce salt in Alicante County (Spain). *Curr. Res. Microb. Sci.* 3:100136. doi: 10.1016/j.crmicr.2022.100136

Martínez-Espinosa, R., Richardson, D., and Bonete, M. (2015). Characterisation Characterization of chlorate reduction in the haloarchaeon Haloferax mediterranei. *Biochim. Biophys. Acta* 1850, 587–594. doi: 10.1016/j.bbagen.2014.12.011

Martínez-Espinosa, R. M., Lledó, B., Marhuenda-Egea, F. C., and Bonete, M. J. (2007). The effect of ammonium on assimilatory nitrate reduction in the haloarchaeon *Haloferax mediterranei*. *Extremophiles* 11, 759–767. doi: 10.1007/s00792-007-0095-9

Matarredona, L., Camacho, M., Zafrilla, B., Bonete, M. J., and Esclapez, J. (2020). The role of stress proteins in haloarchaea and their adaptive response to environmental shifts. *Biomolecules* 10:1390. doi: 10.3390/biom10101390

Menasria, T., Aguilera, M., Hocine, H., Benammar, L., Ayachi, A., Si Bachir, A., et al. (2018). Diversity and bioprospecting of extremely halophilic archaea isolated from Algerian arid and semi-arid wetland ecosystems for halophilic-active hydrolytic enzymes. *Microbiol. Res.* 207, 289–298. doi: 10.1016/j.micres.2017.12.011

Miralles-Robledillo, J., Bernabeu, E., Giani, M., Martínez-Serna, E., Martínez-Espinosa, R., and Pire, C. (2021). Distribution of denitrification among haloarchaea: A comprehensive study. *Microorganisms* 9:1669. doi: 10.3390/microorganisms9081669

Modern, D., Ebel, C., and Zaccai, G. (2000). Halophilic adaptation of enzymes. *Extremophiles* 4, 91–98. doi: 10.1007/s007920050142

Moopantakath, J., Imchen, M., Kumavath, R., and Martínez-Espinosa, R. M. (2021). Ubiquitousness of *Haloferax* and carotenoid producing genes in Arabian sea coastal biosystems of India. *Mar. Drugs* 19:442. doi: 10.3390/md19080442

Moopantakath, J., Imchen, M., Siddhardha, B., and Kumavath, R. (2020). 16s rRNA metagenomic analysis reveals predominance of Crtl and CruF genes in Arabian Sea coast of India. *Sci. Total Environ.* 743:140699. doi: 10.1016/j.scitotenv.2020.140699

Moopantakath, J., Imchen, M., Sreevalsan, A., Siddhardha, B., Martínez-Espinosa, R. M., and Kumavath, R. (2022). Biosynthesis of silver chloride nanoparticles (AgCl-NPs) from extreme halophiles and evaluation of their biological applications. *Curr. Microbiol.* 79:266. doi: 10.1007/s00284-022-02970-x

Moran-Reyna, A., and Coker, J. A. (2014). The effects of extremes of pH on the growth and transcriptomic profiles of three haloarchaea. *F1000Res.* 3:168. doi: 10.12688/f1000research.4789.1

Mormile, M. R., Hong, B. Y., and Benison, K. C. (2009). Molecular analysis of the microbial communities of Mars analog lakes in Western Australia. *Astrobiology* 9, 919–930. doi: 10.1089/ast.2008.0293

Mukherji, S., Ghosh, A., Bhattacharyya, C., Mallick, I., Bhattacharyya, A., Mitra, S., et al. (2020). Molecular and culture-based surveys of metabolically active hydrocarbon-degrading archaeal communities in Sundarban mangrove sediments. *Ecotoxicol. Environ. Saf.* 195:110481. doi: 10.1016/j.ecoenv.2020.110481

Nagar, D. N., Ghosh, N. N., and Braganca, J. M. (2022). Green synthesis of selenium nanospheres and nanoneedles by halophilic archaea. *Appl. Nanosci.* 12, 3983–3994. doi: 10.1007/S13204-022-02665-6

Nercessian, D., Di Meglio, L., De Castro, R., and Paggi, R. (2015). Exploring the multiple biotechnological potential of halophilic microorganisms isolated from two Argentinean salterns. *Extremophiles* 19, 1133–1143. doi: 10.1007/s00792-015-0785-7

Ng, W. V., Kennedy, S. P., Mahairas, G. G., Berquist, B., Pan, M., Shukla, H. D., et al. (2000). Genome sequence of *Halobacterium* species NRC-1. *Proc. Natl. Acad. Sci.U.S.A.* 97, 12176–12181. doi: 10.1073/pnas.190337797

Ogan, A., Danis, O., Gozuacik, A., Cakmar, E., and Birbir, M. (2012). Production of cellulase by immobilized whole cells of *Haloarcula*. *Appl. Biochem. Microbiol.* 48, 440–443. doi: 10.1134/S0003683812050092

Oh, D., Porter, K., Russ, B., Burns, D., and Dyall-Smith, M. (2010). Diversity of *Haloquadratum* and other haloarchaea in three, geographically distant, Australian saltern crystallizer ponds. *Extremophiles* 14, 161–169. doi: 10.1007/s00792-009-0295-6

Oren, A. (2002b). Molecular ecology of extremely halophilic Archaea and Bacteria. *FEMS Microbiol. Ecol.* 39, 1–7. doi: 10.1016/S0168-6496(01)00200-8

Oren, A. (2002a). *Halophilic microorganisms and their environments*. Dordrecht: Springer, doi: 10.1007/0-306-48053-0

Oren, A. (2013). "Life at high salt concentrations," in *The prokaryotes: Prokaryotic communities and ecophysiology*, eds E. Rosenberg, E. F. DeLong, S. Lory, E. Stackebrandt, and F. Thompson (Berlin: Springer), 421–440. doi: 10.1007/978-3-642-30123-0_57

Osman, J. R., Regeard, C., Badel, C., Fernandes, G., and DuBow, M. S. (2019). Variation of bacterial biodiversity from saline soils and estuary sediments present near the Mediterranean Sea coast of Camargue (France). *Antonie Van Leeuwenhoek* 112, 351–365. doi: 10.1007/s10482-018-1164-z

Patel, S., Bagai, R., and Madamwar, D. (1996). Stabilization of a Halophilic α-Amylase by Calcium Alginate Immobilization. *Biocatal. Biotransformation* 14, 147–155. doi: 10.3109/10242429609106882

Patil, S., Fernandes, J., Tangasali, R., and Furtado, I. (2014). Exploitation of *Haloferax Alexandrinus* for biogenic synthesis of silver nanoparticles antagonistic to human and lower mammalian pathogens. *J. Clust. Sci.* 25, 423–433. doi: 10.1007/s10876-013-0621-0

Patra, J. K., Das, G., Fraceto, L. F., Campos, E. V. R., Rodriguez-Torres, M., del, P., et al. (2018). Nano based drug delivery systems: Recent developments and future prospects. *J. Nanobiotechnol.* 16:71. doi: 10.1186/s12951-018-0392-8

Pérez-Pomares, F., Bautista, V., Ferrer, J., Pire, C., Marhuenda-Egea, F. C., and Bonete, M. J. (2003). α-Amylase activity from the halophilic archaeon *Haloferax mediterranei*. *Extremophiles* 7, 299–306. doi: 10.1007/s00792-003-0327-6

Popescu, G., and Dumitru, L. (2009). Biosorption of some heavy metals from media with high salt concentrations by halophilic *Archaea*. *Biotechnol. Biotechnol. Equip.* 23, 791–795. doi: 10.1080/13102818.2009.10818542

Quillaguamán, J., Guzmán, H., Van-Thuoc, D., and Hatti-Kaul, R. (2010). Synthesis and production of polyhydroxyalkanoates by halophiles: Current potential and future prospects. *Appl. Microbiol. Biotechnol.* 85, 1687–1696. doi: 10.1007/s00253-009-2397-6

Rhodes, M. E., Oren, A., and House, C. H. (2012). Dynamics and persistence of Dead Sea microbial populations as shown by high-throughput sequencing of rRNA. *Appl. Environ. Microbiol.* 78, 2489–2492. doi: 10.1128/AEM.06393-11

Sahli, K., Gomri, M. A., Esclapez, J., Gómez-Villegas, P., Bonete, M. J., León, R., et al. (2022). Characterization and biological activities of carotenoids produced by three haloarchaeal strains isolated from Algerian salt lakes. *Arch. Microbiol.* 204:6. doi: 10.1007/s00203-021-02611-0

Salem, N. F., Abouelkheir, S. S., Yousif, A. M., Meneses-Brassea, B. P., Sabry, S. A., Ghozlan, H. A., et al. (2020). Large scale production of superparamagnetic iron oxide nanoparticles by the haloarchaeon *Halobiforma* sp. N1 and their potential in localized hyperthermia cancer therapy. *Nanotechnology* 32:09LT01. doi: 10.1088/1361-6528/abc851

Salgaonkar, B. B., Das, D., and Bragança, J. M. (2016). Resistance of extremely halophilic archaea to zinc and zinc oxide nanoparticles. *Appl. Nanosci.* 6, 251–258. doi: 10.1007/s13204-015-0424-8

Salgaonkar, B. B., Mani, K., and Bragança, J. M. (2013). Accumulation of polyhydroxyalkanoates by halophilic archaea isolated from traditional solar salterns of India. *Extremophiles* 17, 787–795. doi: 10.1007/S00792-013-0561-5

Santorelli, M., Maurelli, L., Pocsfalvi, G., Fiume, I., Squillaci, G., La Cara, F., et al. (2016). Isolation and characterisation characterization of a novel alpha-amylase from the extreme haloarchaeon *Haloterrigena turkmenica*. *Int. J. Biol. Macromol.* 92, 174–184. doi: 10.1016/j.ijbiomac.2016.07.001

Schäfer, G., Purschke, W., and Schmidt, C. L. (1996). On the origin of respiration: Electron transport proteins from archaea to man. *FEMS Microbiol. Rev.* 5, 223–234. doi: 10.1016/0168-6445(96)00010-1

Serrano, S., Mendo, S., and Caetano, T. (2022). Haloarchaea have a high genomic diversity for the biosynthesis of carotenoids of biotechnological interest. *Res. Microbiol.* 173:103919. doi: 10.1016/j.resmic.2021.103919

Shukla, H. D. (2006). Proteomic analysis of acidic chaperones, and stress proteins in extreme halophile *Halobacterium* NRC-I: A comparative proteomic approach to study heat shock response. *Proteome Sci.* 4:6. doi: 10.1186/1477-5956-4-6

Simó-Cabrera, L., García-Chumillas, S., Hagagy, N., Saddiq, A., Tag, H., Selim, S., et al. (2021). Haloarchaea as cell factories to produce bioplastics. *Mar. Drugs* 19:159. doi: 10.3390/md19030159

Singh, A., and Singh, A. K. (2017). Haloarchaea: Worth exploring for their biotechnological potential. *Biotechnol. Lett*. 39, 1793–1800. doi: 10.1007/s10529-017-2434-y

Singh, J., Dutta, T., Kim, K. H., Rawat, M., Samddar, P., and Kumar, P. (2018). 'Green' synthesis of metals and their oxide nanoparticles: Applications for environmental remediation. *J. Nanobiotechnol.* 16:84. doi: 10.1186/s12951-018-0408-4

Siroosi, M., Amoozegar, M. A., Khajeh, K., Fazeli, M., and Habibi Rezaei, M. (2014). Purification and characterization of a novel extracellular halophilic and organic solvent-tolerant amylopullulanase from the haloarchaeon, *Halorubrum* sp. strain Ha25. *Extremophiles* 18, 25–33. doi: 10.1007/s00792-013-0589-6

Somboonna, N., Assawamakin, A., Wilantho, A., Tangphatsornruang, S., and Tongsima, S. (2012). Metagenomic profiles of free-living archaea, bacteria and small eukaryotes in coastal areas of Sichang island, Thailand. *BMC Genomics* 13(Suppl. 7):S29. doi: 10.1186/1471-2164-13-S7-S29

Sorokin, D. Y., Khijniak, T. V., Kostrikina, N. A., Elcheninov, A. G., Toshchakov, S. V., Bale, N. J., et al. (2018). *Natronobiforma cellulositropha* gen. nov., sp. nov., a novel haloalkaliphilic member of the family Natrialbaceae (class Halobacteria) from hypersaline alkaline lakes. *Syst. Appl. Microbiol.* 41, 355–362. doi: 10.1016/j.syapm.2018.04.002

Sorokin, D. Y., Toshchakov, S. V., Kolganova, T. V., and Kublanov, I. V. (2015). Halo(natrono)archaea isolated from hypersaline lakes utilize cellulose and chitin as growth substrates. *Front. Microbiol.* 6:942. doi: 10.3389/fmicb.2015.00942

Sorokin, D. Y., Yakimov, M., Messina, E., Merkel, A. Y., Koenen, M., Bale, N. J., et al. (2022). *Natranaeroarchaeum sulfidigenes* gen. nov., sp. nov., carbohydrate-utilizing sulfur-respiring haloarchaeon from hypersaline soda lakes, a member of a new family Natronoarchaeaceae fam. nov. in the order Halobacteriales. *Syst. Appl Microbiol.* 45:126356. doi: 10.1016/j.syapm.2022.126356

Srivastava, P., Braganca, J., Ramanan, S. R., and Kowshik, M. (2014b). Green Synthesis of Silver Nanoparticles by Haloarchaeon *Halococcus salifodinae* BK6. *Adv. Mater. Res.* 938, 236–241. doi: 10.4028/www.scientific.net/AMR.938.236

Srivastava, P., Braganca, J. M., and Kowshik, M. (2014a). In vivo synthesis of selenium nanoparticles by *Halococcus salifodinae* BK18 and their antiproliferative properties against HeLa cell line. *Biotechnol. Prog.* 30, 1480–1487. doi: 10.1002/btpr.1992

Srivastava, P., Nikhil, E. V. R., Bragança, J. M., and Kowshik, M. (2015). Anti-bacterial TeNPs biosynthesized by haloarcheaon *Halococcus salifodinae* BK3. *Extremophiles* 19, 875–884. doi: 10.1007/s00792-015-0767-9

Szabó, A., Korponai, K., Kerepesi, C., Somogyi, B., Vörös, L., and Bartha, D. (2017). Soda pans of the Pannonian steppe harbor unique bacterial communities adapted to multiple extreme conditions. *Extremophiles* 21, 639–649. doi: 10.1007/s00792-017-0932-4

Tag, H. M., Saddiq, A. A., Alkinani, M., and Hagagy, N. (2021). Biosynthesis of silver nanoparticles using *Haloferax* sp. NRS1: Image analysis, characterization, in vitro thrombolysis and cytotoxicity. *AMB Express* 11:75. doi: 10.1186/s13568-021-01235-3

Taran, M., Monazah, A., and Alavi, M. (2017). Using petrochemical wastewater for synthesis of cruxrhodopsin as an energy capturing nanoparticle by *Haloarcula* sp. IRU1. *Prog. Biol. Sci*. 6, 151–157. doi: 10.22059/PBS.2016.590017

Taran, M., Rad, M., and Alavi, M. (2018). Biosynthesis of TiO2 and ZnO nanoparticles by *Halomonas elongata* IBRC-M 10214 in different conditions of medium. *BioImpacts* 8, 81–89. doi: 10.15171/bi.2018.10

Thombre, R. S., Shinde, V. D., Oke, R. S., Dhar, S. K., and Shouche, Y. S. (2016). Biology and survival of extremely halophilic archaeon *Haloarcula marismortui* RR12 isolated from Mumbai salterns, India in response to salinity stress. *Sci. Rep.* 6:25642. doi: 10.1038/srep25642

Tiquia-Arashiro, S., and Rodrigues, D. (2016). "Halophiles in Nanotechnology," in *Extremophiles: applications in nanotechnology*, eds. S. Tiquia-Arashiro and D. Rodrigues (Switzerland: Springer, Cham), 53–88. doi: 10.1007/978-3-319-45215-9_2

Torregrosa-Crespo, J., Pire Galiana, C., and Martínez-Espinosa, R. M. (2017). "Biocompounds from Haloarchaea and their uses in biotechnology," in *Archaea-new biocatalysts, novel pharmaceuticals and various biotechnological applications*, eds. H. Sghaier, A. Najjar, and K. Ghedira (London: IntechOpen), 63–82. doi: 10.5772/intechopen.69944

Uthandi, S., Saad, B., Humbard, M. A., and Maupin-Furlow, J. A. (2010). LccA, an Archaeal Laccase Secreted as a Highly Stable Glycoprotein into the Extracellular Medium by *Haloferax volcanii*. *Appl. Environ. Microbiol.* 76, 733–743. doi: 10.1128/AEM.01757-09

Ventosa, A. (2006). "Unusual microorganisms from unusual habitats: Hypersaline environments," in *Prokaryotic diversity mechanisms and significance*, eds N. A. Logan, H. M. Lappin-Scott, and P. C. F. Oyston (Cambridge: Cambridge University Press), 223–254. doi: 10.1017/CBO9780511754913.015

Ventosa, A., Sánchez-Porro, C., Martín, S., and Mellado, E. (2005). "Halophilic Archaea and Bacteria as a Source of Extracellular Hydrolytic Enzymes," in *Adaptation to life at high salt concentrations in archaea, bacteria, and eukarya*, eds N. Gunde-Cimerman, A. Oren, and A. Plemenitaš (Berlin: Springer), 337–354. doi: 10.1007/1-4020-3633-7_23

Vera-Bernal, M., and Martínez-Espinosa, R. M. (2021). Insights on cadmium removal by bioremediation: The case of Haloarchaea. *Microbiol. Res.* 12, 354–375. doi: 10.3390/microbiolres12020024

Verma, D. K., Chaudhary, C., Singh, L., Sidhu, C., Siddhardha, B., Prasad, S. E., et al. (2020). Isolation and taxonomic characterization of novel haloarchaeal isolates from indian solar saltern: A brief review on distribution of bacteriorhodopsins and V-Type ATPases in haloarchaea. *Front. Microbiol.* 11:554927. doi: 10.3389/fmicb.2020.554927

Voica, D. M., Bartha, L., Banciu, H. L., and Oren, A. (2016). Heavy metal resistance in halophilic Bacteria and Archaea. *FEMS Microbiol. Lett.* 363:fnw146. doi: 10.1093/femsle/fnw146

Wang, G., Kennedy, S. P., Fasiludeen, S., Rensing, C., and DasSarma, S. (2004). Arsenic resistance in *Halobacterium* sp. strain NRC-1 examined by using an improved gene knockout system. *J. Bacteriol.* 186, 3187–3194. doi: 10.1128/JB.186.10.3187-3194.2004

Wei, W., Hu, X., Yang, S., Wang, K., Zeng, C., Hou, Z., et al. (2022). Denitrifying halophilic archaea derived from salt dominate the degradation of nitrite in salted radish during pickling. *Int. Food Res. J.* 152:110906. doi: 10.1016/j.foodres.2021.110906

Williams, G. P., Gnanadesigan, M., and Ravikumar, S. (2013). Biosorption and bio-kinetic properties of solar saltern halobacterial strains for managing Zn2+, As2+ and Cd2+ metals. *Geomicrobiol. J.* 30, 497–500. doi: 10.1080/01490451.2012.732663

Yadav, A. N., Sharma, D., Gulati, S., Singh, S., Dey, R., Pal, K. K., et al. (2015). Haloarchaea endowed with phosphorus solubilization attribute implicated in phosphorus cycle. *Sci. Rep.* 5:12293. doi: 10.1038/srep12293

Yatsunami, R., Sato, M., Orishimo, K., Hatori, Y., Zhang, Y., Takashina, T., et al. (2010). Gene expression and characterization of a novel GH family 18 chitinase from extremely halophilic archaeon *Halobacterium salinarum* NRC-1. *J. Jpn. Soc. Extrem.* 9, 19–24. doi: 10.3118/jjse.9.19

Zafrilla, B., Martínez-Espinosa, R. M., Alonso, M. A., and Bonete, M. J. (2010). Biodiversity of archaea and floral of two inland saltern ecosystems in the Alto Vinalopó Valley, Spain. *Saline Syst.* 6:10. doi: 10.1186/1746-1448-6-10

Zalazar, L., Pagola, P., Miró, M. V., Churio, M. S., Cerletti, M., Martínez, C., et al. (2019). Bacterioruberin extracts from a genetically modified hyperpigmented *Haloferax volcanii* strain: Antioxidant activity and bioactive properties on sperm cells. *J. Appl. Microbiol.* 126, 796–810. doi: 10.1111/jam.14160

Zenke, R., von Gronau, S., Bolhuis, H., Gruska, M., Pfeiffer, F., and Oesterhelt, D. (2015). Fluorescence microscopy visualization of halomucin, a secreted 927 kDa protein surrounding *Haloquadratum walsbyi* cells. *Front. Microbiol.* 6:249. doi: 10.3389/fmicb.2015.00249

Zhang, T., Datta, S., Eichler, J., Ivanova, N., Axen, S. D., Kerfeld, C. A., et al. (2011). Identification of a haloalkaliphilic and thermostable cellulase with improved ionic liquid tolerance. *Green Chem.* 13, 2083–2090. doi: 10.1039/c1gc15193b

Zhao, Y., Rao, Z., Xue, Y., Gong, P., Ji, Y., and Ma, Y. (2015). Biosynthesis, property comparison, and hemocompatibility of bacterial and haloarchaeal poly (3-hydroxybutyrate-co-3-hydroxyvalerate). *Sci. Bull.* 60, 1901–1910. doi: 10.1007/s11434-015-0923-8

Zhao, Y. X., Rao, Z. M., Xue, Y. F., Gong, P., Ji, Y. Z., and Ma, Y. H. (2015). Poly (3-hydroxybutyrate-co-3-hydroxyvalerate) production by haloarchaeon *Halogranum amylolyticum*. *Appl. Microbiol. Biotechnol.* 99, 7639–7649. doi: 10.1007/s00253-015-6609-y

frontiers | Frontiers in Microbiology

TYPE Original Research
PUBLISHED 01 June 2023
DOI 10.3389/fmicb.2023.1112247

OPEN ACCESS

EDITED BY
Andreas Teske,
University of North Carolina at Chapel Hill, United States

REVIEWED BY
Jing Han,
Chinese Academy of Sciences (CAS), China
Shaoxing Chen,
Anhui Normal University, China

*CORRESPONDENCE
Alexander G. Elcheninov
✉ elcheninov.ag@gmail.com

†These authors have contributed equally to this work

RECEIVED 30 November 2022
ACCEPTED 15 May 2023
PUBLISHED 01 June 2023

CITATION
Elcheninov AG, Ugolkov YA, Elizarov IM, Klyukina AA, Kublanov IV and Sorokin DY (2023) Cellulose metabolism in halo(natrono)archaea: a comparative genomics study.
Front. Microbiol. 14:1112247.
doi: 10.3389/fmicb.2023.1112247

Cellulose metabolism in halo(natrono)archaea: a comparative genomics study

Alexander G. Elcheninov[1]*, Yaroslav A. Ugolkov[1], Ivan M. Elizarov[1], Alexandra A. Klyukina[1], Ilya V. Kublanov[1†] and Dimitry Y. Sorokin[1,2†]

[1]Winogradsky Institute of Microbiology, Federal Research Centre of Biotechnology, Russian Academy of Sciences, Moscow, Russia, [2]Department of Biotechnology, Delft University of Technology, Delft, Netherlands

Extremely halophilic archaea are one of the principal microbial community components in hypersaline environments. The majority of cultivated haloarchaea are aerobic heterotrophs using peptides or simple sugars as carbon and energy sources. At the same time, a number of novel metabolic capacities of these extremophiles were discovered recently among which is a capability of growing on insoluble polysaccharides such as cellulose and chitin. Still, polysaccharidolytic strains are in minority among cultivated haloarchaea and their capacities of hydrolyzing recalcitrant polysaccharides are hardly investigated. This includes the mechanisms and enzymes involved in cellulose degradation, which are well studied for bacterial species, while almost unexplored in archaea and haloarchaea in particular. To fill this gap, a comparative genomic analysis of 155 cultivated representatives of halo(natrono)archaea, including seven cellulotrophic strains belonging to the genera *Natronobiforma, Natronolimnobius*, *Natrarchaeobius*, *Halosimplex*, *Halomicrobium* and *Halococcoides* was performed. The analysis revealed a number of cellulases, encoded in the genomes of cellulotrophic strains but also in several haloarchaea, for which the capacity to grow on cellulose was not shown. Surprisingly, the cellulases genes, especially of GH5, GH9 and GH12 families, were significantly overrepresented in the cellulotrophic haloarchaea genomes in comparison with other cellulotrophic archaea and even cellulotrophic bacteria. Besides cellulases, the genes for GH10 and GH51 families were also abundant in the genomes of cellulotrophic haloarchaea. These results allowed to propose the genomic patterns, determining the capability of haloarchaea to grow on cellulose. The patterns helped to predict cellulotrophic capacity for several halo(natrono)archaea, and for three of them it was experimentally confirmed. Further genomic search revealed that glucose and cellooligosaccharides import occurred by means of porters and ABC (ATP-binding cassette) transporters. Intracellular glucose oxidation occurred through glycolysis or the semi-phosphorylative Entner-Dudoroff pathway which occurrence was strain-specific. Comparative analysis of CAZymes toolbox and available cultivation-based information allowed proposing two possible strategies used by haloarchaea capable of growing on cellulose: so-called specialists are more effective in degradation of cellulose while generalists are more flexible in nutrient spectra. Besides CAZymes profiles the groups differed in genome sizes, as well as in variability of mechanisms of import and central metabolism of sugars.

KEYWORDS

haloarchaea, cellulotrophic, genomics, CAZymes, cellulose, polysaccharides degradation

Introduction

Extremely halophilic archaea, belonging to the class *Halobacteria* (*Euryarchaeota* phylum), are abundant in natural terrestrial and deep-see hypersaline lakes, men-made solar salterns, rock salt deposits and saline soils. The well-studied majority of cultivated haloarchaea are growing aerobically on rich media containing peptides or simple sugars. Recently, however, a number of novel metabolic capacities of haloarchaea were discovered, including capability to grow anaerobically by sulfur respiration (Sorokin et al., 2016, 2017, 2021) or to grow aerobically with insoluble polysaccharides as the sole substrate (Sorokin et al., 2015, 2018, 2019a,b). Still, the haloarchaea bearing novel metabolic features are in total minority among cultivated representatives of this class with their unique metabolic machinery practically unexplored on biochemical or genomic level. Another question is whether the numerous haloarchaea growing on simple substrates may have any of the mentioned above properties, more specifically would the saccharolytic haloarchaea be capable of growth on insoluble polysaccharides.

Polysaccharides are degraded under the action of different types of enzymes, belonging to so-called carbohydrate-active enzymes (CAZymes, Drula et al., 2022). CAZymes included glycosidases (GHs), polysaccharide lyases (PLs), carbohydrate esterases (CEs), glycosyl transferases (GTs, mostly involved in carbohydrate biosynthesis) as well as auxiliary proteins (AAs) and proteins with carbohydrate binding domains (CBMs). Hydrolysis of exogenous insoluble polysaccharides demand extracellular CAZymes (in total majority – GHs), responsible for initial degradation steps occurred outside the cell. Currently, four model of CAZymes export and the consequent mechanisms of polysaccharides degradation in bacteria are suggested (Gardner and Schreier, 2021): (a) CAZymes are exported *via* outer-membrane vesicles (Elhenawy et al., 2014), (b) CAZymes are exported from periplasm *via* type II secretion system (Gardner and Keating, 2010), (c) cellulosome – CAZymes and specific carbohydrate-binding proteins are attached to the scaffoldins anchored to the cytoplasmic membrane (Artzi et al., 2017), and (d) S-layer-bound CAZymes and tapirins (specific binding protein) are attached to S-layer glycoproteins and pili (Conway et al., 2016; Lee et al., 2019). In turn, the mechanisms and enzymes, involved in polysaccharides hydrolysis in archaea and specifically in halophilic archaea are almost unknown. In particular, this is true for one of the most abundant polysaccharide on Earth – cellulose. Cellulose is a recalcitrant structural homopolysaccharide consisted of beta-1,4-linked D-glucose residues. Despite no variation in primary structure, different forms of celluloses distinguished from each other by degree of crystallinity and ratio and layout of crystalline and amorphous domain – so-called allomorphs (Uusi-Tarkka et al., 2021) which defines the variability of the enzymes involved in cellulose hydrolysis.

Extracellular cellulose hydrolysis resulted in formation of cellooligosaccharides (maximal – C6, Zhong et al., 2020), cellobiose and glucose. The last is less preferable since it is more accessible for competitors and accounts for the preference of cellulotrophic microorganisms to carry out the final steps of cellooligosaccharides hydrolysis intracellularly. Although, a few studies on cellooligosaccharides and cellobiose import in hyperthermophilic archaea *Pyrococcus furiosus* (Koning et al., 2001) and *Sulfolobus solfataricus* (Elferink et al., 2001) revealed that high-affinity ATP-binding cassette (ABC) transporters to be involved in this process, but nothing is known about haloarchaea. The mechanisms of glucose import into the cells as well as proteins involved in this process also are very poorly studied in haloarchaea. It seems the ABC transporters play a key role (Williams et al., 2019) in glucose import in halophilic archaea. Glucose is a single final product of cellulose hydrolysis, and its oxidation in haloarchaea occurred by means of (a) semi-phosphorylative Entner-Doudoroff pathway (Johnsen et al., 2001; Pickl et al., 2014), (b) modified glycolysis involving ketohexokinase and 1-phosphofructokinase (Altekar and Rangaswamy, 1991; Pickl et al., 2012) or (c) canonical glycolysis with ADP-dependent phosphofructokinase.

Recent developments in sequence technologies as well as the overall interest to haloarchaea resulted in a high number of available haloarchaeal genome sequences, both cultivated and uncultured (metagenome assembled genomes - MAGs). This is a good background for a comprehensive comparative genomic study to reveal the mechanisms of cellulose utilization in haloarchaea. The aim of this work was to use comparative genomics for comprehensive annotation of haloarchaeal CAZymes, involved in cellulose hydrolysis to reveal their cellulolytic machinery in the strains capable of growing on cellulose and to be able predicting this possibility for strains, for which it was not verified experimentally. Finally, basing on the sets of GHs and other CAZymes and auxiliary proteins we attempted to predict haloarchaea's strategies of polysaccharides decomposing in hypersaline environments.

Materials and methods

Genome sequencing

Genomic DNA isolation, Illumina sequencing as well as genome assembly were performed as described earlier (Sorokin et al., 2018).

For strain AArcel5 additional sequencing using nanopore techonology (Oxford Nanopore Technology) was done. Genomic DNA of the strain was isolated using phenol-chloroform extraction (Gavrilov et al., 2016) and futher repurified using MagAttract HMW DNA Kit (Qiagen) according to manufacturer protocol. The DNA library was prepared with Rapid Barcoding Kit (SQK-RBK004, Oxford Nanopore Technologies). Sequencing was performed with FLO-MIN-106D flow cell (R9.4.1) and MinION device. Basecalling was performed using Guppy basecaller v.2.3.5 with flipflop model. In total of 94,910 reads were obtained by ONT sequencing (~152 Mbp). Assembly was performed as follows: Canu v.1.8 (Koren et al., 2017) was used to obtain *de novo* assembly using long ONT reads followed by Nanopolish v.0.11 (Loman et al., 2015) polishing with raw fast5 reads as well as several rounds of Pilon v.1.23 (Walker et al., 2014) polishing with Illumina reads.

Genome and phylogenetic analyses

High quality genomes of cultivated haloarchaea were downloaded from IMG/M system (Chen et al., 2019); genomes, which were *de novo* sequenced during this work, were also previously annotated using IMG/M system. To exclude almost identical genomes AAI matrix was constructed using aai_matrix.sh (Rodriguez-R and Konstantinidis, 2016). Completeness levels of assemblies with >95% AAI with each

other were estimated with CheckM v.1.1.5 (Parks et al., 2015): one assembly with better quality from each group will be selected for the further analysis.

For phylogenomic analysis based on the "ar122" set of conserved archaeal proteins, the sequences were identified and aligned in *in silico* proteomes of strains from AArcel and HArcel groups as well as described species within *Halobacteria* using the GTDB-tk v.1.2.0 with reference data v.89 (Chaumeil et al., 2019). The phylogenomic tree was constructed using RAxML v.8.2.12 (Stamatakis, 2014) with the PROTGAMMAILG model of amino acid substitution; local support values were 1,000 rapid bootstrap replications. Phylogenetic tree was visualized using iTOL v.6.5.2 (Letunic and Bork, 2019).

CAZymes genes were identified in the genomes using dbCAN v.2.0.11 (Zhang et al., 2018). Comparative analysis was performed with the complete set of revealed in each genome CAZymes as well as with families containing the enzymes with targeted (eg. endoglucanases) activities. Enzymes localization was predicted using SignalP v.6.0 (Teufel et al., 2022). Isoelectric points were estimated with IPC 2.0 (Kozlowski, 2021).

Putative carbohydrate-specific transporters as well as enzymes involved in central catabolism pathways were detected using blastp with characterized reference proteins, obtained from SwissProt (Boutet et al., 2016) and TCDB (Saier et al., 2014) databases, as queries and haloarchaeal genomes as subjects (e-value $<10^{-5}$). Positive hits were manually checked with blast against SwissProt database. For ABC transporters only the gene clusters encoding at least substrate-binding protein and permease subunits were taken into account (ATPase was not since it is relatively nonspecific component).

Clusters of Orthologous Groups (COGs) were identified with IMG Pipeline (Chen et al., 2019). NMDS ordination was performed with vegan package.[1]

Experimental support

Neutrophilic and alkaliphilic haloarchaea were cultivated on the medium prepared according to Sorokin et al. (2015). For the haloarchaea from salt lakes, a mineral base medium contained the following ($g\,l^{-1}$): 240 NaCl, 5 KCl, 0.25 NH_4Cl, 2.5 K_2HPO_4, pH 6.8. The medium was heat sterilized at 120°C for 30 min and after cooling supplemented with vitamin and trace metal mix (Pfennig and Lippert, 1966) (1 $mL\,l^{-1}$ each) and 2 mM $MgSO_4$. For alkaliphilic natronoarchaea from soda lakes, a sodium carbonate/bicarbonate buffered mineral base medium containing 4 M total Na^+ included ($g\,l^{-1}$): 190 Na_2CO_3, 30 $NaHCO_3$, 16 NaCl, 5 KCl and 1 K_2HPO_4 with a final pH 10 after heat sterilization was supplemented with the same additions as the neutral base medium, except that the amount of Mg was two times lower and that 4 mM NH_4Cl was added after sterilization. Finally, the ready to use alkaline base medium was mixed 1:3 with the neutral medium, resulting in the final pH of 9.6. Various forms of insoluble celluloses with different degrees of crystallinity were used as growth substrates at the final concentration of 1–2 $g\,l^{-1}$.

1 https://CRAN.R-project.org/package=vegan

Results and discussion

General genome properties and phylogenetic analysis

Genome properties of two cellulotrophic haloarchaeal groups, AArcel (alkaliphilic haloarchaea from soda lakes) and HArcel (neutrophilic haloarchaea from neutral salt lakes), were compared (Table 1). Two genome assemblies were obtained earlier [*Natronobiforma cellulositropha* AArcel2 (Sorokin et al., 2018) and *Halococcoides cellulosivorans* HArcel1 (Sorokin et al., 2019a)], one genome was resequenced and reassembled in the course of this work (*Natronobiforma cellulositropha* AArcel5^T, see *Material and Methods* section) and the others (*Natronolimnobius* sp. AArcel1, *Natrarchaeobius* sp. AArcel7, *Halosimplex* sp. HArcel2 and *Halomicrobium* sp. HArcel3) were sequenced *de novo* in the course of this work. The G + C content of all the genome assemblies laid within rather narrow boundaries: 58.85–68.31%. In turn the genome sizes greatly varied from 2.72 Mbp (HArcel1) to 5.12 Mbp (AArcel7) leading to fairly broad range of a number of a protein-coding genes: 2641–4,769.

Currently all haloarchaea are affiliated with the class *Halobacteria* within the *Euryarchaeaota* phylum. Phylogenomic analysis of cellulotrophic strains based on "ar122" set of conserved proteins showed that natronoarchaeal AArcel strains belong to the order *Natrialbales*, while neutrophilic HArcel strains – to the order *Halobacteriales* (Figure 1) thus confirming the results of 16S rRNA gene and RpoB protein sequence-based phylogenetic analyses (Sorokin et al., 2018, 2019a). The seven cellulotrophic haloarchaea were relatively equally distributed on the haloarchaeal tree indicating polyphyletic origin of cellulotrophy in this class. To estimate occurence of this capability among haloarchaea 155 genomes of cultivated representatives of *Halobacteria* class, including 7 cellulotrophic strains were analyzed in respect to the presence of cellulose-active CAZymes.

Cellulolytic capabilities of AArcel/HArcel strains compared with other haloarchaea

Currently there are 26 known CAZymes families (22 glycoside hydrolases and 4 polysaccharide monooxygenases) harboring the enzymes with confirmed cellulolytic activities *sensu lato* (including hydrolysis of cellooligosaccharides, e.g., beta-glucosidase or cellobiose phosphorylase, http://www.cazy.org; Supplementary Table S1): beta-glucosidase (GH1, GH2, GH3, GH30, GH39, GH116), endoglucanase (GH5, GH6, GH7, GH8, GH9, GH10, GH12, GH44, GH45, GH48, GH51, GH74, GH124, GH131, GH148), cellobiose/cellodextrin phosphorylase (GH94) and lytic cellulose monooxygenase (AA9, AA10, AA15, AA16). Among them, 13 families contain archaeal sequences and only 6 families contained biochemically characterized cellulases and related enzymes found in archaea (GH1, GH2, GH3, GH5, GH12 and GH116). Besides cellulases there is a number of auxiliary proteins responsible for binding and transportation of oligomers and glucose inside the cell.

To reveal the distribution of the cellulases *sensu lato* among the haloarchaeal genomes, the genes encoding selected GHs and AAs families members were searched in 155 high-quality genomes of representatives of *Halobacteria* class including 7 genomes of AArcel/

TABLE 1 General properties of genomes of haloarchaeal AArcel/HArcel strains.

Strain	IMG Genome ID	Genome size, bp	Gene count	Scaffold count	G+C, %	Reference
AArcel1	2,681,813,540	4,560,092	4,555	18	58.85	*de novo* sequencing
AArcel2	2,642,422,534	3,732,973	3,776	42	65.43	Sorokin et al., 2018
AArcel5	2,868,148,463	3,829,432	3,854	5	65.42	resequencing
AArcel7	2,808,606,451	5,121,137	4,820	22	62.82	*de novo* sequencing
HArcel1	2,681,813,541	2,723,120	2,757	1	65.74	Sorokin et al., 2019a
HArcel2	2,808,606,450	4,572,180	4,633	68	68.31	*de novo* sequencing
HArcel3	2,867,963,358	4,205,126	4,230	19	66.23	*de novo* sequencing

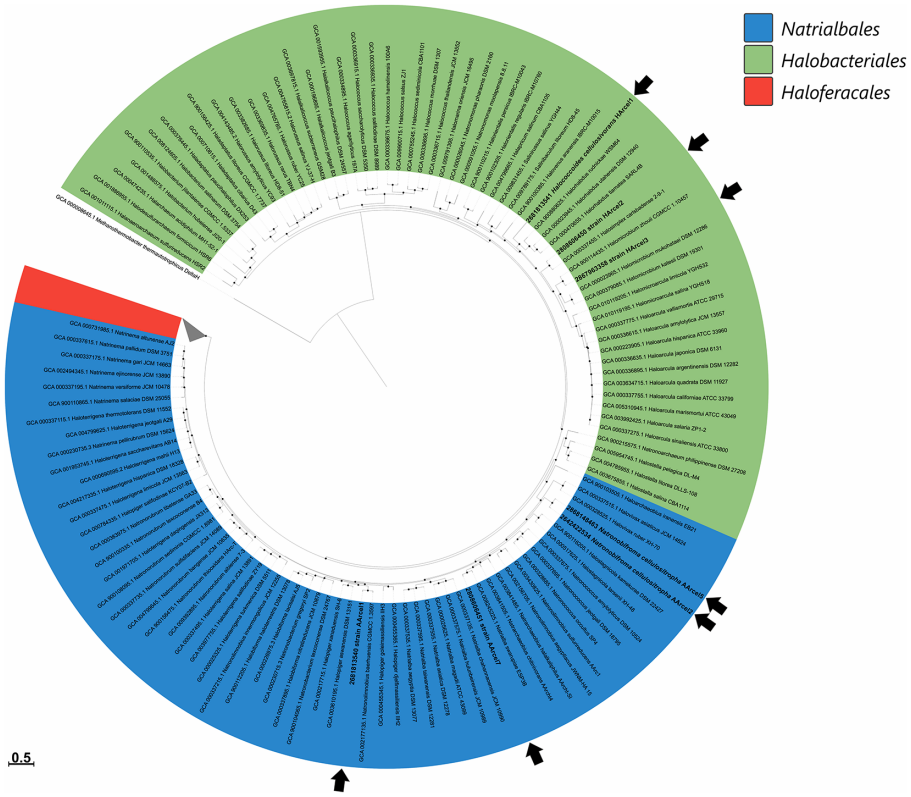

FIGURE 1
Maximum-likelihood phylogenetic tree of *Halobacteria* class based on 122 concatenated sequences of conservative archaeal proteins. Strains from AArcel/HArcel groups were marked by black arrows. The branch lengths correspond to the number of substitutions per site according to the corrections associated with the PROTGAMMAILG model in RAxML. The black circles at nodes indicate that the percentage of corresponding support values (1,000 rapid bootstrap replications) was above 50. *Methanothermobacter thermautotrophicus* DeltaH was used as an outgroup.

HArcel strains, playing a role of positive controls as they are known to be cellulose-utilizing organisms (Sorokin et al., 2015; Supplementary Figure S1). The search showed that 117 of 155 genomes possess at least one gene encoding protein from the abovementioned families (11 families were found).

The cellulases genes were unequally distributed within these 117 genomes and the AArcel/HArcel strains with the confirmed ability to utilize native insoluble forms of cellulose (Sorokin et al., 2015) were among the top in the number of such genes per genome. Among other haloarchaea for which this capacity is yet unknown there were examples with high number of cellulase genes per genome as well as genomes encoded single or few cellulases and the transition from the first to the latter variaty was seamless. With such distribution, it appeared impossible to distinguish genuine cellulotrophic representatives using this cellulases *sensu lato* dataset which is, most probably, related to the fact that besides cellulases these GH families contain enzymes which only indirectly involved in cellulose decomposition. In this regard, a set of query CAZymes was limited to CAZymes families containing endoglucanases – enzymes, playing crucial role in cellulose depolymerization (Mandeep et al., 2021) and which can be considered as signature enzymes for cellulotrophic organisms. The search with the endoglucanases set (Figure 2) resulted in selection of a much narrower group of haloarchaeal genomes with a high probability to be capable of degrading cellulose, not only its

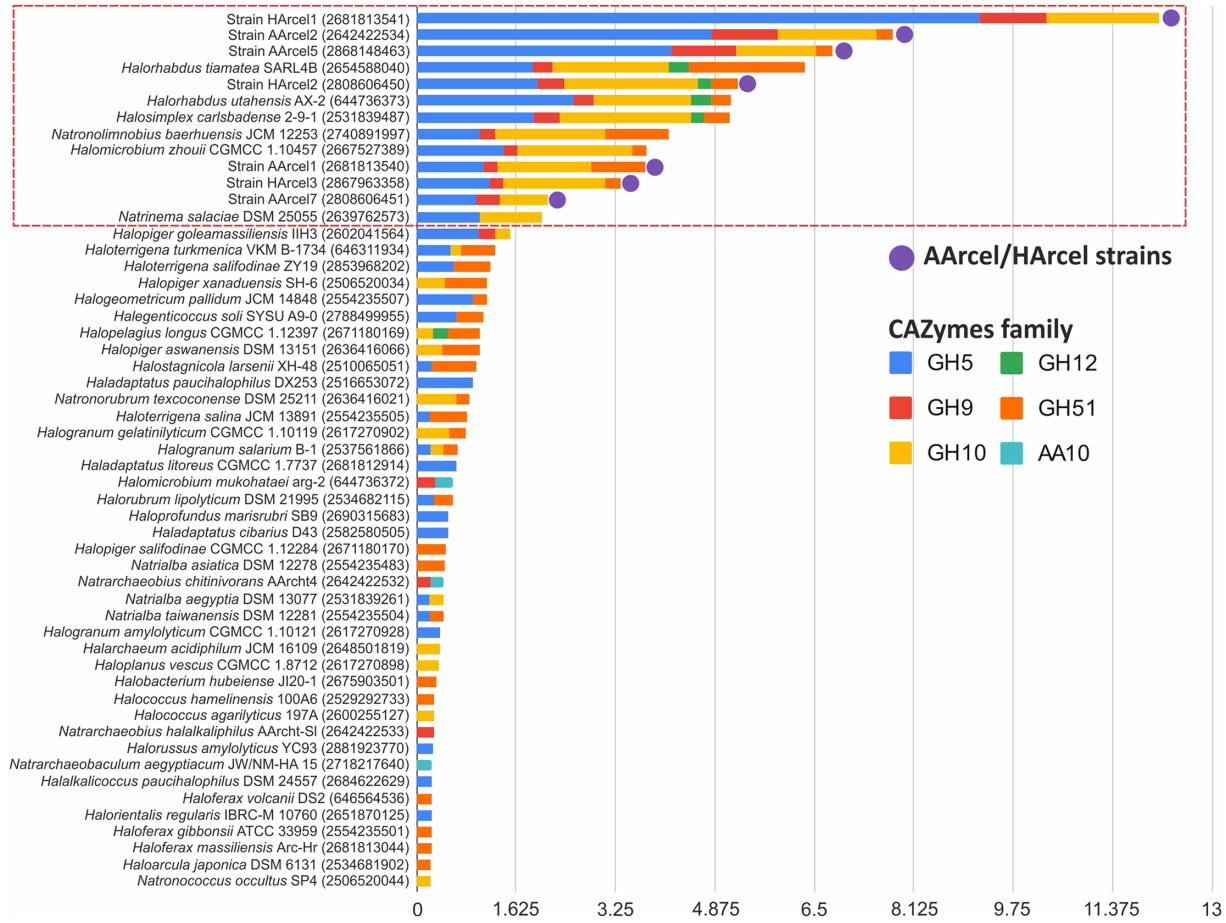

FIGURE 2
Relative abundance (gene number per1 Mbp) of putative endoglucanase genes found in 53 genomes of haloarchaea.

smaller and soluble derivatives as cellobiose, cellooligosacharides or heteropolysaccharides, containing beta-1,4-glucose linkages in their backbone or side chains. In total, 13 strains were found capable of degrading cellulose including all AArcel/HArcel strains, for which an ability to grow on native celluloses was experimentally approved (Sorokin et al., 2015). Besides AArcel and HArcel strains, the following haloarchaea were predicted to be cellulotrophic: *Halosimplex carlsbadense* 2–9-1, *Halorhabdus tiamatea* SARL4B, *Halorhabdus utahensis* AX-2, *Halomicrobium zhouii* CGMCC 1.10457, *Natronolimnobius baerhuensis* JCM 12253 and *Natrinema salaciae* DSM 25055. Three of them, *N. baerhuensis* JCM 12253, *H. carlsbadense* 2–9-1 (JCM 11222) and *H. zhouii* CGMCC 1.10457 (JCM 17095), were acquired from the Japan Collection of Microorganisms (JCM, https://jcm.brc.riken.jp/en/) and their ability to grow on amorphous cellulose was confirmed in our laboratory, while the other three still need to be tested.

While inspecting the reference endoglucanase sets of these cellulotrophic strains, including both AArcel/HArcel with the confirmed growth on cellulose and *de novo* predicted cellulotrophs it became apparent that the true cellulotrophic archaea must possess multiple and variable GH5 and GH10 families glycosidases, as well as at least several representatives from the GH9 family [excluding *Natrinema salaciae* DSM 25055 (2639762573)]. It should be noted that characterized proteins from GH5 and GH9 are mainly endoglucanases, while the majority of GH10 glycosidases are endoxylanases (despite several endoglucanases are also known (Xue et al., 2015; Zhao et al., 2019) being the reason to include this family into the "endoglucanases" set). It is possible that the latter are indeed cellulases in haloarchaea or involved in hemicelluloses decomposition, which might contribute to a better availability of cellulose for cellulases.

All putative endoglucanases encoded in the genomes of cellulotrophic haloarchaea were highly acidic having isoelectric point (pI) values from 3.86 to 4.56 (Figure 3; Supplementary Figure S2) which is linked with high salinity of their environments. Several alkaliphilic strains (AArcel1, AArcel2 and AArcel5) possessed slightly lower median pI values compared with neutrophilic haloarchaea, while AArcel7 and *Natronolimnobius baerhuensis* JCM 12253 had median pI values similar to neutrophiles indicating that environmental pH is not influencing the ratio of charged amino acids in these enzymes.

The genes encoding GH5 family glycosidases were the most numerous GH-encoding genes found in the genomes of 13 proven and predicted cellulotrophic haloarchaea. The number of GH5-encoding genes varied from 5 to 25 per genome. According to PFAM the length of a single GH5 catalytic domain is around 406 amino acids, while the lengths of the GH5-containing proteins in 13 cellulotrophic haloarchaea varied from 326 to 2,101 amino acids (Supplementary Figure S3). The data indicated that many of these proteins contained additional substrate-binding or other yet undetectable domains which can provide novel functionalities (Supplementary Table S2).

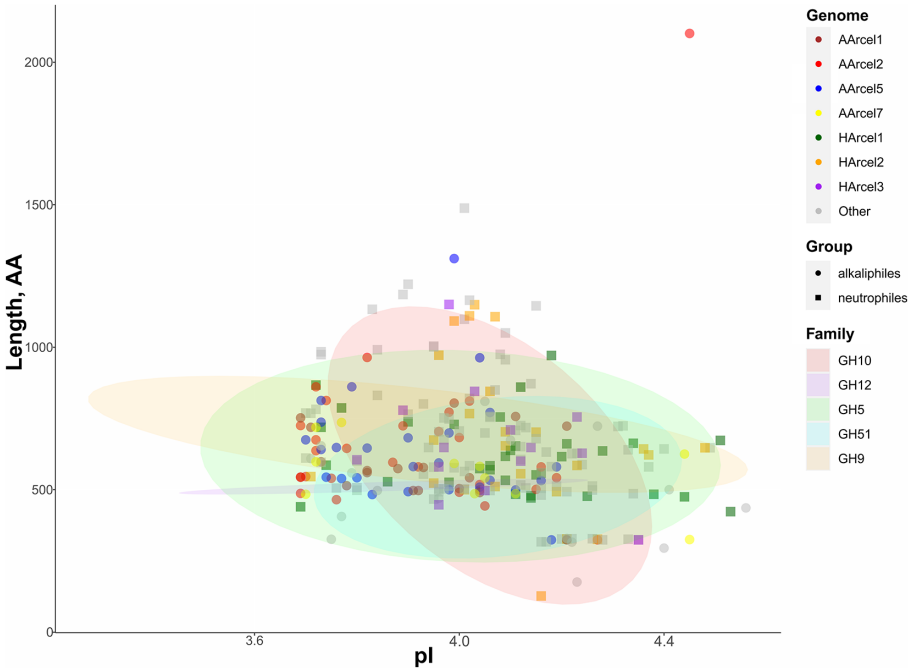

FIGURE 3
Characteristics of putative endoglucanases found in 13 genomes of cellulotrophic haloarchaea. Colors of the dots – genome assignment, shapes of the dots – assignment to neurtrophiles or alkaliphiles (based on literature data), ellipse color – enzyme family.

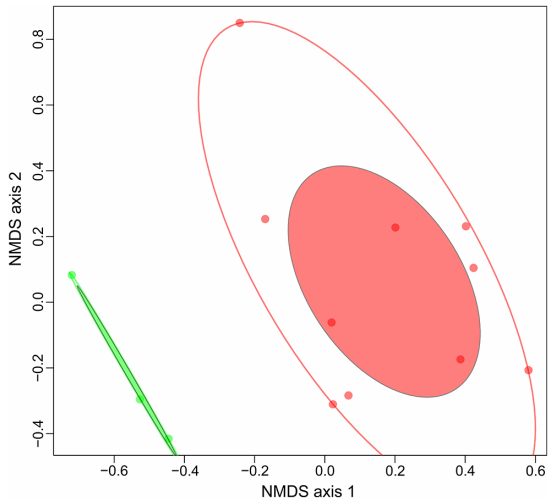

FIGURE 4
NMDS ordination plot (Bray, k=2, stress value=0.1263) of 13 haloarchaeal cellulolytic genomes based on CAZymes sets (with exception of GTs).

Ecological strategies of cellulose-utilizing haloarchaea

In our previous work on polysaccharidolytic haloarchaea (Sorokin et al., 2015) we proposed to divide all strains growing on cellulose into two groups: cellulotrophic and cellulolytic. The first are highly effective cellulose degraders, while the second are opportunists with broader substrate specificities, devouring many different oligo- and polysaccharides including the cellooligosaccharides released due to the action of the first group. In this respect, for 13 haloarchaea which either authoritatively or with high degree of probability being cellulotrophic an attempt has been made to reveal their lifestyle through the comparison of their CAZymes repertoire. Genome clustering of 13 genomes of cellulotrophic haloarchaea with NMDS ordinations was performed based on (i) a complete set of COGs found in the genomes and (ii) a set of CAZymes (excluding glycosyl transferases). Genome clusterization based on COGs gave no results since a relatively similar metabolism in terms of COGs functional categories was observed in all strains. Different results were obtained when CAZymes distribution among the genomes were used for clustering: two clearly separated groups comprised of (i) a compact cluster containing three strains (HArcel1, AArcel2 and AArcel5) and (ii) a larger and more diffused cluster comprising of other ten strains (Figure 4) were observed. We propose that the cellulose-utilizing microorganisms from the first group can be assigned to "specialists" while the second one contained "generalists." Remarkably, the genomes of cellulotrophic specialists are smaller than the generalists: 2.7–3.8 Mb and 4.2–5.1, respectively (Table 1) supporting our assumptions on their behavior.

Moreover, these two groups can be clearly distinguished not only by CAZymes repertoires and genome sizes but also by direct observation of ability to degrade cellulose. When growing on amorphous cellulose specialists form much larger hydrolysis zones in comparison with generalists (Figure 5).

Because of the action of numerous CAZymes cellulose is depolymerized to a single monomer, glucose. The question arose whether the central carbohydrate metabolism of cellulotrophic strains is uniform or the opposite is true. *In silico* reconstruction of the glucose/cellobiose/cellooligosaccharides import and glucose oxidation pathways in AArcel/HArcel strains with confirmed capability to grow on cellulose showed that glucose was transported into the cells by two

10.3389/fmicb.2023.1112247

different transport systems: (a) porters (superfamily 2.A according to TCDB) and ATP-binding cassette (ABC) transporters (superfamily 3.A.1 according to TCDB). Genes of phosphotransferase transport system (PTS) were absent in all genomes. In turn, cellooligosaccharides could be transported into the cells *via* ABC transporters as it was described for hyperthermophilic archaea (Koning et al., 2001). The number of genes encoding presumable carbohydrate transport systems components varied greatly between the genomes (Figure 6; Supplementary Table S3): HArcel1 possessed only 4 transporters (2 porters and 2 ABC transporters), while in the genome of AArcel7 35 transporters-encoding genes (9 porters and 26 ABC transporters) were found. A general observation is that the strains affiliated to specialists have less number of transporters than the generalists.

Genome analysis (Figure 7) revealed that glucose is metabolized *via* canonical-like glycolysis with ADP-phosphofructokinase (strains AArcel1 and AArcel7), haloarchaeal type of glycolysis (strains HArcel1 and HArcel3) or semi-phosphorylative Entner-Doudoroff pathway (all strains with exception of strain HArcel1).

Strain AArcel1 oxidizes glucose *via* glycolysis with ADP-phosphofructokinase as well as by complete semi-phosphorylative Entner-Doudoroff (KDPG) pathway. In the genomes of two closely related strains, AArcel5 and AArcel2, the genes encoding ADP-phosphofructokinase or 1-phosphofructokinase were absent indicating both glycolysis variants cannot be functional in this microorganism. Still, the genes of all KDPG pathway enzymes were found in the genomes of these haloarchaea. The glycolysis with ADP-phosphofructokinase as well as semi-phosphorylative KDPG pathway were predicted for AArcel7. Strain HArcel1 probably catabolized glucose only *via* glycolysis with phosphoglucomutase (performed the conversion of fructose-6-phosphate to fructose-1-phosphate, Lowry and Passonneau, 1969) and 1-phosphofructokinase and lacked KDPG pathway because KDPG aldolase gene was not found in the genome. Strain HArcel2 did not possess any variant of glycolysis due to the absence of the ADP-phosphofructokinase and 1-phosphofructokinase genes. Glucose was oxidized *via* KDPG-pathway in this microorganism. The genes encoding 1-phosphofructokinase and phosphoglucomutase were found in the genome of strain HArcel3 and thus it can utilize glucose *via* glycolysis like strain HArcel1. Complete semi-phosphorylative KDPG pathway was also predicted for this strain. Enzymes catalyzed common reactions for both the glycolysis and the KDPG pathway were present while glyceraldehyde-3-phosphate ferredoxin oxidoreductase (GAPOR), which often found in hyperthermophilic archaea, was absent in all studied strains. A gene of nonphosphorylating glyceraldehyde-3-phosphate dehydrogenase (GAPN) was found only in the AArcel7.

Summarizing the distribution of glucose oxidation pathways among the studied cellulotrophic haloarchaea it appears that specialists possessed only one glucose oxidation pathway, either

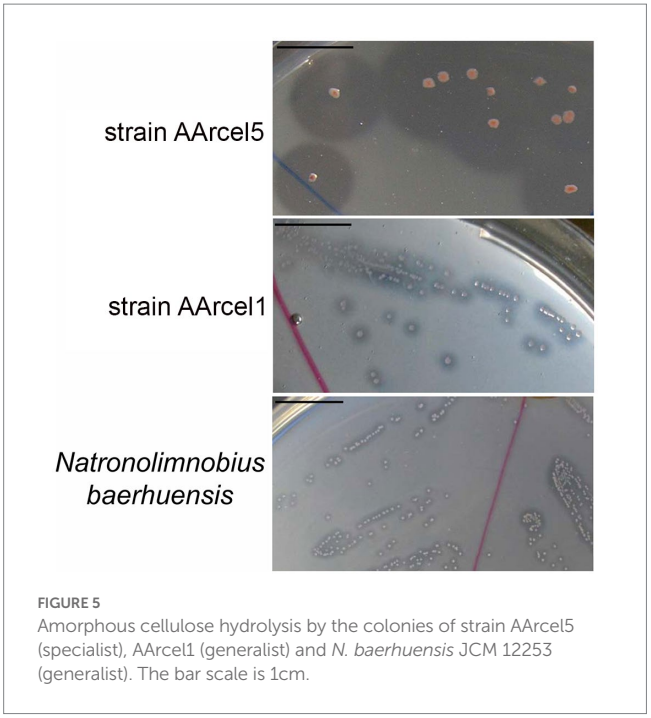

FIGURE 5
Amorphous cellulose hydrolysis by the colonies of strain AArcel5 (specialist), AArcel1 (generalist) and *N. baerhuensis* JCM 12253 (generalist). The bar scale is 1cm.

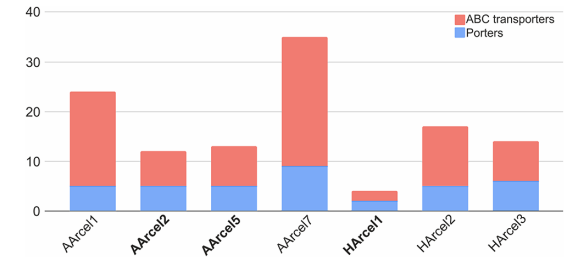

FIGURE 6
Number of putative transport system involved in carbohydrate transport AArcel/HArcel strains. Specialists are in bold.

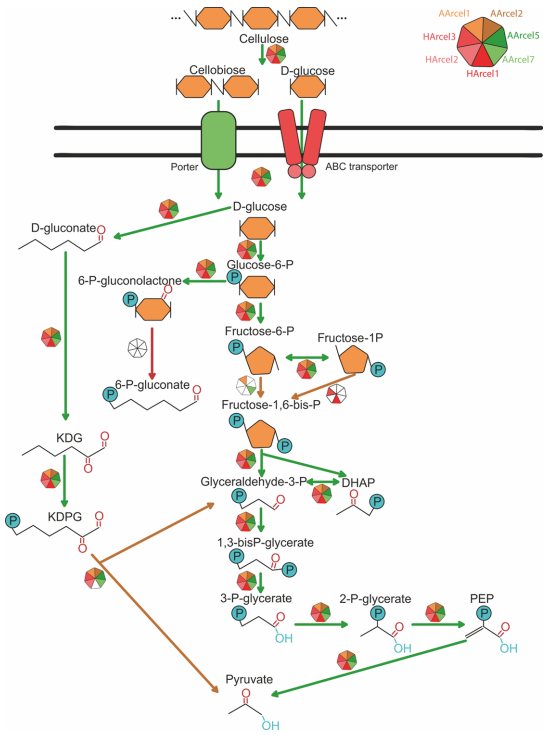

FIGURE 7
Glucose import and catabolism pathways found in AArcel/HArcel strains.

glycolysis (HArcel1) or KDPG (AArcel2 and AArcel5). Generalists, in turn, possess two pathways (AArcel1, AArcel7 and HArcel3) with the only exception – HArcel2, oxidizing glucose *via* KDPG pathway. This seems to be associated with narrower metabolism of specialists. These results are in accordance with other findings, distinguished these two groups: specialists characterized by a narrow specialization on cellulose degradation, smaller genomes, larger repertoire of genes encoding putative endoglucanases and lower number and variety in sugar transporters. Generalists include less specialized strains with a much broader substrate spectrum, larger genomes encoding lower number of cellulases but higher number and variability of sugar transporters.

Conclusion

The capacity of halophilic archaea to degrade various recalcitrant polysaccharides is of considerable interest for the understanding of their role in the mineralization of organic compounds in hypersaline environments and for search of extremely halo(alkali)stable extracellular CAZymes, attractive for the production of biofuel from lignocellulosic wastes since the pre-treatment step of this process is accomplished either with alkali or ionic liquids (Zavrel et al., 2009).

Large-scale analysis of all known CAZymes families containing cellulases encoded in the high-quality genomes of cultivated haloarchaea allowed to predict putative cellulotrophic strains. Since the dataset included the genomes of haloarchaea for which growth on and degradation of cellulose were experimentally confirmed and which therefore can be used as positive markers, these predictions allowed to propose a set of CAZymes-encoding genes indicative of the potential cellulotrophic lifestyle with a high degree of probability. Experimental validation of three out of seven cellulotrophic strains for which this property was not shown before confirmed their ability to grow on cellulose. The CAZymes patterns characteristic to cellulotrophic haloarchaea can serve as a tool for the comparative genomics-based identifying other haloarchaea carrying this trait.

Finally, genomic analysis followed by experimental verification of cellulase activity allowed dividing the cellulotrophic haloarchaea into two groups differed in strategies of cellulose utilization - specialists and generalists. The groups differed in efficiency of cellulose hydrolysis, CAZyme profiles, genome sizes, as well as in variability of mechanisms of import and central metabolism of sugars. Both groups are capable of growth on cellulose but specialists are more effective in cellulose degradation while generalists are more flexible to environmental changes, particularly to the changes in nutrient sources.

Data availability statement

The datasets presented in this study can be found in online repositories. The names of the repository/repositories and accession number(s) can be found in the article/Supplementary material.

Author contributions

AE, YU, and IK analyzed the genomes and run phylogenetic analysis. IE and AK were responsible for DNA isolation and genome sequencing libraries preparation. DS performed microbiological experiments. IK supervised the study. AE, IK, and DS wrote the manuscript. All authors contributed to the article and approved the submitted version.

Funding

The work was supported by the Ministry of Science and Higher Education of the Russian Federation.

Conflict of interest

The authors declare that the research was conducted in the absence of any commercial or financial relationships that could be construed as a potential conflict of interest.

Publisher's note

Supplementary material

The Supplementary material for this article can be found online at: https://www.frontiersin.org/articles/10.3389/fmicb.2023.1112247/full#supplementary-material

References

Altekar, W., and Rangaswamy, V. (1991). Ketohexokinase (ATP: D-fructose 1-phosphotransferase) initiates fructose breakdown via the modified EMP pathway in halophilic archaebacteria. *FEMS Microbiol. Lett.* 83, 241–246. doi: 10.1111/j.1574-6968.1991.tb04471.x

Artzi, L., Bayer, E. A., and Moraïs, S. (2017). Cellulosomes: bacterial nanomachines for dismantling plant polysaccharides. *Nat. Rev. Microbiol.* 15, 83–95. doi: 10.1038/nrmicro.2016.164

Boutet, E., Lieberherr, D., Tognolli, M., Schneider, M., Bansal, P., Bridge, A. J., et al. (2016). UniProtKB/Swiss-Prot, the manually annotated section of the UniProt KnowledgeBase: how to use the entry view. *Methods Mol. Biol.* 1374, 23–54. doi: 10.1007/978-1-4939-3167-5_2

Chaumeil, P.-A., Mussig, A. J., Hugenholtz, P., and Parks, D. H. (2019). GTDB-Tk: a toolkit to classify genomes with the genome taxonomy database. *Bioinformatics* 36, 1925–1927. doi: 10.1093/bioinformatics/btz848

Chen, I. A., Chu, K., Palaniappan, K., Pillay, M., Ratner, A., Huang, J., et al. (2019). IMG/M v. 5.0: an integrated data management and comparative analysis system for microbial genomes and microbiomes. *Nucleic Acids Res.* 47, D666–D677. doi: 10.1093/nar/gky901

Conway, J. M., Pierce, W. S., Le, J. H., Harper, G. W., Wright, J. H., Tucker, A. L., et al. (2016). Multidomain, surface layer-associated glycoside hydrolases contribute to plant polysaccharide degradation by caldicellulosiruptor species. *J. Biol. Chem.* 291, 6732–6747. doi: 10.1074/jbc.M115.707810

Drula, E., Garron, M.-L., Dogan, S., Lombard, V., Henrissat, B., and Terrapon, N. (2022). The carbohydrate-active enzyme database: functions and literature. *Nucleic Acids Res.* 50, D571–D577. doi: 10.1093/nar/gkab1045

Elferink, M. G., Albers, S. V., Konings, W. N., and Driessen, A. J. (2001). Sugar transport in *Sulfolobus solfataricus* is mediated by two families of binding protein-dependent ABC transporters. *Mol. Microbiol.* 39, 1494–1503. doi: 10.1046/j.1365-2958.2001.02336.x

Elhenawy, W., Debelyy, M. O., and Feldman, M. F. (2014). Preferential packing of acidic glycosidases and proteases into Bacteroides outer membrane vesicles. *MBio* 5, e00909–e00914. doi: 10.1128/mBio.00909-14

Gardner, J. G., and Keating, D. H. (2010). Requirement of the type II secretion system for utilization of cellulosic substrates by *Cellvibrio japonicus*. *Appl. Environ. Microbiol.* 76, 5079–5087. doi: 10.1128/AEM.00454-10

Gardner, J. G., and Schreier, H. J. (2021). Unifying themes and distinct features of carbon and nitrogen assimilation by polysaccharide-degrading bacteria: a summary of four model systems. *Appl. Microbiol. Biotechnol.* 105, 8109–8127. doi: 10.1007/s00253-021-11614-2

Gavrilov, S. N., Stracke, C., Jensen, K., Menzel, P., Kallnik, V., Slesarev, A., et al. (2016). Isolation and characterization of the first xylanolytic hyperthermophilic euryarchaeon Thermococcus sp. strain 2319x1 and its unusual multidomain glycosidase. *Front. Microbiol.* 7:552. doi: 10.3389/fmicb.2016.00552

Johnsen, U., Selig, M., Xavier, K. B., Santos, H., and Schonheit, P. (2001). Different glycolytic pathways for glucose and fructose in the halophilic archaeon *Halococcus saccharolyticus*. *Arch. Microbiol.* 175, 52–61. doi: 10.1007/s002030000237

Koning, S. M., Elferink, M. G., Konings, W. N., and Driessen, A. J. (2001). Cellobiose uptake in the hyperthermophilic archaeon *Pyrococcus furiosus* is mediated by an inducible, high-affinity ABC transporter. *J. Bacteriol.* 183, 4979–4984. doi: 10.1128/JB.183.17.4979-4984.2001

Koren, S., Walenz, B. P., Berlin, K., Miller, J. P., Bergman, N. H., and Philippy, A. (2017). Canu: scalable and accurate long-read assembly via adaptive k-mer weighting and repeat separation. *Genome Res.* 27, 722–736. doi: 10.1101/gr.215087.116

Kozlowski, L. P. (2021). IPC 2.0 : prediction of isoelectric point and pKa dissociation constants. *Nucleic Acids Res.* 49, W285–W292. doi: 10.1093/nar/gkab295

Lee, L. L., Hart, W. S., Lunin, V. V., Alahuhta, M., Bomble, Y. J., Himmel, M. E., et al. (2019). Comparative biochemical and structural analysis of novel cellulose binding proteins (tapirins) from xxtremely thermophilic *Caldicellulosiruptor* species. *Appl. Environ. Microbiol.* 85, e01983–e01918. doi: 10.1128/AEM.01983-18

Letunic, I., and Bork, P. (2019). Interactive tree of life (iTOL) v4: recent updates and new developments. *Nucleic Acids Res.* 47, W256–W259. doi: 10.1093/nar/gkz239

Loman, N. J., Quick, J., and Simpson, J. T. (2015). A complete bacterial genome assembled de novo using only nanopore sequencing data. *Nat. Methods* 12, 733–735. doi: 10.1038/nmeth.3444

Lowry, O. H., and Passonneau, J. V. (1969). Phosphoglucomutase kinetics with the phosphates of fructose, glucose, mannose, ribose, and galactose. *J. Biol. Chem.* 244, 910–916. doi: 10.1016/s0021-9258(18)91872-7

Mandeep, , Liu, H., and Shukla, P. (2021). Synthetic biology and biocomputational approaches for improving microbial endoglucanases toward their innovative applications. *ACS Omega* 6, 6055–6063. doi: 10.1021/acsomega.0c05744

Parks, D. H., Imelfort, M., Skennerton, C. T., Hugenholtz, P., and Tyson, G. W. (2015). CheckM: assessing the quality of microbial genomes recovered from isolates, single cells, and metagenomes. *Genome Res.* 25, 1043–1055. doi: 10.1101/gr.186072.114

Pfennig, N., and Lippert, K. D. (1966). Über das vitamin B12-bedürfnis phototropher schwefelbakterien. *Arch. Microbiol.* 55, 245–256.

Pickl, A., Johnsen, U., Archer, R. M., and Schönheit, P. (2014). Identification and characterization of 2-keto-3-deoxygluconate kinase and 2-keto-3-deoxygalactonate kinase in the haloarchaeon *Haloferax volcanii*. *FEMS Microbiol. Lett.* 361, 76–83. doi: 10.1111/1574-6968.12617

Pickl, A., Johnsen, U., and Schönheit, P. (2012). Fructose degradation in the haloarchaeon *Haloferax volcanii* involves a bacterial type phosphoenolpyruvate-dependent phosphotransferase system, fructose-1-phosphate kinase, and class II fructose-1,6-bisphosphate aldolase. *J. Bacteriol.* 194, 3088–3097. doi: 10.1128/JB.00200-12

Rodriguez-R, L., and Konstantinidis, K. (2016). The enveomics collection: a toolbox for specialized analyses of microbial genomes and metagenomes. *PeerJ Prepr.* 4:e1900v1. doi: 10.7287/peerj.preprints.1900

Saier, M. H., Reddy, V. S., Tamang, D. G., and Västermark, A. (2014). The transporter classification database. *Nucleic Acids Res.* 42, D251–D258. doi: 10.1093/nar/gkt1097

Sorokin, D. Y., Elcheninov, A. G., Toshchakov, S. V., Bale, N. J., Sinninghe Damsté, J. S., Khijniak, T. V., et al. (2019b). *Natrarchaeobius chitinivorans* gen. Nov., sp. nov., and *Natrarchaeobius halalkaliphilus* sp. nov., alkaliphilic, chitin-utilizing haloarchaea from hypersaline alkaline lakes. *Syst. Appl. Microbiol.* 42, 309–318. doi: 10.1016/j.syapm.2019.01.001

Sorokin, D. Y., Khijniak, T. V., Elcheninov, A. G., Toshchakov, S. V., Kostrikina, N. A., Bale, N. J., et al. (2019a). *Halococcoides cellulosivorans* gen. Nov., sp. nov., an extremely halophilic cellulose-utilizing haloarchaeon from hypersaline lakes. *Int. J. Syst. Evol. Microbiol.* 69, 1327–1335. doi: 10.1099/ijsem.0.003312

Sorokin, D. Y., Khijniak, T. V., Kostrikina, N. A., Elcheninov, A. G., Toshchakov, S. V., Bale, N. J., et al. (2018). *Natronobiforma cellulositropha* gen. Nov., sp. nov., a novel haloalkaliphilic member of the family *Natrialbaceae* (class *Halobacteria*) from hypersaline alkaline lakes. *Syst. Appl. Microbiol.* 41, 355–362. doi: 10.1016/j.syapm.2018.04.002

Sorokin, D. Y., Kublanov, I. V., Gavrilov, S. N., Rojo, D., Roman, P., Golyshin, P. N., et al. (2016). Elemental sulfur and acetate can support life of a novel strictly anaerobic haloarchaeon. *ISME J.* 10, 240–252. doi: 10.1038/ismej.2015.79

Sorokin, D. Y., Messina, E., Smedile, F., La Cono, V., Hallsworth, J. E., and Yakimov, M. M. (2021). Carbohydrate-dependent sulfur respiration in halo(alkali)philic archaea. *Environ. Microbiol.* 23, 3789–3808. doi: 10.1111/1462-2920.15421

Sorokin, D. Y., Messina, E., Smedile, F., Roman, P., Damsté, J. S. S., Ciordia, S., et al. (2017). Discovery of anaerobic lithoheterotrophic haloarchaea, ubiquitous in hypersaline habitats. *ISME J.* 11, 1245–1260. doi: 10.1038/ismej.2016.203

Sorokin, D. Y., Toshchakov, S. V., Kolganova, T. V., and Kublanov, I. V. (2015). Halo(natrono)archaea isolated from hypersaline lakes utilize cellulose and chitin as growth substrates. *Front. Microbiol.* 6:942. doi: 10.3389/fmicb.2015.00942

Stamatakis, A. (2014). RAxML version 8: a tool for phylogenetic analysis and post-analysis of large phylogenies. *Bioinformatics* 30, 1312–1313. doi: 10.1093/bioinformatics/btu033

Teufel, F., Almagro Armenteros, J. J., Johansen, A. R., Gíslason, M. H., Pihl, S. I., Tsirigos, K. D., et al. (2022). SignalP 6.0 predicts all five types of signal peptides using protein language models. *Nat. Biotechnol.* 40, 1023–1025. doi: 10.1038/s41587-021-01156-3

Uusi-Tarkka, E.-K., Skrifvars, M., and Haapala, A. (2021). Fabricating sustainable all-cellulose composites. *Appl. Sci.* 11:10069. doi: 10.3390/app112110069

Walker, B. J., Abeel, T., Shea, T., Priest, M., Abouelliel, A., Sakthikumar, S., et al. (2014). Pilon: an integrated tool for comprehensive microbial variant detection and genome assembly improvement. *PLoS One* 9:e112963. doi: 10.1371/journal.pone.0112963

Williams, T. J., Allen, M. A., Liao, Y., Raftery, M. J., and Cavicchioli, R. (2019). Sucrose metabolism in haloarchaea: reassessment using genomics, proteomics, and metagenomics. *Appl. Environ. Microbiol.* 85, e02935–e02918. doi: 10.1128/AEM.02935-18

Xue, X., Wang, R., Tu, T., Shi, P., Ma, R., Luo, H., et al. (2015). The N-terminal GH10 domain of a multimodular protein from *Caldicellulosiruptor bescii* is a versatile xylanase/β-glucanase that can degrade crystalline cellulose. *Appl. Environ. Microbiol.* 81, 3823–3833. doi: 10.1128/AEM.00432-15

Zavrel, M., Bross, D., Funke, M., Büchs, J., and Spiess, A. C. (2009). High-throughput screening for ionic liquids dissolving (ligno-)cellulose. *Bioresour. Technol.* 100, 2580–2587. doi: 10.1016/j.biortech.2008.11.052

Zhang, H., Yohe, T., Huang, L., Entwistle, S., Wu, P., Yang, Z., et al. (2018). dbCAN2: a meta server for automated carbohydrate-active enzyme annotation. *Nucleic Acids Res.* 46, W95–W101. doi: 10.1093/nar/gky418

Zhao, F., Cao, H.-Y., Zhao, L.-S., Zhang, Y., Li, C.-Y., Zhang, Y.-Z., et al. (2019). A novel subfamily of endo-β-1,4-glucanases in glycoside hydrolase family 10. *Appl. Environ. Microbiol.* 85, e01029–e01019. doi: 10.1128/AEM.01029-19

Zhong, C., Ukowitz, C., Domig, K. J., and Nidetzky, B. (2020). Short-chain cello-oligosaccharides: intensification and scale-up of their enzymatic production and selective growth promotion among probiotic bacteria. *J. Agric. Food Chem.* 68, 8557–8567. doi: 10.1021/acs.jafc.0c02660

Frontiers in Microbiology

Explores the habitable world and the potential of microbial life

The largest and most cited microbiology journal which advances our understanding of the role microbes play in addressing global challenges such as healthcare, food security, and climate change.

Discover the latest Research Topics

See more →

Frontiers

Avenue du Tribunal-Fédéral 34
1005 Lausanne, Switzerland
frontiersin.org

Contact us

+41 (0)21 510 17 00
frontiersin.org/about/contact